On the Risk Assessment of German Covered Bonds in a One-Period Setting

Dissertation

zur Erlangung des akademischen Grades

Dr. rer. nat.

eingereicht an der

Mathematisch- Naturwissenschaftlich- Technischen Fakultät

der Universität Augsburg

von

Maximilian Hughes

Erstgutachter:	Prof. Dr. Ralf Werner
Zweitgutachter:	Prof. Dr. Georg Schlüchtermann
Tag der mündlichen Prüfung:	05. November 2019

To my mum who provided me with everything a son could wish for.

> By this means all knowledge degenerates into probability; and this probability is greater or less, according to our experience of the veracity or deceitfulness of our understanding, and according to the simplicity or intricacy of the question.

(David Hume, A Treatise of Human Nature, 1739-40)

> It isn't that they can't see the solution. It's that they can't see the problem. They can't see the problem if they are looking in the wrong place. They can't see the problem if they have blinders on — for 'none are so blind as those that will not see'.

(Gilbert K. Chesterton, Scandal of Father Brown, 1935)

> Complete realism is clearly unattainable, and the question whether a theory is realistic enough can be settled only by seeing whether it yields predictions that are good enough for the purpose in hand or that are better than predictions from alternative theories.

(Milton Friedman, The Methodology of Positive Economics, 1953)

Acknowledgements

First and foremost, I would like to thank my supervisor Prof. Dr. Ralf Werner for the immense support and trust placed in me, enabling me to write about this remarkable and highly interesting topic and guiding me into the fields of covered bonds and mathematical finance.

Special thanks to Yan Yang, Dr. Dirk Banholzer, Dr. Manuela Spangler, Dr. Jan Natolski, Prof. Dr. Georg Schlüchtermann and participants of numerous conferences, seminars and workshops for their valuable input. My expression of gratitude to the department of computer science and mathematics of the University of Applied Sciences Munich and the institute of mathematics of the University of Augsburg that gave me the opportunity to complete my thesis within the framework of a joint research project in mathematical finance.

This research is part of the project regarding the modelling of the Pfandbriefe (German covered bonds), financially supported by the Bayerische Staatsministerium für Wissenschaft, Forschung und Kunst and backed by the corporate partners Allianz Deutschland AG, Deutsche Pfandbriefbank AG and DEVnet GmbH.

On behalf of Andreas Kokott and Jan Leuchter I would like to express my gratitude to whole of DEVnet GmbH where, alongside my thesis, I could pursue a career as a consultant and quantitative analyst with many interesting and exiting projects. The flexibility regarding working hours and the degrees of freedom I was given was highly appreciated.

I would like to take the opportunity to highlight several books which gave me great insights and inspiration in their respective fields for which I am very grateful: financial modelling — Björk (2004), Wilmott (2006), Hull (2009) & interest rate modelling — Brigo and Mercurio (2007), Schlüchtermann and Pilz (2010) & credit risk modelling — Bluhm et al. (2002), Lando (2004), McNeil et al. (2005) & financial calculus — Baxter and Rennie (1996), Shreve (2004), Shreve (2012) & numerical methods — Glasserman (2004), Korn et al. (2010), Kloeden and Platen (2011) & covered bonds — Golin (2006), Spangler and Werner (2014).

Above all, many thanks go to all my friends and family for supporting me throughout this work. Especially, without the patience, moral backing and continual encouragement from my mother Carole, my brother Rupert and my partner in life Veronika, this endeavour I set out on could not have been realised.

Abstract

This research examines the events of mortgage Pfandbrief defaults occurring due to asset-liability mismatches on the balance sheet of Pfandbrief banks. The risk assessment of the Pfandbrief in a one-period and risk-neutral setting is based on advanced structural and reduced-form modelling approaches. In its over 200 year history not one single Pfandbrief has ever defaulted, however, this practically risk-free perception has changed since the recent financial crises. Investors seek methods to carry out their own credit quality analysis instead of relying on ratings from third parties, e.g. rating agencies, and basing their investment decisions thereupon. A generic modelling framework is proposed and adapted to the mortgage type of Pfandbrief. Certain characteristics attributed specifically to the Pfandbrief and cover pool risks, for example, refinancing risk, interest rate risk and asset default risk are incorporated into the introduced models. The first model is based on Merton's structural approach. Significant improvements wrt to computation time and accuracy of the underlying stochastic process are accomplished as well as an enhanced least square Monte Carlo application is established. The innovative reduced-form approach adopts techniques from CDO modelling which are applied to the underlying cover pool. A large homogeneous portfolio is postulated for the cover pool where stochastic recovery rates are included. Forecasting future default probabilities in continuous time is accomplished via generator matrices where updated credit quality information regarding the cover pool assets can be integrated. Furthermore, the well-established JLT model is extended allowing stochastic risk premiums to be exogenously considered. Dependency between asset positions is captured via copulas. The profound advantage of the reduced-form model over its structural counterpart is the more accurate modelling of the Pfandbrief's downside risk.

Table of Contents

List of Tables

List of Figures

List of Acronyms

A	assets
a.e.	almost everywhere
a.s.	almost surely
ABS	asset backed security
ACP	aircraft cover pool
AD	Anderson-Darling
AIC	Akaike information criterion
APB	aircraft Pfandbrief
ATM	at-the-money
ATS	affine term structure
BaFin	Bundesanstalt für Finanzdienstleistungsaufsicht
BAM	best approximation of the annual transition matrix
BIC	Bayesian information criterion
CB	covered bond
CBPP	covered bond purchase programme
CDO	collateralised debt obligations
CIR1F	Cox-Ingersoll-Ross one-factor model
CLO	collateralised loan obligation
CP	cover pool
CPT	conditional pass-through
CRR	Capital Requirements Regulation
DA	diagonal adjustment
EAD	exposure at default
ECB	European Central Bank
ECBC	European Covered Bond Council
EJLT	extended Jarrow-Lando-Turnbull
EL	expected loss
EONIA	Euro OverNight Index Average
EQ	equity
ESG	economic scenario generator
EU	European Union
EURIBOR	Euro InterBank Offered Rate
EVT	extreme value theory
GCD	Global Credit Data
GGB	government guaranteed bond
GPD	generalised Pareto distribution

HJM	Heath-Jarrow-Morton
HW1F	Hull-White one-factor model
i.i.d.	independent identically distributed
iff	if and only if
IRB	internal ratings-based (IRB) approach
JLT	Jarrow-Lando-Turnbull
KK	Kijima-Komoribayashi
KS	Kolmogorov-Smirnov
KW	Kruskal-Wallis
KWG	Kreditwesengesetz
L	liabilities
LCR	liquidity coverage ratio
LGD	loss given default
LHP	large homogeneous portfolio
LSMC	least square Monte Carlo
LTRO	long-term refinancing operations
LtV	loan-to-value
MBS	mortgage backed security
MC	Monte Carlo
MCP	mortgage cover pool
ML	maximum likelihood
MPB	mortgage Pfandbrief
NIG	normal inverse Gaussian
NMC	nested Monte Carlo
OA	other assets
OC	overcollateralisation
ODE	ordinary differential equation
OL	other liabilities
OO	object oriented
OOP	object oriented programming
OTC	over the counter
PB	Pfandbrief
PCP	public cover pool
PCR	principle component regression
PD	probability of default
PfandBG	Pfandbriefgesetz
PLSR	partial least squares regression
PPB	public Pfandbrief
QE	Quadratic-Exponential

RCMM	regular credit migration model
RMBS	residential mortgage backed security
RMSE	root mean squared error
RWA	risk weighted asset
SABR	stochastic alpha, beta, rho
SARIMA	seasonal auto regressive integrated moving average
SCP	ship cover pool
SDE	stochastic differential equation
SME	small and medium enterprise
SPB	ship Pfandbrief
SPV	special purpose vehicle
SVD	singular value decomposition
TG	Truncated-Gaussian
UL	unexpected loss
vdp	Verband deutscher Pfandbriefbanken
WA	weighted adjustment
wrt	with respect to
ZCB	zero-coupon bond

List of Symbols

β_k	regression coefficients
B_t	bank account process
$\boldsymbol{C}$	multivariate copula
chol	Cholesky decomposition operator
d	derivative operator
δ	recovery rate
Δt	discrete time increment
$\mathfrak{d}$	time difference operator
$\mathrm{d}t$	infinitesimal time increment
$\mathrm{d}W(t)$	infinitesimal Brownian increment
$\mathrm{d}Y$	Poisson process
$\mathbb{E}$	expectation operator
$\boldsymbol{F}$	N-dimensional distribution function
f	function
$\mathcal{F}_t$	history of Brownian motion up to time t / filtration
$\boldsymbol{G}$	generator matrix
$\mathfrak{g}_t$	Girsanov kernel
g	function
$\circ$	Hadamard product
Im	imaginary part of a complex number
K	strike
κ	mean reversion speed
λ	jump intensity
$\mathcal{L}^p$	$\mathcal{L}^p$ spaces / Lebesgue spaces for $0 < p \leq \infty$
μ	mean
Ω	sample space
$f = O(g)$	asymptotic order symbol; there exists a n_0 and a constant c such that for all $n > n_0$, $\lvert f(n)\rvert \leq c\lvert g(n)\rvert$, with the result $\lim_{n\to\infty} f(n)/g(n) \neq \infty$
$f = o(g)$	asymptotic order symbol; for all $c > 0$, there exists an n_0 such that for all $n > n_0$, $\lvert f(n)\rvert \leq cg(n)$, with the result $\lim_{n\to\infty} f(n)/g(n) = 0$

$\otimes$	Dyadic / Kronecker product
$\mathcal{P}$	real-world probability measure
$\boldsymbol{P}$	transition matrix
$P(t,T)$	zero-coupon bond
∂	partial derivative operator
$\boldsymbol{\Phi}$	standard normal distribution function, $\boldsymbol{\Phi}(z) = \text{Prob}(\text{N}(0,1) \leq z)$
φ_t	market price of risk
Π	jump amplitude of the jump process
Prob	probability operator
$\mathcal{Q}$	risk-neutral probability measure
$\mathcal{Q}_T$	forward probability measure
$\boldsymbol{R}$	correlation matrix
$\mathbb{R}$	set of real numbers
r	(risk-free) interest rate
Re	real part of a complex number
$r(t)$	(risk-free) interest rate process
S	maturity / exercise time of a derivative
s	time
$\boldsymbol{\Sigma}$	covariance matrix
σ	standard deviation
σ^2	variance
$\varsigma^2(t)$	volatility process
T	maturity / exercise time of a derivative
t	time
T_1	maturity of liabilities
T_2	maturity of assets
τ	default time
θ	mean reversion level
$\theta(t)$	initial yield curve
$\mathcal{T}$	set of maturities
U	uniform random variable
u	realisation of the uniform random variable
$V(t,T)$	risky zero-coupon bond
$\mathbb{V}$	variance operator
v	positive constant
$V(t)$	state variable process; present value
$W(t), \widetilde{W}(t)$	Brownian motion
X	random variable
x	realisation / variable

Y	random variable
y	realisation / variable
Z	random variable (usually standard-normal if not stated otherwise)
z	realisation / variable (usually standard-normal if not stated otherwise)

1. Introduction

Pfandbriefe are covered bonds issued on the basis of the German Pfandbriefgesetz (PfandBG). In contrast to many other European covered bonds, the fundamentals of the Pfandbrief and its emission are regulated by law instead of only by contract. The two most important classes of German Pfandbriefe are the mortgage Pfandbriefe and public sector Pfandbriefe, which are characterised by the type of available collateral (cover pool). In 2016, Germany represents the second largest covered bond market, after Denmark, with an outstanding volume (including all types of Pfandbriefe) of approximately €373.8 bn with a market share of 15.6% — the worldwide covered bond volume totalling €2.4 tn. In addition to the significant size of the Pfandbrief market, the following points underline the high social and economic relevance:

- Pfandbriefe represent one of the most cost-efficient refinancing options — e.g. compared to unsecured bonds they allow a much more favourable refinancing for the issuer — in the classical banking business (lending), and thus promote both the lending amount as well as the conditionality of lending by banks due to lower refinancing costs. This is especially true in times of liquidity bottlenecks and financial crises, since Pfandbriefe were one of the most stable and liquid asset classes even in hight of the financial crisis, referring to VDP (2010) and VDP (2011). Likewise, according to VDP (2011), the issue volume of German Pfandbriefe was hardly affected by the financial crisis and the emissions expectations of the vdp (Verband deutscher Pfandbriefbanken) member banks were essentially fulfilled.

- Due to their structural advantages over other securitisation structures, German Pfandbriefe in the financial market are regarded as similarly safe investments as German government bonds. This assessment of Pfandbriefe being highly qualitative (i.e. practically fail-safe) and extremely liquid investments in the financial market is also confirmed by the liquidity guidelines of the supervisory authorities in Basel III (BIS, 2013). Inline with Basel III, Pfandbriefe are permitted to be part of the liquidity buffer of a bank and to be included for calculating its LCR (liquidity coverage ratio) under specific criteria (EBA, 2016, p. 91). The favourable treatment of the covered bond, enabled by the LCR Delegated Act, came into effect in July 2018 by the European Commission and represents an EU-wide implementation of the Basel's LCR rules.

- Pfandbriefe represent one of the most important asset classes, in particular for German insurance companies and pension funds. One example is Allianz Deutschland AG which holds approximately 15.6% of its investments in Pfandbriefe, amounting to €89.9 billion, in 2016, compare Allianz SE (2016). This means that the surplus yields of the insurance companies, and thus, for example, the returns on life insurance contracts or the costs for private health insurance depend to a large extent on the performance of German Pfandbriefe.

1.1. Problem Statement

Since Pfandbriefe were regarded as ‘largely non-hazardous’ until a few years ago, their spread differences to German government bonds were usually interpreted as pure liquidity premiums. However, due to the increase in the fluctuations in the spreads of German Pfandbriefe observed in recent years (see FIGURE 1.1), this interpretation was questioned in academic examinations where alternative explanatory approaches were presented for the widening of spreads phenomenon. Some reasons for a shift of opinions amongst

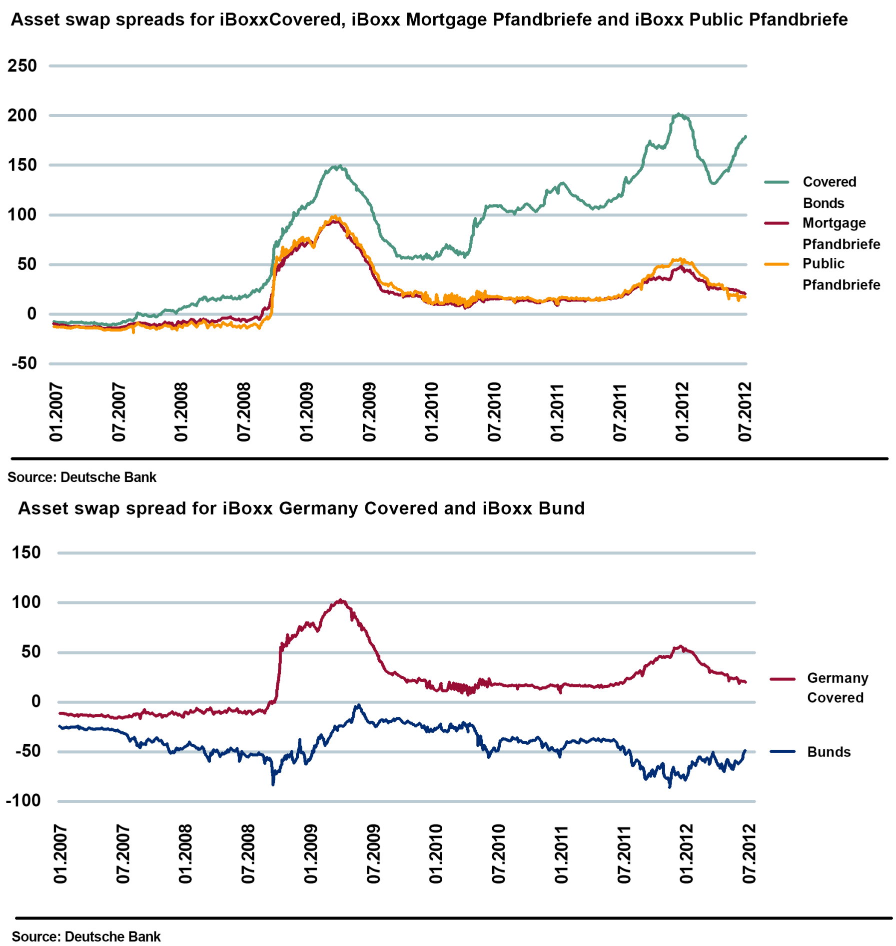

FIGURE 1.1.: Performance of Pfandbrief spreads in comparison to covered bonds and bunds (Source: (VDP, 2012)). Top: iBoxx Mortgage/Public Pfandbrief versus iBoxx Covered; Bottom: iBoxx Germany covered versus iBoxx Bund

researchers and investors, especially since the financial crisis, are:

- Up to the recent past, i.e. until the onset of the financial crisis, the Pfandbrief market was one of the most liquid bond markets in Germany. The spreads between German Pfandbriefe and German government bonds were very low and also had very low volatility (see FIGURE 1.1). Thus, now there exists a more urgent need for the pricing of German Pfandbriefe, similarly to structured but illiquid and more volatile credit derivatives of Collateralized Debt Obligations (CDOs) or (Mortgage-Backed Securities) MBSs.

- In the same way as for other credit derivatives, such as CDOs or MBSs, investors in their investment decision essentially depended on the judgement of rating agencies. Due to the loss of trust in third party gradings or at least having an increased awareness of an underlying potential bias, investors are now willing to carry out their own risk assessments, even though the overall consent over the excellent credit quality of German Pfandbriefe evidently still remains.
- The Pfandbriefgesetz was established on May 22nd, 2005 with its latest amendment on January 3rd, 2018. It regulates, among other things, the transparency requirements for Pfandbrief issuers and specifies which information issuers are required to publish on a quarterly basis. However, it is important to emphasise that only since the vdp transparency initiative in third quarter 2010 has resulted in a uniform interpretation of these requirements across all vdp member banks. This allows to carry out a coherent and consistent modelling of Pfandbriefe on the basis of such granular data.

Despite the high popularity of the Pfandbrief, in contrast to CDOs or MBSs, there is neither an adequate mathematical modelling framework, nor software tools for the assessment and / or risk analysis of German Pfandbriefe. This gap is to be partially bridged by this work on the basis of innovative financial mathematical and information technology methods in order to answer current questions about the Pfandbrief on a quantitative basis where CDO and MBS modelling concepts are adopted.

1.2. Related Work

To this end, quantitative studies on the Pfandbrief remain scarce. In Siewert and Vonhoff (2011) the authors on the one hand confirm the historical view to the extent that liquidity remains the central driving factor for spread differences, but on the other hand the issuer's default risk (thus the balance sheet structure) and the quality of the cover pool also have a strong influence on the valuation differences to German government bonds. The analysis in Siewert and Vonhoff (2011) is carried out empirically by means of regression approaches based on available market information in the form of spreads and cover pool assets / loans. A comparable study is also given in Prokopczuk and Vonhoff (2012). In the PhD thesis of Sünderhauf (2006), the question is investigated whether the mortgage Pfandbrief can be described as a failure risk independent of the issuer's credit rating. Sünderhauf (2006), and likewise Siewert and Vonhoff (2011), conclude that this is not the case. Main driver of the issuer's risk structure is the constitution of the balance sheet with its asset-liability and maturity mismatches. In Sünderhauf (2006)'s risk assessment a structural model based on the Merton (1974) approach is applied where various stress scenarios are simulated. Given the issuer has defaulted, it is then of interest if the Pfandbrief itself has defaulted. The third major work on this topic complex by Rudolf and Saunders (2009) compares the structural differences between mortgage Pfandbriefe, CDOs and MBSs. The authors conclude that German Pfandbriefe have a much lower credit risk than comparable financial instruments due to the structural concept. Kenyon (2009) provides pricing methods for covered bonds based on a 'Triggered Refreshed CDO' with 'Issuer Risk model' solely focussing on public-/sovereign-related sector case. The model concentrates on asset replacement by the issuer resulting in a significant change to the default distribution described by the factor Copula approach. However, requirements on asset-liability matches on issuances, e.g.

duration, cash flows, etc. are ignored. A more recent study on covered bonds, in general, is provided by Tasche (2016) based on the balance sheet segmentation of Chan-Lau and Oura (2014). Thereby, emphasis is laid upon the impact of the asset encumbrance by the cover pool on the loss characteristics of the issuer's senior unsecured debt. It is shown that an exact calibration of the two asset case may be impossible based on a one-period structural modelling approach. Likewise to Kenyon (2009), the assumption of a well-managed cover pool is postulated (non consideration of asset-liability mismatches). A first multi-period simulation-based Pfandbrief model is introduced by Spangler (2018) providing a flexible framework to adequately account for Pfandbrief's most important characteristics and risks. Calibration and simulation results are analysed.
An extensive risk analysis of the Pfandbrief is given in Spangler and Werner (2014) where certain risks are prioritised, based on the legislative framework of the Pfandbrief issuance. This is of great significance to the overall modelling process. For example, in the event of an issuer defaulting Pfandbrief holders are ring fenced from other creditors. Homey and Soldera (2010) also give some insights on the legal framework (PfandBG). A more general view of the covered bond market (not only in Germany) can be found in Golin (2006), Packer et al. (2007), Philipp (2008), Volk (2009), Volk (2011), Pinedo and Tanenbaum (2010a), Pinedo and Tanenbaum (2010b) and Bertalot et al. (2011), whereas Beckers (2009) and Just and Maennig (2012) give specific background information on the German mortgage market and the product of the mortgage Pfandbrief. Dübel (2010) argues that a need to reform the Pfandbrief product itself and Pfandbrief banks is necessary in the wake of the financial crisis.

1.3. Thesis Structure

An outline of the thesis structure is detailed for orientation purposes. Apart from the main body of the thesis an appendix is provided for outsourcing elements which do not contribute to the general setup and flow of reading, however, provide extra insight to certain topics.
Appendix A is dedicated to the object orientated implementation side of the complete Pfandbrief framework in MATLAB[1] and a proposal of efficient programming thereof. More in-depth theory on certain topics and derivations of some important formulas are provided in Appendix B. Essential to the complete modelling process is to establish a data catalogue (Appendix C) where all required data is documented. Supplementary graphics can be found in Appendix D.
In the main part we first give an overview of the covered bond and Pfandbrief market and examine a mortgage Pfandbrief bank more closely wrt its balance sheet. The findings thereof are then incorporated into the investigation of the Pfandbrief default process consisting of the Pfandbrief modelling framework, its models and its applications to available data. One main result from the statistical market analysis is the rise in market share of the mortgage type Pfandbriefe. Thus, solely mortgage Pfandbrief banks (banks with a predominant mortgage Pfandbrief business) are subject to the default investigation in a one-period setting. Methods essential to the framework are first described in theory then backed by extensive applications where appropriate. Often examples, identifiable by a separate example environment, are included providing a better understanding

[1]Copyright © R2017a
MATLAB®is a registered trademark of MathWorks, Inc.™

of the underlying theory and adding a common theme to the overall thesis structure. By selecting and connecting examples one can deduce the default determination of the Pfandbrief product from beginning to end. This thesis is structured as follows:

- *Chapter 2 — Market and Bank Analysis* provides a worldwide review of the covered bond and in particular of the Pfandbrief market in Germany. Some interesting developments in recent years are extracted and taken into consideration for educing suitable modelling concepts. Further, on a micro level the balance sheet setup is analysed by the example of the selected mortgage Pfandbrief bank Münchener Hypothekenbank eG. Historical time series of balance sheet positions are statistically analysed in order to make assertions about past and future business developments.
- *Chapter 3 — A Pfandbrief Modelling Framework* describes the underlying theory of the Pfandbrief modelling in a one-period setting, namely, how a Pfandbrief bank's balance sheet is embedded into a general default framework. The Pfandbrief framework produces the fundamental ground work for any financial models taken into consideration. Emphasis is laid upon providing a structure which constitutes crucial features restricted by the boundaries of the underlying Pfandbrief law, yet at the same time keeping it generic for allowing a flexible interpretation on choosing applicable models from a mathematical perspective. An analysis of suitable interest rate models in general is taken into account by taking past and current interest rate market environments into consideration. It turns out that, according to well defined model selection criteria, the (affine) one-factor Hull-White interest rate model is most suitable in fulfilling the requirements for assessing the default profile of the Pfandbrief in a one-period setting. An application to market data is carried out in a risk-neutral setup.
- *Chapter 4 — Structural Model* reviews the one-period Pfandbrief model introduced by Sünderhauf (2006). An advanced least-square Monte Carlo approach is implemented and advantageous numerical methods for the stochastic volatility and jump process are developed where vast computational improvements wrt to accuracy and speed are achieved. Furthermore, we provide mathematical formulations of the underlying stochastic differential equations in the forward and real-world measure adding additional modelling possibilities. As aforementioned, we only take the mortgage business of a Pfandbrief bank into account, as opposed to Sünderhauf (2006) who also included the public sector, thus reducing the simulation effort. However, any presented amendments can easily be extended to public sector financing of a Pfandbrief bank.
- *Chapter 5 — Reduced-Form Model* is the newly proposed model based on the reduced form approach. The major advantage stems from the fact that the distribution of the cover pool is directly determined by ratings, obtained for example from internal ratings-based (IRB) approach, of its assets which are incorporated in the credit risk assessment of the Pfandbrief product. This renders expensive simulations unnecessary. The mortgage cover pool marginal distribution is linked by a copula with the other assets position capturing the underlying dependence structure. Model complexity is significantly reduced by postulating a large homogeneous portfolio for the cover pool assets. Additionally, by allowing stochastic recovery rates more emphasis can be laid upon the downside risk of the loss distribution. At the same time more reliable information on cover pool assets can be injected into the loss distribution, and thus more control over resulting default probabilities of the Pfandbrief can be

obtained. Thereby, a great deal of attention is dedicated to obtaining forward and risk-neutral default probabilities in a Markovian modelling environment. The novelties of this chapter are represented by an extension to the standard JLT model by incorporating stochastic risk premiums paired with optimisation techniques for transforming the given annual transition matrix to a valid generator matrix.

- *Chapter 6 — Default Analysis* applies the Pfandbrief framework with the structural and the reduced form model to a selection of mortgage Pfandbrief banks, with Münchener Hypothekenbank eG at the centre of attention. The model outcomes are examined on realistic and stressed scenarios applied to available balance sheet and §28 PfandBG data. Thereby, interest rate risk is accounted for by calibrating to today's market. The overall aim is to investigate under which circumstances the bank's asset-liability management is not sufficiently adapted or equipped preventing Pfandbriefe from defaulting. Should an event of default occur, the loss given default and expected loss are then of interest.

Finally, *Chapter 7 — Conclusion* summarises the thesis and suggests promising future research areas.

2. Market and Bank Analysis

This section can be viewed as supplementary to standard providers of market statistics, for example the fact books of the ECBC[1] ((ECBC, 2016) and (ECBC, 2017)) or VDP[2] ((VDP, 2016) and (VDP, 2017)), where the depicted graphics provide an overall development in an ‘at a glance manner’[3]. Additionally, this statistical analysis can be viewed as extension of the Pfandbrief market section in Spangler and Werner (2014). Moreover, a thorough market analysis is crucial for any modelling attempts at a later stage.
Emphasis is laid upon the public sector and mortgage type of covered bonds and Pfandbriefe. Other types (including ship, aircraft and mixed assets issued in France) do not play a significant role in the overall market or have just recently emerged, for instance the aircraft and ship Pfandbrief in the German market. Evidently, from FIGURE 2.1 the covered bond in 2016 is dominated by the public sector (12% after 15% in 2015) and mortgage type[4] (86% after 85% in 2015). This snapshot reveals the importance of the mortgage type covered bond internationally over the public sector type. The German Pfandbrief market (FIGURE 2.2) is more balanced between mortgage (55%) and public sector (43%) types, however, coming a long way from a dominated public sector market contributing three-quarters of the share in 2003. Further analysis throughout this section will reveal that there is a clear trend towards a mortgage covered bond / Pfandbrief driven market.
Despite a low interest rate environment (see for example FIGURE 2.29), fixed rate bonds continue to make up the majority of the covered bond market, see FIGURE 2.3 which is also the case for the domestic German market (FIGURE 2.4) regarding outstanding and new issuance bonds. According to ECBC (2016) “an even more pronounced shift towards fixed rates in our statistics in the coming years” is expected due to repo haircuts reflecting the actual maturity of a bond.
In the German Pfandbrief market the larger amount of outstanding volume and new issuance is denominated in Euro (FIGURE 2.6) which, being situated in the EU, comes with no surprise. Internationally, the picture is slightly different where domestic currencies have gained more market share. This has largely got to do with contractions in volume of large Euro markets, e.g. Germany, France and Spain whereas Denmark has gained a higher impact on the covered bond market with its Danish krone, compared to

[1] `http://ecbc.hypo.org`

[2] `http://www.pfandbrief.de`

[3] One of the more complex produced plots for the market analysis is a bubble plot in order to display the short (x-axis) and long (y-axis) term developments of the respective markets and market players. This comparison is obtained by calculating the relative percentage changes of outstanding volume in comparison to the average change of the total market. Additionally, today’s market (here 4th quarter 2016) is represented as bubbles of the total outstanding volume. The desired effect is to receive a chart where under and over performing markets and market players are easily identified wrt the average performance of the underlying market by allocation to the newly defined quadrants of the coordinate system.

[4] Figures in this section will occasionally exhibit other types than public sector and mortgage but will be widely ignored in this statistical analysis.

2015 (Figure 2.5).
A noteworthy salience of 2016 is the rise of newly issued soft bullet covered bonds compared to the traditional hard bullet maturity structures which have dominated the covered bond markets with a two thirds market share (Figure 2.7). New issues of soft bullet covered bonds account for 50% while hard bullet covered bonds are a mere 45% in 2016. Conditional pass-through (CPT) maturity structures still remain a niche product. Germany is a traditional hard bullet market making up 100% of outstanding Pfandbriefe[5]. A soft bullet maturity structure has not been seen necessary, since, in case of an insolvency the trustee has different means to meet the timely reimbursement of the outstanding payments. These include, e.g. making use of the 180-day liquidity buffer and taking out of covered loans from other credit institutions or the Central Bank, amongst others (Spangler and Werner, 2014). However, the vdp proposes a PfandBG amendment (Hagen, 2018) which includes the possibility of maturity postponements of Pfandbriefe in the event of the insolvency of a Pfandbrief bank. This can be seen as an additional protection of the cover pool, converging towards a soft bullet maturity structure.

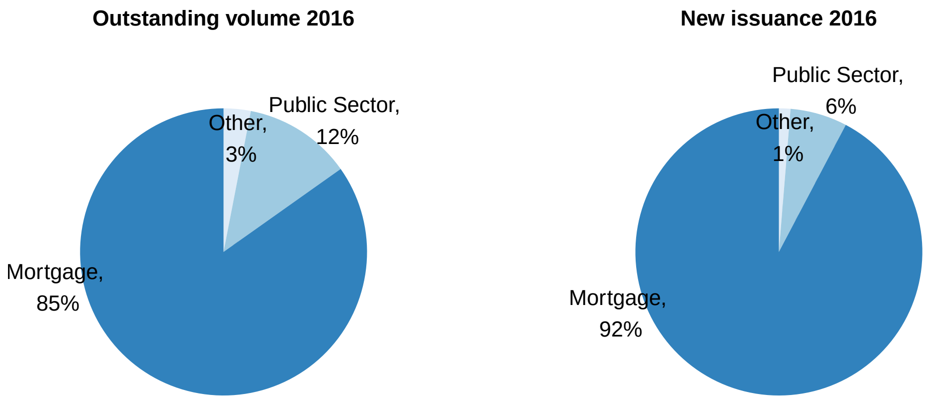

Figure 2.1.: Share of outstanding covered bond volume and new issuance split by collateral type, in 2016

2.1. Covered Bond Market

The covered bond market is the most important privately issued bond segment in Europe's capital markets. Prior to the intensification of the financial crisis in September 2008, covered bonds were a key source of funding for Euro area banks. The market had grown to over €2.2 tn by the end of 2008 and further expand to €2.4 tn in 2016 with 32 issuing countries. Despite the recent financial turmoil, the covered bond asset class has proven to be a reliable investment instrument guaranteeing financial stability with a 200 year long history. Both, issuers and investors, widely benefit from this stable and long-term investment opportunity, particularly in real estate loans and public sector debt. In fact, the covered bond asset class restored investor confidence and ensured European issuers access to debt capital markets. They are characterised by the double

[5] An additional figure for the Pfandbrief market is therefore omitted.

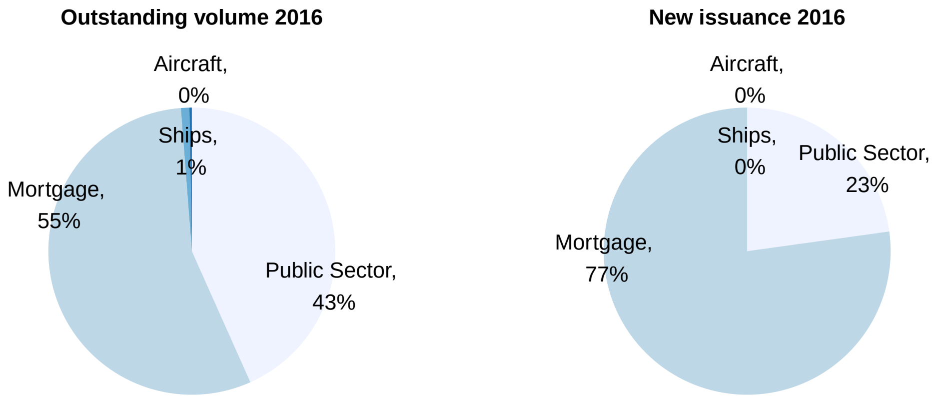

FIGURE 2.2.: Share of outstanding Pfandbrief volume and new issuance split by collateral type, in 2016

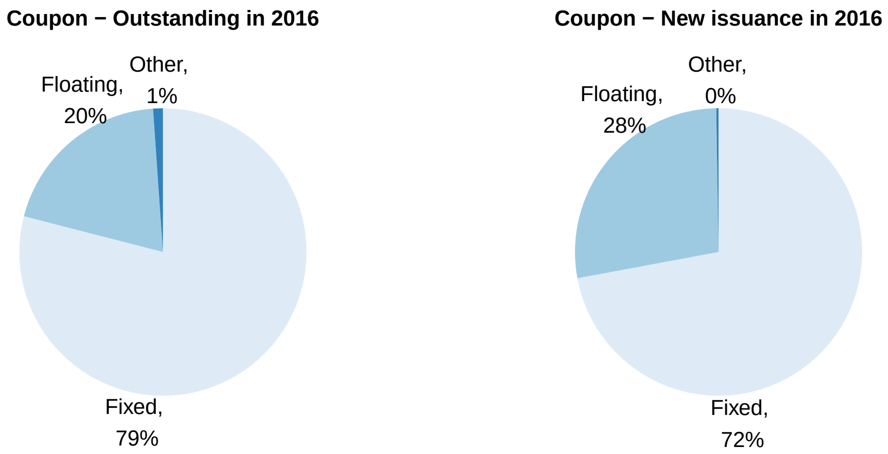

FIGURE 2.3.: Coupon shares of outstanding covered bond volume and new issuance, in 2016

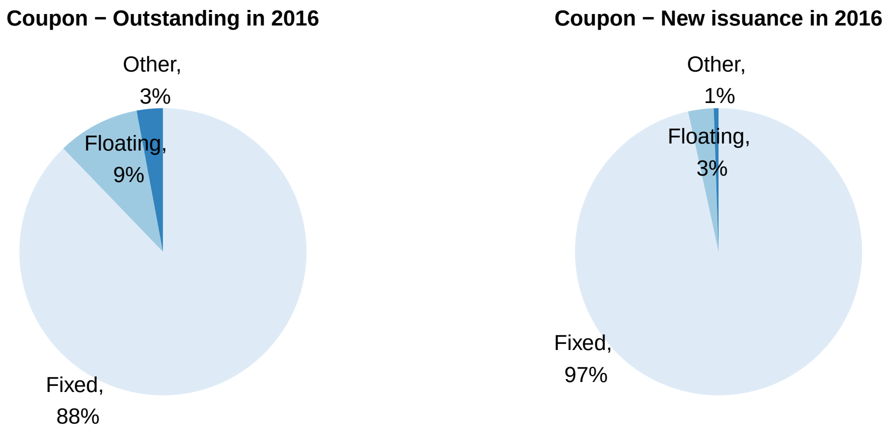

FIGURE 2.4.: Coupon shares of outstanding Pfandbrief volume and new issuance, in 2016

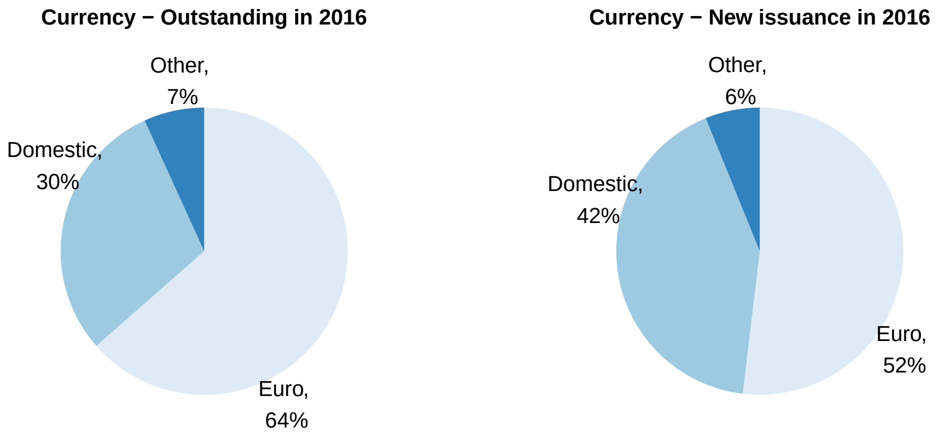

FIGURE 2.5.: Currency shares of outstanding covered bond volume and new issuance, in 2016

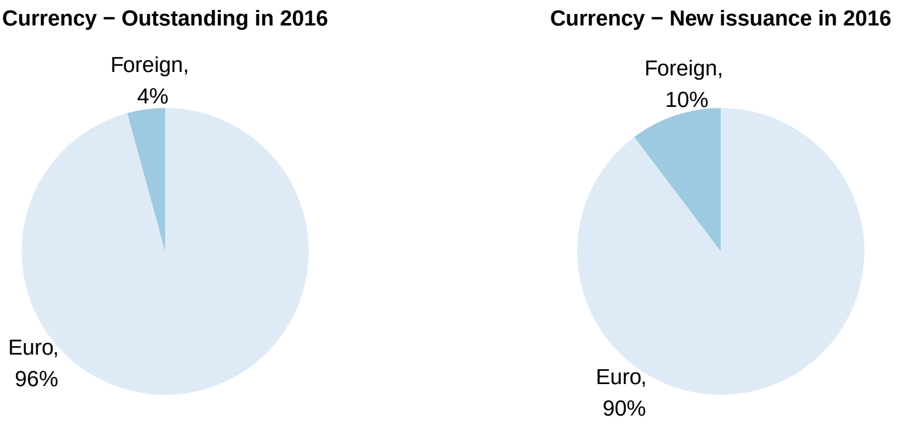

FIGURE 2.6.: Currency shares of outstanding Pfandbrief volume and new issuance, in 2016

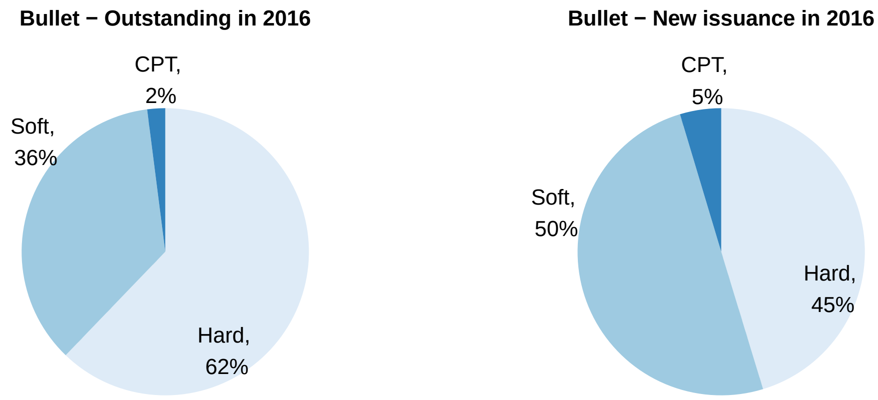

FIGURE 2.7.: Bullet shares of outstanding covered bond volume and new issuance, in 2016

protection offered to their holders, the separation of collateralised assets in a cover pool that is dynamically managed, and strict regulatory and supervisory frameworks.

2.1.1. An Overview

At first we take a macro view of the market of 2016 with the following main observations, compare FIGURE 2.8, FIGURE 2.9 and FIGURE 2.10:

- A seismic shift has occurred from 2015 to 2016. Denmark (€391 bn) has overtaken Germany (€374 bn) as the largest covered bond market. Denmark has steadily grown its covered bond market predominantly consisting of mortgage covered bonds. For the mortgage type Denmark already dominated the market over a longer period.
- UK (€102 bn) dropped by two positions to number nine. Switzerland (€118 bn) and Norway (€115 bn) consequently moved up by one position to take number seven and eight, respectively.
- Turkey has entered the covered bond market as a newest member totalling 31 countries with outstanding covered bonds.
- Nordic countries, including Denmark, have further enlarged their market share compared to the traditional markets of Germany, France and Spain.

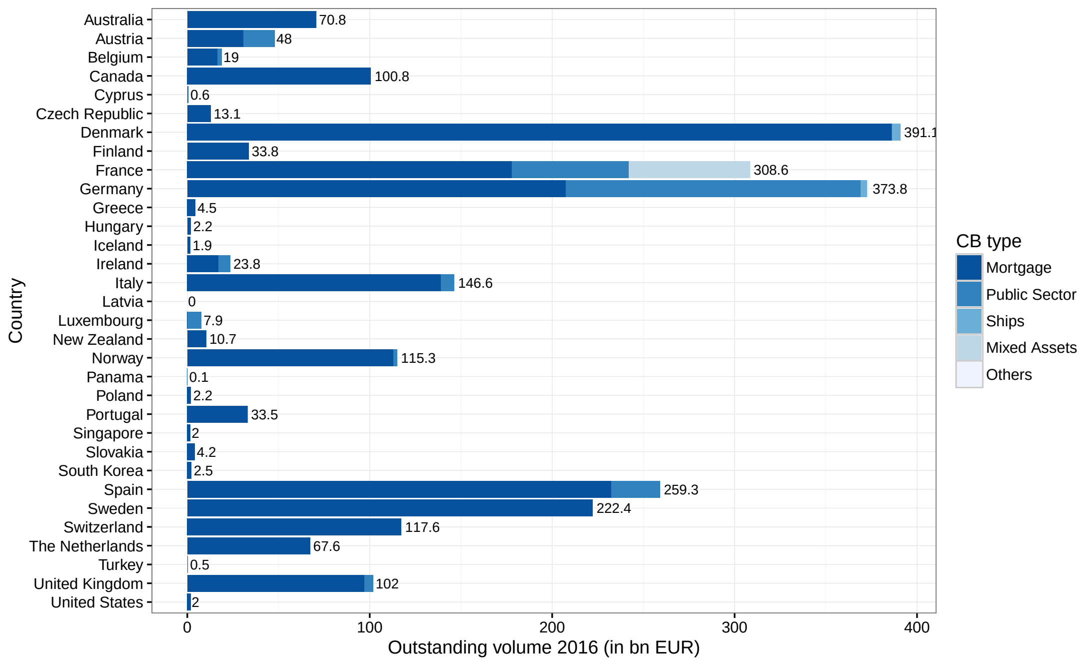

FIGURE 2.8.: Outstanding covered bond volume of issuing countries split into different collateral types, in 2016

An overview of long-term trends since 2003 are given stacked by covered bond types, compare FIGURE 2.11 and FIGURE 2.12:

- Even during the financial crisis up until 2013 a clear upward trend in the covered bond market could be observed.

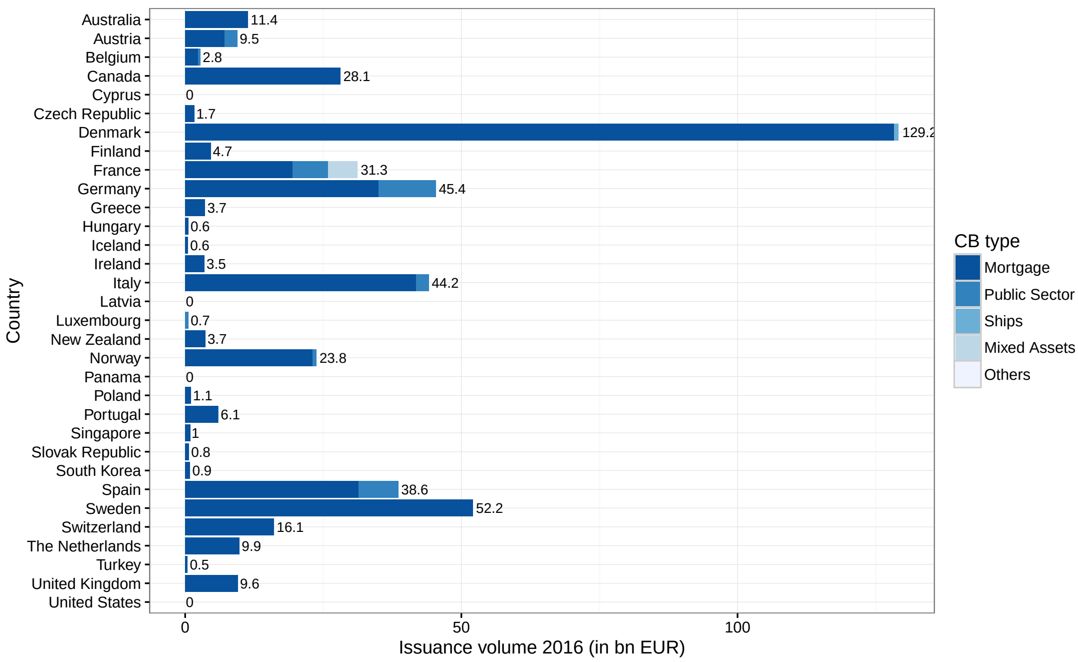

FIGURE 2.9.: New issuance of covered bonds of issuing countries split into different collateral types, in 2016

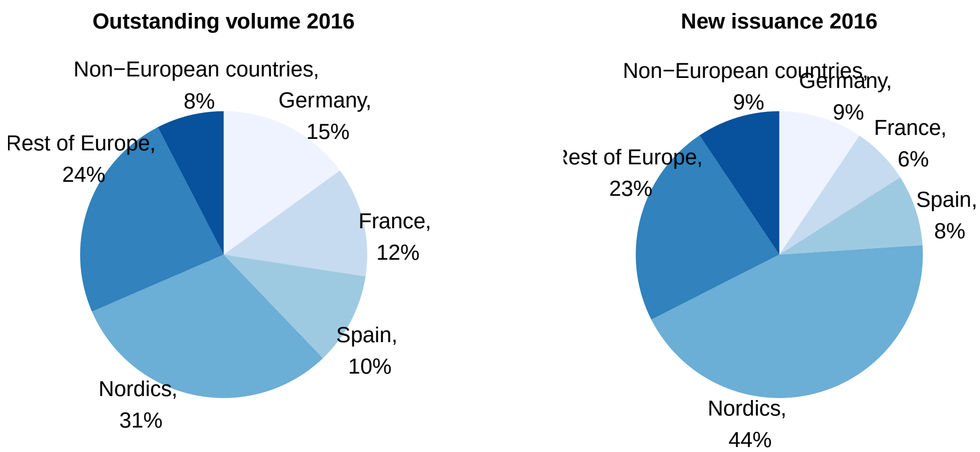

FIGURE 2.10.: Share of outstanding covered bond volume and new issuance split by country groups, in 2016

- The upward trend came to an end in 2013 when the market contracted by 8% for the first time.

- Since 2015 the downward trend in outstanding volumes has been stopped where since 2016 we see a sideways drift.

- At 310 active issuers (that operate a total of 426 covered bond programmes), the net number has gone down by 6. This number has nearly tripled since 2003 climaxing in 2011 before flattening towards 2016 and correlating positively with the overall outstanding covered bond volume.

The ongoing steady growth between 2008 and 2012 can be largely explained by the intervention of the ECB into the covered bond market (Beirne et al., 2011). After the bail-out of four German banks all together during the time period April 2008 to the end of 2011 a certain uneasiness was widely spread amongst investors raising concerns about the stability of the market. Simultaneously, funding conditions of issuers deteriorated. This situation gave enough reason for the ECB to act by establishing the covered bond purchase programme (CBPP) amounting to €60 bn of covered bond purchases between July 2009 and June 2010. This restored liquidity to the market, re-launched issuances and reduced spreads. Two further programmes CBPP2 (from November 2011 to October 2012) and CBPP3 started at the end of October 2014. The programme size of CBPP2 amounted to €40 bn where an amount of €16.4 bn of covered bonds was purchased. CBPP3 is still ongoing. As of July 7$^{\text{th}}$, 2017, the ECB held a volume of €223.0 bn covered bonds under the CBPP3, compare Volk (2017). The total volume of CBPP3 eligible covered bonds in the ECB's database amounts to €1,080 bn (as of July 14$^{\text{th}}$, 2017) where the CBPP3 ECB share then is 21%. Since the ECB can buy covered bonds up to 70% share per issue, there still exists plenty of room for further CBPP3 purchases.

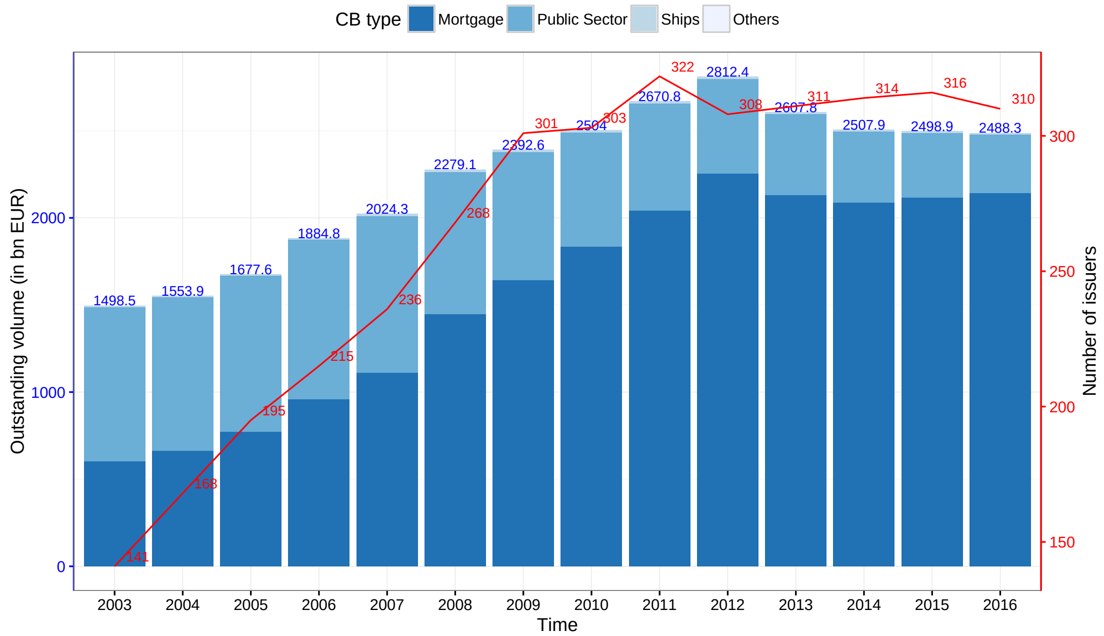

FIGURE 2.11.: Outstanding covered bond volume split into different collateral types, with number of issuers over time

2.1.2. Legal Frameworks

In EPRS (2015), the call for a 'common European framework' is expressed. Particularly, it is criticised that "there is no single, harmonised, legal framework for covered bonds. Industry participants note that this can partly be explained by the fact that the cultural, legal and economic fundamentals vary from country to country and as a result, real-estate finance systems and the role of covered bonds as funding instruments

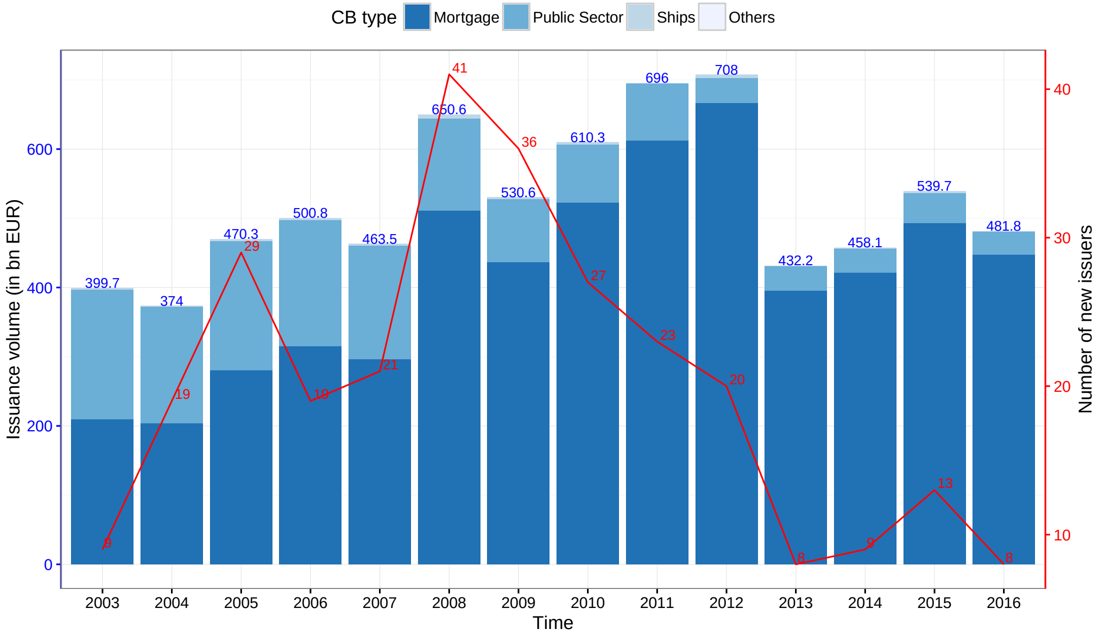

FIGURE 2.12.: New issuance of covered bonds split into different collateral types, with number of issuers over time

for housing mortgages vary accordingly.", cf. (EPRS, 2015). Although efforts have been undertaken of standardising the various differing frameworks, at least on EU level, we shall display the current main legal frameworks in place today.
Golin (2006) gives two fundamental categories with which covered bonds can be associated. These are 'statutory' and 'structured' covered bonds which categorise the legal frameworks under which the covered bonds are issued. The latter allows issuers and bond holders to construct their own bilateral agreement of the legal contract regarding the covered bond purchase and is, e.g., well established in the United Kingdom. However, many countries, thereof most European countries, have adopted a statutory regulatory framework which applies to all market participants issuing covered bonds. Germany has its own Pfandbrief law, the 'PfandBG', which came into effect on May 22$^{\text{nd}}$ 2005. So called 'enhanced' covered bonds are considered to be a mixture between 'statutory' and 'structured' covered bonds where a covered bond legal framework is implemented but also allows contractual degrees of freedom between investors and issuers. The 'enhanced' category has emerged, for example, in Spain.
Recently, most European countries have undertaken amendments (ECBC, 2016, p. 131) to their covered bond laws. Also outside of Europe attempts have been made to introduce the covered bond as an investment product, notably in Australia, Canada, Japan, New Zealand, South Korea and the USA. A more differentiated view on the respective legal structures is given in Stöcker (2011) which is based on the work by Lassen (2005). An overview of these models can be seen in TABLE 2.1 and a brief description of the models is given by the following (Stöcker, 2011):

- Model I: Origination and servicing of eligible assets and management of covered bond issuing institute by the parent bank where the funding institute has no other function than holding eligible assets. In the case of insolvency the covered bond issuer is separated from the parent bank.

- Model II: Issuer originates, services and funds eligible business where loan origination is restricted by law to mortgages and public sector loans. In the case of insolvency the cover assets are segregated from insolvency estate.

- Model III: Issuer originates, services and funds eligible and non-eligible business where covered bond license is granted only to banks complying with legal license requirements. Strict eligibility criteria apply for identifying eligible cover assets. In the case of insolvency the cover assets are segregated from insolvency estate.

- Model IV: Issuer originates, services and funds eligible and non-eligible business where no issuing license is required or license is granted without any requirements. Strict eligibility criteria apply for identifying eligible cover assets. In the case of insolvency the cover assets are segregated from insolvency estate.

- Model V: Issuer originates, services and funds eligible and non-eligible loans. Assets are transferred onto a legally separated entity, a special purpose vehicle (SPV) without bank status.

Remark 2.1. *The models of* TABLE *2.1 are subject to minor modifications compared to Stöcker (2011). Firstly, model III of Stöcker (2011) — the issuer is an universal credit institution — is further distinguished where a qualified covered bond license is needed, specifying model III, and not needed which defines model IV in* TABLE *2.1. Further, the 'pooling model' in Stöcker (2011) is omitted for a more clear distinction of categories as it can be combined with any other model in* TABLE *2.1. A similar legal model classification to Stöcker (2011) can be found in Hillenbrand (2013).*

A clear dissociation of above listed models is not always given. As already alluded in Remark 2.1, pooling models are also implemented in several countries, particularly in Austria, Denmark, France, Germany, Hungary, Spain and Switzerland. Here, the covered bond issuer, in most cases, is a credit institution cooperating with several or even many originators which keep on servicing the cover assets. Eligibility criteria apply to the cover assets and the issuance is governed by a special legal framework. Furthermore, different pooling models exist wrt their transfer techniques. For more details on pooling models refer to Stöcker (2011). Besides, some countries have adopted more than one kind of model which, in some cases, are running parallel. Increasingly, the type where the issuer is an universal credit institution (models III and IV) is the favoured choice, referring to Stöcker (2011). This applies to Denmark, Finland, Luxembourg and Sweden where legislation has already been passed or is on its way. However, the old frameworks are still in place so that these original models are recorded in TABLE C.1. Model V can be viewed as a convergence towards the product of an asset backed security (ABS). Superficially, the products are similar, since ABSs are also backed by pools of loans. The decisive difference is that ABSs use SPVs. Unlike covered bonds, the asset encumbrance of banks' balance sheets is non-existent or small. The embraced 'bail-in' policy after the financial crises requires unencumbered balance sheets where bondholders and/or depositors — not taxpayers as in the 'bail-out' case — are subject to the insolvency process. Yet, ABSs, apart from CDOs, are regarded as the cause for the US subprime mortgage crisis and forfeited trust amongst investors. Moreover, the risk of 'bail-in' is less attractive from an investor perspective[6]. Markets where the model affiliation is not clear or are not classified by Stöcker (2011) are defined as ‘other’. New model assignments, according to the respective framework descriptions in ECBC (2016), are Australia — model V, Belgium — model III, Canada — model V, Cyprus — model III, New Zealand — model V, Panama — other, Singapore — model V, South Korea — model IV and United States — other. A complete list of countries with corresponding models is given in TABLE C.1. Noteworthy is the fact that non-European countries, belonging to the more recent covered bond issuing members, tend to opt for model V. Concluding, the article ‘An anatomy of a successful covered bond jurisdiction’ (ECBC, 2016) covers necessary pre-conditions needed for successfully introducing a covered bond legislation.

Model	Description
I	Issuer is completely specialized funding institute
II	Issuer is specialized credit institution by law
III	Issuer is universal credit institution with a qualified license
IV	Issuer is universal credit institution without a qualified license
V	Issuer is using SPV to achieve insolvency segregation of cover assets

TABLE 2.1.: Legal framework models

2.1.3. Covered Bonds by Legal Framework and Country

We extend the covered bond market overview of Section 2.1.1 by including the information gathered in Section 2.1.2. Thereby, we apply the described ‘at a glance’ format[3] based on data going back as far as 2008. At first the total covered bond market is examined which is then broken down in a public sector and mortgage covered bond type review. This allows a more differentiated analysis of the empirical developments.

2.1.3.1. Total

In total €2,488,299 mn of outstanding covered bonds are registered according to ECBC (2017). Here we shall focus our attention on the public sector and mortgage covered bonds only. As already mentioned above, the market for ship covered bonds is negligibly small with €8,295 mn in 2016 where Denmark (€4,744 mn) and Germany (€3,551 mn) are the single two issuing countries. This also applies to the aircraft where Germany has an outstanding volume of €1,006 mn in 2016. France additionally issues a mixed asset type of covered bond amounting to €66,587 mn.
In FIGURE 2.13 the top ten markets in 2016 are displayed in a stacked graph (in a cumulative sense) which have a 82% share of the total covered bond market. Denmark has taken the lead as the largest issuing country of covered bonds overtaking Germany. Interestingly, new markets such as Canada (the only non-European country) in 2007, Norway in 2007, Italy in 2004 and Sweden in 2005 have fairly recently joined the covered bond market and have established themselves under the top ten by 2016. Furthermore,

[6]A more complete comparison of securitisation markets and German covered bond, particularly mortgage-backed, is given in Staff Team of IMF (2011)

while the old markets, Germany, Spain and France, have steadily declined, especially since 2012 the new members have counterbalanced this negative trend, simultaneously, increasing their market share.

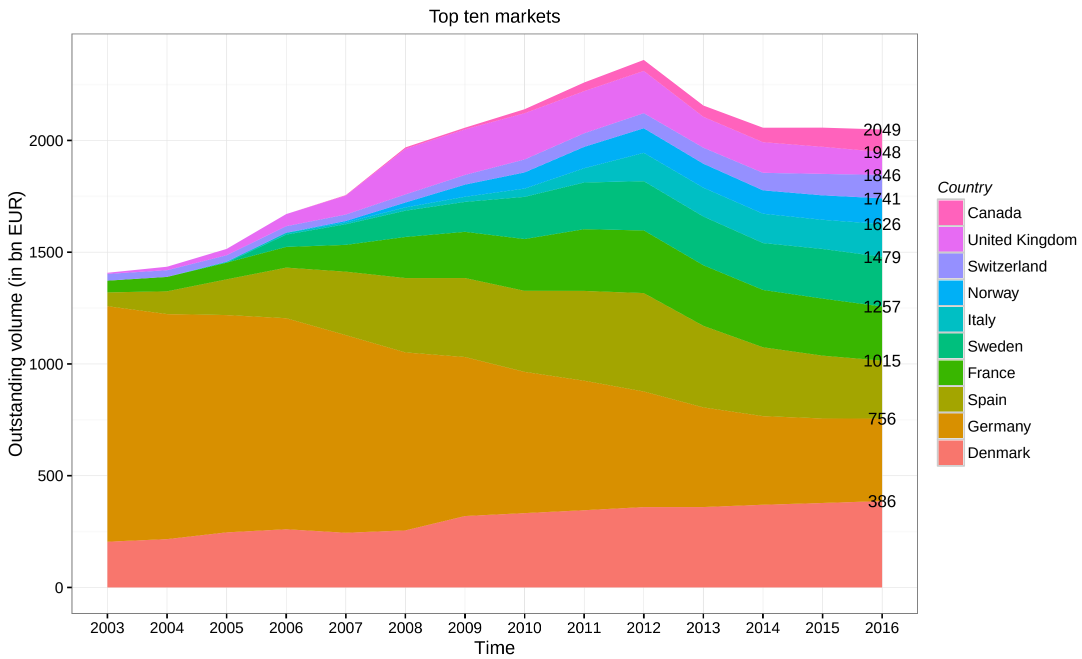

FIGURE 2.13.: Total outstanding covered bond volume over time of top ten markets in 2016

An overview of short (since 2014) and long (since 2008) term changes of covered bond markets[7] can be found in FIGURE 2.14. On average all covered bond issuing countries have lost -0.3% (or approximately stayed the same) on the short term and have gained 10.0% on the long term which is marked by the blue circle with 'ECBC'. Since 2003 Germany's covered bond market has nearly dropped by two thirds in outstanding volume (€-682.9 bn), since 2008 by -53.6% (€-431.8 bn) and since 2014 by -6.8% (€-28.5 bn). Germany with its large absolute volume losses pulls the market as a whole to the bottom left corner of the coordinate system of FIGURE 2.14. Spain (x: -15.8%, y: -22.1%) and the United Kingdom (x: -25.5%, y: -50.0%) (both under the top ten markets, see FIGURE 2.13) underperform on a short as well as a long-term horizon compared to the overall market. The Nordics, represented by Denmark, Norway, Sweden and Finland, all outperform the market. A further observation is that countries in the first quadrant, which possess a significant outstanding covered bond volume, are either categorised 'model I' — Finland (x: 5.5%, y: 488.2%), Norway (top 10; x: 10.3%, y: 425.6%), Sweden (top 10; x: 6.0%, y: 89.1%) and Switzerland (top 10; x: 33.8%, 190.2%) — or 'model V' — Australia (x: 9.3%, y: 2756,4%), Canada (top 10; x: 55.5%, y: 1433.7%), Italy (top 10; x: 11.7%, y: 906.3%) and The Netherlands (x: 14.9%, y: 229.2%).

[7] Not included are Latvia, Singapore and Turkey. These either have no outstanding volume in 2016 or do not show a long enough history. Country ISO codes marked with '*' have a shorter long-term time horizon for the simple reason that no covered bond market existed prior. The differing onset dates (other than 2008) can be extracted from TABLE C.1.

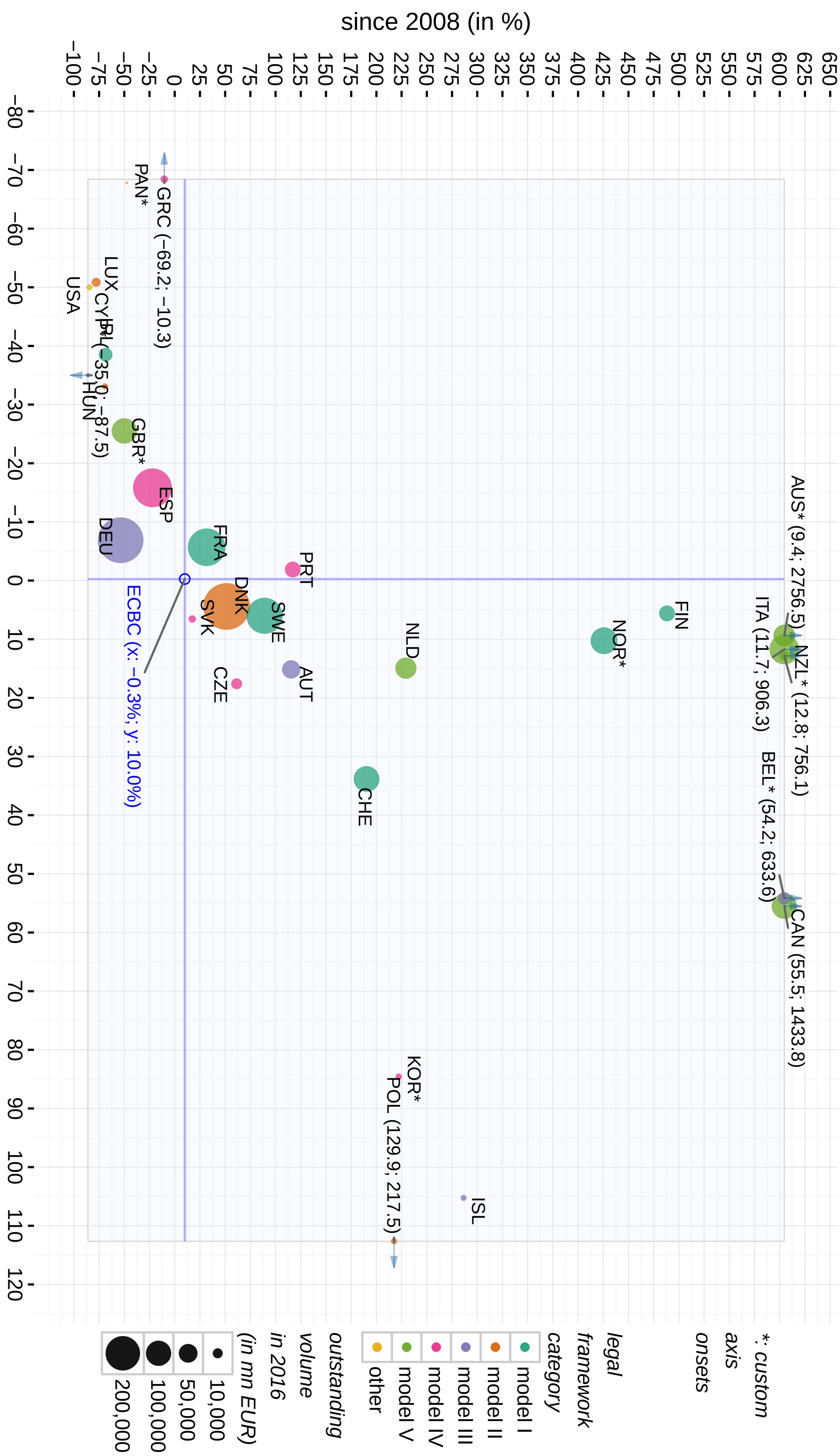

Figure 2.14.: Total outstanding covered bond volume, with short and long term development of issuing countries, in 2016

2.1.3.2. Public Sector

Taking a closer look at the public sector market we find that Germany and France are the major players in this segment. Germany accounts for 53.6% and France for 21.3% of the market share in 2016, amounting to three quarters put together (subsequent markets are Spain (8.9%), Austria (5.6%), Luxembourg (2.6%) and Italy (2.5%)). However, their developments are inverse. While France has increased its volume and gaining a larger market share since 2003, Germany has suffered a substantial loss, especially over the last ten years, see FIGURE 2.15. Still both Germany (€10.3 bn) and France (€6.4 bn) together with Spain (€7.3 bn) are by far the largest markets in terms of new issuance in 2016, see FIGURE 2.9. According to ECBC (2017, p. 136), particularly in Germany and France, local government investments (around 30% of loans) are financed by covered bonds. In total, "more than €250 bn European Union local government loans, an equivalent of close to 14% of the total European Union local government debt, are refinanced via the covered bond market.", cf. (ECBC, 2017, p. 136).

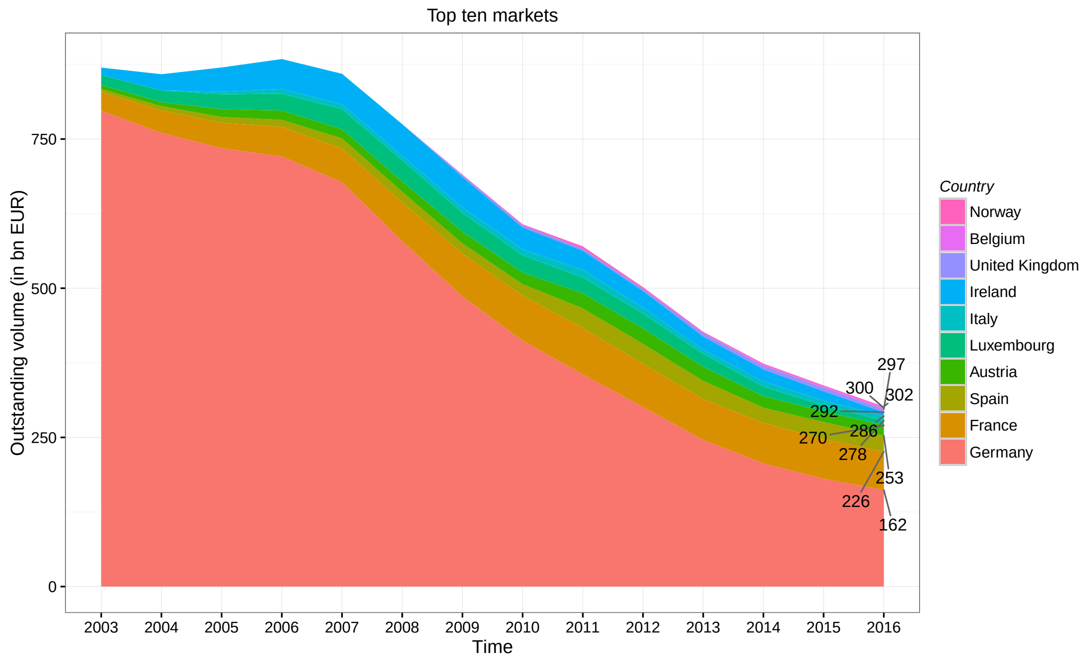

FIGURE 2.15.: Outstanding public sector covered bond volume over time of top ten markets in 2016

Altogether, only eleven countries had outstanding public sector covered bonds in 2016, see FIGURE 2.16. Poland still had a volume of €35.2 mn outstanding public sector covered bonds in 2015 which has fallen to zero in 2016. Belgium is also not considered in FIGURE 2.16 since its public sector outstanding volume history only dates back to 2014. Refer to TABLE C.1 for countries marked[7] with '*'. It is now evident that the bulk of established total losses in the German covered bond market (Section 2.1.3.2) is explained by the contraction of the public sector. Since 2003, -79.7% (€-635,6 bn), since 2008 -72.0% (€-417.1 bn) and since 2014 -21.6% (€-44.6 bn). Once again Germany is the main driver of the short as well as long term negative trend where the average market is denoted by 'ECBC' (x: -19.2%, y: -61.0%). Long term wise the United Kingdom (x:

-20.4%, 42.3%) and Spain (x: 5.4%, y: 51.4%) can show a substantial positive trend being two major markets (both in top ten list). Austria (x: -11.0, y: -0.9), France (x: -5.1, y: -0.8) and Italy (x: -12.9, y: -6.0) do not show large movements in the short nor long term.
As already stated by Spangler and Werner (2014) two main factors for the negative trend in the German market have been identified, the

- EU decision on the end of guarantees for the German Landesbank sector by 2015, in 2001 (abolishment of the 'Gewährträgerhaftung'), and the

- ongoing sovereign crisis of EU states (mainly Portugal, Italy, Ireland, Spain and Greece) leading to a reduction cover pool assets from these countries.

Particularly, for the German market the decline has potentially more, yet weaker, reasons:

- Rescue of Hypo Real Estate AG, Germany's largest issuer of Pfandbriefe, in 2009 where a re-structuring of its balance sheet and operating structure became necessary. In general, Banks' future "(...) losses which in certain cases run into several billions might continue to have an impact on the business strategies (...)", cf. (PBB, 2009, p. 65).

- Short-term introduction of alternative funding instruments during the financial crises provided by the ECB and issuance of Government Guaranteed Bonds (GGBs), cf. (VDP, 2009).

- German re-unification inflated the issuance of public sector covered bonds which could not be sustained over time, cf. (ECBC, 2016, p. 120).

These points, paired with a general risk aversion and market weariness in a post-Lehman Brothers financial era has led to this dramatic public sector flight. However, there might be light at the end of the tunnel and a bottom limit reached in the near future. The article 'Refinancing local public sector investments and export loans — a key role for covered bonds' in ECBC (2016) indicates public sector covered bonds will remain a source of funding especially for local authorities and a key pillar for public investments, also for other European countries. In ECBC (2017, p. 139) the hope is expressed that export loans might be eligible for covered bond refinancing reviving the public sector market if the loans meet the criteria stated in Capital Requirements Regulation (CRR) of Article 129(1), thus "benefiting from a state guarantee or a guarantee provided by an export credit agency (ECA)", cf. (ECBC, 2017, p. 138). Nevertheless, many outlooks of the public sector covered bond remain pessimistic, see for example Schönfeld (2012). Furthermore, new markets for the public sector type have not emerged, or at least established themselves. For example, the US has not been able to pass a suitable covered bond legislation to this date, although this has been apparently attempted several times, according to ECBC (2016, p. 495). Furthermore, referring to the year 2017, "all previously issued structured covered bonds (...) have now matured and there are currently no outstanding US covered bonds.", cf. (ECBC, 2017, p. 519).

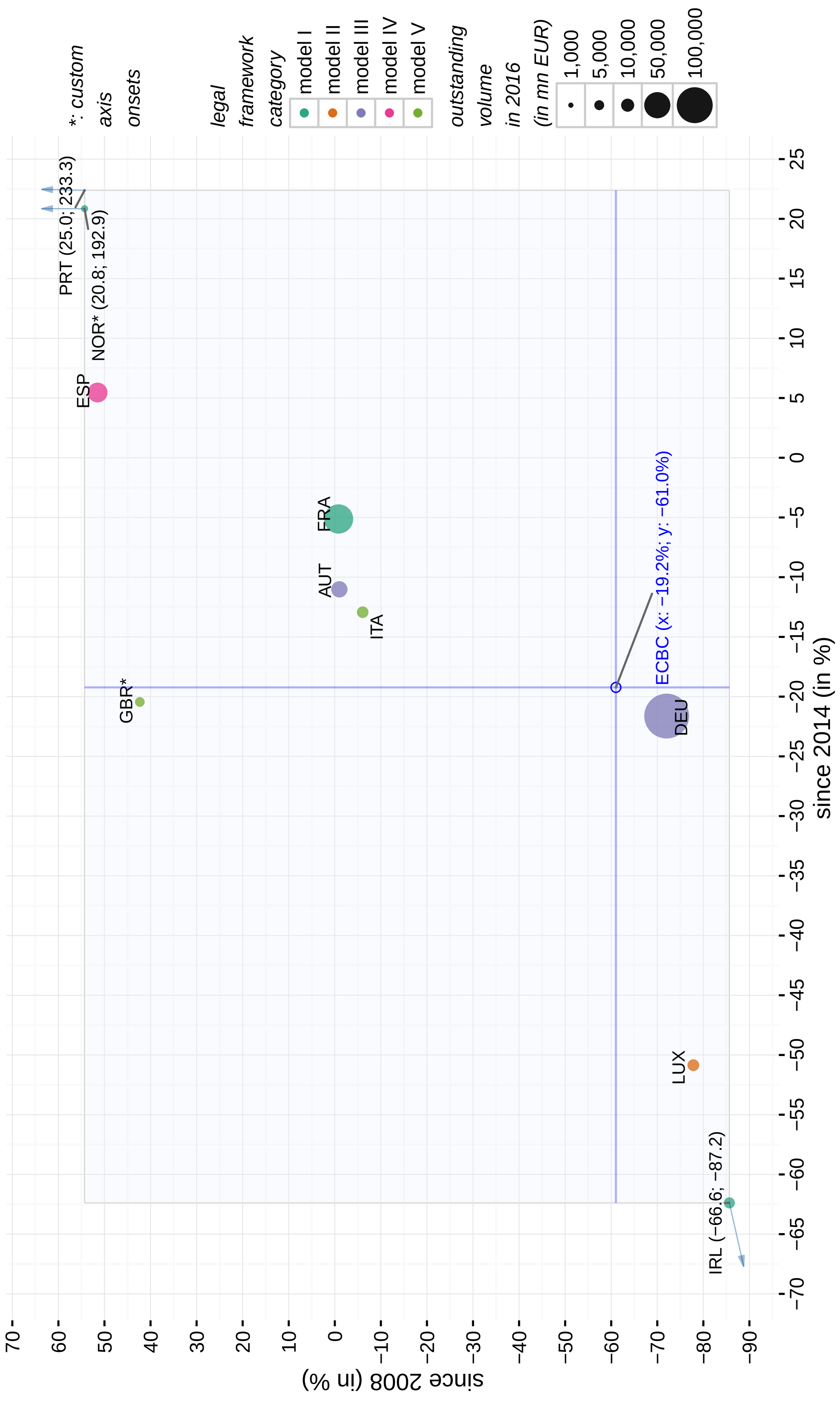

FIGURE 2.16.: Outstanding public sector covered bond volume, with short and long term development of issuing countries, in 2016

2.1.3.3. Mortgage

A complete opposite picture to the public sector covered bonds in Section 2.1.3.2 is produced by the mortgage type. This segment has seen considerable growth since 2003. Newer markets (in 2016), represented by Sweden (€222.4 bn), Italy (€138.9 bn), Norway (€113.1 bn) and Canada (€100.8 bn) have contributed enormously to the overall volume increase, see FIGURE 2.17. Currently, Denmark (€386.3 bn) has volume wise the largest impact on the mortgage market. Germany (€207.3 bn) and France (€177.8 bn) could maintain a stable development over a longer period while Spain's market contracted since 2012 (€232.5 bn in 2016). The United Kingdom (€97.1 bn in 2016), traditionally a MBS market, could establish itself in the top ten group with a steep growth rate of factor 40 from 2003 to 2010. However, it will be interesting to see how 'Brexit' will affect the covered bond market as negative impacts are already starting to appear, compare ECBC (2016, p. 501).

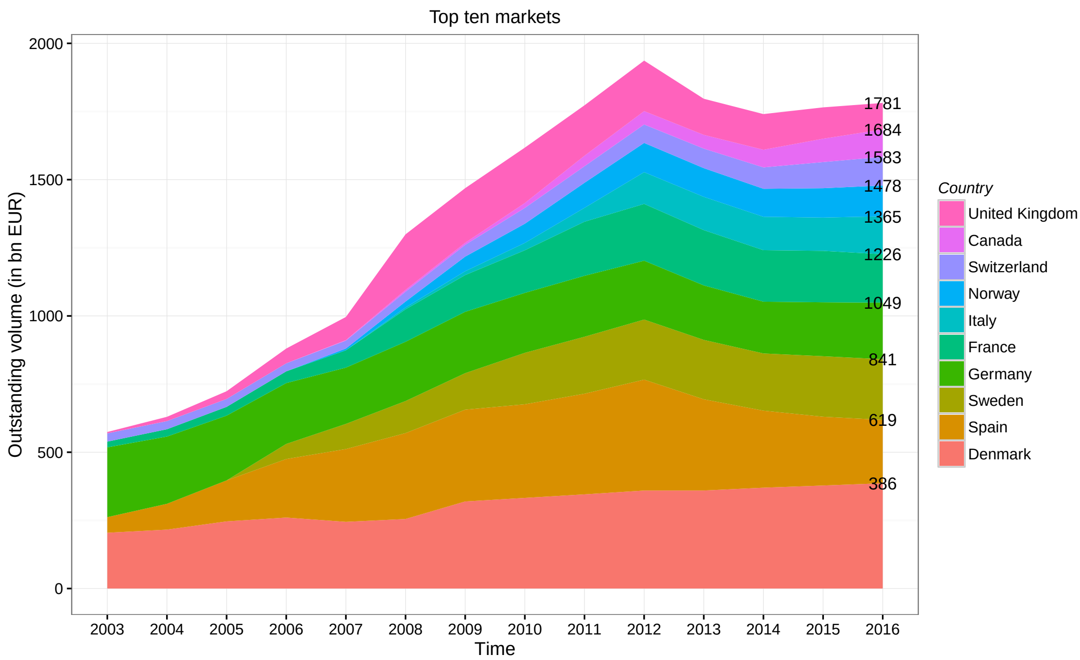

FIGURE 2.17.: Outstanding mortgage covered bond volume over time of top ten markets in 2016

A rather similar picture to the total market of FIGURE 2.14 is also depicted by the mortgage type, compare FIGURE 2.18. This is easily explained since the covered bond market is dominated by the mortgage type, see FIGURE 2.1, FIGURE 2.8 and FIGURE 2.11. We see an average growth rate of 49.1% since 2008 and 3.2% since 2014 denoted by 'ECBC' which nearly exactly coincides with Denmark — the largest mortgage market. Contributing to the Danish covered bond success story is a certain degree of flexibility wrt refinancing and repayment (ECBC, 2016, p. 68-69):

- "Mainly bullet bonds and to an extent floaters are refinanced by the issuance of new bonds at refinancing auctions over the life of the loan.", cf. (ECBC, 2016, p. 68-69).

- "Any Danish covered bond can be bought back by the borrower[8] at the current market price and delivered to the issuing mortgage bank — the buyback option.", cf. (ECBC, 2016, p. 68-69).

The rest of the Nordics outperform the market, situated in the first quadrant of the coordinate system, with Finland (x: 5.5%, y: 488.2%), Norway (top 10; x: 10.0%, y: 415.6%) and Sweden (top 10; x: 6.0%, y: 89.1%), all belonging to the same legal framework 'model I'. Switzerland, one of the top ten markets and also belonging to 'model I', can likewise lock in a positive growth rate of 33.8% short-term and 190.2% long-term. Further countries with extraordinary market gains and substantial market volumes are Australia (x: 37.6%, y: 521.2%), Canada (top 10; x: 55.5%, y: 1433.7%), Italy (top 10; x: 13.5%, y: 2038.1%), New Zealand (x: 12.8%, y: 756.1%) and The Netherlands (x: 14.9%, y: 229.2%) — all issuing under 'model V'.
As for the German market we see an expansion of 9.1% since 2014 and a contraction of -4.6% since 2008. Referring to Spangler and Werner (2014), two main characteristics of its robustness are

- attractive refinancing possibilities. Cheap funding can be obtained at comparably low costs, and

- new issuers, such as saving banks and international players are joining the market.

Further reasons are

- "a benign constellation of Germany's housing market" (DGHYP, 2012, p. 6), and

- offering "ready availability of financing at the longest tenors possible and the lowest price feasible" (ECBC, 2016, p. 137).

2.1.4. Jumbo Market

The first Jumbo (benchmark format with > €1 bn) was issued in 1995. This format of the German Pfandbrief was primarily created to provide more liquidity to investors — particularly having a direct impact on secondary liquidity — and increased funding for public sector lending. "Jumbo size, e.g., have on average double the trading volume than benchmarks with less than €1 bn of nominal outstanding.", cf. (ECBC, 2017, p. 61). Wolf (2010) shows when and how many new countries have followed suit since the introduction of the Jumbo Pfandbrief, reshaping the covered bond market as a whole. In 2016, the largest issuing countries of Jumbos are Denmark (€240.3 bn), France (€188.5 bn), Sweden (€177.3 bn), Spain (€129.7 bn) and Canada (€84.2 bn). Taking a closer look at the placements in FIGURE 2.19, we see for 2016 that the Jumbo nearly accounts for half of all outstanding covered bonds. The Jumbos, in total, saw a decline in 2016 (€174 bn in 2016 after €217 bn in 2015) continuing the trend since 2012 (FIGURE 2.20). While Jumbos are are considered to be more liquid due to their size, from an issuer's perspective "smaller benchmark issues are more favourable in the context of asset liability management and legal requirements regarding liquidity holdings", cf. (Spangler and Werner, 2014, p. 26). Until 2013, we have seen a steady growth for all categories, see FIGURE 2.20. According to ECBC (2017), during the years of the financial and the Euro sovereign crisis many banks in various countries used retained covered bonds as repo

[8]The borrower is referred to as the covered bond issuer.

FIGURE 2.18.: Outstanding mortgage covered bond volume, with short and long term development of issuing countries, in 2016

collateral, partly, accounting for this overall upward trend. The biggest increase compared to 2014 took place in the €500-999 m benchmark category. Outstanding covered bonds in this category increased by €66 bn or 24%. “In 2015, the rise in gross supply of Euro benchmark covered bonds was merely due to increased issuance from banks located within the Euro area. This is related (at least partly) to the Eurosystem’s third covered bond purchase programme (CBPP3), which has made it increasingly attractive for banks to issue covered bonds.”, (ECBC, 2017, p. 74).
In 2013, a large drop in the private placement category occurred (€-85 bn or -11%) because “European lenders paid back part of their long-term refinancing operations (LTRO) money and consequently cancelled out retained covered bonds”, cf. ECBC (2017, p. 582). The gross issuance decline in 2013 is also reflected in FIGURE 2.21. In 2014 this category did continue to fall (€-26 bn or -4%) but similar to the overall market it has stabilised in 2015. In 2016, private placements increased slightly from €115 bn to €126bn.

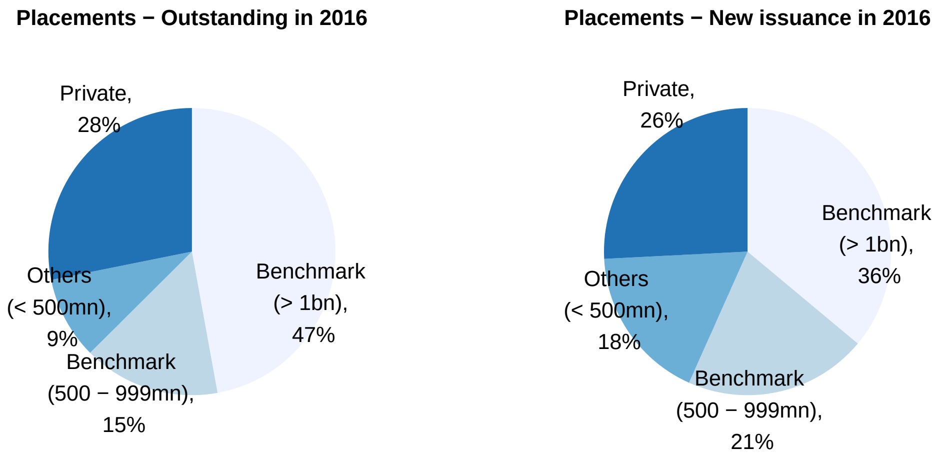

FIGURE 2.19.: Placement shares of outstanding covered bond volume and new issuance, in 2016

2.2. Pfandbrief Market

Let us now solely view the sub-segment of Section 2.1 the German covered bond market, respectively the Pfandbrief market, where the attention is largely shifted to the issuing Pfandbrief banks themselves. In total there exist 35 Pfandbrief issuing banks in Germany (TABLE C.2) in 2016. When dissecting the Pfandbrief market in recent years it is noteworthy that “there never has been a German Pfandbrief default, and nor has a German Pfandbrief bank ever failed. In fact, prior to the crisis, the only covered bond issuer bankruptcy was in 1883 — the Austrian issuer Böhmische Bodenkredit. In that case, the failed bank’s covered bond obligations were transferred to another bank two years later, interest payments were reduced, and the bonds redeemed in full in 1901.”, cf. (Staff Team of IMF, 2011). The trust of investors in the Pfandbrief and the issuing banks stems from this well acknowledged circumstance that no Pfandbrief has ever defaulted.
Yet, it is evident (from Section 2.1) that since the financial crisis of 2008 and the consecutive Euro crisis the Pfandbrief market in Germany has changed significantly. During

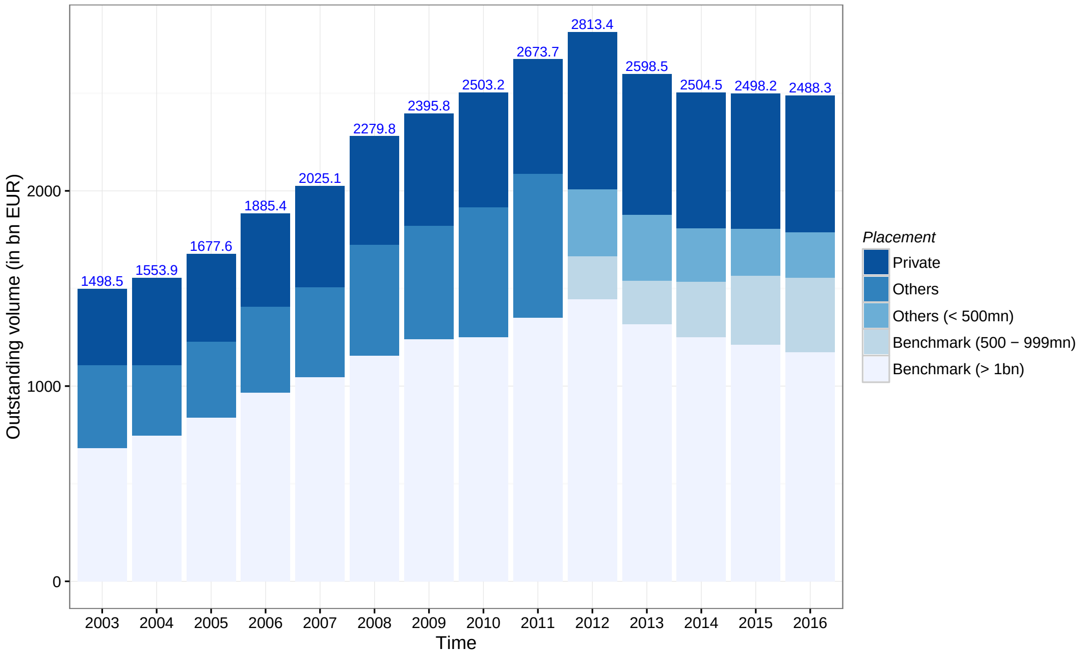

FIGURE 2.20.: Placement shares of outstanding covered bond volume over time

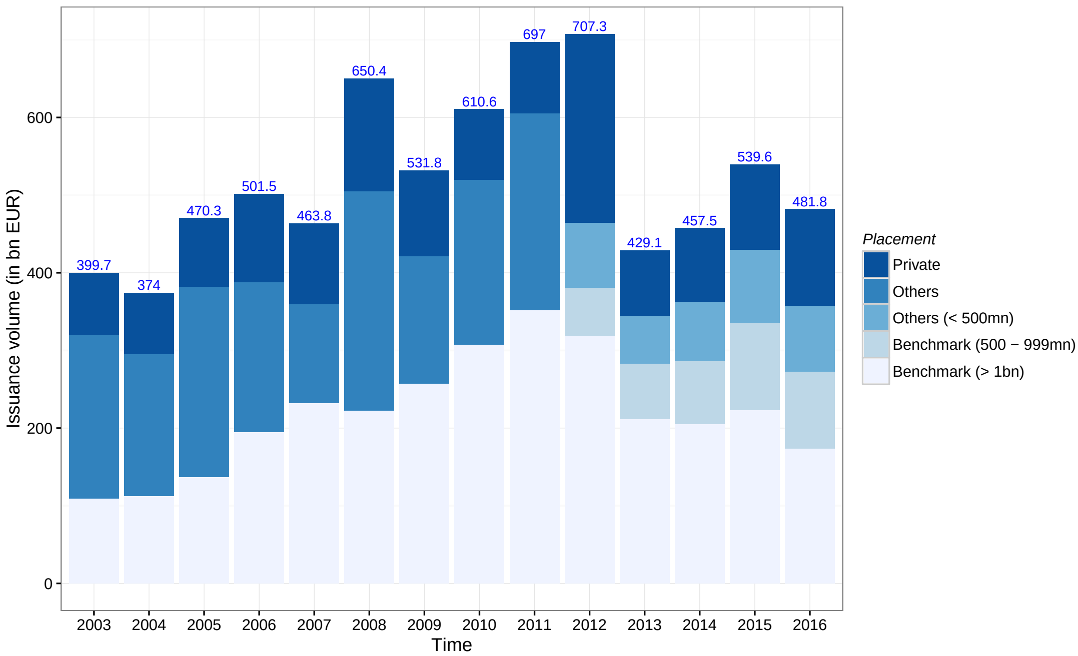

FIGURE 2.21.: Placement shares of covered bond new issuance over time

the financial crisis certain banks, including one of the largest issuers the Hypo Real Estate Group, were subject to bank bailouts by the German government. “The banks in question included Düsseldorfer Hypothekenbank (April 2008), Hypo Real Estate Group (October 2008), and EuroHypo AG (May 2009). For example, in the case of Hypo Real Estate Group, the covered bonds were seen as being sufficiently collateralised, but there were questions regarding the ability to liquidate it in the wake of the Lehman Brothers bankruptcy.”, cf. (Staff Team of IMF, 2011). Consequently, the affected banks had to go through painful recovery and resolution regimes neglecting their daily business of issuing new Pfandbriefe. Naturally, the bailouts also eroded trust amongst investors (evidently from FIGURE 1.1).
In the following we shall further dissect the Pfandbrief market by viewing Pfandbrief types separately in order to obtain a more complete picture thereof. Not included in the analysis are in general DVB, EH and PSD. DVB only issues ship Pfandbriefe. For PSD Pfandbrief data is only available since 4$^{\text{th}}$ quarter 2015 where Pfandbriefe of €15 mn were issued and totalling €163 mn in 4$^{\text{th}}$ quarter 2016. All significant assets and liabilities of EH, Hypothekenbank Frankfurt AG, were transferred to DSB, Commerzbank AG, and the banking license was returned in May 2016.

2.2.1. An Overview

At first we take a macro view[9] of the market of 2016 with the following main observations, compare FIGURE 2.22 and FIGURE 2.23:

- Deutsche Pfandbriefbank AG, formerly known as Hypo Real Estate Group, thus the abbreviation HRE, is still the largest issuing bank of Pfandbriefe with a total of €30.3 bn where mortgage and public sector are evenly split (mortgage €14.1 bn; public sector €16.2 bn).
- Interestingly, there exist banks (APO, DIBA, HASP, MMW, NAT, SKB, WBP) only issuing mortgage type Pfandbriefe, but no bank solely focusing on the public sector type, only in combination with the mortgage type.
- Eligible cover pool assets are predominately situated in Germany — mortgage (82%) and public sector (81%). Mainly, this has to do with that the PfandBG sets geographical restrictions. For example, a 10% limit is in place for foreign lending outside the EU (compare Spangler and Werner (2014)). Only 2% - 3% of assets lie outside of Europe.
- Ship Pfandbriefe have a total outstanding volume of €3,590.7 mn (BRL: €102.1 mn, DSB: €1,135.4 mn, DVB: €720.0 mn, HSH: €1,553.2 mn, NLB: €80.0 mn). DVB is the only bank solely issuing ship Pfandbriefe.
- The first and only issuing bank of aircraft Pfandbriefe is NLB with an outstanding (and new issuance) volume of €1,006 mn.

An overview of long-term trends since 2003, stacked by Pfandbrief types, are given, compare FIGURE 2.24 and FIGURE 2.25:

[9] Note that due to non-existing data of newly issued Pfandbriefe in the context of PfandBG §28 it is not possible to produce FIGURE 2.9 as in the overview of the covered bond market (Section 2.2.1).

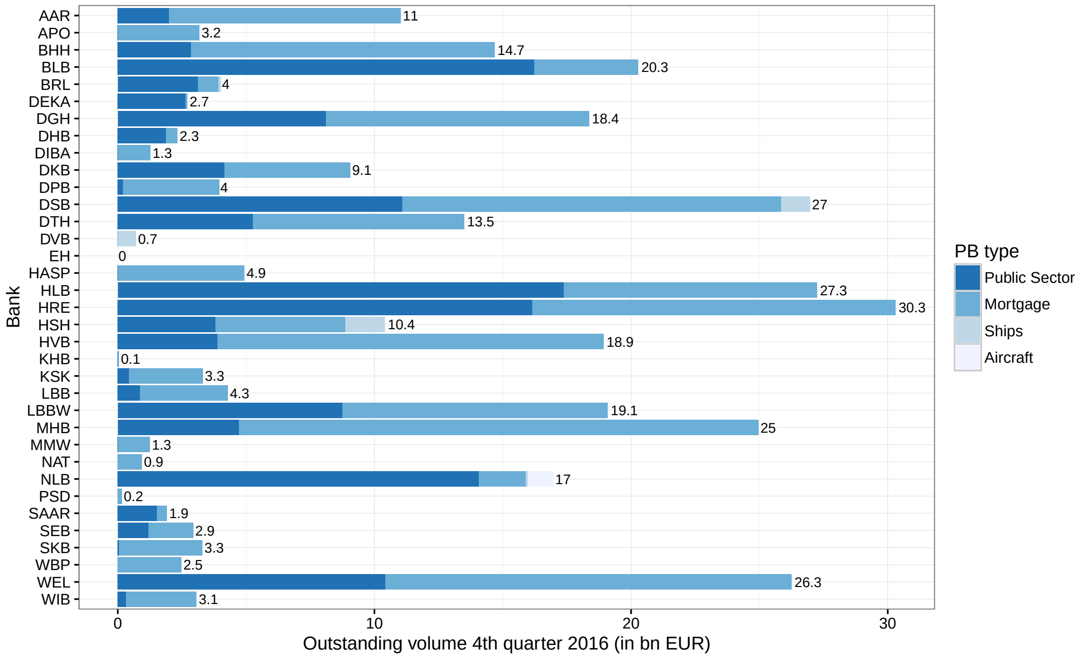

FIGURE 2.22.: Outstanding Pfandbrief volume of Pfandbrief banks split into different collateral types, in 4th quarter 2016

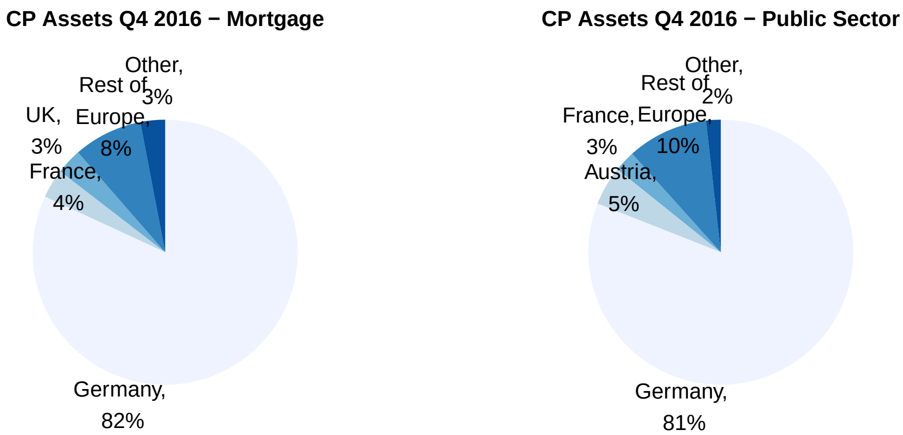

FIGURE 2.23.: Mortgage and public sector cover pool assets split by country groups, in 4th quarter 2016

- Compared to the overall development of the covered bond market (Section 2.2.1) we see an inverse trend specifically for the German market. This has solely to do with the stark decline of the public sector Pfandbriefe (contracting by nearly 80% as already pointed out in Section 2.1.3.2). Taking a glance at the issuance figures reveals that in 2003 ten times as many public Pfandbrief were issued than in the more recent years. On average the issuance volume between 2012 and 2016 amounts to approx. €14 bn.

- In terms of volume the mortgage type Pfandbriefe more or less stayed constant (moving below and above €200 bn) throughout the years since 2003, however, substantially enlarging its market share from approx. 20% in 2003 to 55% in 2016. Taking a look at the issuance figures suggests a similar interpretation where on average approx. €40 bn of new mortgage Pfandbrief have been issued over the time period 2003 to 2016.

- During the crisis years, beginning 2007 with the financial crisis and ending 2013 with the European sovereign crisis, the largest drop in outstanding Pfandbriefe is recorded with over 50%.
- Since 2014 a flattening out of the outstanding volume can be observed which is paired with stabilised sizes of new Pfandbriefe issuances since 2012.
- Interesting is the persisting positive trend of longer maturity terms for Pfandbriefe (red line in Figure 2.24 and Figure 2.25), rising from 4.6 years in 2003 to 7.1 years in 2016.

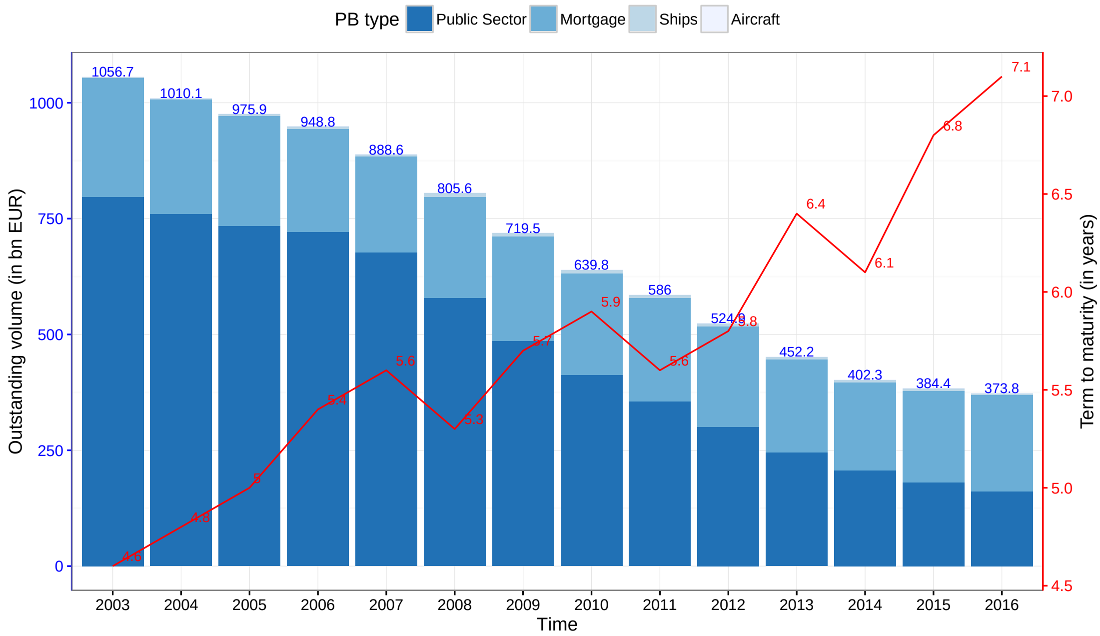

Figure 2.24.: Outstanding Pfandbrief volume split into different collateral types, with term to maturity over time

2.2.2. An Investor's Perspective

The Pfandbrief is widely considered to be a safe investment. From an investor's perspective some advantages of the Pfandbrief include the double recourse to issuer and cover pool and therefore higher recovery in case of liquidation. Furthermore, there is no risk of bailing-in, generally, there exists better liquidity through larger issue size and higher rating and higher rating stability than unsecured debt.

A main feature of the security behind the Pfandbrief is its cover pool and overcollateralisation (OC) thereof. Per PfandBG it is mandatory to hold a minimum of 2% OC over the total outstanding Pfandbriefe in each asset type class. Many Pfandbrief issuers even maintain voluntary OC exceeding the 2% level. Higher levels of OC may also have a positive impact on the overall credit rating and is favourably recognised amongst Pfandbrief investors. However, since it is voluntarily the issuer may reduce the created

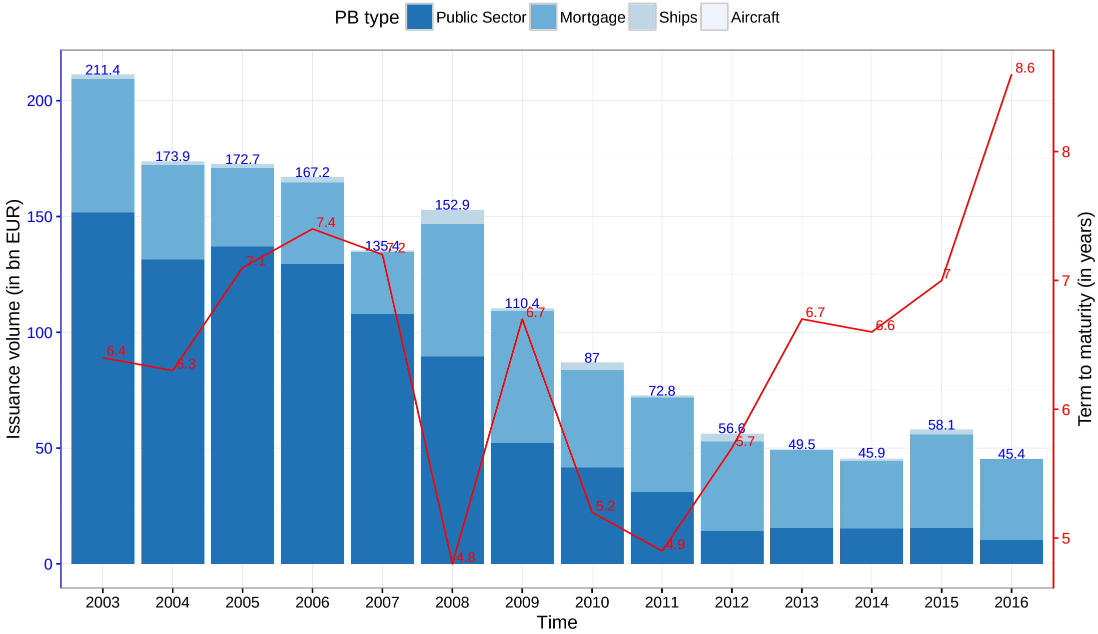

FIGURE 2.25.: New issuance of Pfandbriefe split into different collateral types, with term to maturity over time

buffer at any time, also in case of default. A more elaborate analysis of OC and its implications can be found in Spangler and Werner (2014). The average OC over all issuing banks of mortgage Pfandbriefe is 53.9% and 63.9% of public sector Pfandbriefe. In FIGURE 2.26 we see the total cover pool divided in total outstanding Pfandbriefe and share of OC held by each bank for the public sector type and mortgage type Pfandbriefe, respectively. Further, it can be extracted that there exists a wide range of voluntary OC between issuers. For the mortgage type BHH holds an OC of 7.0% whereas DEKA holds 263.0% OC. For the public sector type MHB maintains a OC slightly above the the 2% mandatory level (2.5%) whereas SKB has an additional buffer over 440%.
Further, it is natural to take a closer look at the spreads of the Pfandbrief compared to other covered bond markets and other financial products. FIGURE 1.1 depicts the time period of the financial crisis and shortly before and after. Clearly, two spikes can be observed in FIGURE 1.1 wrt the Pfandbrief. Once in the first half of 2009, abruptly widening after the collapse of Lehman Brothers, moving from below zero to 100 bp. The second larger spread widening occurred during the European sovereign crisis between 2011 and 2012. Currently, spreads have moved back to pre-crisis levels of below zero bp, see FIGURE 2.27. Yet, compared to other financial products with high seniority, including covered bonds from other issuing countries, spreads of the Pfandbrief — mortgage or public sector — are significantly lower throughout turbulent and benign markets. On average mortgage spreads are slightly lower than public spreads.
A similar picture is depicted of the Jumbo market (FIGURE 2.28). Germany, Denmark, Spain, France and the United Kingdom account for most very large issues trading in liquid secondary markets that are dominated by OTC trading. For German Jumbo Pfandbriefe daily average spreads are published including benchmark issuances with a minimum size of €500 mn and with a residual maturity of at least one year as part of

the transparency initiative by the vdp[10].
Although, the analysis of spreads restore trust into the Pfandbrief, the poor return on investment has given investors reason to look for alternative opportunities. Pfandbrief yields[11] have fallen due to the zero interest rate policy of the ECB in recent years, see FIGURE 2.29. On the x-axis we see the historical interest rates where a peak was reached for 2008 and after declined until reaching practically zero for lower maturities, even turning slightly negative for maturities of one to five years. On the y-axis the daily yield curve is depicted where a higher rate is expected for longer maturities. Interestingly, humped and inverted yield curves[12] can also be observed for 2008 reflecting the market's uncertainty in a turbulent period. Currently, the earnings of a Pfandbrief investor for Pfandbriefe with longer maturities are around 1% for ten years and higher.

2.2.3. Pfandbriefe by Issuing Category and Bank

Similarly to Section 2.1.3, we incorporate additional information in the 'at a glance' format[3] based on data going back as far as 2008. We define three issuing categories, namely 'Hyp' — banks having a predominant mortgage Pfandbrief business, 'Hyp-Oef' — banks largely issuing a mixture of mortgage and public sector Pfandbriefe and 'Other' — banks where the Pfandbrief business plays a minor role in relation to other balance sheet positions. These classifications are based on the shares of Pfandbriefe in the banks' balance sheets summarised in TABLE C.2. Deducing from TABLE C.2, currently, seven Pfandbrief banks in total are suitable for modelling the Pfandbrief's default which predominantly issue mortgage liabilities and consequently hold mortgage related assets in their balance sheet. The selected mortgage Pfandbrief banks, with some recent Pfandbrief related business strategies, are:

AAR The business model of AAR consists of real estate financing and refinancing activities which belongs to their structured property financing segment. In this segment, AAR supports national and international clients with their real estate investments and is active in Europe, North America and Asia. Aareal Bank provides financing for commercial real estate, in particular office buildings, hotels, retail, logistics and residential real estate. In 4$^{\text{th}}$ quarter 2016, AAR has €9,036.7 mn outstanding mortgage

[10]According to vdp's website (`https://www.pfandbrief.de/site/de/vdp/statistik/statistik/spread.html`) the spread determination is based on mid-asset swap versus 6-month Euribor. In particular, "for each Jumbo Pfandbrief and issues with min. issuance volume of €500 mn outstanding with a residual life of more than one year, the participating banks report every trading day within a given time window a spread on the basis mid-asset swap versus 6-month Euribor. A clearly defined procedure is used to calculate an average secondary market spread every trading day for each involved Pfandbrief. This spread is then published on the vdp's website.", cf. vdp (above link).

[11]The underlying data of the Deutsche Bundesbank (`https://www.bundesbank.de/Navigation/DE/Statistiken/Zeitreihen_Datenbanken/Geld_und_Kapitalmaerkte/geld_und_kapitalmaerkte_list_node.html?listId=www_skms_it04a`) are the series BBK01.WT3311 - BBK01.WT3339 from 01/01/2004 to 30/12/2016 consisting of the daily term structure of interest rates in the debt securities market based on estimated values by the Deutsche Bundesbank. "Interest rates on (notional) zero-coupon bonds without a default risk, estimated by the procedure described in the definitions of the Statistical Supplement Capital Market Statistics. The estimates are based on the prices of Pfandbriefe (Mortgage and Public Pfandbriefe) with residual maturities of at least 3 months. The interest rates are estimated using a non-linear parametric approach", cf. Deutsche Bundesbank (above link). A more detailed description and structure of the securities can be found in Schich (1996). The time series consist of 15 data points, which are distributed equally between 1 and 15 years.

[12]Compare also FIGURE 3.4 in Section 3.7.1.

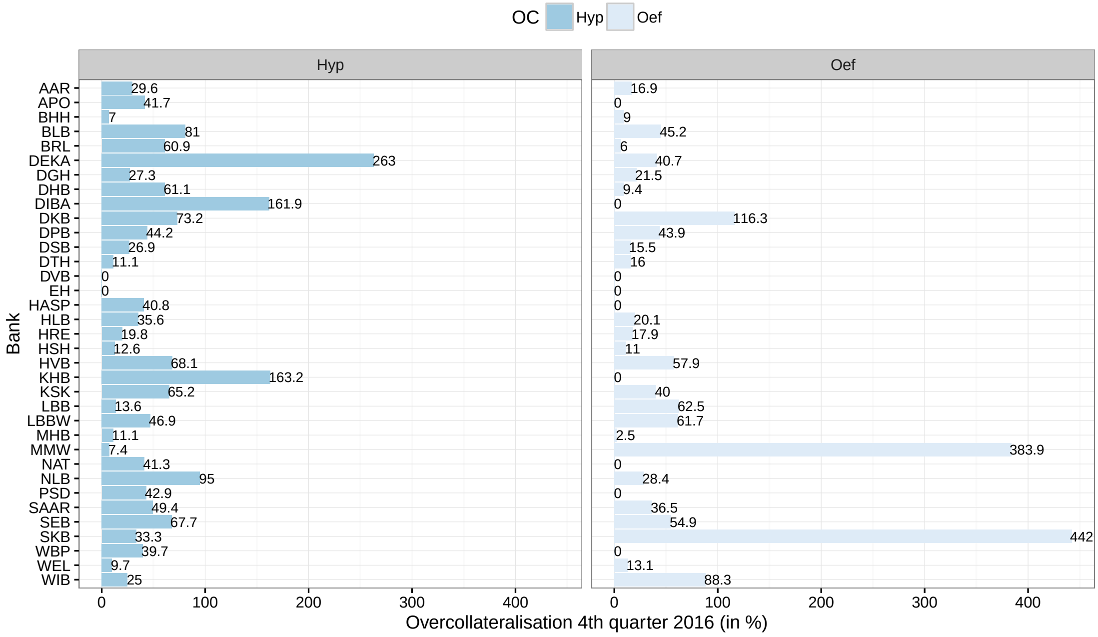

FIGURE 2.26.: Overcollateralisation of mortgage (left) and public sector (right) cover pool, in 4th quarter 2016

Pfandbriefe and the nominal value of the cover pool amounts to €11,712.0 mn with an OC of 29.6% (FIGURE 2.26). The purchase of Westdeutsche ImmobilienBank AG (WIB) which specialises in commercial real estate financing was completed effective on May 31, 2015 (AAR, 2015). In addition to the German Pfandbrief and unsecured bank bonds, housing deposits represent an important pillar in the bank's long-term refinancing mix (AAR, 2016).

BHH Berlin Hyp is a financial institution specialising in commercial real estate finance, combining the experience gained in around 150 years of real estate lending business and the corresponding feel for current market trends in order to design future-oriented products and services for professional clients. April 27, 2015 marks the day the bank issued a seven-year term €500 mn mortgage Pfandbrief which was the first 'Green Pfandbrief'. This is a mortgage Pfandbrief in the sense of the Pfandbrief Act, to which the 'Green Bond Principles' — particularly sustainable buildings – are additionally applied (BHH, 2015). In total €11,839.1 mn outstanding mortgage Pfandbriefe are in circulation covered by €12,664.6 mn which amounts to an OC of 7%.

MHB MHB focuses on residential real estate finance in Germany. Central partners in this business area are the banks of the Genossenschaftliche Finanzgruppe. Around two-thirds of business is accounted for by private residential property financing. MHB profited from continued low interest rates, high demand for real estate and real estate financing as well as the strong market position of brokerage partners, especially the cooperative banks. Due to MHB's business strategy wrt the public-sector Pfandbriefe, no public Pfandbriefe were issued in 2016. Further, more mortgage Pfandbriefe in foreign currencies were issued (around 40% of funding volume were not denominated in euros), compare MHB (2016). MHB is the largest issuer of mortgage Pfandbriefe (FIGURE 2.34) with a relatively small voluntary OC of 11.1% (FIGURE 2.26).

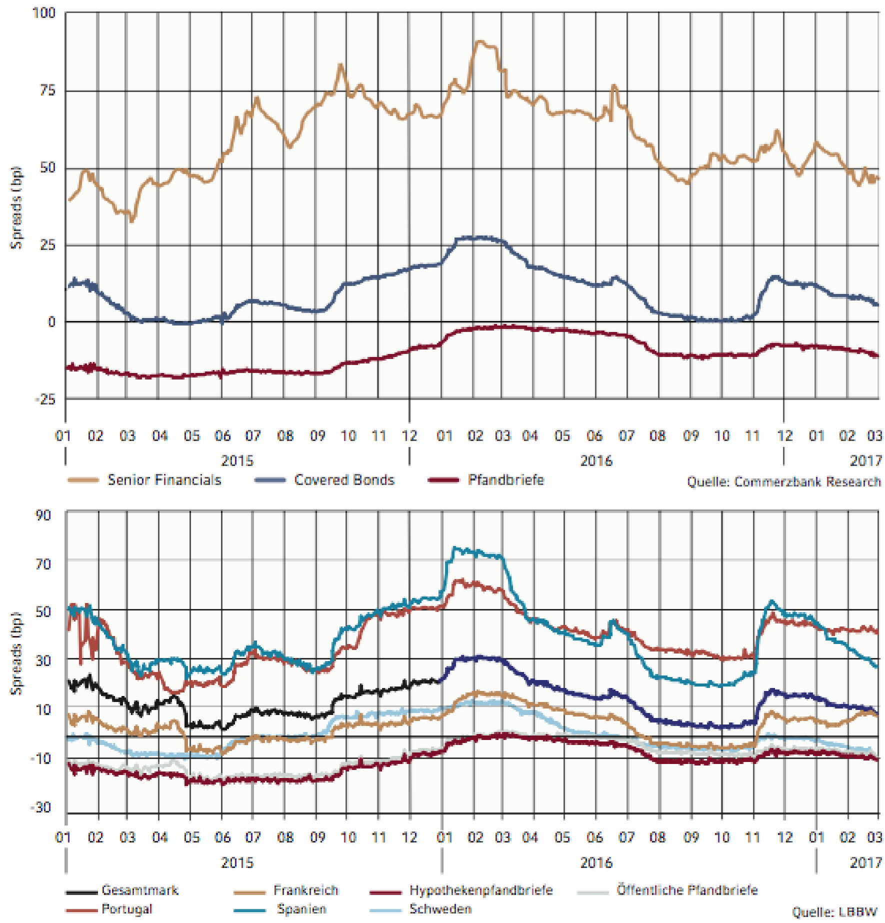

FIGURE 2.27.: Performance of Pfandbrief spreads in comparison to covered bonds and uncovered debt (Source: (VDP, 2016)). Top: Uncovered bank debt versus covered funding; Bottom: Development of the swap spreads of Pfandbriefe compared to other covered bonds

MMW MMW, founded in 1995, is a bank focused on long-term real estate financing and the refinancing of these businesses. Investors are mainly banks, pension funds and insurances in Germany; Private investors play a subordinate role. In general, the main refinancing instrument remains the Pfandbrief. Given the particular structure of the asset side, but also with regard to the management of the liability side, small-volume registered Pfandbriefe — responding to the needs of smaller institutional investors — have always made up a large part of the issue volume. In 2016, MHB continued to expand its real estate financing similar to previous years on the basis of a successful Pfandbrief business (MMW, 2016). The outstanding mortgage Pfandbrief volume is relatively small of €1,250.4 mn with an OC of 7.4%.

NAT One of the decisive legal bases for the activities of the bank is the Pfandbrief Act (PfandBG). The bank mainly operates only those transactions that can be reclassified into Pfandbrief coverage under the Pfandbrief Act. The business of NAT in the real estate lending sector continues to be generated mainly from the countries of France and Germany. The focus of lending is on the issue of commercial loans with mortgage collateral. The refinancing of NAT is carried out in line with its business model through

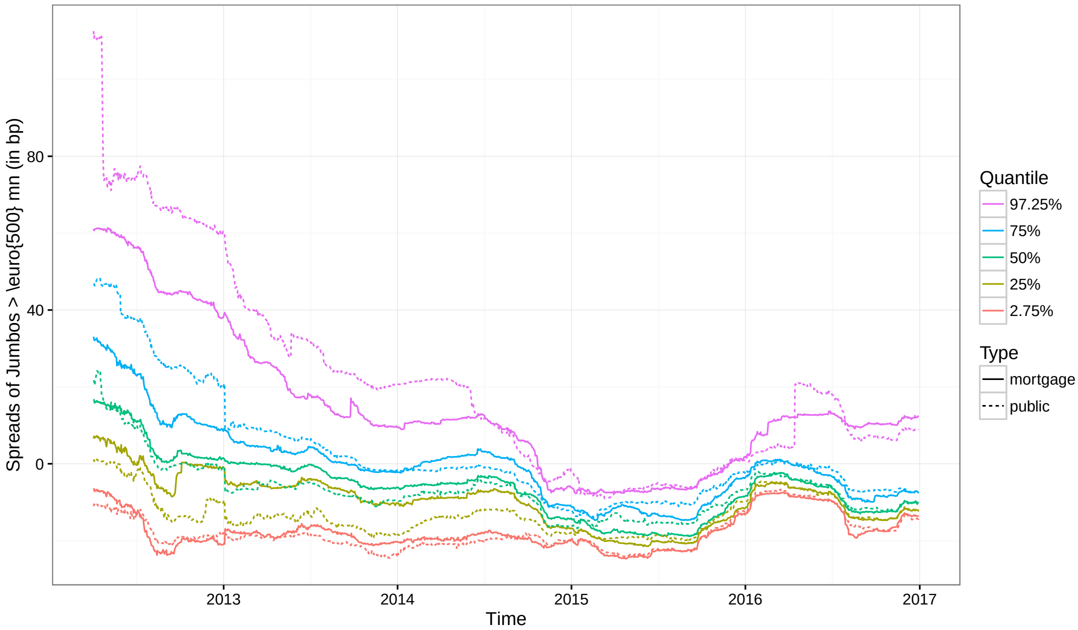

FIGURE 2.28.: Spreads of mortgage jumbos larger than €500 mn over time

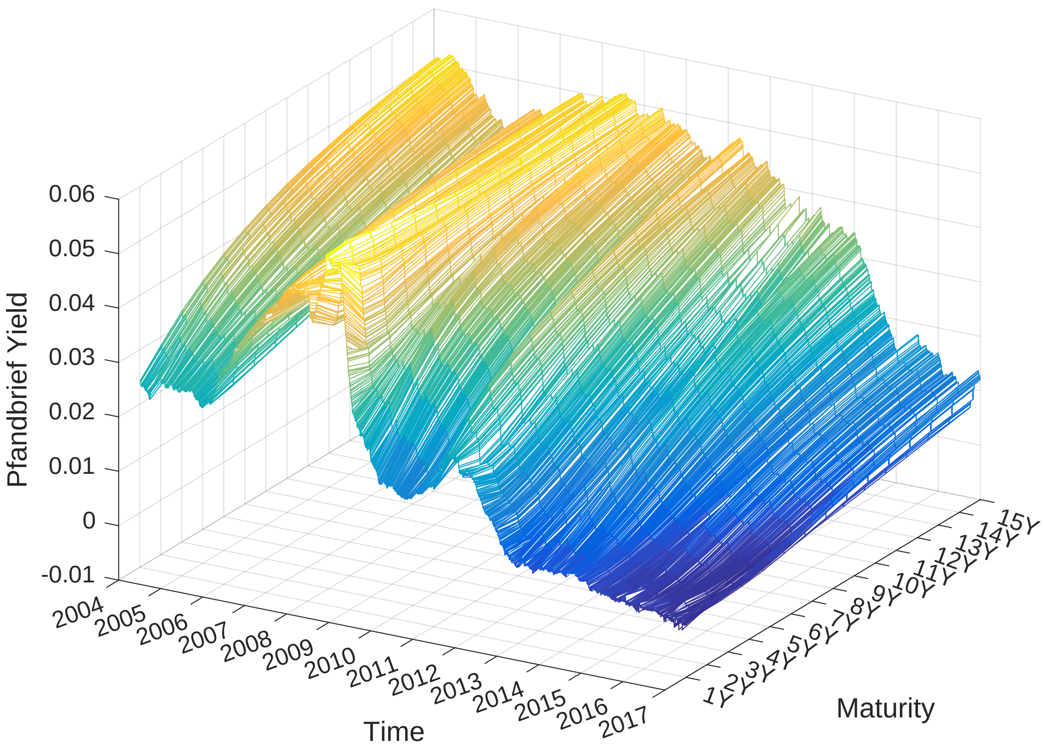

FIGURE 2.29.: Daily Pfandbrief interest rates from 07/01/2004 to 30/12/2016 for different maturities (1Y - 15Y)

the issue of Pfandbriefe. Outstanding mortgage Pfandbrief volume amounts to €947.7 mn with a corresponding cover pool of €1339.4 mn and OC of 41.3% (see FIGURE 2.26). Of the 'Hyp' type issuers the bank has zero outstanding public sector Pfandbrief, thus solely concentrating on the mortgage type.

WBP WBP was founded in 1968 as a special institute for mortgage lending and supported clients of Wüstenrot Bausparkasse AG in the financing of their real estate projects. In 2005, Wüstenrot Bank AG Pfandbriefbank, one of the first universal banks with a Pfandbrief license, emerged from the merger with Wüstenrot Hypothekenbank. The Pfandbrief portfolio amounted to €2.5 bn (previous year: €3.4 bn) and contains only mortgage Pfandbriefe in 2016. The public sector Pfandbriefe business was discontinued as of June 30, 2016 where the cover pool was fully settled (WBP, 2016). In the products and asset classes of the proprietary business, the focus is on fixed income, i.e. covered and unsecured bonds, e.g. government and bank bonds and Pfandbriefe. In addition, only a small amount is invested in foreign currencies. The refinancing of the lending business is carried out in particular via Pfandbriefe (WBP, 2015).

WIB The credit portfolio of WIB is distributed primarily to the German, European markets and North America. WIB primarily finances office and retail real estate, shopping centers, logistics centers, hotels, residential properties and public facilities. The loan portfolio also includes a portfolio of private mortgage lending. The past financial year was marked by the further integration of WIB into the AAR Group. Here we depict WIB still as stand-alone bank — although taken over by AAR — with its own Pfandbrief business (outstanding volume according to vdp amounts to €2,745.4 mn) independent of AAR since the data source is mainly vdp where both banks are still treated separately on vdp's website[13] in the 4th quarter of 2016 (WIB, 2016).

At first the total Pfandbrief market is examined which is then broken down in a public sector and mortgage covered bond type review. This allows a more differentiated analysis of the empirical developments.

2.2.3.1. Total

The total Pfandbrief market of the top ten issuers in 4th quarter 2016, see FIGURE 2.30, consists of the sum of public sector and mortgage type of Pfandbrief types. The top ten issuers account for €227 bn of outstanding Pfandbrief volume which makes up 60% of the Pfandbrief market. HRE, the Deutsche Pfandbriefbank AG (formerly known as the Hypo Real Estate Bank AG), is still the largest issuer in Germany. The merging of Hypo Real Estate Bank AG and DEPFA Deutsche Pfandbriefbank AG to Deutsche Pfandbriefbank AG in mid 2009 is reflected in the time series of FIGURE 2.30 by the jump in 2nd quarter 2009. Also the incorporation of EH into DSB can clearly be observed in 2nd quarter 2016, letting DSB become the forth largest issuer in 4th quarter 2016. Also, DSB is the bank with the largest gain since 4th quarter 2008 with over 1600%. LBBW has substantially forfeited its market share compared to 4th quarter 2008 when it was the largest issuer. In 4th quarter 2008 its Pfandbrief volume amounted to €75.0 bn which is reduced by -74.5% to €19.1 bn in 4th quarter 2016. In total the volume size of the group of top ten issuers has contracted by 38.1%.

[13] `https://www.pfandbrief.de/site/de/vdp/statistik/statistik/statistiken-pfandbg-vdp.html`

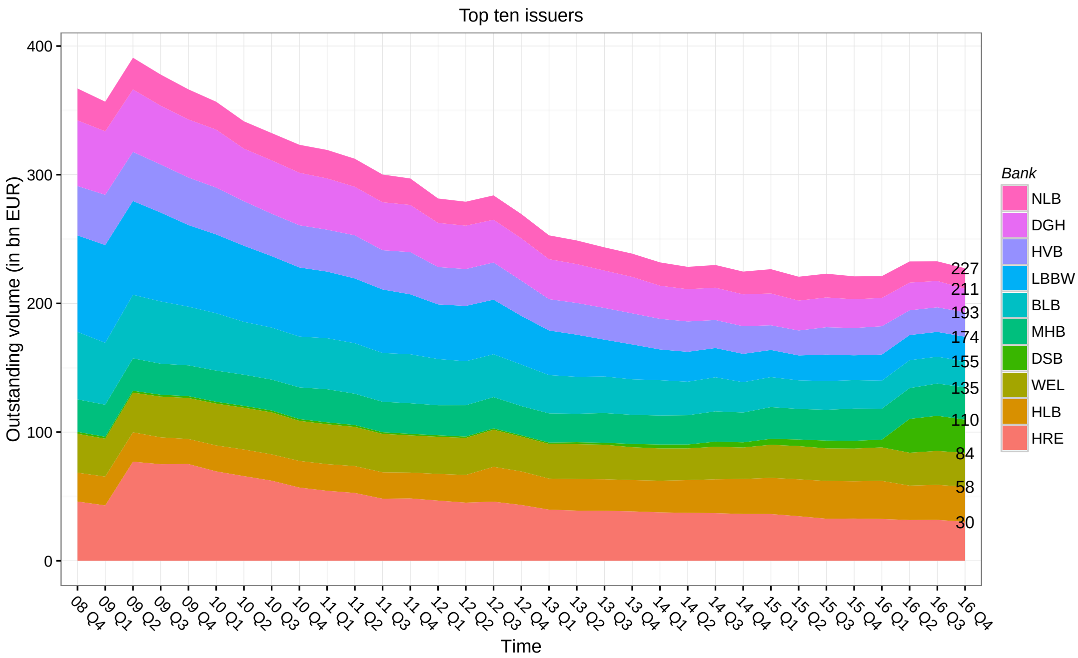

Figure 2.30.: Total outstanding Pfandbrief volume over time of top ten issuers in Q4 2016

In Figure 2.31 the depiction of the public sector and mortgage Pfandbrief market is given where Pfandbrief banks of Table C.2 are visualised[14] in comparison to the average over banks development (depicted by the blue circle and labeled vdp) of Pfandbrief banks with -7.9% in short and -53.5% in long term changes. BLB (top 10; x: -13.9, y: -61.3), DGH (top 10; x: -25.8, y: -64.0) and LBBW (top 10; x: -13.2, y: -74.5) are three banks with the largest losses in volume pulling the overall market to the bottom left corner of the coordinate system. Four banks belonging to the issuing category 'Hyp' outperform the market, situated in the first quadrant of the coordinate system, with NAT* (x: 75.4, y: 1795.4), MMW (x: 12.5, y: 31.9), MHB (top 10; x: 7.8, y: -0.9) and BHH (x: 5.6, y: -41.6). Also WEL (x: 7.5, y: -13.3) categorised as 'Hyp-Oef' can be found in the first quadrant. It needs to be noted that the outlier DSB has no impact on the overall average changes as its volume increase is only a shift from EH to DSB.

2.2.3.2. Public Sector

We now focus on the public sector Pfandbrief market. A similar picture as in Figure 2.24 is also depicted for the top ten markets in Figure 2.32. The top ten issuers account for approx. 70% of market share with an accumulated outstanding volume of €112.2 bn. Unlike in the total market of Section 2.2.3.1, HRE is only in third place in the public sector market. HLB is the largest issuer with an outstanding volume €17.4 bn (share 10.7%) followed by BLB with €16.2 bn (share 10.0%) so that the top three hold approx. one third of the market share. For HLB one can observe a significant jump in

[14]Banks marked with '*' have a shorter long-term time horizon (y-axis): DIBA* since 3rd quarter 2011, DKB* since 3rd quarter 2009, LBB* since 1st quarter 2010, NAT* since 1st quarter 2013 and SAAR* since 1st quarter 2010.

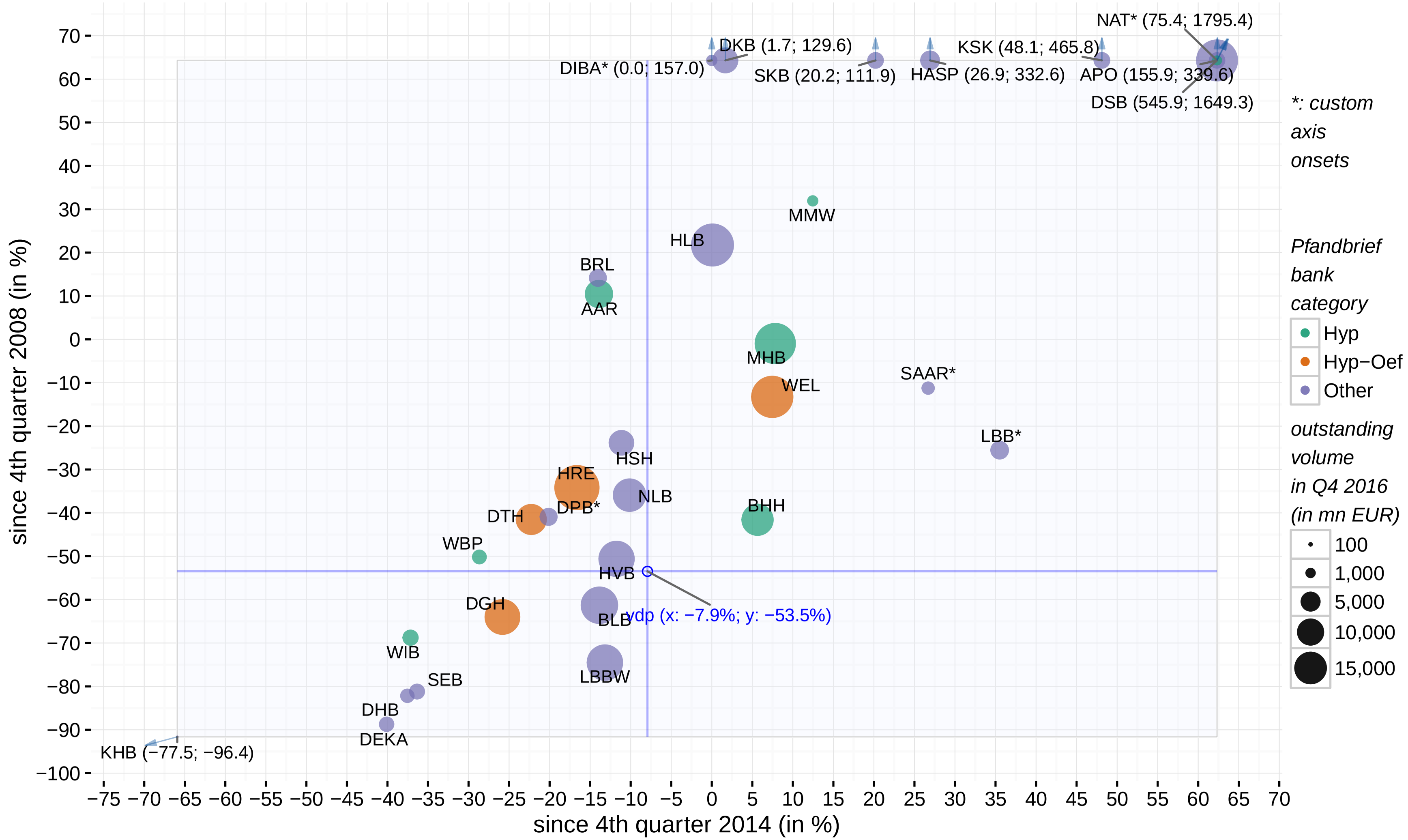

FIGURE 2.31.: Total outstanding Pfandbrief volume, with short and long term development of Pfandbrief banks, in Q4 2016

Figure 2.32 as well as Figure 2.24 from 2nd quarter 2012 (€15.6 bn) to 3rd quarter 2012 (€21.3 bn) in public sector volumes. On July 1st, 2012, HLB has taken over significant parts of refinancing funds — including outstanding issues of Pfandbriefe — from WestLB's Verbundbank activities.

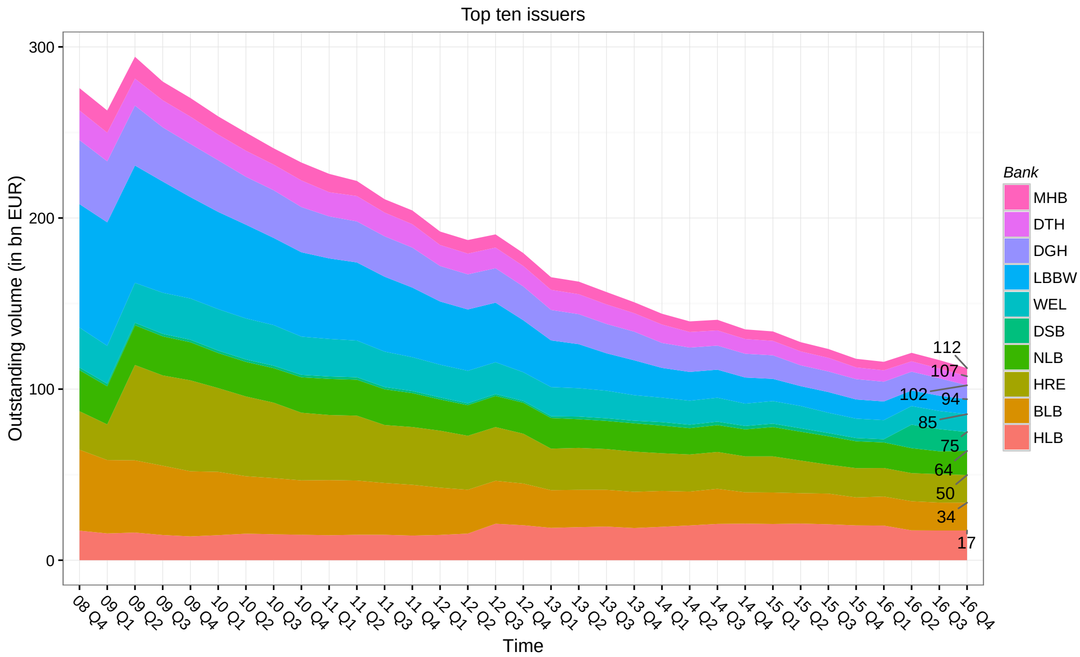

Figure 2.32.: Outstanding public sector Pfandbrief volume over time of top ten issuers in Q4 2016

In Figure 2.33 the depiction of the public sector Pfandbrief market is given where Pfandbrief banks of Table C.2 are visualised[15] in comparison to the total development (vdp) of Pfandbrief banks with -26.7% in short and -72.2% in long term changes. Once again three players, LBBW (top 10; x: -42.5, y: -87.9), DGH (top 10; x: -41.6, y: -78.3) and DTH (top 10; x: -39.0, y: -69.7), from the top ten list account for the larger volume losses, amounting to over €60 bn in total since 4th quarter 2008 and over €2 bn in total since 4th quarter 2014. The only two banks which show a positive growth rate — short and long term — are DSB (top 10; x: 453.2, y: 649.6) and KSK (x: 0.9, y: 465.0) whereas DSB's exorbitant growth is a consequence of the takeover of EH.

2.2.3.3. Mortgage

For the mortgage type Pfandbriefe we see a rather stable sideways shift on the long term under the top ten market players and a growth period in the short term since 4th quarter 2014 which is inline with Figure 2.24. The top ten issuers in 4th quarter 2016 account for 63.3% of the mortgage Pfandbrief market share. HVB, in 4th quarter 2008 the largest issuer, has forfeited half its market share by 4th quarter 2016 from 14.2% to

[15] Banks marked with '*' have a shorter long-term time horizon (y-axis): DPB* since 3rd quarter 2009, LBB* since 1st quarter 2010 and SAAR* since 1st quarter 2010. Not included in analysis are APO, DIBA, HASP and NAT which do not issue public Pfandbriefe. KHB does not issue public Pfandbriefe after 1st quarter 2010 and WBP ceased their public sector Pfandbrief program in 2nd quarter 2016.

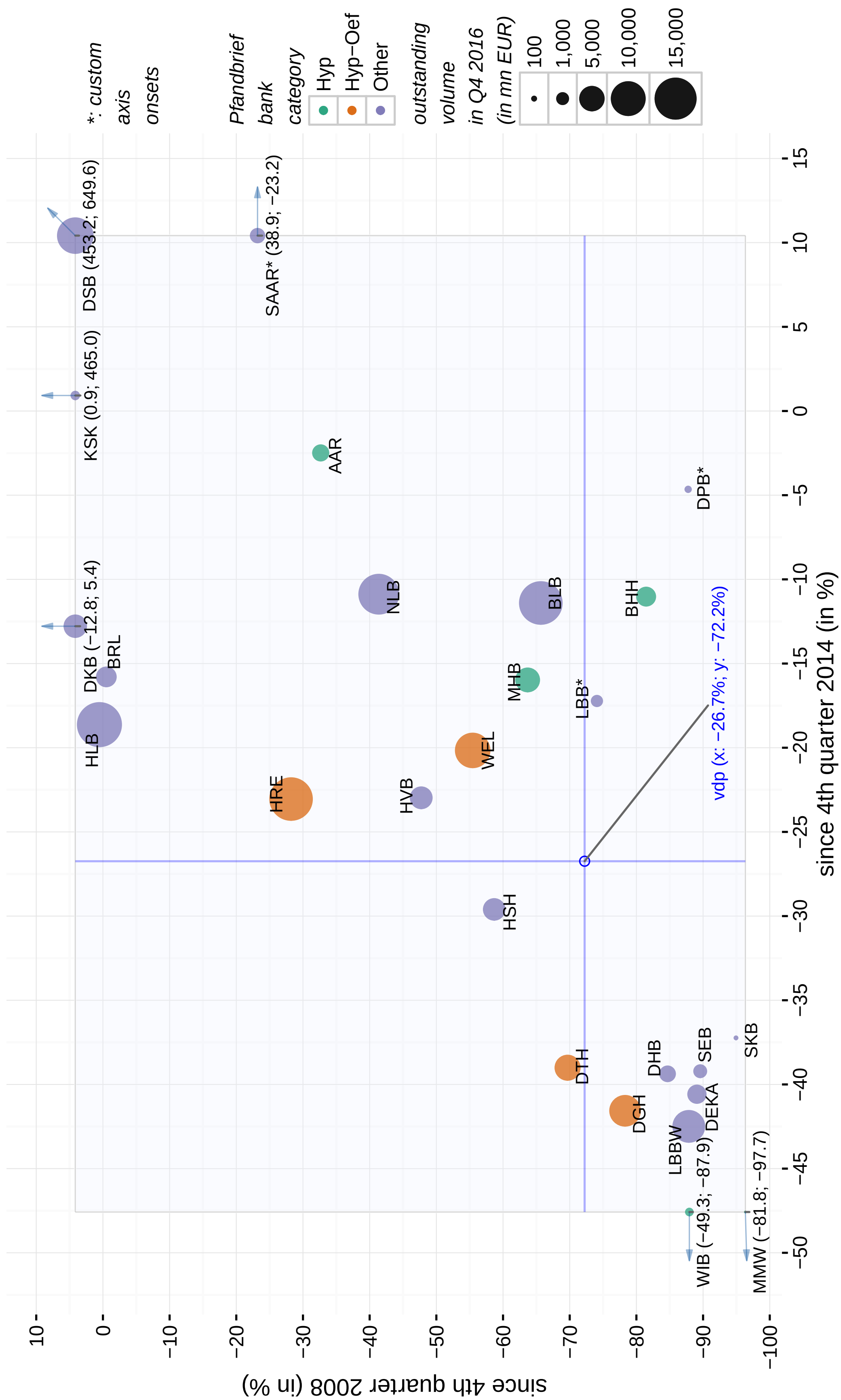

Figure 2.33.: Outstanding public sector Pfandbrief volume, with short and long term development of Pfandbrief banks, in Q4 2016

7.2% ranking third. First place goes to MHB with a market share of 9.8% in 4th quarter 2016 which is labeled as a predominant 'Hyp' type issuer according to TABLE C.2. Also categorised as 'Hyp' and under the top ten issuers are BHH (5.7%) and AAR (4.4%). As in FIGURE 2.30 and FIGURE 2.32 we again see the significant gain in market share of DSB since 1st quarter 2016.

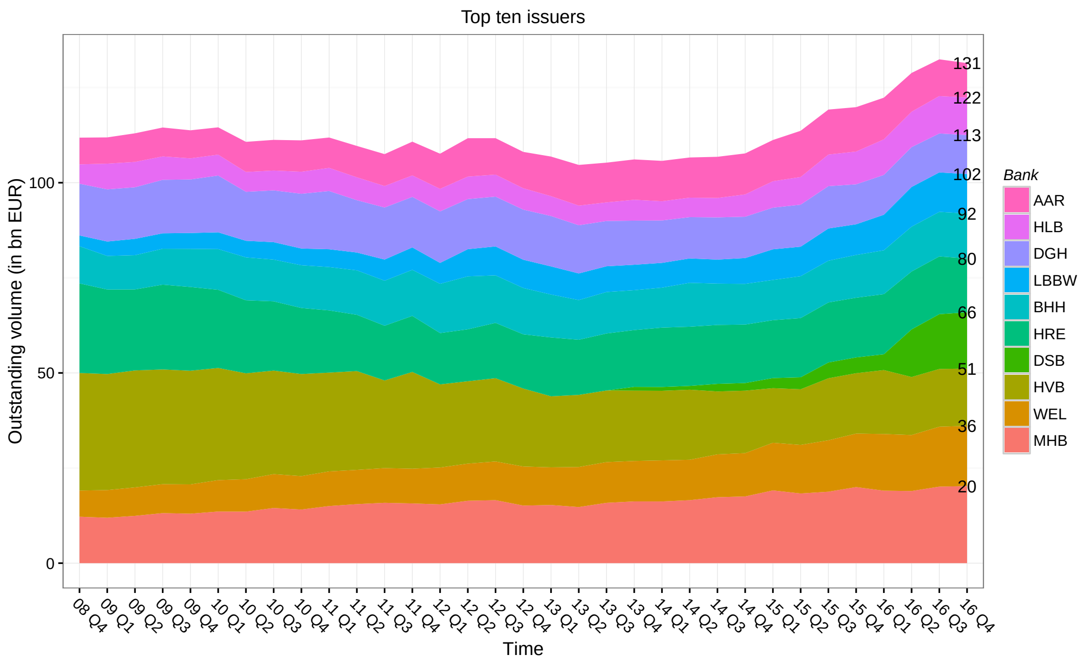

FIGURE 2.34.: Outstanding mortgage Pfandbrief volume over time of top ten issuers in Q4 2016

In FIGURE 2.35 the depiction of the mortgage Pfandbrief market is given where Pfandbrief banks of TABLE C.2 are visualised[16] in comparison to the total development (vdp) of Pfandbrief banks with 13.9% in short and -6.2% in long term changes. In the bottom left quadrant we find WIB (x: -35.2, y: -61.2) and WBP (x: -28.5, y: -44.6) of the issuer category 'Hyp'. For AAR (top 10; x: -16.1, y: 28.8) we only see on the short term a negative sign. A rather stable and slightly above market average growth rate — long and short term — can be observed for BHH (top 10; x: 10.6, y: 21.3), MHB (top 10; x: 15.5, 65.9) and MMW (x: 15.4, y: 84.7). NAT* (x: 75.4, y: 1795.4) once again is marked as outlier in the top right corner.

2.2.4. Jumbo Market

Continuing the coverage of the Jumbo market of Section 2.1.4, now specifically for the German market, we immediately spot the stark decline of the Jumbo Pfandbrief (FIGURE 2.37). Compared to 2003, totalling €383.2 bn in outstanding Pfandbriefe, over 90% in outstanding volume has been lost, amounting to €34.6 bn in 2016. Germany

[16] Banks marked with '*' have a shorter long-term time horizon (y-axis): DIBA* since 3rd quarter 2011, DKB* since 3rd quarter 2009, DSB* since 4th quarter 2013, LBB* since 1st quarter 2010, NAT* since 1st quarter 2013 and SAAR* since 1st quarter 2010.

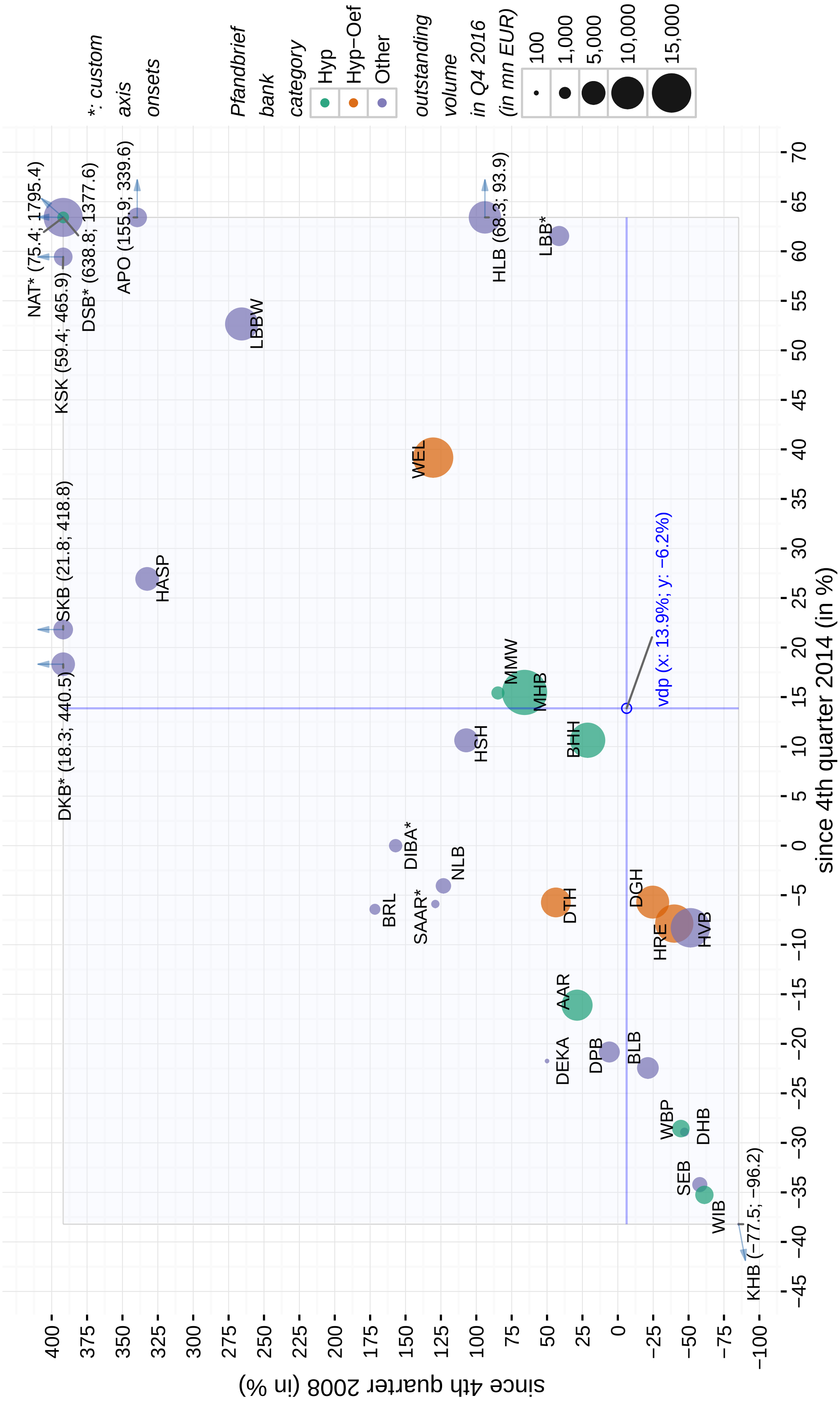

Figure 2.35.: Outstanding mortgage Pfandbrief volume, with short and long term development of Pfandbrief banks, in Q4 2016

is therefore not included in the top ten Jumbo issuing countries in 2016. Traditionally, Jumbos are issued as the public sector type of Pfandbriefe, thus, the trend is correlated with that of the public sector (Section 2.2.3.2). In the late 1990s and 2000, the predominant Jumbo to be issued was the public-sector type, with a share of over 90% of all Jumbos issued, compare Mastroeni (2000). This is simply due to the higher issued volume of public-sector Pfandbriefe (over 80% at that time; compare also FIGURE 2.24) and the difficulty involved in pooling the necessary €1 bn or higher in mortgage loans.
In 2016, the market for benchmark Pfandbriefe of €500 mn or higher has changed dramatically. A total of €22,3 bn were issued thereof €18,5 bn (83.0%) mortgage and only €3.8 bn (17.0%) public-sector Pfandbriefe. The benchmark with size €500-€999 mn has significantly gained influence and popularity since 2012, see FIGURE 2.37 and FIGURE 2.38. As alluded above, especially, for mortgage type Pfandbriefe it is easier to bundle smaller amounts of mortgages together rather than sums of €1 bn or higher contributing to the rise of the lower benchmark category. The top five banks wrt outstanding volume of mortgage benchmark Pfanbriefe of €500 mn or higher are DSB (€6.8 bn), MHB (€6.6 bn), WEL (€6.0 bn), PBB (€5.0 bn) and BHH (€4.9 bn).
In 2016, the Pfandbrief market consists predominantly of private placements making up over half of outstanding Pfandbriefe (FIGURE 2.36) which clearly contrasts to the picture of all covered bond markets in FIGURE 2.19. In 2003, private placements only accounted for 36.4% of all outstanding Pfandbriefe.

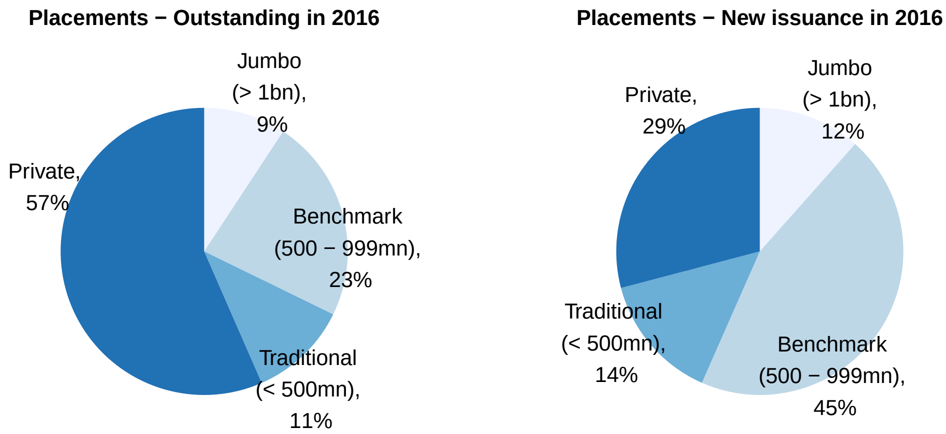

FIGURE 2.36.: Placement shares of outstanding Pfandbrief volume and new issuance, in 2016

2.3. Münchener Hypothekenbank eG (MHB)

Exemplary for the 'Hyp' issuer category in TABLE C.2 we analyse the balance sheet positions of MHB, simply because it is the largest mortgage Pfandbrief issuer in 2016, see FIGURE 2.34. One finding from above sections (Section 2.1 and Section 2.2) is a persistent trend of a declining public covered bond, respectively, Pfandbrief which will likely become even less significant in the future. This also applies to MHB. MHB's decrease of the public Pfandbrief since the 4^{th} quarter 2008 has amounted to -63.7% and since 4^{th} quarter 2014 to -16.0% (FIGURE 2.33). The time series data of MHB is available on its website (`www.muenchenerhyp.de`) and VDP's website (`www.pfandbrief.de`), with

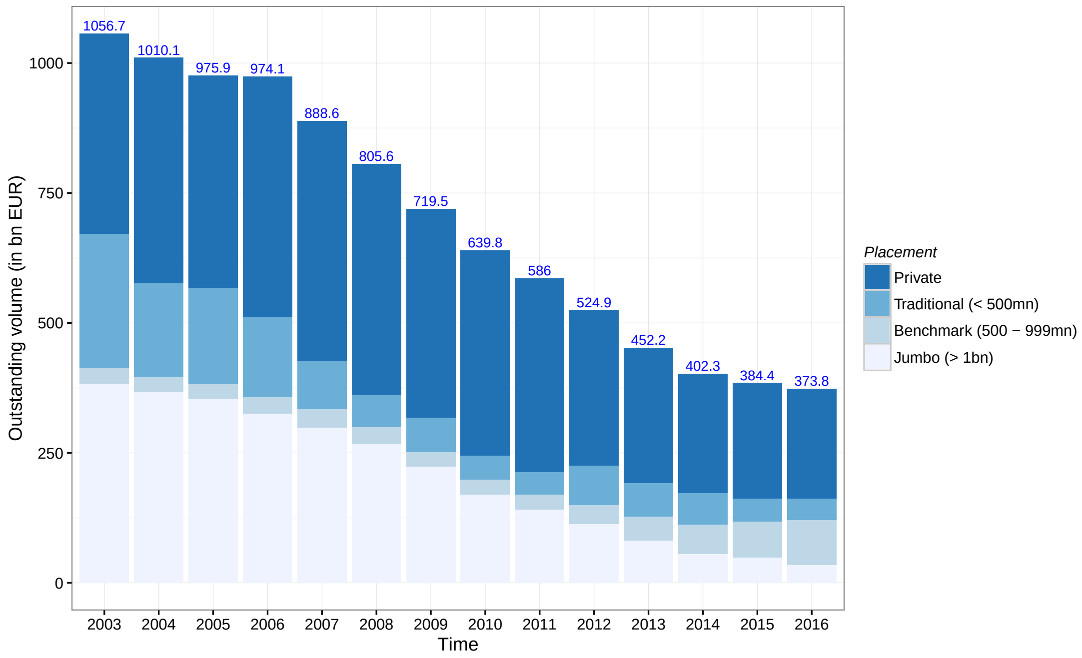

FIGURE 2.37.: Placement shares of outstanding Pfandbrief volume over time

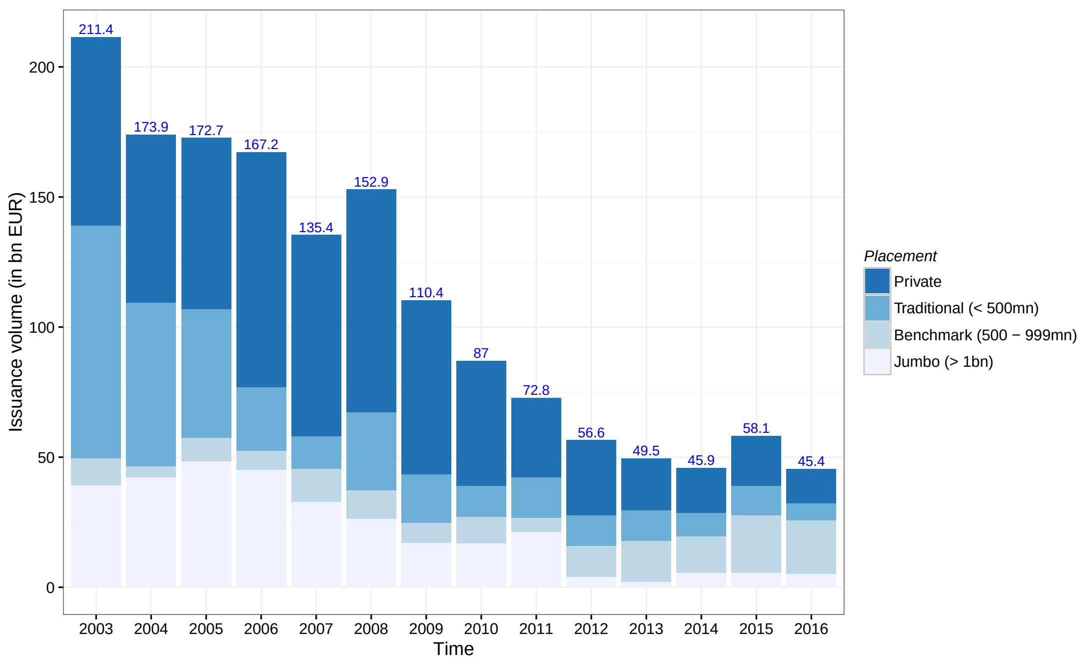

FIGURE 2.38.: Placement shares of Pfandbrief new issuance over time

onset 4^{th} quarter 1999. A linear interpolation procedure is conducted for filling missing data, prior to 4^{th} quarter 2008.
In this bank level investigation, methods from time series analysis and the field of econometrics are applied. Emphasis is laid upon the bank's development of balance sheet positions relative to time. Thereby, it is of high interest to statistically derive two main features by extracting the information contained in the series:

Structural changes The analysis of structural changes has two reasons. First it is of interest if statistically detected changes coincide with actual break dates, for example the beginning of the recent financial crisis, the introduction of the 'New Pfandbrief Act' (PfandBG) or realignment of internal business strategies. Secondly, when structural changes are present forecasts can be made based on the series as of the breakpoint instead of the complete series, thus relying on more recent data. Translated into a parametric time series model, this means that the parameters of the model are not stable throughout the sample period but change over time. Throughout, structural breakpoints are computed with a linear regression on lagged series. The F-statistic on the obtained residuals is then consulted where the null hypothesis has no structural change boundaries. "Tests based on F-statistics (...) are designed to have good power for single-shift alternatives (of unknown timing). The basic idea is to compute an F-statistic (or Chow statistic) for each conceivable breakpoint in a certain interval and reject the null hypothesis of structural stability if any of these statistics (or some other functional such as the mean) exceeds a certain critical value (...).", cf. (Kleiber and Zeileis, 2008). Visually, the original series with its corresponding fitted values are depicted. The located breaks by the F-statistic are included with a 95% confidence interval. Additionally, a linear regression is conducted before and after the break quantifying the change in the slope regression coefficient. Zeileis et al. (2002) provide an excellent R package for detecting potential structural breaks.

Forecasting Predictions on the future behaviour of the asset and liability positions are established. Thereby, it is important to find an adequate time series model which captures the underlying information. Moreover, the stationary property needs to hold for guaranteeing non-biased estimates. R provides several packages for time series analysis. Here, the forecasts rely on the (S)ARIMA (seasonal auto regressive integrated moving average) technique where differentiating takes place for integrated series and automatic best fit algorithms are implemented, according to either AIC, AICc or BIC value. The (S)ARIMA model is the seasonal version of the ARIMA model taking the seasonality present in the time series into consideration. To fix the notation (Peña et al., 2001)

$$\text{ARIMA}\ \underbrace{(p,d,q)}_{\substack{\text{non-seasonal}\\ \text{part}}}\ \underbrace{(P,D,Q)[s]}_{\substack{\text{seasonal}\\ \text{part}}}, \tag{2.1}$$

with

$$\Phi(L^s)\phi(L)(1-L^s)^D(1-L)^d y_t = c + \theta(L)\Theta(L^s)\epsilon_t, \tag{2.2}$$

where

- the non-seasonal AR (autoregressive) part is given by the pth order polynomial $\phi(L) = 1 - \phi_1 L - \ldots - \phi_p L^p$,
- the non-seasonal MA (moving average) part is given by the qth order polynomial

$\theta(L) = 1 + \theta_1 L + \ldots + \theta_q L^q$,

- d is the order of differencing for the non-seasonal part,
- the seasonal AR part is given by the Pth order polynomial $\Phi(L^s) = 1 - \Phi_1 L^s - \ldots - \Phi_P L^{Ps}$,
- the seasonal MA part is given by the Qth order polynomial $\Theta(L^s) = 1 + \Theta_1 L^s + \ldots + \Theta_Q L^{Qs}$,
- D is the order of differencing for the seasonal part,
- s number of periods per season,
- c is some constant, and
- L is the lag operator so that for a given time series $y = \{y_1, y_2, \ldots\}$ then $Ly_t = y_{t-1}$ and $\Delta y_t = y_t - y_{t-1} = (1 - L)y_t$ holds.

An univariate analysis is preferred because an independent view on the position series is necessary due to differing breaking points in the series. Numerous literature on time series analysis exists. Peña et al. (2001), Tsay (2010) and Tsay (2013) cover most essential approaches.

2.3.1. Total Assets and Liabilities

Before we take a closer look at the asset and liability positions we analyse the total sum of assets and liabilities as accounted on its quarterly balance sheet. With a lag of two the F-test in Table 2.2 finds a structural break at 2nd quarter 2008 with a rather wide confidence interval between 4th quarter 2006 and 2nd quarter 2009.

	statistic	p-value	lag	date
F-test	14.08	0.02	2	Q2 2008

Table 2.2.: Structural change test of total asset and liability positions

MHB first addresses the sub-prime and beginning of the financial crisis in the interim financial report of MHB (2007b), the first half of 2007. According to MHB its business was not directly affected by the crisis in the sub-prime segment of the credit market, as it operates exclusively in the commercial sector and in rental property construction and does not finance homes or condominiums in the US. In accordance with its risk strategy MHB is primarily involved in the financing of office real estate and focus on top-tier financing tranches. However, indirectly MHB, as every other financial intermediate, felt the liquidity crunch due to the general crisis of confidence in the financial markets. Worldwide investors withdrew investments from bonds. In Figure 2.39 we see the structural change depicted with its vertical red dashed line and its corresponding confidence interval (horizontal red line). In the post crisis era a sluggish growth rate with €87.1 mn per quarter can be observed compared to €174.4 mn per quarter prior which is double the amount prior to 2nd quarter 2008.
The model ARIMA(2,0,0)(2,1,0)[4] is fitted to the time series as of the detected structural change in 2nd quarter 2008. In Table 2.3 we see from the unit root test results that all information contained in the series in Figure 2.39 has been extracted so that only white noise is left over (see also Figure D.1 in Appendix D). In Figure 2.40 we see

the forecast for the time series for the next three years with a corresponding confidence interval resulting in a sideways shift without a clear upward or downward trend. Next we apply the same procedure for each asset and liability position separately. This way we can further investigate in an isolated manner by extracting the information contained in each position.

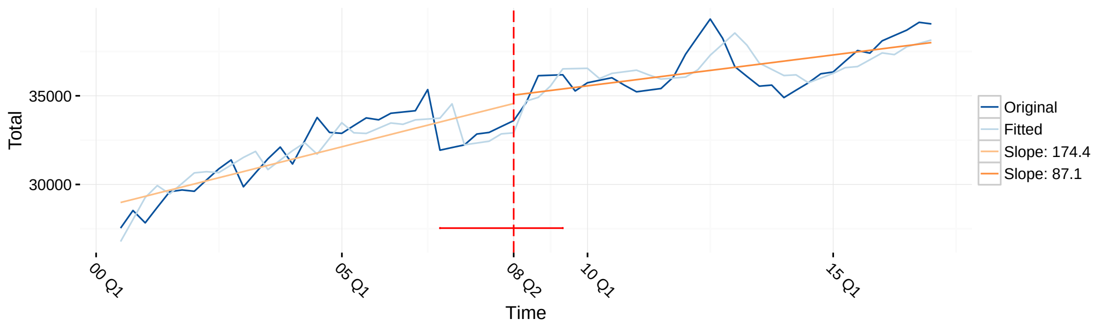

FIGURE 2.39.: Depiction of significant structural change of total asset and liability positions, in mn EUR

ADF-Test		PP-Test		KPSS-Test	
statistic	p-value	statistic	p-value	statistic	p-value
-7.63	0.01	-7.61	0.01	0.21	0.10

TABLE 2.3.: Unit root tests of total asset and liability positions

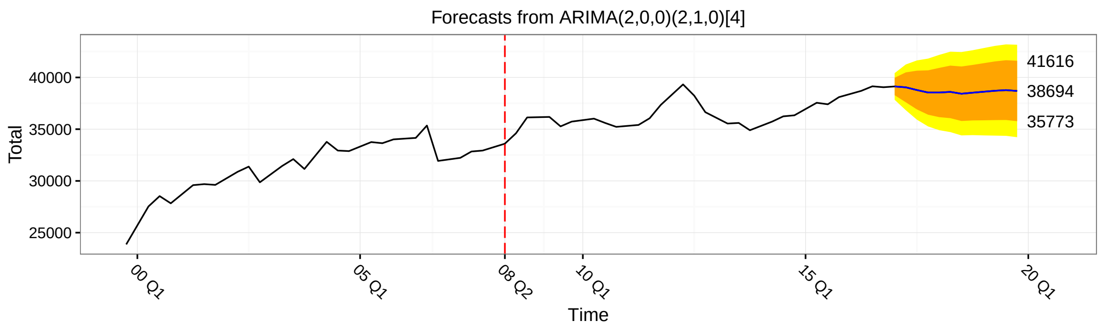

FIGURE 2.40.: Depiction of significant structural change of total asset and liability positions, in mn EUR

2.3.2. Assets

On the asset side emphasis is laid upon the three positions mortgage (Hyp) CP, public sector (Oef) CP and other assets (OA). OA simply contains all other assets which are not in CP-Hyp or CP-Oef. TABLE 2.4 contains the F-statistics with corresponding p-values and break dates of all three positions. The null hypothesis of no structural change is rejected where the break dates turn out to lie close to each other within a time span just over a year. For CP-Hyp we choose a lag of two while for CP-Oef and OA a lag of one is sufficient.

F-Test	CP-Hyp	CP-Oef	OA
statistic	20.67	31.78	30.46
p-value	0.00	0.00	0.00
lag	2	1	1
date	Q4 2007	Q3 2006	Q1 2007

TABLE 2.4.: Structural change test of asset positions

From FIGURE 2.33 and FIGURE 2.35 we already know the adverse developments of the public sector and mortgage assets of MHB. In FIGURE 2.41 the structural changes are visualised. Until the time period approx. between 3rd quarter in 2006 and 4th quarter in 2007 both positions were positively correlated possessing a positive upward trend where the public sector even had a double growth rate than its mortgage counterpart. This drastically changed from then on. Since the 3rd quarter in 2006, CP-Oef dropped by €-297.4 mn per quarter. An accelerated growth can be seen for the mortgage cover pool after the 4th quarter of 2007 by a factor of over three. Another observation is that OA fluctuate between €4 and €6 bn up to the 2nd quarter of 2007 before growing by €121.5 mn per quarter.
In the annual reports of MHB some explanations can be found for the structural changes on the asset side. We mainly refer to MHB (2005), MHB (2006) and MHB (2007a) where the public and mortgage new business is emphasised upon. Further, there exists a certain lag on business decisions from previous quarters or years before their impacts are reflected on the overall development of the balance sheet positions as in the time series of FIGURE 2.41.
Evidently from the annual reports the main business of MHB on the asset side is the funding of real estate which can be roughly divided into private residential financing and commercial mortgages. Overall, new business in 2007 increased to €4.14 bn (MHB, 2007a). The engine of new business in private housing finance was the strong demand for forward financing, which increased again in 2007. The main reason for this was the development of interest rates. On the one hand, the flat interest-rate structure meant that the premiums for forward loans were low and, on the other, rising interest rates prompted many customers to secure favorable interest rates before the end of their financing. Taking into account the purchase of the Corealcredit Bank AG portfolio in the new business, the volume of commitments in the private residential construction segment amounted to €2.33 bn. Furthermore, growth in international business was particularly pronounced. New business rose by 49.5%, or €361.2 mn, to €1.09 bn which for the most part was achieved in the USA. The US business's share of total foreign new business was around 77%.
In general, MHB does not pursue any volume targets in the public sector (state and municipal) lending business, see MHB (2006) and MHB (2007a). Commitments by MHB, which include in particular tradable promissory notes issued by federal states, local authorities and public-sector banks, are solely based on terms of revenue and profitability considerations. In MHB (2005) we find some explanations for the retreat of MHB in the public sector segment: The persistently weak margin situation compared to the previous years and the lower market volume due to the abolition of state liability for Landesbanken has led to declining loan commitments from €5.3 bn in the previous year to €1.9 bn in 2005. By the 2nd quarter 2007, overall, public sector commitments dropped

to volume of €1,052.3 mn which was €1,687.0 mn in the same period of the previous year.
We fit the models of TABLE 2.5 on the univariate time series data of the individual time series data where the structural changes are detected onward. The corresponding unit root tests can be found in TABLE 2.6 and ACF plots in FIGURE D.2. For CP-Hyp and CP-Oef we see a clear upward and downward trend for the forecast of three years. Similar to the overall trend of FIGURE 2.39 no clear direction can be determined for OA, thus, the rather larger confidence interval.

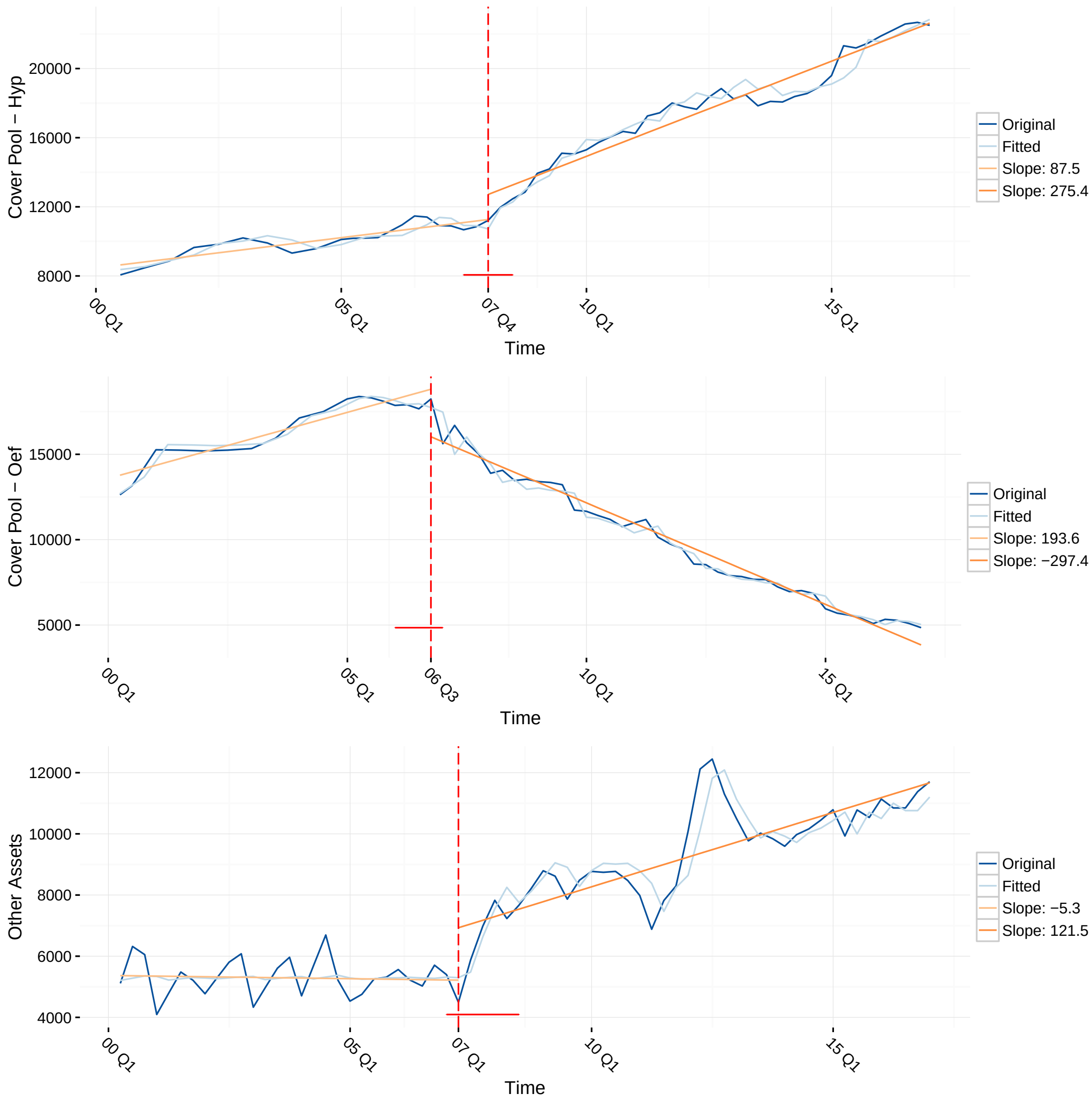

FIGURE 2.41.: Depiction of significant structural change of asset positions, in mn EUR

2.3.3. Liabilities

We now draw our attention to the refinancing business — the liability side. We observe that the structural changes of PB-Hyp and PB-Oef coincide with their counterparts on the asset side (CP-Hyp and CP-Oef) having similar quarterly rates before and after the

position	model
CP-Hyp	ARIMA(1,0,0)(1,1,0)[4] with drift
CP-Oef	ARIMA(1,1,0) with drift
OA	ARIMA(1,1,0)

Table 2.5.: SARIMA model fits of asset positions

		CP-Hyp	CP-Oef	OA
ADF-test	statistic	-7.27	-8.33	-7.41
	p-value	0.01	0.01	0.01
PP-test	statistic	-7.35	-8.33	-7.40
	p-value	0.01	0.01	0.01
KPSS-test	statistic	0.24	0.19	0.03
	p-value	0.10	0.10	0.10

Table 2.6.: Unit root tests of asset positions

break dates. This should not be too surprising since there exists a causality between the amount of assets available and issuing of Pfandbriefe — per definition a Pfandbrief only can be issued on the basis of the assets by which it is covered. In Table 2.7 the detected structural changes with the corresponding break dates are given which are visualised in Figure 2.43. The position other liabilities (OL), the counterpart of OA, has an earlier break date, yet, with a broader forward leaning 95% confidence interval in the range of 3rd quarter 2003 and 2nd quarter 2006. For equity (EQ) we can see a continuous moderate quarterly growth rate with a more recent larger jump in 4th quarter 2013.
Again we relate to the annual reports of MHB during the period of the structural changes. One would expect that the sale of Pfandbriefe, particularly larger benchmark issues (Section 2.2.4), is considerably more difficult during the financial crises triggered by the sub-prime crisis of 2007. The financial market crisis and its further exacerbation due to the insolvency of Lehman Brothers hampered the refinancing business for credit institutions worldwide. As a result, the money and capital markets came to a complete standstill at times. However, according to the annual reports, particularly (MHB, 2008) MHB got off lightly. This has to do with having a reliable customer, the German insurance industry, being the most important buyer of structured issues for MHB. In this sector, MHB is able to place high volumes, especially in the case of long-dated, multi-callable bonds (MHB, 2005). Furthermore, especially during this time, MHB could largely rely on the cooperative 'FinanzVerbund'[17] which turned out to be very beneficial to its liquidity management. In 4th quarter 2008, large parts of emissions could be placed with the 'FinanzVerbund'. Lastly, due to the good reputation as a reliable issuer, MHB was also able to refinance itself outside the 'FinanzVerbund'.
Fitting the models of Table 2.8 to the time series posterior to the break dates we obtain the parameters for forecasting future developments in Figure 2.44. Again a rather similar picture is given as in Figure 2.42. The corresponding unit root tests can be found in Table 2.9 and ACF plots in Figure D.3.

[17] The 'FinanzVerbund' relates to the financial network of the Volksbanken Raiffeisenbanken.

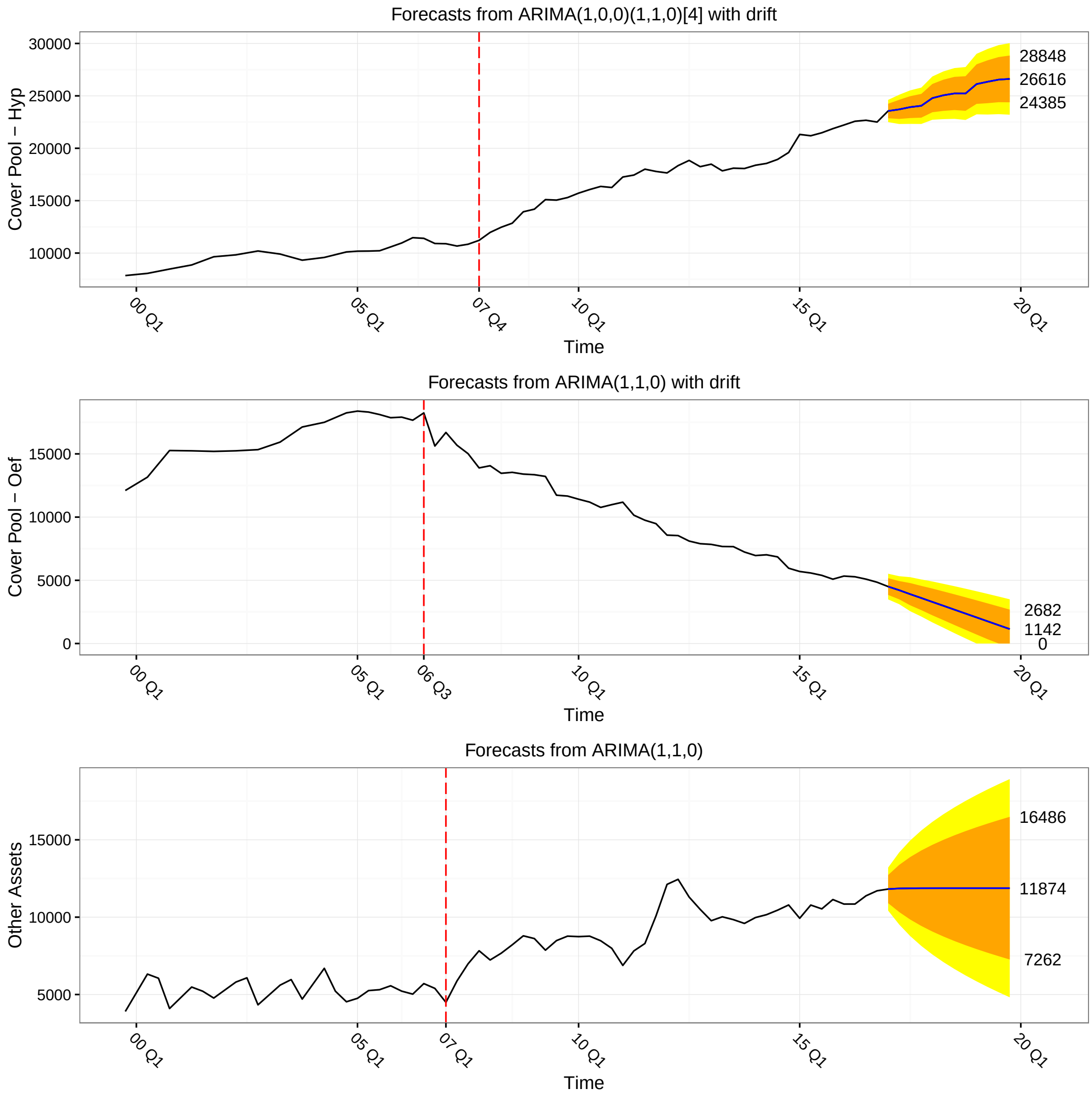

Figure 2.42.: Depiction of significant structural change of liability positions, in mn EUR

F-Test	PB-Hyp	PB-Oef	OL	EQ
statistic	24.67	22.51	15.17	30.24
p-value	0.00	0.00	0.01	0.00
lag	3	1	1	1
date	Q3 2007	Q3 2006	Q4 2003	Q4 2013

Table 2.7.: Structural change test of liability positions

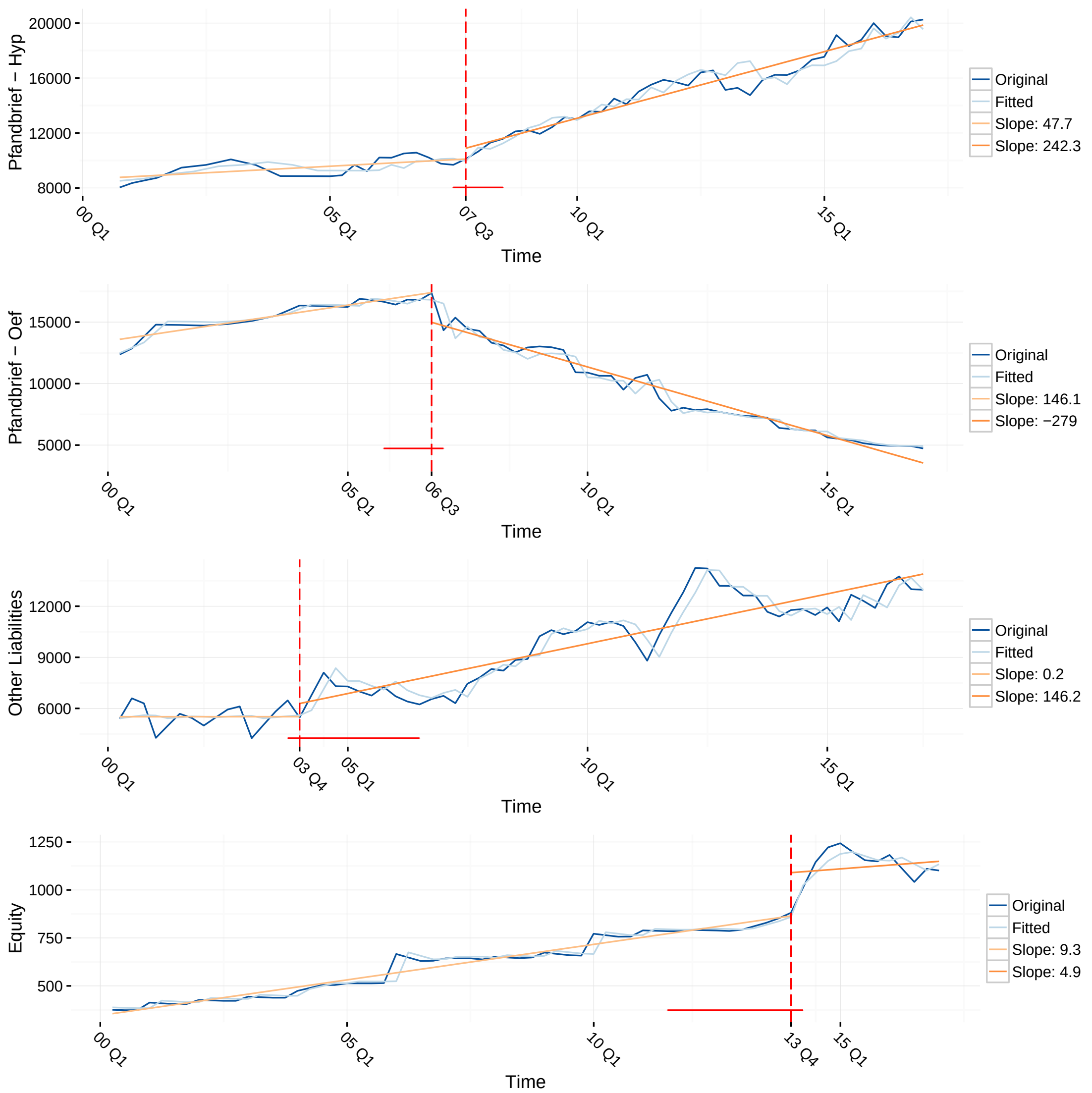

FIGURE 2.43.: Depiction of significant structural change of liability positions, in mn EUR

position	model
PB-Hyp	ARIMA(1,0,0)(1,1,0)[4] with drift
PB-Oef	ARIMA(0,1,1) with drift
OL	ARIMA(2,0,1)(2,1,0)[4] with drift
EQ	ARIMA(0,2,0)(0,1,0)[4]

TABLE 2.8.: SARIMA model fits of liability positions

		PB-Hyp	PB-Oef	OL	EQ
ADF-test	statistic	-5.78	-6.23	-6.90	-3.15
	p-value	0.01	0.01	0.01	0.13
PP-test	statistic	-5.81	-6.24	-6.93	-2.94
	p-value	0.01	0.01	0.01	0.21
KPSS-test	statistic	0.10	0.58	0.09	0.08
	p-value	0.10	0.02	0.10	0.10

TABLE 2.9.: Unit root tests of liability positions

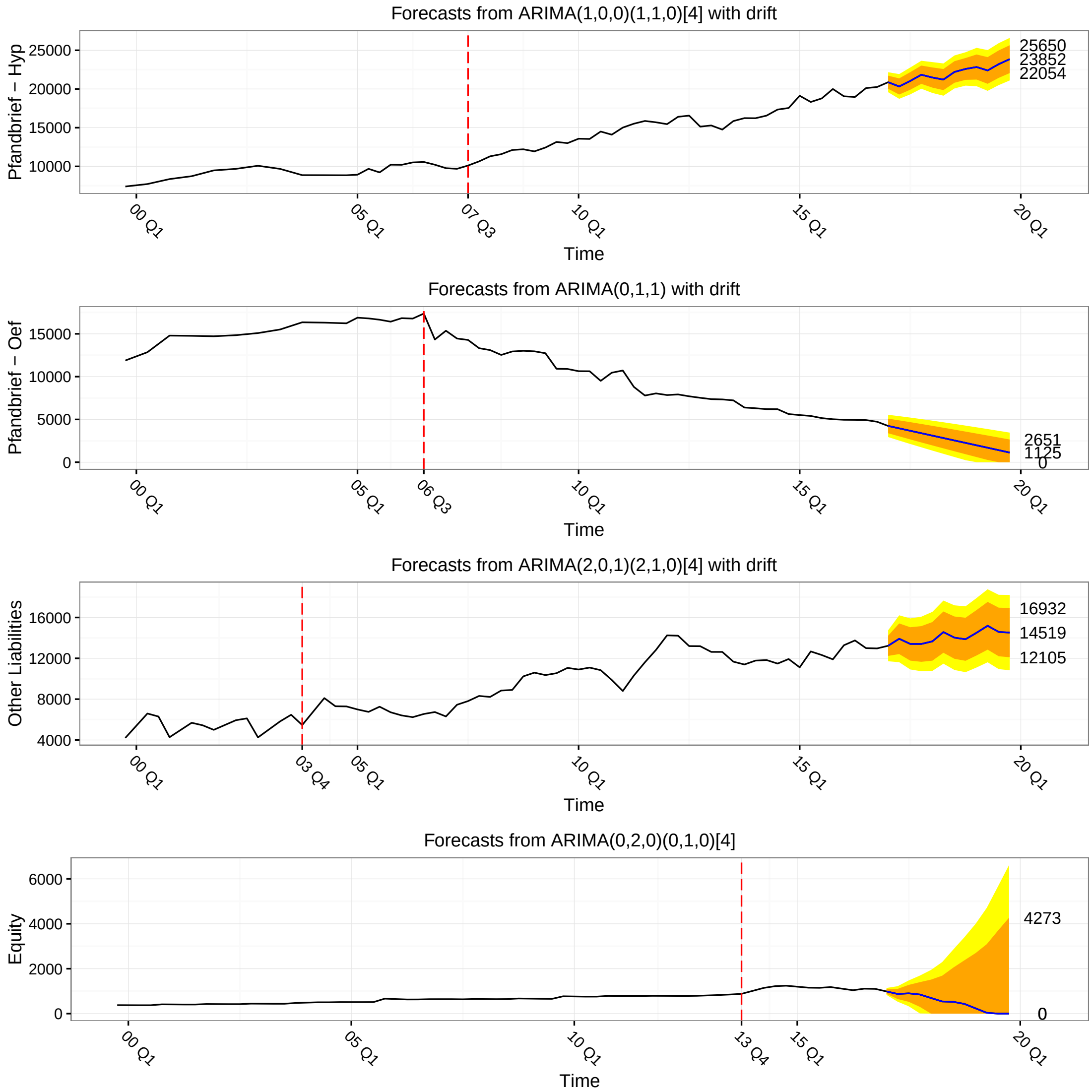

FIGURE 2.44.: Depiction of significant structural change of liability positions, in mn EUR

2.4. Summary

Two main takeaways from the market and bank analysis can be stated: Firstly, the rising importance of the mortgage covered bond / Pfandbrief business and, secondly, the simultaneous decline of the public covered bond / Pfandbrief business. Both trends have been sufficiently verified by current and past market developments. On the international scale it will be interesting to see whether Denmark can further claim its position as largest covered bond issuer in total and in the mortgage segment. Furthermore, in view of the existing legal frameworks implemented in each country, it will also be interesting to see which will establish itself, or at least to be taken as blue print for enforcing a consolidation wrt an universal framework on the European stage.

Evidently, the financial crisis, starting as sub-prime crisis in 2007, had an impact also on the covered bond market in general and its aftermath is still felt today reflected by the exceptionally low interest rates (see Figure 2.29) due to an expansive monetary policy by the ECB and other central banks. Yet, the complete magnitude of the financial crisis on the covered bond can not be fully assessed since the further interference of the ECB with its CBPP resulted in a distorted market view. Surely, on the one hand this was a necessary move to restore liquidity and confidence back into the market, however, a clear assessment of true covered bond sales is not really possible. Moreover, a distortion among banks arises, between those making use of state and central bank bailout funds and those that do not. On the long run the low interest rate environment may be more harmful to covered bond issuing banks.

On the bank level we have learnt that it is even harder to pin point one or more macro economic influences as in the case of MHB. While regarding the balance sheet development as a whole – the sum of assets or liabilities — the conclusion might well be that the financial and Euro crisis may have a sluggish impact on the bank's overall growth rate since the break point of the time series coincides with the onset of the financial turbulences dating back to 2008. However, dissecting the balance sheet positions separately we see the adverse developments of public and mortgage balance sheet positions on both sides. According to the annual reports this has largely to do with the business strategy of MHB at that time — the concentration on residential construction and commercial lending. Besides, MHB claims the sub-prime crisis and its consequences for the international financial markets did not affect MHB directly. Investments in the sub-prime segment were and are not included in its portfolio due to careful risk policy. MHB even goes on by stating that the financial crisis, rather, offered attractive additional business opportunities, as the traditional securitisation business — especially the syndication business — experienced a certain renaissance due to the weakening securitisation markets (MHB, 2007a).

3. A Pfandbrief Modelling Framework

The modelling of the Pfandbrief requires specific characteristics attributed to a financial intermediary issuing Pfandbriefe in a one-period setting. This includes the incorporation of the underlying legal framework and cover pool risks, a risk-neutral modelling setup, the application of different credit risk — structural and reduced-form — approaches, a simplified Pfandbrief bank's balance sheet structure and a default waterfall scheme wrt to the bank itself as well as the Pfandbrief as a financial product. In the wake of negative interest rates and due to its role as a fundamental component of the underlying models, interest rate risk is examined more closely. At the core, standard market assumptions are postulated. Merton (1974), in his seminal work, assumes perfect capital markets with no arbitrage possibilities, rational market participants, the existence of a risk-free investment opportunity and the strict absolute priority rule is held, amongst other restrictions.

3.1. Legal Requirements and Cover Pool Risks

The Pfandbrief product is, apart from the Kreditwesengesetz (KWG), embedded in the Pfandbriefgesetz (PfandBG) which regulates the legal requirements for the issuance of the Pfandbrief. An extensive analysis of the Pfandbrief's legal framework (PfandBG) and related cover pool risks are given in Spangler and Werner (2014). Here we shall briefly address the main characteristics and properties which need to be considered in any model setup. The focus lies upon the investor's perspective should the bank and its issued Pandbriefe default. A Pfandbrief investor also accounts losses if there is not sufficient collateral to prevent Pfandbriefe from defaulting. All applied models must be conform to the PfandBG, fulfilling the following main requirements:

Characterisation 3.1 (Legal requirements).

- *The Pfandbrief investor has a preferential claim over the cover pool and cross-collateralisation does not exist, thus cover pools are ring-fenced.*
- *The nominal amount of the cover pool must at any time cover — greater or equal — the nominal amount of all outstanding Pfandbriefe.*
- *The net present value*[1] *of the cover pool must at any time cover — greater than 2% — the net present value of all outstanding Pfandbriefe (including interest and amortization commitments).*

Key elements of cover pool risks in a post-issuer insolvency environment are identified in descending order (Spangler and Werner, 2014):

[1] This is legally specified in the net present value regulation ('PfandBarwertV').

Characterisation 3.2 (Cover pool risks).

1. *Refinancing risk (and market value risk) — Should the amortization of the cover pool assets be insufficient to match the outstanding Pfandbriefe at maturity then mismatches between assets and liabilities exist, referring to as refinancing risk. The market value of real estates may also differ during booming markets and times of economic recessions.*

2. *Interest rate and currency risk — Interest rate and currency risk refer to losses due to adverse interest rate and, respectively, exchange rate movements. Losses are casued by interest rate and currecny mismatches between the cover pool and outstanding Pfandbriefe, or by mark-to-market losses in case of a forced sale.*

3. *Asset default risk (and real estate risk) — Losses can occur when the credit quality of cover pool assets deteriorate over time and even default, known as asset default risk or asset credit risk. The risk of losses arising from changing real estate prices is referred to as real estate risk.*

4. *Reinvestment risk — Uncertainty arises on whether cover pool earnings can be reinvested if these are not needed to fund Pfandbrief payments where, in the long run, interest payments to Pfandbrief holders might be insufficient if wrongly allocated.*

5. *Prepayment and counterparty risk — Prepayment risk arises from the early repayment of cover pool debt. When there exist high counterparty concentrations of derivatives in the cover pool which are positively correlated to the Pfandbrief issuer then this results in counterparty risk.*

Remark 3.1. *Other risks related to the default of the Pfandbrief exist, such as issuer risks which are relevant in the pre-issuer insolvency period, see Spangler and Werner (2014). However, we shall concentrate on the above cover pool risks 1. to 3. of Characterisation 3.2 in a post-insolvency environment since "issuer default triggers the Pfandbrief holder's direct exposure to cover pool risks" (Spangler and Werner, 2014) and simply because of the reason that not all risks can be adequately modelled in a one-period setting as many risks are conditional on different time points.*

3.2. Real-World vs Risk-Neutral Setting

During the conceptional development of the underlying Pfandbrief framework an important question arises whether to model under the real-world or risk-neutral measure. In Hull (2015) we find a compact description of the concepts of valuation (risk-neutral) and scenario analysis (real-world) which are both used for estimating future cash flows, however, are distinguished by:

- "In valuation, a financial institution is interested in estimating the present value of future cash flows. It does this by calculating the expected values (i.e., average values) of the future cash flows across all alternative outcomes and discounting the expected values back to today.", cf. (Hull, 2015, p. 137).

- "In scenario analysis, a financial institution is interested in exploring the full range of situations that might exist at a particular future time.", cf. (Hull, 2015, p. 137).

Typically, risk-neutral valuation is used for projections of evolving asset prices through time. Monte Carlo simulations are widely applied to simulate, for example, the situation of a company defaulting at a discrete point in time. As alluded already above in Section 3.1 (Characterisation 3.1), we are dealing with present values of a bank's asset and liability side of the balance sheet (see for example TABLE C.6 displaying the input data of Münchener Hypothekenbank eG). It is then natural to resort to the risk-neutral measure for pricing of today's and future present values. Thus, the existence of the risk-neutral probability measure $\mathcal{Q}$ is postulated. The 'Fundamental Theorem of Asset Pricing' guarantees the risk-neutral measure $\mathcal{Q}$ because it is assumed that the capital market is arbitrage free (see for example Bingham and Kiesel (2013)). Under the assumption of a complete market there exists an unique equivalent martingale. In general, we relate to the risk-neutral measure $\mathcal{Q}$ henceforth if not stated otherwise. Switching between the risk-neutral and real-world measure can be achieved by a change of measure represented by the Radon-Nikodým derivative.
In general, one can relate the applied setup to a economic scenario generator (ESG) to project future scenarios[2]. When utilising ESG, all derivatives must be priced within those scenarios using the risk-neutral measure. Besides a structural approach, the risk-neutral setting can also be applied in a reduced-form based approach, both of which are introduced in the next section.

3.3. Structural vs Reduced-Form Approach

Here we shall give a brief review of the structural and reduced-form approaches and the implications thereof on the modelling of the Pfandbrief default. The difference between the two approaches is as follows:

- "Structural models are based on the information set available to the firm's management, which includes continuous-time observations of both asset values and liabilities.", cf. (Guo et al., 2009).
- "Reduced-form models are based on the information set available to the market, typically including only partial observations of both the firm's asset values and liabilities.", cf. (Guo et al., 2009).

Put in other words the main differences are: Structural models provide the link between the probability of default and the firms' fundamental financial situation incorporated in their assets and liabilities structure whereas reduced-form lack this link between credit risk and the firms' balance sheet information. Due to the assumption of complete information investors, usually, are able to predict the arrival of default in structural models. In reduced-form models default is an unpredictable event — characterising its main feature and advantage. Relying on market information reduced-form models use market prices of the firms' defaultable instruments, such as bonds or credit default swaps, to extract both their default probabilities and their credit risk dependencies.
The classical structural approach in determining the bank's and Pfandbrief default is applied by Sünderhauf (2006). Sünderhauf (2006) argues that this is the more suitable modelling approach since it allows an impact and causal analysis. Should a default event occur then it can be directly allocated to one or more endogenous risk factors.

[2]ESG is used, for example, in the modelling of life insurances.

This may be true when it comes to modelling the overall bank and Pfandbrief default profile. However, the innovative reduced-form model in this work addresses solely the asset side, namely emphasising on the quality of the cover pool (referring to 3. of Characterisation 3.2). The cover pool is modelled as a risky zero-coupon bond consisting of a large amount of mortgage assets. Thus, we regard the reduced-form approach wrt the cover pool as a superior modelling choice since the default probabilities of each single asset can be incorporated into the default analysis in an aggregated manner. This allows a much more direct access to the overall risk profile of the cover pool capturing the down side risks more adequately. Furthermore, stressed scenarios can be simulated by letting the mortgage credit ratings deteriorate over time.

3.4. One-Period vs Multi-Period Setting

When setting up a modelling framework, naturally, a trade-off between applicability and complexity arises. Realistically, the overall default process of a bank stretches over a longer time period of several weeks or even months. During the default process, a financial institution has the possibility of acquiring additional liquidity, apart from its own mandatory liquidity cushion, either from external sources or by restructuring its own balance sheet. For example, a bank has access to unsecured — overnight borrowings and the issuance of certificates of deposit or commercial papers — and secured — repurchase agreements (repos) or collateralised central bank open market operations where assets are deposited as collateral in exchange for cash — external funding. The option of debt roll-over is another way of delaying or even preventing an actual default. The multi-period model of Spangler (2018), for example, adequately accounts for the most important additional funding possibilities to the default modelling of a Pfandbrief bank, respectively Pfandbrief product.

While a multi-period model can account for different stages of a defaulting bank where counter measures are established to keep the bank alive, a one-period model can essentially only take a snap shot of the bank's solvency at a certain point in time. Thus, a one-period model is a simplification where the default of the Pfandbrief bank and its cover pool is examined simultaneously at the maturity of liabilities. This additionally implies that Pfandbriefe with different maturities are not considered. Resorting to a one-period setting means modelling default due to over-indebtedness. Arguably, a multi-period approach is the more realistic modelling choice. An approximation thereof is advantageous when it comes to obtaining a fast and simplified risk assessment. Furthermore, it might be of interest to obtain scenarios where additional funding options are deliberately not wanted, thus obtaining blunt and sober risk assessments of the current balance sheet constitution and, consequently, revealing potential asset-liability mismatches for one time period.

A more recent one-period modelling approach of a covered bond issuing bank is given by Tasche (2016) based on the balance sheet classification by Chan-Lau and Oura (2014). Similarly to Sünderhauf (2006)'s one-period model (based on the work by Anderson and Cakici (1999)), the asset side consists of one position of encumbered assets (cover pool) and one position of unencumbered assets (other assets). Likewise, the liability side is identically structured divided into three positions with secured debt (Pfandbrief), unsecured debt (other liabilities) and equity. Actually, compared to Chan-Lau and Oura (2014), Tasche (2016) adds the refinement of splitting the unsecured debt into senior

and junior unsecured debt. Yet, it is in our interest to use actual published data according to §28 PfandBG and bank's balance sheet where a clear distinction of senior and junior unsecured debt is not obtainable. Additionally, both models, Tasche (2016) and Sünderhauf (2006), are based on structural credit risk approaches where the recovery is determined endogenously. However, one striking difference is that Tasche (2016) does not account for asset-liability mismatches (1. of Characterisation 3.2), thus assuming that the cover pool is well-managed. Further, Tasche (2016) does not distinguish between nominal and present values (Characterisation 3.1) and does not account for risk-neutral modelling (see Section 3.2). Moreover, Tasche (2016) makes the assumption of log-normal distributions for the cover pool and other assets positions on the asset side which may be a bit over-simplified.
The framework in a one-period setting that we propose[3] refers to Sünderhauf (2006) and captures the main features of Characterisation 3.1 and Characterisation 3.2. The assessment of over-indebtedness is accomplished by defining an exogenous default barrier, namely the total liability nominal. The seniority of the Pfandbrief investor over the cover pool is considered. In the case of default the Pfandbrief investor has full claim over the cover pool, and furthermore the issuer has the obligation to fulfil certain cover requirements which are explicitly incorporated into the one-period model.

3.5. Balance Sheet Structure

A general and theoretical balance sheet of a mortgage-Pfandbrief bank is depicted in Figure 3.1. The asset side is divided into the cover pool (CP), which is segmented into mortgage (MCP), public (PCP), ship (SCP) and aircraft (ACP) loans and other assets (OA). Correspondingly, the liability side consists of the issued Pfandbriefe (PB), subdivided into mortgage (MPB), public (PPB), ship (SPB) and aircraft (APB) issuances, other liabilities (OL) and equity (EQ). The general balance sheet equation (in terms of present value) then amounts to

$$\begin{aligned}(V_{MCP} + V_{PCP} + V_{SCP} + V_{ACP}) + V_{OA} =& \\ &(V_{MPB} + V_{PPB} + V_{SPB} + V_{APB}) + V_{OL} + V_{EQ}, \quad (3.1)\end{aligned}$$

for any given point in time. The asset and liability side always match. From a modelling perspective, the more balance sheet positions are considered the more complex suitable models become. Moreover, an underlying dependence structure between positions needs to be incorporated. An aggregation of positions may be desirable, possibly even necessary. The concept of a simplified balance sheet to an assessable amount of positions is adopted from Sünderhauf (2006). However, any simplification of the balance sheet needs to be consistent with actual business characteristics of a mortgage Pfandbrief bank.
SPB and APB are in general negligible small (see Figure 2.2) so that these play no major part in the overall default process of the selected banks in Table C.2. The remaining positions are MPB and PPB where four modelling possibilities are formulated wrt the balance sheet:

[3]The introduced framework was first presented at the Operations Research (OR) 2013 in Rotterdam on September 3rd, 2013.

Assets (A)	**Liabilities (L)**
Cover Pool (CP)	Pfandbriefe (PB)
- Mortgage (MCP)	- Mortgage (MPB)
- Public (PCP)	- Public (PPB)
- Ship (SCP)	- Ship (SPB)
- Aircraft (ACP)	- Aircraft (APB)
	Other Liabilities (OL)
Other Assets (OA)	Equity (EQ)

FIGURE 3.1.: General balance sheet of a mortgage Pfandbrief bank.

1. Model MPB and PPB with corresponding MCP and PCP separately. Strictly speaking, this is the most reasonable choice, since the cover pool positions should be treated separately according to Characterisation 3.1. However, from a modelling perspective an extra asset position can be significantly more cumbersome on a computational level where additional underlying dependency structures between asset positions need to be considered.

2. Aggregate MPB with PPB on the liability side to one Pfandbrief position and MCP with PCP on the asset side to one cover pool position. This summary is accompanied by a certain modelling bias, however, cover pool assets and Pfandbrief liabilities are consistently pooled wrt to their corresponding risk profiles.

3. Encumber public Pfandbrief cover pool assets to a new position which is not eligible for the overall cover pool upon default. This means basically to 'cut out' the public sector (PCP and PPB) from the balance sheet entirely which is then refrained from being included in the overall bank and Pfandbrief default analysis.

4. Aggregate PPB with OL and corresponding PCP with OA. This simplification poses a gross inconsistency since the property of homogeneous risk profiles is not given any more. Furthermore, OA can potentially be utilised as additional collateral for the Pfandbrief. Consequently, adding PCP to OA means that a larger amount of assets is available for the coverage of Pfandbriefe in case of the bank's default, meaning defaulting Pfandbriefe become even more unlikely. This case then becomes a biased scenario in favour of the Pfandbrief.

Certainly, the first modelling possibility makes the most sense, widely complying with the requirements of PfandBG (see Characterisation 3.1). Possibilities two to four constitute considerable approximations where the balance sheet is aggregated even further. However, this group of simplifications have different biases within. We argue that the third and fourth points pose a higher degree of distortion compared to the second. The second is at least homogeneous wrt to cover pool assets and on the other side Pfandbrief liabilities, and largely inline with Characterisation 3.1. Further, we know from the findings in TABLE C.2 that 'pure' mortgage Pfandbrief banks also have a predominant mortgage cover pool and Pfandbrief position compared to their public sector holdings. Moreover, market trends and bank specific forecasts (see Chapter 2) suggest that the public sector position will become even less significant in the future.
Thus, we deduce the fundamental Assumption 3.1 for modelling the default of the

Pfandbrief. Assumption 3.1 can be considered as a substantial simplification of a mortgage Pfandbrief bank's balance sheet and has a major impact on the model complexity amounting to only five balance sheet positions which need to be taken into account.

Assumption 3.1 (Balance Sheet Aggregation).

(a) The present value of the cover pool is aggregated over all cover pool segments to

$$V_{CP} = V_{MCP} + V_{PCP} + V_{SCP} + V_{ACP}$$

and, likewise, all Pfandbrief segments to one total Pfandbrief

$$V_{PB} = V_{MPB} + V_{PPB} + V_{SPB} + V_{APB}.$$

(b) Equation (3.1) simplifies (for any point in time) to

$$V_{CP} + V_{OA} = V_{PB} + V_{OL} + V_{EQ}. \tag{3.2}$$

Remark 3.2. *We want to stress at this point that the upcoming models in a one-period setting can always be extended where public sector cover pool and Pfandbrief positions can additionally be considered if desired.*

3.6. Default Waterfall Scheme

The objective of this section is implementing a viable mathematical framework for modelling the Pfandbrief based on Assumption 3.1. This setup is essential to the overall modelling process and can be regarded as the core foundation in the one-period setting. Firstly, the proposed framework needs to meet the requirements in Section 3.1 and secondly, needs to be generic in the sense so that various financial models may be applied and substituted. The derived formulations are set in the risk-neutral measure $\mathcal{Q}$. Broadly, the proposed framework is based on the work by Sünderhauf (2006) which originates from Anderson and Cakici (1999). However, an amendment is undertaken wrt the change of measure from risk-neutral to the forward measure ensuring a mathematical sound formulation. In addition, an extension is provided in the form of the reduced-form modelling representation.
Assets naturally have a longer maturity period than liabilities, thus the bank's balance sheet implies an asset-liability mismatch, see 1. of Characterisation 3.2. This problem can intensify and, in a worst case scenario, lead to the default of the bank, if the bank does not intervene accordingly, or it may be inevitable due to extraordinary circumstances. When modelling the default of a Pfandbrief bank two stages need to be taken into consideration. At the maturity of the Pfandbriefe, T_1, one checks if the bank defaulted or not. This is the case iff — after taking into account the priority claim of the Pfandbrief holders — the liabilities cannot be fully paid back. Expressed in a formula, default occurred when $V_{CP}(T_1, T_2) + V_{OA}(T_1) < N_{PB}(T_1) + N_{OL}(T_1)$, meaning if the sum of present values of the cover pool (cover pool values are modelled as a risky zero-coupon bond with maturity T_2, thus discounting until T_1 becomes necessary; more details will follow in Section 3.6.1) and other assets is smaller than the sum of nominals of the Pfandbriefe and other liabilities. Once this event has occurred, then it becomes

necessary to proceed to the second stage where one needs to check if the Pfandbrief defaulted or not, expressed by formula $V_{CP}(T_1,T_2)+V_{OA}(T_1) < N_{PB}(T_1)$. This is the case iff — also taking into account that the Pfandbriefe have to maintain a certain cover at all times — the Pfandbriefe cannot be paid back in full. When this occurs, the Pfandbrief investor will account a loss, with a certain recovery rate (the complete default scheme is depicted in FIGURE 3.2). To incorporate the above default structure (FIGURE 3.2) of

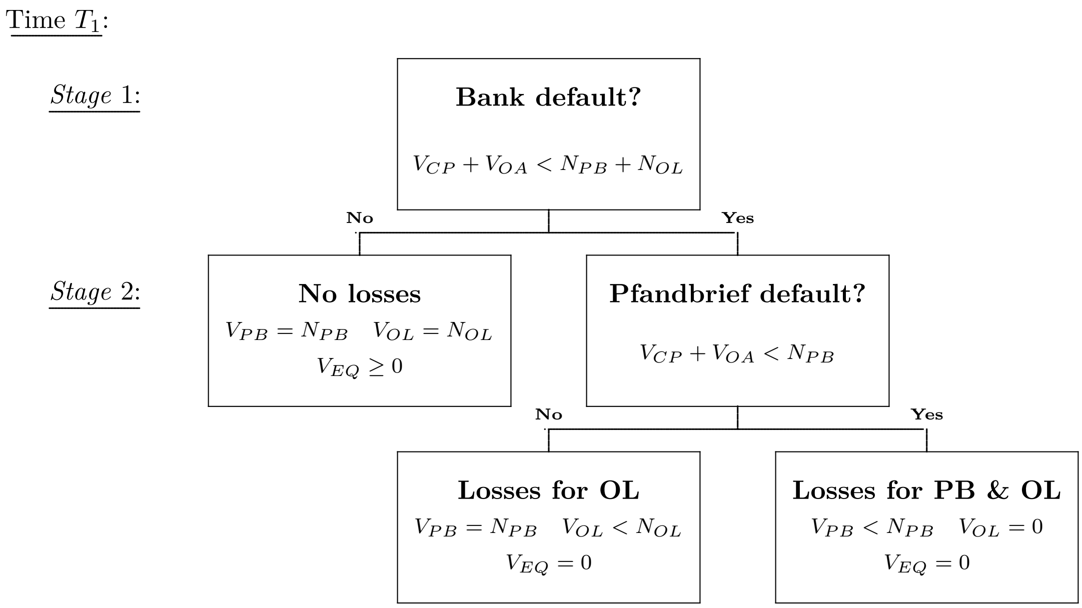

FIGURE 3.2.: Default waterfall scheme. *Stage 1* depicts the default of a bank and *Stage 2* of the Pfandbrief at time T_1 (maturity of the liabilities).

two stages into a viable setup, structural credit risk models are considered based on the seminal work of Merton (1974). Merton considers three balance sheet positions in his original model. V_A represents the asset value total[4] (aggregating V_{CP} with V_{OA}, thus $V_A = V_{CP} + V_{OA}$). The liability values V_{PB} and V_{OL} are aggregated to V_D (representing the total debt-structure). The equity position stays as it is, namely V_{EQ} (completing the liability side with $V_L = V_D + V_{EQ} = V_{PB} + V_{OL} + V_{EQ}$). Obviously, equation $V_A = V_D + V_{EQ}$ holds. Now default is examined at maturity of debts being T_1, where the firm must pay a promised payment of N. Consequently, if $V_A(T_1) \geq N$ the creditor receives his money in full and equity gets the payment of $V_A(T_1) - N \geq 0$, otherwise if $V_A(T_1) < N$ the firm is bankrupt as it cannot meet its obligations (and $V_{EQ} = 0$). Resulting from this the debt value can be expressed as a risky zero-coupon bond with

$$V_D(T_1) := \min[V_A(T_1), N], \tag{3.3}$$

which is equivalent to a put option. On the other hand the equity position corresponds to a call option on the firm's asset values with

$$V_{EQ}(T_1) := \max[V_A(T_1) - N, 0]. \tag{3.4}$$

[4]The dynamics for the value of the firm are described by log-normal diffusion, see Merton (1974).

3.6.1. Assets

Continuing Merton's idea of modelling a bank's credit risk the present values of the bank's asset side, the cover pool (CP) and other assets (OA) ($V_x,\ x \in \{CP, OA\}$), are now introduced, where $V_A = V_{CP} + V_{OA}$.

3.6.1.1. Cover Pool

The cover pool is modelled as a risky zero-coupon bond with nominal N_{CP} and maturity T_2 ($T_2 \geq T_1$). Two approaches arise for determining the cover pool value at T_1 where $\frac{B_{T_1}}{B_{T_2}} = \exp\left(-\int_{T_1}^{T_2} r(s)\mathrm{d}s\right)$ is the stochastic discount factor, B_{T_1} is a bank account process (Definition B.5) at T_1 with $B_0 = 1$ and $r(t)$ is the underlying risk-free (instantaneous) short rate process.

Structural Approach Following Sünderhauf (2006), based on the idea proposed by Anderson and Cakici (1999), the cover pool defaults if $V_{CP}(T_2, T_2) < N_{CP}$. In this case the recovery value is then given by $V_{CP}(T_2, T_2)$. Otherwise, the nominal can be fully repaid. Discounting to time T_1 under the risk-neutral measure and calculating the conditional expectation given the information at time T_1 yields the present value of the cover pool at time T_1

$$V_{CP}(T_1, T_2) = \mathbb{E}_{\mathcal{Q}}\left(\frac{B_{T_1}}{B_{T_2}} \min[V_{CP}(T_2, T_2), N_{CP}] \,\middle|\, \mathcal{F}_{T_1}\right), \tag{3.5}$$

where V_{CP} is a state variable process and $\mathcal{F}_{T_1}$ is the information given at T_1 with $T_1 \leq T_2$.

Reduced-Form Approach For pricing the risky zero-coupon bond price of the cover pool the reduced-form approach formulation by Jarrow et al. (1997) is adopted. The pricing formula at time T_1 amounts to

$$V_{CP}(T_1, T_2) = \mathbb{E}_{\mathcal{Q}}\left(\frac{B_{T_1}}{B_{T_2}} \left(\delta \mathbb{1}_{\{\tau \leq T_2 \,|\, \tau > T_1\}} + \mathbb{1}_{\{\tau > T_2 \,|\, \tau > T_1\}}\right) \,\middle|\, \mathcal{F}_{T_1}\right) \tag{3.6}$$

where $T_1 \leq T_2$, $\mathcal{F}_{T_1}$ is the information given at T_1, τ denotes the random default time and $\delta \in [0, 1]$ the recovery rate (initially assumed to be exogenously given which for now is constant). The indicator function $\mathbb{1}_{\{\tau \leq T_2 \,|\, \tau > T_1\}}$ is one if the cover pool defaults as a whole no later than T_2, given no default until T_1 and zero otherwise. The opposite is the case for $\mathbb{1}_{\{\tau > T_2 \,|\, \tau > T_1\}}$ which represents the survival. Thus, information on the credit-worthiness of the cover pool is needed for determining the value of its corresponding risky zero-coupon bond.

Formulas (3.5) and (3.6) incorporate the typical credit portfolio characteristics meaning the majority of loans and bonds have a fixed maturity where payments are capped at T_2, the maturity of asset cash flows, including nominal payments and in some cases interest payments (Sünderhauf, 2006).

Remark 3.3. *From formulas (3.5) and (3.6) we can see that a log-normal assumption for the CP as in Chan-Lau and Oura (2014), respectively Tasche (2016) is not justifiable since the formulas account for the asset-liability mismatch.*

Conclusively, in order to calculate the present values at time t the T_1-forward (martingale) measure, derived in (B.15) in Appendix B.2.2, is required. The issue is that over the interval $[t, T_1]$, the stochastic processes $V(t, T_1)$ and $r(t)$ are (almost) never independent so that the conditional expectation cannot be computed without enormous computational undertaking. The idea is to use a T_1-bond (for a fixed T_1) as numeraire rather than using the money market as numeraire, as in the risk-neutral case. Plugging in the values at T_1 from (3.5) and (3.6) the resulting formula under the T_1-forward measure $\mathcal{Q}_{T_1}$, is given by

$$\begin{aligned} V_{CP}(t, T_1) &= \mathbb{E}_{\mathcal{Q}_{T_1}}\left(\frac{B_t}{B_{T_1}} V_{CP}(T_1, T_2)\left(\frac{\mathrm{d}\mathcal{Q}}{\mathrm{d}\mathcal{Q}_{T_1}}_{|\mathcal{F}_t}\right)\middle|\,\mathcal{F}_t\right) \\ &= \mathbb{E}_{\mathcal{Q}_{T_1}}\left(\frac{B_t}{B_{T_1}} V_{CP}(T_1, T_2)\left(\frac{B_{T_1} P(t, T_1)}{P(T_1, T_1) B_t}\right)\middle|\,\mathcal{F}_t\right) \\ &= P(t, T_1)\mathbb{E}_{\mathcal{Q}_{T_1}}\left(V_{CP}(T_1, T_2)\,|\,\mathcal{F}_t\right), \end{aligned} \tag{3.7}$$

where $t \leq T_1 \leq T_2$.

3.6.1.2. Other Assets

Other asset present values, on the other hand, are simply fixed at T_1, where we denote any future random variable — simulated from today to T_1 or randomly drawn at T_1 — by $V_{OA}(T_1, T_1)$ so that

$$V_{OA}(T_1) := V_{OA}(T_1, T_1), \tag{3.8}$$

as the majority of mortgage banks typically do not have a loan-like payment profile, cf. Sünderhauf (2006). Calculating today's present values results to

$$V_{OA}(t, T_1) = \mathbb{E}_{\mathcal{Q}}\left(\frac{B_t}{B_{T_1}} V_{OA}(T_1)\middle|\,\mathcal{F}_t\right), \tag{3.9}$$

where $t \leq T_1$ and $\frac{B_t}{B_{T_1}} = \exp\left(-\int_t^{T_1} r(s)\mathrm{d}s\right)$.

3.6.2. Liabilities

We assume that at time T_1 the values $V_{CP}(T_1, T_2)$ and $V_{OA}(T_1)$ are known from (3.5) or (3.6) and (3.8) respectively. Applying Merton's idea to the more complex structure of the balance sheet of a mortgage Pfandbrief bank, one obtains equations (3.11), (3.14) and (3.15) for the liability side. Again, debt is modelled as zero-coupon bonds with maturity T_1 and again the debtors' maximum claims $N_x, x \in \{PB, OL\}$ are repaid, or not, depending on the value of the bank's assets.
According to the waterfall scheme of Figure 3.2 Pfandbrief holders rank senior wrt the cover pool (Characterisation 3.1). The uniqueness of the PB payment profile lies therein that at first PB creditors have full recourse over the CP and then additionally on OA in order to cover the claim of N_{PB} — the nominal zero-coupon bond value of the Pfandbrief. In a one-period setting, at T_1, the issuer has no other possibility to tap monetary sources except OA where the issuer is required by PfandBG to maintain cover requirements with a minimum of 2% of overcollateralization. More precisely, the

present value of CP is denoted by $V_{CP}(T_1, T_2)$ on which the mortgage PB investor has preferential claim. Now, should the CP not be sufficient, i.e. there exists a shortfall given by

$$SF_{CP} = \max[N_{PB} - V_{CP}(T_1, T_2), 0], \tag{3.10}$$

then the OA present values, $V_{OA}(T_1)$, can also be tapped. In total, the PB creditor's payout is defined by the minimum over N_{PB} and appertained recoverable assets — consisting of CP and OA — with

$$V_{PB}(T_1) := \min[V_{CP}(T_1, T_2) + V_{OA}(T_1), N_{PB}]. \tag{3.11}$$

The creditors of OL receive in T_1 the minimum of the nominal zero-coupon bond value N_{OL} and the present value of the appertained collateral. Their share amounts, firstly, to the part of OA which is not needed to fill up the shortfall of the CP in (3.10), so that

$$OA_{Rest} = \max[V_{OA}(T_1) - \max[N_{PB} - V_{CP}(T_1, T_2), 0], 0]. \tag{3.12}$$

Secondly, OL creditors can potentially be paid by what is left over from the CP, known as overcollateralization, which amounts to

$$OC_{CP} = \max[V_{CP}(T_1, T_2) - N_{PB}, 0]. \tag{3.13}$$

With (3.12) and (3.13) it follows the payment profile of OL with

$$\begin{aligned} V_{OL}(T_1) := \min[\max[V_{OA}(T_1) - \max[N_{PB} - V_{CP}(T_1, T_2), 0], 0] + \\ \max[V_{CP}(T_1, T_2) - N_{PB}, 0], N_{OL}]. \end{aligned} \tag{3.14}$$

The simplest liability payment profile is that of the equity (EQ) position. It is unaffected by the priority payments of the financing with outside capital. Analogously to Merton (1974)'s formula (3.4), the present values of EQ is represented by a call option of the total asset position present values subtracted by the nominal amounts of all liability positions in T_1, see (3.15). Hence, (3.15) is positive iff the bank does not default at T_1, with (compare also FIGURE 3.2)

$$V_{EQ}(T_1) := \max[V_{CP}(T_1, T_2) + V_{OA}(T_1) - N_{PB} - N_{OL}, 0]. \tag{3.15}$$

The present value of a liability position $x \in \{PB, OL, EQ\}$ at time t can be determined by

$$V_x(t, T_1) = \mathbb{E}_{\mathcal{Q}}\left(\frac{B_t}{B_{T_1}} V_x(T_1) \,\middle|\, \mathcal{F}_t \right), \tag{3.16}$$

where $t \leq T_1$.

Remark 3.4. *The extended version of above waterfall scheme with the additional public sector Pfandbrief type with positions PCP and PPB can be found in Sünderhauf (2006, p. 140).*

3.7. Interest Rate Risk

The mathematical formulation of the Pfandbrief modelling framework under Section 3.6 relies on modelling interest rate risk[5] — addressing 2. of Characterisation 3.2. Ultimately, an adequate and correct risk assessment of the Pfandbrief product needs to be ensured. Both, the structural and reduced-form approach in Section 3.6.1 have the underlying interest rate market as a common factor. More precisely, we want to find suitable stochastic discount factors (Definition B.6) in form of

$$D(t,T_1) = \frac{B_t}{B_{T_1}} = \exp\left(-\int_t^{T_1} r(s)\mathrm{d}s\right), \quad 0 \le t \le T_1,$$

and, respectively,

$$D(T_1,T_2) = \frac{B_{T_1}}{B_{T_2}} = \exp\left(-\int_{T_1}^{T_2} r(s)\mathrm{d}s\right), \quad 0 \le T_1 \le T_2,$$

for equations (3.5), (3.6), (3.7), (3.9) and (3.16). Now, we do not know much about the component $r(s)$, respectively $r(t)$, at some point in time s or t yet, other than being the instantaneous spot interest rate arising from taking the limit $T \to t^+$ of the yield curve $R(t,T)$ of Definition B.10 (see also Remark B.7). Furthermore, the above discount factors, $D(t,T_1)$ and $D(T_1,T_2)$, are embedded in equations consisting of calculating the conditional expectation of some risky zero-coupon bond price V_x, $x \in \{CP, OA, PB, OL\}$ under the risk-neutral measure $\mathcal{Q}$ which, at this stage, we do not know how to handle. There exist numerous interest rate models to choose from. Certain model selection criteria are analysed and formulated as modelling requirements in order to find a suitable interest rate model. In-depth theory and derivations of the established requirements are largely outsourced to Appendix B.2.3, Appendix B.2.4 and Appendix B.2.5. Before continuing our analysis of finding an appropriate model we can already state that we are dealing with spot interest rates which is formulated in Requirement 3.1.

Requirement 3.1. *An underlying short rate, $r(t)$, more precisely an instantaneous spot rate model needs to be postulated.*

In the upcoming section we shall concentrate on the current — extraordinary — market situation of negative interest rates. This embodies one of the higher prioritised requirements which need to be met. The analysis of the modelling requirements is then summarised where the model choice is revealed. It turns out, the (affine) one-factor Hull-White interest rate model (Hull and White, 1990), respectively extended Vašìček model, poses a promising option of taking on the task of modelling the current interest rate environment and, additionally, possesses favourable modelling features. Furthermore, emphasis is laid upon a practitioner's perspective for applying the Pfandbrief modelling framework. Thus, we purposely only give examples in the cases of calibration of the well-known and widely used Hull-White model. However, due to the negativity of the yield curve in the short term, the standard calibration approach is not applicable. An alternative to the 'Black-76' model (Black, 1976) for obtaining input market prices is

[5] Currency risk is deliberately omitted. Outstanding Pfandbriefe (FIGURE 2.6) as well as cover pool assets are largely denominated in Euros where the majority of real estates are situated in Germany or EU countries (compare Spangler and Werner (2014)).

given. For a more extensive numerical analysis of the applied methods and resulting parameter estimates we refer to the literature.
The theory and notation is mainly based on the books by Björk (2004) and Brigo and Mercurio (2007). Fundamental contributors to the evolution of various stochastic interest rate models, amongst many others, are Vašìček (1977), Brennan and Schwartz (1982), Cox et al. (1985), Ho and Lee (1986), Hull and White (1990) and Heath et al. (1992).

3.7.1. Market Resemblance

Analysing and understanding the interest rate market is crucial in order to choose a suitable interest rate model. Furthermore, market shocks, such as the default of the Lehman Brothers Holdings Inc., may have significant impacts on the resulting model parameters when estimating or calibrating.
Figure 3.3 gives an insight of the interest rate market movements of the past 18 years, represented by the Euro InterBank Offered Rate (EURIBOR). Two central points can be extracted. Clearly, a structural change in rates has occurred in a short time period of eight months after September 2008, when the base rates were lowered seven consecutive times by the ECB, accumulating to 3.25% points. Only during 2011 there was a period of rising rates before returning to 1% in the same year again. Since then, the ECB gradually lowered the base rate, being just about above zero in 2014 before finally reaching 0% on March 10th, 2016. Similar base rate reductions in similar time intervals can be observed from the Bank of England and the Fed. The specific dates and corresponding base rates are given in Table 3.1 which unambiguously is reflected in Figure 3.3. The pre

Date	Rate	Date	Rate	Date	Rate
Jul. 3rd, 2008	4.25%	Apr. 2nd, 2009	1.25%	Jul. 5th, 2012	0.75%
Oct. 8th, 2008	3.75%	May 7th, 2009	1.00%	May 2nd, 2013	0.50%
Nov. 6th, 2008	3.25%	Apr. 7th, 2011	1.25%	Nov. 7th, 2013	0.25%
Dec. 4th, 2008	2.50%	Jul. 7th, 2011	1.50%	Jun. 5th, 2014	0.15%
Jan. 15th, 2009	2.00%	Nov. 3rd, 2011	1.25%	Sep. 4th, 2014	0.05%
Mar. 5th, 2009	1.50%	Dec. 8th, 2011	1.00%	Mar. 10th, 2016	0.00%

Table 3.1.: ECB base rates

Lehmann default mean over all rates with different maturities thereby dropped from 3.34% to 0.70% since. The second noteworthy observation is the recent phenomenon of negative interest rates which only has been observed in the Japanese market thus far. The zero interest rate policy by the ECB (as of 2014, see Table 3.1) subsequently affected the market rates, starting with short termed rates to become negative. Onset dates of corresponding EURIBORs turning negative for different maturities (as in Figure 3.3), are

- EURIBOR1W: September 5th, 2014,
- EURIBOR1M: January 19th, 2015,
- EURIBOR3M: April 21th, 2015,
- EURIBOR6M: November 6th, 2015,

- EURIBOR9M: November 27^{th}, 2015, and
- EURIBOR12M: February 5^{th}, 2016.

The dramatic change since the financial crisis, climaxing in the default of Lehmann Brothers on 15/09/2008, is also reflected in present term structures of interest rates. Benchmark fixed income securities in the form of EONIA, EURIBOR1M, EURIBOR3M, EURIBOR6M and EURIBOR12M are depicted in Figure 3.4. Exemplarily, the yield curves of 16/09/2008 and 31/12/2016 are compared and interpreted in an economic context. The yield curves from 16/09/2008 are all positive (as expected from Figure 3.3), mostly in the range of 4% and 5% and show a 'humped' and 'inverted' shape. A 'humped' yield curve usually indicates that investors are uncertain about the future of the general economic state, and where a current transitioning form a 'normal' to 'inverted' state is reflected. Here the yield curves become slightly 'inverted' after approximately 15 years which heralds a potential looming economic recession as investors accept a lower interest rate although longer-term securities generally bear a greater investment risk. The yield curves from 31/12/2016 are negative in the short term which become positive in the longer term and show a 'normal' shape where investors have a more benign expectation of the future economic growth. It is also an indicator that central banks are increasing the supply of money, thus an easing monetary policy which has clearly been the case in recent months and years.
Concluding, it is apparent that any chosen interest rate model needs to be adaptable to recent market developments as a result of zero interest rate policies imposed by central banks around the world. Moreover, there is no reason to believe that base rates are likely to be raised in the near future. Thus, modelling of negative interest rates must be a central feature for any eligible model, see Requirement 3.2.

Requirement 3.2. *An adequate interest rate model needs to be able to handle negative interest rates which includes calibration of the model parameters to the market and simulation of the instantaneous spot interest rate.*

Remark 3.5. *The assumption of normal short rates (Vašìček (1977) or extended Vašìček (Hull and White, 1990), see Remark B.12) in a negative interest rate market environment is plausible where negative rates are allowed. Moving back to the economical commonplace of positive rates other distributions where positivity can be guaranteed are needed. From Remark B.14 we know that Dothan (1978), Black et al. (1990) and Black and Karasinski (1991) are log-normally distributed yielding positive interest rates. However, apart from not having a closed form solution, log-normal models have an explosive nature since the exponential function is applied twice on $r(t)$, once for the log-normal distribution and once for the bank account process in (B.16). Thus, it may be more advisable to resort to square-root diffusions, for example, the CIR1F (Remark B.12) interest rate model (Cox et al., 1985) which has an underlying non-central chi-square distribution.*

3.7.2. Model Choice

Now let us summarise the findings of Appendix B.2.3, Appendix B.2.5 and Section 3.7.1 to establish modelling requirements in order to choose an adequate interest rate model to be utilised for the Pfandbrief framework in a one-period setting.

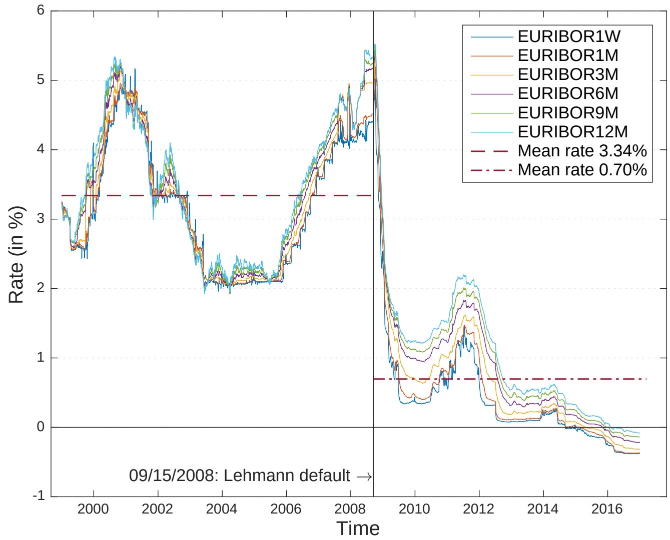

FIGURE 3.3.: Daily EURIBOR interest rates for different maturities (1W, 1M, 3M, 6M, 9M, 12M), from 31/12/1998 to 02/01/2017 (data source: `http://www.bundesbank.de`)

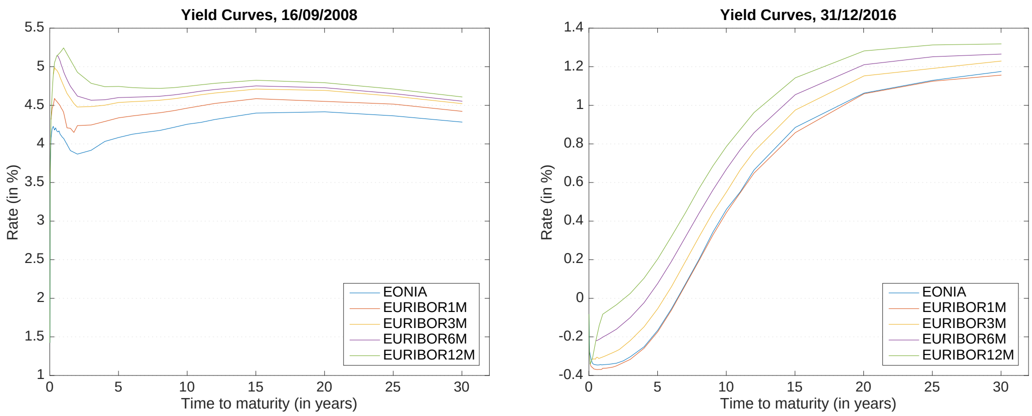

FIGURE 3.4.: Selection of yield curves represented by EONIA and EURIBOR (1M, 3M, 6M, 12M). Left: 16/09/2008; Right: 31/12/2016 (data source: Bloomberg)

Since we are dealing with spot interest rates, as formulated in Requirement 3.1, we can already rule out any other type of model. Now one may argue that the Heath-Jarrow-Morton (HJM) framework (Heath et al., 1992) where the state variable is represented by the forward rate curve may also be a viable modelling option. In fact, it is possible to move from short rate[6] to forward rate model and back. A short term rate is simply a particular forward rate. The converse is not necessarily true. Even if compatibility exists, analytical derivations from short rate to HJM types of models is not possible where numerical methods need to be established instead. Derivable short rate models are for example Vašìček (Vašìček, 1977), extended Vašìček (Hull and White, 1990), extended Cox-Ingersoll-Ross (Hull and White, 1990) and also the Ho and Lee (1986) model.

[6] A list of affine short rate models can be found in Björk (2004, p. 375) or Schlüchtermann and Pilz (2010, p. 332).

Remark 3.6. *Ho and Lee (1986) is the discrete time version of the HJM framework (Heath et al., 1992) which was the first forward curve based model in order to model the forward rate stochastic process* $\{f(t,T)\}_{0\leq t\leq T}$.

Both approaches, short rate and forward rate, have advantages and disadvantages wrt modelling interest rate risk. However, one main advantage of the above short rate based models is their tractability given by the ATS representation of Definition B.15 of Appendix B.2.3.2. More precisely, closed form solutions for bond prices and other interest rate derivatives such as caps / floors or swaptions can be derived. This feature is certainly advantageous wrt calibrating and pricing, leading to Requirement 3.3. Thus, we shall opt for short rate based models and leave HJM framework to further research in the context of the modelling of the Pfandbrief. For further comparisons one can, for example, refer to Björk (2004).

Requirement 3.3. *The ATS representation of short rate based models guarantees analytical pricing formulas which is well-deemed when modelling interest rate risk.*

When fitting the initial term structure a dimensionality issue arises (Appendix B.2.5.1) since one equation needs to be solved for each yield curve maturity, potentially resulting in a large calibration problem. Furthermore, in Example B.1 we see that fitting the initial term structure is not always satisfactory. The Hull-White model can be calibrated exactly to any initial term structure. By design, the time dependent function $\theta(t)$ solves the dimensionality issue since each time step t can be interpreted as a parameter which is fitted to the yield curve. Thus, we can confidently state that Requirement 3.4, where the objective is to optimally calibrate the model parameters to match the market, is covered by the Hull-White model.

Requirement 3.4. *The theoretical prices of the model need to coincide with the observed prices of today. In more detail, we want to choose the parameter vector* ϑ *such that*

$$P(0,T;\vartheta) \approx P^M(0,T), \quad \forall T \geq 0. \tag{3.17}$$

Further, we look at potential extensions (Requirement 3.5) introduced in Appendix B.2.5.2. Answering the question whether extensions are beneficial or not needs to be evaluated more closely. In general, a trade off between model flexibility and tractability remains. When considering one or more factors, the issue of high correlation is not an immediate problem in a one-period modelling setting. The default assessment of a Pfandbrief bank solely takes place at maturity T_1. Consequentially, potential shocks are only passed on from model term structure in $[t, T_1]$ to the term structure in $[T_1, T_2]$. This may not be the case when modelling in a multi-period time setting. Also the gain in accuracy with taking more than one factor into consideration is negligible. Thus, we assume that one single source of uncertainty, the single state variable being the instantaneous spot rate, is sufficient to explain the movements of the term structure. When considering time varying model parameters, the extension of the Vašìček model makes absolutely sense. More flexibility is gained while at the same time retaining a tractable model. In (B.27) κ and σ are made constant while the mean reversion level parameter, $\theta(t)$, is time dependent gaining more degrees-of-freedom.

Requirement 3.5. *Model extensions need to be easily realisable where important model features are retained and tractability is not lost.*

Lastly, a more recent but not less important requirement is the handling of negative interest rates (Requirement 3.2). The Vašìček (Vašìček, 1977) and the extended Vašìček (Hull and White, 1990) short rate models, for example, allow negative interest rates. This was broadly seen as weakness of the models since, until recently, negativity was regarded as not possible or at least highly unlikely. Now however, particularly the Hull-White model has seen a renaissance in increasing popularity.
Concluding, in view of all above requirements a logical and appropriate model choice is the Hull-White one factor (HW1F) model due to its favourable modelling criteria on the one hand, and relative simplicity on the other. Model definition, properties and parameter calibration of the HW1F model shall be presented more closely in the next section.

Remark 3.7. *A trade off between several modelling factors will always be persistent. For now the HW1F model takes on the role of a favourable modelling choice. The combination of completely fitting the observed bond data and allowing for negative interest rates in the current market environment makes it indispensable. However, should modelling scenarios change in the future then other more favourable models might emerge. A natural extension to the HW1F is represented by the G2++ model. As already alluded above the HJM framework poses an interesting modelling option. Should interest rates return to the normal state of being positive again then, for example, the CIR++ model may be considered since it guarantees positive short rates.*

3.7.3. Hull-White One Factor (HW1F) Model

The Hull-White model (Hull and White, 1990) belongs to the class of no arbitrage models which is designed to be exactly consistent with today's term structure of interest rate. Thus, today's term structure of interest rates is directly inserted into the model where the drift is dependent on time and where the shape of the inserted zero curve governs the average path taken by the short rate in the future. Other extending features of the model are placed into Appendix B.2.4 where a complete derivation of the zero-coupon bond pricing formula (Appendix B.2.4.1) and the real-world and forward measure representations of the short rate SDEs (Appendix B.2.4.2) are given.

3.7.3.1. Model Definition

Hull and White (1994) assume that the instantaneous short-rate process evolves under the risk-neutral measure $\mathcal{Q}$ according to

$$\mathrm{d}r(t) = (\theta(t) - \kappa r(t))\mathrm{d}t + \sigma \mathrm{d}W^{\mathcal{Q}}(t), \quad r(0) = r_0, \tag{3.18}$$

where κ, $\sigma > 0$ are constants and $\theta(t)$ is given by

$$\theta(t) = \frac{\partial f^M(0,t)}{\partial T} + \kappa f^M(0,t) + \frac{\sigma^2}{2\kappa}(1 - \exp(-2\kappa t)), \tag{3.19}$$

where $f^{\mathrm{M}}(0,t) := \frac{-\partial \ln P^{\mathrm{M}}(0,t)}{\partial t}$ is the market instantaneous forward rate prevailing at time 0 for the maturity t and $P^{\mathrm{M}}(0,t)$ is the (risk-free) market discount factor at maturity t. This shows that r follows the initial forward curve. When the short rate process deviates from the mean reversion level $\frac{\theta(t)}{\kappa}$ it is reverted back at rate κ. The SDE of (3.18) can also be formulated under the forward and real-world measure, see Appendix B.2.4.2. Integration of (3.18) yields

$$\begin{aligned} r(t) &= r(s)\mathrm{e}^{-\kappa(t-s)} + \int_s^t \mathrm{e}^{-\kappa(t-u)}\theta(u)\mathrm{d}u + \sigma \int_s^t \mathrm{e}^{-\kappa(t-u)}\mathrm{d}W^{\mathbb{Q}}(u) \\ &= r(s)\mathrm{e}^{-\kappa(t-s)} + \alpha(t) - \alpha(s)\mathrm{e}^{-\kappa(t-s)} + \sigma \int_s^t \mathrm{e}^{-\kappa(t-u)}\mathrm{d}W^{\mathbb{Q}}(u), \end{aligned} \tag{3.20}$$

where

$$\alpha(t) = f^M(0,t) + \frac{\sigma^2}{2\kappa^2}(1-\mathrm{e}^{-\kappa t})^2. \tag{3.21}$$

Remark 3.8. *Originally, in Hull and White (1990) the short rate dynamics (3.18) included deterministic time dependent functions of mean reversion speed, $\kappa(t)$, and volatility level, $\sigma(t)$, amounting to (B.27), with $\beta = 0$, which is widely referred to as the Hull-White extended Vašiček model. However, as pointed out by Brigo and Mercurio (2007) this extension must be handled with caution where an additional exact fit to the volatility may be 'dangerous' when emphasising on fitting the term structure of interest rates, as pointed out already in Section B.2.5.2. Thus, the model (3.18) with constants κ and σ is preferred.*

After integrating (3.18) one obtains that $r(t)$ conditional on $\mathcal{F}_s$ is normally distributed with mean and variance given respectively by

$$\begin{aligned} \mathbb{E}\left(r(t)\,|\,\mathcal{F}_s\right) &= r(s)\exp(-\kappa(t-s)) + f^M(0,t) + \frac{\sigma^2}{2\kappa^2}(1-\exp(-\kappa t))^2, \\ \mathbb{V}\left(r(t)\,|\,\mathcal{F}_s\right) &= \frac{\sigma^2}{2\kappa}\left(1-\exp(-2\kappa(t-s))\right). \end{aligned} \tag{3.22}$$

We have an affine structure so by Theorem B.10 bond prices are given by Definition B.15 where A and B solve (B.37) and (B.38). The solutions to these equations yield the zero-coupon terms for the HW1F model, given by

$$A(t,T) = \ln\left(\frac{P^M(0,T)}{P^M(0,t)}\right) + B(t,T)f^M(0,t) - \frac{\sigma^2}{4\kappa}(1-\exp(-2\kappa t))B^2(t,T) \tag{3.23}$$

$$B(t,T) = \frac{1}{\kappa}\left(1-\exp(-\kappa(T-t))\right), \tag{3.24}$$

completing the analytical pricing formula of (B.28). A complete derivation of (3.23) and (3.24) is given in Appendix B.2.4.1.

3.7.3.2. Calibration

When calibrating, in the case of negative forward rates one can, for example, resort to the Bachelier model, instead of the Black model, for obtaining cap / floor market prices in combination with normal cap / floor volatility quotes. Should only log-normal volatilities be available then it is also possible to convert these to normal volatilities, as in Schachermayer and Teichmann (2008). Other alternatives are the normal SABR model, displaced models and free boundary models in order to deal with the issue of negative rates. Here we concentrate on the Black (log-normal) and Bachelier (normal) models and set $\mathcal{T} := \{T_\alpha, \ldots, T_\beta\}$ containing the reset and payment dates of a cap / floor and $\mathfrak{d} := \{\mathfrak{d}_{\alpha+1}, \ldots, \mathfrak{d}_\beta\}$ the corresponding year fractions (Definition B.9). N is the nominal value, F is the forward rate (e.g. of the floating rate to be capped) and K is the strike level (e.g. the cap rate). $\sigma_{\alpha,\beta}$ denotes the common volatility parameter which is retrieved from market quotes. The ATM strike level is determined as in Definition 3.1.

Definition 3.1. *Consider a cap (floor) with payment times $T_{\alpha+1}, \ldots, T_\beta$ associated year fractions $\mathfrak{d}_{\alpha+1}, \ldots, \mathfrak{d}_\beta$ and strike K. The cap (floor) is said to be at-the-money (ATM) if and only if*

$$K = K_{\text{ATM}} := S_{\alpha,\beta}(0) = \frac{P(0,T_\alpha) - P(0,T_\beta)}{\sum_{i=\alpha+1}^{\beta} \mathfrak{d}_i P(0,T_i)}, \tag{3.25}$$

where $S_{\alpha,\beta}(0)$ is the forward swap rate at time t for the sets of times $\mathcal{T}$ and year fractions $\mathfrak{d}$. The cap is instead said to be in-the-money (ITM) if $K < K_{\text{ATM}}$, and out-of-the-money (OTM) if $K > K_{\text{ATM}}$, with the converse holding for a floor.

Positive rate modelling The standard way of quoting prices on caps / floors (and swaptions) is in terms of Black's model (Black, 1976) which is a version of the Black-Scholes model (Black and Scholes, 1973) adapted to deal with forward underlying assets. Here interest rates must not become negative. Cap and floor formulas of the Black model to be applied are

$$\text{Cap}^{\text{Bl}}(0, \mathcal{T}, \mathfrak{d}, N, K, \sigma_{\alpha,\beta}) = N \sum_{i=\alpha+1}^{\beta} P(0,T_i)\mathfrak{d}_i \text{BlC}(K, F(0, T_{i-1}, T_i, v_i)) \tag{3.26}$$

and

$$\text{Floor}^{\text{Bl}}(0, \mathcal{T}, \mathfrak{d}, N, K, \sigma_{\alpha,\beta}) = N \sum_{i=\alpha+1}^{\beta} P(0,T_i)\mathfrak{d}_i \text{BlP}(K, F(0, T_{i-1}, T_i, v_i)) \tag{3.27}$$

respectively, where the Black call and put prices amount to

$$\text{BlC}(K, F, v_i) = F\Phi(d_1(K, F, v_i)) - K\Phi(d_2(K, F, v_i)), \tag{3.28}$$

and

$$\text{BlP}(K, F, v_i) = K\Phi(-d_2(K, F, v_i)) - F\Phi(-d_1(K, F, v_i)), \tag{3.29}$$

with

$$d_1(K, F, v_i) = \frac{\ln(F/K) + v_i^2/2}{v_i},$$
$$d_2(K, F, v_i) = \frac{\ln(F/K) - v_i^2/2}{v_i},$$

and

$$v_i = \sigma_{\alpha,\beta}\sqrt{T_{i-1}}.$$

Negative rate modelling The normal model, referred to as the Bachelier model (Bachelier, 1900), allows valuation of options with negative strikes and negative current forward rates, in contrast to the log-normal model. The formulas for the caps and floors are the same as for the Black model where instead the Bachelier call and put prices are inserted, so that

$$\mathrm{Cap}^{\mathrm{Ba}}(0, \mathcal{T}, \mathfrak{d}, N, K, \sigma_{\alpha,\beta}) = N \sum_{i=\alpha+1}^{\beta} P(0, T_i)\mathfrak{d}_i \mathrm{BaC}(K, F(0, T_{i-1}, T_i, v_i)) \tag{3.30}$$

and

$$\mathrm{Floor}^{\mathrm{Ba}}(0, \mathcal{T}, \mathfrak{d}, N, K, \sigma_{\alpha,\beta}) = N \sum_{i=\alpha+1}^{\beta} P(0, T_i)\mathfrak{d}_i \mathrm{BaP}(K, F(0, T_{i-1}, T_i, v_i)), \tag{3.31}$$

where the Bachelier call and put prices amount to

$$\mathrm{BaC}(K, F, v_i) = (F - K)\Phi(d_1(K, F, v_i)) + v_i\phi(d_1(K, F, v_i)) \tag{3.32}$$

and

$$\mathrm{BaP}(K, F, v_i) = (K - F)\Phi(-d_1(K, F, v_i)) + v_i\phi(d_1(K, F, v_i)) \tag{3.33}$$

respectively, with

$$d_1(K, F, v_i) = \frac{F - K}{v_i}$$

and

$$v_i = \sigma_{\alpha,\beta}\sqrt{T_{i-1}}.$$

Using the results of Section B.2.4.2 we can derive the pricing formulas of the needed derivatives of the HW1F model. To be able to obtain the closed form solutions we need to know the distribution of the process r under the T-forward measure $\mathcal{Q}_T$ which is given by (B.47). The expectation and variance under $\mathcal{Q}_T$ (as for the above (3.22) under $\mathcal{Q}$) can be found for example in Brigo and Mercurio (2007). Following Brigo and Mercurio (2007) the price at time t of a European call and put option that mature at time T on a zero-coupon bond with strike price K maturing at time S is under the Hull-White model given by

$$\mathrm{ZBC}(t,T,S,X) = P(t,S)\Phi(h) - XP(t,T)\Phi(h-\sigma_p) \tag{3.34}$$

and

$$\mathrm{ZBP}(t,T,S,X) = XP(t,T)\Phi(-h+\sigma_p) - P(t,S)\Phi(-h) \tag{3.35}$$

respectively, where

$$\begin{aligned}\sigma_p &= \sigma\sqrt{\frac{1-\mathrm{e}^{-2\kappa(T-t)}}{2\kappa}}B(T,S),\\ h &= \frac{1}{\sigma_p}\log\frac{P(t,S)}{P(t,T)X} + \frac{\sigma_p}{2},\end{aligned}$$

with

$$B(T,S) = \frac{1}{\kappa}(1-\mathrm{e}^{-\kappa(S-T)}).$$

Cap and floor prices amount to

$$\mathrm{Cap}(t,\mathcal{T},N,X) = N\sum_{i=1}^{n}(1+X\mathfrak{d}_i)\mathrm{ZBP}\left(t,t_{i-1},t_i,\frac{1}{1+X\mathfrak{d}_i}\right) \tag{3.36}$$

and

$$\mathrm{Floor}(t,\mathcal{T},N,X) = N\sum_{i=1}^{n}(1+X\mathfrak{d}_i)\mathrm{ZBC}\left((t,t_{i-1},t_i,\frac{1}{1+X\mathfrak{d}_i}\right) \tag{3.37}$$

respectively, where

$$\begin{aligned}\sigma_p^i &= \sigma\sqrt{\frac{1-\mathrm{e}^{-2\kappa(t_{i-1}-t)}}{2\kappa}}B(t_{i-1},t_i),\\ h_i &= \frac{1}{\sigma_p^i}\log\frac{P(t,t_i)(1+X\mathfrak{d}_i)}{P(t,t_{i-1})} + \frac{\sigma_p^i}{2},\end{aligned}$$

with

$$B(t_{i-1},t_i) = \frac{1}{\kappa}(1-\mathrm{e}^{-\kappa(t_i-t_{i-1})}).$$

Calibrating the Hull-White model means choosing the model parameters, κ and σ, such that the model prices for caps and floors given by equations (3.36) and (3.37) coincide, in a well-defined way, with market prices of cap and floor prices determined from quoted cap / floor volatilities of the Black model with (3.26) and (3.27) or Bachelier model with (3.30) and (3.31). The non-linear least-squares problem is formulated in Problem 3.1. The corresponding calibration procedure is given in FIGURE 3.7. Mean reversion and volatility parameters are calibrated simultaneously by using the analytical prices. This means we perform one 2-dimensional minimisation.

Problem 3.1 (HW1F calibration).

$$\begin{aligned} &\min_{\vartheta} \|\Pi(\vartheta) - C\|_2^2, && (3.38)\\ \text{subject to} \quad &\vartheta \in \Theta \subset \mathbb{R}_+^2 \end{aligned}$$

where

- $\Theta \subset \mathbb{R}_+^2$ *is a non-empty and compact set,*
- $\vartheta = (\kappa, \sigma)$ *is a vector containing the HW1F parameters to be calibrated,*
- $\Pi(\vartheta) : \Theta \to \mathbb{R}^m$ *is a vector of price functions of calibration instruments depending on the parameter* ϑ *and*
- $C \in \mathbb{R}^m$ *the corresponding vector of observed cap / floor market prices.*

Remark 3.9. *A more intuitive representation of the objective functions in Problem 3.1 is*

$$SSR = \sum_{k=1}^{m} \left(\mathrm{Cap}_k^{\mathrm{HW}}(t, \mathcal{T}, N, X) - \mathrm{Cap}_{\mathrm{k}}^{\mathrm{Market}}(0, \mathcal{T}, \mathfrak{d}, N, K, \sigma_{\alpha,\beta})\right)^2$$

or

$$SSR = \sum_{k=1}^{m} \left(\mathrm{Floor}_k^{\mathrm{HW}}(t, \mathcal{T}, N, X) - \mathrm{Floor}_{\mathrm{k}}^{\mathrm{Market}}(0, \mathcal{T}, \mathfrak{d}, N, K, \sigma_{\alpha,\beta})\right)^2$$

where m *is the number of calibration instruments and SSR is the sum of squared residuals.*

Concluding, with the results from Example 3.1 more research needs to be invested in the relatively new, yet persisting, situation of negative interest rates. The calibration outcome based on Bachelier model cap market prices still leaves room for improvement. However, the available volatility surfaces (FIGURE 3.5) as input data were mostly incomplete which could have a negative effect on the calibration outcome. Nevertheless, the Bachelier model provides an adequate remedy for confronting the current market of low interest rates. Simulating short rates in the HW1F model is straightforward since short rates are normally distributed with expectation and variance as in (3.22).

Example 3.1 (Calibration HW1F). *The Hull-White one-factor model (HW1F) parameters,* κ *and* σ*, are calibrated to cap market prices with corresponding yields curves EURIBOR3M in* FIGURE *3.4 according to the calibration procedure of* FIGURE *3.7. Throughout 2016, negative interest rates can be observed so that normal volatilities in combination with the Bachelier model are chosen as the Black model is not applicable. For 2008 we resort to the traditional approach of the Black model. Cap market prices (*FIGURE *3.6) are obtained via the Black model with (3.26) and log-normal volatilities (*FIGURE *3.5) and via the Bachelier model with (3.30) and normal volatilities (*FIGURE *3.5). ATM strikes are calculated according to Definition 3.1.*
We conduct two calibration procedures for each date where at first we fix $\kappa = 0.5$ *which is common practice and then calibrate* κ *and* σ *with no fixation. The reason for this is that the calibration based on the Bachelier model market prices predominantly calibrates a small mean reversion speed parameter relative to the volatility level which was*

confirmed also for other dates in 2016. So by fixing κ one obtains a more reasonable result with little loss in accuracy. In general, results based on the Black model have been overall more promising, also in the non-fixed case. We use the inbuilt MATLAB *solver* `lsqnonlin()` *with* `'trust-region-reflective'` *algorithm and set the starting values to* $(\kappa_0, \sigma_0) = (0.5, 0.5)$. *Calibration results can be viewed in* TABLE *3.2.*

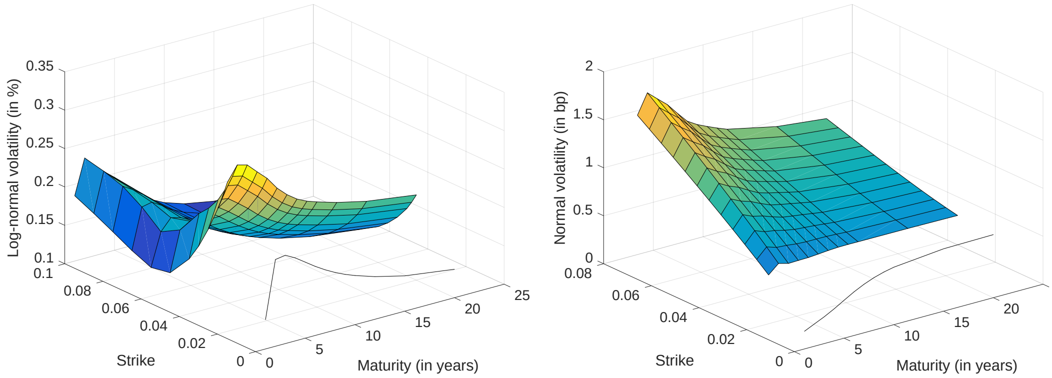

FIGURE 3.5.: Volatility surfaces. Left: Log-normal on 16/09/2008; Right: Normal on 31/12/2016 (data source: Bloomberg)

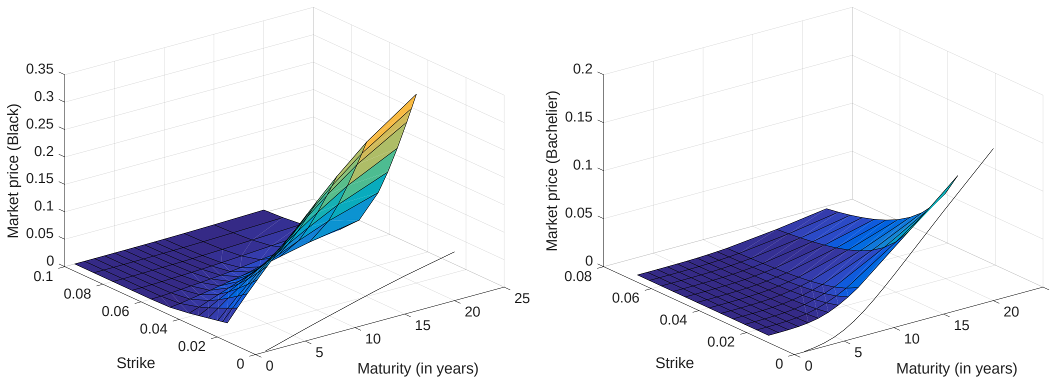

FIGURE 3.6.: Cap market prices. Left: Black model on 16/09/2008; Right: Bachelier model on 31/12/2016

Model	Date	Fixed κ			Non-fixed κ		
		$\widehat{\kappa}$	$\widehat{\sigma}$	Error	$\widehat{\kappa}$	$\widehat{\sigma}$	Error
Black	16/09/2008	0.5	0.018	$1.16 \cdot 10^{-3}$	0.078	0.009	$3.57 \cdot 10^{-4}$
Bachelier	31/12/2016	0.5	0.022	$1.22 \cdot 10^{-2}$	$1.00 \cdot 10^{-6}$	0.007	$3.44 \cdot 10^{-3}$

TABLE 3.2.: Calibration results of HW1F for fixed and non-fixed κ

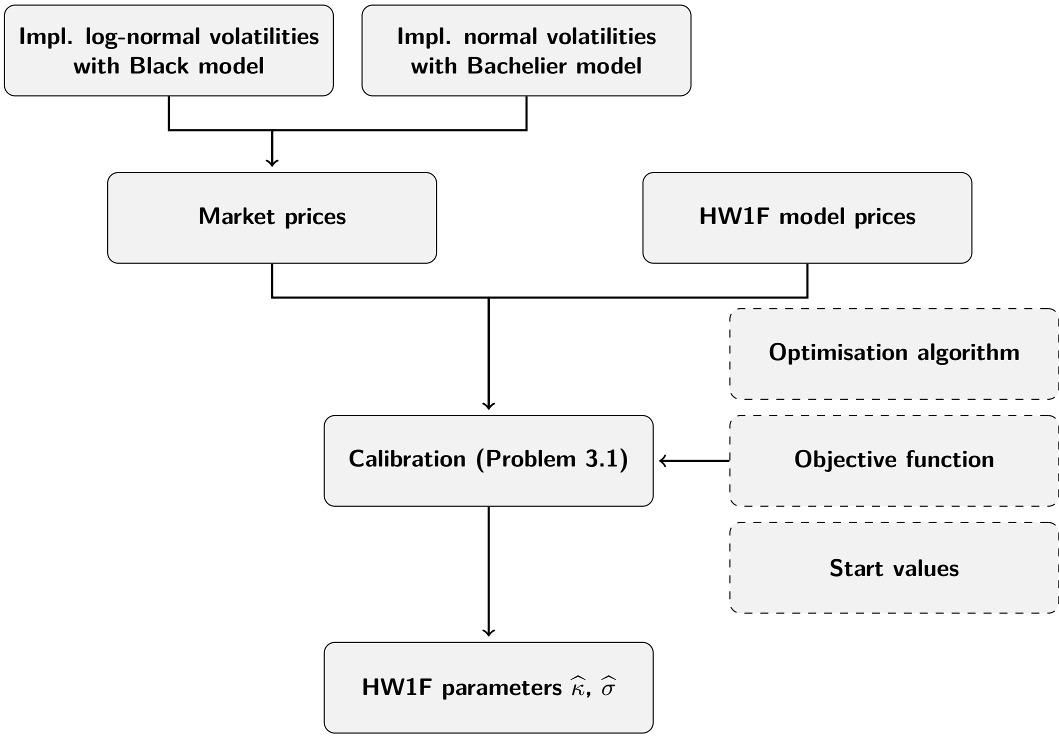

FIGURE 3.7.: Calibration process of the HW1F model

4. Structural Model

In the first approach, a bank's one-period balance sheet is modelled by applying Monte Carlo simulations as proposed by Sünderhauf (2006), based on the work of Bates (1996), Zhou (1997) and Zhou (2001), amongst others and going back as far as Merton (1976). Apart from reviewing this model wrt the asset positions CP and OA of a mortgage Pfandbrief bank, we present advantageous simulation algorithms wrt to computation time and an advanced least square Monte Carlo method. Fixating a benchmark of 10,000 paths — representing a sufficient amount to be able to conduct proper valuations thereupon — in a Monte Carlo setting, it was possible to significantly reduce the computation time during the implementation process[1]. An initial implementation in a nested Monte Carlo setting took approx. twelve minutes, by already taking MATLAB's programming language features — preallocation of storage, vectorisation and parallelisation (see Appendix A) — into consideration. The techniques introduced in Appendix A are the basis of any implementation throughout this framework. Particularly, without exploiting the vector-based advantages the simulations turn out to be rather inefficient, taking hours not minutes. Additional inclusion of efficient numerical methods could further reduce the computation time by a factor of six to approx. two minutes for the nested case (Section 4.1). Moreover, the modelling approximation in form of the least square Monte Carlo method (Section 4.3.2) could reduce the overall processing to a few seconds (even under one second depending on the regression method). This amounts to a gain of at least a factor of 14. However, the least square Monte Carlo method comes at a cost in accuracy compared to the nested case. Therefore, we propose a stepwise regression which amounts to just under ten seconds for simulating 10,000 paths at T_1 (maturity of liabilities) which explains over 99% variability of its nested counterpart. A gross summary of computation times and gains in this chapter is given in TABLE 4.1. The refined performance analyses can be found in the respective sections. Furthermore, alternative measures, in terms of a forward risk-neutral and real-world representation of the underlying SDEs are formulated, providing more modelling flexibility and simultaneously a more complete picture of the overall Pfandbrief modelling framework in a one-period setting (Section 4.2).

	Non-vectorised	Appendix A	Section 4.1	Section 4.3.2
Time	~hours	~12min	~2min	~10sec
Gain factor	-	>60	>6	>14

TABLE 4.1.: Summary of approximate computation times and gains in the structural model.

[1] First numerical results including computation times of the structural model were presented at the Operations Research (OR) 2013 in Rotterdam on September 3$^{\text{rd}}$, 2013.

4.1. Model Setup

Sünderhauf (2006) resorts to various SDEs, consisting of model advancements introduced in Section 4.1.1, in order to simulate the present values $V_{CP}(T_1, T_2)$ (Section 3.6.1.1) and $V_{OA}(T_1)$ (Section 3.6.1.2) of the Pfandbrief framework in Chapter 3. The model components can also be viewed as risk drivers, namely interest rate, volatility, correlation and credit quality. Sünderhauf (2006) argues that these are necessary to obtain realistic scenarios of a bank's day-to-day operational business, hence its creditworthiness and ultimately the creditworthiness of its Prandbrief issuances. Sünderhauf (2006)'s model is embedded in a risk-neutral setting.

4.1.1. Model Evolution

Before giving a detailed description of the underlying model we state a brief review of the model's developments in the context of historical time line and research literature. The final model is a geometric jump-diffusion process whose risk-free interest rate, conditional on no-jump, follows a mean-reverting Ornstein-Uhlenbeck process and whose instantaneous variance follows a mean-reverting square-root process. The jump contribution is modelled through a Poisson shock arrival and a random log-normal amplitude. In principle all Black-Scholes model (Black and Scholes, 1973) hypotheses hold. However, specific restrictions to the jump-diffusion process as specified by Merton (1976) need to be imposed in form of Assumption 4.1.

Assumption 4.1 (Zhou (1997)). *The capital asset pricing model (CAPM) holds for equilibrium security returns and the jump component of a firm's value equation is purely firm specific and is uncorrelated with the market.*

Assumption 4.1 has further implications, namely (compare Merton (1976), Bates (1991), Bates (1996), (Zhou, 1997) and (Zhou, 2001)):

- The jump part is diversifiable (or unsystematic). Thus, the jump risk does not require a risk premium in principle (market price of zero) and consequently the assumption that the expected return on a portfolio equals the riskless rate under the CAPM holds.
- Uniqueness of the equivalent martingale measure (EMM) is guaranteed under diversifiable firm-jumps, thus choosing one specific EMM by leaving the jump part unchanged.
- Deriving a closed-form expression for the price of a call option becomes feasible, if jump risk is diversifiable. Otherwise, the market would be incomplete, the payoffs of the option cannot be replicated, and consequently the option cannot be priced, since jumps in the stock price cannot be hedged using traded securities.

Remark 4.1. *Refer to Bates (1991), Bates (1996) and Zhou (2001) where systematic jumps are allowed and differences between jump size parameters under $\mathcal{P}$ and $\mathcal{Q}$ are analysed.*

The additional source of uncertainty when pricing options, in order to capture additional skewed behaviour of the implied volatility of options which cannot be explained by diffusion-based continuous-path models, is modelled by a Poisson process as specified in Assumption 4.2.

Assumption 4.2 (Merton (1976)). *The Poisson-distributed 'event' is the arrival of an important piece of information about the stock. It is assumed that the arrivals are independently and identically distributed. Therefore, the probability of an event occurring during a time interval of length h (where h is as small as you like) can be written as*

$$\begin{aligned}\text{Prob}(\textit{the event does not occur in the time interval } (t, t+h))) &= 1 - \lambda h + o(h),\\ \text{Prob}(\textit{the event occurs once in the time interval } (t, t+h)) &= \lambda h + o(h),\\ \text{Prob}(\textit{the event occurs more than once in the time interval } (t, t+h)) &= o(h),\end{aligned}$$

where $o(h)$ is the asymptotic order symbol defined by $\psi(h) = o(h)$ if $\lim_{h\to 0}[\psi(h)/h] = 0$, and λ is the mean number of arrivals per time unit.

4.1.1.1. Merton (1976) Model

The first representation of the model can be found in the seminal work of Merton (1976). Let V denote the total market value of the assets of the firm. The dynamics of V under the risk-neutral measure $\mathcal{Q}$ are given by the following jump-diffusion process

$$\frac{\mathrm{d}V(t)}{V(t)} = (r - \lambda v)\mathrm{d}t + \sigma_V \mathrm{d}W_V^{\mathcal{Q}}(t) + (Y(t) - 1)\mathrm{d}N(t), \tag{4.1}$$

where

- r is the (constant) riskless interest rate,
- σ_V is the (constant) instantaneous volatility of the return (conditional on no arrivals of important new information, i.e. the Poisson event does not occur),
- $W_V^{\mathcal{Q}}(t)$ is a standard Brownian motion,
- $N(t)$ is an (independent) Poisson process with (constant) intensity parameter λ (mean number of arrivals per time unit),
- $Y(t) > 0$ is the jump amplitude and is log-normally distributed with $\log(Y(t)) \overset{iid}{\sim} N(\mu_Y, \sigma_Y^2)$,
- $v = \mathbb{E}(Y(t) - 1) = \exp(\mu_Y + \sigma_Y^2/2) - 1$ is the (constant) expected value of the jump component $(Y(t) - 1)$ (random variable percentage change in the asset value if the Poisson event occurs), and
- $W_V^{\mathcal{Q}}(t)$, $N(t)$ and $Y(t)$ are assumed to be mutually independent.

The convenient result of $Y(t)$ being log-normally distributed is that the distribution of $\mathrm{d}V(t)/V(t)$ is again log-normal (as in Merton (1974)). Concluding, model (4.1), consisting of a mixture of both continuous (accounting for 'normal' price changes) and jump (accounting for 'abnormal' price changes) processes, "has most of the attractive features of the original Black-Scholes formula in that it does not depend on investor preferences or knowledge of the expected return on the underlying stock", cf. (Merton, 1976).

Remark 4.2. *Initially, Merton (1976) formulated (4.1) under the real-world measure $\mathcal{P}$, setting $\mu_V = r$ where μ_V is the (constant) instantaneous expected return on the asset. Assuming that jumps of the stock prices are diversifiable (Assumption 4.1) allows one to simply swap the diffusion drift μ_V with r (and vice versa) while all other parameters, including those of the jump component, remain unchanged (compare also Korn et al. (2010, p. 337)). In other words, statistical properties of the jump part under $\mathcal{Q}$ or $\mathcal{P}$ are identical so that*

$$\lambda^{\mathcal{Q}} = \lambda^{\mathcal{P}} \qquad \textit{and} \qquad \mu_Y^{\mathcal{Q}} = \mu_Y^{\mathcal{P}},$$

and where the variance parameter σ_Y^2 is invariant to any measure change.

Remark 4.3. *If we assume that $\lambda = 0$, then also $\mathrm{d}N(t) = 0$ and then $V(t)$ has the same dynamics as in the Black-Scholes (Black and Scholes, 1973) and Merton (Merton, 1974) approaches.*

4.1.1.2. Bates (1996) Model

The first introduced extension to Merton (1976)'s model in Section 4.1.1.1 comprises of an added stochastic volatility process, $\varsigma(t)$, where the assumption of a constant volatility parameter of (4.1), σ_V, gets relaxed (compare also Heston (1993)). Bates (1996) argues that a combination of stochastic variance with a jump-diffusion process can explain the 'volatility smile' when pricing options. However, by resorting to a mean-reverting square root process (refer to Cox et al. (1985) and Brigo and Mercurio (2007) for further details) the resulting jump-diffusion type model also takes on a higher level of complexity. Pricing formulas for European options are derived via moment generating functions. The risk neutral process of the firm's asset value is given by

$$\begin{aligned} \frac{\mathrm{d}V(t)}{V(t)} &= (r - \lambda v)\mathrm{d}t + \varsigma(t)\mathrm{d}W_V^{\mathcal{Q}}(t) + (Y(t) - 1)\mathrm{d}N(t), \qquad (4.2) \\ \mathrm{d}\varsigma^2(t) &= \kappa(\theta - \varsigma^2(t))\mathrm{d}t + \sigma_\varsigma \sqrt{\varsigma^2(t)}\mathrm{d}W_\varsigma^{\mathcal{Q}}(t), \\ \mathrm{d}W_V^{\mathcal{Q}}(t)\mathrm{d}W_\varsigma^{\mathcal{Q}}(t) &= \rho_{V,\varsigma}\mathrm{d}t. \end{aligned}$$

where $W_V^{\mathcal{Q}}(t)$ and $W_\varsigma^{\mathcal{Q}}(t)$ are independent of $N(t)$ and $Y(t)$ and the correlation $\rho_{V,\varsigma}$ is some constant in $[-1, 1]$. Otherwise, the same assumptions hold as in Section 4.1.1.1 for the rest of model components.

Remark 4.4. *If the SDE of $V(t)$ in (4.2) is solely driven by*

$$\frac{\mathrm{d}V(t)}{V(t)} = \varsigma(t)\mathrm{d}W_V^{\mathcal{Q}}(t),$$

thus setting the drift and jump part to zero (as in the Heston (1993) model), then $\varsigma^2(t)$ can be interpreted as the instantaneous variance of relative changes to $V(t)$. More precisely, the quadratic variation of $\mathrm{d}V(t)/V(t)$ over an instantaneous time period $[t, t+\mathrm{d}t]$ is then $\varsigma^2(t)\mathrm{d}t$.

4.1.1.3. Zhou (1997) Model

Zhou (1997) relaxes the assumption of a constant risk-free interest rate r of (4.1) by assuming that the instantaneous risk-free interest follows a diffusion process of the well known Vašìček (1977) interest rate model (for more details on the Vašìček (1977) model refer to Brigo and Mercurio (2007)). This was first proposed by Longstaff and Schwartz (1995) for the Merton (1974) model which incorporates both default and interest rate risk. Thereby, Longstaff and Schwartz (1995) found out, inter alia, that correlation between changes in firm's value and interest rates have a significant effect on credit spreads. The jump-diffusion model with short-term interest rate dynamics amounts to

$$\begin{aligned}
\frac{\mathrm{d}V(t)}{V(t)} &= (r(t) - \lambda v)\mathrm{d}t + \sigma_V \mathrm{d}W_V^{\mathcal{Q}}(t) + (Y(t) - 1)\mathrm{d}N(t), \qquad (4.3)\\
\mathrm{d}r(t) &= \kappa\left(\theta - r(t)\right)\mathrm{d}t + \sigma_r \mathrm{d}W_r^{\mathcal{Q}}(t),\\
\mathrm{d}W_V^{\mathcal{Q}}(t)\mathrm{d}W_r^{\mathcal{Q}}(t) &= \rho_{V,r}\mathrm{d}t,
\end{aligned}$$

where $W_V^{\mathcal{Q}}(t)$ and $W_r^{\mathcal{Q}}(t)$ are independent of $N(t)$ and $Y(t)$ and the correlation $\rho_{V,r}$ is some constant in $[-1, 1]$. Otherwise, the same assumptions hold as in Section 4.1.1.1 for the rest of model components.

4.1.1.4. Zhou (2001) Model

Finally, Zhou (2001) combines all three models of (4.1), (4.2) and (4.3) where he permits interest rates to be stochastic, in form of the Vašìček model (Vašìček, 1977) and a variance process, in form of CIR1F model (refer to Cox et al. (1985) and Brigo and Mercurio (2007) for further details). While offering a high amount of flexibility, derivations of closed form solutions wrt pricing options and other derivatives are not feasible. The complete jump-diffusion model comprises of

$$\begin{aligned}
\frac{\mathrm{d}V(t)}{V(t)} &= (r(t) - \lambda v)\mathrm{d}t + \varsigma(t)\mathrm{d}W_V^{\mathcal{Q}}(t) + (Y(t) - 1)\mathrm{d}N(t), \qquad (4.4)\\
\mathrm{d}r(t) &= \kappa_r\left(\theta_r - r(t)\right)\mathrm{d}t + \sigma_r \mathrm{d}W_r^{\mathcal{Q}}(t),\\
\mathrm{d}\varsigma^2(t) &= \kappa_\varsigma(\theta_\varsigma - \varsigma^2(t))\mathrm{d}t + \sigma_\varsigma\sqrt{\varsigma^2(t)}\mathrm{d}W_\varsigma^{\mathcal{Q}}(t),\\
\mathrm{d}W_r^{\mathcal{Q}}(t)\mathrm{d}W_\varsigma^{\mathcal{Q}}(t) &= \rho_{r,\varsigma}\mathrm{d}t,\\
\mathrm{d}W_V^{\mathcal{Q}}(t)\mathrm{d}W_\varsigma^{\mathcal{Q}}(t) &= \rho_{V,\varsigma}\mathrm{d}t,\\
\mathrm{d}W_V^{\mathcal{Q}}(t)\mathrm{d}W_r^{\mathcal{Q}}(t) &= \rho_{V,r}\mathrm{d}t.
\end{aligned}$$

where $\mathrm{d}W_V^{\mathcal{Q}}(t)$, $W_r^{\mathcal{Q}}(t)$ and $W_\varsigma^{\mathcal{Q}}(t)$ are independent of $N(t)$ and $Y(t)$ and the correlation parameters $\rho_{r,\varsigma}$, $\rho_{V,\varsigma}$ and $\rho_{V,r}$ are some constants in $[-1, 1]$. Otherwise the same assumptions hold as in Section 4.1.1.1 for the rest of model components.

4.1.2. Interest Rate Component

While (4.1) and (4.2) rely on a constant interest rate component in their models, (4.3) and (4.4) lift this restriction allowing interest rates, more precisely instantaneous spot

rates, evolve stochastically. Therefore, the Vašìček (1977) model is introduced to model $r(t)$. However, as pointed out by Zhou (1997) and Zhou (2001) other models can be used instead in this context. With the current market situation of low interest rates and the reasons derived in Section 3.7 we resort to the HW1F model (which was also the choice of Sünderhauf (2006)). Incorporating a stochastic short rate model permits an overall more realistic modelling since interest rates themselves are of stochastic nature (compare FIGURE 3.3). Merton was one of the first to acknowledge this fact: "It [interest rate] is observable, satisfies the condition of being stochastic over time, and while it is surely not the sole determinant of yields on other assets, it is an important factor. Hence, one should interpret the effects of a changing interest rate in the forthcoming analysis in the way economists have generally done in the past: namely, as a single (instrumental) variable representation of shifts in the investment opportunity set.", (Merton, 1973).
Concluding, the relaxation of assuming a constant interest rate is one of the more noteworthy progressions in the model evolution review (Section 4.1.1) of Merton's initial model of (Merton, 1976), respectively (Merton, 1974).

4.1.3. Volatility Component

The Cox-Ingersoll-Ross model (Cox et al., 1985) belongs to the class of so called equilibrium models for modelling instantaneous spot rates, compare Hull (2009). In the one-factor case (CIR1F) the short rate process involves only one source of uncertainty and is described by an Itô process. The instantaneous drift and standard deviation are assumed to be functions of the short rate but are independent of time. The most important feature is the avoidance of negative rates. The volatility term decreases when the spot rate approaches zero. This implies a higher (lower) volatility in case of higher (lower) interest rates compared to models with constant volatility, for example the model of Vašìček (Vašìček, 1977). Also, when interest rates are zero, the volatility term is zero, thereby disabling the random feature of the model and implying that rates shift deterministically in positive direction.
Although originally intended to be an interest rate model, the motivation of applying this model in the context of stochastic volatilities is obvious, due to its favourable property of non-negativity (Heston, 1993). In the following we give a brief model definition with its main characteristics in the context of the affine term structure introduced in Section B.2.3.2. Thereby, we use the notation $\varsigma^2(t)$ to define the variance process in from of the CIR1F model. Emphasis is laid upon simulation which is computationally burdensome, due to an underlying non-central chi-squared distribution of the evolving process.

4.1.3.1. Model Definition

The model formulation (Brigo and Mercurio, 2007) under the risk-neutral measure $\mathcal{Q}$ is

$$\mathrm{d}\varsigma^2(t) = \kappa \left(\theta - \varsigma^2(t)\right) \mathrm{d}t + \sigma\sqrt{\varsigma^2(t)}\mathrm{d}W^{\mathcal{Q}}(t), \quad \varsigma^2(0) = \varsigma_0^2, \tag{4.5}$$

with positive constants ς_0^2, κ, θ and σ. The Feller condition

$$2\kappa\theta > \sigma^2 \tag{4.6}$$

has to be imposed to ensure that the origin is inaccessible to the process (4.5), so that we can guaranty that $\varsigma^2(t)$ remains positive.
The mean reverting process of (4.5) has an underlying non-central χ^2-distribution as defined in Definition B.23 with the non-centrality parameter proportional to $\varsigma^2(t)$ where the transition density has a closed form expression. Following Cox et al. (1985), the density of $\varsigma^2(t)$ at time t, given $\varsigma^2(s)$ at time s $(s < t)$, is

$$\begin{aligned} p_{(\varsigma^2(t)\,|\,\varsigma^2(s))}(x) &= p_{\chi_\nu'^2(\lambda(s,t))/c(s,t)}(x) = c(s,t)p_{\chi_\nu'^2(\lambda(s,t))}(c(s,t)\cdot x), \\ c(s,t) &= \frac{4\kappa}{\sigma^2(1-\exp(-\kappa(t-s)))}, \\ \lambda(s,t) &= c(s,t)\exp(-\kappa(t-s))\varsigma^2(s), \\ \nu &= 4\kappa\theta/\sigma^2, \end{aligned} \tag{4.7}$$

with ν denoting the degrees of freedom and where now the non-centrally parameter λ in Definition B.23 is a time dependent stochastic variable $\lambda(s,t)$. Consequently, $\varsigma^2(t)$ can be expressed as

$$\varsigma^2(t) = (c(s,t))^{-1}\chi_\nu'^2(\lambda(s,t)) \quad s < t.$$

In words, conditional on $\varsigma^2(s)$, $\varsigma^2(t)$ is distributed as $(c(s,t))^{-1}$ times a non-central χ^2-distribution with ν degrees of freedom and non-centrality parameter $\lambda(s,t)$. Equivalently, the cumulative distribution function of $\varsigma^2(t)\,|\,\varsigma^2(s)$ is

$$\mathrm{Prob}(\varsigma^2(t) \leq x\,|\,\varsigma^2(s)) = F_{\chi_\nu'^2(\lambda(s,t))}(c(s,t)\cdot x) \quad s < t,$$

with the cdf of $\chi_\nu'^2(\lambda)$ and $\lambda = \lambda(s,t)$ (Johnson et al., 1995)

$$\begin{aligned} \mathrm{Prob}(\chi_\nu'^2(\lambda) \leq x) &= F_{\chi_\nu'^2(\lambda)}(x) \\ &= \mathrm{e}^{-\lambda/2}\sum_{j=0}^{\infty}\frac{(\frac{1}{2}\lambda)^j/j!}{2^{\nu/2+j}\Gamma(\frac{1}{2}\nu+j)}\int_0^x y^{\nu/2+j-1}\mathrm{e}^{-y/2}\mathrm{d}y, \quad x > 0, \end{aligned}$$

where $\Gamma(\cdot)$ is the (complete) gamma function with

$$\Gamma(\alpha) = \int_0^\infty \mathrm{e}^{-u}u^{\alpha-1}\mathrm{d}u.$$

This setup allows us to simulate (4.5) analytically on a discrete time grid. This means sampling from the non-central χ^2-distribution which is looked at more closely in the next section.

Remark 4.5. *In Johnson et al. (1995) it is stated that for $\nu \to \infty$ (λ remaining constant) or $\lambda \to \infty$ (ν remaining constant) the non-central χ^2-distribution of Definition B.23 converges to a normal distribution (or in both cases when ν and λ approach infinity). See Definition B.23 for more details.*
Transferred to the CIR1F model of (4.5) this implies that for large $\varsigma^2(t)$ that the underlying non-central χ^2-distribution converges to the normal distribution, since the non-centrality parameter $\lambda(s,t)$ depends on $\varsigma^2(t)$.

The mean and variance of $\varsigma^2(t)$ conditional on $\mathcal{F}_s$ $(s < t)$ are given by

$$\mathbb{E}\left(\varsigma^2(t)\,\middle|\,\mathcal{F}_s\right) = \varsigma^2(s)\exp(-\kappa(t-s)) + \theta\left(1-\exp(-\kappa(t-s))\right), \tag{4.8}$$

$$\mathbb{V}\left(\varsigma^2(t)\,\middle|\,\mathcal{F}_s\right) = \varsigma^2(s)\frac{\sigma^2}{\kappa}\left(\exp(-\kappa(t-s)) - \exp(-2\kappa(t-s))\right) + \theta\frac{\sigma^2}{2\kappa}\left(1-\exp(-\kappa(t-s))\right)^2 \tag{4.9}$$

where $\varsigma^2(t)$ grows with increasing σ (volatility level) and decreasing κ (mean reversion speed).

Remark 4.6. *Belonging to the class of affine term structure models we can, in an abbreviated manner due to Corollary B.2, derive the closed form solution to the zero-coupon bond price equation of (B.28) which is outlined in the following. Inserting $\mu(r,t) = \kappa(\theta - \varsigma^2(t))$ and $\sigma(r,t) = \sigma\sqrt{\varsigma^2(t)}$ in (B.30) one obtains*

$$\left[\frac{\partial A(t,T)}{\partial t} - \kappa\theta B(t,T)\right] - \left(1 + \frac{\partial B(t,T)}{\partial t} - \kappa B(t,T) - \frac{1}{2}\sigma^2 B^2(t,T)\right) r = 0.$$

When $\varsigma^2(t)$ converges to zero the terms in brackets should be equal zero, so that equations (B.37) and (B.38) emerge. Making use of Theorem B.10 by setting $\alpha(t) = -\kappa$, $\beta(t) = \kappa\theta$, $\gamma(t) = \sigma^2$ and $\delta(t) = 0$ one comes to the same results, namely

$$\begin{cases} \dfrac{\partial B(t,T)}{\partial t} = \kappa B(t,T) + \dfrac{1}{2}\sigma^2 B^2(t,T) - 1 \\ B(T,T) = 0 \end{cases} \tag{4.10}$$

and

$$\begin{cases} \dfrac{\partial A(t,T)}{\partial t} = \kappa\theta B(t,T) \\ A(T,T) = 0. \end{cases} \tag{4.11}$$

Solving the partial differential equation for the CIR1F model is quite cumbersome, especially the solution to (4.11) meaning integrating with respect to t over an interval $[t,T]$. However, having only constant parameters $\alpha(t) = -\kappa$, $\beta(t) = \kappa\theta$, $\gamma(t) = \sigma^2$ and $\delta(t) = 0$ Corollary B.2 can be applied, where

$$B(t,T) = \frac{2(\mathrm{e}^{c_1(T-t)} - 1)}{(\kappa + c_1)(\mathrm{e}^{c_1(T-t)} - 1) + 2c_1}, \tag{4.12}$$

with $c_1 = \sqrt{\kappa^2 + 2\sigma^2}$. For $A(t,T)$ we postulate

$$A(t,T) = \frac{2\kappa\theta}{\sigma^2}\ln\left(\frac{2c_1\mathrm{e}^{\frac{1}{2}(\kappa+c_1)(T-t)}}{(\kappa+c_1)(\mathrm{e}^{c_1(T-t)} - 1) + 2c_1}\right) \tag{4.13}$$

as correctly given by Cox et al. (1985) and reverse engineer the solution by computing the derivative of (4.13) wrt time t. We set $C = (\kappa + c_1)(\mathrm{e}^{c_1(T-t)} - 1) + 2c_1$ so that after *applying the chain rule*

$$\begin{aligned}
\frac{\partial A(t,T)}{\partial t} &= \frac{2\kappa\theta}{\sigma^2}\cdot\frac{C}{2c_1 \mathrm{e}^{\frac{1}{2}(\kappa+c_1)(T-t)}}\cdot\frac{(c_1^3-\kappa^2 c_1)\mathrm{e}^{\frac{1}{2}(\kappa+3c_1)(T-t)}+(\kappa^2 c_1-c_1^3)\mathrm{e}^{\frac{1}{2}(\kappa+c_1)(T-t)}}{C^2}\\
&= \frac{2\kappa\theta}{\sigma^2}\cdot\frac{(c_1^3-\kappa^2 c_1)(\mathrm{e}^{\frac{1}{2}(\kappa+3c_1)(T-t)}-\mathrm{e}^{\frac{1}{2}(\kappa+c_1)(T-t)})}{2c_1\mathrm{e}^{\frac{1}{2}(\kappa+c_1)(T-t)}C}\\
&= \frac{2\kappa\theta}{\sigma^2}\cdot\frac{2c_1\sigma^2\mathrm{e}^{\frac{1}{2}(\kappa+c_1)(T-t)}(\mathrm{e}^{c_1(T-t)}-1)}{2c_1\mathrm{e}^{\frac{1}{2}(\kappa+c_1)(T-t)}C}\\
&= \kappa\theta\frac{2(\mathrm{e}^{c_1(T-t)}-1)}{C}\\
&= \kappa\theta B(t,T)
\end{aligned}$$

equals (4.11). Inserting (4.13) and (4.12) with c_1 into (B.28) finally yields the zero-coupon bond price for the CIR model.

4.1.3.2. Simulation

For obtaining the exact solution of the CIR1F model ones needs to draw from the non-central chi-squared distribution (Definition B.23), as the process paths are distributed accordingly. The density function for a non-central chi-square random variable takes on an interesting form consisting of an infinite weighted sum of central Chi-square densities with Poisson weights. This comes with a huge computational burden[2]. Thus, generating multiple CIR1F paths will have an multiplicative effect on the overall simulation time. It is the objective, and crucial in the case of CIR1F, to find alternative methods which are faster but have little loss in accuracy. A trade-off between accuracy and computational efficiency naturally arises. Additionally, to the well-known 'Euler-Maruyama', 'Milstein' or 'Milstein-Implicit' discretisations (see Remark 4.7 for the generic formulations thereof) and the 'Analytic' approach, the 'Truncated-Gaussian' and 'Quadratic-Exponential' schemes are compared. The two latter schemes provide expeditious algorithms which feature desirable efficiency and accuracy properties. For more information see Andersen (2008) and Andersen et al. (2010). Moreover, we need to analyse if the introduced schemes can guarantee positivity of (4.5). More precisely, it needs to be analysed if $\mathrm{Prob}(\varsigma^2(t) > 0, \forall t > 0) = 1$ holds even if the Feller condition (4.6) is imposed. We divide the proposed schemes into two (homogeneous) approximating groups wrt the 'Analytic' scheme, namely the 'standard' discretisations of 'Euler-Maruyama', 'Milstein' and 'Milstein-Implicit' and the 'moment-matching' techniques of 'Truncated-Gaussian' and 'Quadratic-Exponential'. Main simulation results[3] of the five schemes are first presented before going into more detail of the algorithms themselves and their computations below.

First we take a look at convergence rates of the schemes 'Euler-Maruyama', 'Milstein' and 'Milstein-Implicit' for different time steps. Strong and weak convergence for SDEs are applied which are the two most widely used convergence concepts determining the

[2] A detailed description on drawing random numbers for the chi-squared and non-central chi-squared distribution e.g. via a Poisson distribution is given in Johnson et al. (1994) and Johnson et al. (1995), respectively.

[3] More extensive numerical tests on pricing of European call options in the Heston model are provided in Andersen (2008).

accuracy of SDE simulation methods (Kloeden and Platen, 2011). Time steps are chosen so that 2^n, $n = \{5, 6, \ldots, 14\}$ at which the convergence formulas are applied. As expected, FIGURE 4.1 reveals that 'Euler-Maruyama' compared to its more sophisticated counterparts 'Milstein' and 'Milstein-Implicit' is inferior in the weak as well as strong convergence case (compare also Higham (2001)). Noteworthy is the fact that the 'Euler-Maruyama' scheme has a convergence order of 1, the same as 'Milstein' and 'Milstein-Implicit', in the weak case. However, "this should not be viewed as a deficiency of Milstein's method; rather the Euler scheme is better than it 'should' be, achieving order-1 weak convergence without expanding all terms to $O(h)$", (Glasserman, 2004). For the schemes 'Analytic', 'Quadratic-Exponential' and 'Truncated-Gaussian' we can

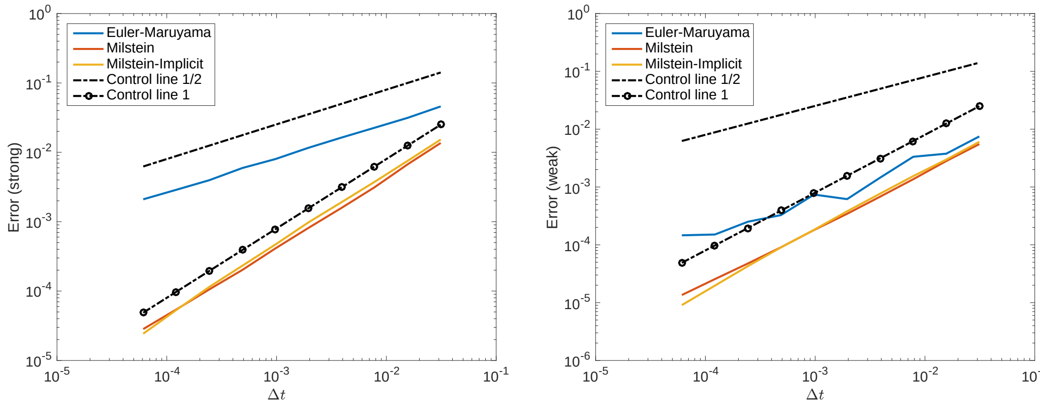

FIGURE 4.1.: Strong and weak convergence error plots of schemes 'Euler-Maruyama', 'Milstein' and 'Milstein-Implicit'. Left: Strong convergence; Right: Weak convergence

reproduce the plots given in Andersen (2008) and Andersen et al. (2010) where the cumulative distribution functions of the respective schemes are depicted. For comparison reasons we also include the Gaussian and log-normal distributions where the conditional mean (4.8) and variance (4.9), the first two moments of $\varsigma^2(t)$, are parametrised. As stated in Andersen (2008), neither of these distributions are particularly good proxies for the true distribution of $\varsigma^2(t)$ where the Gaussian also turns negative. However, they do reveal how close the more elaborate schemes of 'Quadratic-Exponential' and 'Truncated-Gaussian' are to the analytical simulation (blue graph in FIGURE 4.2) with the true underlying non-central chi-squared distribution of (4.7). As pointed out in Andersen (2008), in typical applications condition (4.6) is mostly not met, thus very small values (close to zero) are very likely. Inherently, it is the area close to zero where any scheme has difficulties matching the random numbers of Algorithm 4.4 which is evidently the case in FIGURE 4.2. However, we find that the 'Quadratic-Exponential' scheme fairly accurately emulates the true underlying cumulative distribution of the 'Analytic' scheme for different parameter settings (compare left and right picture of FIGURE 4.2). A performance analysis is undertaken where one path consisting of 10 years with 250 business days for each year is generated and repeated 100 times. Taking a look at the resulting computation times (TABLE 4.2) of the introduced methods we find that the more elaborate the scheme the longer it takes to generate the process path. Even though we compute the cache in the case of the 'Truncated-Gaussian' (Algorithm 4.1) at a pre-loop stage, as suggested by Andersen (2008), the lookup of ψ^* still consumes a large amount of time. Thereby, the smallest absolute difference to the cache values is determined and indexed, yielding the wanted cached value (see also Remark 4.9). However, reducing

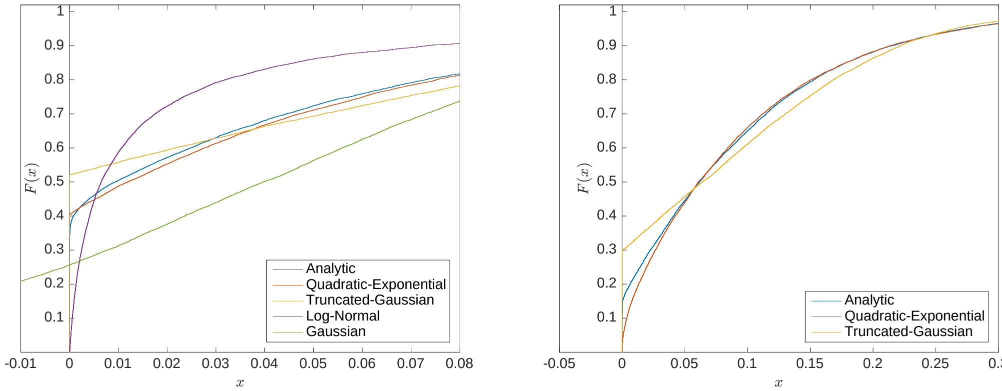

FIGURE 4.2.: Cumulative distribution function for $\varsigma^2(T)$ given $\varsigma^2(0)$, with $T = 0.1$ of schemes 'Analytic', 'Quadratic-Exponential' and 'Truncated-Gaussian'. Model parameters are $\theta = 0.04$, $\kappa = 0.5$, and $\sigma = 1$. Left: $\varsigma^2(0) = 0.04$ and including the Gaussian and log-normal distributions; Right: $\varsigma^2(0) = 0.09$

equidistant partitions of the interval ψ from 1,000 reduces the computation time substantially. The same simulation with 100 partitions yields the computation time of only 36.83 seconds (compared to 327.10 seconds in TABLE 4.2). The less granular the segmentation of I_ψ is the larger the distance between to the 'true' values of ψ becomes. The less accurate schemes 'Euler-Maruyama', 'Milstein' and 'Milstein-Implicit' are the fasted where differences are small amongst each other. A symbolic summary of the accuracy measurements of the underlying schemes is also depicted in TABLE 4.2.

To summarise: Conditional on accuracy and speed the 'Quadratic-Exponential' scheme is the most favourable, reducing the computational burden of the 'Analytic' scheme by a factor of over twelve. However, if speed is of utmost importance the one might want to resort to 'Milstein-Implicit' (factor of approximately up to 450 over 'Analytic') in the class of 'standard' discretisations. Utilising the 'Analytic' scheme in situations where accuracy may be of concern it still poses a manageable simulation duration. There is no reason opting for 'Euler-Maruyama', 'Milstein' or 'Truncated-Gaussian'.

	Euler-Maruyama	Milstein	Milstein-Implicit	Truncated-Gaussian	Quadratic-Exponential	Analytic
Time (sec)	0.20	0.21	0.08	327.10	3.02	36.72
Accuracy	$-$	$\circ$	$\circ$	$\circ$	$+$	$+$

TABLE 4.2.: Computation times and accuracy depiction ('$-$': bad, '$\circ$': moderate and '$+$': good) of the CIR1F simulation schemes of 'Euler-Maruyama', 'Milstein', 'Milstein-Implicit', 'Truncated-Gaussian', 'Quadratic-Exponential' and 'Analytic'. Simulations are based on 2500 time points and 100 repetitions.

Remark 4.7. *For the schemes 'Euler-Maruyama', 'Milstein' or 'Milstein-Implicit' we state the generic formulations wrt to the process $X(t)$. (Refer to Glasserman (2004) or Kloeden and Platen (2011) for derivations and more details on the proposed approxima-*

tions.) Consider the following (scalar) stochastic differential equation (SDE)

$$\mathrm{d}X(t) = a(X(t))\mathrm{d}t + b(X(t))\mathrm{d}W(t). \tag{4.14}$$

We define a time grid $0 = t_0 < t_1 < \cdots < t_n$, $Z_i \sim \mathrm{N}(0,1)$, $i = 1, \ldots, n$ *then for* $i = 0, \ldots, n-1$ *the time-discretised approximations* $\hat{X}$ *of* X *with* $\hat{X}(0) = X(0)$ *and* $\Delta t = t_{i+1} - t_i$ *are:*

- *Euler-Maruyama:*

$$\hat{X}(t_{i+1}) = \hat{X}(t_i) + a(\hat{X}(t_i))\Delta t + b(\hat{X}(t_i))\sqrt{\Delta t} Z_{i+1} \tag{4.15}$$

- *Milstein:*

$$\begin{aligned}\hat{X}(t_{i+1}) = \hat{X}(t_i) + a(\hat{X}(t_i))\Delta t + b(\hat{X}(t_i))\sqrt{\Delta t} Z_{i+1} &+ \\ \frac{1}{2} b'(\hat{X}(t_i)) b(\hat{X}(t_i)) \Delta t (Z_{i+1}^2 - 1)&\end{aligned} \tag{4.16}$$

- *Milstein-Implicit:*

$$\begin{aligned}\hat{X}(t_{i+1}) = \hat{X}(t_i) + a(\hat{X}(t_{i+1}))\Delta t + b(\hat{X}(t_i))\sqrt{\Delta t} Z_{i+1} &+ \\ \frac{1}{2} b'(\hat{X}(t_i)) b(\hat{X}(t_i)) \Delta t (Z_{i+1}^2 - 1)&\end{aligned} \tag{4.17}$$

In summary 'Milstein' and 'Milstein-Implicit' expand 'Euler-Maruyama' by the term

$$\frac{1}{2} b'(\hat{X}(t_i)) b(\hat{X}(t_i)) \Delta t (Z_{i+1}^2 - 1).$$

Notice the difference between 'Milstein' and 'Milstein-Implicit' where the former possesses the drift term $a(\hat{X}(t_i))$ *depending on the past time point* t_i *and the latter is driven by the drift term* $a(\hat{X}(t_{i+1}))$ *at current time* t_{i+1}*. Replacing*

$$\begin{aligned} X(t) &= \varsigma^2(t), \\ a(X(t)) &= \kappa\left(\theta - \varsigma^2(t)\right), \\ b(X(t)) &= \sigma\sqrt{\varsigma^2(t)} \end{aligned}$$

in (4.14) we receive the SDE discretisation schemes (4.15), (4.16) and (4.17) for (4.5).

Euler-Maruyama The stochastic 'Euler-Maruyama' method is the simplest discretisation method for stochastic differential equations. The method is a stochastic differential equation that maps a random variable $\varsigma^2(t_{i-1})$ of the CIR1F process (4.5) into a new random variable $\varsigma^2(t_i)$ where $\mathrm{d}\varsigma^2(t) \approx \Delta\varsigma^2(t)$, $\mathrm{d}t \approx \Delta t$ and $\mathrm{d}W(t) \approx \Delta W(t)$ (Δ denoting the difference operator). This is accomplished using a recursive discrete version of Equation (4.5) at discretisation times t_i, $i = 1, \ldots, n$:

$$\begin{aligned}\varsigma^2(t_i) &= \varsigma^2(t_{i-1}) + \kappa(\theta - \varsigma^2(t_{i-1}))\Delta t + \sigma\sqrt{\varsigma^2(t_{i-1})\Delta t} Z_{t_i} \\ &= \kappa\theta\Delta t + (1 - \kappa\Delta t)\varsigma^2(t_{i-1}) + \sigma\sqrt{\varsigma^2(t_{i-1})\Delta t} Z_{t_i},\end{aligned} \tag{4.18}$$

where $\Delta t = t_i - t_{i-1} = \int_{t_{i-1}}^{t_i} 1\mathrm{d}s$ and $\Delta W(t) = W(t_i) - W(t_{i-1}) = \int_{t_{i-1}}^{t_i} 1\mathrm{d}W(s) = Z_{t_i}$ with $Z \sim \mathrm{N}(0,1)$. The probability of $\varsigma^2(t_i)$ turning negative when $\varsigma^2(t_{i-1}) > 0$ is then (compare also Lord et al. (2006))

$$\mathrm{Prob}(\varsigma^2(t_i) < 0) = \Phi\left(-\frac{(1-\kappa\Delta t)\varsigma^2(t_{i-1}) + \kappa\theta\Delta t}{\sigma\sqrt{\varsigma^2(t_{i-1})\Delta t}}\right)$$

where Φ is the cdf of the standard normal distribution. With $\Delta t \to 0$ then also $\mathrm{Prob}(\varsigma^2(t_i) < 0) \to 0$, thus with decreasing step size the less likely negative values occur. An illustration of the process behaviour of (4.5) under the 'Euler-Maruyama' scheme for two different parameter sets is given in Example 4.1. To address the non-positivity issue some (rather crude) numerical solutions are proposed within the 'Euler-Maruyama' scheme:

· Deelstra and Delbaen (1998):

$$\varsigma^2(t_i) = \kappa\theta\Delta t + (1-\kappa\Delta t)\varsigma^2(t_{i-1}) + \sigma\sqrt{\max(\varsigma^2(t_{i-1}),0)\Delta t}Z_{t_i}$$

· Higham and Mao (2005):

$$\varsigma^2(t_i) = \kappa\theta\Delta t + (1-\kappa\Delta t)\varsigma^2(t_{i-1}) + \sigma\sqrt{|\varsigma^2(t_{i-1})|\Delta t}Z_{t_i}$$

· Berkaoui et al. (2008):

$$\varsigma^2(t_i) = |\kappa\theta\Delta t + (1-\kappa\Delta t)\varsigma^2(t_{i-1}) + \sigma\sqrt{\varsigma^2(t_{i-1})\Delta t}Z_{t_i}|$$

In Lord et al. (2006) and Dereich et al. (2012) one finds a more thorough analysis (and additional schemes) of above amendments wrt positivity preservation and convergence rates. Noteworthy is the fact that the scheme under Deelstra and Delbaen (1998) still cannot completely rule out occurring negative values. Lord et al. (2006) state that an expansion of Deelstra and Delbaen (1998) to

$$\varsigma^2(t_i) = \kappa\theta\Delta t + (1-\kappa\Delta t)\max(\varsigma^2(t_{i-1}),0) + \sigma\sqrt{\max(\varsigma^2(t_{i-1}),0)\Delta t}Z_{t_i}$$

works best under the proposed fixings to the 'Euler-Maruyama' scheme (for more details see Lord et al. (2006)). Although being the easiest to implement, it does raise the question if these amendments to the 'Euler-Maruyama' produce permissible realisations of a paths of (4.5). Thus, we turn our focus to other, potentially more promising, schemes.

Example 4.1. *Due to, potentially, occurring negative values under the root, the real valued part of the process* ($\mathrm{Re}(\varsigma^2(t))$) *is plotted in* FIGURE *4.3. On the left side we have* $2\kappa\theta = 0.36 \not> 1.00 = \sigma^2$ *so that condition (4.6) is not fulfilled for given parameters where on multiple occasions (as expected) the non-negativity criterium of the CIR1F is not met. On the right picture of* FIGURE *4.3 the Feller condition (4.6) is satisfied with* $2\kappa\theta = 0.40 > 0.25 = \sigma^2$ *for given parameters. However, although positivity should be ensured by (4.6) we observe a breach of the zero boundary, marked in red.*

Milstein The next proposed scheme is the 'Milstein' scheme of (4.16). It makes use of Itô's formula (Theorem B.3) to increase the accuracy of the approximation by adding

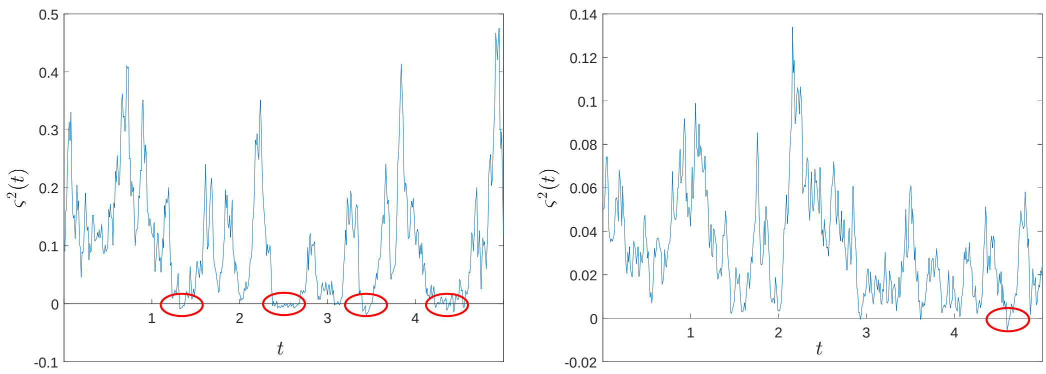

FIGURE 4.3.: Example path of 'Euler-Maruyama' scheme. Left: Condition (4.6) not fulfilled, with $\varsigma^2(0) = 0.09$, $\kappa = 2$, $\theta = 0.09$ and $\sigma = 1$; Right: Condition (4.6) fulfilled, with $\varsigma^2(0) = 0.05$, $\kappa = 5$, $\theta = 0.04$ and $\sigma = 0.5$

a second order term of the Taylor expansion. It can be regarded as a refinement to 'Euler-Maruyama' where a convergence rate of h) is achieved for the drift term (compare Glasserman (2004)). For (4.5) the discretisation amounts to

$$\begin{aligned}\varsigma^2(t_i) &= \varsigma^2(t_{i-1}) + \kappa(\theta - \varsigma^2(t_{i-1}))\Delta t + \sigma\sqrt{\varsigma^2(t_{i-1})\Delta t} Z_{t_i} + \frac{1}{4}\sigma^2\Delta t(Z_{t_i}^2 - 1)\\ &= \kappa\theta\Delta t + (1 - \kappa\Delta t)\varsigma^2(t_{i-1}) + \sigma\sqrt{\varsigma^2(t_{i-1})\Delta t} Z_{t_i} + \frac{1}{4}\sigma^2\Delta t(Z_{t_i}^2 - 1),\end{aligned}$$

where $Z \sim \mathrm{N}(0, 1)$. As in the case of the 'Euler-Maruyama' scheme, 'Milstein' also generates, with positive probability, negative values of (4.5) (compare Andersen et al. (2010)). Numerical adjustments, as already proposed in 'Euler-Maruyama', wrt to absolute or maximum values also become necessary. However, under certain circumstances when all conditions (see for example Kahl (2008)) in Remark 4.8 are met, then also (4.5) is guaranteed to be positive under the 'Milstein' scheme.

Remark 4.8. *The generic 'Milstein' method of (4.16) guarantees positivity if the conditions for $i = 0, \ldots, n-1$*

$$\begin{aligned} b(\hat{X}_{t_i})b'(\hat{X}_{t_i}) &> 0,\\ \hat{X}_{t_i} &> \frac{b(\hat{X}_{t_i})}{2b'(\hat{X}_{t_i})},\\ \Delta t &< \frac{2}{b(\hat{X}_{t_i})b'(\hat{X}_{t_i}) - 2a(\hat{X}_{t_i})}\left(\hat{X}_{t_i} - \frac{b(\hat{X}_{t_i})}{2b'(\hat{X}_{t_i})}\right)\end{aligned}$$

are fulfilled. (The last condition is only necessary if the denominator is positive.)

Milstein-Implicit A notable improvement over 'Euler-Maruyama' and 'Milstein' is the 'Milstein-Implicit' scheme. It can be shown than under the Feller condition (4.6) retaining positivity for (4.5) is feasible. The difference to 'Milstein' lies with the treatment of the drift term. Applying Ito's formula (Theorem B.3) yields

$$\varsigma^2(t_i) = \frac{1}{1+\kappa\Delta t}\left(\varsigma^2(t_{i-1}) + \kappa\theta\Delta t + \sigma\sqrt{\varsigma^2(t_{i-1})\Delta t}Z_{t_i} + \frac{1}{4}\sigma^2\Delta t(Z_{t_i}^2 - 1)\right), \quad (4.19)$$

where $Z \sim \mathrm{N}(0,1)$. Since the denominator of (4.19) is positive it leaves us to show that the numerator is positive. Thereby, we aggregate all stochastic parts (depending on Z_{t_i}) of (4.19) to a (quadratic polynomial) function f

$$f(Z_{t_i}) := \sigma\sqrt{\varsigma^2(t_{i-1})\Delta t}Z_{t_i} + \frac{1}{4}\sigma^2\Delta t Z_{t_i}^2.$$

Since the second derivative of f is $f''(Z_{t_i}) > 0$ and the root of $f'(Z_{t_i})$ ($f'(Z_{t_i}) \stackrel{!}{=} 0$) is

$$Z_{t_i} = -\frac{2\sqrt{\varsigma^2(t_{i-1})}}{\sigma\sqrt{\Delta t}},$$

we obtain the (global) minimum of $-\varsigma^2(t_{i-1})$ for $f(Z_{t_i})$. Thus, we can approximate the numerator of (4.19) by

$$\begin{aligned}
&\varsigma^2(t_{i-1}) + \kappa\theta\Delta t + \sigma\sqrt{\varsigma^2(t_{i-1})\Delta t}Z_{t_i} + \frac{1}{4}\sigma^2\Delta t(Z_{t_i}^2 - 1)\\
&= \varsigma^2(t_{i-1}) + \left(\kappa\theta - \frac{1}{4}\sigma^2\right)\Delta t + f(Z_{t_i})\\
&\geq \varsigma^2(t_{i-1}) + \left(\kappa\theta - \frac{1}{4}\sigma^2\right)\Delta t - \varsigma^2(t_{i-1})\\
&= \left(\kappa\theta - \frac{1}{4}\sigma^2\right)\Delta t > 0.
\end{aligned}$$

Concluding, we can state that 'Milstein-Implicit' is the first scheme in our selection of altogether five proposed schemes where the Feller condition (4.6) is fulfilled.

Truncated-Gaussian Andersen (2008)'s idea for a 'Truncated-Gaussian' (TG) method stems from the already established fact of Remark 4.5 that for $\lambda(s,t) \to \infty$ the non-central χ^2-distribution approaches a normal distribution so that for large $\varsigma^2(t)$ the first two Gaussian moments provide a suitable fit, hence the name 'Gaussian' in TG. However, relying entirely on large $\varsigma^2(t)$ is predestined for failure. A first impression of a pure 'Gaussian' (postulating a normal distribution) approximation with moments (4.8) and (4.9) can be viewed in FIGURE 4.2 (left picture). Clearly, as $\varsigma^2(t)$ approaches zero the 'Gaussian' approximation is not able to produce a satisfying result in resembling a 'χ^2-kind of density' around the origin (compare the 'Analytic' curve which resembles the 'true' underlying distribution). Furthermore, negative values are not permitted for (4.5). Thus, it would be advantageous to impose a boundary at the origin as a first measure, hence the name 'Truncated' in TG. This step of "shifting the left tail mass of a Gaussian into a delta-function at zero" (Andersen, 2008) is comparable to the additional necessary amendments under the 'Euler' scheme. However, we are not done yet. The name 'Truncated-Gaussian' may be somewhat misleading since Andersen (2008) additionally adds the advancement of sampling from a moment-matched Gaussian density where "for small $\varsigma^2(t)$, the resulting scheme will approximate the chi-square density in (B.61) by a mass in 0 combined with an upper density tail proportional to $\mathrm{e}^{-x^2/2}$", (Andersen, 2008). Consequently, the overall success of TG will be attributed to the handling of small values of $\varsigma^2(t)$ as then $\lambda(s,t) \to 0$ and the non-central approaches the central χ^2-distribution with $\nu = 4\kappa\theta/\sigma^2$ (Definition B.22). When additionally $\nu \to 0$ the χ^2-distribution shifts more mass to the origin and as pointed out by Andersen (2008) the more frequent case is $\nu = 4\kappa\theta/\sigma^2 << 2$. In summary, Andersen (2008) uses a combination of Gaussian and central χ^2 approximations where the TG scheme is defined as follows:

$$\begin{aligned}\varsigma^2(t_i) &= \Big(\mu(\varsigma^2(t_{i-1})) + \sigma(\varsigma^2(t_{i-1}))Z_{t_i}\Big)^+ \\ &= \max\Big(\mu(\varsigma^2(t_{i-1})) + \sigma(\varsigma^2(t_{i-1}))Z_{t_i}, 0\Big) \end{aligned} \tag{4.20}$$

where $Z \sim \mathrm{N}(0,1)$ and the still unknown parameters μ and σ depend on the process $\varsigma^2(t_{i-1})$ at time t_{i-1}. Note that positivity of (4.5) is ensured by (4.20). The specification of $\mu(\varsigma^2(t_{i-1})$ and $\sigma(\varsigma^2(t_{i-1}))$ with the complete computation steps of TG are now introduced (for more details and corresponding proofs refer to Andersen (2008)).
The moment-matching procedure consists of approximating the exact first two conditional moments of (4.8) and (4.9) by the unconditional moments $\mathbb{E}(\varsigma^2(t_i))$ and $\mathbb{V}(\varsigma^2(t_i))$ in order to obtain the parameters μ and σ of (4.20). The proposed moment-matching function and solution is given in Theorem 4.1 (refer to Andersen (2008) for corresponding proof).

Theorem 4.1 (Moment-matching 'Truncated-Gaussian'). *Let $\phi(x) = (2\pi)^{-1/2}\mathrm{e}^{-x^2/2}$ be the standard Gaussian density, and define a function $g : \mathbb{R} \to \mathbb{R}$ by the relation*

$$g(x)\phi(g(x)) + \Phi(g(x))\Big(1 + g(x)^2\Big) = (1+x)\left(\phi(g(x)) + g(x)\Phi(g(x))\right)^2 \tag{4.21}$$

Also set

$$\psi := \frac{m^2}{s^2} > 0. \tag{4.22}$$

with $m = \mathbb{E}(\varsigma^2(t_i) \,|\, \varsigma^2(t_{i-1}))$ and $s^2 = \mathbb{V}(\varsigma^2(t_i) \,|\, \varsigma^2(t_{i-1}))$. If $\varsigma^2(t_i)$ is generated by the TG scheme (4.20), with parameter settings

$$\mu = \frac{m}{\phi(g(\psi))g(\psi)^{-1} + \Phi(r(\psi))}, \quad \sigma = \frac{m}{\phi(g(\psi)) + g(\psi)\Phi(r(\psi))},$$

then $\mathbb{E}(\varsigma^2(t_i)) = m$ and $\mathbb{V}(\varsigma^2(t_i)) = s^2$.

A greater portion of computations can be done outside of the loop over discretised time steps, saving on computational time. These prerequisites involve solving (4.21) for $\psi \in [1/\alpha^2, \sigma^2/(2\kappa\theta)] = I_\psi$ (a sufficient discretisation of the interval is for example 1,000 equidistant partitions) and $\alpha = 4.5$ (according to Andersen (2008) the confidence multiplier α needs to be "a number around 4 or 5") and computing

$$f_\mu(\psi) = \frac{g(\psi)}{\phi(g(\psi)) + g(\psi)\Phi(g(\psi))}, \quad f_\sigma(\psi) = \frac{\psi^{-1/2}}{\phi(g(\psi)) + g(\psi)\Phi(g(\psi))}$$

which consists of the values than can be cached together with I_ψ into the main memory for later lookup, see left picture of FIGURE 4.4 and Remark 4.9 for more details. The interpretation of interval I_ψ is subtended. Large values of ψ correspond to small values of ς^2. Since we are more interested in small values (near to zero) the corresponding upper region of I_ψ is, likewise, of higher importance. Lower and upper boundaries are obtained via limits of (4.22) where

$$\lim_{\varsigma^2(t_{i-1})\to\infty} \frac{\left(\mathbb{E}(\varsigma^2(t_i)\,|\,\varsigma^2(t_{i-1}))\right)^2}{\mathbb{V}(\varsigma^2(t_i)\,|\,\varsigma^2(t_{i-1}))} = 0$$

and

$$\lim_{\varsigma^2(t_{i-1})\to 0} \frac{\left(\mathbb{E}(\varsigma^2(t_i)\,|\,\varsigma^2(t_{i-1}))\right)^2}{\mathbb{V}(\varsigma^2(t_i)\,|\,\varsigma^2(t_{i-1}))} = \frac{\sigma^2}{2\kappa\theta}.$$

However, the case for $\varsigma^2(t_{i-1}) \to \infty$ (large values of $\varsigma^2(t_{i-1})$) is of less importance since it is covered by the Gaussian distribution approximation of Remark 4.5. Therefore, the confidence multiplier α is introduced to define the relevant domain for mapping the function $g(\psi)$ which is given by I_ψ. Consequently, if $\psi \leq 1/\alpha^2$ then $f_\mu = f_\sigma = 1$ and $\mu = m$ and $\sigma = s$. The complete cache range of f_μ and f_σ is depicted in the left picture of Figure 4.4 where for $\varsigma^2(t_{i-1}) = 0$ the corresponding values are $f_\mu = -49.4$ and $f_\sigma = 6.65$ marking the range end points. On the right picture of Figure 4.4 we see the impact of f_μ and f_σ on μ and σ in comparison to m and s. An interval of sorted $\varsigma^2(t_{i-1})$ values with $\varsigma^2(t_{i-1}) \in [0, 0.01]$ is chosen for visualisation. For $\varsigma^2(t_{i-1}) > 0.01$ visual differences between m and μ as well as between s and σ are not detectable. Thus, for larger values of $\varsigma^2(t_{i-1})$ the parameters (m, s, μ, σ) converge as expected. The purpose of f_μ and f_σ is to counteract the behaviour of the simplified shifting of (4.20) when $\mu = m$ and $\sigma = s$ which would result in a larger mean and smaller variance in relation to the (original) Gaussian distribution. The right picture of Figure 4.4 reveals that the moment-matching procedure of Theorem 4.1 will firstly shift probability mass further to the left by a mean < 1 and raise the variance of small $\varsigma^2(t_{i-1})$. This is the desired outcome for emulating a central χ^2-distribution around the origin. Concluding, Andersen (2008) states the following final result: “Naïve truncation schemes (such as certain Euler schemes) that assume $f_\mu \approx f_\sigma \approx 1$ not surprisingly have large biases.” The additional necessary computation steps for TG are presented in Algorithm 4.1.

Algorithm 4.1 (Truncated-Gaussian).

1. *Given $\varsigma^2(t_{i-1})$, compute (moments (4.8) and (4.9))*

$$\begin{aligned} m &= \theta + (\varsigma^2(t_{i-1}) - \theta)\mathrm{e}^{-\kappa\Delta t} \\ s^2 &= \frac{\varsigma^2(t_{i-1})\sigma^2\mathrm{e}^{-\kappa\Delta t}}{\kappa}\left(1 - \mathrm{e}^{-\kappa\Delta t}\right) + \frac{\theta\sigma^2}{2\kappa}\left(1 - \mathrm{e}^{-\kappa\Delta t}\right)^2 \end{aligned}$$

   and plug into

$$\psi^* = \frac{s^2}{m^2}.$$

2. *Look up ψ^* in the cache and extract the corresponding function evaluations $f_\mu(\psi)$ and $f_\sigma(\psi)$ and compute*

$$\begin{aligned} \mu &= f_\mu(\psi)m \\ \sigma &= f_\sigma(\psi)s. \end{aligned}$$

3. Compute $\varsigma^2(t_i) = (\mu + \sigma Z)^+$, *where* $Z \sim \mathrm{N}(0,1)$.

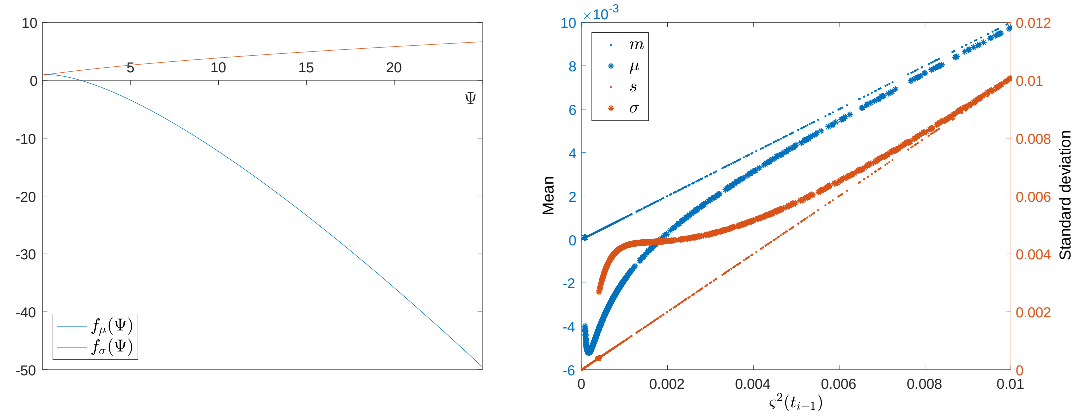

FIGURE 4.4.: Left: Cache for $f_\mu(\psi)$ and $f_\sigma(\psi)$ of the 'Truncated-Gaussian' scheme; Right: Comparison of the parameters m and s to the 'Truncated-Gaussian' parameters μ, and σ for small $\varsigma^2(t)$, with $\varsigma^2(0) = \theta = 0.04$, $\kappa = 5$, and $\sigma = 0.5$

Remark 4.9. *Look up procedure of* ψ^* *in the cache involves the following simple computations where the index of corresponding* $f_\mu(\psi)$ *and* $f_\sigma(\psi)$ *is returned. Let us assume the values of* $f_\mu(\psi)$ *and* $f_\sigma(\psi)$ *together with* I_ψ *are successfully cached.*
The first implementation attempt of simulating one path of the CIR1F model comprises of the intuitive computation of the absolute differences of I_ψ *and* ψ^* *and looking for the smallest difference.*

```
% Intuitive implementation
[~,positionMu] = min(abs(cacheMu(:,1) - psiParameter));
[~,positionSigma] = min(abs(cacheSigma(:,1) - psiParameter));
```

This procedure can be expanded to a simulation setting with more than one path in a vectorised fashion. Therefore, MATLAB*'s inbuilt* `bsxfun()` *function is utilised to avoid a* `for` *loop over each* ψ.

```
% Vectorised implementation
[~,positionMu] = min(abs(bsxfun(@minus,cacheMu(:,1),psiParameter)));
[~,positionSigma] = min(abs(bsxfun(@minus,cacheSigma(:,1),psiParameter)));
```

Finally, we resort to MATLAB*'s inbuilt function* `histc()` *to speed up the computation (approximately by a factor of two).* `histc()` *returns the bin number that each entry in* ψ^* *sorts into with* ψ *representing the bin range.*

```
% Fastest  implementation
[~,positionMu] = histc(psiParameter,cacheMu(:,1));
[~,positionSigma] = histc(psiParameter,cacheSigma(:,1));
```

Quadratic-Exponential A further advancement to the above TG scheme is represented by 'Quadratic-Exponential' (QE) algorithm (Andersen, 2008). QE has its root in the above introduced TG scheme where the common ground is a moment-matching technique. However, QE allows for a slower density decay of $\varsigma^2(t_{i-1})$ when approaching zero. Thus, QE adds an additional, more accurate, approximation step as opposed to TG resulting to two different distributions for approximating the distribution of the variance on the lower tail. More precisely, the refinements of QE include:

- A non-central χ^2-distribution approximation by, firstly, a moment-matching approach via a quadratic function applied to a Gaussian variable (hence the name 'Quadratic' in QE) and, secondly, an exponential distribution approximation (hence the name 'Exponential' in QE).
- A switching rule between the two approximation steps (moment-matching and exponential distribution) is established to obtain a reasonable approximation for small values of the variance process (4.5).

Furthermore, the advantage wrt to memory and speed of QE over TG is the fact that pre-caching (functions f_μ and f_σ in TG) is not necessary. With the knowledge from TG over computation of ψ via (4.22) the proposed QE scheme is divided into computation steps, namely:

- Case $\psi \leq 2$: The first case covers the more moderate values of $\varsigma^2(t_{i-1})$. From Remark 4.5 we know that the Gaussian distribution is a suitable approximation (see also TG scheme). Here a quadratic function is chosen in the form of

$$\varsigma^2(t_i) = a(\varsigma^2(t_{i-1}))\left(b(\varsigma^2(t_{i-1})) + Z_{t_i}\right)^2 \tag{4.23}$$

  where a and b are dependent on $\varsigma^2(t_{i-1})$ and Z_{t_i} is a standard normal random variable. Notice that (4.23) precludes any negative values (if $a(\varsigma^2(t_{i-1})) > 0$ and $b(\varsigma^2(t_{i-1})) > 0$). The specification of $a(\varsigma^2(t_{i-1})) > 0$ and $b(\varsigma^2(t_{i-1}))$ is given in Theorem 4.2 (see Andersen (2008) for corresponding proof).

  Theorem 4.2 (Moment-matching 'Quadratic-Exponential': $\psi \leq 2$). *Let m and s be as defined in Theorem 4.1 (equations (4.8) and (4.9)), and set $\psi = s^2/m^2$. Provided that $\psi \leq 2$, set*

$$b^2 = 2\psi^{-1} - 1 + \sqrt{2\psi^{-1}}\sqrt{2\psi^{-1} - 1} \geq 0 \tag{4.24}$$

  and

$$a = \frac{m}{1+b^2}. \tag{4.25}$$

  Let $\varsigma^2(t_i)$ be as defined in (4.23), then $\mathbb{E}(\varsigma^2(t_i)) = m$ and $\mathbb{V}(\varsigma^2(t_i)) = s^2$.

- Case $\psi \geq 1$: This case covers the very small values of $\varsigma^2(t_{i-1})$. Here Andersen (2008) resorts to an approximation by an exponential distribution for the lower tail arising from the asymptotic behaviour of the non-central χ^2-distribution. More precisely, the proposed density is a mixture of a Dirac delta-function and an exponential distribution. For more details on its derivation refer to Andersen (2008)). The resulting pdf, cdf and inverse cdf of this approximation read as follows:

$$\begin{aligned}\mathrm{Prob}(\varsigma^2(t_i) \in [x, \mathrm{d}x]) &\approx \left(p\delta(0) + \zeta(1-p)\mathrm{e}^{-\zeta x}\right)\mathrm{d}x, \quad x \geq 0,\\ \Psi(x) = \mathrm{Prob}(\varsigma^2(t_i) \leq x) &= p + (1-p)\left(1 - \mathrm{e}^{-\zeta x}\right), \quad x \geq 0,\end{aligned}$$

and

$$\Psi^{-1}(u) = \Psi^{-1}(u; p, \zeta) = \begin{cases} 0, & 0 \leq u \leq p \\ \zeta^{-1} \ln\left(\frac{1-p}{1-u}\right), & p < u \leq 1 \end{cases}$$

where δ is a Dirac delta-function, $p \in [0, 1]$ and $\zeta \geq 0$. Finally, we simply can sample the future value $\varsigma^2(t_i)$ by

$$\varsigma^2(t_i) = \Psi^{-1}(U_{t_i}; p(\varsigma^2(t_{i-1})), \zeta(\varsigma^2(t_{i-1}))) \tag{4.26}$$

where p and ζ depend on $\varsigma^2(t_{i-1})$ and U_{t_i} is an uniform random number. Notice that negative values are not possible under (4.26). The computations of p and ζ are given in Theorem 4.3 (see Andersen (2008) for corresponding proof).

Theorem 4.3 (Exponential distribution 'Quadratic-Exponential': $\psi \geq 1$). *Let m, s and ψ be as defined in Theorem 4.1. Assume that $\psi \geq 1$ and set*

$$p = \frac{\psi - 1}{\psi + 1} \in [0, 1), \tag{4.27}$$

and

$$\zeta = \frac{1-p}{m} = \frac{2}{m(\psi + 1)} > 0. \tag{4.28}$$

Let $\varsigma^2(t_i)$ be as defined in (4.26), then $\mathbb{E}(\varsigma^2(t_i)) = m$ and $\mathbb{V}(\varsigma^2(t_i)) = s^2$.

Lastly, we need to find a rule of when to use the moment-matching approach and when to use the exponential distribution approximation. This can be easily found since both cases have a common domain of $\psi \in [1, 2]$. It is natural to choose the mean of this interval yielding the critical value $\psi_c = 1.5$. A visual impression of the switching rule and imposed approximations is given in Figure 4.5. Therefore, a path of ten years with 250 business days for each year is simulated using the same parameter settings as in Figure 4.4. For clarity reasons the values of $\varsigma^2(t)$ are capped at 0.04 and values of exactly zero are omitted. Setting the switching rule to $\psi_c = 1.5$ it is expected to have, to some extent, an overlapping region for $\varsigma^2(t)$. However, overall a high degree of selectivity between both above cases can be observed. The domain for small values is assigned to (4.26) with Theorem 4.3, and likewise for large values to (4.23) with Theorem 4.2. The complete computation steps are given in Algorithm 4.2.

Algorithm 4.2 (Quadratic-Exponential).

1. *Compute $\psi = \frac{s^2}{m^2}$, with m and s^2 as in step 1. of Algorithm 4.1.*
2. ***if*** $\psi \leq \psi_c$
   a) *Compute a and b according to equations (4.25) and (4.24).*
   b) *Set $\varsigma^2(t_i) = a(b + Z_{t_i})^2$.*
3. ***otherwise*** $\psi > \psi_c$
   a) *Compute ζ and p according to equations (4.28) and (4.27).*

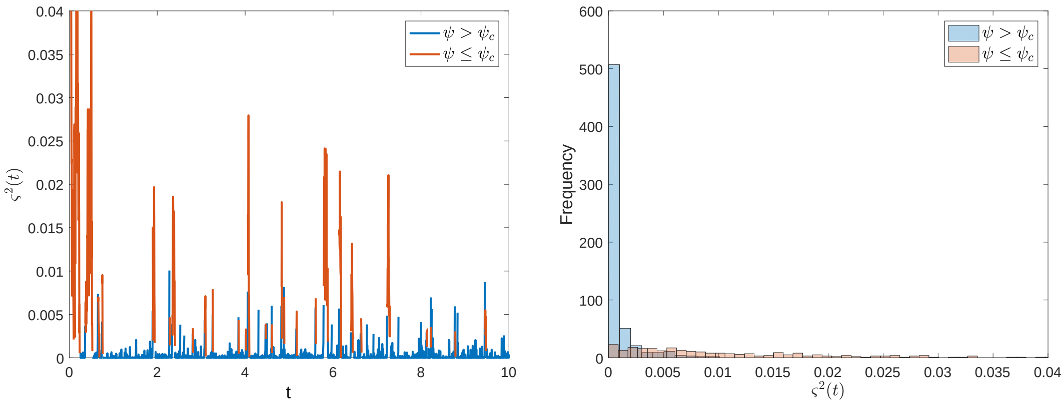

FIGURE 4.5.: Switching rule for 'Quadratic-Exponential' scheme, with $\psi_c = 1.5$ and $\varsigma^2(0) = \theta = 0.04$, $\kappa = 5$, and $\sigma = 0.5$; Left: Time series; Right: Histogram

b) Set $\varsigma^2(t_i) = \Psi^{-1}(U; p, \zeta)$*, where* $U \sim \mathrm{Unif}(0, 1)$ *and*

$$\Psi^{-1}(u) = \Psi^{-1}(u; p, \zeta) = \begin{cases} 0, & 0 \leq u \leq p \\ \zeta^{-1} \ln\left(\frac{1-p}{1-u}\right), & p < u \leq 1. \end{cases}$$

Remark 4.10. *Now, Algorithm 4.2 is fairly straight forward to implement. However, from an implementation perspective a loop over each* ψ *value is needed as the '*`if else`*' statement only can handle scalars which makes the code slow. Instead, by indexing arrays with conditions* $\psi \leq \psi_c$*,* $\psi > \psi_c$ *and* $p < u \leq 1$ *respectively an efficient vectorisation (see Appendix A.2) can be achieved. A* MATLAB *code excerpt of Algorithm 4.2 is given where* `procVola` *denotes the underlying variance process (note one single loop over time with index* `i` *is still required and random numbers are here uniformly distributed):*

```
% 2. b):
idx1 = psi <= psi_c;
procVola(i,idx1) = a(idx1).*(sqrt(b(idx1)) + norminv(RN(i,idx1),0,1)).^2;
```

```
% 3. b):
idx2 = RN(i,:) <= p & psi > psi_c;
procVola(i,idx2) = 0;

idx3 = RN(i,:) > p & psi > psi_c;
procVola(i,idx3) = log((1 - p(idx3))./(1 - RN(i,idx3)))./zeta(idx3);
```

Analytic The 'Analytic' approach involves simulating the square-root diffusion (4.5) by sampling from the transition density (4.7) on a (discretised) time grid $0 = t_0 < t_1 < \ldots < t_n$. From Section 4.1.3.1 we know that $c(t_{i-1}, t_i)\varsigma^2(t_i) \,|\, \varsigma^2(t_{i-1}) \sim \chi_\nu'^2(\lambda(t_{i-1}, t_i))$. With the parameters defined in (4.7) we have all necessary tools and inputs available to successfully implement the procedure. However, as pointed out by Glasserman (2004) it would be advantageous splitting the sampling from the non-central χ^2-distribution into sampling from a central χ^2-distribution and a Poisson random variable or from a central χ^2-distribution and a standard normal random variable so that two separate algorithms can be proposed for the 'Analytic' approach. Note that for the Algorithm specification we change the notation of the degrees of freedom parameter from ν to d. The two cases are (Glasserman, 2004):

- Case $\nu > 1$: The first case samples from a central χ^2- and a standard normal distribution. As outlined in Definition B.23 it is possible to decompose $\chi_\nu'^2(\lambda)$ to

$$\chi_\nu'^2(\lambda) = (Z_1 + \delta)^2 + Z_2^2 + \ldots + Z_\nu^2 = \chi_1'^2(\lambda) + \chi_{\nu-1}^2$$

for when ν only takes on integers. In the general case where ν takes on any real number $\nu > 1$ we then have (compare also Johnson et al. (1995))

$$\chi_\nu'^2(\lambda) = (Z + \sqrt{\lambda})^2 + \chi_{\nu-1}^2$$

where Z is a standard normal variable and $\chi_{\nu-1}^2$ a central chi-square random variable with $\nu - 1$ degrees of freedom. Following Glasserman (2004), the sampling from an non-central χ^2-distribution can be formulated as in Algorithm 4.3 which now consists of drawing a central chi-square and an (independent) standard normal random variable.

Algorithm 4.3 (Analytic Simulation ($d > 1$)).

1. *Draw a standard normal random variable Z, with mean $\frac{1}{2}\lambda(t_{i-1}, t_i)$.*
2. *Draw a central chi-square (Definition B.22) random variable χ_d^2, with $d = \nu - 1$ degrees of freedom.*
3. *Set $\varsigma^2(t_i) = c(t_{i-1}, t_i))^{-1}[(Z + \sqrt{\lambda(t_{i-1}, t_i)})^2 + \chi_d^2]$.*

- Case $\nu \leq 1$: The second case, which is also the general case as it would cover $\nu > 0$, involves drawing from a central χ^2- and a Poisson distribution. However, since we have covered $\nu > 1$ in Algorithm 4.3 we only need to consider the values $(0 <)\nu \leq 1$. As stated in Johnson et al. (1995) one can decompose $F_{\chi_\nu'^2(\lambda)}(x)$ (for $x > 0$) of the non-central χ^2-distribution "as a weighted sum of central χ^2 probabilities with weights equal to the probabilities of a Poisson distribution with expected value $\frac{1}{2}\lambda$" (Johnson et al., 1995), thus

$$\begin{aligned} F_{\chi_\nu'^2(\lambda)}(x) &= \sum_{j=0}^{\infty} \left(\frac{\left(\frac{1}{2}\lambda\right)^j}{j!} \mathrm{e}^{-\lambda/2} \right) \mathrm{Prob}(\chi_{\nu+2j}^2 \leq x) \\ &= \sum_{j=0}^{\infty} \left(\frac{\left(\frac{1}{2}\lambda\right)^j}{j!} \mathrm{e}^{-\lambda/2} \right) F(x; \nu + 2j, 0) \qquad (4.29) \end{aligned}$$

where with $\lambda = 0$, non-central χ^2-distribution takes on a central χ^2-distribution with $\nu + 2j$ degrees of freedom (compare also Definition B.23). Glasserman (2004) offers a derivation of (4.29), namely: We define a Poisson random variable N with mean $\frac{1}{2}\lambda$ then the probability of $N = j$ is

$$\mathrm{Prob}(N = j) = \frac{\left(\frac{1}{2}\lambda\right)^j}{j!} \mathrm{e}^{-\lambda/2}, \quad j = 0, 1, 2, \ldots.$$

Conditional on $N = j$, the random variable $\chi^2_{\nu+2N}$ has a central χ^2-distribution with $\nu + 2j$ degrees of freedom, so that

$$\mathrm{Prob}(\chi^2_{\nu+2N} \leq x \,|\, N = j) = \frac{1}{2^{\nu/2+j}\Gamma(\nu/2 + j)} \int_0^x \mathrm{e}^{-y/2} y^{\nu/2+j-1} \mathrm{d}y.$$

Then we obtain the unconditional distribution

$$\sum_{j=0}^{\infty} \mathrm{Prob}(N = j)\, \mathrm{Prob}(\chi^2_{\nu+2N} \leq x \,|\, N = j) = F_{\chi'^2_\nu(\lambda)}(x),$$

resulting to (4.29). In summary when $\nu \leq 1$ one then follows the steps as in Algorithm 4.4 (which also can be found in Andersen et al. (2010)).

Algorithm 4.4 (Analytic Simulation ($d \leq 1$)).

1. *Draw a Poisson random variable N, with mean $\frac{1}{2}\lambda(t_{i-1}, t_i)$.*
2. *Given N, draw a central chi-square (Definition B.22) random variable χ^2_d, with $d = \nu + 2N$ degrees of freedom.*
3. *Set $\varsigma^2(t_i) = (c(t_{i-1}, t_i))^{-1} \cdot \chi^2_d$.*

Concluding the description of the 'Analytic' case leaves us to mention that the case $\nu > 1$ is hardly relevant in practice since $\nu = 4\kappa\theta/\sigma^2 << 2$ (Andersen, 2008). However, it is good to know that the case exists since computation times can be significantly reduced (drawing a standard normal instead of a Poisson random variable) and switching between $\nu > 1$ and $\nu \leq 1$ is easily implemented should the case $\nu > 1$ apply at some point. Yet, if we are talking of the 'Analytic' scheme from here on after we mean the Algorithm 4.4 with $\nu \leq 1$.

4.1.4. Jump Component

Before introducing the full model with its risk components it appears necessary to give more theoretical insight to the underlying jump component of the model as well as efficient simulation algorithms thereof.

4.1.4.1. Model Definition

In Glasserman (2004) we find the theoretical basis for a jump-diffusion type model. A simple representation of a jump process is assumed in Definition 4.1.

Definition 4.1 (Jump-diffusion process). *The jump process J is given by*

$$J(t) = \sum_{j=1}^{N(t)} (Y_j - 1) \tag{4.30}$$

where $Y_1, Y_2, \ldots$ are random variables and $N(t)$ is a counting process. This means that there are random arrival times

$$0 < \tau_1 < \tau_2 < \cdots$$

and

$$N(t) = \sup\{n : \tau_n \leq t\}$$

counts the number of arrivals in $[0, t]$*. The size of a jump is* $Y_j - 1$ *if* $t = \tau_j$ *and 0 if* t *does not coincide with any of the* τ_j*.*

We now postulate a distribution for the underlying counting process $N(t)$ of the jump process $J(t)$ (Assumption 4.3).

Assumption 4.3. $N(t)$ *is a (homogeneous) Poisson process (having an underlying Poisson distribution) with rate* λt *(and constant* λ*).*

1. *Inter-arrival times are* $\tau_{j+1} - \tau_j$ *independent with a common exponential distribution*

$$\mathrm{Prob}(\tau_{j+1} - \tau_j \geq t) = 1 - \mathrm{e}^{-\lambda t}, \quad t \geq 0.$$

2. $\mathbb{E}[N(t)] = \mathbb{V}[N(t)] = \lambda t$ *(Expectation and variance are both dependent on time* t*.)*
3. Y_j *are i.i.d. and independent of* N*.*

Under Assumption 4.3, J is called a compound Poisson process. For Y_j we assume a log-normal distribution (Assumption 4.4). This choice goes back to Merton (1976), appointing tractability to the model as the product of a log-normal random variable is again log-normal (compare also Glasserman (2004)).

Assumption 4.4. *If* $Y_j \sim \mathrm{LN}(\mu, \sigma^2)$ *(so that* $\log Y_j \sim \mathrm{N}(\mu, \sigma^2)$*) then for any fixed* n*,*

$$\prod_{j=1}^{n} Y_j \sim \mathrm{LN}(n\mu, n\sigma^2).$$

Since we are modelling under the risk neutral measure we need to show that the underlying compound jump process is a martingale. Therefore we borrow the general Property 4.1 from Glasserman (2004).

Property 4.1. *A standard property of the Poisson process is that* $N(t) - \lambda t$ *(a 'compensated Poisson process' with* $\mathbb{E}[N(t) - \lambda t] = 0$*) is a martingale. A generalisation of this property is*

$$\sum_{i=1}^{N(t)} h(Y_j) - \lambda \mathbb{E}[h(Y)]t,$$

being a martingale for i.i.d. Y*,* Y_1*,* Y_2 *and any function* h *for which* $\mathbb{E}[h(Y)]$ *is finite. Accordingly, the process*

$$J(t) - \lambda v t$$

is a martingale if $v = \mathbb{E}[Y_j] - 1$*.*

Certain Properties 4.2 can be deduced from the defined jump process wrt to Y_j and the models of $V(t)$ under Section 4.1.1, cf. (Glasserman, 2004).

Property 4.2.

1. *Y_j are the ratios of the asset price before and after a jump and jumps are multiplicative wrt $V(t)$.*
2. *The process $V(t)$ is continuous from the right.*
3. *By restricting Y_j to be positive random variables, the process $V(t)$ can never become negative.*

Remark 4.11. *Properties 4.2 imply (Glasserman, 2004):*
Right continuousness means

$$V(t) = \lim_{u \searrow t} V(u),$$

which contains the jump at time t and the value instantaneously before a jump takes on the limit

$$V(t-) = \lim_{u \nearrow t} V(u)$$

approaching from the left where $t-$ denotes the time just before a potential jump. The jump in V at τ_j is

$$V(\tau_j) - V(\tau_j-) = V(\tau_j-)[J(\tau_j) - J(\tau_j-)] = V(\tau_j-)(Y_j - 1),$$

so that

$$V(\tau_j) = V(\tau_j-)Y_j$$

which is equivalent to

$$\log(V(\tau_j)) = \log(V(\tau_j-)) + \log(Y_j).$$

This explains the $Y_j - 1$ term (rather than simply Y_j) in Definition 4.1. "$Y_j - 1$ random variable percentage change in the stock price if the Poisson event occurs", cf. (Merton, 1976).

Consequential from Definition 4.1, Assumption 4.3, Assumption 4.4 and Properties 4.2 we can write

$$\mathrm{d}J(t) = (Y(t) - 1)\mathrm{d}N(t) = \sum_{j=1}^{\mathrm{d}N(t)} (Y_j - 1),$$

as in models of $V(t)$ under Section 4.1.1, which stands for the jump at time t. Also the solutions to the SDEs of the generalised (with jump component) geometric Brownian motions can be stated by applying Itô's formula, namely

$$V(t) = V(0)\exp(X(t)) \prod_{j=1}^{N(t)} Y_j,$$

where:

- Merton (1974), respectively model (4.1), with constant interest rate and volatility:

$$X(t) = (r - \frac{1}{2}\sigma_V^2 - \lambda v)\mathrm{d}t + \sigma_V \mathrm{d}W_V^Q(t)$$

- Bates (1996), respectively model (4.2), with constant interest rate and stochastic volatility:

$$X(t) = (r - \frac{1}{2}\varsigma^2(t) - \lambda v)\mathrm{d}t + \varsigma(t)\mathrm{d}W_V^Q(t)$$

- Zhou (1997), respectively model (4.3), with stochastic interest rate and constant volatility:

$$X(t) = (r(t) - \frac{1}{2}\sigma_V^2 - \lambda v)\mathrm{d}t + \sigma_V \mathrm{d}W_V^Q(t)$$

- Zhou (2001), respectively model (4.4), with stochastic interest rate and volatility:

$$X(t) = (r(t) - \frac{1}{2}\varsigma^2(t) - \lambda v)\mathrm{d}t + \varsigma(t)\mathrm{d}W_V^Q(t).$$

4.1.4.2. Simulation

We now turn our focus on producing efficient algorithms for the jump component. From Section 4.1.3 we know that simulating with an underlying Poisson distribution (the non-central chi-squared distribution relies on drawing from a Poisson distribution) is slow. Evidently, the jump process of Definition 4.1 with Assumption 4.3 also draws random numbers from a Poisson distribution. Glasserman (2004) offers two standard algorithms (Algorithm 4.5 and Algorithm 4.6) in the context of the Poisson jump process which are slightly modified. The major difference between both algorithms is that once we simulate at fixed dates $0 = t_0 < t_1 < \cdots < t_n$ where the increment $N(t_{i+1}) - N(t_i)$ has a Poisson distribution with mean $\lambda(t_{i+1} - t_i)$ and each increment is independent of each other (Algorithm 4.5). The other simulates at jump times $\tau_1, \tau_2, \ldots$ and uses the fact that these are exponentially distributed (Algorithm 4.6).

Algorithm 4.5 (Poisson process — simulating at fixed dates). *Simulating from t_i to t_{i+1} consists of the following steps:*

1. *Generate $N \sim \mathrm{Po}(\lambda\Delta t)$ with mean $\lambda\Delta t$ where λ is the jump intensity and $\Delta t = t_{i+1} - t_i$ is the discretised time difference.*
2. *Generate $\log Y_j \sim \mathrm{N}(\mu, \sigma^2)$ for $j = \{1, \ldots, N\}$ and compute*

$$J(t_{i+1}) = \sum_{j=N(t_i)+1}^{N(t_{i+1})} \log Y_j,$$

with $Z \sim \mathrm{N}(0,1)$.

Algorithm 4.6 (Poisson process — simulating jump times). *Simulating at jump times $\tau_1, \tau_2, \ldots$ consists of the following steps:*

1. *Generate* $\Delta t = R_{j+1}$ *from the exponential distribution* $R_{j+1} \sim \mathrm{Exp}(\lambda)$ *with mean* $1/\lambda$ *and set* $t_{j+1} = t_j + R_{j+1}$.

2. *Generate* $\log Y_{j+1} \sim \mathrm{N}(\mu, \sigma^2)$ *and set* $J(t_{i+1}) = \log Y_{j+1}$.

Since Δt gets replaced by R_{j+1} in Algorithm 4.6 and consequently is dependent on λ, it is not further pursued as we want to keep an adequate discretisation of dt for the full process $V(t)$ under our control. We shall concentrate on Algorithm 4.5 where further advancements are made.

From an implementation and simulation perspective Algorithm 4.5 is inefficient as in every loop a new random variable N needs to be drawn with mean $\lambda\Delta t$. This issue is addressed by showing that the complete Poisson process up to time T, on the complete interval $[0, T]$, with arrival times $\tau_1, \tau_2, \ldots, \tau_n$ can be generated. The foundation for this idea is the 'order statistics property of the Poisson process', generally formulated in Theorem 4.4, with Lemma 4.1 (Mikosch, 2009). Corresponding proof of Theorem 4.4 is stated in Mikosch (2009).

Lemma 4.1 (Joint density of order statistics). *If the i.i.d.* X_i, $i = 1, \ldots, n$ *have density* f *then the density of the vector* $(X_{(1)}, \ldots, X_{(n)})$ *is given by*

$$f_{X_{(1)},\ldots,X_{(n)}}(x_1, \ldots, x_n) = n! \prod_{i=1}^{n} f(x_i) \mathbb{1}_{\{x_1 < \cdots < x_n\}}.$$

Theorem 4.4 (Order statistics property of the Poisson process). *Consider the Poisson process* $N = (N(T))_{T \geq 0}$ *with continuous a.e. positive intensity function* λ *and arrival times* $0 < \tau_1 < \tau_2 < \cdots$ *a.s. Then the conditional distribution of* $(\tau_1, \ldots, \tau_n)$ *given* $\{N(T) = n\}$ *is the distribution of the ordered sample* $(X_{(1)}, \ldots, X_{(n)})$ *of an i.i.d. sample* $X_1, \ldots, X_n$ *with common density* $\lambda(x)/\mu(T)$, $0 < x \leq T$*:*

$$(\tau_1, \ldots, \tau_n \,|\, N(T) = n) \stackrel{d}{=} (X_{(1)}, \ldots, X_{(n)}).$$

In other words, the left-hand vector has the conditional density

$$f_{\tau_1,\ldots,\tau_n}(x_1, \ldots, x_n \,|\, N(T) = n) = \frac{n!}{(\mu(T))^n} \prod_{i=1}^{n} \lambda(x_i), \quad 0 < x_1 < \cdots < x_n < T$$

where μ *is the linear mean value function.*

In the case of a homogeneous Poisson process, with $\mu(T) = \lambda T$, intensity $\lambda > 0$ and arrival times τ_i, $i = 1, \ldots, n$, the joint conditional density amounts to

$$f_{\tau_1,\ldots,\tau_n}(x_1, \ldots, x_n \,|\, N(T) = n) = \frac{n!}{T^n}, \quad 0 < x_1 < \cdots < x_n < T, \tag{4.31}$$

resulting from Theorem 4.4. From Lemma 4.1 it follows that (4.31) resembles the joint density of a uniform ordered sample $X_{(1)}, \ldots, X_{(n)}$ of $X_1, \ldots, X_n \stackrel{iid}{\sim} \mathrm{unif}(0, T)$ with

$$f(x_1, x_2, \ldots, x_n) = \frac{1}{T^n}, \quad 0 < x_1 < \cdots < x_n < T$$

because each X_i has the density function $1/T$ and are independent. Conclusively, given that the number of arrivals in $[0, T]$ is n, it follows that the arrival times $\tau_1, \ldots, \tau_n$ are jointly distributed as an ordered random sample of size n from a $\text{unif}(0, T)$ distribution. It is also important to note that this property is independent of the jump rate λ. With the result from Theorem 4.4 we can rewrite Algorithm 4.5 to Algorithm 4.7 (compare also Korn et al. (2010, p. 312)).

Algorithm 4.7 (Poisson process). *Simulating a Poisson process at rate λ up to time T consists of following steps:*

1. *Determine number of event occurrences on the complete interval $[0, T]$, by:*
   a) *Generate $N(T) \sim \text{Po}(\lambda T)$ with mean λT.*
   b) *Generate $U_1, \ldots, U_{N(T)} \overset{iid}{\sim} \text{unif}(0, T)$.*
   c) *Sort in ascending order to obtain the order statistics $U_{(1)} < U_{(2)} < \cdots < U_{(N(T))}$ and set $t_i = U_{(i)}$, $i \in \{1, \ldots, N(T)\}$.*
2. *Generate $\log(Y_1, \ldots, Y_{N(T)}) \sim \text{N}(\mu, \sigma^2)$ and assign to each corresponding t_i, $i = \{1, \ldots, N(T)\}$. Compute the compound Poisson process (over all time points in the interval [0,T]).*

Evident from Table 4.3, a significant reduction in computation time (by a factor of over 400) can be achieved by Algorithm 4.7 for the compound Poisson process, as opposed to Algorithm 4.5. Even when utilising Matlab's loop avoidance functions, e.g. `arrayfun()` the inferior Algorithm 4.5 could not be improved. An example of a Poisson process, and its corresponding (homogeneous) Poisson process is depicted in Figure 4.6 where five path realisations are generated, based on Algorithm 4.7. On the left picture solely the arrivals are displayed while the right picture also includes the compounded jump heights from a log-normal distribution. The interval on which the arrivals occur is $[0, 1]$ (one year with 252 business days) and the intensity is given by $\lambda = 20$, so that $\mathbb{E}[N(T)] = \lambda T = 20 \cdot 1 = 20$. Thereby, due to Theorem 4.4, the arrivals are distributed according to an ordered sample from an i.i.d. $\text{unif}(0, 1)$ sequence on each path. Lastly, we seek to improve the drawing of random numbers from the Poisson distribution directly wrt to generation time. Again we refer to Glasserman (2004) where an alternative Algorithm 4.8 is given based on the inverse transformation method.

Algorithm 4.8 (Inverse transformation method — Poisson distribution). *For discrete distributions the inverse transformation method amounts to the sequential search for the smallest n at which $F(n) \leq U$, where F denotes the cumulative distribution function and $U \sim \text{unif}(0, 1)$. In the case of a Poisson distribution, $F(n)$ is calculated as $\text{Prob}(N = 0) + \cdots + \text{Prob}(N = n)$; rather than calculating each term in this sum we can use the relation $\text{Prob}(N = k + 1) = \text{Prob}(N = k)\lambda/(k + 1)$. This leads to following algorithm:*

1. *Set $p = \exp(-\lambda)$, $F = p$ and $N = 0$.*
2. *Generate $U \sim \text{unif}(0, 1)$.*
3. *Compute loop*

   while *$U > F$*

$N = N + 1$; $p = p\lambda/N$; $F = F + p$;

return N.

We compare Algorithm 4.8 MATLAB's inbuilt random number generator function of the Poisson distribution `poissrnd()`. Results are displayed in TABLE 4.4 where 100 repetitions were run to obtain the average time. Concluding, using Algorithm 4.8 one can potentially further reduce the computation time in TABLE 4.3 of the already highly efficient Algorithm 4.7 by a factor of 2.

	Algorithm 4.5	Algorithm 4.7
Time (sec)	38.66	0.09

TABLE 4.3.: Comparison of Poisson process algorithms with $T = 7$ and $\Delta t = 0.004$, totalling 1,764 time points. 1,000 paths were generated for each algorithm in this experiment.

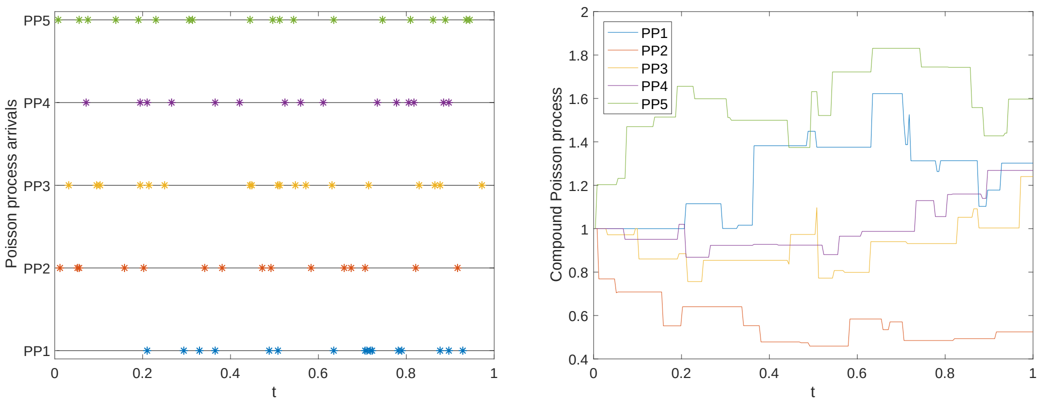

FIGURE 4.6.: Five paths of a Poisson process on interval $[0, 1]$ and $\lambda = 20$, based on Algorithm 4.7. Left: Arrivals of a Poisson process; Right: Compound Poisson process, with $\mu = 0$ and $\sigma = 0.1$.

	MATLAB	Algorithm 4.8
Time (sec)	4.49	2.13

TABLE 4.4.: Comparison of Poisson random variables drawing with 100,000 numbers

4.1.5. Full Model

All model components are summarised here and notations are adapted to make these components distinguishable. Thereby, we resort to the theoretical groundwork provided by Section 3.7.3, Section 4.1.1, Section 4.1.2, Section 4.1.3 and Section 4.1.4. Sünderhauf (2006) incorporates the following risk factors:

Interest rate risk Fluctuating interest rates let bonds be exposed to certain market risks. The balance sheet position values of Section 3.6 are also sensitive to interest rate changes in the market, depending on the time to maturity and coupon rate. Due to the current market situation with interest rates being close or below zero and other model cirteria derived in Section B.2.5 we resort to the HW1F. HW1F is also the choice of Sünderhauf (2006). In order to distinguish model parameters, the Hull-White model parameters are denoted as κ_r (mean reversion speed) and σ_r (volatility level). The Brownian motion is reformulated as $\mathrm{d}W_r^{\mathcal{Q}}(t)$.

Volatility risk The Cox-Ingersoll-Ross (CIR) model (Cox et al., 1985) in Section 4.1.3 is widely used for incorporating stochastic volatilities, see Hull and White (1988). It is popular for modelling volatilities for the simple reason of its property of non-negativity. We expand the notation of Section 4.1.3 to $\varsigma_x(t)$ for $x \in \{OA, CP\}$. κ_{ς_x} denotes the mean reversion speed, θ_{ς_x} the mean reversion level and σ_{ς_x} the volatility level being the model parameters (> 0), whereas $\mathrm{d}W_{\varsigma_x}^{\mathcal{Q}}(t)$ represents the Brownian motion, for $x \in \{OA, CP\}$. Motivating stochastic time-dependent volatilities, as opposed to a constant parameter, arises from the assumption that "also the volatilities of assets returns are exposed to unexpected fluctuations", cf. (Sünderhauf, 2006).

Credit risk The creditworthiness of a financial intermediate is expressed by the state variable process $V_x(t)$, for $x \in \{OA, CP\}$. The complete state variable process consists of a interest rate, a variance and a jump process where the drift is adjusted by $-\lambda_x v_x$ (see Section 4.1.1.1 for further details). The jump process is constructed by, firstly,

- a Poisson process, denoted by $\mathrm{d}N_x(t)$ with intensity $\lambda_x \geq 0$, for $x \in \{OA, CP\}$ and secondly,
- the corresponding jump size is log-normally distributed with $\ln[Y_x(t)] \overset{\text{iid}}{\sim} \mathrm{N}\left(\mu_{Y_x}, \sigma_{Y_x}^2\right)$, where $v_x = \mathbb{E}_Q[Y_x(t) - 1] = \exp\left(\mu_{Y_x} + 0.5\sigma_{Y_x}^2\right) - 1$ and $\sigma_{Y_x}^2 \geq 0$, for $x \in \{OA, CP\}$.

In summary, the underlying jump-diffusion process accounts for marginal fluctuations of a mortgage Pfandbrief bank's asset values which are caused by 'normal' market developments and exogenous economical conditions. Ad-hoc announcements may have extraordinary high impacts on the bank's asset values which are characterised by the jump process. The arrival of important new information can consist of, for example, a judicial decision or other legal amendments concerning the bank's business, with positive or negative outcome for a Pfandbrief bank. Furthermore, we are particularly interested in the downside risk of assets (losses on the asset side will negatively affect the liability side, see Section 3.6). This can be accomplished by assigning a negative sign to the mean jump size parameter μ_{Y_x}.

Correlation risk The dependencies between given independent Brownian motions $\mathrm{d}\widetilde{W}_r^{\mathcal{Q}}(t)$, $\mathrm{d}\widetilde{W}_{\varsigma_{OA}}^{\mathcal{Q}}(t)$, $\mathrm{d}\widetilde{W}_{\varsigma_{CP}}^{\mathcal{Q}}(t)$, $\mathrm{d}\widetilde{W}_{V_{OA}}^{\mathcal{Q}}(t)$ and $\mathrm{d}\widetilde{W}_{V_{CP}}^{\mathcal{Q}}(t)$ are also considered. For incorporating the dependencies between Brownian motions a Cholesky decomposition of the correlation matrix $\boldsymbol{R} = \boldsymbol{L}\boldsymbol{L}^\top$, being a positive semidefinite matrix, needs to be conducted which is then multiplied by the Brownian motions. Also following Sünderhauf (2006) the processes $\mathrm{d}N_x(t)$ and $Y_x(t)$ are independent as well as $\mathrm{d}\widetilde{W}_r^{\mathcal{Q}}(t)$, $\mathrm{d}\widetilde{W}_{\varsigma_x}^{\mathcal{Q}}(t)$ and $\mathrm{d}\widetilde{W}_{V_x}^{\mathcal{Q}}(t)$ with $\mathrm{d}N_x(t)$ and $Y_x(t)$, for $x \in \{OA, CP\}$.

The full model, under the risk neutral measure $\mathcal{Q}$ with the cash account numeraire, in a vectorised formulation results to

$$\mathrm{d}\begin{pmatrix} r(t) \\ \varsigma_{OA}^2(t) \\ \varsigma_{CP}^2(t) \\ V_{OA}(t) \\ V_{CP}(t) \end{pmatrix} = \begin{pmatrix} [\theta_r(t) - \kappa_r r(t)] \\ \kappa_{\varsigma_{OA}}\left[\theta_{\varsigma_{OA}} - \varsigma_{OA}^2(t)\right] \\ \kappa_{\varsigma_{CP}}\left[\theta_{\varsigma_{CP}} - \varsigma_{CP}^2(t)\right] \\ V_{OA}(t)\left[r(t) - \lambda_{OA} v_{OA}\right] \\ V_{CP}(t)\left[r(t) - \lambda_{CP} v_{CP}\right] \end{pmatrix} \mathrm{d}t + \begin{pmatrix} \sigma_r \\ \sigma_{\varsigma_{OA}}\sqrt{\varsigma_{OA}^2(t)} \\ \sigma_{\varsigma_{CP}}\sqrt{\varsigma_{CP}^2(t)} \\ V_{OA}(t)\varsigma_{OA}(t) \\ V_{CP}(t)\varsigma_{CP}(t) \end{pmatrix} \circ \begin{pmatrix} \mathrm{d}W_r^{\mathcal{Q}}(t) \\ \mathrm{d}W_{\varsigma_{OA}}^{\mathcal{Q}}(t) \\ \mathrm{d}W_{\varsigma_{CP}}^{\mathcal{Q}}(t) \\ \mathrm{d}W_{V_{OA}}^{\mathcal{Q}}(t) \\ \mathrm{d}W_{V_{CP}}^{\mathcal{Q}}(t) \end{pmatrix} + \begin{pmatrix} 0 \\ 0 \\ 0 \\ V_{OA}\left[Y_{OA}(t) - 1\right]\mathrm{d}N_{OA}(t) \\ V_{CP}\left[Y_{CP}(t) - 1\right]\mathrm{d}N_{CP}(t) \end{pmatrix} \tag{4.32}$$

where $\circ$ represents the Hadamard product and

$$\begin{pmatrix} \mathrm{d}W_r^{\mathcal{Q}}(t) \\ \mathrm{d}W_{\varsigma_{OA}}^{\mathcal{Q}}(t) \\ \mathrm{d}W_{\varsigma_{CP}}^{\mathcal{Q}}(t) \\ \mathrm{d}W_{V_{OA}}^{\mathcal{Q}}(t) \\ \mathrm{d}W_{V_{CP}}^{\mathcal{Q}}(t) \end{pmatrix} = \mathrm{chol}(\boldsymbol{R})\mathrm{d}t \cdot \begin{pmatrix} \mathrm{d}\widetilde{W}_r^{\mathcal{Q}}(t) \\ \mathrm{d}\widetilde{W}_{\varsigma_{OA}}^{\mathcal{Q}}(t) \\ \mathrm{d}\widetilde{W}_{\varsigma_{CP}}^{\mathcal{Q}}(t) \\ \mathrm{d}\widetilde{W}_{V_{OA}}^{\mathcal{Q}}(t) \\ \mathrm{d}\widetilde{W}_{V_{CP}}^{\mathcal{Q}}(t) \end{pmatrix},$$

with

$$\boldsymbol{R} = \begin{pmatrix} 1 & \rho_{r,\varsigma_{OA}} & \rho_{r,\varsigma_{CP}} & \rho_{r,V_{OA}} & \rho_{r,V_{CP}} \\ \rho_{\varsigma_{OA},r} & 1 & \rho_{\varsigma_{OA},\varsigma_{CP}} & \rho_{\varsigma_{OA},V_{OA}} & \rho_{\varsigma_{OA},V_{CP}} \\ \rho_{\varsigma_{CP},r} & \rho_{\varsigma_{CP},\varsigma_{OA}} & 1 & \rho_{\varsigma_{CP},V_{OA}} & \rho_{\varsigma_{CP},V_{CP}} \\ \rho_{V_{OA},r} & \rho_{V_{OA},\varsigma_{OA}} & \rho_{V_{OA},\varsigma_{CP}} & 1 & \rho_{V_{OA},V_{CP}} \\ \rho_{V_{CP},r} & \rho_{V_{CP},\varsigma_{OA}} & \rho_{V_{CP},\varsigma_{CP}} & \rho_{V_{CP},V_{OA}} & 1 \end{pmatrix}.$$

Note that for each state variable process the jump process needs to be added, i.e. $[Y_x(t) - 1]\,\mathrm{d}N_x(t)$ for $x \in \{OA, CP\}$.
Concluding, we state which methods have proven to be advantageous, so far, in simulating (4.32) appropriately and we propose to use. For the interest rate component we can simulate the HW1F with the exact solution of (3.22) generating normally distributed short rates as defined in (3.18) at no noteworthy computational cost. The jump component is best simulated under Algorithm 4.7 hugely reducing the computational burden, compared to the conventional method of Algorithm 4.5. Optionally, one can additionally enhance Algorithm 4.7 by making use of Algorithm 4.8 depending on the software used. When simulating the CIR1F model the choice of algorithm is a bit ambiguous due to the trade off between accuracy and speed. However, two methods stand out, namely the 'Milstein-Implicit' and 'Quadratic-Exponential' schemes. When one prefers speed over accuracy then 'Milstein-Implicit' is the better option, otherwise, 'Quadratic-Exponential' represents a rational choice wrt to speed and accuracy.

4.2. Alternative Measures

It may become desirable to represent model (4.32) in different measures, as modelling narratives might change. We will derive SDEs of (4.32) in

- T_2-forward (martingale) measure ($\mathcal{Q}_{T_2}$), and

· real-world (objective) measure ($\mathcal{P}$).

In general, changes of measure in continuous time affects the drift part of the SDE. Thus, a suitable numeraire needs to be found for the drift term which is represented by the HW1F interest rate model (Section 3.7.3). In order to find this numeraire, we make use of Girsanov's Theorem B.4. Note that under Assumption 4.1 the jump component (Section 4.1.4) is unaffected by the change of measure since the jump process is independent from the market. Consequently, parameters of the jump amplitude and frequency are the same under $\mathcal{Q}$, $\mathcal{Q}_{T_2}$ and $\mathcal{P}$.
For illustration purposes, we consider the three dimensional stochastic process where the dynamics of the processes $r(t)$, $\varsigma_x^2(t)$ and $V_x(t)$ can also be expressed in terms of three independent Brownian motions $\widetilde{W}_r^{\mathcal{Q}}(t)$, $\widetilde{W}_{\varsigma_x}^{\mathcal{Q}}(t)$ and $\widetilde{W}_{V_x}^{\mathcal{Q}}(t)$ with $x \in \{CP, OA\}$ (Cholesky decomposition) where

$$
\begin{aligned}
\boldsymbol{R} &= \begin{pmatrix} 1 & \rho_{r,\varsigma_x} & \rho_{r,V_x} \\ \rho_{\varsigma_x,r} & 1 & \rho_{\varsigma_x,V_x} \\ \rho_{V_x,r} & \rho_{V_x,\varsigma_x} & 1 \end{pmatrix} \\
&= \begin{pmatrix} l_{11} & 0 & 0 \\ l_{21} & l_{22} & 0 \\ l_{31} & l_{32} & l_{33} \end{pmatrix} \begin{pmatrix} l_{11} & l_{12} & l_{13} \\ 0 & l_{22} & l_{23} \\ 0 & 0 & l_{33} \end{pmatrix} \\
&= \boldsymbol{L}\boldsymbol{L}^\top,
\end{aligned}
$$

with

$$
\begin{aligned}
l_{11} &= 1, \\
l_{22} &= \sqrt{1-\rho_{\varsigma_x,r}^2}, \\
l_{33} &= \sqrt{1-\left(\rho_{V_x,r}^2 + \frac{1}{\sqrt{1-\rho_{\varsigma_x,r}^2}}(\rho_{V_x,\varsigma_x} - \rho_{V_x,r}\rho_{\varsigma_x,r})\right)}
\end{aligned}
$$

and

$$
\begin{aligned}
l_{21} &= \rho_{\varsigma_x,r} \\
l_{31} &= \rho_{V_x,r} \\
l_{32} &= \frac{1}{\sqrt{1-\rho_{\varsigma_x,r}^2}}(\rho_{V_x,\varsigma_x} - \rho_{V_x,r}\rho_{\varsigma_x,r})
\end{aligned}
$$

so that

$$
\begin{aligned}
\mathrm{d}W_r^{\mathcal{Q}}(t) &= \mathrm{d}\widetilde{W}_r^{\mathcal{Q}}(t), \\
\mathrm{d}W_{\varsigma_x}^{\mathcal{Q}}(t) &= \rho_{\varsigma_x,r}\mathrm{d}\widetilde{W}_r^{\mathcal{Q}}(t) + \sqrt{1-\rho_{\varsigma_x,r}^2}\,\mathrm{d}\widetilde{W}_{\varsigma_x}^{\mathcal{Q}}(t) \\
\mathrm{d}W_{V_x}^{\mathcal{Q}}(t) &= \rho_{V_x,r}\mathrm{d}\widetilde{W}_r^{\mathcal{Q}}(t) + \frac{1}{\sqrt{1-\rho_{\varsigma_x,r}^2}}(\rho_{V_x,\varsigma_x} - \rho_{V_x,r}\rho_{\varsigma_x,r})\mathrm{d}\widetilde{W}_{\varsigma_x}^{\mathcal{Q}}(t) + \\
&\quad \sqrt{1-\left(\rho_{V_x,r}^2 + \frac{1}{\sqrt{1-\rho_{\varsigma_x,r}^2}}(\rho_{V_x,\varsigma_x} - \rho_{V_x,r}\rho_{\varsigma_x,r})\right)}\,\mathrm{d}\widetilde{W}_{V_x}^{\mathcal{Q}}(t).
\end{aligned} \tag{4.33}
$$

This decomposition makes it easier to perform a measure change where the above dependent Brownian motions (4.33) are inserted in our underlying state variable process of (4.32) which is reformulated to

$$\begin{aligned} \mathrm{d}r(t) &= (\theta_r(t) - \kappa_r r(t))\mathrm{d}t + \sigma_r \mathrm{d}W_r^{\mathcal{Q}}(t) \\ \mathrm{d}\varsigma_x^2(t) &= \kappa_{\varsigma_x}(\theta_{\varsigma_x} - \varsigma_x^2(t))\mathrm{d}t + \sigma_{\varsigma_x}\sqrt{\varsigma_x^2(t)}\mathrm{d}W_{\varsigma_x}^{\mathcal{Q}}(t) \\ \mathrm{d}V_x(t) &= V_x(t)\left[(r(t) - \lambda_x v_x)\mathrm{d}t + \varsigma_x(t)\mathrm{d}W_{V_x}^{\mathcal{Q}}(t) + (Y_x(t)-1)\mathrm{d}N_x(t)\right]. \end{aligned} \tag{4.34}$$

Remark 4.12. *The complete procedure can easily be extended to the five dimensional case of (4.32) for deriving the forward and real-world measures. In the following only the tree-dimensional cases are considered (for illustration purposes).*

4.2.1. Forward Measure

Suppose $V_{CP}(T_2, T_2)$ is a $\mathcal{F}_{T_2}$-measurable random variable of some future cover pool value. Further, we restrict the σ-field to $\mathcal{F}_{T_1}$. Then according to Definition B.14 in Appendix B.2.2 we have

$$\frac{\mathrm{d}\mathcal{Q}_{T_2}}{\mathrm{d}\mathcal{Q}} = \frac{P(T_2,T_2)B(0)}{P(0,T_2)B(T_2)} = \frac{\exp\left(-\int_0^{T_2} r(u)\mathrm{d}u\right)}{P(0,T_2)}$$

and under the T_2-forward (martingale) measure we can rewrite the structural asset pricing formula (3.5) to

$$\begin{aligned} V_{CP}(T_1,T_2) &= B_{T_1}\mathbb{E}_{\mathcal{Q}}\left(B_{T_2}^{-1}V_{CP}(T_2,T_2)\,\Big|\,\mathcal{F}_{T_1}\right) \\ &= P(T_1,T_2)\mathbb{E}_{\mathcal{Q}_{T_2}}\left(V_{CP}(T_2,T_2)\,|\,\mathcal{F}_{T_1}\right), \end{aligned}$$

with $T_1 \leq T_2$. Computing the expectation under the forward measure allows us to discount by multiplying with $P(T_1, T_2)$. The apparent result simplifies matters since discounting now is of deterministic nature, thus simulating a discount factor as it is the case in the risk-neutral setting (where the numeraire is a bank account process as in Definition B.5), becomes unnecessary. The numeraire, in form of the discount factor $P(T_1, T_2)$, may then be observed in the market.
Following Brigo and Mercurio (2007) we can define a process x,

$$\mathrm{d}x(t) = -\kappa_r x(t)\mathrm{d}t + \sigma_r \mathrm{d}W_r^{\mathcal{Q}}(t), \quad x(0) = 0,$$

and by integrating we have for each $s < t$,

$$x(t) = x(s)\mathrm{e}^{-\kappa_r(t-s)} + \sigma_r\int_s^t \mathrm{e}^{-\kappa_r(t-u)}\mathrm{d}W^{\mathcal{Q}}(u),$$

so that with (3.21), (3.20) is the sum of

$$r(t) = x(t) + \alpha(t)$$

for each t. Furthermore, we borrow the following solution of the integral

$$\int_t^{T_2} x(u)\mathrm{d}u = \frac{1-\mathrm{e}^{-\kappa_r(T_2-t)}}{\kappa_r} x(t) + \frac{\sigma_r}{\kappa_r} \int_t^{T_2} \left(1-\mathrm{e}^{-\kappa_r(T_2-u)}\right) \mathrm{d}W^{\mathcal{Q}}(u) \tag{4.35}$$

from Brigo and Mercurio (2007). By denoting by $f^M(0,T_2)$ as the instantaneous forward rate at time 0 for a maturity T_2 implied by the term structure $T_2 \to P^M(0,T_2)$ we also have

$$\alpha(T_2) = f^M(0,T_2) + \frac{\sigma_r^2}{2\kappa_r^2}\left(1-\mathrm{e}^{-\kappa_r T_2}\right)^2, \tag{4.36}$$

in order to exactly fit the observed term structure, see also (3.21). Having all ingredients we need, with (4.35) and (4.36), we can derive the change of measure from risk neutral to T_2-forward measure, based on Brigo and Mercurio (2007). Applying the probability measure, defined by the Radon-Nikodym derivative above, gives us

$$\begin{aligned}
\frac{\mathrm{d}\mathcal{Q}_{T_2}}{\mathrm{d}\mathcal{Q}} &= \frac{\exp\left(-\int_0^{T_2} r(u)\mathrm{d}u\right)}{P(0,T_2)} \\
&= \frac{\exp\left(-\int_0^{T_2} x(u)\mathrm{d}u - \int_0^{T_2} \alpha(u)\mathrm{d}u\right)}{P(0,T_2)} \\
&= \exp\left(-\frac{\sigma_r}{\kappa_r}\int_0^{T_2}\left(1-\mathrm{e}^{-\kappa_r(T_2-u)}\right)\mathrm{d}\widetilde{W}_r^{\mathcal{Q}}(u) - \int_0^{T_2}\frac{\sigma_r^2}{2\kappa_r^2}\left(1-\mathrm{e}^{-\kappa_r u}\right)^2\mathrm{d}u\right)\cdot \\
&\qquad \frac{\exp\left(-\int_0^{T_2} f^M(0,u)\mathrm{d}u\right)}{P(0,T_2)} \\
&= \exp\left(-\frac{\sigma_r}{\kappa_r}\int_0^{T_2}\left(1-\mathrm{e}^{-\kappa_r(T_2-u)}\right)\mathrm{d}\widetilde{W}_r^{\mathcal{Q}}(u) - \right. \\
&\qquad \left. \int_0^{T_2}\frac{\sigma_r^2}{2\kappa_r^2}\left(1-\mathrm{e}^{-\kappa_r(T_2-u)}\right)^2\mathrm{d}u\right),
\end{aligned} \tag{4.37}$$

as with $t=0$ it follows that $x(0)=0$ and from Definition B.13 we know that $P^M(0,T_2) = \exp\left(-\int_0^{T_2} f^M(0,u)\mathrm{d}u\right)$. Further, substitution of $(1-\mathrm{e}^{-\kappa_r u})^2$ with $\left(1-\mathrm{e}^{-\kappa_r(T_2-u)}\right)^2$ takes place in the last integral (not affecting the integration outcome).
Girsanov's Theorem B.4 yields the independent Brownian motions $\widetilde{W}_r^{\mathcal{Q}_{T_2}}$, $\widetilde{W}_{\varsigma_x}^{\mathcal{Q}_{T_2}}$ and $\widetilde{W}_{V_x}^{\mathcal{Q}_{T_2}}$, defined by

$$\begin{aligned}
\mathrm{d}\widetilde{W}_r^{\mathcal{Q}_{T_2}}(t) &= \mathrm{d}\widetilde{W}_r^{\mathcal{Q}}(t) + \frac{\sigma_r}{\kappa_r}\left(1-\mathrm{e}^{-\kappa_r(T_2-t)}\right)\mathrm{d}t \\
&= \mathrm{d}\widetilde{W}_r^{\mathcal{Q}}(t) + \sigma_r B_r(t,T_2)\mathrm{d}t \\
\mathrm{d}\widetilde{W}_{\varsigma_x}^{\mathcal{Q}_{T_2}}(t) &= \mathrm{d}\widetilde{W}_{\varsigma_x}^{\mathcal{Q}}(t) \\
\mathrm{d}\widetilde{W}_{V_x}^{\mathcal{Q}_{T_2}}(t) &= \mathrm{d}\widetilde{W}_{V_x}^{\mathcal{Q}}(t).
\end{aligned} \tag{4.38}$$

Finally, by inserting (4.33) and (4.38) into (4.34) the joint dynamics of r, ς_x^2 and V_x under $\mathcal{Q}_{T_2}$ are

$$
\begin{aligned}
\mathrm{d}r(t) &= (\theta_r(t) - \kappa_r r(t) - \sigma_r^2 B_r(t,T_2))\mathrm{d}t + \sigma_r \mathrm{d}W_r^{\mathcal{Q}_{T_2}}(t),\\
\mathrm{d}\varsigma_x^2(t) &= \left[\kappa_{\varsigma_x}(\theta_{\varsigma_x} - \varsigma_x^2(t)) - \sigma_r B_r(t,T_2)\rho_{\varsigma_x r}\sigma_{\varsigma_x}\sqrt{\varsigma_x^2(t)}\right]\mathrm{d}t + \\
&\qquad\qquad\qquad\qquad \sigma_{\varsigma_x}\sqrt{\varsigma_x^2(t)}\mathrm{d}W_{\varsigma_x}^{\mathcal{Q}_{T_2}}(t),\\
\mathrm{d}V_x(t) &= V_x(t)\left[r(t) - \lambda_x v_x - \sigma_r B_r(t,T_2)\rho_{V_x r}\varsigma_x(t)\right]\mathrm{d}t + \\
&\qquad\qquad V_x(t)\varsigma_x(t)\mathrm{d}W_{V_x}^{\mathcal{Q}_{T_2}}(t) + V_x(t)(Y_x(t)-1)\mathrm{d}N_x(t).
\end{aligned}
\tag{4.39}
$$

4.2.2. Real-World Measure

Simulating under the real-world measure is useful when real-world based assessments are desired which can be obtained individually by a Pfandbrief bank. The aim is to uncover real-world (or actual) probabilities of the Pfandbrief, since under the risk-neutral valuation default probabilities are overestimated. The main reason for this deviation is that risk-neutral probabilities compensate investors for their unobservable aversion to bad outcomes. With the help of Girsanov's theorem (Theorem B.4) we can derive a SDE under the real-world measure $\mathcal{P}$ from the risk-neutral measure $\mathcal{Q}$ by applying a change of measure to the drift term. Thereby, we set $\mathrm{d}W^{\mathcal{Q}}(t) = \mathrm{d}W^{\mathcal{P}}(t) - \varphi(t)$ where φ denotes the market price of risk[4]. With the findings of Section B.2.4.2 for the HW1F model we can reformulate the independent Brownian motions $\widetilde{W}_r^{\mathcal{P}}$, $\widetilde{W}_{\varsigma_x}^{\mathcal{P}}$ and $\widetilde{W}_{V_x}^{\mathcal{P}}$ at first, defined by

$$
\begin{aligned}
\mathrm{d}\widetilde{W}_r^{\mathcal{P}}(t) &= \mathrm{d}\widetilde{W}_r^{\mathcal{Q}}(t) + \varphi r(t)\mathrm{d}t\\
\mathrm{d}\widetilde{W}_{\varsigma_x}^{\mathcal{P}}(t) &= \mathrm{d}\widetilde{W}_{\varsigma_x}^{\mathcal{Q}}(t)\\
\mathrm{d}\widetilde{W}_{V_x}^{\mathcal{P}}(t) &= \mathrm{d}\widetilde{W}_{V_x}^{\mathcal{Q}}(t)
\end{aligned}
\tag{4.40}
$$

By inserting (4.33) and (4.40) into (4.34) the joint dynamics of r, ς_x^2 and V_x under $\mathcal{P}$ are

$$
\begin{aligned}
\mathrm{d}r(t) &= [\theta_r(t) - (\kappa_r + \sigma_r\varphi)r(t)]\mathrm{d}t + \sigma_r \mathrm{d}W_r^{\mathcal{P}}(t)\\
\mathrm{d}\varsigma_x^2(t) &= \left[\kappa_{\varsigma_x}(\theta_{\varsigma_x} - \varsigma_x^2(t)) - \varphi r(t)\rho_{\varsigma_x r}\sigma_{\varsigma_x}\sqrt{\varsigma_x^2(t)}\right]\mathrm{d}t + \sigma_{\varsigma_x}\sqrt{\varsigma_x^2(t)}\mathrm{d}W_{\varsigma_x}^{\mathcal{P}}(t)\\
\mathrm{d}V_x(t) &= V_x(t)\left[r(t)(1 - \varphi\rho_{V_x r}\varsigma_x(t)) - \lambda_x v_x\right]\mathrm{d}t + \\
&\qquad\qquad V_x(t)\varsigma_x(t)\mathrm{d}W_{V_x}^{\mathcal{P}}(t) + V_x(t)(Y_x(t)-1)\mathrm{d}N_x(t).
\end{aligned}
\tag{4.41}
$$

4.3. Monte Carlo Simulation

Due to the continuous development of computers and, therefore, computational power and memory storage, it has become feasible to compute complex problems via Monte Carlo simulations. Moreover, in the area of finance this approach has become more

[4]Note the following relationship between the market price of risk (φ) the Girsanov kernel ($\mathfrak{g}$): $\varphi(t) = -\mathfrak{g}(t)$.

and more significant over, at least, the past three decades. Particularly, in the case of underlying models without closed form solutions, practically, no other real alternatives exist to Monte Carlo. A first application of Monte Carlo, specifically, in the field of (corporate) finance is attributed to Hertz (1964). In this work we shall utilise Monte Carlo in the form of

- nested Monte Carlo (NMC), and
- least square Monte Carlo (LSMC).

4.3.1. Nested Monte Carlo (NMC)

For obtaining the asset (A) present values at maturity T_1 of model (4.32), denoted by formulas (3.5) and (3.8) a nested Monte Carlo (NMC) simulation is conducted (as depicted in FIGURE 4.7). Here l paths are generated until maturity of liabilities T_1 and from there, for each ith path another m paths until maturity of assets T_2. The conditional expectation (3.5) can then be easily computed by calculating the mean after discounting by the risk-free interest rate. Note that the nested case of FIGURE 4.7 only applies to the cover pool (CP).

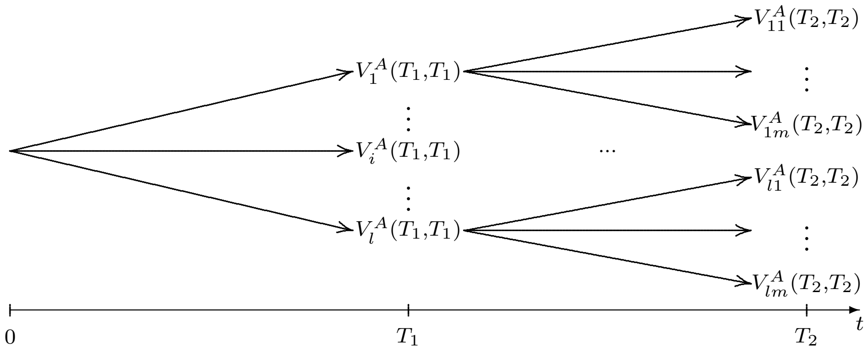

FIGURE 4.7.: Illustration of a nested Monte Carlo simulation setting. The other asset (OA) positions mature at time T_1 and the cover pool (CP) positions mature at time T_2, with $i = 1, \ldots, l$ and $j = 1, \ldots, m$ being the number of paths and $t = 0, \ldots, T_1, \ldots, T_2$, with $0 \leq T_1 \leq T_2$ being the time index.

4.3.1.1. Application

A stylised example of the complete procedure, including the modelling of the liability side, of applying the structural model in a NMC setting can be seen in Example 4.2. It is stylised in the sense that no real data of a Pfandbrief bank's balance sheet or according to §28 PfandBG is taken into account and parameters are chosen with the basic scenario set defined by Sünderhauf (2006) in TABLE C.14. So far the application can be summarised in three steps in order to obtain information on creditworthiness of the Pfandbrief which are graphically accompanied in Example 4.2. Here, as depicted in FIGURE 4.10 of Example 4.2, no defaults occurred for the Pfandbrief (PB) position, most other liability (OL) creditors are fully paid out and equity (EQ) also receives some incoming cash flows (compare also the waterfall default scheme of Figure 3.2). Ideally, this is how it should be from an investor's perspective. However, at a later stage we shall also consider real data and apply different scenarios by stressing the parameter set of Table C.14 to selected Pfandbrief banks.

Example 4.2 (Application of structural model (stylised)). *Applying the structural model (in a NMC setting) consists of three basic steps:*

1. *Simulate model (4.32) with basic scenario parameter set of* Table *C.14. Therefore, we choose $l = 10,000$ and $m = 100$ numbers of paths (see* Figure *4.7) so that we hold a vector of 10,000 at T_1 values for $V_{CP}(T_1, T_2)$ and $V_{OA}(T_1)$. For illustration purposes the depiction of the simulated paths is thinned out to $l = 10$ and $m = 3$ in* Figure *4.8. Shown as dashed red lines, we set the nominal $N_{CP} = 1$ and simulate $V_{OA}(T_1)$ only to T_1.*

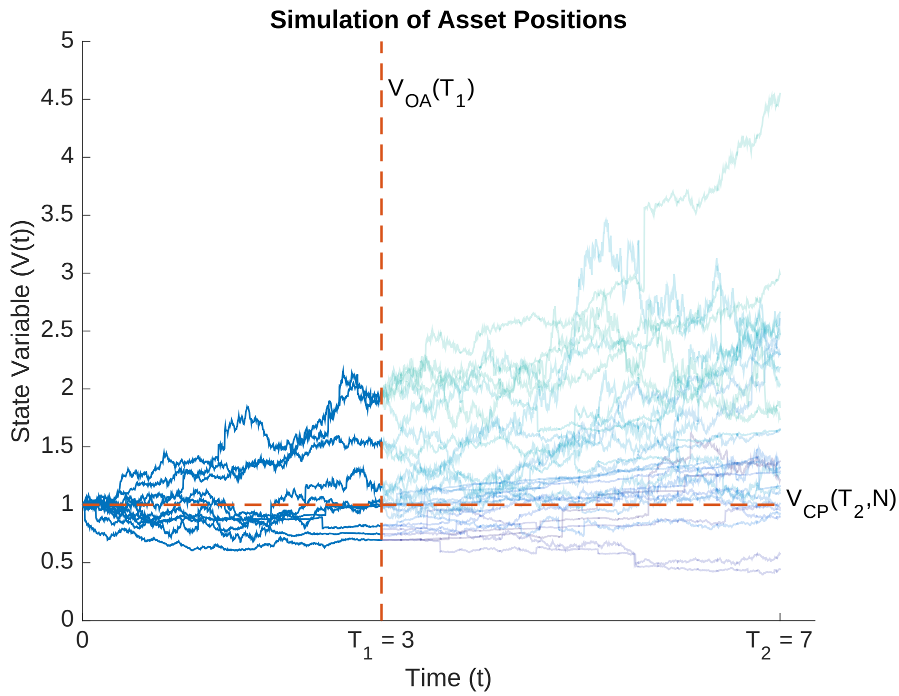

Figure 4.8.: NMC simulation of $V_{CP}(t)$ and $V_{OA}(t)$ in model (4.32) with $t \in [0, T_2]$

2. *Apply formulas (3.5) and (3.8). In T_1 (*Figure *4.9) we obtain the joint asset distribution with marginals cover pool ($V_{CP}(T_1, T_2)$) and other assets ($V_{OA}(T_1)$).*

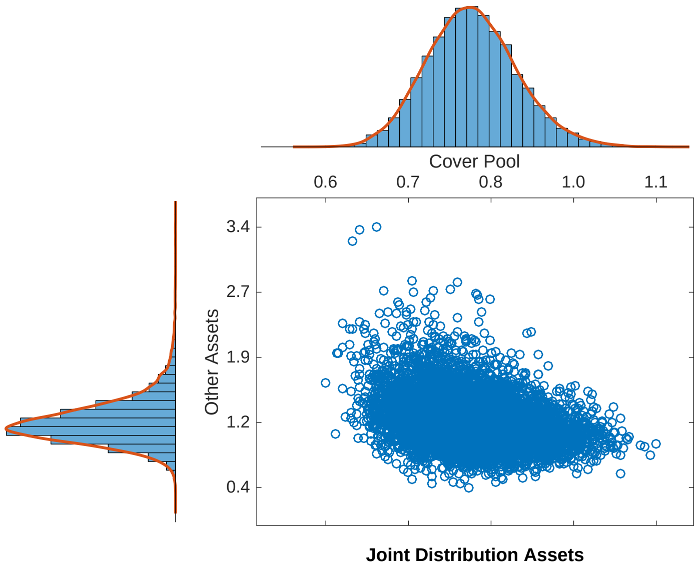

FIGURE 4.9.: Joint asset distribution with marginals cover pool (3.5) and other assets (3.8) at time T_1

3. *Apply formulas (3.11), (3.14) and (3.15), with $N_{PB} = 1$ and $N_{OL} = 1$. In T_1 (FIGURE 4.10) the desired output of the liability present values are received for further default assessments.*

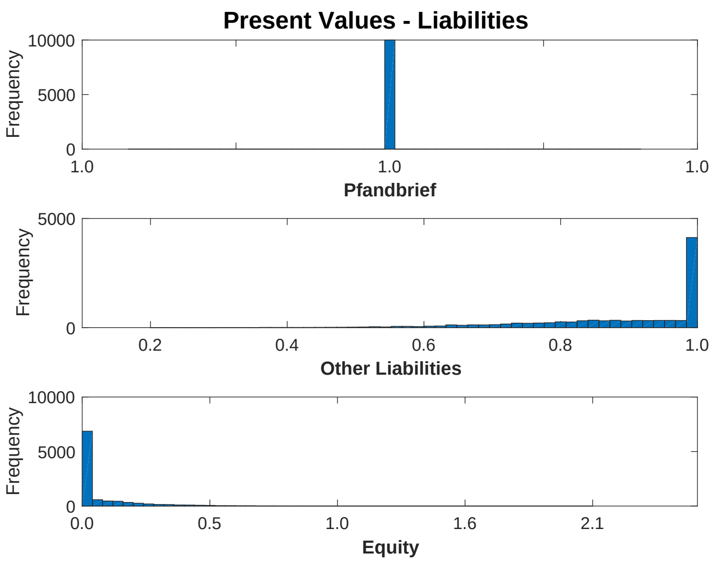

FIGURE 4.10.: Liability present values of Pfandbrief (3.11), other liabilities (3.14) and equity (3.15) at time T_1

4.3.1.2. Code Efficiency

NMC, also known as Monte Carlo on Monte Carlo, may become numerically cumbersome, evident from FIGURE 4.7. In general, but even more so in a nested path generation setting, it is crucial constructing efficient simulation environments. We already have significantly enhanced algorithms regarding the CIR1F model (Section 4.1.3.2) and jump process (Section 4.1.4.2) from a mathematical standpoint. Additionally, we will now give some insights on efficient programming, respectively an object oriented implementation yielding satisfactory results wrt computation times and code readability. We shall illustrate the object oriented implementation proposal by applying a NMC simulation to the CP position (since only CP is simulated until T_2). For reasons of clarity and comprehensibility, the most important code snippets are presented in an aggregated manner rather than displaying the complete source code, due to the complexity of model (4.32). Thus, the pseudo code in MATLAB's programming language is not executable. Firstly, we can easily expand the preparatory work of Appendix A.2 to an additional dimension which is required for the interval $[T_1, T_2]$ (compare FIGURE 4.7). We define an array of dimension $((T_2 - T_1) * \frac{1}{\Delta t} \times m \times l)$ for each process object `objIR` $(r(t))$, `objVola` $(\varsigma^2_{CP}(t))$, `objJump` $(N_{CP}(t))$ and `objStateVar` $(V_{CP}(t))$.
For $\texttt{X} \in \{\texttt{IR}, \texttt{Vola}, \texttt{StateVar}\}$ some preparations need to be made first. Drawing standard normal random numbers of dimension $((T_2 - T_1) * \frac{1}{\Delta t} \times m \times l)$ and computing the Wiener process increments of `objIR`, `objVola` and `objStateVar` prior to any time costly computations (e.g. loops) will further enhance the implementation. For simplifying matters we assume that the Brownian motions of model (4.32) are independent for now.

```
% Preallocate storage
procX = nan(nTimeSteps,nPathsNested,nPaths);
% Draw random numbers and compute Wiener increments
wienerX = randn(nTimeSteps,nPathsNested,nPaths)*deltat;
```

Similarly, for the `objJump` process we draw over the complete interval $[T_1, T_2]$ (compare Algorithm 4.7), resulting in computational gains as stated in TABLE 4.3.

```
% Draw random numbers
poissRN = poissrnd(intensity*(T2 - T1),nPathsNested,nPaths);
```

An object oriented programming implies that each process, `objIR`, `objVola`, `objJump` and `objStateVar` is wrapped in its own function where the processes are generated. Thereby, each function goes through the basic steps of preallocating storage, drawing random numbers and assigning the initial values of each process before any computation of the respective model are handled. Exemplary, this is shown by means of the `objIR` object (compare also Example A.2 in Appendix A.2.2).

```
function irProc = objIR(nTimeSteps,nPathsNested,nPaths,initialValue,deltat
    ,...)
   % Preallocate storage
   irProc = nan(nTimeSteps,nPathsNested,nPaths);
   % Assign initial value
   irProc(1,:,:) = repmat(initialValue',nPathsNested,1);
   % Draw random numbers and compute Wiener increments
   wienerIR = randn(nTimeSteps,nPathsNested,nPaths)*deltat;

   % Generate short rates (here Euler discretisation)
```

```
   for i = 2:nTimeSteps
      irProc(i,:,:) = irProc(i-1,:,:) + ...;
   end

% eof
end
```

For the state `objStateVar` the situation is slightly different, as it depends on the processes `objIR`, `objVola` and `objJump` which can be generated independently of each other. A `for` loop over time is not necessary for `objStateVar`, as shown for the simplified Example A.3 in Appendix A.2.2.

```
function stateVarProc = objStateVar(procIR,procVola,procJump,...)
   % Preallocate storage
   stateVarProc = nan(nTimeSteps,nPathsNested,nPaths);
   % Assign initial value
   stateVarProc(1,:,:) = repmat(log(initialValue)',nPathsNested,1);
   % Draw random numbers
   wienerStateVar = randn(nTimeSteps,nPathsNested,nPaths)*deltat;

   % Generate state variables
   stateVarProc(2:end,:,:) = ...;
   stateVarProc = exp(cumsum(stateVarProc));

% eof
end
```

Lastly, a code parallelisation[5] is suggested for further code optimisation. The `parfor` loop allows to parallelise any statements contained within. Since `objIR`, `objVola` and `objJump` are independent we are able to call the underlying processes in an efficient parallelisation environment.

```
% Call process objects via parallelised loop
parfor loopvar = 1:3
   % Call interest rate object
   procIR = objIR(...);
   % Call volatility object
   procVola = objVola(...);
   % Call jump object
   procJump = objJump(...);
end
```

Remark 4.13. *Above implementation proposal can easily be alternated so that correlated Brownian motions can be modelled too. Simply, draw the standard normal random numbers outside of each function of the objects `objIR`, `objVola` and `objStateVar`. Compute the Cholesky decomposition of the correlation matrix and multiply with the Brownian increments at each time step t. Then the correlated $((T_2 - T_1) * \frac{1}{\Delta t} \times m \times l)$ dimensional Brownian increments, `wienerCorrIR`, `wienerCorrVola` and `wienerCorrStateVar`, can be passed on as additional function argument of the corresponding object, for example:*

```
function volaProc = objVola(...,wienerCorrVola,...)
   ...
```

[5]Note that parallelisation depends on MATLAB's Parallel Computing Toolbox™.

```
% eof
end
```

Concluding, from above example it becomes evident that combining the findings of Appendix A.2 with an object oriented implementation yields an efficient programming style wrt functional and modular design, readability and, most importantly, computational time. Alternatively, one could also implement (4.32) in one big loop over time. This, however would not take advantage of complete vectorisation nor parallelisation techniques. Furthermore, object oriented programming (OOP) allows one to recycle any object to be used in any other type of model, setting or framework.

4.3.2. Least Square Monte Carlo (LSMC)

An alternative to the NMC simulation above (Section 4.3.1) is the least square Monte Carlo (LSMC) approach which is the method utilised by Sünderhauf (2006). The main advantage is that it is only necessary to simulate l paths for the complete interval $[0, T_2]$ (compare FIGURE 4.7). However, being an approximation over the nested paths, a loss in accuracy has to be accounted for. An example of the complete procedure and more details on the LSMC method itself is given in the seminal work of Longstaff and Schwartz (2001).
In the case of modelling a bank's default in the one-period setting and having a Markovian process, Equation (3.5) is embedded in the general regression equation

$$\underbrace{\mathbb{E}_{\mathcal{Q}}\left[\frac{B_{T_1}}{B_{T_2}}\min\left[N_{CP}; V_{CP}(T_2,T_2)\right]\,\middle|\, X_{T_1}\right]}_{\mathbb{E}[Y\,|\,X_{T_1}]} = \underbrace{\sum_{k=0}^{p}\beta_k f_k(V_{CP}(T_1,T_1), r(T_1), \varsigma^2_{CP}(T_1))}_{C(\cdot)}, \quad (4.42)$$

where $f_k(\cdot),\ k = 0,\dots,p$ are the predictor functions with $V_{CP}(T_1,T_1)$, $r(T_1)$ and $\varsigma^2_{CP}(T_1)$ as arguments (see also FIGURE 4.11). Subsequently, one minimises the residuals, being the difference of the dependent variable ($Y \in \mathbb{R}$) and independent variables ($X_{T_1} \in \mathbb{R}^{p+1}$)

$$\min_{\beta_k}\left\| \frac{B_{T_1}}{B_{T_2}}\min\left[N_{CP}; V_{CP}(T_2,T_2)\right] - \sum_{k=0}^{p}\beta_k f_k(V_{CP}(T_1,T_1), r(T_1), \varsigma^2_{CP}(T_1))\right\|_2^2. \quad (4.43)$$

In more detail, we model the conditional expectation $\mathbb{E}[Y\,|\,X_{T_1}]$ of Y (dependent on covariates X_{T_1}), thus the expectation is a function of covariates denoted by $\mathbb{E}[Y\,|\,X_{T_1}] = C(X_{T_1})$ (see Equation (4.42)). The dependent variable Y can be decomposed in $Y = \mathbb{E}[Y\,|\,X_{T_1}] + \epsilon = C(X_{T_1}) + \epsilon$ where in the (classical) linear regression model the residuals ϵ (non explainable deviation) are normally distributed with $\mathbb{E}[\epsilon_i] = 0$ and $\mathbb{V}[\epsilon_i] = \sigma^2$ for $i = 1,\dots,l$ observations. Further, the (least squares) minimisation problem of the residuals with $\beta_k \in \mathbb{R}$ can be formulated as $\min\limits_{\beta_k}\|Y - C(X_{T_1})\|_2^2$ (see Equation (4.43)), since $\epsilon = Y - C(X_{T_1})$.
Once each $\hat\beta_k$, $k = 0,\dots,p$ has been determined, the conditional expectation $\mathbb{E}[Y\,|\,X_{T_1}]$ of (4.42) can easily be computed. The vector of fitted values can be computed with $\hat y = \sum_{k=0}^{p}\hat\beta_k f_k(V_{CP}(T_1,T_1), r(T_1), \varsigma^2_{CP}(T_1))$ yielding the desired cover pool values $V_{CP}^{LSMC}(T_1,T_2)$. So far we have not made any assumptions for $f_k(\cdot),\ k = 0,\dots,p$.

Longstaff and Schwartz (2001) resorts to basis functions, here referring to factored polynomial equations in a linear function, as a suitable choice. Clearly, the overall success of the regression-based approach depends on the choice of the constellation of the predictor $f_k(\cdot),\ k = 0, \ldots, p$ with its basis functions. This issue shall be addressed in what follows and can be regarded as extensions to the LSMC approach in Sünderhauf (2006).
Expected improvements of the overall LSMC fit may be achieved by resorting to

1. higher polynomial degrees and additional variables for $f_k(\cdot),\ k = 0, \ldots, p$,

2. alternative basis functions $f_k(\cdot),\ k = 0, \ldots, p$, or

3. alternative regression methods,

or a combination of all. To test these proposals, a robustness analysis of the LSMC method is conducted in the following. Thereby, the obtained LSMC values from Equation (4.43) are compared to the values from the NMC simulation which are interpreted as 'true' values at time T_1. The

· root mean squared error (RMSE) $\left(\frac{1}{l}\sum_{i=1}^{l}\left(V_{i\,CP}^{\mathrm{NMC}}(T_1,T_2) - V_{i\,CP}^{\mathrm{LSMC}}(T_1,T_2)\right)^2\right)^{1/2}$ and

· coefficient of determination (R^2) from regressing the LSMC values to the NMC values with $V_{CP}^{\mathrm{NMC}}(T_1,T_2) = \beta_0 + \beta_1 V_{CP}^{\mathrm{LSMC}}(T_1,T_2) + \epsilon$

are calculated as the reference measures.
The procedure is as follows. The full NMC is conducted as in Figure 4.7 with $l = 10,000$ and $m = 100$, generating 1,000,000 paths in total. At T_2, 10,000 paths are randomly drawn from the 1,000,000 paths simulated, on which the LSMC method is applied. Subsequently, the LSMC values are compared to the 'true' NMC values at T_1 (which are discounted from T_2 in a previous step). Initially, computations are based on the basis parameter set defined in Table C.14. In order to obtain additional insight into the behaviour of the underlying LSMC methods, variance and jump parameters are stressed which are given in Table 4.5.
Regarding the used regression method, in general, a removal procedure is implemented. If covariates with linear dependence are present then these are simply filtered and the corresponding coefficients are set to zero, else a standard linear regression is conducted. This way the effected covariates are removed when multiplying with the vector of coefficients. This procedure is based on the orthogonal-triangular decomposition and is referred to 'removal of covariates' throughout the analysis, if not stated otherwise.

	$\varsigma_{CP}^2(0)$	$\theta_{\varsigma CP}$	$\kappa_{\varsigma CP}$	$\sigma_{\varsigma CP}$	λ_{CP}
Stressed I	0.06	0.06	-	-	1
Stressed II	0.09	0.09	1	1	1

Table 4.5.: Stressed sets for variance and jump process parameters, while all other parameters in Table C.14 remain unchanged.

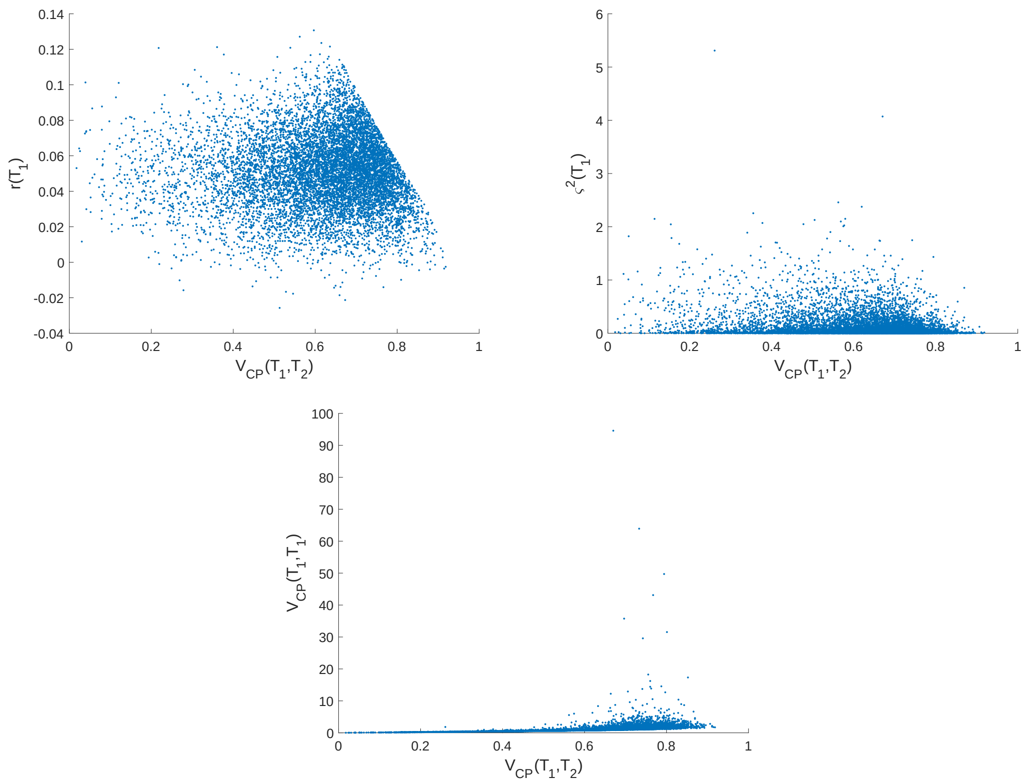

FIGURE 4.11.: Cover pool present values $V_{CP}(T_1, T_2)$ vs covariates; top left: $V_{CP}(T_1, T_2)$ vs $r(T_1)$; top right: $V_{CP}(T_1, T_2)$ vs $\varsigma^2(T_1)$; bottom middle: $V_{CP}(T_1, T_2)$ vs $V_{CP}(T_1, T_1)$

4.3.2.1. Polynomial Degrees and Variables

The power basis function $W_n(x) = x^n$ with $n = 2$ is the proposed polynomial[6] of Sünderhauf (2006) where V and r are inserted as arguments[7]. The suggested solution is analysed wrt the NMC values and compared to the following adjustments. Arising from the general regression formulas (4.42) and (4.43) a third variable, the stochastic variance (ς^2), is additionally considered in the regression, in conjunction with higher polynomial degrees as basis functions. Each regression model has an intercept denoted by c and interaction combinations of the corresponding input variables (V, r) or (V, r, ς^2) are allowed.

At first a benchmark computation based on the basic parameter set adopted from Sünderhauf (2006) in TABLE C.14 is performed. FIGURE 4.12 depicts the LSMC performances of $W_n(x)$, in the form of RMSE (left side) and R^2 (right side) with $n = 1, \ldots 5$, where also the sets of $x = \{V, r\}$ and $x = \{V, r, \varsigma^2\}$ are compared. As expected the LSMC fit improves with higher degree and by inserting the stochastic variance which achieves an (almost) parallel shift in performance.

Next, a direct comparison of $W_2(V, r)$ (model proposed by Sünderhauf (2006)) and $W_5(V, r, \varsigma^2)$ (best model so far) to the NMC values in FIGURE 4.13 is conducted. Arguably, the differences between $W_2(V, r)$ and $W_5(V, r, \varsigma^2)$ may seem negligible at first

[6]The polynomial degree n is to be interpreted in an accumulated sense, e.g. if $n = 2$ this also includes the terms 0 and 1, i.e. all terms up until $n = 2$, if not explicitly stated otherwise.

[7]For the sake of brevity a simpler notation, omitting CP and $t = T_1$, is used.

sight. However, when deviating slightly from the basis parameter set given in Table C.14 by stressing the variance and jump parameters to ‘Stressed I’ from Table 4.5, it becomes more evident in Figure 4.14 that $W_2(V, r)$ cannot sufficiently match the ‘true’ NMC values while $W_5(V, r, \varsigma^2)$ remains widely insensitive to the parameter change. Larger deviations to the ‘true’ values can be explained by the higher fluctuations in the generated simulation paths which largely can be compensated for by considering the corresponding variance, ς^2, as additional explanatory variable in the regression (4.43). Concluding, basis functions of higher polynomial degree perform better than lower. Certainly, by increasing the polynomial degree ($n \to \infty$) one might eventually receive a perfect fit. Moreover, taking the variance variable (V, r, ς^2) into account, instead of only two (V, r), optimises the overall fit.

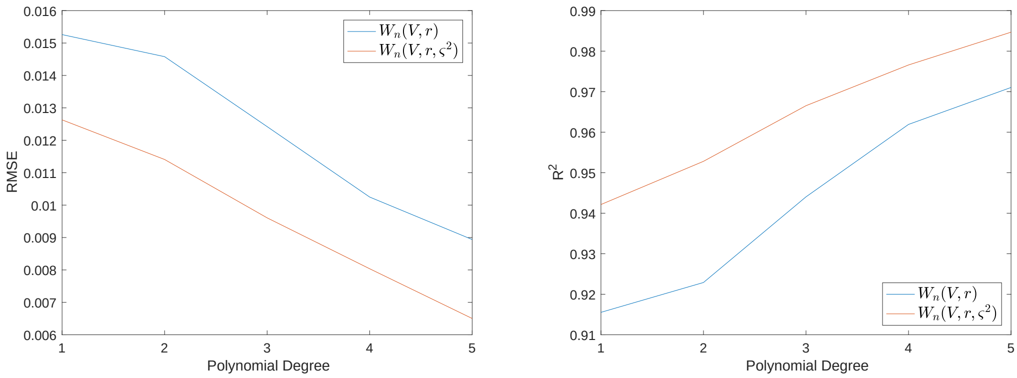

Figure 4.12.: LSMC results of $W_n(x)$ for $n = 1, \ldots, 5$, $x = \{V, r\}$ for the two variable case and $x = \{V, r, \varsigma^2\}$ for the three variable case, with basis parameter set in Table C.14 and $l = 10,000$ simulation paths.

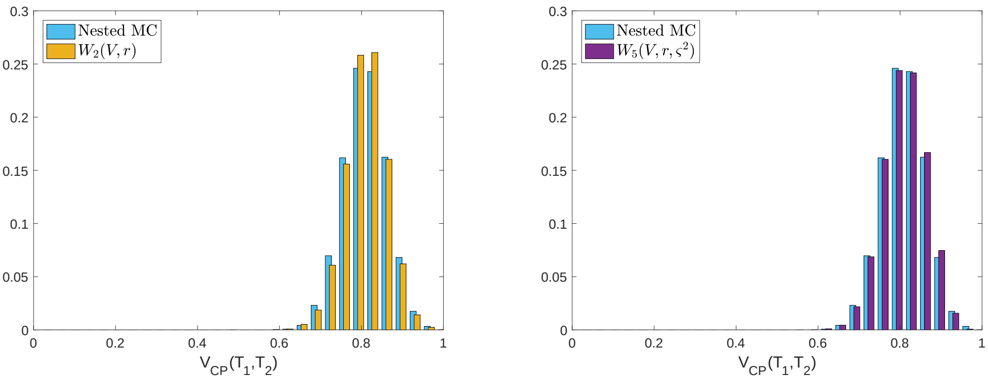

Figure 4.13.: LSMC results of $W_2(V, r)$ and $W_5(V, r, \varsigma^2)$ compared to NMC, with basis parameter set in Table C.14 and $l = 10,000$ simulation paths.

4.3.2.2. Basis Functions

The best-known and widely used basis functions are, apart from the power function ($W_n(x)$) in Section 4.3.2.1, Laguerre, Legendre, Hermite and Chebyshev which are in-

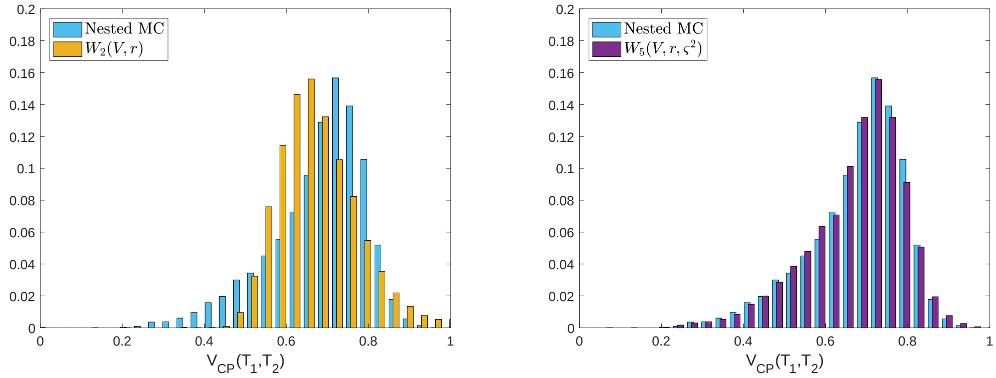

FIGURE 4.14.: LSMC results of $W_2(V, r)$ and $W_5(V, r, \varsigma^2)$ compared to NMC based on the basis parameter set in TABLE C.14 with stressed parameters $\varsigma^2_{CP}(0) = \theta_{\varsigma_{CP}} = 0.06$ and $\lambda_{CP} = 1$ ('Stressed I' set of TABLE 4.5) and $l = 10,000$ simulation paths.

troduced in TABLE 4.6 in the Rodrigues representation:

$$f_n(x) = \frac{1}{a_n g(x)} \frac{\mathrm{d}^n}{\mathrm{d}x^n} \left[p(x) \left(g(x)\right)^n\right].$$

Further, the polynomials of TABLE 4.6 are weighted by $\exp(-x/2)$, as proposed by Longstaff and Schwartz (2001)). For example, the first three Laguerre polynomials amount to

$$\begin{aligned}
P_0(x) &= \exp\left(-\frac{x}{2}\right)\\
P_1(x) &= \exp\left(-\frac{x}{2}\right)(1-x)\\
P_2(x) &= \exp\left(-\frac{x}{2}\right)\left(1-2x+\frac{x^2}{2}\right).
\end{aligned}$$

In Section 4.3.2.1 we established that the three variable case in general performs better. Therefore, the basis function comparisons are based on $x = \{V, r, \varsigma^2\}$. The weighted polynomial functions of TABLE 4.6 improve the regression fit compared to the simple power functions. However, no significant differences can be seen between the basis functions of TABLE 4.6 (all functions lie on each other).
Concluding, the basis functions in TABLE 4.6 manage to obtain fairly reasonable results already for low polynomial degrees, so that a less complex regression function (less covariates) for Equation (4.43) seems feasible. For example, $W_5(x)$ has a similar outcome as $P_2(x)$, with $x = \{V, r, \varsigma^2\}$.

4.3.2.3. Regression Methods

Multicollinearity poses an issue wrt the usage of basis functions as linear dependence arises, especially with high n. Repeating similar transformations of the underlying variable will eventually yield a singular regressor matrix. Without addressing this issue the regression can lead to distorted (very large) coefficients, resulting in completely different

Family	$f_n(x)$	a_n	$p(x)$	$g(x)$
Laguerre	$P_n(x)$	$(-1)^n 2^n n!$	1	$1-x^2$
Legendre	$L_n(x)$	$n!$	e^{-x}	x
Hermite	$H_n(x)$	$(-1)^n$	e^{-x^2}	1
Chebyshev	$T_n(x)$	$(-1)^n 2^n \frac{\Gamma(n+\frac{1}{2})}{\sqrt{\pi}}$	$(1-x^2)^{-1/2}$	$1-x^2$

TABLE 4.6.: Basis functions in the Rodrigues representation, compare Moreno and Navas (2003).

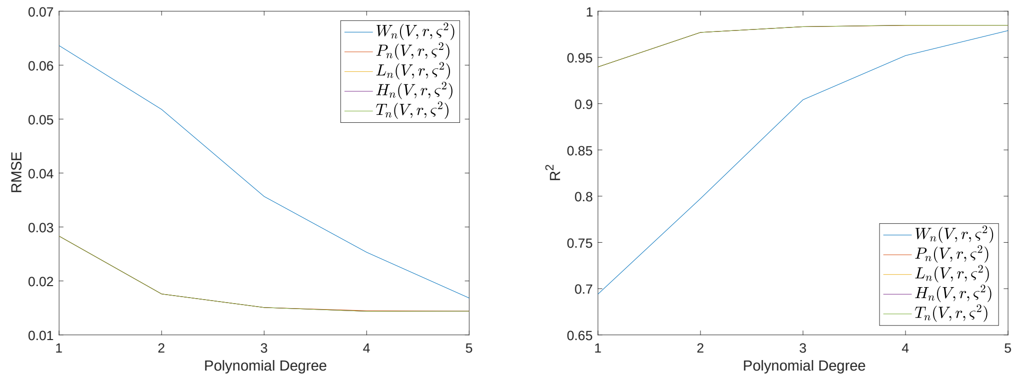

FIGURE 4.15.: LSMC results of various basis functions ($W_n(x)$, $P_n(x)$, $L_n(x)$, $H_n(x)$ and $T_n(x)$) for $n = 1,\dots,5$ and $x = \{V, r, \varsigma^2\}$ for the three variable case, based on the basis parameter set in TABLE C.14 with stressed parameters $\varsigma^2_{CP}(0) = \theta_{\varsigma_{CP}} = 0.06$ and $\lambda_{CP} = 1$ ('Stressed I' set of TABLE 4.5) and $l = 10,000$ simulation paths.

predicted values than expected, thus the LSMC approximation might fail. A desired solution would be to establish a regression procedure guaranteeing:

1. The method yields a stable solution and is easy to use.
2. Any collinearity can be precluded.
3. The optimal solution is found for any given set of covariates (dependent on the inserted variables, basis functions and number of terms), while at the same time keeping the complexity of the regression equation low.

Here are four proposed solutions, amongst others, of handling high correlation in between covariates (for a more detailed description, see Draper and Smith (1998), Fahrmeir et al. (1996) and Fahrmeir et al. (2013)).

Singular value decomposition (SVD) regression Here the design matrix is decomposed into two orthogonal and one diagonal matrix. One needs to find the low rank approximation in terms of the SVD of the design matrix. This method is used by Moreno and Navas (2003) to overcome the cases where singular matrices are existent.

Principle component regression (PCR) An also widely used technique, where the regressors are orthogonally transformed in space while at the same time maximising the variance described by the covariates and resulting in independent variables, called principle components.

Partial least squares regression (PLSR) Similarly to PCR, it projects the covariates into a new space, but additionally does this with the predictor variable, by finding the direction for explaining the maximum of variance.

Stepwise regression Starting with an initial model the stepwise regression will add or remove covariates incrementally to then compare the explanatory power of the previous with the updated model. This is done by comparing the F-statics, Akaike information criterion (AIC) or Bayesian information criterion (BIC), in each step.

Now it is the objective to compare above regression techniques on the Laguerre $P_n(V, r, \varsigma^2)$ function (from the results in Section 4.3.2.2, any of the functions in TABLE 4.6 would be suitable). Therefore, the variance process parameters are stressed with 'Stressed II' from TABLE 4.5. The visual results are given in FIGURE 4.16 where the methods 'Removal', 'SVD', 'PLSR' and 'PCR' do not differ to a large amount, so that any would deliver a fairly reasonable fit[8]. As can be inferred from FIGURE 4.16 the gain in accuracy for $n > 2$ is neglectable for the regression methods other than stepwise. The stepwise regression does not improve vastly for $n > 1$. A direct comparison of $P_2(V, r, \varsigma^2)$ with removal method and $P_1(V, r, \varsigma^2)$ with stepwise method is given in FIGURE 4.17 and their correspondong regression formulas in TABLE 4.7. It is worth while to also have

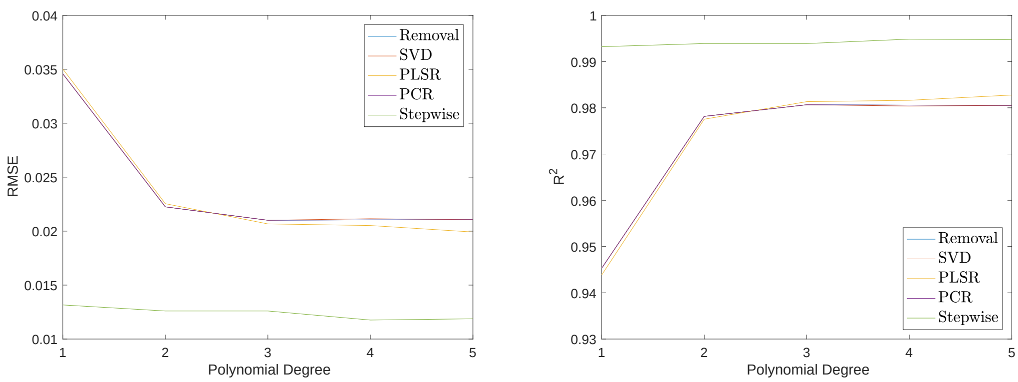

FIGURE 4.16.: LSMC results of various regression methods ('Removal', 'SVD', 'PLSR', 'PCR' and 'Step'), with $P_n(x)$ for $n = 1, \dots, 5$ and $x = \{V, r, \varsigma^2\}$ for the three variable case, based on the basis parameter set in TABLE C.14 with stressed parameters $\varsigma^2_{CP}(0) = \theta_{\varsigma CP} = 0.09$ and $\kappa_{\varsigma CP} = \sigma_{\varsigma CP} = \lambda_{CP} = 1$ ('Stressed II' set of TABLE 4.5) and $l = 10,000$ simulation paths.

a closer look at computation times of all regression methods. TABLE 4.8 summarises the times in seconds where as reference the NMC method is also given. Evidently, the NMC takes the longest, while the regression models reduce the computational burden significantly, but comes with loss in precision. In the end the decision on what to use, will remain a trade-off between accuracy and speed. As a reasonable compromise to, on the one hand make sure that the approximation is as accurate as possible and, on the other to have a relatively fast computation, one might opt for the stepwise regression[9].

[8]For the methods 'PLSR' and 'PCR' the full regression model with all covariates are considered.

[9]Surely, this would not apply to the conventional usage of the LSMC approximation for valuing American or other exotic options, as each time step needs to be considered, but may well be a solution

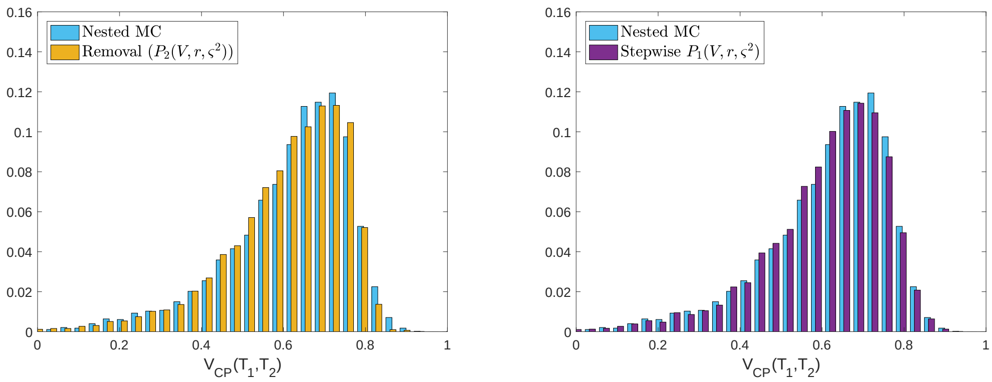

FIGURE 4.17.: LSMC results of $P_2(V, r, \varsigma^2)$ with removal method and $P_1(V, r, \varsigma^2)$ with stepwise method compared to NMC based on the basis parameter set in TABLE C.14 with stressed parameters $\varsigma^2_{CP}(0) = \theta_{\varsigma_{CP}} = 0.09$ and $\kappa_{\varsigma_{CP}} = \sigma_{\varsigma_{CP}} = \lambda_{CP} = 1$ ('Stressed II' set of TABLE 4.5) and $l = 10,000$ simulation paths.

	Formula	RMSE	R^2
Removal ($n = 2$)	$y \sim 1 + P_0(V) + P_1(V) + P_2(V) + P_0(r) + P_1(r) + P_2(r) + P_0(\varsigma^2) + P_1(\varsigma^2) + P_2(\varsigma^2) + V \cdot r + V \cdot \varsigma^2 + r \cdot \varsigma^2 + V \cdot r \cdot \varsigma^2$	0.0222	0.9781
Stepwise ($n = 1$)	$y \sim 1 + V \cdot r \cdot \varsigma^2 + P_1(V) * P_0(r) + P_1(V) * P_1(\varsigma^2) + P_0(r) * P_1(r) + P_0(r) * P_1(\varsigma^2) + P_1(r) * P_1(\varsigma^2)$	0.0132	0.9932

TABLE 4.7.: Comparison of LSMC methods removal and stepwise regression of $P_n(x)$ and $x = \{V, r, \varsigma^2\}$, for the three variable case, based on the basis parameter set in TABLE C.14 with stressed parameters $\varsigma^2_{CP}(0) = \theta_{\varsigma_{CP}} = 0.09$ and $\kappa_{\varsigma_{CP}} = \sigma_{\varsigma_{CP}} = \lambda_{CP} = 1$ ('Stressed II' set of TABLE 4.5) and $l = 10,000$ simulation paths. The expressions in the Formula column is based on Wilkinson notation for regression models (i.e. $a * b$ means $a, b, a \cdot b$ in standard notation and 1 is the intercept term).

Furthermore, the stepwise regression fulfills all three posed requirements from above. Also, during the analysis it could be observed that the methods 'SVD', 'PLSR' and 'PCR' did not deliver stable results all the time.
Lastly, this extensive analysis clearly suggests that a careful regression analysis needs to be conducted beforehand to obtain a sufficiently well approximation by the LSMC approach for any given parameter set.

	Removal	SVD	PLSR	PCR	Stepwise	Nested
Time (sec)	1.95	4.88	0.07	0.05	9.51	133.83

TABLE 4.8.: Computation times of the LSMC methods (Removal, SVD, PLSR, PCR, Stepwise) and NMC, for $n = 5$. All methods are based on generating $l = 10,000$ present values $t = T_1$ (the NMC generates another $m = 100$ for each i in the interval $[T_1, T_2]$).

for a one-period setting as is the case here.

4.4. Summary

Above review of Sünderhauf (2006)'s structural model has revealed the following improvements:

- A sound mathematical formulation of the underlying one-period Pfandbrief model is provided in Chapter 3, building the foundation of the structural modelling proposal. When discounting the cover pool's present values (3.5) to today, a change of measure is required to obtain the valuation formula (3.7).
- Embedding of the SDEs into the real-world and forward-measure for additional modelling flexibility and consistency are additionally considered, see Section 4.2.
- Enhanced simulation algorithms, particularly for the volatility component (Section 4.1.3) and jump component (Section 4.1.4), are implemented so that the computational burden is significantly reduced while at the the same time keeping accuracy high.
- Reassessing the LSMC technique (Section 4.3.2) has led to significant corrections in simulation accuracy compared to the 'true' simulated values of the NMC technique. Thereby, the inclusion of $\varsigma^2_{CP}(T_1)$ as independent variable, the utilisation of Laguerre polynomial functions and the application of the stepwise regression technique have proven to be the decisive factors in goodness-of-fit gains.
- Computation inefficiencies can be ruled out by exploiting given features, for example pre-allocation of storage, parallelisation and vector based programming in MATLAB's software environment, see Appendix A.2.

Of course, there exist many other modelling advancements when it comes to efficient simulation techniques. For example, various variance reduction techniques come to mind in order to enhance the efficiency of Monte Carlo simulation. For example, importance sampling, stratified sampling, moment matching methods or control variates are some of the methods (Glasserman, 2004). Tractable features of a model are presumed to be able to conduct adjustments or correct simulation outputs. Model (4.32) is by construction rather complex, thus applying any variance reduction technique could actually lead to no improvements at all without exactly knowing the starting point. In recent years, the alternative of quasi Monte Carlo has received greater attention. Compared to variance reduction techniques quasi Monte Carlo suppresses randomness in order to seek for more accuracy. Furthermore, from an implementation stand point it is easily realisable as the random numbers from the (ordinary) Monte Carlo simulation just need to be replaced. However, an initial implementation in combination with a Brownian bridge in combination with a Sobol sequence have not shown noteworthy improvements (compared to the gains under (Section 4.3.2) so that it has been omitted and left for future research.

5. Reduced-Form Model

The newly proposed model in the context of modelling the German Pfandbrief is introduced here. In general, we incorporate information on credit migrations into bond prices — a rating based approach. Before commencing on modelling aspects in greater depth we dedicate a motivational section on the idea of applying a reduced-form type of model. Next we give an initial and simplified version of the reduced-form model. Certain shortcomings of this simplification are identified and addressed which are revisited in proposed remedies in sections thereon. Some effort is dedicated to obtaining appropriate default probabilities and future scenarios. Furthermore, a large homogeneous portfolio is postulated reflecting the balance sheet's asset side of a Pfandbrief bank consisting of individual mortgages.

5.1. Motivation

A call for an innovative valuation model in the context of the Pfandbrief framework (Chapter 3) arises from three motivational aspects having the mutual goal of gaining improvements on risk assessments of the bank's cover pool and ultimately of the Pfandbrief product itself. Thereby, emphasis is laid upon asset default risk, the third most important cover pool associated risk according to Spangler and Werner (2014), see also Section 3.1. Firstly, modelling advancements are motivated from the insights gained in the review of the structural model proposed by Sünderhauf (2006). Secondly, we find that major rating agencies have advanced analysis tools implemented for assessing the credit quality of a Pfandbrief bank's cover pool in their covered bond rating methodologies which can be regarded as modelling standards. Thirdly, new developments in the covered bond, respectively, Pfandbrief market as well as in the banking and also real estate industry, along with imposed regulatory requirements, make a more refined modelling approach, particularly, of the cover pool necessary.

5.1.1. Modelling Advancements

From a modelling perspective the introduced structural based credit risk model of Chapter 4 relies on large-scale simulations which can potentially exhaust available resources. Without the modelling enhancements, for example, consisting of efficient algorithms introduced for the volatility component in Section 4.1.3 or for the jump component in Section 4.1.4 first simulations of model (4.32) applying the nested Monte Carlo approach in Section 4.3.1 amounted to several minutes. Although significant improvements wrt computational time have been accomplished the Monte Carlo simulation approach of the structural model still poses a considerable burden on storage allocation. Resorting to the LSMC (Section 4.3.2) technique may provide some effective tools in reducing the number of paths necessary for adequately modelling the balance sheet positions at

T_1. However, even though this numerically advanced technique is readily realisable, the amount of storage (random access memory) needed will be in the range of several gigabytes[1] since (4.32) is a five dimensional process. Furthermore, incorporating additional cover pool positions or also applying the structural model to a multi-period modelling setting will substantially contribute to more involved computational requirements and considerations.
Moreover, the model (4.32) possesses 24 parameters (six cover pool, six other assets, two interest rate market and ten dependency parameters) where a complete calibration of the model to market data, respectively, estimation to internal bank data becomes more art than science. Consequently, parameters (except for the interest rate market model, see Section 3.7) are chosen subjectively, rather than objectively. This fact, apart from the aforementioned computational issues, embodies the greatest weakness of the structural model in Chapter 4. Thus, it would be advantageous to derive a more tangible model, in particular, focussing on obtaining more accurate risk assessments of the underlying cover pool portfolio.

5.1.2. Rating Methodologies

In their covered bond rating methodologies major rating agencies have some type of asset risk assessment tool implemented for analysing assets contained in the Pfandbrief bank's cover pool. Often cover pool assets are further stressed in order to evaluate the impact of deteriorating asset quality on covered bond ratings. Rating agencies periodically publish their risk reports of covered bonds and covered bond issuers where various other risk factors are taken into consideration. Due to their complexity a brief reflection on relevant parts in the context of credit risk assessments of cover pool assets are extracted form the respective rating methodologies. We mainly refer to ECBC (2016, p. 501-542) where the methodologies of five rating agencies, DBRS, Fitch, Moody's, S&P and Scope Ratings, are accurately described. Here, the focus lies upon the methodologies of DBRS and Scope Ratings due to their similar modelling features compared to the newly proposed reduced-form model. An excerpt of their implemented cover pool modelling practices are:

DBRS The cover pool credit assessment in DBRS's covered bond rating methodology is comparable to the analysis of residential mortgage backed securities (RMBSs) or collateralized loan obligations (CLOs) of small and medium sized enterprises (SMEs), thus other forms of securitisation (as opposed to the Pfandbrief) of homogeneous asset pools. The assessment mainly consists of (ECBC, 2016):

1. Estimates of the probability of default (PD) and loss given default (LGD) for each rating category of the underlying assets are established.
2. Analysis of the stressed asset cash flows (including interest rates and exchange rates) from the underlying assets is conducted.
3. An analysis is undertaken of the manner in which the cash flows are allocated to the liabilities based on transaction documents.

[1] Suppose we want to simulate 100,000 paths of seven years with a discretisation of 250 days with the LSMC method in Section 4.3.2. We need to preallocate storage space for the five process objects and again for the dependent random number objects amounting to an object of total size with $2 \times 5 \times 7 \times 250 \times 100,000 \approx 14$GB.

Jointly, the probability of default of the issuer and the cover pool credit assessment, are taken into account to determine the probability of default of covered bonds. Furthermore, DBRS incorporates a certain time lag for covered bonds receiving cover pool cash flows with a certain recovery rate attached, thus cash flows are not always paid out in full.

Scope Ratings Main focus of Scope Ratings' asset credit analysis is laid upon assessing the performance of relevant assets in the cover pool which are highly issuer-specific where additionally, for example, country-specific aspects are incorporated. Besides relying on Monte Carlo methods for simulating asset default and other market-standard modelling approaches to evaluate concentrated portfolios, respectively cover pools, Scope Ratings utilises the large homogeneous portfolio (LHP) approximation approach assuming homogeneous, granular cover pools, which typically consist of residential and commercial mortgage loans. Stress scenarios applied to the cover pool are triggered in order to find out about the perseverance of cover pool cash flows and the credit differentiation a cover pool can support.

In summary, we retain the following main features of above utilised methods of the rating agencies DBRS and Scope Ratings which constitute important parts of the proposed reduced form approach for modelling the Pfandbrief:

- Incorporating probabilities of default of cover pool assets categorised by rating classes,
- assuming a LHP approximation for the cover pool, and
- conducting stress tests on the cover pool distribution by shifting probability mass to lower rating classes.

5.1.3. Market, Industry and Regulatory Developments

Recent market developments (Chapter 2) in the Pfandbrief (Section 2.2) as well as in the covered bond (Section 2.1) market as a whole have contributed to shifting more attention to the mortgage type of Pfandbriefe due to the persistent decline of public sector Pfandbriefe and non-existent relevance of ship and aircraft Pfandbriefe. Thus, a more refined assessment of the mortgage Pfandbrief and subsequently of the mortgage cover pool in the Pfandbrief modelling framework of Chapter 3 becomes necessary.

The necessity of banks complying with Basel II regulations issued by the 'Basel Committee on Banking Supervision' implies that also ratings wrt bonds contained in the cover pool are mandatory, be it externally from rating agencies (see Section 5.1.1) or internally, in order to perform the IRB (internal ratings-based) approach to calculate capital requirements for credit risk. Thereby, entirely relying on credit risk information from rating agencies may be problematic since ratings are usually updated not more than once a year. Although having access to credit information of individual banks, presumably, rating agencies will however not have a complete picture of single assets contained in the mortgage cover pool. Consequently, only crude credit risk aggregations are feasible.

However, when dealing with mortgage loans banks conduct their own scoring assessments of individual mortgage borrowers or of businesses mortgaging residential and commercial properties. Based on these credit scores eligibility for granting a mortgage loan and the charge to the borrower are established. This is confirmed by the study of EBF (2014) where, apart from scoring models, the main drivers of PD, are the length of

historical defaults in internal databases, PD calibration and cyclical adjustment, regulatory/supervisory constraints, the scope of the definition of default used by banks and the importance of back-testing. Notably, since 2005 data collections regarding PD and LGD on mortgage portfolios have intensified. Building up a consistent and continuous internal database of historical defaults is advantageous since PDs and LGDs are main inputs for the determination of risk weights in the IRB ansatz.
Furthermore, efforts have been undertaken to develop a common LGD-grading data base of member institutes of the VDP for assessing losses of real estate financiers to value, primarily, the collateral of Pfandbriefe. LGD-grading is an essential part of the advanced IRB approach of Basel II and specifies the amount of the expected loss if the debtor fails to repay his or her loan. A common data base of mortgage banks, firstly, allows all members of the VDP to have access to the same information on which they base their counterparty's credit risk and, secondly, assures a higher standard of data quality. Two main features are (Hagen and Marburger, 2002):

- Data on losses of different types of real estate in various regions are historically accumulated.

- Real estate market forecasts, necessary to assess how certain types of properties in particular regional markets will develop in the future, are based on transaction data of the mortgage banks.

An expansion of including PD-rating to the LGD-grading data base is also taken into consideration: "At the moment, the association is considering the possibility to develop a PD-rating for the real estate customer segment in addition to LGD-grading. In this way, the member institutes, which would require or wish for support for a PD rating, would have a 'one-size-fits-all' system that would be recognized for applying the advanced IRB approach in Basel.", (Hagen and Marburger, 2002). Additionally, in the interview of Hagen (2002) it is also held out in prospect that the data base may be accessed by third parties, other than VDP members, contributing to the transparency initiative of the Pfandbrief[2]. More recent articles suggest that the database is already in use, see Eilers (2017a) and Eilers (2017b), upon which real estate market forecasts are conducted. To determine the required regulatory capital, WIB for example, has been applying the IRB approach estimating not only PDs but also LGDs which is based on internal historical data and the LGD-grading database provided by vdpExpertise GmbH (WIB, 2015, p. 10). On an international scale Global Credit Data (GCD) (formerly named PECDC or the Pan-European Credit Data Consortium) is an important initiative in the area of EAD and LGD modelling where currently over 50 member banks across Europe, Africa, Asia, Australia and North America are working on a joint data pool. The project created 'by banks, for banks' originated in 2004. GCD also claims to have "the world's largest database of defaults and PD estimates for large corporates, banks, SMEs and specialised lending" on there website[3]. Separate asset classes are installed, including a real estate finance class, where in each segment calculations on default rates, migration rates and average PDs can be conducted.
In summary, we can confidently assume that a sufficient amount of IRB related data

[2]The data base today is operated by vdpExpertise GmbH (`https://www.vdpexpertise.de`) which is a service company of the VDP. The current data pool (as of 2015) comprises more than 60,000 real estate realisations in Germany and allows a profound statistical risk analysis of the most important LGD parameters.

[3]`https://www.globalcreditdata.org`

exists, in particular, PD-ratings on a micro level of mortgage loans which we are interested in. At the latest since the onset of Basel II regulations, data bases are per default internally implemented at Pfandbrief banks (see EBF (2014)). In addition, we have learnt that pooling initiatives by organisations like the VDP or GCD have been established where multiple banks commit to share their counterparty credit risk measures. In fact one of the main criticisms of EBF (2014) is the lack of standardised and consistent approaches wrt risk weighted asset (RWA) computations of banks' mortgage IRB models across Europe. Common data pools contribute to counteract data related inconsistencies to which member banks can contrast, for example, their internal PD systems. Although not having access to bank internal or conglomerate data bases it is sufficient for our purposes to know that they at least exist.

5.2. A Simplified Model

During the review of Sünderhauf (2006)'s one-period model of Chapter 4, FIGURE 4.9 emerged as motivation for developing an innovative approach for modelling the Pfandbrief in a one-period setting. The first modelling attempt stems from the idea to significantly simplify the structural model (Chapter 4) while preserving its main features. Primarily, the overall aim is achieving a considerable parameter reduction and, simultaneously, gaining degrees-of-freedom.
An important property of our simplified model is assuming a real-world modelling setting (Assumption 5.1). This is necessary because we estimate model parameters from historical time series and simply project the obtained estimates into the future.

Assumption 5.1. *Analysis is conducted under the real-world measure $\mathcal{P}$.*

Largely, we orientate ourselves to the modelling considerations and mathematical formulations of the Pfandbrief modelling framework (Chapter 3). Thus, as in the structural model (Chapter 4), the asset side consisting of CP and OA are likewise at the core of the model's redesign in a one-period setting. Assumption 5.2 provides the setup of the simplified model.

Assumption 5.2. *Assume that at T_1 (maturity of liabilities) the following distributions hold:*

- *The cover pool position is modelled by a Vašiček distribution (see Definition B.24 at T_1, so that*

$$V_{CP}(T_1, T_2) \sim \text{Vasi}(p_{CP}, \varrho_{CP})[= F_{CP}(x_{CP})],$$

  where $p_{CP} \in [0, 1]$ and $\varrho_{CP} \in [0, 1]$, denote the probability and correlation parameter of the Vašiček distribution.

- *A log-normal distribution is postulated for the other asset position at T_1 with*

$$V_{OA}(T_1) \sim \text{LN}(\mu_{OA}, \sigma_{OA}^2)[= F_{OA}(x_{OA})],$$

  where $\mu_{OA} \in \mathbb{R}$ and $\sigma_{OA}^2 > 0$ are the mean and variance parameters of the log-normal distribution.

· *The joint cdf of* $V_{CP}(T_1, T_2)$ *and* $V_{OA}(T_1)$ *is provided by the bivariate copula, denoted by*

$$V_A(T_1) \sim C(F_{CP}(x_{CP}), F_{OA}(x_{OA}))$$

where $V_A(T_1)$ *stands for the asset values at* T_1 *of the joint distribution and* C *can take on any copula defined in Appendix B.5.*

We intentionally leave it open for now to specify a suitable copula from Appendix B.5. This gap will be filled during an estimation example to real data below. First, emphasis is laid upon analysing the justification of the marginal distribution specifications in Assumption 5.2 for the cover pool and other assets positions. Thereby, we utilise the structural model of Chapter 4 as reference with the basic parameter setting in Table C.14. The procedure consists of fitting the postulated distributions to the simulated values and applying equations (3.5) and (3.8). Therefore, the values of the respective asset position are divided into two sets, a calibration and a validation set from the same sample of structural simulation in Chapter 4. For example, if we simulate 10,000 paths with the NMC (Section 4.3.1) or LSMC (Section 4.3.2) technique then the two sets are equally divided in 5,000 values each. The distribution parameters are fitted to the calibration set. With the resulting estimates a new sample of 5,000 random numbers are drawn which are then compared to the validation set. The comparison is conducted by applying appropriate test procedures. The following goodness-of-fit tests are taken into consideration:

Kruskal-Wallis (KW) test Returns the p-value for the null hypothesis that the data comes from the same distribution. The alternative hypothesis is that not all samples come from the same distribution.

Kolmogorov-Smirnov (KS) test Non-parametric test of the equality of continuous, one-dimensional probability distributions that can be used to compare two samples. The test rejects the null hypothesis at the 5% significance level.

Anderson-Darling (AD) test Anderson-Darling k-sample procedure to test whether k sampled populations are identical. The Anderson-Darling k-sample procedure assumes that i-th sample has a continuous distribution function and we are interested in testing the null hypothesis that all sampled populations have the same distribution, without specifying the nature of that common distribution:

$$H_0 : F_1 = F_2 = \ldots = F_k \tag{5.1}$$

5.2.1. Cover Pool Distribution

In Section 3.6.1.1 we laid the groundwork for modelling the cover pool taking on values of a risky zero-coupon bond. The structural model utilises MC techniques (Section 4.3) to generate the desired present values at T_1. This is to be replicated. Zero-coupon bonds are normally bounded by one since 'money today is worth more than money tomorrow'. Consequently, it is natural to assume a cover pool distribution on a domain of $[0, 1]$. The Vašìček distribution of Assumption 5.2 is suitable to fulfil this task. However, with the full model of (4.32), including the HW1F model, the boundedness at one for $V_{CP}(T_1, T_2)$ is not necessarily guaranteed. This phenomenon can be observed in FIGURE 5.1. It follows from the fact that we allow negative short rates to occur by simulating $r(t)$ with the HW1F model. When decreasing $r(0)$ and $f^M(0,t)$ by -100 bp, -200 bp and -300 bp respectively, it clearly shifts the distributions of the present values to the right, exceeding the value of one. This may seem an unsatisfactory result at first. Yet, if we move to a more normalised market environment of non-negative interest rates then also the expected situation of 'capped' $V_{CP}(T_1, T_2)$ values sets in. This can be simulated by exchanging the HW1F model by the CIR1F model (Section 4.1.3) due to it's non-negativity property. Repeating the experiment of shifting the initial short rate value ($r(0)$) and mean reversion level (θ_r) towards zero we observe that $V_{CP}(T_1, T_2)$ does not breach the predefined boundary of one. Letting $r(0)$ and θ_r converge to zero will, simultaneously, let $V_{CP}(T_1, T_2)$ converge to one (leaving all other parameters unchanged in TABLE C.14), as depicted in FIGURE 5.1. With the basic parameter set of

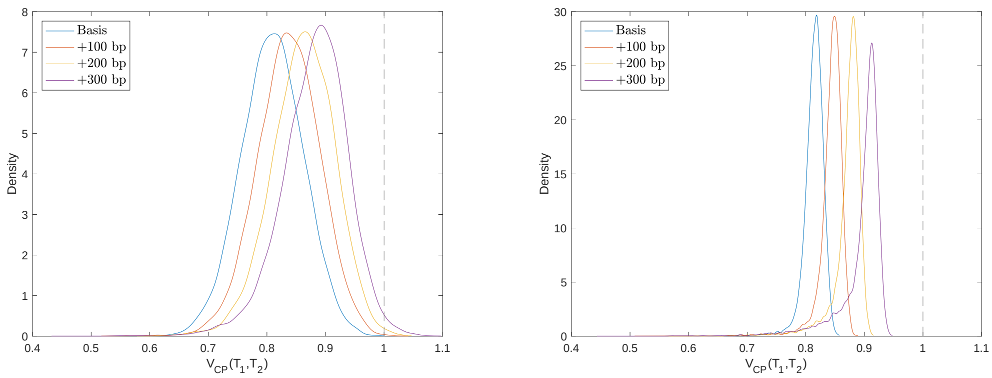

FIGURE 5.1.: Comparison of $V_{CP}(T_1, T_2)$ densities, where the initial interest rate and mean reversion level parameters in TABLE C.14 are changed by $r(0) = f^M(0,t) = 0.05 + x$, with $x = \{-100, -200, -300\}$ basis points (bp) for the HW1F model (left picture) and $r(0) = \theta_r = 0.05 + x$, with $x = \{-100, -200, -300\}$ basis points (bp) for the CIR1F model (right picture), where θ_r is the mean reversion parameter.

TABLE C.14, FIGURE 5.2 reveals that the Vašiček distribution overall does a good job of fitting the simulated values where maturities, T_1 and T_2, are further apart. Only when the time gap decreases the peakedness of the simulated values can not be fully captured. Also when choosing different parameter sets we see that the Vašiček distribution has difficulties adapting to the new situation. For example, we can reuse the stressed values of TABLE 4.5 to show the rather poor goodness-of-fit outcome. As described above, the Vašiček distribution is fitted to the calibration set providing the estimates of TABLE 5.1. Vašiček parameters are obtained via ML estimation. Sampling from the fitted Vašiček distribution and comparing to the validation set yields the test statistics of TABLE 5.2. We see that for the 'Basic' scenario the KW test can not reject the H_0 of equal median and equal distributions, thus an alignment of both sets can be assumed. KS and AD tests do reject this hypothesis. When moving towards more extreme scenario sets ('Stressed I' & 'Stressed II') the outcome is not in favour of our initial assumption of emulating the one-period structural approach of simulating the cover pool distribution at T_1. The peakedness and poor adaptability to parameter changes is explainable by the naturally given low parametrisation of the Vašiček distribution. We shall summarise further observations at the end of Section 5.2.

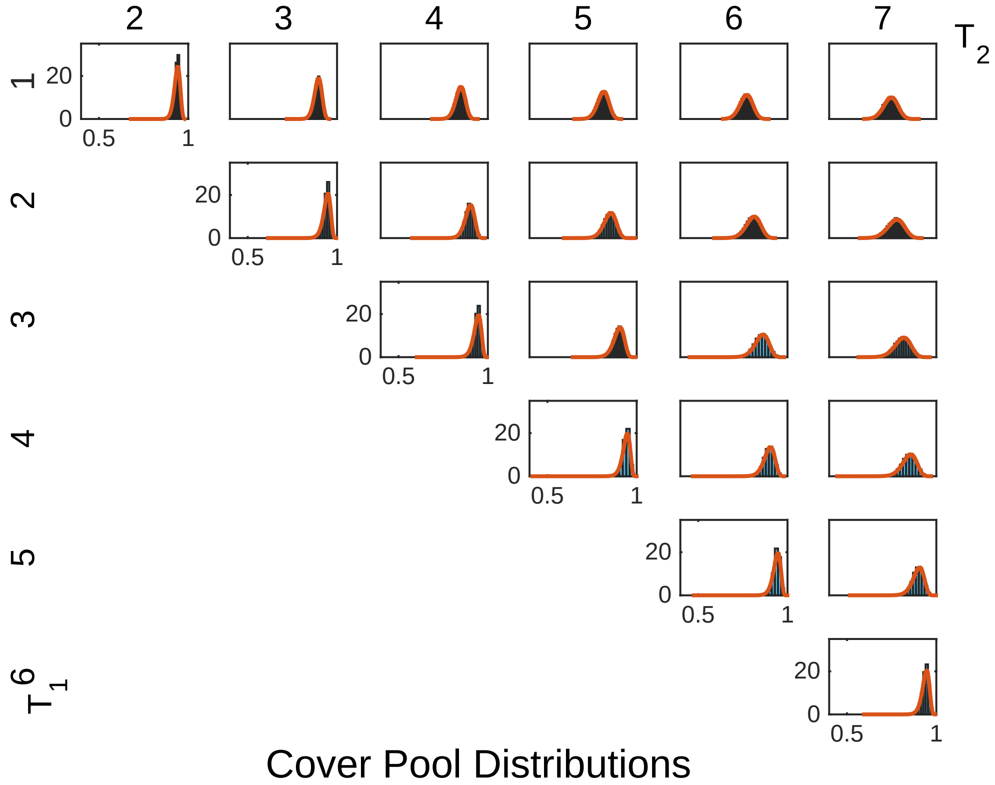

FIGURE 5.2.: Depiction of the cover pool present values ($V_{CP}(T_1, T_2)$)) of the Monte Carlo simulations (blue histograms) with the corresponding distribution fit of the Vašiček distribution (red curves) for different maturities.

Parameter	Basic	Stressed I	Stressed II
$\hat{p}$	0.809	0.677	0.613
$\hat{\varrho}$	0.040	0.094	0.139

TABLE 5.1.: Vašiček fit for 'Basic' (TABLE C.14), 'Stressed I' and 'Stressed II' (TABLE 4.5) parameter sets.

	KW test		KS test		AD test	
	p-value	H_n	p-value	D_n	p-value	A_n
Basic	0.205	1.609	0.015	0.031	0.003	6.705
Stressed I	0.001	11.726	0	0.073	0	24.158
Stressed II	0.001	11.438	0	0.080	0	35.528

TABLE 5.2.: Goodness-of-fit tests of the Vašiček distribution at confidence level $\alpha = 0.05$.

5.2.2. Other Assets Distribution

Let us now take a closer look at the other assets distribution at T_1. We can confidently assume that the other assets position (approximately) takes on the log-normal distribution. This is due to the fact of the established definition in Section 3.6.1.2 of not possessing a loan-like payment profile, in line with Merton's (Merton, 1974) approach where a firm's assets value is assumed to obey a log-normal diffusion process. Still the log-normal assumption with a parametrisation of two variables (as in the Vašiček case of the previous section) is a gross simplification to the SDEs with stochastic interest rates, volatility and jumps in (4.32). However, this is intentional. The results are similar to those of Section 5.2.1, yet, overall better wrt the goodness-of-fit tests. In FIGURE 5.3 we see the same behaviour of not fully reaching the peakedness when T_1 and T_2 are further apart. Again, we divide the sample set from Section 4.3.1 at T_1 into two sets as described above. The parameter estimates, obtained via ML estimation, for the log-normal distribution on the calibration set can be viewed in TABLE 5.3. These are used to simulate the corresponding samples to compare to the validation sets. The results are mixed. While for 'Stressed I' the test results unanimously keep the assumption of a log-normal distribution this can not be confirmed by the more stricter tests of KS and AD test for 'Basic' and 'Stressed II' scenarios.

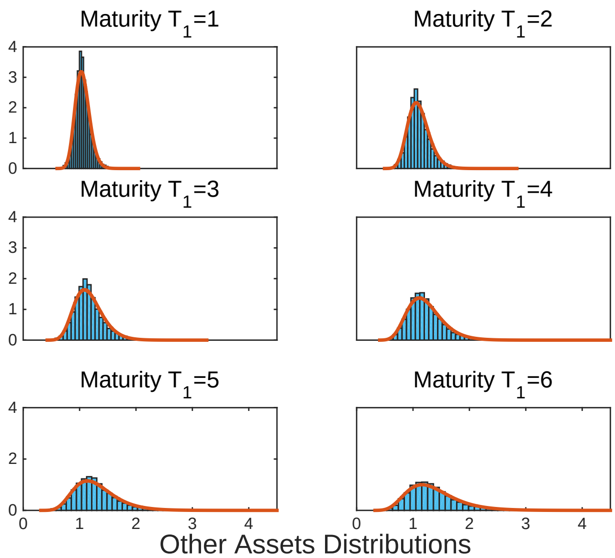

FIGURE 5.3.: Depiction of the other assets present values ($V_{OA}(T_1)$) of the Monte Carlo simulations (blue histograms) with the corresponding distribution fit of the log-normal distribution (red curves) for different maturities.

Parameter	Basic	Stressed I	Stressed II
$\hat{\mu}$	0.130	0.014	-0.022
$\hat{\sigma}$	0.215	0.550	0.600

TABLE 5.3.: Log-normal fit for 'Basic' (TABLE C.14), 'Stressed I' and 'Stressed II' (TABLE 4.5) parameter sets.

	KW test		KS test		AD test	
	p-value	H_n	p-value	D_n	p-value	A_n
Basic	0.195	1.682	0.003	0.036	0	6.453
Stressed I	0.180	1.797	0.134	0.023	0.163	1.561
Stressed II	0.317	1.000	0	0.068	0	25.038

TABLE 5.4.: Goodness-of-fit tests of the log-normal distribution at confidence level $\alpha = 0.05$.

5.2.3. An Estimation Example to Real Data

The salient, overall advantage of this simplified version is the fact that it can be easily estimated to market data and only a handful of parameters need to be estimated (altogether five parameters). The selected Pfandbrief bank is the Münchener Hypothekenbank eG. Beforehand it is necessary to take a closer look at the input data (see Appendix C) used for calibration.

TABLE C.11 contains the ratings of the cover pool assets divided into regional segments which in turn are divided into sub-segments containing the mortgage type. Given are the default probabilities (pd_i), intra-correlations (ic_i) and weights (w_i) of the corresponding asset segments. These rating and correlation specifications are provided by Moody's[4]. These data will be used for the purpose of calibrating the parameters of the Vašíček distribution, respectively cover pool position. For modelling the other assets and dependency between the cover pool and other assets an obvious choice would be to resort to the time series of these positions obtained from §28 PfandBG and respective balance sheets. Unfortunately, the data have only quarterly time steps[5], so that only 60 observations in the period Q4 1999 to Q4 2016 (FIGURE 2.42 in Section 2.3) could be retrieved which proved to be insufficient for conducting a proper time series analysis (especially in the case of the dependency structure as a filtering process, based on GARCH estimation, needed to be applied). Instead, proxies are utilised in the form of the RX-REIT-Index[6] and RX-Real-Estate-Index[7] (left picture of FIGURE 5.4). To take an index related to real estate seems to be an appropriate choice for the cover pool. Also the other assets will consist, to some extent, largely of real estate assets, so that a similar index may be a good choice. It can be assumed that these particular indices will be positively correlated, which is a reasonable assumption to make. Daily data is available since November 7$^{\text{th}}$, 2007 (base year starting level at 1,000).

To filter any kind of autocorrelation and/or heteroskedasticity a so called AR-GJR-GARCH model is fitted to the return data, to hopefully, produce a series of i.i.d. observations. The filtering procedure is as follows:

1. Fit an AR(1) (first order autoregressive) model to the conditional mean of the returns

$$R_t = \varphi_0 + \varphi_1 R_{t-1} + \epsilon_t,$$

accounts for autocorrelation.

[4] `www.moodys.com`

[5] A Pfandbrief bank will, internally, have the means to provide more granular observations based on daily data, due to the mandatory daily liquidity checks of PfandBG.

[6] `http://www.boerse-frankfurt.de/index/kurshistorie/RX-REIT-Index`

[7] `http://www.boerse-frankfurt.de/index/kurshistorie/RX-Real-Estate-Index`

2. Fit a GJR(1)-GARCH(1,1) (asymmetric GARCH, with $p = q = r = 1$) model to the conditional variance (cf. (Glosten et al., 1993))

$$\sigma_t^2 = \alpha_0 + \alpha_1 \epsilon_{t-1}^2 + \beta \sigma_{t-1}^2 + \gamma[\epsilon_{t-1} < 0]\epsilon_{t-1}^2,$$

accounts for heteroskedasticity. The GJR(1) term $\gamma[\epsilon_{t-1} < 0]\epsilon_{t-1}^2$ incorporates asymmetry (leverage) into the variance by a boolean indicator that takes the value 1 if the prior model residual is negative and 0 otherwise.

3. To compensate for the fat tails often associated with equity returns distributions are considered which can account for extreme values. The standardized residuals are modelled as a standardised Student's t distribution

$$v_t = \epsilon_t / \sigma_t \overset{\text{iid}}{\sim} \mathrm{t}(\nu),$$

where $\nu > 0$ is the degrees-of-freedom parameter.

The calibration procedure is outlined below, with the corresponding results:

Cover pool Strictly speaking, Table C.11 displays a heterogeneous finite portfolio with weights w_i where the probability bucketing approach in the one factor Gaussian model would be a realistic modelling choice resembling the underlying data ((Andersen et al., 2003) and (Hull and White, 2004)). For simplicity reasons, we intentionally ignore the granularity of the portfolio and instead compute the weighted probability mean with $\hat{p} = 1 - \sum_{i=1}^{n} pd_i w_i = 0.9949$ (probability of not defaulting). Further, we average the intra-correlations by means of Fisher's z-transformation ((Bushman and Wang, 1995) and (Corey et al., 1998)) with $\hat{\varrho} = \tanh^{-1}(\sum_{i=1}^{n} \tanh(c_i)/n) = 0.2747$ (correlation). These approximations allow us to obtain the needed parameters of the Vašiček distribution.

Other assets The complete AR-GJR-GARCH estimation is conducted on the RX-REIT-Index time series as specified above. The mean of the log-normal distribution is computed as the average of the sum over the log-returns $\hat{\mu} = \frac{1}{n}\sum_{i=1}^{n} \ln \frac{RX_i}{RX_{i-1}} = 3.4685 \cdot 10^{-04} \approx 0$. The long-term variance can be extracted from the GARCH(1,1) part of the model, with $\hat{\sigma}^2 = V_L = \frac{\hat{\alpha}_0}{1-\hat{\alpha}_1-\hat{\beta}_1} = 0.0148$ and estimates $\hat{\alpha}_0 = 0.0004$, $\hat{\alpha}_1 = 0.0546$, $\hat{\beta}_1 = 0.9169$.

Asset position dependency Due to its flexibility of the copula approach it is possible to replace the copula family with a preferred choice. A selection of suitable copulas is given in the following, with their corresponding bivariate density and parameter ranges in Appendix B.5.

- *Elliptical copulas* — The most prominent copulas in this family are the Gaussian and Student's t copula possessing elliptical distributions, as its name already states, and therefore are symmetric in the tails.
- *Archimedean copulas* — The three main Archimedean copulas are the Clayton, Frank and Gumbel copulas. The Frank copula is a symmetric copula, whereas Clayton and Gumbel copulas are asymmetric. The Clayton exhibits greater dependence in the negative, and the Gumbel in the positive tail.

The euclidean distance (L^2 norm) to the empirical copula is then computed in order to have a goodness-of-fit measure which is valid for comparing all above introduced copulas. The estimated copula distributions and goodness-of-fit can be seen in Table 5.5.

Remark 5.1. *A more refined analysis of the dependency structure would be to include tail dependency. An extreme value theory (EVT) can be utilised for obtaining the tail dependence structure and easily amended to the above asymmetric GARCH model. Specifically, when modelling the tails of a distribution with a generalised Pareto distribution (GPD) it is necessary to have approximately independent and identically distributed (i.i.d.) observations. This allows for capturing the residuals lying in the upper and lower tail (*$\mathrm{Prob}(X \leq x) \leq \alpha$ *and* $\mathrm{Prob}(X \leq x) \geq 1-\alpha$*, where* $\alpha = 0.1$*). The parametric GPD is fitted, via maximum likelihood (ML) estimation, to the extreme tail values (also known as the distribution of peaks over threshold method) with*

$$\epsilon_t \overset{\text{iid}}{\sim} \mathrm{GPD}(\mu, \sigma, \xi), \tag{5.2}$$

where ϵ_t *are the standardised residuals,* $\mu \in \mathbb{R}$ *is the location,* $\sigma > 0$ *is the scale and* $\xi \in \mathbb{R}$ *is the shape parameter, The CDF of the GPD is defined as*

$$F_{(\xi,\mu,\sigma)}(x) = 1 - \left(1 + \frac{\xi(x-\mu)}{\sigma}\right)^{-1/\xi}, \tag{5.3}$$

where x *are the exceeding values.*

Remark 5.2. *In the 2016 appeared scientific paper by Tasche (2016) an alternative, yet quite similar, estimation approach is proposed. In Tasche (2016), one-period structural modelling approaches for covered bonds and senior unsecured debt losses are investigated. He also acknowledges the fact that "(...) two-assets models with separate values of the cover pool (as we refer to 'CP') and the issuer's remaining portfolio (as we refer to 'OA') allow for more realistic modelling.", cf. (Tasche, 2016). The extra dimension adds additional complexity where an exact calibration is nearly impossible according to Tasche (2016). The method of moments technique is applied where a joint distribution of CP and OA values is fitted to given PD and LGD data. Alternatively, "the cover pool is reflected by a risk-based adjustment of the encumbrance ratio of the issuer's assets" (Tasche, 2016) reducing to an one-asset model.*

	Gaussian	t	Clayton	Frank	Gumbel
Estimate	0.4338	0.4419	0.6567	2.9974	1.3740
L^2 norm	6.5289	5.7113	18.3302	8.8995	14.1877

Table 5.5.: Copula fit — estimates and euclidean distance between the empirical and fitted copula.

From Table 5.5 we can deduce that the t-copula (having the smallest L^2 norm) is the appropriate modelling choice with regard to the underlying dependence structure. Having completed the real world calibration procedure, it is now possible to obtain the bivariate joint distribution of the assets which is depicted in the right picture of Figure 5.4.

5.2.4. Summary

The introduced simplified reduced-form model provides a first insight to a novel Pfandbrief modelling approach in a one-period setting. It purposely reduces the complexity of

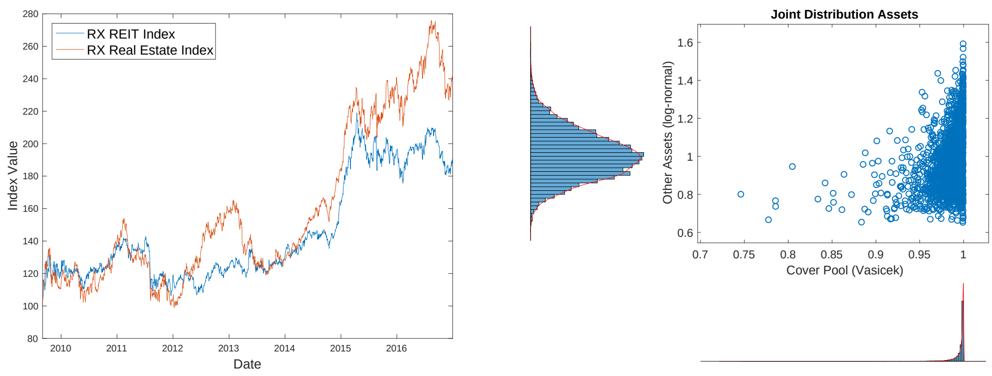

FIGURE 5.4.: Estimation of simplified model to real data. Left side: Proxy index values for cover pool and other assets; Right side: Joint distribution of assets with estimated parameters.

the structural model (4.32) in Chapter 4 at the cost of some shortcomings (as opposed to its structural) counterpart which will be addressed in following:

- Currently, the market is in an abnormal phase of negative interest rates (Section 3.7.1). Resorting to the HW1F model (Section 3.7.3) in (4.32) represents a more realistic modelling environment allowing negative short rates. Consequently, cover pool values ($V_{CP}(T_1, T_2)$) greater than one may occur at T_1. The Vašiček distribution can only handle values $V_{CP}(T_1, T_2) \in [0, 1]$ which restricts the modelling to market situation of positive interest rates or one knowingly blends out the zero interest rate policy of recent years. As pointed out above (FIGURE 5.1) the CIR1F model lets $V_{CP}(T_1, T_2)$ be bounded below one for (4.32).

- The drastic parameter reduction from 24 parameters in (4.32) to five in Assumption 5.2 cannot account for all market situations as revealed by the poor outcomes of the goodness-of-fit tests in the numerical comparison of the two approaches. This observation applies to the cover pool values as well as the other asset values. The log-normal assumption for OA performing only slightly better than the Vašiček assumption for CP. Further tests have shown when maturities of liabilities and assets (T_1 and T_2) are chosen more closely the distribution fit for the cover pool values further deteriorates. But in reality, the maturity gap is usually observed to be larger than three years.

Arguably, comparing the structural model of (4.32) to the simplified model of Assumption 5.2 feels more like 'comparing apples to oranges'. It is not surprising when contrasting the distributions from both worlds the outcome is not very satisfactory, especially, when moving to more extreme scenarios (see TABLE 4.5) for (4.32). Allowing for greater flexibility one could opt for distributions which have a higher parametrisation (e.g. the normal inverse Gaussian (NIG) distribution possesses four parameters (Kalemanova et al., 2007) which, potentially, could be a candidate in case of modelling the cover pool. However, this comes at the cost of additional complexity. Also, the Vašiček distribution holds desired credit risk related properties which other distributions may not.

Concluding, we can state that our first modelling attempt has achieved the goal of significantly simplifying the structural model of, yet, at the cost of some of some noteworthy insufficiencies as mentioned above. Furthermore, it strongly resembles the model of Tasche (2016) in the sense that two asset positions, CP and OA, are modelled as two marginal distributions with an underlying dependency structure between both positions which is embedded in a one-period setting at T_1. Nevertheless, some unanswered questions remain:

· The simplified version of this model is based on the real-world measure $\mathcal{P}$. However, as we have specified in Section 3.2, based on Characterisation 3.1, we want to model under the risk-neutral measure. The question of how to accomplish this is one of the central challenges throughout the next sections where necessary modelling advancements and complexities are introduced.

· How is asset-liability mismatch accounted for? Assets naturally have longer maturities than liabilities, thus how is the term transformation ($0 \leq T_1 \leq T_2$) adequately incorporated?

· What are suitable parameter estimates for p_{CP}, ϱ_{CP}, μ_{OA}, σ^2_{OA} and ρ as well as suitable data for the estimation thereof? Particularly, what are the correct cover pool default probabilities, p_{CP}, at some future point in time T_1?

· Postulating a recovery rate of zero ($\delta = 0$) for the Vaš̂íček distribution in Assumption 5.2 raises some doubt that this is a justifiable choice, since cover pool assets are mortgage loans backed by the value of the real estate. What is the accurate recovery rate for cover pool assets and how can it be adequately incorporated into (3.6)?

· The above simplified model does not account for a proper modelling of the established reduced form model of (3.6) in Section 3.6.1.1. Formula (3.6) can be divided into two components, a riskless interest rate component represented by the stochastic discount factor and a risky factor represented by the defaults occurring in the underlying cover pool (with a certain discovery rate). Lastly, what would such a model look like where a strict distinction between both components is maintained?

5.3. Model Setup

Conceptually, for the reduced-form model we postulate a bivariate distribution for modelling the complete asset side with the cover pool (CP) and other assets (OA) postions as marginals linked by a (bivariate) copula for capturing the underlying dependence structure. Figure 5.5 depicts the default process where random numbers are drawn from the joint asset distribution at T_1, yielding $V_A(T_1)$. Formulas (3.11), (3.14) and (3.15) are then applied so that the liability values $V_{PB}(T_1)$, $V_{OL}(T_1)$ and $V_{EQ}(T_1)$ can be obtained. This procedure requires that equations (3.6) and (3.8) are specified appropriately linked by a suitable copula. Ultimately, the overall aim is to reproduce Figure 4.9 of the structural model in Example 4.2 at T_1 in order to obtain the corresponding liability values of Figure 4.10.

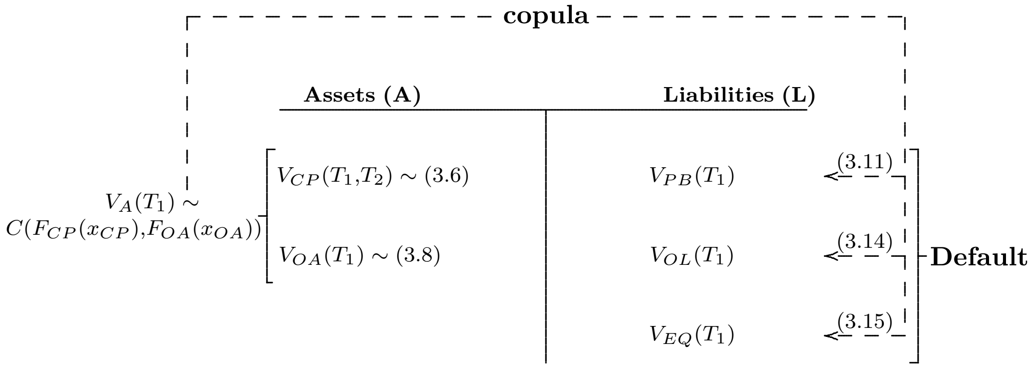

FIGURE 5.5.: Overview of the reduced-form model.

5.3.1. Linking Cover Pool and Other Assets

Proceeding the framework specifications in Chapter 3, more specifically in Section 3.6.1, we regard cover pool and other assets as two separate entities with an underlying dependence structure. Each possessing a marginal distribution, a natural choice of linkage is via bivariate copulas (Mai and Scherer, 2012). The motivation of using copulas also arises from the modelling of collateralised debt obligations (CDOs), see for example Li (2000), Hull and White (2004) and Laurent and Gregory (2005), amongst many others. Equivalently to the tranche structure of a CDO with different assigned ratings, for example senior (AAA), junior (AA, A, BBB) and residual (lower than BBB), the asset structure of a Pfandbrief bank can be divided similarly. The cover pool asset composition and the range of eligible collateral is restrictively regulated by the PfandBG which stipulates high quality requirements[8] and represents the senior tranche. Everything else, including mortgage loans not considered in the cover pool, constitute the other assets defining the junior tranche.
Given the fact that no Pfandbrief has ever defaulted in its over 200 year history it is of importance to resort to modelling options which are able to capture extreme events. Wrt to copulas the t-copula and likewise Archimedean copulas (Appendix B.5) would be suitable choices being leptokurtic (thickness in the tails) and which are able to model tail dependency. See Example 5.1 for the contrast of the behaviour at the distribution tails of the normal and t-copula.

Example 5.1 (Normal vs t-copula). *We choose the t-copula (5.4) with appropriate given marginal distributions for CP and OA where*

$$C(x_{CP}, x_{OA}; \rho, \nu) = t_{\rho,\nu}(F_{CP}(x_{CP}), F_{OA}(x_{OA})), \tag{5.4}$$

with $\nu > 0$ degrees of freedom and $\rho \in [-1, 1]$. FIGURE *5.6 illustrates the difference in tail behaviour of the t-copula compared to the Gaussian copula with linear dependency coefficient of $\rho = 0.5$. Evidently from (3.11), the tail behaviour of the asset positions is passed on to the resulting Pfandbrief distribution. The chosen copula can then be plugged into the asset model,* FIGURE *5.5.*

[8] On the eligibility of cover pool assets and its requirements refer to Spangler and Werner (2014).

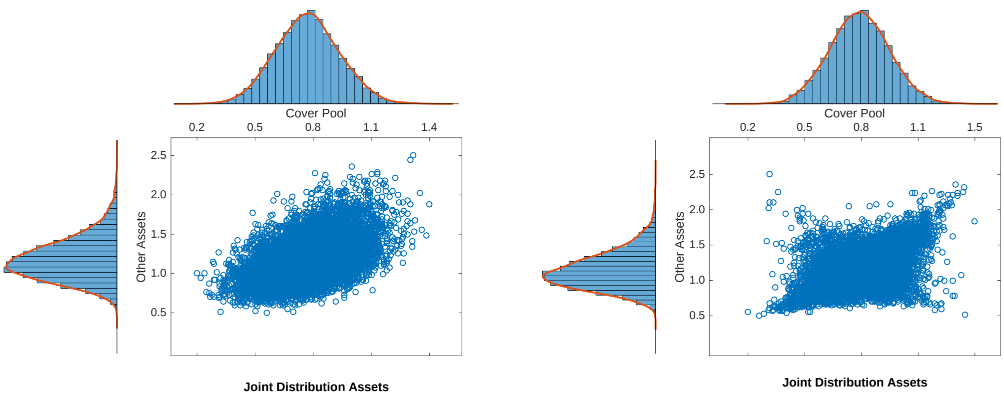

FIGURE 5.6.: Depiction of a stylised example of the joint asset distribution with given marginal distributions of the cover pool and other assets. Left side: Gaussian copula with $\rho = 0.5$. Right side: T-copula with $\rho = 0.5$ and $\nu = 2$.

5.3.2. Cover Pool

The foundation of (3.6) lies in the seminal reduced-form approach by Jarrow et al. (1997), which has its origins in Litterman and Iben (1991) and Jarrow and Turnbull (1995). Jarrow et al. (1997)'s model, also referred to as JLT model, postulates a firm's bankruptcy process as exogenously given which is independent of the firm's underlying assets. Thereby, the bankruptcy process is modelled as a finite state Markov process. More precisely, information in form of a firm's credit ratings and default probabilities is taken into account for pricing corporate bonds. In the context of modelling a Pfandbrief bank's default and the default of issued Pfandbriefe by the respective bank, we once again replace 'firm' with 'asset' where particularly assets contained in the cover pool are of interest. Thus, instead of pricing a corporate bond, as in the case of the JLT model, we are modelling the risky zero-coupon bond price(s) of a Pfandbrief bank's cover pool. As in Jarrow et al. (1997), we consider a frictionless economy with a finite horizon $[0, T^*]$ where trading can be in discrete or continuous time. Specifying the model of Jarrow et al. (1997) we refer to Bielecki and Rutkowski (2004) where we find a more exact mathematical formulation concerning the filtration included in the underlying probability space. This elaboration becomes necessary, firstly, due to an applied change of measure from real world to EMM. Secondly, we are dealing with several sources of market and credit risk which also have an impact on the Markovian assumption of Section B.3. In order to separate market and credit risk in a proper manner we need to again take additional considerations regarding the filtration into account. We define the following notation (Bielecki and Rutkowski, 2004):

- We introduce the filtration $\mathcal{H}$ where the associated sub-filtrations $\mathcal{F}$ and $\mathcal{F}^X$ of $\mathcal{H}$ are formally identified by $\mathcal{F}$ with $\mathcal{F} \otimes \{\emptyset, \hat{\Omega}\}$ and by $\mathcal{F}^X$ with $\{\emptyset, \widetilde{\Omega}\} \otimes \mathcal{F}^X$. Thereby, we set $\Omega = \widetilde{\Omega} \otimes \hat{\Omega}$ and $\mathcal{H} = \mathcal{F} \otimes \mathcal{F}^X$, where $\mathcal{F}$ ($\mathcal{F}^X$, respectively) is a filtration of events in $\widetilde{\Omega}$ (in $\hat{\Omega}$, respectively).

- $\mathcal{F}$ denotes the filtration of the market risk, whereas $\mathcal{F}^X$ represents the corresponding credit risk filtration which support the assumption of independence between market risk and default risk. Assuming independence implies $\mathcal{H} = \mathcal{F} \otimes \mathcal{F}^X$ where the required Markov property holds while incorporating market and credit related risks.

· In such a model, the migration process X is essentially supported by $\hat{\Omega}$. An appropriate change of the product probability measure with $\mathcal{P} = \widetilde{\mathcal{P}} \otimes \hat{\mathcal{P}}$ to an equivalent product probability measure $\mathcal{Q} = \widetilde{\mathcal{Q}} \otimes \hat{\mathcal{Q}}$ would preserve the $\mathcal{H}$-Markov property of X as well as the independence assumption of $\mathcal{F}$ and $\mathcal{F}^X$.

Hereinafter, we will simply use the $\mathcal{H}$ filtration admitting both, market and credit risk, where any distinction thereof is explicitly mentioned. Apart from this standard setup we state three main assumptions wrt reduced form modelling (Bielecki and Rutkowski, 2004):

Assumption 5.3. *There exists a (unique) equivalent martingale measure $\mathcal{Q}$, equivalent to $\mathcal{P}$ on $(\Omega, \mathcal{H}_{T^*})$, such that all default-free and risky zero-coupon bond prices follow $\mathcal{H}$-martingales, after discounting by the savings account.*

Assumption 5.4. *The interest rate risk is modelled by means of an $\mathcal{F}$-adapted stochastic process $r(t)$ of the default-free short-term interest rate, where $\mathcal{F}$ is some sub-filtration of $\mathcal{H}$.*

Assumption 5.5. *The default time τ is a random variable (the bankruptcy process) independent of the default-free interest rate process r, conditionally upon the filtration $\mathcal{H}$ under the martingale measure $\mathcal{Q}$.*

Other than the original model specification of Jarrow et al. (1997) we relax the assumption of a constant recovery coefficient, allowing random recovery rates denoted as $\tilde{\delta}$. Hence, there exists a dependency between recovery and default, compare Andersen and Sidenius (2004). The adjusted JLT pricing formula (3.6) at time T_1 results to

$$
\begin{aligned}
V_{CP}(T_1, T_2) &= \mathbb{E}_{\mathcal{Q}}\left(\frac{B_{T_1}}{B_{T_2}}\left(\tilde{\delta}\mathbb{1}_{\{\tau \le T_2 \,|\, \tau > T_1\}} + \mathbb{1}_{\{\tau > T_2 \,|\, \tau > T_1\}}\right) \middle| \mathcal{H}_{T_1}\right) \\
&= \mathbb{E}_{\mathcal{Q}}\left(\frac{B_{T_1}}{B_{T_2}} - \frac{B_{T_1}}{B_{T_2}}\left((1-\tilde{\delta})\mathbb{1}_{\{\tau \le T_2 \,|\, \tau > T_1\}}\right) \middle| \mathcal{H}_{T_1}\right) \\
&= P(T_1, T_2) - \mathbb{E}_{\mathcal{Q}}\left(\frac{B_{T_1}}{B_{T_2}}\left((1-\tilde{\delta})\mathbb{1}_{\{\tau \le T_2 \,|\, \tau > T_1\}}\right) \middle| \mathcal{H}_{T_1}\right) \\
&= P(T_1, T_2) - P(T_1, T_2)\mathbb{E}_{\mathcal{Q}}\Big[(1-\tilde{\delta}) \,|\, \{\tau \le T_2 \,|\, \tau > T_1\}; \mathcal{H}_{T_1}\Big] \cdot \\
&\qquad Q(\tau \le T_2 \,|\, \tau > T_1). \qquad (5.5)
\end{aligned}
$$

In other words, Equation (5.5) is the value of a riskless zero-coupon bond minus the value of the conditional expected recovery on default loss under the risk-neutral measure.

Remark 5.3. *With constant recovery rate δ (5.5) reduces to*

$$V_{CP}(T_1, T_2) = P(T_1, T_2) - P(T_1, T_2)(1-\delta)Q(\tau \le T_2 \,|\, \tau > T_1).$$

5.3.2.1. Forward Measure

Assuming that the default time is independent of the interest rate process (Assumption 5.5) is unrealistic and far stretched. In order to relax Assumption 5.5 we apply a change of measure, from risk-neutral to forward measure (see also in Bielecki and

Rutkowski (2004)), in form of the Radon-Nikodým derivative in Definition B.14. This is a similar way to what we have seen in Section 4.2.1 by means of zero-coupon bonds. The risky zero-coupon bond value of the cover pool under the forward measure amounts to

$$\begin{aligned} V_{CP}(T_1,T_2) &= P(T_1,T_2) - \\ &\qquad \mathbb{E}_{\mathcal{Q}_{T_2}}\left(\frac{B_{T_1}}{B_{T_2}}\left((1-\tilde{\delta})\mathbb{1}_{\{\tau\le T_2\,|\,\tau>T_1\}}\right)\left(\frac{\mathrm{d}Q}{\mathrm{d}Q_{T_2}}\right)_{|\mathcal{H}_{T_1}}\middle|\,\mathcal{H}_{T_1}\right) \\ &= P(T_1,T_2) - \\ &\qquad \mathbb{E}_{\mathcal{Q}_{T_2}}\left(\frac{B_{T_1}}{B_{T_2}}\left((1-\tilde{\delta})\mathbb{1}_{\{\tau\le T_2\,|\,\tau>T_1\}}\right)\left(\frac{B_{T_2}P(T_1,T_2)}{P(T_2,T_2)B_{T_1}}\right)\middle|\,\mathcal{H}_{T_1}\right) \\ &= P(T_1,T_2) - P(T_1,T_2)\mathbb{E}_{\mathcal{Q}_{T_2}}\Big[(1-\tilde{\delta})\,|\,\{\tau\le T_2\,|\,\tau>T_1\};\mathcal{H}_{T_1}\Big]\cdot \\ &\qquad Q_{T_2}(\tau\le T_2\,|\,\tau>T_1) \end{aligned} \tag{5.6}$$

where $\mathcal{Q}_{T_2}$ is the forward martingale measure for $T_1 \le T_2 \le T^*$.

5.3.2.2. Loss Distribution

Continuing on the modelling of the cover pool we rely on the forward measure as formulated in Section 5.3.2.1. Further, we assume the cover pool is a portfolio consisting of single assets m, $m = 1, \dots, M$ in an universe of M assets, with an intrinsic value of a risky zero-coupon bond $V_{CP}^m(T_1,T_2)$. Thereby, Equation (5.6) consists of two components, namely

- the riskless zero-coupon bond $P(T_1,T_2)$, and
- the expected default loss

$$\mathbb{E}_{\mathcal{Q}_{T_2}}\Big[(1-\tilde{\delta}_m)\,|\,\{\tau_m\le T_2\,|\,\tau_m>T_1\};\mathcal{H}_{T_1}\Big]Q_{T_2}(\tau_m\le T_2\,|\,\tau_m>T_1), \tag{5.7}$$

  representing the risk of the bank holding a cover pool asset m.

The latter, (5.7), is modelled as a loss distribution embedded in a large homogeneous portfolio (LHP) which is specified in the upcoming section. According to Andersen and Sidenius (2004), negative correlation between recovery rates and default frequencies exists which calls for the necessity of taking random recovery rates into account. Moreover, in the context of the Pfandbriefe cover pool assets are likely to have a high recovery at default of the outstanding mortgages. A certain assurance is given by the mortgage lending limit of 60% (compare Spangler and Werner (2014)). This is considered as an extension to the well known Gaussian copula model of the portfolio default loss.
In general, the Gaussian copula approach transforms τ_m, the default time of an asset m, into new standard normal random variables X_m via a 'percentile-to-percentile' transformation. Asset m defaults at time τ_m, when

$$X_m \le \Phi^{-1}(F_m(\tau_m)), \qquad m = 1, \dots, M,$$

where F_m is the distribution function (e.g. the exponential distribution) of the default time τ_m. This allows a multivariate normal interpretation of X_m with an underlying correlation matrix $\mathbf{\Sigma}$. Consequently, the complex correlation structure of τ_m is replaced by a more manageable one, where X_m can be interpreted as some kind of standardised asset returns. Instead of computing the pairwise correlation between X_m and X_n for each pair m, n, underlying correlation structure can be substituted by using a common market factor Z (here representing housing market data of a specific economy, or similar, adequately characterising the systematic credit risk of the portfolio). This represents the simplifying idea behind the factor copula model first introduced by Vašìček (1987), and Li (2000) being the first to apply the Gaussian model to multi-name credit derivatives. We apply the extended version of factor copula model under stochastic recovery rates for the period $(T_1, T_2]$ and state the LHP representation thereof. For a complete derivation of the Gaussian copula model and LHP with stochastic recovery rates, refer to Andersen and Sidenius (2004).

Following Andersen and Sidenius (2004), consider a portfolio of M default-risky cover pool assets. For a fixed time horizon $(T_1, T_2]$ default occurs before T_2 and after T_1. We connect X_m and τ_m by the known[9] forward default probabilities

$$q_m := Q_{T_2}(\tau_m \in (T_1, T_2] \,|\, \tau_m > T_1), \qquad m = 1, \ldots, M$$

for each cover pool asset m. The one factor Gaussian copula model with random recovery is given in Definition 5.1 where factor loadings remain constant over time and idiosyncratic factors for asset m are mutually independent random variables. Under this copula model the variable X_m is mapped to default time τ_m of the mth asset using a percentile-to-percentile transformation, i.e. the asset m defaults when

$$\Phi(X_m) \leq q_m \qquad \Leftrightarrow \qquad X_m \leq \Phi^{-1}(q_m), \qquad m = 1, \ldots, M.$$

Definition 5.1 (One factor Gaussian copula with random recovery). *Consider a cover pool portfolio of M assets. The standardised asset return for the time period $(T_1, T_2]$ of the mth asset in the portfolio, X_m, is assumed to be of the form*

$$X_m = a_m Z + \sqrt{1 - a_m^2}\epsilon_m, \tag{5.8}$$

where

- $Z \overset{iid}{\sim} \mathrm{N}(0, 1)$ *is the systemic common market factor,*
- $0 \leq a_m < 1$, $m = 1, \ldots, M$ *are factor loadings,*
- $\epsilon_m \overset{iid}{\sim} \mathrm{N}(0, 1)$, $m = 1, \ldots, M$ *are idiosyncratic factors and*
- Z *and* ϵ_m *are independent.*

The loss of the mth asset is modelled as

$$\begin{aligned} l_m &= l_m^{\max}(1 - \tilde{\delta}_m) \\ &= l_m^{\max}(1 - \Phi_m(\mu_m + b_m Z + \xi_m)), \end{aligned} \tag{5.9}$$

where

[9] A detailed description on how to obtain risk-neutral forward probabilities is provided in the succeeding sections.

- *each* l_m *is bounded, i.e.* $l_m \in [0, l_m^{\max}]$*, with* $l_m^{\max} \in \mathbb{R}_+$,
- $\tilde{\delta}_m \in [0,1]$ *are random recovery rates,*
- μ_m*,* $m = 1, \ldots, M$ *are constants,*
- $b_m \geq 0$*,* $m = 1, \ldots, M$ *are factor loadings, and*
- $\xi_m \overset{iid}{\sim} \mathrm{N}(0, \sigma^2_{\xi_m})$*,* $m = 1, \ldots, M$ *are idiosyncratic factors and independent of* Z *and* ϵ_m*.*

Given a common market factor Z, it follows from above specification and Definition 5.1, that (Andersen and Sidenius, 2004)

$$\begin{aligned} Q_m(Z = z) &= \mathrm{Prob}(X_m \leq \Phi^{-1}(q_m) \,|\, Z = z) \\ &= \mathrm{Prob}(\tau_m \in (T_1, T_2] \,|\, \tau_m > T_1, Z = z) \\ &= \Phi\left(\frac{\Phi^{-1}(q_m) - a_m z}{\sqrt{1 - \|a_m\|}}\right), \qquad m = 1, \ldots, M \end{aligned}$$

and

$$l_m(Z = z) = l_m^{\max}\left(1 - \Phi\left(\frac{\mu_m + b_m z}{\sqrt{1 + \sigma^2_{\xi_m}}}\right)\right), \qquad m = 1, \ldots, M.$$

Remark 5.4. *More sophisticated models other than the Gaussian copula model may well be utilised and can easily be further extended. However, emphasis is laid upon recovery rates and providing an initial modelling groundwork.*

Now, we assume that each asset m has the same default probability, the same factor loadings and the same recovery rate and that assets are equally weighted, meaning there exists no asset m dominating the total portfolio amount whereas a sufficiently large number of assets M exists. Then, according to Andersen and Sidenius (2004) the total portfolio loss experienced on $(T_1, T_2]$ is

$$L = \sum_{m=1}^{M} l_m^{\max}(1 - \tilde{\delta}_m)\mathbb{1}_{\{\tau_m \leq T_2 \,|\, \tau_m > T_1\}}$$

which can be approximated by the homogeneous portfolio of Definition 5.2.

Definition 5.2 (Large Homogeneous Portfolio (LHP) under random recovery rates). *Consider a homogeneous portfolio in an one-factor version of the cumulative Gaussian model, with*

$$\begin{aligned} F_\infty(y) = \lim_{M \to \infty} \mathrm{Prob}\left(L/M \leq y\right) &= \Phi\left(-h^{-1}(y)\right) \\ h(z)/l^{max} &= Q(z) l\left(z\right) \\ &= \Phi\left(\frac{\Phi^{-1}\left(q\right) - az}{\sqrt{1 - a^2}}\right)\left(1 - \Phi\left(\frac{\mu_{\tilde{\delta}} + b_{\tilde{\delta}} z}{\sqrt{1 + \sigma^2_{\tilde{\xi}}}}\right)\right) \end{aligned}$$

for constants a, $\mu_{\tilde{\delta}}$, $b_{\tilde{\delta}}$, σ^2_{ξ}, where $0 \leq y \leq 1$, $0 < a < 1$ and $b_{\tilde{\delta}} \geq 0$.

Remark 5.5. *Since $Q(z)$ and $l\,(z)$ are continuous and strictly decreasing, $h(z) = y$ in Definition 5.2 has a unique solution z^* for $0 \leq y \leq 1$ and $\{Q(z)l\,(z) \leq y\} = \{z \geq z^*\}$. Thus, we have*

$$\begin{aligned}\text{Prob}(L \leq y) &= \mathbb{E}[\text{Prob}(Q(z)l\,(z) \leq y \,|\, z)] \\ &= \mathbb{E}[\text{Prob}(z \geq z^* \,|\, Z)] \\ &= \text{Prob}(z \geq z^*) = 1 - \Phi(z^*).\end{aligned}$$

Remark 5.6. *With constant recovery rate δ, the LHP model reduces to*

$$h(z) = y = \Phi\left(\frac{\Phi^{-1}(q) - az}{\sqrt{1-a^2}}\right) l^{max}(1-\delta)$$

$\Leftrightarrow$

$$\frac{\Phi^{-1}(q) - az}{\sqrt{1-a^2}} = \Phi^{-1}\left(\frac{y}{l^{max}(1-\delta)}\right)$$

$\Leftrightarrow$

$$\Phi^{-1}(q) - az = \Phi^{-1}\left(\frac{y}{l^{max}(1-\delta)}\right)\sqrt{1-a^2}$$

$\Leftrightarrow$

$$z = \frac{\Phi^{-1}(q) - \Phi^{-1}\left(\frac{y}{l^{max}(1-\delta)}\right)\sqrt{1-a^2}}{a}$$

$\Rightarrow$

$$P(L \leq y) = \Phi\left(\frac{\Phi^{-1}\left(\frac{y}{l^{max}(1-\delta)}\right)\sqrt{1-a^2} - \Phi^{-1}(q)}{a}\right), \tag{5.10}$$

yielding a closed form solution to Definition 5.2.

The expectation and variance of the recovery rate and dependence between recovery rate and asset returns is given by

$$\begin{aligned}\mathbb{E}(\tilde{\delta}) &= \Phi\left(\frac{\mu_{\tilde{\delta}}}{\sqrt{1+\sigma^2}}\right) \\ \mathbb{V}(\tilde{\delta}) &= \Phi_2\left(\frac{\mu_{\tilde{\delta}}}{\sqrt{1+\sigma^2}}, \frac{\mu_{\tilde{\delta}}}{\sqrt{1+\sigma^2}}; \frac{\sigma^2}{1+\sigma^2}\right) - \Phi\left(\frac{\mu_{\tilde{\delta}}}{\sqrt{1+\sigma^2}}\right)^2 \\ \tau(\tilde{\delta}, X) &= 2\pi^{-1}\sin^{-1}(b_{\tilde{\delta}}a/\sigma).\end{aligned}$$

Example 5.2 (Gaussian model with stochastic recovery rate). *To illustrate the difference between stochastic recovery and constant recovery ($b_{\tilde{\delta}} = 0$) we set $\mathbb{E}(\tilde{\delta}) = 0.6$, $\mathbb{V}(\tilde{\delta}) = 0.01$ and $\tau(\tilde{\delta}, X) = \{0, 0.3, 0.8\}$. q and the parameter a are determined with the help of* Table *C.11 containing the interdependencies and default probabilities of m cover pool assets grouped by s segments and sub-segments with corresponding weights. We conduct the same calculation as in Section 5.2.3. The average factor loading and the weighted sums one-year default probability are $\hat{a} = \tanh^{-1}(\sum_{i=1}^{n}\tanh(c_i)/n) = 0.2747$ and $\hat{q}(0,1) = \sum_{s=1}^{S} pd_s w_s = 0.0051$, respectively. However, we are interested in the conditional forward default probability of q on the interval $(T_1, T_2]$. For reasons of simplifi-*

cations we assume a constant hazard rate model with $\hat{\lambda} = \hat{q}(0,1) = 0.0051$ *for computing the forward default probabilities which amounts to* $\hat{q}(\tau \leq 7 \,|\, \tau > 3) = 0.0201$.

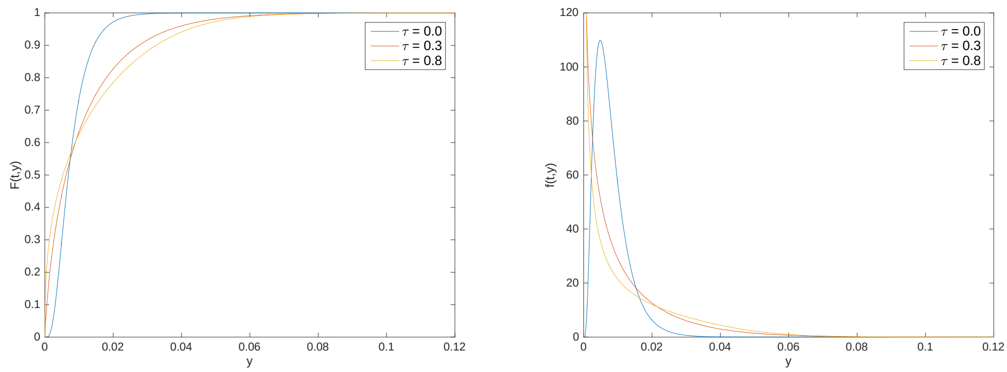

FIGURE 5.7.: Loss distributions of random recovery model with given values $\mathbb{E}(\tilde{\delta}) = 0.6$, $\mathbb{V}(\tilde{\delta}) = 0.01$, $\tau(\tilde{\delta}, X) = \{0, 0.3, 0.8\}$ and estimated values $\hat{a} = 0.2387$, $\hat{q}(\tau \leq 7 \,|\, \tau > 3) = 0.0201$.

5.3.3. Other Assets

Since we only simulate to T_1 for the other assets the computational burden is manageable. Thus, there is no immediate need of changing the proposed full model of (4.32) for $V_{OA}(t)$, respectively (3.8). However, other assets only account for a smaller amount of the overall asset side of a mortgage Pfandbrief bank (see type 'Hyp' in TABLE C.2) so that a complexity reduction of (4.32) for V_{OA} at T_1 seems reasonable. Nonetheless, the position of OA still plays an important role in the overall Pfandbrief modelling framework. Sünderhauf (2006) concludes that it is advisable for a Pfandbrief bank to hold a minimum percentage of other assets in its asset portfolio in order to have additional collateral for the Pfandbrief as Pfandbrief investors also have, amongst other potential creditors, a privileged claim over it, compare formula (3.11) and FIGURE 3.2. Thus, we are seeking a viable model which accounts for the modelling considerations and mathematical properties of Chapter 3 and at the same time using less parameters to approximately achieve a similar outcome of the structural model of Chapter 4. Inline with classical financial modelling of log-normal prices (Hull (2009) and Wilmott (2006)) and, simultaneously, inline with Tasche (2016)'s assumption of a log-normal distribution for the issuer's remaining portfolio (OA), we also apply this simplification for modelling (3.8). Furthermore, the results of the goodness-of-fit tests of Section 5.2.2 are reassuring to postulate this approximation of (4.32) for OA.
Following the groundbreaking works of Samuelson (1965) and Black and Scholes (1973) and since no further restrictions are imposed to the other assets (Equation (3.8)), the values at time T_1 resemble future stock prices, which are assumed to be a geometrical Brownian motion and log-normally distributed

$$\ln V_{OA}(T_1) \sim \mathrm{N}\left[\ln V_{OA}(0) + \left(r - \frac{\sigma_{V_{OA}}^2}{2}\right) T_1, \sigma_{V_{OA}}^2 T_1\right]. \tag{5.11}$$

Remark 5.7. *For a more realistic modelling approach one can opt for at least including stochastic interest rates as in Briys and de Varenne (1997)'s model where we modify the original model with time-dependent $\kappa(t)$ and $\sigma(t)$ parameters to be constant, amounting to (5.12). (5.12) can be regarded as a compromise between (4.32) and (5.11) with*

$$\begin{aligned}\frac{\mathrm{d}V_{OA}(t)}{V_{OA}(t)} &= r(t)\mathrm{d}t + \sigma_{V_{OA}}\mathrm{d}W^{\mathcal{Q}}_{V_{OA}}(t), \qquad (5.12)\\ \mathrm{d}r(t) &= (\theta(t) - \kappa r(t))\,\mathrm{d}t + \sigma_r \mathrm{d}W^{\mathcal{Q}}_r(t),\\ \mathrm{d}W^{\mathcal{Q}}_{V_{OA}}(t)\mathrm{d}W^{\mathcal{Q}}_r(t) &= \rho_{V_{OA},r}\mathrm{d}t.\end{aligned}$$

Remark 5.8. *When utilising the model specified with constant interest rates r there is no need to apply the change into the forward measure. Should, however, stochastic interest rates be incorporated as in (5.12) then the derivation of the forward measure can be applied analogously to Section 4.2.1.*

5.4. Obtaining Future Probabilities

One of the issues of the simplified approach in Section 5.2 wrt modelling the cover pool is obtaining default probabilities at some time in the future. Crucial to the rating based model is assessing default probabilities correctly. More precisely, the forward default / survival probabilities need to be calculated which arises from (5.6). Given a default time τ, the probability of survival in T years is $\mathrm{Prob}(\tau > T) = 1 - \mathrm{Prob}(\tau \leq T) = 1 - \mathbb{E}[\mathbb{1}_{\{\tau \leq T\}}]$. Several other related quantities can be derived from the basic probability. For instance

$$\mathrm{Prob}(S \leq \tau \leq T) = \mathrm{Prob}(\tau > S) - \mathrm{Prob}(\tau > T)$$

is the unconditional probability of default occuring in the time interval $[S, T]$. Using Bayes's rule for conditional probability, one can deduce that the probability of survival in T years conditioned on survival up to $S \leq T$ years is

$$\mathrm{Prob}(\tau > T \,|\, \tau > S) = \frac{\mathrm{Prob}(\{\tau > T\} \cap \{\tau > S\})}{\mathrm{Prob}(\tau > S)} = \frac{\mathrm{Prob}(\tau > T)}{\mathrm{Prob}(\tau > S)},$$

since $\{\tau > T\} \subset \{\tau > S\}$. From this we can define the forward default probability for the interval $[S, T]$ as

$$\mathrm{Prob}(S \leq \tau \leq T \,|\, \tau > S) = 1 - \mathrm{Prob}(\tau > T \,|\, \tau > S) = 1 - \frac{\mathrm{Prob}(\tau > T)}{\mathrm{Prob}(\tau > S)}.$$

Assuming that $\mathrm{Prob}(\tau > T)$ is strictly positive and differentiable in T, we define the forward default rate function as

$$h(T) = -\frac{\partial \log \mathrm{Prob}(\tau > T)}{\partial T}.$$

It then follows that $\mathrm{Prob}(\tau > T \,|\, \tau > S) = \exp\left(-\int_S^T h(u)\mathrm{d}u\right)$. The forward default rate measures the instantaneous rate of arrival for a default event at time T conditioned on survival up to T. Indeed, if $h(T)$ is continuous we find that for a short time interval

$[T, T + \Delta T]$

$$h(T)\Delta T \approx \text{Prob}(T \leq \tau \leq T + \Delta T \,|\, \tau > T).$$

5.4.1. Historical Mortgage Defaults

At first, we consider macroeconomic mortgage default rates for inferring future default probabilities based on (constant) hazard rate computations. Certainly, this practice represents a gross simplification and generalisation of the underlying default structure of a Pfandbrief bank's mortgage cover pool, however, a first entry point in forecasting required probabilities in a reduced form modelling framework is thereby provided and can be viewed as an initial benchmark evaluation.
Most recent (years 2014 and 2015) default rates for Germany are given by the Bundesanstalt für Finanzdienstleistungsaufsicht (BaFin), see Table 5.6. Here a distinction between residential and commercial properties is undertaken where a slightly higher risk profile can be observed for commercial mortgages in 2015. Hagen and Marburger (2002) state[10] similar average default rates for commercial finance for multi-purpose office and office buildings in Germany are 0.08%, or only 0.05% for up to 60% of the borrowing outflows which constitutes exceptionally low contingency risks. Interestingly, mortgage default rates have not changed dramatically over the years — at least in Germany. This observation is reflected in Table 5.7 where "overall, default rates for German securitisation transactions on residential mortgages, consumer loans and SME credits, which form the largest share of issuance activity, are around 0.30% — or less than half of the European average of 0.65%" (Staff Team of IMF, 2011) even during the years of the financial crises. While mortgage default rates are traditionally low in Germany and rest of Europe, the USA reveals a completely different picture. Rates doubled twice in two consecutive years from 2.27% to 8.43% since the onset of subprime mortgage crisis.
In Section B.3.1 we have introduced the hazard rate. Survival analysis relies on the exponential distribution with parameter λ and mean $1/\lambda$. The simplest possible survival distribution is obtained by assuming a constant risk over time, so the hazard, survival function and distribution amount to

$$\begin{aligned} \lambda(t) &= \lambda \\ S(t) &= \exp(-\lambda t) \\ f(t) &= \lambda \exp(-\lambda t) \end{aligned}$$

for all t. The density is obtained by multiplying the survivor function by the hazard rate.
Inserting the values of Table 5.6 or Table 5.7 for $\lambda(t) = \lambda$ into (B.55) we are, in generic terms, able to forecast sector or country wide future default probabilities. More plausible results can be obtained by resorting to Pfandbrief bank related data. Therefore, we utilise Moody's default data given in Table C.11 of Münchener Hypothekenbank eG. The one-year default probability is computed by $\hat{p}(0, 1) = \sum_{i=1}^{M} pd_i w_i = 0.0051$. We set, as in Section 5.2.3, $\hat{\lambda} = \hat{p}(0, 1) = 0.0051$ which again can be plugged into (B.55) resulting in, for example, the conditional forward default probability $\hat{p}(\tau \leq 7 \,|\, \tau > 3) = 0.0201$ of the time period $t \in (3, 7]$ years.

[10] Unfortunately, it is not explicitly stated on which year or years the default rates are based on, but presumably 2001 preceding the year of publication of Hagen and Marburger (2002).

		CCR upper limit	2015	2014
Residential	Art. 125 (3) a) & 199 (3) a)	0.30%	0.04%	0.05%
	Art. 125 (3) b) & 199 (3) b)	0.50%	0.07%	0.10%
Commercial	Art. 126 (3) a) & 199 (4) a)	0.30%	0.04%	0.05%
	Art. 126 (3) b) & 199 (4) b)	0.50%	0.15%	0.10%

Table 5.6.: Default rates for real estate risk positions in Germany, according to Art. 125, 126 and 199 Regulation (EC) No. 575/2013 according to the Capital Requirements Regulation (CRR) (source: www.bafin.de[11])

Country	2007 (%)	2008 (%)	2009 (%)
Germany	0.30	0.30	0.30
France	0.44	0.40	0.44
United Kingdom	1.88	2.42	2.45
USA	2.27	4.66	8.43
Poland	1.20	1.00	3.20
EU ∅	0.65	0.65	0.65

Table 5.7.: Evolution of mortgage default rates of selected countries during the financial crisis (source: Commission Staff Working Paper (2011))

Remark 5.9. *We have found a simple way of forecasting default probabilities based on historical macro economic figures. Yet, we still owe an approach for risk-neutral modelling under $\mathcal{Q}$. In Lando (2004), for example, we find the formula*

$$S(t,T) = \text{Prob}(\tau > T \mid \mathcal{H}_t) = \mathbb{E}_{\mathcal{Q}}\left(\exp\left(-\int_t^T \lambda(s)\mathrm{d}s\right) \middle| \mathcal{H}_t\right).$$

This reduced-form model framework constitutes the relation between the stochastic intensity process $\lambda(t)$ and the random survival probabilities at future times t provided $\tau > t$. It allows us to model the default probability of a Pfandbrief bank's cover pool surviving at time t of which we have no knowledge at time 0. Thus, the expectation is constructed where λ is a process which is adapted to (in fact predictable with respect to) the filtration $\mathcal{H}_t$.

Duffie (1999) also proposes a model based on constant default hazard rates where a risk-neutral valuation is feasible by knowing the asset swap spread value instead of the risky bond price. The amount by which the value of the risk-free bond exceeds the value of the risky bond is the asset swap spread. This fact allows to obtain risk-neutral constant hazard rates of λ. "In that case, default occurs at a time that, under 'risk-neutral probabilities' is the first jump time of a Poisson process with intensity λ", (Duffie, 1999).

[11] `https://www.bafin.de/SharedDocs/Downloads/DE/Auslegungsentscheidung/dl_ae_161222_verlustraten_2015_ba.pdf?__blob=publicationFile&v=3`

5.4.2. Cover Pool Credit Ratings

From Section 5.1.3 we know that mortgage loan ratings exist, either within a Pfandbrief bank itself or submitted to external data pools consisting of multiple intermediaries, ensuing Assumption 5.6.

Assumption 5.6. *Credit risk transition matrices aggregated into rating classes are readily available. More precisely, default and migration (from higher to lower rating classes and vice versa) probabilities of mortgage cover pool assets are given, or can be estimated from historical default data.*

Assumption 5.6 requires some additional insight into Markovian theory wrt transition matrices[12] and their estimation which is outsourced to Appendix B.3. Ideally, modelling is embedded in continuous time which complicates matters but solutions thereof are made available. The very basic approach of Section 5.4.1 can be refined to more suitably reflect the cover pool's risk profile of a Pfandbrief bank where forecasting cover pool default probabilities are treated in a granular sense. The major advantage of a rating based approach is being able to divide the cover pool assets into different rating classes. Moreover, continuous probabilities, meaning at any point in time, are obtainable.

5.4.2.1. Embedding Problem

Forecasting default probabilities can be accomplished by projecting Markov chain transition matrices into the future. In discrete time, a t-step transition probability denotes the probability that in t time units later the chain will be in state j, given it is now in state i. In the case of homogeneity the t-step transition probabilities can be computed by the t-th power of the (one-period) transition matrix (basically Theorem B.12 in matrix notation), i.e.

$$p_{ij}^{(t)} := \text{Prob}(X_t = j \mid X_0 = i) = \left(P^t\right)_{ij},$$

or in matrix notation

$$p_{ij}^{(t)} := \boldsymbol{P}^t = \underbrace{\boldsymbol{P} \cdots \boldsymbol{P}}_{t-\text{times}}, \tag{5.13}$$

where $p_{ij}^{(t)} > 0$, $\sum_{j=1}^{K} p_{ij}^{(t)} = 1$, for $i, j = 1, \ldots, K \in \mathcal{S}$ (discrete state set) and $t \in \mathbb{N}_0$. However, for the continuous time case, when $t \geq 0$ or $t \in \mathbb{R}_0^+$, it becomes necessary to transform the given one-year transition matrix to a generator matrix.

Remark 5.10. *This section can also be regarded as supplementing theoretical background to Hughes and Werner (2016).*

[12] A note on notation of the underlying Markov chains: In general we use $\{X_t\}$ for discrete-time and $\{X(t)\}$ for continuous-time Markov chains. However, to avoid any confusion with the price of a zero-coupon bond, $P(t, T)$, we denote transition matrices in general in bold font $\boldsymbol{P}$. Further, we denote the n-step transition matrix in discrete time by $\boldsymbol{P}_{0,n}$ with $n \in \mathbb{N}_0$. E.g. $\boldsymbol{P}_{0,1}$ is the given one-year transition matrix published by rating agencies which is frequently used in upcoming sections. The t-step transition matrix in continuous time is denoted by $\boldsymbol{P}_t$ with $t \in \mathbb{R}_0^+$. Inline again with the Markov chain in continuous time the generator matrix is given as $\boldsymbol{G}(t)$, $\forall t \geq 0$ for the inhomogeneous case.

The common approach, in the context of embedding a transition matrix in continuous time, is based on the notion of the generator of a continuous-time Markov process (Definition B.17). Bielecki and Rutkowski (2004) offer this compact definition of the embedding problem:

Definition 5.3 (Embedding Problem). *Find a $K \times K$ matrix $\boldsymbol{G}$ satisfying (a) and (b) of Properties B.3 (non-negative off-diagonal entires and all rows summing to* 0*), such that* $\exp(\boldsymbol{G}) = \boldsymbol{P}$*.*

As $\boldsymbol{P}_{0,1} = \exp(\boldsymbol{G})$ from Definition 5.3 needs to hold, a feasible candidate may be the matrix logarithm of a given transition matrix. However, this is most times not the case in the context of credit migration matrices, as more restrictive conditions of the embedding problem itself will reveal. Consequently, it becomes necessary to apply techniques in order to satisfy (a) and (b) of Properties B.3. In many publications, e.g. Jarrow et al. (1997) or Israel et al. (2001), it is suggested to simply compute the matrix logarithm and do some adjustments (diagonal adjustment (DA) and weighted adjustment (WA)) to the resulting matrix, eliminating negative off-diagonal entries by simply adding these to the diagonal. This seems a rather crude approach. Hughes and Werner (2016) show that Definition 5.3 can be formulated as a non-linear optimisation problem and be solved numerically with sufficient accuracy, thus rendering approximations unnecessary. Furthermore, this direct approach via non-linear optimisation allows one to consider credit risk-relevant constraints.
Having received a valid generator (for example in Table C.13) one can easily compute future default probabilities for any $t > 0$, namely by (B.60). The numerical calculation then can be conducted via the eigenvalue decomposition of $\boldsymbol{G}$, yielding

$$\boldsymbol{G} = \boldsymbol{U}\mathrm{diag}(d_1, \dots, d_K)\boldsymbol{U}^{-1}, \tag{5.14}$$

where $\boldsymbol{U}$ are the eigenvectors and $\mathrm{diag}(d_1, \dots, d_K)$ is the diagonal matrix containing the eigenvalues. Then the transition matrix can be obtained by

$$\boldsymbol{P}(t) = \boldsymbol{U}\mathrm{diag}(\mathrm{e}^{d_1 t}, \dots, \mathrm{e}^{d_K t})\boldsymbol{U}^{-1}. \tag{5.15}$$

Next, existence and uniqueness conditions are formulated wrt the matrix logarithm $\boldsymbol{M}$, with $\boldsymbol{P} = \exp(\boldsymbol{M})$ and generator matrix $\boldsymbol{G}$, with $\exp(\boldsymbol{G}) = \boldsymbol{P}$. The motivation of computing the matrix logarithm is twofold. First, computing the matrix logarithm may yield a valid generator and second, the upcoming optimisation approaches rely on the matrix logarithm as start matrix. In either cases a resulting real-valued solution is needed. In this context, it may also occur that more than one feasible matrix logarithm may exist, from which it follows that multiple solutions to the generator may be derived. Culver (1966) gives two necessary and sufficient conditions on the existence and uniqueness (corresponding proofs are also stated in Culver (1966)):

Theorem 5.1 (Existence of the Logarithm). *Let $\boldsymbol{P}$ be a real square matrix. Then there* exists *a real solution $\boldsymbol{M}$ to the equation $\boldsymbol{P} = \exp(\boldsymbol{M})$ if and only if*

(a) $\boldsymbol{P}$ is non-singular, and

(b) each elementary divisor (Jordan block) of $\boldsymbol{P}$ belonging to a negative eigenvalue occurs an even number of times.

Theorem 5.2 (Uniqueness of the Logarithm). *Let $\boldsymbol{P}$ be a real square matrix. Then the equation $\boldsymbol{P} = \exp(\boldsymbol{M})$ has a* unique *real solution $\boldsymbol{M}$ if and only if*

(a) all the eigenvalues of $\boldsymbol{P}$ are positive real and

(b) no elementary divisor (Jordan block) of $\boldsymbol{P}$ belonging to any eigenvalue appears more than once.

Remark 5.11. *It follows from Theorem 5.1 and Theorem 5.2 that if $\boldsymbol{P}_{0,1}$ is diagonalisable and if all eigenvalues are positive, real and distinct then the matrix logarithm uniquely exists.*

The existence of the logarithm is given for all three annual transition matrices from Table C.12, meaning all matrices have full rank and in all three cases the eigenvalues are positive thus fulfilling Theorem 5.1 (a) and (b). Israel et al. (2001) state that repeated eigenvalues are commonly not observed for credit risk transition matrices. Also both 8×8 matrices have a unique real solution as Theorem 5.2 (a) and (b) are satisfied, due to positive, real and distinct eigenvalues. However, $\boldsymbol{P}_{0,1}^{\text{Moodys XXL}}$ yields a complex conjugate eigenvalue pair ($0.5932 - 0.0201i$ and $0.5932 + 0.0201i$), hence (a) does not hold. A summary of the conditions for the matrix logarithm is given in Table 5.8. Lastly, we

	Theorem 5.1 — Existence		Theorem 5.2 — Uniqueness	
	(a)	(b)	(a)	(b)
$\boldsymbol{P}_{0,1}^{\text{S\&P}}$	✓	✓	✓	✓
$\boldsymbol{P}_{0,1}^{\text{Moodys}}$	✓	✓	✓	✓
$\boldsymbol{P}_{0,1}^{\text{Moodys XXL}}$	✓	✓	×	–

Table 5.8.: An overview of where the existence (Theorem 5.1) and uniqueness (Theorem 5.2) conditions on the matrix logarithm apply to the given annual transition matrices from Table C.12.

need to show that simply computing the matrix logarithm may not yield valid generator matrices. This is usually observed specifically for transition matrices in credit risk as negative off-diagonal entries arise, compare Israel et al. (2001). For real eigenvalues the principal logarithm[13] is simply computed which is the case for $\boldsymbol{P}_{0,1}^{\text{S\&P}}$ and $\boldsymbol{P}_{0,1}^{\text{Moodys}}$. For $\boldsymbol{P}_{0,1}^{\text{Moodys XXL}}$ the situation is different. Here a complex conjugate eigenvalue pair exists so that one needs to search in every branch of the matrix logarithm. Applying the search algorithm proposed by Singer and Spilerman (1976) and Israel et al. (2001) three real-valued solutions of the matrix logarithm can be found for this particular matrix. Yet, not one single valid generator according to (a) and (b) of Properties B.3 arises. The smallest negative off-diagonal entries of the corresponding matrix logarithm are given in Table 5.9.

At this point many publications addressing the matter resort to the diagonal adjustments (DA and WA) to eliminate the negative off-diagonal entries. Both methods are thoroughly described for example in Israel et al. (2001). Also it becomes evident that the embedding problem itself relies on more restrictive conditions for obtaining valid generators, as analysed in the next section. To this end many publications address the

[13]For computing the principal logarithm Matlab's inbuilt function `logm()`, which is based on the Schur-Parlett algorithm, is utilised.

Branch	$m_{\min}^{\text{S\&P}}(0,1)$	$m_{\min}^{\text{Moodys}}(0,1)$	$m_{\min}^{\text{Moodys XXL}}(0,1)$
-1	–	–	-13.390
0	-0.0003	-0.0003	-0.0013
1	–	–	-19.061

TABLE 5.9.: Minimum off-diagonal values of the resulting matrix logarithm computations, where $m_{\min}(0,1) = \min m_{ij}(0,1), i \neq j, \forall i, j = 1, \ldots, K$ in all branches of the logarithm function.

embedding problem, consisting of the existence of an embeddable matrix in continuous time and its uniqueness (also referred to as identification), reaching back as far as Elfving (1937). In these works the authors give conditions as to when a discretely obtained transition matrix can be embedded in a continuous time setting. Thus far necessary and sufficient conditions have only been formulated for 2×2 (see Kingman (1962) attributed to D. G. Kendall, and Guerry (2013)) and 3×3 matrices (see Cuthbert (1973), Johansen (1974), Frydman (1980), Carette (1995) and Guerry (2014)). For higher dimensions the issue still remains vague.
Necessary conditions (Lin (2011) also states the same list in her dissertation) for the existence in chronological order are (corresponding proofs are given in the stated references):

Theorem 5.3 (Necessary conditions for existence of a generator $\boldsymbol{G}$ with $\exp(\boldsymbol{G}) = \boldsymbol{P}$). *Let $\boldsymbol{P}$ be a transition matrix.*

(a) No eigenvalue λ_i of $\boldsymbol{P}$ can satisfy $|\lambda_i| = 1$ other than $\lambda_i = 1$. In addition, any negative eigenvalue must have even (algebraic) multiplicity. (cf. Elfving (1937))

(b) If $p_{ij} = 0$, then $p_{ij}^{(n)} = 0$ for any integer $n \geq 2$. If $p_{ij} \neq 0$, then $p_{ij}^{(n)} \neq 0$ for any integer $n \geq 2$. (cf. Chung (1960))

(c) For every pair of states i and j such that j is accessible from i, $p_{ij} > 0$. (cf. Chung (1960) and Grimmett and Stirzaker (2001))

(d) $\det(\boldsymbol{P}) > 0$ *(cf. Kingman (1962))*

(e) All eigenvalues of $\boldsymbol{P}$ must lie inside a heart-shaped region H_n in the complex plane whose boundary is the curve $x(v) + iy(v)$, where $0 \leq v \leq \pi / \sin(2\pi/n)$ and

$$
\begin{aligned}
x(v) &= \exp(-v + v\cos(\frac{2\pi}{n}))\cos(v\sin(\frac{2\pi}{n})),\\
y(v) &= \exp(-v + v\cos(\frac{2\pi}{n})\sin(v\sin(\frac{2\pi}{n})),
\end{aligned}
$$

together with its symmetric image with respect to the real axis. (cf. Runnenberg (1962))

(f) $\det(\boldsymbol{P}) \leq \prod_{i=1}^{K} p_{ii}$ *(cf. Goodman (1970))*

(g) If $\boldsymbol{P}$ has distinct eigenvalues, then each eigenvalue λ_i of $\boldsymbol{P}$ satisfies $|\lambda_i| \leq |\log(\det(\boldsymbol{P}))|$. (cf. Singer and Spilerman (1976) and Israel et al. (2001))

(h) *For any $K \times K$ transition matrix $\boldsymbol{P}$ which can be embedded in a continuous time Markov chain, there exist distinct indices i, j such that for all k*

$$p_{ik} = 0 \quad \textit{implies} \quad p_{jk} = 0,$$

and likewise distinct indices i', j' such that, for all k,

$$p_{ki'} = 0 \quad \textit{implies} \quad p_{kj'} = 0.$$

(cf. Fuglede (1988))

(i) *The entries of $\boldsymbol{P}$ must satisfy*

$$p_{ik} \geq m^m r^r (m+r)^{-m-r} \sum_j (p_{ij} - b_m)(p_{jk} - b_r) \mathbf{1}_{p_{ij} > b_m,\, p_{jk} > b_r},$$

for any positive integers m and r. Here $b_m = \sum_{l=m+1}^{\infty} \mathrm{e}^{-\mu} \mu^l / l! = 1 - \sum_{l=0}^{m} \mathrm{e}^{-\mu} \mu^l / l!$ which equals the probability that $N' > m$, where N' is a Poisson random variable with mean $\mu \equiv max_i(-g_{ii})$, with $max_i(-g_{ii}) \leq -\mathrm{trace}(\boldsymbol{G}) = -\log(\det(\boldsymbol{P}))$. Furthermore $\mathbf{1}_B$ is the indicator function of the Boolean event B. (cf. Israel et al. (2001))

The necessary conditions of Theorem 5.3 can be divided into two classes: conditions (a), (d), (e), (f) and (g) examine the eigenvalues (respectively determinant), while conditions (b), (c), (h) and (i) look at the matrix entries themselves more closely.
Following Israel et al. (2001) the most important conditions to be checked are (c), (d) and (f). While conditions (d) and (f) of Theorem 5.3 are satisfied by all given matrices in TABLE C.12, condition (c) is not. For example, in $\boldsymbol{P}_{0,1}^{\text{S\&P}}$ it is possible to migrate from class AAA to CCC-C via class A ($p_{1,3}^{\text{S\&P}}(0,1) > 0$ and $p_{3,7}^{\text{S\&P}}(0,1) > 0$), but not directly, as $p_{1,7}^{\text{S\&P}}(0,1) = 0$. This violation is a frequently observed phenomenon when examining credit risk transition matrices (due to non-observable defaults for high ratings in historical data, as also pointed out in Israel et al. (2001)). Therefore, Israel et al. (2001) established a more quantitative version of (c), being the most recent condition added to the list, (i). For example, we get the new probabilities for $p_{7,1}^{\text{Moodys}}(0,1) \geq 4.9210 \cdot 10^{-9}$, $p_{7,2}^{\text{Moodys}}(0,1) \geq 1.2563 \cdot 10^{-7}$, $p_{1,4}^{\text{Moodys}}(0,1) \geq 7.0681 \cdot 10^{-7}$, $p_{1,6}^{\text{Moodys}}(0,1) \geq 1.6223 \cdot 10^{-7}$, $p_{1,7}^{\text{Moodys}}(0,1) \geq 1.6473 \cdot 10^{-10}$, $p_{2,7}^{\text{Moodys}}(0,1) \geq 1.6348 \cdot 10^{-8}$ and $p_{1,8}^{\text{Moodys}}(0,1) \geq 2.6519 \cdot 10^{-8}$ for the original zero entries. Similarly, for $\boldsymbol{P}_{0,1}^{\text{S\&P}}$ new lower bounds with moderately low integer values (m and r) could be extracted. However, as also indicated by Israel et al. (2001) the bounds are not sufficiently large to rule out the possibility that the observed zero entries are due to rounding off. Also replacing the zero entries of $\boldsymbol{P}_{0,1}^{\text{Moodys}}$ with the newly obtained bounds and computing the matrix logarithm thereof have not resulted in a valid generator, as still negative off-diagonal values occur, corroborating the claim of the new bounds not being large enough. In fact tests have shown that only values larger than 10^{-4} make the negative values disappear. In the case of the large matrix $\boldsymbol{P}_{0,1}^{\text{Moodys XXL}}$ integer values m and r needed to be set very high (e.g. $m, r = 80$) in order to even get strictly positive bounds. With positive higher integers also lower probabilities are obtained, vanishing to zero. When computing the matrix power, for any given RCMM (Properties B.2) and $n \geq 2$, it can not always be guaranteed that zero entries remain zero entries so that (b) does not hold. A further important condition specifically addresses the situation when complex eigenvalues occur

(condition (e)). Here the Runnenberg boundary (cf. Runnenberg (1962)) is not to be exceeded. FIGURE 5.8 depicts the Runnenberg boundary with the real eigenvalues of $\boldsymbol{P}_{0,1}^{\text{S\&P}}$ and $\boldsymbol{P}_{0,1}^{\text{Moodys}}$. Also the complex conjugate eigenvalue pair of $\boldsymbol{P}_{0,1}^{\text{Moodys XXL}}$ lies within this boundary (see FIGURE 5.9). An extensive analysis of complex eigenvalues is given in Singer and Spilerman (1976). Checking the necessary condition (h), ac-

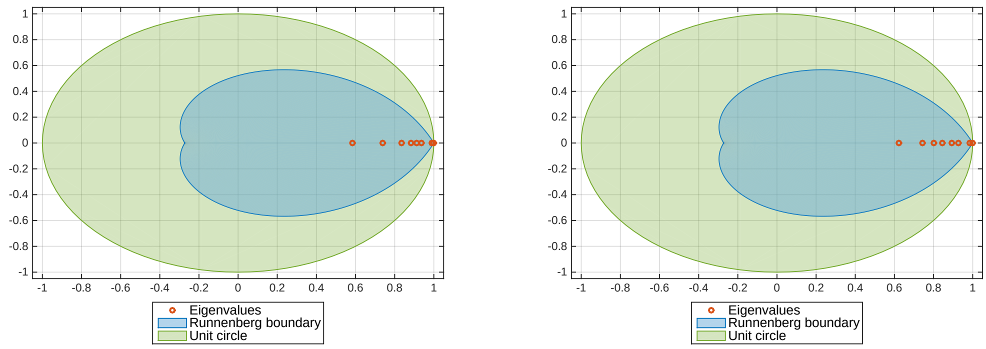

FIGURE 5.8.: Depiction of the eigenvalues pair of $\boldsymbol{P}_{0,1}^{\text{S\&P}}$ (left side) and $\boldsymbol{P}_{0,1}^{\text{Moodys}}$ (right side) lying within the Runnenberg boundaries of a 8×8 matrix (Theorem 5.3 (e)).

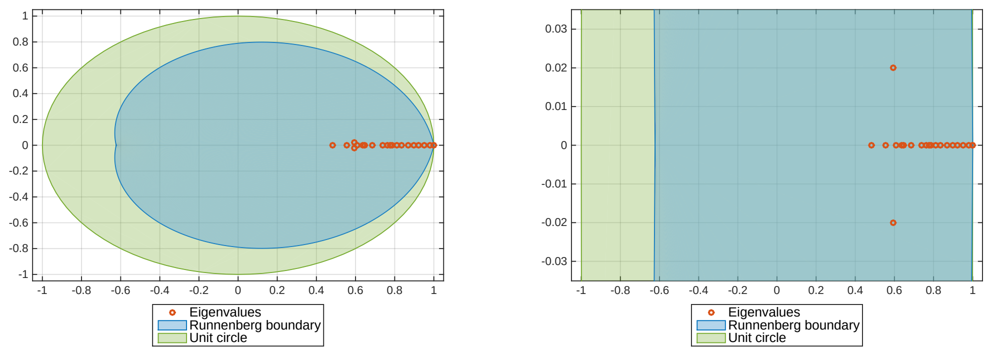

FIGURE 5.9.: Depiction of the eigenvalues of $\boldsymbol{P}_{0,1}^{\text{Moodys XXL}}$ lying within the Runnenberg boundaries of a 21×21 matrix (Theorem 5.3 (e)). Right plot rescales the imaginary axis, revealing the complex conjugate pair lying in close proximity.

cording to Fuglede (1988), reveals that the right stochastic matrices $\boldsymbol{P}_{0,1}^{\text{S\&P}}$, $\boldsymbol{P}_{0,1}^{\text{Moodys}}$ and $\boldsymbol{P}_{0,1}^{\text{Moodys XXL}}$ possess the same pattern of zero entries, satisfying this necessary criterium. The least restrictive condition is (a), as it relates closely to the existence of the matrix logarithm in Theorem 5.1. Negative eigenvalues in general are usually not observed for credit risk transition matrices and $\lambda_K = 1$, so that $|\lambda_K| = 1$. A summary of all existence conditions of the embedding problem is given in TABLE 5.10.

Remark 5.12. *From this rather brief, although representative investigation of common credit risk transition matrices it becomes evident that especially conditions (b) and (c) will, with high probability never apply to credit migration matrices. However, a longer history of default data would mean a higher probability that defaults have occurred even for higher rating classes. Also (i) gives a certain amount of assurance to be able to*

	Theorem 5.3 — Existence								
	(a)	(b)	(c)	(d)	(e)	(f)	(g)	(h)	(i)
$\boldsymbol{P}_{0,1}^{\text{S\&P}}$	✓	×	×	✓	✓	✓	✓	✓	×
$\boldsymbol{P}_{0,1}^{\text{Moodys}}$	✓	×	×	✓	✓	✓	✓	✓	×
$\boldsymbol{P}_{0,1}^{\text{Moodys XXL}}$	✓	×	×	✓	✓	✓	✓	✓	×

Table 5.10.: An overview of where the existence (Theorem 5.3) conditions for the embedding problem apply to the given annual transition matrices from Table C.12.

correct these entries (yet these need to be sufficiently large).

It can be concluded that specifically credit risk transition matrices have problems fulfilling the conditions class of matrix entries ((b), (c), and (i)) while on the other hand the eigenvalue related conditions are usually all met.
To this end, we need to ascertain the fact that theoretically no valid generators for our given transition matrices exist as three out of nine necessary conditions do not hold. However, for the sake of completeness and to show the feasibility of checking we will also discuss the case where more than one generator might arise, hence non-uniqueness (Theorem 5.4). It is sufficient (compare Singer and Spilerman (1976)) to show that if at least one of the conditions holds then only one valid generator exists (corresponding proofs are given in the stated references):

Theorem 5.4 (Sufficient conditions for uniqueness of a generator $\boldsymbol{G}$ with $\exp(\boldsymbol{G}) = \boldsymbol{P}$). *Let $\boldsymbol{P}$ be a transition matrix.*

(a) If $\boldsymbol{P}$ has distinct eigenvalues and $\det(\boldsymbol{P}) > \mathrm{e}^{-\pi} (\approx 0.0432)$, then only one possible generator for $\boldsymbol{P}$ exists. (cf. Cuthbert (1972), Cuthbert (1973) and Israel et al. (2001))

(b) If $\min_i(\boldsymbol{P})_{ii} > 1/2 \; \forall i = 1, \ldots, K$, and $\boldsymbol{P}$ is diagonally dominant, then it can be guaranteed that the generator is unique. (cf. Cuthbert (1972) and Cuthbert (1973))

(c) If the eigenvalues of $\boldsymbol{P}$ are distinct, real, and positive, then only one possible generator for $\boldsymbol{P}$ exists. (cf. Singer and Spilerman (1976))

(d) If $\det(\boldsymbol{P}) > 1/2$, then $\boldsymbol{P}$ has at most one generator. (cf. Israel et al. (2001))

(e) If $\det(\boldsymbol{P}) > 1/2$ and $\|\boldsymbol{P} - \boldsymbol{I}\| < 1/2$ (using any matrix norm), then only one possible generator for $\boldsymbol{P}$ exists. (cf. Israel et al. (2001))

All matrices in Table C.12 do not fulfil Theorem 5.4 (d) nor (e) by Israel et al. (2001). These conditions seem to be quite restrictive as the threshold of 1/2 is rather high, as compared to condition (a) ($\boldsymbol{P}_{0,1}^{\text{S\&P}}$ and $\boldsymbol{P}_{0,1}^{\text{Moodys}}$ yield a determinant value of 0.269 and 0.256 respectively). In general, requirement (b) is in most cases satisfied as in credit risk the annual transition matrix has the larger amount of probability mass on the diagonal. Also if $p_{ii} > 0.5$, for all $i = 1, \ldots, K$ then also $\det(P) > 0$, cf. Israel et al. (2001)[14]. Regarding condition (c), it is simply due to the fact that should real eigenvalues exist only the principal branch of the logarithm can be computed.

[14]For further interesting relations of strictly diagonally dominant matrices refer to Israel et al. (2001).

Remark 5.13. *Should however, more than one valid generator be obtained then Israel et al. (2001) propose to minimise the possibility of "jumping too far too quickly", based on some simple calculations.*

A summary of all uniqueness conditions of the embedding problem is given in TABLE 5.11.

	Theorem 5.4 — Uniqueness				
	(a)	(b)	(c)	(d)	(e)
$\boldsymbol{P}_{0,1}^{\text{S\&P}}$	✓	✓	✓	×	×
$\boldsymbol{P}_{0,1}^{\text{Moodys}}$	✓	✓	✓	×	×
$\boldsymbol{P}_{0,1}^{\text{Moodys XXL}}$	×	✓	×	×	×

TABLE 5.11.: An overview of where the uniqueness (Theorem 5.4) conditions for the embedding problem apply to the given annual transition matrices from TABLE C.12.

5.4.2.2. Forecast Procedure with Updated PDs

In Hughes and Werner (2016) we show how credit risk migration matrices in continuous time are received for any given one-year transition matrix based on a non-linear optimisation procedure. Furthermore, constraints are imposed so that not only a valid generator matrix results, but also the outcome is manipulated to a more desirable structure of matrix entries of $\boldsymbol{G}$, respectively $\boldsymbol{P}_{0,1}$, before forecasting into the future. A general forecast procedure may be as follows:

1. Obtain an one-year transition matrix $\boldsymbol{P}_{0,1}$ either via estimation (Section B.3.2) or assume as given.
2. Embed $\boldsymbol{P}_{0,1}$ in continuous time to obtain the corresponding generator $\boldsymbol{G}$ by using an accurate numerical embedding procedure as in Hughes and Werner (2016) where additional constraints can be incorporated if desired.
3. Use formula (B.60) or the numerical more efficient formula (5.15) in combination with (5.14) to obtain a future (or past < 1 year) transition matrix version, $\boldsymbol{P}_{0,t}$, with $t \in \mathbb{R}_0^+$.

Here we add another optimisation problem where updated PDs are incorporated into an existing one-year transition matrix. Subsequently, we shall forecast into the future and compare the non-updated PDs to the updated PDs. Needless to say that any other constraint introduced in Hughes and Werner (2016) can be applied a priori.

Remark 5.14. *This additional optimisation problem of updated default probabilities has its origin in Kealhofer et al. (1998) and is picked up again by Bluhm et al. (2002). The conclusion of Kealhofer et al. (1998) is: "There is a wide range of default probabilities within a rating range because the rating agencies are slow in upgrading and downgrading firms whose default probabilities have changed." These findings are based on KMV's expected default frequencies (EDF) methodology. Translated to our modelling setting of rating mortgage assets contained in the cover pool we can incorporate the exogenous* *changes in default probabilities and redistribute probability mass to the rest of the transition matrix in order to obtain a valid transition matrix as in Definition B.16 where the row sums amount to one.*

As in Hughes and Werner (2016) we rely on the best approximation of the annual transition matrix (BAM) method. Until 2010, it remained open if there were a (weak/strong) relation between BAM and its approximation QOG. Then, Davies (2010) derived Theorem 5.5, which gives the distance of any solution of a generator matrix $\boldsymbol{G}$ to the matrix logarithm $\boldsymbol{M} = \log(\boldsymbol{P})$. In the context of optimisation, it follows that should $\boldsymbol{G}$ be close to $\log(\boldsymbol{P}_{0,1})$, then so is $\exp(\boldsymbol{G})$ to $\boldsymbol{P}_{0,1}$.

Theorem 5.5. *Let $\boldsymbol{P}$ be a transition matrix such that all eigenvalues are strictly positive, and put $\boldsymbol{M} = \log(\boldsymbol{P})$. If $\boldsymbol{G}$ lies within the set of (a) and (b) of Properties B.3 and $\|\boldsymbol{M} - \boldsymbol{G}\|_\infty = \epsilon$, then:*

$$\|\boldsymbol{P} - \exp(\boldsymbol{G})\|_\infty \leq \min\{2, \exp(\epsilon) - 1\} \leq \min\{2, 2\epsilon\},$$

where the used norm is $\|\boldsymbol{A}\|_\infty = \max\{\|\boldsymbol{A}\nu\|_\infty : \|\nu\|_\infty \leq 1\} = \max\limits_{1 \leq i \leq n} \{\sum_{j=1}^n |A_{i,j}|\}$.

For the optimisation problems, we need to define the set of all valid generators, thus Definition 5.4 is derived from (a) and (b) of Properties B.3.

Definition 5.4 (Generator matrix constraints).

$$\mathcal{G} := \Big\{ \boldsymbol{X} \in \mathbb{R}^{K \times K} : \sum_{j=1}^{K} x_{ij} = 0, \quad i = 1, \ldots, K; \tag{G1}$$

$$x_{ij} \geq 0, \quad \forall i \neq j \text{ and } i, j = 1, \ldots, K \Big\} \tag{G2}$$

Now lets assume new PDs are estimated, for example due to external shocks, which need to be incorporated into a subsequent risk assessment. An ad-hoc solution is to update an existing one-year transition matrix with the new PDs in order to retain the benefits of a modified generator matrix. Even though the condition of a right stochastic matrix of each row summing to one ($\sum_{j=1}^{K} p_{ij} = 1$ for $i, j = 1, \ldots, K \in \mathcal{S}$) is violated at first by the updated PDs, the non-linear optimisation approach is able to rectify this with (G1) and (G2) of Definition 5.4. Definition 5.5 defines the required PD update constraint.

Definition 5.5 (Updated default probability constraint).

$$\mathcal{U} := \Big\{ \boldsymbol{P} \in \mathbb{R}^{K \times K} : \boldsymbol{P}_{i,K} = \boldsymbol{P}_{i,K}^{\text{update}}, \quad i = 1, \ldots, K-1 \Big\} \tag{U1}$$

Remark 5.15. *Definition 5.5 can easily be rewritten to that the update resembles a change of the diagonal, so that*

$$\mathcal{U} := \Big\{ \boldsymbol{P} \in \mathbb{R}^{K \times K} : \boldsymbol{P}_{i,i} = \boldsymbol{P}_{i,i}^{\text{update}}, \quad i = 1, \ldots, K-1 \Big\}, \tag{U2}$$

or even a combination of both (U1) and (U2). For illustration purposes we only show (U1).

The constraint of Definition 5.5 together with the constraint of the generator matrix in Definition 5.4 we can now formulate the optimisation problem of BAM (Problem 5.1).

Problem 5.1 (Best approximation of the annual transition matrix (BAM)). *Find a generator matrix $\boldsymbol{G}$ that, when exponentiated (by the matrix exponential), most closely matches a given annual transition matrix $\boldsymbol{P}_{0,1}$, with:*

$$\begin{aligned} \boldsymbol{G} = \underset{\boldsymbol{X}\in\mathcal{G}}{\arg\min} \quad & \| \exp(\boldsymbol{X}) - \boldsymbol{P}_{0,1}\|_{\mathrm{F}}^2, \\ \text{subject to} \quad & \exp(\boldsymbol{X}) \in \mathcal{U} \end{aligned} \tag{BAM}$$

where $\|\cdot\|_{\mathrm{F}}$ denotes the Frobenius norm.

For illustration purposes lets suppose the PDs of $\boldsymbol{P}_{0,1}^{\text{Moodys}}$ in Table C.12 may have risen by 20bp for investment (Aaa, Aa, A, Baa) and 50bp for speculative (Ba, B, Caa-C) grades so that $\boldsymbol{P}_{i,K}^{\text{update}} = [0.0020, 0.0023, 0.0021, 0.0036, 0.0196, 0.0756, 0.2666]$, with $i = 1, \ldots, K-1$ in Definition 5.5. The results are given in Table 5.12 where the range of deviation from the $\boldsymbol{P}_{i,K}^{\text{update}}$ PDs lie in the interval $[2bp; 8bp]$. It seems also that the PDs obtained from optimisation are underestimated wrt to the updated PDs which other outcomes for various $\boldsymbol{P}_{i,K}^{\text{update}}$, $i = 1, \ldots, K-1$ have, in general, confirmed. Adding to the PDs has forced the optimisation to subtract the equivalent probability mass from previous states in each row. This can be clearly seen when comparing $\boldsymbol{P}_{0,1}^{\text{update}}$ in Table 5.12 to $\boldsymbol{P}_{0,1}^{\text{Moodys}}$ in Table C.12. Definition 5.5 can also be combined with any other constraint defined in Hughes and Werner (2016) and applied to larger transition matrices, e.g. $\boldsymbol{P}_{0,1}^{\text{Moodys XXL}}$.

A five-year forecast is conducted on the non-updated $\boldsymbol{P}_{0,1}^{\text{Moodys}}$ and updated $\boldsymbol{P}_{0,1}^{\text{update}}$ transition matrices as in the described procedure above. Comparisons of the non-updated and updated default probabilities are depicted in Figure 5.10. It can be concluded that an update of PDs, thus taking new information on default changes into account, has a significant impact on any subsequent risk assessments.

$\boldsymbol{P}_{0,1}^{\text{update}}$	Aaa	Aa	A	Baa	Ba	B	Caa-C	D
Aaa	0.8861	0.1024	0.0096	0.0003	0.0001	0.0001	0.0000	0.0015
Aa	0.0105	0.8868	0.0952	0.0032	0.0011	0.0011	0.0000	0.0020
A	0.0003	0.0285	0.9018	0.0589	0.0071	0.0015	0.0000	0.0018
Baa	0.0003	0.0031	0.0704	0.8521	0.0603	0.0098	0.0006	0.0033
Ba	0.0000	0.0001	0.0049	0.0561	0.8350	0.0802	0.0047	0.0190
B	0.0000	0.0000	0.0010	0.0058	0.0652	0.8263	0.0269	0.0749
Caa-C	0.0000	0.0001	0.0057	0.0097	0.0297	0.0603	0.6289	0.2658
D	0.0000	0.0000	0.0000	0.0000	0.0000	0.0000	0.0000	1.0000

$\boldsymbol{G}^{\text{update}}$	Aaa	Aa	A	Baa	Ba	B	Caa-C	D
Aaa	-0.1216	0.1156	0.0046	0.0000	0.0000	0.0000	0.0000	0.0015
Aa	0.0118	-0.1226	0.1067	0.0000	0.0009	0.0012	0.0000	0.0020
A	0.0002	0.0318	-0.1077	0.0672	0.0058	0.0011	0.0000	0.0017
Baa	0.0003	0.0023	0.0803	-0.1651	0.0711	0.0082	0.0004	0.0025
Ba	0.0000	0.0000	0.0029	0.0664	-0.1865	0.0964	0.0046	0.0163
B	0.0000	0.0000	0.0007	0.0041	0.0780	-0.1960	0.0370	0.0763
Caa-C	0.0000	0.0000	0.0070	0.0114	0.0371	0.0815	-0.4656	0.3287
D	0.0000	0.0000	0.0000	0.0000	0.0000	0.0000	0.0000	0.0000

Table 5.12.: Result of the 8×8 matrices $\boldsymbol{P}_{0,1}^{\text{update}}$ and $\boldsymbol{G}^{\text{update}}$.

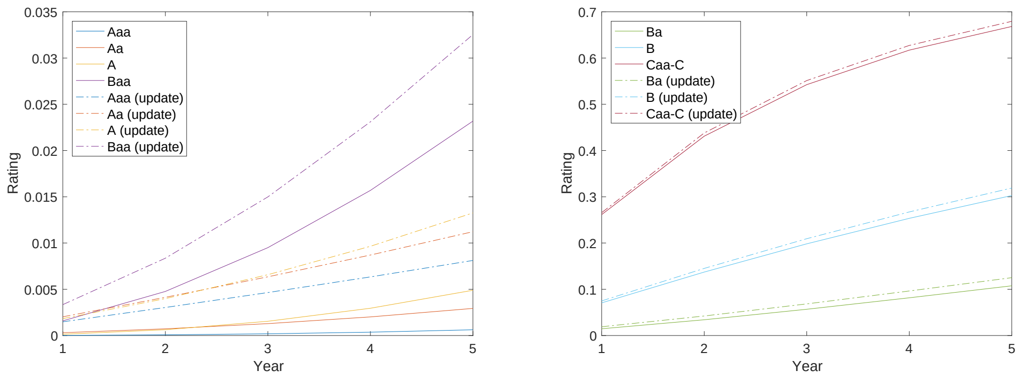

FIGURE 5.10.: Comparison of non-updated and updated default probabilities with a five-year forecast horizon. Left: Investment grade rating classes Aaa - Baa; Right: Speculative grade rating classes Ba - Caa-C.

5.5. Obtaining Risk-Neutral Probabilities

A crucial component of the proposed model of Section 5.3, in particular Section 5.3.2, is the conversion form real-world to risk-neutral probabilities. This is also a weakness of the simplified model in Section 5.2 which could only handle PDs based on historical time series yielding estimates in a real-world setting. Essentially, the upcoming reduced-form approach models spreads between a riskless and a risky bond for which Assumption 5.5 is of central importance. This shall be briefly illustrated in the following where we additionally assume, for reasons of simplicity, zero recovery $\delta = 0$ (bonds are not redeemed in the event of default).

Remark 5.16. *To be inline with the model specification and notation of Jarrow et al. (1997) we return to the assumption of a constant recovery rate, δ, for this section. See also Remark 5.3.*

Let $V(t,T)\mathbb{1}_{\{\tau>T\}}$ be the price at time $t \leq T$ of a defaultable zero-coupon bond with maturity T and face value equal to one unit of currency. Then, with $\delta = 0$, the JLT pricing formula (Jarrow et al., 1997) amounts to

$$V(t,T)\mathbb{1}_{\{\tau>T\}} = \mathbb{E}_{\mathcal{Q}}\left(\exp\left(-\int_t^T r(s)\mathrm{d}s\right)\mathbb{1}_{\{\tau>T\}}\,\middle|\,\mathcal{H}_t\right).$$

Applying Assumption 5.5 this simplifies to

$$V(t,T)\mathbb{1}_{\{\tau>T\}} = P(t,T)Q(\tau > T \,|\, \mathcal{H}_t).$$

Therefore, as long as $\tau > t$ the risk-neutral survival probability is given by

$$Q(\tau > T \,|\, \mathcal{H}_t) = \frac{V(t,T)}{P(t,T)} = \exp\left(-\int_t^T \left(f^d(t,s) - f(t,s)\right)\mathrm{d}s\right). \tag{5.16}$$

Comparing (5.16) to the credit spread measure

$$s(t,T) = -\frac{1}{T-t}\log\frac{V(t,T)}{P(t,T)} = -\frac{1}{T-t}\int_t^T h(t,s)\mathrm{d}s, \tag{5.17}$$

which is the difference of the continuously compounded yield to maturity of a default-free zero-coupon bond $P(t,T)$ and of a defaultable zero-coupon bond $V(t,T)$ with $h(t,s) = f^d(t,s) - f(t,s)$, we see that the term structure of risk-neutral survival probabilities is determined by the term structure of both defaultable and default-free zero-coupon bonds. Further, we can state that depending on the credit-worthiness of a risky zero-coupon bond it will sell for less than a riskless zero-coupon bond which will be useful for modelling the credit risk of the underlying cover pool assets.
Following Jarrow et al. (1997), the idea now is to let $Q(\tau > T \,|\, \mathcal{H}_t)$ depend on a rating class i of allocated cover pool assets where $Q_i(\tau > T \,|\, \mathcal{H}_t)$ denotes the probability of survival past T given the information up to time t under the risk-neutral measure $\mathcal{Q}$ for assets starting out in category i. Let $V_i(t,T)$ be the value of a zero-coupon bond issued by an asset in credit class i at time t, then

$$V_i(t,T) = P(t,T)(\delta + (1-\delta)Q_i(\tau > T \,|\, \mathcal{H}_t)). \tag{5.18}$$

With (5.16) and (5.17) it follows from the pricing formula (5.18) that

$$s_i(t,T) = -\frac{1}{T-t}\log\left(\delta + (1-\delta)Q_i(\tau > T \,|\, \mathcal{H}_t)\right) \tag{5.19}$$

where $Q_i(\tau > T) = 0$ if $\tau \leq t$. The forward rate for the risky zero-coupon bond in credit class i by inserting (5.18) is

$$\begin{aligned} f_i(t,T) &= -\log\left(\frac{V_i(t,T+1)}{V_i(t,T)}\right) \\ &= f(t,T) + \mathbb{1}_{\{\tau>t\}}\log\left(\frac{\delta + (1-\delta)Q_i(\tau > T \,|\, \mathcal{H}_t)}{\delta + (1-\delta)Q_i(\tau > T+1 \,|\, \mathcal{H}_t)}\right) \end{aligned} \tag{5.20}$$

where in bankruptcy $f_K(t,T) = f(t,T)$. To get the spot rate, set $T = t$ in Equation (5.20) and simplify

$$r_i(t) = r(t) + \mathbb{1}_{\{\tau>t\}}\log\left(\frac{1}{1-(1-\delta)q_{iK}(t,t+1)}\right) \tag{5.21}$$

where in bankruptcy $r_K(t) = r(t)$.
We now need to give some more theoretical background on how to obtain the risk-neutral survival probabilities $Q_i(\tau > T \,|\, \mathcal{H}_t)$. In general there exist larger differences between real-world and risk-neutral default probabilities. The difference between actual and risk-neutral probabilities is reflected in risk-premiums required by market participants to take risks. In the real-world, investors demand risk premiums, whereas under the risk-neutral probabilities all assets have the same expected rate of return, the risk-free rate (or short rate), and thus do not incorporate any such premium. Consequently, risk-neutral default probabilities must be higher than actual real-world probabilities.

5.5.1. Discrete Time

The narrative of mainly being interested in modelling in continuous time has not changed, however, it makes sense, from a comprehensibility perspective, to consider the discrete case first before moving on to its continuous counterpart. One of the central assumptions of Jarrow et al. (1997) is the independence of a particular bond on the history of the market or past ratings, thus future credit ratings of this bond depend only on the current rating of a bond. Following Bielecki and Rutkowski (2004), this key forgetfulness feature in Markovian theory is reflected in Assumption 5.7.

Assumption 5.7. *The migration process X_t, with $0 \leq t \leq T^*$ follows a time-homogeneous Markov chain under the real-world probability $\mathcal{P}$. The transition matrix of the migration process X_t under $\mathcal{P}$ is defined as in Definition B.16 with Properties B.1.*

However, under the equivalent martingale measure, more precisely moving from the real-world to the risk-neutral measure, two potential issues concerning the Markov chain X_t arise, namely forfeiting

1. the property of time-homogeneity, and
2. of greater concern the Markov property itself.

The loss of the homogeneity property is less problematic. In order to prepare for the change of measure we formulate the general case of a inhomogeneous transition matrix from time t to time $t+1$ under the equivalent martingale probability with $q_{ij}(t, t+1) = Q(X^*_{t+1} = j \mid X^*_t = i)$ for every $t = 0, \dots, T^* - 1$ which leads to Assumption 5.8 (Bielecki and Rutkowski, 2004).

Assumption 5.8. *The migration process X^*_t, with $0 \leq t \leq T^*$ follows a time-inhomogeneous Markov chain under the martingale measure $\mathcal{Q}$, with the time-dependent transition matrix*

$$\boldsymbol{Q}_{t,t+1} = (q_{ij}(t, t+1))_{1 \leq i,j \leq K} \tag{5.22}$$

where

$$\boldsymbol{Q}_{t,t+1} = \begin{pmatrix} q_{1,1}(t,t+1) & q_{1,2}(t,t+1) & \cdots & q_{1,K}(t,t+1) \\ q_{2,1}(t,t+1) & q_{2,2}(t,t+1) & \cdots & q_{2,K}(t,t+1) \\ \vdots & \vdots & \ddots & \vdots \\ q_{K-1,1}(t,t+1) & q_{K-1,2}(t,t+1) & \cdots & q_{K-1,K}(t,t+1) \\ 0 & 0 & \cdots & 1 \end{pmatrix},$$

and

$$q_{ii}(t,t+1) = 1 - \sum_{\substack{j=1 \\ j \neq i}}^{K} q_{ij}(t,t+1),$$

with $i = 1, \dots, K$.

Property 5.1.

(a) $q_{ij}(t,t+1) \geq 0, \quad \forall i \neq j$ *and* i, j

(b) $\sum_{j=1}^{K} q_{ij}(t,t+1) = 1, \quad i = 1,\dots,K$

(c) $q_{Kj}(t,t+1) = 0$ *for every* $j < K$ *and* $t = 0,\dots,T^*-1$*, so that once more the state* K *is absorbing*

(d) $q_{ij}(t,t+1) > 0$ *if and only if* $p_{ij} > 0$ *for* $0 \le t \le T^* - 1$

Also computing future transition matrices can easily be accomplished. The cumulative transition matrix, that is the T^*-step $K \times K$ transition matrix $\boldsymbol{Q}_{0,T^*}$ whose i,jth entry is $q_{ij}(0,T^*)$, satisfies

$$\boldsymbol{Q}_{0,T^*} = \boldsymbol{Q}_{0,1}\boldsymbol{Q}_{1,2}\cdots\boldsymbol{Q}_{T^*-1,T^*} = \prod_{t=0}^{T^*-1}\boldsymbol{Q}_{t,t+1}, \tag{5.23}$$

for inhomogeneous matrices $\boldsymbol{Q}_{t,t+1}$, $t = 0,\dots,T^*-1$. Lemma 5.1 computes the survival probability at any future date T, starting from credit class i at time t, with (5.23) where $Q_i(\tau > T \,|\, \mathcal{H}_t)$ denotes the conditional probability on the filtration $\mathcal{H}_t$. The result of Lemma 5.1 becomes useful when calibrating the model.

Lemma 5.1 (Probability of Solvency in Terms of $\boldsymbol{Q}$). *Let a mortgage asset be in state* i *at time* t*, denoted by* $X_t^* = i$ *and define* $\tau := \inf\{t \in \{0,\dots,T^*\} : X_t^* = K\}$*, which represents the first time of bankruptcy. Then, the probability that default occurs after time* T *is*

$$Q_i(\tau > T \,|\, \mathcal{H}_t) = \sum_{j \neq K} q_{ij}(t,T) = 1 - q_{iK}(t,T).$$

Addressing the issue of preserving the Markov property is more complex where additional restrictions need to be imposed. As pointed out by Bielecki and Rutkowski (2004) we are dealing with different sources of uncertainty (market risk, credit risk and other economic factors) when switching from one measure to another. More precisely, “the Radon-Nikodým densities are assumed to be only adapted wrt the natural filtration of the Markov chain, rather than adapted to the filtration $\mathcal{H}$”, (Bielecki and Rutkowski, 2004). The potential effect thereof on the risk-neutral transition probabilities of Assumption 5.8 is unknown to this end. In fact, Bielecki and Rutkowski (2004) present two sufficient conditions for the preservation of the Markov property yielding a more rigorous theoretical background to the issue. We orientate ourselves towards the readily established concept of risk premium adjustments constituting the solution to our problem, as proposed by Jarrow et al. (1997). The transition probabilities are, in general, given by

$$q_{ij}(t,t+1) = \pi_{ij}(t)p_{ij}, \qquad i,j \in \mathcal{S}, \tag{5.24}$$

where $\pi_{ij}(t)$ are the risk-premia adjustments that may depend on the whole history up to time t and p_{ij} are the actual transition probabilities of the observed time-homogeneous Markov chain $\{X_t : 0 \le t \le T^*\}$. We see that the underlying chain of $q_{ij}(t,t+1)$, conditional on the history up to time t, is then no longer of Markovian nature. Jarrow et al. (1997) impose the restriction

$$\pi_{ij}(t) = \pi_i(t), \qquad i \neq j, \tag{5.25}$$

with $\pi_i(t)$ being deterministic functions of time t. This ensures that after risk neutralisation the process $\{X_t^* : 0 \le t \le T^*\}$ is a non-homogeneous Markov chain. Further, the independence of j (column-independence) provides additional analytical tractability to the model. The column-independence restriction only requires the estimation of $K-1$ unknowns, instead of $(K-1)^2$. However, this assumption is not necessarily realistic as pointed out by Jarrow et al. (1997). Risk premiums, $\pi_i(t)$, are interpreted as proportionality factor which may depend on i and t but not on j since for any state i, the probability under the martingale measure $\mathcal{Q}$ of jumping to the state $j \neq i$ is assumed to be proportional to the corresponding probability under the real-world probability $\mathcal{P}$ (moving from i to j receives the same risk premium as moving from i to K). In matrix form we can write (5.24) with (5.25) as

$$\boldsymbol{Q}_{t,t+1} = \boldsymbol{I} + \boldsymbol{\Pi}(t)[\boldsymbol{P} - \boldsymbol{I}]$$

where $\boldsymbol{I}$ is the $K \times K$ identity matrix and $\boldsymbol{\Pi}(t) = \operatorname{diag}(\pi_1(t), \ldots, \pi_{K-1}(t), 1)$ is a $K \times K$ diagonal matrix.

Remark 5.17. *It is immediately clear that higher risk premiums cause higher default probabilities. Higher default probabilities imply lower prices for defaultable zero-coupon bonds, through (5.18).*

Remark 5.18. *Since, the last row in the transition matrix for $\boldsymbol{Q}_{t,t+1}$ in conjunction with Equation (5.25) implies that $\pi_K(t) \equiv 1$ for any t, we shall refer to the vector $(\pi_1(t), \ldots, \pi_{K-1}(t))$ as the risk premium at time t.*

Remark 5.19. *In the special case that $\boldsymbol{\Pi}(t)$ is a constant matrix, independent of t, $\boldsymbol{Q}_{0,t} = \boldsymbol{Q}^t$, where $\boldsymbol{Q}^t$ is the t-fold matrix product. Then, $Q_i(\tau > T \,|\, \mathcal{H}_t) = Q_i(\tau > T - t \,|\, \mathcal{H}_0)$, as the process is time-homogeneous.*

5.5.2. Continuous Time

Having sufficiently introduced the discrete-time formulation in Section 5.5.1 we move on to the continuous-time representation of the reduced form model, again referring to Bielecki and Rutkowski (2004). Essentially, Assumption 5.7 and Assumption 5.8 get replaced by Assumption 5.9 and Assumption 5.10.

Assumption 5.9. *Under the real-world probability measure $\mathcal{P}$, the migration process X follows a time-homogeneous Markov chain, with the intensity matrix $\boldsymbol{G}$ as in Definition B.17.*

Assumption 5.10. *Under the spot martingale measure $\mathcal{Q}$, the credit migration process X^* follows a (time-inhomogeneous) Markov chain, with a time-dependent intensity matrix $\widetilde{\boldsymbol{G}}(t)$, where*

$$\widetilde{\boldsymbol{G}}(t) = \begin{pmatrix} \widetilde{g}_{1,1}(t) & \cdots & \widetilde{g}_{1,K-1}(t) & \widetilde{g}_{1,K}(t) \\ \vdots & \ddots & \vdots & \vdots \\ \widetilde{g}_{K-1,1}(t) & \cdots & \widetilde{g}_{K-1,K-1}(t) & \widetilde{g}_{K-1,K}(t) \\ 0 & \cdots & 0 & 0 \end{pmatrix}$$

and the entries of the matrix $\widetilde{\boldsymbol{G}}(t)$ are functions $\widetilde{g}_{ij}(t)$ are functions $\widetilde{g}_{ij}(t) : [0, T^*] \to \mathbb{R}_+$.

As in the discrete-time setting, it is of interest to obtain the risk-neutral generator matrix of Assumption 5.10 where the real-world setting is the initial situation. Once again, it is of importance to retain the Markov property whereas the time-homogeneity will be lost during the conversion. Likewise, at default time τ the Markov chain will migrate to the the absorbing state K, with

$$\tau := \inf\{t \in [0, T^*] : X(t) = K\}.$$

The transition from a real-world to risk-neutral model is then achieved by the multiplication of the risk premia matrix $\boldsymbol{U}(t)$ and the generator matrix $\boldsymbol{G}$ where the risk adjustments transform the actual probabilities into the pseudo-probabilities suitable for valuation purposes, see Assumption 5.11.

Assumption 5.11. *There exists a matrix function $\boldsymbol{U}(t)$ of the form:*

$$\boldsymbol{U}(t) = \begin{pmatrix} u_{1,1}(t) & \cdots & 0 & 0 \\ \vdots & \ddots & \vdots & \vdots \\ 0 & \cdots & u_{K-1,K-1}(t) & 0 \\ 0 & \cdots & 0 & 1 \end{pmatrix}$$

where the entries, u_{ii}, $i = 1, \dots, K-1$, are strictly positive, integrable functions, such that the risk-neutral and real-world intensity matrices satisfy

$$\widetilde{\boldsymbol{G}}(t) = \boldsymbol{U}(t)\boldsymbol{G} \tag{5.26}$$

for every $t \in [0, T^*]$.

Under the assumption in Equation (5.26), the credit rating process is still Markovian, but it is inhomogeneous since the $\boldsymbol{U}(t) = \mathrm{diag}(u_1(t), \dots, u_{K-1}(t), 1)$ is a $K \times K$ diagonal matrix whose first $K-1$ entries are strictly positive deterministic functions of t that satisfy

$$\int_0^T u_i(t)\mathrm{d}t < +\infty$$

for $i = 1, \dots, K-1$, where conditions in Remark B.17 are widely preserved. In conclusion of the continuous-time JLT model, the same bond valuation formula (5.18) can be applied as in the discrete-time case.

Remark 5.20. *Following Jarrow et al. (1997), the $K \times K$ probability transition matrix from time t to time T for $X(t)$ under the equivalent martingale measure is given as the solution to the Kolmogorov differential equations (see Section B.3.1):*

$$\frac{\partial \boldsymbol{Q}(t,T)}{\partial t} = -\widetilde{\boldsymbol{G}}(t)\boldsymbol{Q}(t,T) \tag{5.27}$$

and

$$\frac{\partial \boldsymbol{Q}(t,T)}{\partial T} = \boldsymbol{Q}(t,T)\widetilde{\boldsymbol{G}}(T) \tag{5.28}$$

with the initial condition $\boldsymbol{Q}(t,t) = \boldsymbol{I}$.

5.5.3. Jarrow et al. (1997) Model Calibration

In order to be able to calibrate the Jarrow et al. (1997) model we need to first assume that the following inputs are given, resulting from Equation (5.18):

- the initial term structure of default free-free bonds, that is, the market values $P(t,T)$,
- the observed initial term structures of risky zero-coupon bonds, $V_i(t,T)$, from credit classes $i = 1,\dots,K-1$, and
- the recovery rate δ.

Resuming, the key result of Jarrow et al. (1997) is summarised in Assumption 5.12 which transforms the actual probabilities to probabilities used in (risk-neutral) valuation.

Assumption 5.12. *We assume that the risk premium adjustments are such that the credit rating process under the martingale probabilities satisfy*

$$q_{ij}(t,t+1) = \begin{cases} \pi_i(t)p_{ij}, & j \neq i, \\ 1 + \pi_i(t)(p_{ii}-1), & i = j \end{cases} \tag{5.29}$$

for all $i,j \in \mathcal{S}$ where

- *$\pi_i(t)$ is a time-dependent, deterministic function (interpreted as discrete-time risk premiums), such that*
- *$q_{ij}(t,t+1) \geq 0$ for all $i,j,j \neq i$, and*
- *$\sum_{\substack{j=1 \\ j\neq i}} q_{ij}(t,t+1) \leq 1$ for $i = 1,\dots,K$.*

The positivity of $q_{ij}(t,t+1)$ results from the the equivalence of the two measures $\mathcal{Q}$ and $\mathcal{P}$. In addition, we see that from (5.29) for $i = j$ (and $q_{ij}(t,t+1) > 0$) the risk premium adjustments $\pi_i(t)$ must satisfy the condition

$$0 < \pi_i(t) < \frac{1}{1-p_{ii}}, \quad \forall i \neq K-1, t \in \mathbb{N}. \tag{5.30}$$

Further, we assume a given empirical, usually an one-year, transition matrix $\boldsymbol{P}_{0,1}$ which is abbreviated to $\boldsymbol{P}$ for this segment. With (5.23) and Assumption 5.12 we can compute

$$\boldsymbol{Q}_{0,t+1} = \boldsymbol{Q}_{0,t}[\boldsymbol{I} + \boldsymbol{\Pi}(t)(\boldsymbol{P} - \boldsymbol{I})]. \tag{5.31}$$

From (5.31) and Lemma 5.1 we get

$$Q_i(\tau \leq t+1 \,|\, \mathcal{H}_0) = \sum_{j=1}^{K} q_{ij}(0,t)\pi_j(t)p_{jK}. \tag{5.32}$$

With above specification we can now formulate a recursive procedure given in Algorithm 5.1. Thereby, we mainly refer to Bielecki and Rutkowski (2004) and enrich by some additional details from Jarrow et al. (1997).

Algorithm 5.1 (Calibration JLT in discrete-time). *Assuming that $\boldsymbol{Q}_{0,t}^{-1}$ exists then solving (5.35) leads to the recursive procedure in discrete-time:*

1. *For $t = 0$, compute from (5.35) the initial values of credit risk premiums, i.e. the vector $(\pi_1(0), \ldots, \pi_{K-1}(0))$. In more detail: Equation (5.18) will be matched if $Q_i(\tau \leq T \mid \mathcal{H}_0)$ is selected such that*

$$Q_i(\tau \leq T \mid \mathcal{H}_0) = \frac{P(0,T) - V_i(0,T)}{P(0,T)(1-\delta)} \tag{5.33}$$

for $i = 1, \ldots, K$ and $T = 1, 2, \ldots, T^*$. Given the empirical transition matrix $\boldsymbol{P}$, we have

$$\boldsymbol{Q}_{0,1} = \boldsymbol{I} + \boldsymbol{\Pi}(0)(\boldsymbol{P} - \boldsymbol{I}).$$

From this matrix, and Lemma 5.1, we get

$$Q_i(\tau \leq 1 \mid \mathcal{H}_0) = \pi_i(0) p_{iK}.$$

Substitution into Equation (5.33) and since $\boldsymbol{Q}_{0,0} = \boldsymbol{I}$ gives

$$\pi_i(0) = \frac{P(0,1) - V_i(0,1)}{P(0,1)(1-\delta)p_{iK}}, \tag{5.34}$$

for $i = 1, \ldots, K-1$.

2. *By combining equations (5.29) and (5.23) find the one-step risk-neutral probability matrix $\boldsymbol{Q}_{0,1}$.*

3. *Substituting (5.32) into Equation (5.33) yields*

$$\boldsymbol{Q}_{0,t} \begin{pmatrix} \pi_1(t) p_{1K} \\ \vdots \\ \pi_{K-1}(t) p_{K-1,K} \\ 1 \end{pmatrix} = \begin{pmatrix} \frac{P(0,t+1) - V_1(0,t+1)}{P(0,t+1)(1-\delta)} \\ \vdots \\ \frac{P(0,t+1) - V_{K-1}(0,t+1)}{P(0,t+1)(1-\delta)} \\ 1 \end{pmatrix}, \tag{5.35}$$

where $\boldsymbol{Q}_{0,0} = \boldsymbol{I}$. At time $t = 1$ we solve (5.35) for the credit risk premiums $(\pi_1(t), \ldots, \pi_{K-1}(t))$ where we use the the matrix $\boldsymbol{Q}_{0,1}$ from the 2. step.

4. *Repeat steps 2. and 3. until all vectors of the risk premiums $(\pi_1(t), \ldots, \pi_{K-1}(t))$, $t = 2, \ldots, T^* - 1$, and, simultaneously, all values $\boldsymbol{Q}_{0,t}$, $t = 3, \ldots, T^*$, (and likewise $\boldsymbol{Q}_{t,t+1}$, $t = 2, \ldots, T^* - 1$ from Assumption 5.12) are found.*

Remark 5.21. *Let us examine the JLT model at $t = 0$ in view of formulae (5.34) and inequality (5.30). If p_{iK} are sufficiently close to zero compared to the nominator in (5.34) then condition (5.30) is violated. Clearly, Algorithm 5.1 is valid only if the one-period default probability is non-zero for every credit class. One option to overcome the possibility of exploding risk premiums in the JLT model is to manipulate the default probabilities, hence impose a upward shift as proposed by Jarrow et al. (1997) where p_{iK} are specified to have a minimum value of 0.0001, which again needs to be subtracted from the main diagonal of $\boldsymbol{P}_{0,1}$. One may argue that this is a rather crude approach and does not necessarily reflect the market as it is not unusual that no defaults occur for bonds with high credit ratings within a time period of one year. This may lead to incorrect pricing results and to arbitrage opportunities.*

Finally, we can use Algorithm 5.1 to obtain the continuous-time calibration procedure by taking Assumption 5.11 into consideration in order to find the risk-neutral intensity matrices $\widetilde{\boldsymbol{G}}(t)$ at time t for given δ and $\boldsymbol{G}$. Again, this is accomplished by matching the observed market prices $V_i(0,T)$ with the theoretical values predicted by the model via the starting position given by (5.18), the credit-risky zero-coupon bond price curves. Substituting $T = t + \Delta t$ on the left and right side of the forward equation (5.28) we get for small Δt and $\boldsymbol{Q}(t,t) = \boldsymbol{I}$ (the initial condition) an appropriate approximation where (Jarrow et al., 1997)

$$\boldsymbol{Q}(t, t + \Delta t) \approx \boldsymbol{I} + \widetilde{\boldsymbol{G}}(t)\Delta t = \boldsymbol{I} + \boldsymbol{U}(t)\boldsymbol{G}\Delta t, \tag{5.36}$$

with

$$\frac{\partial \boldsymbol{Q}(t,T)}{\partial T}\Big|_{T=t+\Delta t} \approx \frac{\boldsymbol{Q}(t, t+\Delta t) - \boldsymbol{I}}{\Delta t}$$

and

$$\boldsymbol{Q}(t, t+\Delta t)\widetilde{\boldsymbol{G}}(t+\Delta t) \approx \boldsymbol{Q}(t,t)\widetilde{\boldsymbol{G}}(t) = \widetilde{\boldsymbol{G}}(t).$$

It is assumed that $\boldsymbol{U}(t)$ is right continuous over $[t, t+\Delta t)$ for small Δt (Jarrow et al., 1997). Algorithm 5.2 yields the desired calibration procedure for the risk premia $\boldsymbol{U}(t)$ for the continuous-time pendant of Algorithm 5.1.

Algorithm 5.2 (Calibration JLT in continuous-time). *Follow the recursive procedure in Algorithm 5.1 with steps 1. to 4. by setting (in matrix notation)*

$$\boldsymbol{\Pi}(t) \equiv \boldsymbol{U}(t)$$

in (5.34),

$$\boldsymbol{Q} - \boldsymbol{I} \equiv \boldsymbol{G}\Delta t$$

in (5.35) and taking the approximation (5.36) of the Kolmogorov forward equation into consideration.

Remark 5.22. *To overcome the drawback of Remark 5.21, Kijima and Komoribayashi (1998) (KK) developed a slight modification of the JLT model where the denominator (5.34) allows for small default probabilities p_{iK}. The central difference of the KK to the JLT model is the handling of the risk premiums in (5.24) with (5.25). Kijima and Komoribayashi (1998) assume that the risk premium adjustments are such that the credit rating process under the martingale probabilities satisfy*

$$q_{ij}(t, t+1) = \begin{cases} \pi_i(t)p_{ij}, & \forall j \neq K, \\ 1 + \pi_i(t)(p_{ii} - 1), & j = K \end{cases} \tag{5.37}$$

for all $i, j \in \mathcal{S}$ where

- $\pi_i(t)$ *is a time-dependent, deterministic function (interpreted as discrete-time risk premiums), such that*
- $q_{ij}(t, t+1) \geq 0$ *for all $i, j, j \neq i$, and*

· $\sum_{\substack{j=1\\ j\neq i}} q_{ij}(t,t+1) \leq 1$ *for* $i = 1,\ldots,K$.

Note the difference between (5.29) and (5.37). In (5.29) the risk premium adjustments $\pi_i(t)$ *are independent of* j *for* $j \neq i$*, while in (5.37) they are independent of* j *for* $j \neq K$*. Similarly, to the boundary condition (5.30) in Jarrow et al. (1997) we can state that the risk premium adjustments* $\pi_i(t)$ *in case of Kijima and Komoribayashi (1998) lies within*

$$0 < \pi_i(t) < \frac{1}{1-p_{iK}}, \quad \forall i \neq K-1, t \in \mathbb{N}, \tag{5.38}$$

resulting from (5.37) for $i = j$ *(and* $q_{ij}(t,t+1) > 0$*).*

5.5.4. Constrained Optimisation

During the review of the JLT (and KK) model above we have identified some weaknesses when incorporating risk premiums, moving from $\mathcal{P}$ to $\mathcal{Q}$, which are briefly summarised:

· The resulting adjusted transition matrix under $\mathcal{Q}$ is not a transition probability matrix since Properties B.1 may be violated. Likewise, the one-step transition matrices calculated from cumulative transition probability matrices do not necessarily have to be transition probability matrices.

· Equivalence of $\mathcal{P}$ and $\mathcal{Q}$ is not guaranteed. For example, Assumption 5.3 claims that the underlying probability measures, $\mathcal{P}$ and $\mathcal{Q}$, are equivalent. However, apart from the drawback described in Remark 5.21 it can be frequently observed that Algorithm 5.1 yields values of $\pi_i(t)$ which thereunto result in negative risk-neutral probabilities.

We shall address above issues by introducing constrained optimisation techniques to the JLT and KK model. Imposing constraints to a linear optimisation problem allows us to additionally infer the recovery rate from market prices with the condition that $0 \leq \delta \leq 1$ if desired. Jarrow et al. (1997) already acknowledge the issues related to the Algorithm 5.1 and therefore propose to opt for the constrained optimisation technique where $u_i(t) \geq 0$, $i = 1,\ldots,K-1$ (the risk premiums need to be non-negative for all credit classes i and times t). Furthermore, as pointed out by Jarrow et al. (1997) arbitrage opportunities may arise due to the existence of negative risk premia which caused by the so called 'yield-to-worst issue' when stripping bonds to obtain zero-coupon bond prices. These potential mispriced zero-coupon bonds are taken care of by Problem 5.2 yielding "the best values for the risk premia consistent with no arbitrage", cf. (Jarrow et al., 1997). Here Jarrow et al. (1997)'s constrained optimisation is slightly modified to Problem 5.2 where $\widetilde{\boldsymbol{G}} \in \mathcal{G}$ implies $(u_1(t),\ldots,u_{K-1}(t)) \geq 0$. The proposed optimisation problem amounts to the sum of squared differences between model and market risk zero-coupon bonds using (5.18) at each time step t and each credit class i.

Problem 5.2. *Let* $V_i(0,t;\widetilde{\boldsymbol{G}})$ *be the model zero-coupon bond prices and* $V_i^M(0,t)$ *be the market zero-coupon bond prices, then*

$$\min_{\substack{\widetilde{\boldsymbol{G}}\in\mathcal{G}\\ u_K(t)=1}} \sum_{i=1}^{K} \Big(V_i(0,t;\widetilde{\boldsymbol{G}}) - V_i^M(0,t)\Big)^2 \tag{5.39}$$

where the set $\mathcal{G}$ is defined as in Definition 5.4.

Further, the additional risk-relevant constraints introduced in Hughes and Werner (2016) can be added to the generator matrix $\widetilde{\boldsymbol{G}}$ where the continuous-time modelling properties are met. The best approximation of the annual transition matrix (BAM) is applied at each time step t for (5.39) with selective or all proposed structural corrections to the generator yielding the desired credit risk relevant outcomes. This adds additional flexibility when moving from $\mathcal{P}$ to $\mathcal{Q}$. Note that the 'yield-to-worst issue' due to 'bad data' as described in Jarrow et al. (1997) may also be improved upon when applying the additional constraints in Hughes and Werner (2016) and simultaneously satisfying $\mathcal{G}$ in Definition 5.4 at all times.

5.6. Extended Jarrow et al. (1997) Approach

So far, in the context of the JLT model, we assumed that prices of risky zero-coupon bonds, $V_i(t,T)$, from credit classes $i = 1,\dots,K-1$ are exogenously given. Yet, in our framework we face the problem that the respective present values of the bonds belonging to the corresponding rating classes are unknown to us. Moreover, it is precisely the value we desire to obtain. Thus, we must find a way of incorporating risk premiums exogenously in order to obtain the risk-neutral zero-coupon bond prices. We refer to Dubrana (2011) where an elegant remedy to our issue is proposed allowing for stochastic spreads which originates from Arvanitis et al. (1999). Here, risk premiums are modelled as a stochastic differential equation in form of the CIR1F model as already introduced in Section 4.1.3 and partly in Appendix B.2. This leads us to an extension of the Jarrow et al. (1997) model, the so called extended JLT (EJLT) model.

Remark 5.23. *The classical usage of the CIR1F model is in the context of interest rates. However, it possesses many other application possibilities due to its non-negativity property, for example as variance process (Section 4.1.3), as intensity process (referring to the conversation between a trader and a quantitative analyst in Brigo and Mercurio (2007)) and, as proposed here, as risk premium process.*

Assume the real world generator matrix is diagonalisable,

$$\boldsymbol{G} = \boldsymbol{\Sigma}\boldsymbol{D}\boldsymbol{\Sigma}^{-1}$$

where the column of $\boldsymbol{\Sigma} \in \mathbb{R}^{K\times K}$ are the right eigenvectors of $\boldsymbol{G}$ and $\boldsymbol{D}$ is the diagonal matrix of eigenvalues of $\boldsymbol{G}$. Similarly, assume the risk-neutral generator matrix is given by

$$\widetilde{\boldsymbol{G}}(t) = \boldsymbol{\Sigma}\widetilde{\boldsymbol{D}}(t)\boldsymbol{\Sigma}^{-1},$$

where $\widetilde{\boldsymbol{D}}(t)$ is a time-dependent stochastic diagonal matrix in order to allow for stochastic spreads, considering that

$$\widetilde{\boldsymbol{D}}(t) = \pi(t)\boldsymbol{D}$$

where we postulate $\pi(t)$ to be stochastic risk premiums. I.e. the model of Arvanitis et al. (1999) relies on modifying the eigenvalues of the historical transition rates while leaving the eigenvectors $\boldsymbol{\Sigma}$ unchanged resulting in the generator matrix $\widetilde{\boldsymbol{G}}$ under the martingale measure. The risk-neutral transition matrix is

$$\boldsymbol{Q}_{t,T} = \boldsymbol{\Sigma}\mathbb{E}_{\mathcal{Q}}\left[\exp\left(\int_t^T \widetilde{\boldsymbol{D}}(s)\mathrm{d}s\right)\middle|\mathcal{H}_t\right]\boldsymbol{\Sigma}^{-1}, \tag{5.40}$$

where $\widetilde{\boldsymbol{D}}(t) = \mathrm{diag}(\widetilde{d}_1(t), \widetilde{d}_2(t), \ldots, \widetilde{d}_K(t))$. Default probabilities can be obtained via

$$\begin{aligned} q_{iK}(t,T) &= \sum_{j=1}^{K-1} \sigma_{ij}\hat{\sigma}_{iK}\left\{\mathbb{E}_{\mathcal{Q}}\left[\exp\left(\int_t^T \widetilde{d}_j(s)\mathrm{d}s\right)\middle|\mathcal{H}_t\right] - 1\right\} \\ &= \sum_{j=1}^{K-1} \sigma_{ij}\hat{\sigma}_{iK}\left\{\mathbb{E}_{\mathcal{Q}}\left[\exp\left(d_j\int_t^T \pi(s)\mathrm{d}s\right)\middle|\mathcal{H}_t\right] - 1\right\}. \end{aligned} \tag{5.41}$$

for $1 \leq i \leq K-1$ and where σ_{ij} is the ijth element of $\boldsymbol{\Sigma}$ and $\hat{\sigma}_{iK}$ is the ijth element of $\boldsymbol{\Sigma}^{-1}$, which follows from

$$\boldsymbol{Q}_{t,T} - \boldsymbol{I} = \boldsymbol{\Sigma}\mathbb{E}_{\mathcal{Q}}\left[\exp\left(\int_t^T \widetilde{\boldsymbol{D}}(s)\mathrm{d}s\right) - \boldsymbol{I}\middle|\mathcal{H}_t\right]\boldsymbol{\Sigma}^{-1}$$

and $\widetilde{d}_K = 0$.

Remark 5.24. *Assuming that $\widetilde{\boldsymbol{D}}(t)$ is a deterministic function, then the risk-neutral probabilities are given by*

$$\boldsymbol{Q}_{t,T} = \boldsymbol{\Sigma}\left[\exp\left(\int_t^T \widetilde{\boldsymbol{D}}(s)\mathrm{d}s\right)\right]\boldsymbol{\Sigma}^{-1},$$

and respectively

$$q_{iK}(t,T) = \sum_{j=1}^{K-1} \sigma_{ij}\hat{\sigma}_{iK}\left\{\exp\left(\int_t^T \widetilde{d}_j(s)\mathrm{d}s\right) - 1\right\}.$$

The stochastic short rate spreads for a given rating can be written as

$$(1-\delta)\widetilde{g}_{iK}(t) = (1-\delta)\pi(t)\sum_{j=1}^{K-1} \sigma_{ij}\hat{\sigma}_{jK}d_j.$$

Now, it is the objective to derive a closed form solution of (5.41) for a rating class j, more precisely of the term

$$\mathbb{E}_{\mathcal{Q}}\left[\exp\left(d_j\int_t^T \pi(s)\mathrm{d}s\right)\middle|\mathcal{H}_t\right].$$

Therefore, we resort to the affine term structure solution of Section B.2.3.2, in particular of the CIR1F model derived in Remark 4.6 where we simply can replace $r(t)$ by $\pi(t)$, respectively $\varsigma^2(t)$ by $\pi(t)$, solving the stochastic differential equation for the CIR model

with

$$\mathrm{d}\pi(t) = \alpha_\pi(\mu_\pi - \pi(t))\mathrm{d}t + \sigma_\pi\sqrt{\pi(t)}\mathrm{d}W^{\mathcal{Q}}(t), \quad \pi(0) = \pi_0. \tag{5.42}$$

The square root process $\pi(t)$ ensures that the credit spreads are positive (see Section 4.1.3 and Appendix B.2 for more details on the CIR1F model; we additionally refer to Brigo and Mercurio (2007) and Björk (2004), amongst others, for theoretical supplementation). The ATS, according to Dubrana (2011), takes on the formulation

$$\mathbb{E}_{\mathcal{Q}}\left[\exp\left(d_j\int_t^T \pi(s)\mathrm{d}s\right)\middle|\mathcal{H}_t\right] = \exp(A_j(t,T) - \pi(t)B_j(t,T)), \tag{5.43}$$

where

$$A_j(t,T) = \frac{2\alpha_\pi\mu_\pi}{\sigma_\pi^2}\ln\left(\frac{2\nu_j \mathrm{e}^{\frac{1}{2}(\alpha_\pi+\nu_j)(T-t)}}{(\nu_j+\alpha_\pi)\left(\mathrm{e}^{\nu_j(T-t)}-1\right)+2\nu_j}\right),$$
$$B_j(t,T) = \frac{-2d_j\left(\mathrm{e}^{\nu_j(T-t)}-1\right)}{(\nu_j+\alpha_\pi)\left(\mathrm{e}^{\nu_j(T-t)}-1\right)+2\nu_j}$$

with $\nu_j = \sqrt{\alpha_\pi^2 - 2d_j\sigma_\pi^2}$ and $d_j \leq 0$ a constant value[15]. The proof of (5.43) can be derived analytically[16] in a similar way as already outlined in Remark 4.6.

Proof. Let us reformulate (5.43) to

$$Z_j(t) := \exp\left(d_j\int_0^t \pi(s)\mathrm{d}s\right)F_j(t,\pi(t);T) = \mathbb{E}_{\mathcal{Q}}\left[\exp\left(d_j\int_0^T \pi(s)\mathrm{d}s\right)\middle|\mathcal{H}_t\right]$$

where

$$F_j(t,\pi(t);T) = \mathbb{E}_{\mathcal{Q}}\left[\exp\left(d_j\int_t^T \pi(s)\mathrm{d}s\right)\middle|\mathcal{H}_t\right]$$

which is abbreviated to $F_j(t,\pi;T)$. For $s \leq t \leq T$ and $\mathbb{E}_{\mathcal{Q}}\left[\exp\left(d_j\int_0^T \pi(s)\mathrm{d}s\right)\middle|\mathcal{H}_t\right]$ being finite (see Theorem 4.1 in Dufresne (2001)), by using the tower property of the conditional expectation, we get

$$\begin{aligned}
\mathbb{E}_{\mathcal{Q}}[Z_j(t)\,|\,\mathcal{H}_s] &= \mathbb{E}_{\mathcal{Q}}\left[\exp\left(d_j\int_0^t \pi(u)\mathrm{d}u\right)F_j(t,\pi;T)\middle|\mathcal{H}_s\right]\\
&= \mathbb{E}_{\mathcal{Q}}\left[\mathbb{E}_{\mathcal{Q}}\left[\exp\left(d_j\int_0^T \pi(u)\mathrm{d}u\right)\middle|\mathcal{H}_t\right]\middle|\mathcal{H}_s\right]\\
&= \mathbb{E}_{\mathcal{Q}}\left[\exp\left(d_j\int_0^T \pi(u)\mathrm{d}u\right)\middle|\mathcal{H}_s\right]\\
&= \exp\left(d_j\int_0^s \pi(u)\mathrm{d}u\right)\mathbb{E}_{\mathcal{Q}}\left[\exp\left(d_j\int_s^T \pi(u)\mathrm{d}u\right)\middle|\mathcal{H}_s\right]
\end{aligned}$$

[15] d_j is an eigenvalue of the generator matrix $\boldsymbol{G}$. We know that the spectral radius of the transition matrix is one. The eigenvalues of a generator matrix are thus equal to the logarithm of eigenvalues of the transition matrix, so that we have $d_j \leq 0$.

[16] My expression of gratitude to Yan Yang for providing the proof of the EJLT model.

$$
\begin{aligned}
&= \exp\left(d_j \int_0^s \pi(u)\mathrm{d}u\right) F_j(s,\pi;T) \\
&= Z_j(s). && (5.44)
\end{aligned}
$$

(5.44) explicitly shows that $Z_j(t)$ is a martingale wrt to $\mathcal{Q}$. With $\mu_\pi(t,\pi) = \alpha_\pi(\mu_\pi - \pi(t))$ and $\sigma_\pi(t,\pi) = \sigma_\pi\sqrt{\pi(t)}$ and the product rule of Itô's Lemma we get

$$
\begin{aligned}
\mathrm{d}Z_j(t) &= \left(\mathrm{d}\exp\left(d_j \int_0^t \pi(u)\mathrm{d}u\right)\right) F_j(t,\pi;T) + \exp\left(d_j \int_0^t \pi(u)\mathrm{d}u\right) \mathrm{d}F_j(t,\pi;T) \\
&= \exp\left(d_j \int_0^t \pi(u)\mathrm{d}u\right) \Bigg[\Bigg(d_j\pi(t)F_j(t,\pi;T) + \frac{\partial F_j}{\partial t}(t,\pi) + \\
&\qquad \mu_\pi(t,\pi)\frac{\partial F_j}{\partial \pi}(t,\pi) + \frac{1}{2}\sigma_\pi^2(t,\pi)\frac{\partial^2 F_j}{\partial \pi^2}F_j(t,\pi;T)\Bigg)\mathrm{d}s + \\
&\qquad\qquad \sigma_\pi(t,\pi)\frac{\partial F_j}{\partial \pi}(t,\pi)\mathrm{d}W(t)\Bigg]
\end{aligned}
$$

In order to show that $Z_j(t)$ is a martingale the ‘ds-term’ needs to be zero with

$$
\begin{aligned}
&d_j\pi(t)F_j(t,\pi;T) + \frac{\partial F_j}{\partial t}(t,\pi) + \mu_\pi(t,\pi)\frac{\partial F_j}{\partial \pi}(t,\pi) + \\
&\qquad \frac{1}{2}\sigma_\pi^2(t,\pi)\frac{\partial^2 F_j}{\partial \pi^2}F_j(t,\pi;T) \overset{!}{=} 0. \qquad (5.45)
\end{aligned}
$$

We consider the case where $d_j \in \mathbb{R}$ and $d_j \leq 0$. Further we assume that (5.43) holds. We substitute (5.43) in (5.45) where

$$
\begin{aligned}
&\frac{\partial A_j(t,T)}{\partial t} - \frac{\partial B_j(t,T)}{\partial t}\pi(t) + \mu_\pi(t,\pi)(-B_j(t,T)) + \frac{1}{2}\sigma_\pi^2(t,\pi)B_j^2(t,T) + d_j\pi(t) = 0 \\
&\left(\frac{\partial A_j(t,T)}{\partial t} - \alpha_\pi\mu_\pi B_j(t,T)\right) + \left(d_j - \frac{\partial B_j(t,T)}{\partial t} + \alpha_\pi B_j(t,T) + \frac{1}{2}\sigma_\pi^2 B_j^2(t,T)\right)\pi(t) = 0
\end{aligned}
$$

For all t, T, π the following equations muss hold:

$$
\frac{\partial B_j(t,T)}{\partial t} - \alpha_\pi B_j(t,T) - \frac{1}{2}\sigma_\pi^2 B_j^2(t,T) = d_j \qquad (5.46)
$$

$$
\frac{\partial A_j(t,T)}{\partial t} = \alpha_\pi\mu_\pi B_j(t,T) \qquad (5.47)
$$

We know that (5.46) is a Riccati differential equation. For time independent factor α_π, μ_π we extend Corollary B.2 to (Schlüchtermann and Pilz, 2010, p. 335)

$$
\begin{aligned}
\frac{2}{d_j^2\sigma_\pi^2}A_j(t,T) &= a_2c_2\ln(a_2 + B_j(t,T)/d_j) + c_2a_1\ln\left(\frac{-B_j(t,T)/d_j + a_1}{a_1}\right) - \\
&\qquad a_2c_2\ln a_2 \qquad (5.48)
\end{aligned}
$$

and

$$
B_j(t,T) = \frac{-2d_j(\mathrm{e}^{c_1(T-t)} - 1)}{(\alpha_\pi + c_1)(\mathrm{e}^{c_1(T-t)} - 1) + 2c_1} \qquad (5.49)
$$

with

$$a_1 = -\frac{\alpha_\pi - \sqrt{\alpha_\pi^2 - 2d_j\sigma_\pi^2}}{-d_j\sigma_\pi^2}, \qquad a_2 = -\frac{-\alpha_\pi - \sqrt{\alpha_\pi^2 - 2d_j\sigma_\pi^2}}{-d_j\sigma_\pi^2},$$
$$c_1 = \sqrt{\alpha_\pi^2 - 2d_j\sigma_\pi^2}, \qquad c_2 = \frac{\alpha_\pi\mu_\pi}{a_1 + a_2}.$$

Inserting (5.49) into (5.48) (with a_1, a_2, c_1 and c_2) we get

$$A_j(t,T) = \frac{2\alpha_\pi\mu_\pi}{\sigma_\pi^2}\ln\left(\frac{2c_1 \mathrm{e}^{\frac{1}{2}(\alpha_\pi + c_1)(T-t)}}{(c_1+\alpha_\pi)(\mathrm{e}^{c_1(T-t)}-1)+2c_1}\right). \tag{5.50}$$
□

The above EJLT model (5.40), respectively (5.41), with (5.42) and (5.43) by Dubrana (2011) allows us to obtain yield credit spreads as in (5.19). These yield spreads of credit class $i \in \{AAA, AA, A, BBB, BB, B, CCC\}$ depicted in FIGURE 5.11 assume risk neutrality and can be adjusted to reflect any desired situation, e.g. increasing the risk premiums in stressed times of a Pfandbrief bank's cover pool.

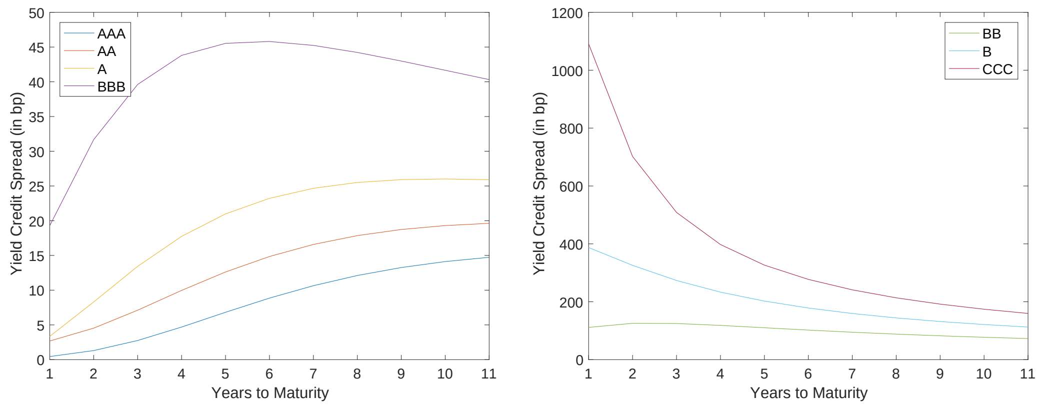

FIGURE 5.11.: Yield credit spreads based on the EJLT model, with given transition matrix $\boldsymbol{P}_{0,1}^{\text{Moodys}}$ of TABLE C.12, recovery rate $\delta = 0.8$, input parameters $\alpha_\pi = 0.1$, $\mu_\pi = 1$, $\sigma_\pi = 1$ and initial value $\pi_0 = 3$. Left: Investment grade yield spreads in basis points as a function of maturity for credit classes AAA, AA, A and BBB; Right: Speculative grade yield spreads in basis points as a function of maturity for credit classes BB, B and CCC.

Remark 5.25. *The proposed calibration method of Arvanitis et al. (1999) can be applied to a constant as well as stochastic generator matrix $\widetilde{\boldsymbol{G}}$ introduced in the EJLT model of Section 5.6. Instead of calibrating a time-dependent intensity matrix at each time step of (5.39) a time-invariant intensity matrix is sought matching a set of pre-specified bond prices as accurately as possible. Additionally, a penalty term is added keeping calibrated transition intensities close to the historical transition intensities. The resulting adjusted intensity matrix and parameters of the SDE in (5.42) are then used to simulate the credit spreads into the future. Each credit class i is extended by $j = 1, \ldots, J$ bonds, expressed* *as*

$$\hat{V}_i^j(\widetilde{\boldsymbol{G}}) = \sum_{h=1}^{T} C_i^j(h) V_i(h, \widetilde{\boldsymbol{G}})$$

where $C_i^j(h)$ *is the coupon of bond* j *in state* i *at date* h *and* $V_i(h, \widetilde{\boldsymbol{G}})$ *is the price of a zero-coupon bond in state* i *with maturity* h*. Again a least squares optimisation is used obtaining a solution closest to the historical generator matrix* $\boldsymbol{G}$*, see Problem 5.3.*

Problem 5.3. *Let* $\hat{V}_i^j(\widetilde{\boldsymbol{G}})$ *be the model bond prices and* $\hat{V}_i^{j,M}$ *be the market bond prices, then*

$$\min_{\substack{\widetilde{\boldsymbol{G}} \in \mathcal{G} \\ \alpha_\pi, \mu_\pi, \sigma_\pi \geq 0 \\ \tilde{d}_K = 0}} \left[\sum_{i=1}^{K} \sum_{j=1}^{J} \left(\hat{V}_i^j(\widetilde{\boldsymbol{G}}) - \hat{V}_i^{j,M} \right)^2 + \underbrace{\sum_{i,j=1}^{K} \left(\frac{(\tilde{g}_{ij} - g_{ij})^2}{\beta_{ij}} \right)}_{\text{penalty term}} \right] \tag{5.51}$$

where the set $\mathcal{G}$ *is defined as in Definition 5.4,* α_π*,* μ_π *and* σ_π *are the parameters of the SDE in (5.42) and* β_{ij} *is some confidence level. A penalty term is added, keeping the eigenvectors close to their historical counterparts.*

5.7. An Application

In the upcoming section we will apply some of the introduced methods from above within the reduced-form model, summarise the modelling outcomes and point out the modelling characteristics. On the one hand with above model specification (Section 5.3 with Figure 5.5, Section 5.4, Section 5.5 and Section 5.6), the weaknesses of the initial model pointed out in Section 5.2 are largely ironed out. However, on the other hand, we have added a higher degree of complexity to the modelling of the Pfandbrief to our reduced-form model, particularly to the CP position. Nonetheless, these advancements turn out to be necessary for an adequate representation of the asset present values at time T_1 in a risk-neutral setting. Here, we purposely apply above theory by means of stylised examples.

Linking Cover Pool and Other Assets As in the model setup of Section 5.3 let us start off with linking of CP and OA. Thereby, let us assume we already have obtained the marginal distributions of CP and OA at time T_1 and build upon Example 5.1. We plug in the simulated joint distribution from the t-copula into equations (3.11), (3.14) and (3.15) to obtain the PVs of the liabilities, see Figure 5.12. Since we are interested in capturing the Pfandbrief defaults adequately, the tail end of the downside risk needs to be focused on. Figure 5.13 depicts the impact the choice of the used copula has on the outcome of the PB distribution. Evidently, the cases of Pfandbrief defaults have increased with the t-copula as opposed to the Gaussian copula since the probability mass has shifted more to the left of the threshold nominal of $N_{PB} = 1$.

Remark 5.26. *Noteworthy, at this point, is the fact that we have no closed solution for the CP distribution at* T_1 *with (5.6) and Definition 5.2 so that we need to resort to numerical methods of the empirical inverse cdf with the* Matlab *function* `ksdensity`*. For the OA values we can simply use the* Matlab *inbuilt function* `logninv`*.*

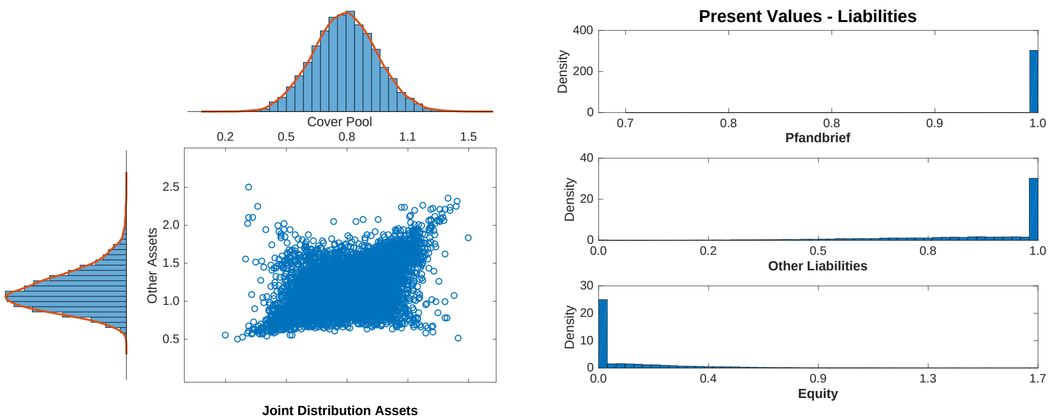

FIGURE 5.12.: Left: Joint distribution of present values of cover pool and other assets at time T_1.; Right: Present values of Pfandbrief, other liabilities and equity at time T_1.

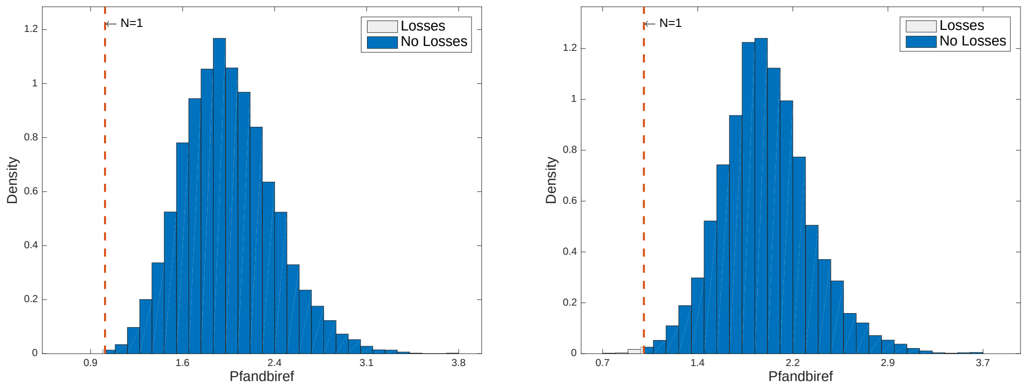

FIGURE 5.13.: Left: Pfandbrief distribution at time T_1, with Gaussian Copula. Right: Pfandbrief distribution at time T_1, with Student's t Copula.

Other Assets For the OA we moved in the opposite direction as in the CP case, taking complexity out compared to the structural model of Chapter 4. We postulate a log-normal distribution for the OA position as specified in Section 5.3.3. In order to obtain suitable model parameters of the other assets distribution at T_1 we resort to Monte Carlo simulations, partly derived on the findings in Chapter 4 of Sünderhauf's structural model (4.32). We calibrate the risk-neutral parameters $m_{V_{OA}}$ and $s^2_{V_{OA}}$ to the distribution of V_{OA} obtained at T_1 from (4.32), so that

$$V_{OA}(T_1) \sim \mathrm{LN}\left(m_{V_{OA}}, s^2_{V_{OA}}\right).$$

FIGURE 5.14 shows densities for different T_1 with corresponding input parameters of the log-normal distribution.

Cover Pool Most modelling advancements and complexities are attributed to the CP to adequately reproduce the PVs of the CP at T_1. Above approaches allow us to simulate downgrading during stressed periods which shall be illustrated in what follows. We shall start off by assuming that the cover pool is classified into different rating buckets to make use of the methods introduced in Section 5.4 and Section 5.6 (based

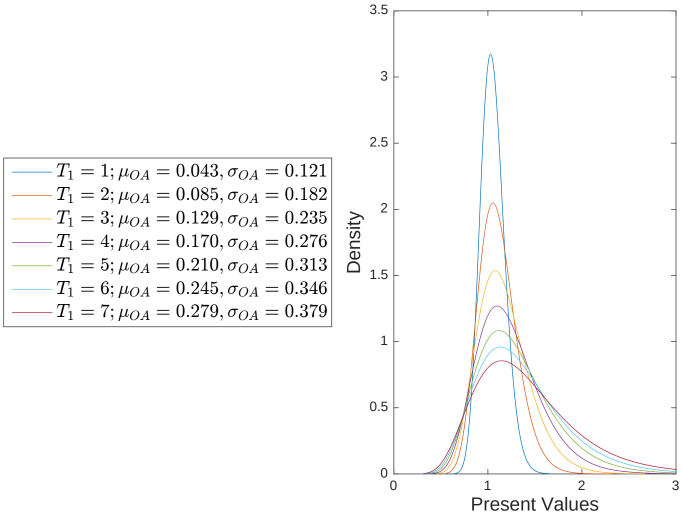

FIGURE 5.14.: Other assets distribution with different input parameters for $T_1 = \{1, 2, \ldots, 7\}$.

on Section 5.5), namely, being able to forecast into the future and model risk-neutrally. After we have successfully forecasted and stressed the portfolio to time T_1 we shall then aggregate over all rating buckets assuming a LHP with stochastic recovery rates as specified in Section 5.3.2.2. A LHP approximation constitutes a considerable modelling simplification. However, there also seems to be evidence to justify the LHP assumption. In TABLE 5.13 the mortgage Pfandbrief credit ratings of the seven mortgage banks defined in TABLE C.2 are displayed. Noticeable is the fact that five of them have been

	AAR	BHH	MHB	MMW	NAT	WBP	WIB
Rating	Aaa	Aaa	Aaa	NA	Aaa	AAA	NA

TABLE 5.13.: Ratings for mortgage Pfandbriefe of 'Hyp' type issuers as defined in TABLE C.2 (sources: AAR: (Lenhard, 2017); BHH: (Widmayer and Yamanaka, 2018); MHB: (Homey and Soriano, 2010); MMW: No ratings found for mortgage Pfandbriefe; NAT: (Rast and Soriano, 2013); WBP: (Isopel and Lanza, 2017); WIB: No ratings found for mortgage Pfandbriefe)

accredited a triple A rating either by Moody's or S&P. Two could not be determined due to lack of information provided by the issuer or rating companies. However, in general it can be observed that a high credit class is attributed to the Pfandbrief over most issuers. The credit quality of the Pfandbrief is highly correlated with the credit quality of its underlying cover pool. Among other factors, also the credit strength of the issuer, the German legal framework for Pfandbriefe and the maintenance of a certain voluntary (above the legal requirements) over-collateralisation contribute to the overall credit quality, compare also Spangler and Werner (2014).
We want to focus on the cover pool. Based on TABLE 5.13, it is fair to assume that a large majority of cover pool assets will consequently also have a triple A status, resulting in a homogeneous cover pool portfolio. Unfortunately, ratings of single nor of bucketed cover pool assets are provided by the Pfandbrief banks. Thus, we need

to establish our own cover pool portfolio with a predominant triple A bucket. In TABLE 5.14 we see the percentage holdings of each credit class. Hence, initially we assume that the cover pool, starting with an overall average credit quality of triple A in $t = 0$. Further, we assume we are given an one year transition matrix $\boldsymbol{P}_{0,1}$ of the corresponding cover pool portfolio. The proposed modelling steps for obtaining a

Rating Category	AAA	AA	A	BBB	BB	B	CCC-C
Holdings (in %)	86.5%	9.7%	2.4%	1.0%	0.2%	0.1%	0.1%

TABLE 5.14.: Cover Pool portfolio quality breakdown to the percentage holdings in the portfolio.

(forward) risk-neutral distribution of $V(T_1, T_2)$ are:

1. The initial term structure of default free bonds $P(T_1, T_2)$ can be obtained under $\mathcal{Q}$ via the HW1F model based on calibration to the market yield curve (see Example 3.1) or under $\mathcal{Q}_{T_2}$ via the given market term structure.
2. We forecast $Q^i_{T_2}(\tau \leq T_2 \,|\, \tau > T_1)$ by using $\boldsymbol{P}_{0,1}$ and the EJLT model (Section 5.6). Suitable parameters of the EJLT model can be obtained by calibrating to bond data as outlined in Problem 5.3. Additional constraints to the generator matrix can be imposed if desired, see Hughes and Werner (2016).
3. We aggregate $Q^i_{T_2}(\tau \leq T_2 \,|\, \tau > T_1)$ to one global default probability of all rating classes i with the help of TABLE 5.14.
4. We apply the LHP model (Section 5.3.2.2) with stochastic recovery rates to obtain the forward risk-neutral CP distribution at T_1.

Let us define scenarios to test our modelling proposal. At first a basis scenario is introduced upon which two stressed scenarios are derived to obtain a CP distribution where the downside risk is focussed upon. Therefore, we stress the PDs of each rating class i and increase the risk premia needed to reflect the risk-neutral PDs correctly. FIGURE 5.15 depicts the impact of the two stressed scenarios compared to the basis scenario. Clearly, the distribution has shifted significantly to the left when simulating under stressed PDs or risk premia. This will prove as a valuable feature should the overall CP credit quality of a Pfandbrief bank deteriorate during, for example, a subprime crisis where adaptions can be made quickly and accurately.

Basis

- The base parametrisation of the factor model under Section 5.3.2.2 is as in FIGURE 5.7 with $\mu_{\tilde{\delta}} = 0.4$, $b_{\tilde{\delta}} = 0.2$, $\sigma_{\xi} = 0.01$, $l^{max} = 1$, $\mathbb{E}(\tilde{\delta}) = 0.6$, $\mathbb{V}(\tilde{\delta}) = 0.01$ and $\tau(\tilde{\delta}, X) = 0.8$.
- We use $\boldsymbol{P}^{\text{Moodys}}_{0,1}$ as given in TABLE C.12.
- For the stochastic risk premia we assume that the parametrisation is as stated in FIGURE 5.11 with $\alpha_{\pi} = 0.1$, $\mu_{\pi} = 1$, $\sigma_{\pi} = 0.75$, $\pi_0 = 3$.
- With $T_1 = 3$ and $T_2 = 7$, the riskless component $P(T_1, T_2) = 0.9409$ obtained via calibration as in Example 3.1 (without constraining $\hat{\kappa}$).
- $\text{Corr}(CP, OA) = 0.5$

Stressed PDs Let us use Definition 5.4 and Definition 5.5 in conjunction with Problem 5.1 to stress the PDs on $\boldsymbol{P}^{\text{Moodys}}_{0,1}$ where now investment (Aaa, Aa, A, Baa) and speculative (Ba, B, Caa-C) grades have risen by 50bp and 100bp, respectively. We obtain the updated default vector $\boldsymbol{P}_{i,K}^{\text{update}} = [0.0050, 0.0053, 0.0051, 0.0066, 0.0246, 0.0806, 0.2716]$, with $i = 1, \dots, K-1$ where we additionally apply all correction constraints as in Hughes and Werner (2016), yielding the valid transition matrix

$$\boldsymbol{P}_{0,1}^{\text{stressed}} = \begin{pmatrix} 0.885 & 0.102 & 0.009 & 0.000 & 0.000 & 0.000 & 0.000 & 0.004 \\ 0.010 & 0.886 & 0.095 & 0.003 & 0.001 & 0.000 & 0.000 & 0.004 \\ 0.001 & 0.028 & 0.901 & 0.058 & 0.007 & 0.001 & 0.000 & 0.004 \\ 0.000 & 0.003 & 0.070 & 0.852 & 0.060 & 0.009 & 0.000 & 0.006 \\ 0.000 & 0.001 & 0.004 & 0.055 & 0.834 & 0.079 & 0.004 & 0.023 \\ 0.000 & 0.001 & 0.002 & 0.007 & 0.063 & 0.824 & 0.025 & 0.078 \\ 0.000 & 0.000 & 0.002 & 0.006 & 0.030 & 0.061 & 0.629 & 0.271 \\ 0.000 & 0.000 & 0.000 & 0.000 & 0.000 & 0.000 & 0.000 & 1.000 \end{pmatrix}$$

which is a stressed version of $\boldsymbol{P}_{0,1}^{\text{Moodys}}$ in TABLE C.12.

Stressed Risk Premia We have the additional possibility to simulate stressed risk premiums by utilising the EJLT model of Section 5.6 where we raise the initial risk premium to $\pi_0 = 7$ leaving $\alpha_\pi = 0.1$, $\mu_\pi = 1$ and $\sigma_\pi = 1$ unchanged.

5.8. Summary

In Section 5.2 we introduced a simplified rating based model which, however, is associated with several issues from a modelling perspective, see summarised in Section 5.2.4. In the sections thereafter (Section 5.3, Section 5.4, Section 5.5 and Section 5.6) we have addressed these problems and, besides, set up a viable reduced-form model which is considered to be a refined alternative to the structural model of Chapter 4, as outlined in Section 5.1. Thereby, we have established two common reduced-form methods, the hazard rate approach and the rating-based approach by utilising transition matrices, in conjunction with the LHP where the relaxed assumption of stochastic recovery rates is postulated. Primarily, we opt for the widely used JLT model where one-year transition matrices given by rating agencies can be inserted serving as a proxy for the credit quality of the cover pool. Further, by extending to the EJLT model (Section 5.6) we can exogenously integrate stochastic risk premiums into the advancement of the reduced-form model for modelling Pfandbriefe. Hence, we have received a model which accounts for forward default probabilities and ensures a risk-neutral modelling environment. These additional complexities are necessary in order to adequately capture the underlying credit risk quality of the cover pool and consequently the Pfandbrief which is effectively revealed in Section 5.7.

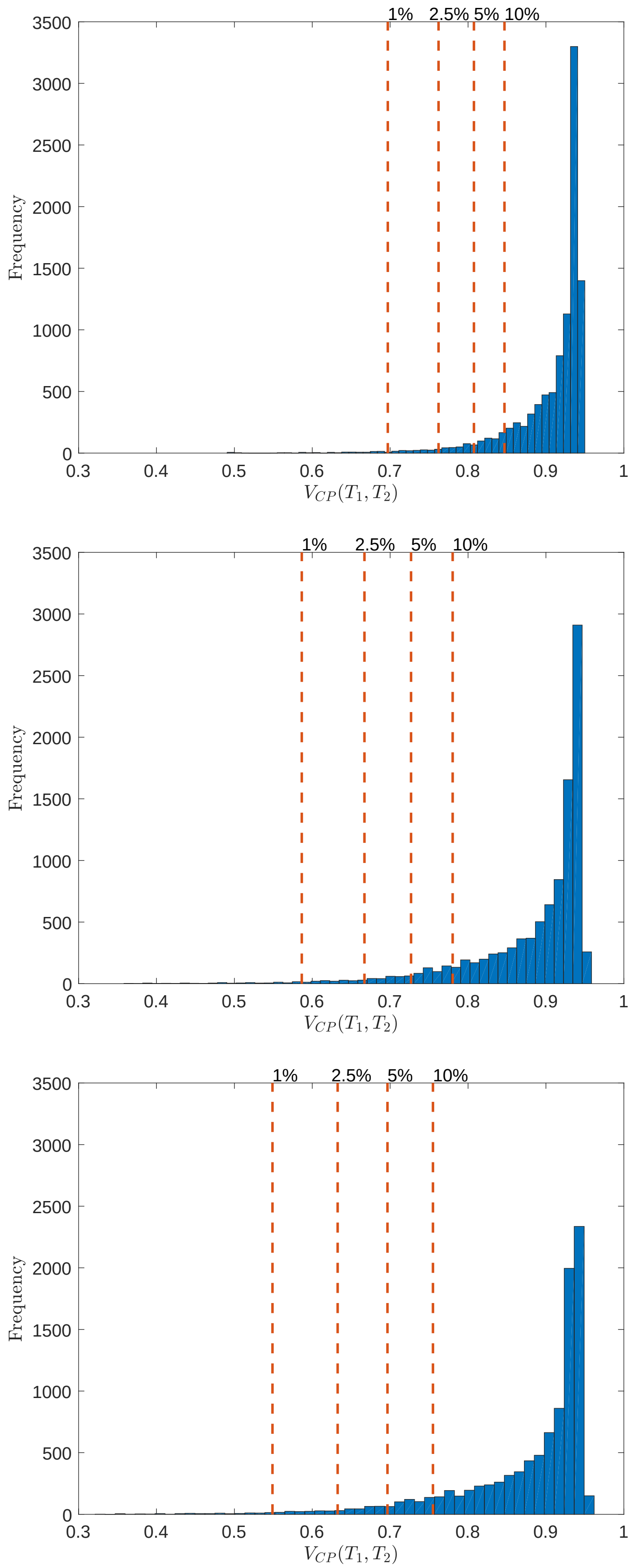

FIGURE 5.15.: CP distributions with scenarios 'Basis' (top), 'Stressed PDs' (middle) and 'Stressed Risk Premia' (bottom).

6. Default Analysis

Risk assessments wrt Pfandbriefe, or more broadly covered bonds, are to this day rare. The simple reason for this is that no reference data exists due to no covered bond defaults in over 100 years. "The extreme scarcity of historical data seriously hampers the analysis of covered bonds and the approximation of PDs", cf. (Golin, 2006) where further a statement by ABN-AMRO reads as follows: "(...) The composition of the collateral pool is of core relevance to the LGD of covered bonds but (...) Basel II prohibits the use of any data provided by the issuer itself effectively making a profound analysis (...) impossible.", cf. (Golin, 2006). Here we shall apply the two introduced one-period models of Chapter 4 and Chapter 5 based on the Pfandbrief framework of Chapter 3 to shed some light, and partly bridge the above mentioned gap, on the overall default modelling of Pfandbriefe. Thereby, we utilise real published data according to §28 PfandBG and balance sheet data from the respective Pfandbrief as gathered in Appendix C. Yet, the available data is still far from complete to conduct fully realistic risk assessments. At first we give some definitions of credit risk measures on which the credit risk assessment of the Pfandbrief is based on. Our main focus lies on the mortgage Pfandbrief bank MHB before we also analyse the other six identified mortgage (type 'Hyp') Pfandbrief banks of TABLE C.2.

6.1. Credit Risk Measures

For our risk assessment in the context of modelling the Pfandbrief in a one-period setting (Chapter 3) we shall mainly orientate ourselves to the described IRB approach in Golin (2006). However, other than Golin (2006, p. 47), we can actually insert the PDs of the Pfandbrief themselves obtained from the application of the structural and reduced-form models instead of the issuer PDs.

Probability of default (PD) Based on (3.11), we define the (risk-neutral) Pfandbrief PDs, for both our approaches by

$$PD_{PB} = \mathrm{Prob}(V_{CP} + V_{OA} < N_{PB}) = \frac{\#\mathrm{Sim}_{\{V_{CP}+V_{OA}<N_{PB}\}}}{\#\mathrm{Sim}_{Total}} \tag{6.1}$$

where #Sim denotes the number of simulated paths or random variables. Hence, (6.1) is simply the frequency of defaults relative to the total events (default and non-default).

Exposure at default (EAD) As a general rule, the Basel Committee on Banking defines EAD (BIS, 2001): "For on-balance sheet transactions, EAD is identical to the nominal amount of exposure." Then, EAD amounts to the (constant) Pfandbrief nominal, with

$$EAD_{PB} = N_{PB}. \tag{6.2}$$

Loss given default (LGD) Under the IRB approach, a predefined LGD ratio of 11.25% for covered bonds (as stated in Capital Requirements Regulation (CRR) Article 161(1), see also Golin (2006) or more recently Izzi et al. (2012) and Gogarn (2015)) has been agreed upon, assuming that covered bonds meet certain criteria (see Capital Requirements Regulation (CRR) Article 129(4) or (5) on covered bonds eligible for the treatment). According to Golin (2006), Germany's mortgage bank association recommend using a lower LGD ration of 7% which is also applied in Ineke et al. (2006). An average LGD of 7% is based on a conducted default analysis consisting of five years of historical data. Thus, we set a constant rate of

$$LGD_{PB} = 0.07 \tag{6.3}$$

which is the fraction of the Pfandbrief's exposure expected to be lost in case of default.

Remark 6.1. *Note that we insert a LGD based on a real-world estimation into our risk-neutral risk assessment models because we simply do not have any other source at our disposal. To obtain an estimate of LGD, for which multiple possibilities exist, it is quite common to resort to a statistical analysis of historical LGD data and to fix it as a deterministic parameter, compare Agrawal et al. (2004) and Izzi et al. (2012).*

Expected Loss (EL) Let us define the Pfandbrief's loss by (Bluhm et al., 2002)

$$\tilde{L}_{PB} = EAD_{PB} \cdot LGD_{PB} \cdot L_{PB} \quad \text{with} \quad L_{PB} = \mathbb{1}_{D_{PB}}, \qquad \text{Prob}(D_{PB}) = PD_{PB} \tag{6.4}$$

where D_{PB} denotes the event that Pfandbriefe default. The expected loss is then defined as (Bluhm et al., 2002)

$$EL_{PB} = \mathbb{E}[\tilde{L}_{PB}] = PD_{PB} \cdot LGD_{PB} \cdot EAD_{PB}, \tag{6.5}$$

with $\mathbb{1}_{D_{PB}}$ being a Bernoulli random variable and equations (6.1), (6.2) and (6.3). For simplicity reasons we assume that the exposure, the loss given default and the default event D_{PB} are independent. EAD_{PB} and LGD_{PB} are considered as constants.

Unexpected Loss (UL) With (6.4), the unexpected loss is defined as (Bluhm et al., 2002)

$$\begin{aligned}
UL_{PB} = \mathbb{V}[\tilde{L}_{PB}]^{\frac{1}{2}} &= \left(\mathbb{E}[\tilde{L}_{PB}^2] - \mathbb{E}[\tilde{L}_{PB}]^2\right)^{\frac{1}{2}} \\
&= \left(\mathbb{E}[EAD_{PB}^2 \cdot LGD_{PB}^2 \cdot L_{PB}^2] - \mathbb{E}[EAD_{PB} \cdot LGD_{PB} \cdot L_{PB}]^2\right)^{\frac{1}{2}} \\
&= \left(EAD_{PB}^2 \cdot LGD_{PB}^2 \cdot PD_{PB} - EAD_{PB}^2 \cdot LGD_{PB}^2 \cdot PD_{PB}^2\right)^{\frac{1}{2}} \\
&= \sqrt{PD_{PB}(1 - PD_{PB})} \cdot LGD_{PB} \cdot EAD_{PB} \qquad (6.6)
\end{aligned}$$

where again we can insert (6.1), (6.2) and (6.3) with EAD_{PB} and LGD_{PB} being constants. Hence, UL_{PB} amounts to the standard deviation of the Pfandbrief loss, or in other words, measures the magnitude of deviation of Pfandbrief losses from the EL_{PB}.

Remark 6.2. *Notice that the unexpected loss representation of (6.6) slightly differs to the definition in Bluhm et al. (2002). We assume that EAD_{PB} and LGD_{PB} are* *constant, whereas in Bluhm et al. (2002) loss given default is the expectation of 'severity of loss in case of default' being a random variable.*

6.2. Adjusted Nominal Values for Coupon Payments

The upcoming proposed procedure provides a more realistic representation of a mortgage Pfandbrief bank's balance sheet at $t = 0$. This basic approach is divided into assets and liabilities. The aim is to calculate adjusted nominal values by allowing coupon payments. Therefore, the given balance sheet and §28 Reporting nominals are discounted by the risk-free rate to today which are equated to the present values according to §28 Reporting. The constant risk-free interest rate of 4^{th} quarter 2016 at $t = 0$ amounts to $r = -0.00218$. Resulting adjusted values of the seven mortgage (type 'Hyp') Pfandbrief banks in TABLE C.2, which can be found in Appendix C.2, are then plugged into the one-period setting of Chapter 3. The computed spreads, s_*^{CP} and s_*^{PB}, are given in TABLE 6.1 of each bank. In TABLE 6.2 the OC and OA shares are displayed which are based on the adjusted balance sheet and §28 Reporting data. TABLE 6.2 will be useful for interpreting the outcomes of the credit risk measures of Section 6.1 when applying the structural (Chapter 4) and reduced-form (Chapter 5) models.

Position	AAR	BHH	MHB	MMW	NAT	WBP	WIB
s_*^{CP}	2.9%	2.6%	1.7%	1.1%	-0.2	2.3%	4.2%
s_*^{PB}	3.1%	2.0%	2.7%	1.5%	1.0	3.1%	3.0%

TABLE 6.1.: Spread estimates of seven mortgage Pfandbrief banks.

Position	AAR	BHH	MHB	MMW	NAT	WBP	WIB
OC	29.4%	7.4%	9.4%	11.9%	50.6%	45.2%	22.6%
OA	71.4%	44.3%	35.1%	29.3%	49.3%	65.1%	30.5%

TABLE 6.2.: Shares of OC and OA of seven mortgage Pfandbrief banks.

6.2.1. Adjusted Asset Nominals

In TABLE 6.3 we denote the cover pool assets with different maturities as $CP_1, \ldots, CP_9$, the cash account as CA and other assets as OA. The maturity ranges are according to §28 Reporting where e.g. for CP_9 the mean over 10 years and 15 years is taken. Further, no maturity over 15 years exists. Cash is only invested until the next point in time so that $T^{CA} = 0$. The maturity of OA is simply set to $T^{OA} = \max_i(T_i^{CP})$. In total we have eleven assets where the buckets for CP amount to nine. Additionally, Assumption 6.1 holds throughout the calculation of the adjusted asset values.

Assumption 6.1. *All CP_i, $i = 1, \ldots, 9$ are zero-coupon bonds. The risk-free rate r and the CP spread s^{CP} are time-independent. CA pays the risk-free rate r.*

	CP_1	CP_2	CP_3	CP_4	CP_5	CP_6	CP_7	CP_8	CP_9	CA	OA
Nom.	N_1^{CP}	N_2^{CP}	N_3^{CP}	N_4^{CP}	N_5^{CP}	N_6^{CP}	N_7^{CP}	N_8^{CP}	N_9^{CP}	N^{CA}	N^{OA}
Mat.	T_1^{CP}	T_2^{CP}	T_3^{CP}	T_4^{CP}	T_5^{CP}	T_6^{CP}	T_7^{CP}	T_8^{CP}	T_9^{CP}	T^{CA}	T^{OA}
Years	0.5	1.0	1.25	1.75	2.5	3.5	4.5	7.5	12.5	0	12.5

TABLE 6.3.: Definitions of the asset types, with corresponding nominals and maturities.

The calculation procedure for the asset side is as follows:

Nominal CA The cover pool nominal cash account equals the values obtained from §28 Reporting with

$$N^{CA} = \widetilde{N}^{CA}. \tag{6.7}$$

Nominal CP According to §28 Reporting, $\widetilde{N}_i^{CP}$ is the nominal for the different maturities. We calculate the adjusted CP nominals N_i^{CP}, $i = 1, \ldots, 9$ of different maturity buckets so that the corresponding present values of §28 Reporting result by discounting the given CP nominals by the risk-free rate r and, simultaneously, considering coupon payments. A problem is that N^{CA} from (6.7) is already included in the total nominal cover pool. As an intermediary step, we assume that N^{CA} is evenly distributed for the first seven maturity buckets in TABLE 6.3, so that

$$\begin{aligned} \widehat{N}_i^{CP} &= \widetilde{N}_i^{CP} - \frac{N^{CA}}{7}, \qquad i = 1, \ldots, 7 \\ \widehat{N}_i^{CP} &= \widetilde{N}_i^{CP}, \qquad i = 8, 9. \end{aligned} \tag{6.8}$$

With $T_0^{CP} = 0$, we compute the accumulated amount of outstanding cover pool nominals in T_i^{CP} by

$$\widehat{M}_i^{CP} = \sum_{j \geq i}^{9} \widehat{N}_i^{CP}, \qquad i = 1, \ldots, 9$$

and

$$\widehat{M}_0^{CP} = \widehat{M}_1^{CP} + N^{CA}.$$

Now, we determine the coupon payment $c_i^{CP}(s^{CP})$ in T_i^{CP} (dependent on the spread s^{CP}) with $c_0^{CP}(s^{CP}) = 0$, no coupon payment in $T_0^{CP} = 0$, and

$$c_i^{CP}(s^{CP}) = \left[e^{s(T_i^{CP} - T_{i-1}^{CP})} - 1\right] \widehat{M}_i^{CP}, \qquad i = 1, \ldots, 9.$$

The sum of payments at $t = 0$ discounted by the riskless rate amount to

$$\hat{V}_i^{CP}(s^{CP}) = N^{CA} + \sum_{i=1}^{9} \left[\widehat{N}_i^{CP} + c_i^{CP}(s^{CP})\right] e^{-rT_i^{CP}}.$$

Determine s_*^{CP}, in order that

$$\hat{V}_i^{CP}(s_*^{CP}) \stackrel{!}{=} \widetilde{V}_i^{CP}, \qquad i = 1, \ldots, 9$$

where $\widetilde{V}_i^{CP}$ denotes the given CP present value from §28 Reporting. Finally, we calculate the adjusted CP nominal by

$$N_i^{CP} = \tilde{N}_i^{CP} + c_i^{CP}(s_*^{CP}), \qquad i = 1, \ldots, 9. \tag{6.9}$$

Nominal OA The balance sheet nominal of OA is obtained by

$$\widetilde{N}^{OA} = \widetilde{N}^A - \widetilde{N}^{CP}$$

where $\widetilde{N}^A$ is the sum of total assets from the bank's balance sheet and $\widetilde{N}^{CP}$ is the nominal cover pool according to §28 Reporting. Since we do not know the present value of OA we increase it by the same ratio as the cover pool with (6.8) and (6.9). It follows the adjusted OA nominal given by

$$N^{OA} = \widetilde{N}^{OA} \frac{\sum_{i=1}^{9} N_i^{CP} + N^{CA}}{\sum_{i=1}^{9} \widehat{N}_i^{CP} + N^{CA}}. \tag{6.10}$$

6.2.2. Adjusted Liability Nominals

As in Section 6.2.1 we specify the liability positions with corresponding maturities, see Table 6.4. We denote the Pfandbriefe with different maturities as $PB_1, \ldots, PB_9$, the other liabilities as OL and equity as EQ. For PB_9 we compute the mean of 10 years and 15 years and assume no maturity over 15 years exists. We set $T^{OL} = T^{EQ} = \max_i(T_i^{PB}) = \max_i(T_i^{CP})$. The total number of liability positions amount to eleven where the Pfandbriefe account for nine different maturity ranges as in §28 Reporting. Additionally, Assumption 6.2 holds throughout the calculation of the adjusted liability values.

Assumption 6.2. *All PB_i, $i = 1, \ldots, 9$ are zero-coupon bonds. The risk-free rate r and the PB spread s^{PB} are time-independent.*

	PB_1	PB_2	PB_3	PB_4	PB_5	PB_6	PB_7	PB_8	PB_9	OL	EQ
Mat.	T_1^{PB}	T_2^{PB}	T_3^{PB}	T_4^{PB}	T_5^{PB}	T_6^{PB}	T_7^{PB}	T_8^{PB}	T_9^{PB}	T^{OL}	T^{EQ}
Nom.	N_1^{PB}	N_2^{PB}	N_3^{PB}	N_4^{PB}	N_5^{PB}	N_6^{PB}	N_7^{PB}	N_8^{PB}	N_9^{PB}	N^{OL}	N^{EQ}
Years	0.5	1.0	1.25	1.75	2.5	3.5	4.5	7.5	12.5	12.5	12.5

Table 6.4.: Definitions of the liability types, with corresponding maturities and nominals.

The calculation procedure for the liability side is as follows:

Nominal PB We calculate the adjusted nominals N_i^{PB}, $i = 1, \ldots, 9$ so that by discounting with the risk-free rate r the present values from §28 Reporting result where coupon payments are considered. $\widetilde{N}_i^{PB}$, $i = 1, \ldots, 9$ denote the nominals for the different maturity ranges from §28 reporting. First, we determine the accumulated amount in T_i^{PB}, $i = 1, \ldots, 9$ outstanding PB nominals with

$$\widehat{M}_i^{PB} = \sum_{j \geq i}^{9} \widetilde{N}_i^{PB}, \qquad i = 1, \ldots, 9.$$

Then determine the coupon payment $c_i^{PB}(s^{PB})$ in T_i^{PB} (dependent on the spread s^{PB})

$$c_i^{PB}(s^{PB}) = \left[e^{s(T_i^{PB}-T_{i-1}^{PB})} - 1\right] \widehat{M}_i^{PB}, \qquad i = 1, \ldots, 9$$

with $T_0^{PB} = 0$. The sum of discounted payments by the risk-free rate r at $t = 0$ amount to

$$\hat{V}_i^{PB}(s^{PB}) = \sum_{i=1}^{9} [\widetilde{N}_i^{PB} + c_i^{PB}(s^{PB})] e^{-rT_i^{PB}}, \qquad i = 1, \ldots, 9.$$

Determine s_*^{PB}, in order that

$$\hat{V}_i^{PB}(s_*^{PB}) \stackrel{!}{=} \widetilde{V}_i^{PB}, \qquad i = 1, \ldots, 9$$

where $\widetilde{V}_i^{PB}$ denote the PB present values from §28 Reporting. Finally, we can compute the adjusted zero-coupon bond nominal with

$$N_i^{PB} = \widetilde{N}^{PB} + c_i^{PB}(s_*^{PB}), \qquad i = 1, \ldots, 9. \tag{6.11}$$

Nominal OL The balance sheet nominal of OL is obtained by

$$\widetilde{N}^{OL} = \widetilde{N}^{L} - \widetilde{N}^{PB} - \widetilde{N}^{EQ}, \qquad i = 1, \ldots, 9$$

where $\widetilde{N}^L (= \widetilde{N}^A)$ is the sum of total liabilities from the bank's balance sheet, $\widetilde{N}^{PB}$ is the balance sheet nominal of PB and $\widetilde{N}^{EQ}$ is the balance sheet nominal of EQ. Since we do not know the present value of OL, it is increased in the same ratio as the PB. Then with (6.11), determine the adjusted nominals

$$N^{OL} = \widetilde{N}^{OL} \frac{\sum_{i=1}^{9} N_i^{PB}}{\sum_{i=1}^{9} \widetilde{N}_i^{PB}}. \tag{6.12}$$

Nominal EQ The adjusted equity nominal is then simply the difference of the adjusted asset nominal (from Section 6.2.1 with (6.7), (6.9) and (6.10)) and the adjusted liability positions consisting of (6.11) and (6.12) with

$$N^{EQ} = \underbrace{N^A}_{=N^{CA}+N^{CP}+N^{OA}} - \sum_{i=1}^{9} N_i^{PB} - N^{OL}. \tag{6.13}$$

6.3. Results of the Structural Model

An extensive sensitivity analysis wrt the model parameters is already covered by Sünderhauf (2006) where numerous scenarios are simulated on different parameter sets which are den compared wrt to their default outcome regarding the Pfandbrief. We also provide stressed scenarios, thereby laying the focus on comparisons between the seven identified mortgage (type 'Hyp') Pfandbrief banks of Table C.2 by applying above above credit risk measures (Section 6.1). Further, one of the main takeaways from Sünderhauf (2006) is the impact of asset-liability mismatch where the larger the maturity gap between assets and liabilities is, the higher the risk of defaulting becomes. Thus, we fix the maturities to $T_1 = 3$ years for the assets and $T_2 = 7$ years for the liabilities which accounts for a realistic setting. In order to sufficiently approximate NMC, the analysis is based on LSMC simulations with 1,000,000 generated paths. For the default analysis of the structural model we define additional scenarios to the basis scenario of TABLE C.14.

Remark 6.3. *The hardware for simulating the structural model of (4.32) with 1,000,000 paths was only available for a certain (short) time period. Consequently, the HW1F model parameters rely on Sünderhauf (2006)'s defined input as in* TABLE *C.14 and not calibrated to the market as outlined in Section 3.7 since the calibration procedure was not implemented into the framework at the time. Likewise, scenarios are only based on* $T_1 = 3$ *and* $T_2 = 7$ *for the reason that other maturities were not considered at time. However, the simulation outcomes for different maturities as well as calibrated HW1F model parameters are obtained by the reduced-form model and displayed in Section 6.4 since it does not depend on higher memory and computing power.*

Apart from adding parallel shifts to the interest rate process we also stress the volatility and jump parameters which are displayed in TABLE 6.5 and TABLE 6.6, respectively. These stressed scenarios are partly derived from Sünderhauf (2006) where similar variations of the parameter sets are given. For example, we apply scenario 'Vola-Jump I' to MHB with balance sheet and §28 Reporting data of the 4^{th} quarter 2016. FIGURE 6.1 depicts the resulting distributions of CP and OA present values at T_1. Thereby, we insert the adjusted nominal values of TABLE C.6 obtained from Section 6.2. By applying the liability formulas of Section 3.6.2 we can produce the desired distributions for further risk analysis as described in Section 6.1. In particular our focus is dedicated to the PB distribution of FIGURE 6.2. For the scenario of 'Vola-Jump I' 70,772 defaults are registered, amounting to a PD of 7.1% with (6.1), as displayed in TABLE 6.7. EL (6.5) and UL (6.6) then result to €138.3 mn and €128.5, respectively.
In TABLE 6.7 results from other simulated scenarios are also given. In general, we can state that parallel shifts, negative and positive, of the yield curve have little to no impact on the the overall credit quality of the Pfandbrief in a one-period setting (compare also Sünderhauf (2006, p. 115)). By stressing the volatility of the underlying processes of (4.32) we see only a slight increase in higher PDs. Other simulations with increased parameter values have shown similar results where the effect of the variance process on the downside risk is limited. This comes without surprise since the resulting underlying state variable processes take on the form of a geometrical Brownian motion which again approximately is log-normal. Increasing the volatility of a log-normal distribution particularly affects the upper tail end while the lower tail end remains largely unaffected. The only component of (4.32) which has a significant influencing leverage on the overall Pfandbrief's downside risk is the jump component. Thereby, we negatively increase the mean jump-amplitude to $\mu_{\pi_{V_{CP}}} = \mu_{\pi_{V_{CP}}} = -0.3$ in 'Vola-Jump I' and $\mu_{\pi_{V_{CP}}} = \mu_{\pi_{V_{CP}}} = -0.5$ in 'Vola-Jump II'. Compared to 'Vola IV' we observe a seven-fold PD increase for 'Vola-Jump I', and another five-fold increase for 'Vola-Jump II' with a PD of 38.7% (TABLE 6.7). In relation to the slightly altered parameter set of 'Vola-Jump I' and 'Vola-Jump II' this seems a considerable rise and reveals one of the most revealing weaknesses of the structural model. Quantifying an appropriate jump amplitude and frequency in order to adequately model the downside risk of the Pfandbrief is evidently a difficult undertaking. An intuitive interpretation and direct linkage of default risk wrt the asset side and how it affects the liability side is, in general, not given

by jump component. Besides, the lack of related Pfandbrief defaults makes it virtually impossible to further investigate what the correct downside impact of jumps should be. A credit risk comparison of the seven identified mortgage Pfandbrief banks (Table C.2) based on the 'Vola-Jump II' parameter set is depicted in Table 6.8. We see that issued Pfandbriefe by MMW have the highest risk of defaulting followed by MHB, WIB and BHH. For AAR, NAT and WBP the risk of defaulting Pfandbriefe is relatively low under this stressed scenario. This outcome is primarily attributed to the amount of OC held by the issuing Pfandbrief bank, and secondarily how much collateral can, potentially, additionally be utilised in the form of OA in the case of default, see Table 6.2. While AAR, NAT and WBP have sufficient amount of additional collateral, BHH, MMW, MHB and WIB do not. Although it is questionable how much of OA is actually appertained to cover the Pfandbrief at default, the analysis gives answers to the general asset-liability management of the underlying bank.

Parameter	Vola I	Vola II	Vola III	Vola IV
$\varsigma_{CP}^2(0)$	0.0081	0.0121	0.02	0.025
$\theta_{\varsigma_{CP}}$	0.0081	0.0121	0.02	0.025
$\varsigma_{OA}^2(0)$	0.0121	0.0225	0.03	0.035
$\theta_{\varsigma_{OA}}$	0.0121	0.0225	0.03	0.035

Table 6.5.: Structural model: Stressed sets for variance process parameters, while all other parameters in Table C.14 remain unchanged.

Parameter	Vola-Jump I	Vola-Jump II
$\varsigma_{CP}^2(0)$	0.025	0.025
$\theta_{\varsigma_{CP}}$	0.025	0.025
$\lambda_{V_{CP}}$	0.2693	0.2693
$\mu_{\pi_{V_{CP}}}$	-0.3	-0.5
$\sigma_{\pi_{V_{CP}}}$	0.1	0.1
$\varsigma_{OA}^2(0)$	0.035	0.035
$\theta_{\varsigma_{OA}}$	0.035	0.035
$\lambda_{V_{OA}}$	0.6484	0.6484
$\mu_{\pi_{V_{OA}}}$	-0.3	-0.5
$\sigma_{\pi_{V_{OA}}}$	0.1	0.1

Table 6.6.: Structural model: Stressed sets for variance and jump process parameters, while all other parameters in Table C.14 remain unchanged.

6.4. Results of the Reduced-Form Model

Now, we shall take a look at the results for the newly proposed reduced-form model of Chapter 5. We already have seen a stylised application of the reduced-form model in Section 5.7. In principal, we attain the procedure described there but apply real balance sheet and §28 Reporting data as in the case of the structural model (Section 6.3).

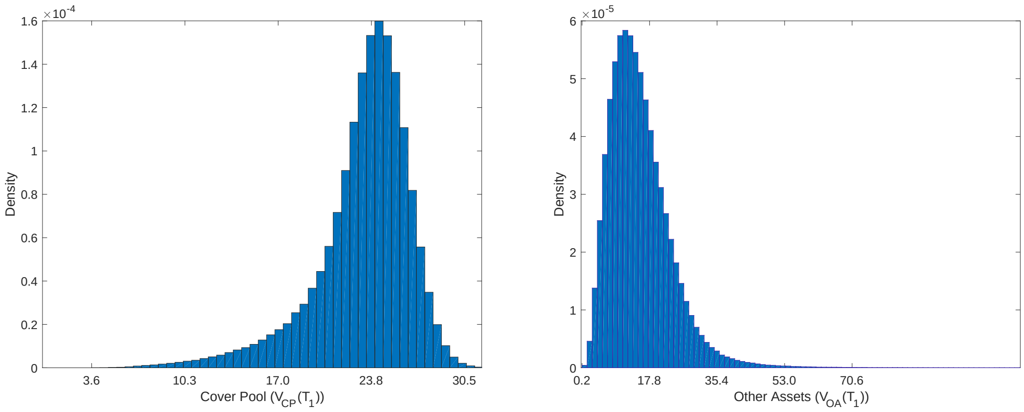

FIGURE 6.1.: Structural model: MHB's asset present values of cover pool (3.5) and other assets (3.8) at time T_1.

Scenario	D_{PB}	PD_{PB} (in%)	EAD_{PB} (in € mn)	LGD_{PB} (in%)	EL_{PB} (in € mn)	UL_{PB} (in € mn)
Basis	542	0.1	27,913.1	7.0	1.1	1.1
IR −200bp	477	0.0	27,913.1	7.0	0.9	0.9
IR −100bp	485	0.0	27,913.1	7.0	0.9	0.9
IR −50bp	517	0.1	27,913.1	7.0	1.0	1.0
IR +200bp	810	0.1	27,913.1	7.0	1.6	1.6
IR +100bp	635	0.1	27,913.1	7.0	1.2	1.2
IR +50bp	581	0.1	27,913.1	7.0	1.1	1.1
Vola I	1,375	0.1	27,913.1	7.0	2.7	2.7
Vola II	2,941	0.3	27,913.1	7.0	5.7	5.7
Vola III	6,868	0.7	27,913.1	7.0	13.4	13.3
Vola IV	10,327	1.0	27,913.1	7.0	20.2	20.0
Vola-Jump I	70,772	7.1	27,913.1	7.0	138.3	128.5
Vola-Jump II	387,049	38.7	27,913.1	7.0	756.3	463.6

TABLE 6.7.: Structural model: Resulting credit risk measures of MHB wrt the PB position for different stressed sets. Simulations are based on LSMC approach of various stressed scenarios with 1,000,000 paths at $T_1 = 3$ and $T_2 = 7$.

Similarly to Section 6.3, we define stressed scenarios on which the credit quality of the Pfandbriefe are tested and conduct comparisons between the seven identified mortgage (type 'Hyp') Pfandbrief banks of TABLE C.2. For the OA position we utilise the results from the structural model in Chapter 4 with the results of FIGURE 5.14 and fix $T_1 = 3$ where also OA mature. Hence, we mainly concentrate on the modelling of the CP position. The results are based on a sample size of 100,000 realisations of random numbers with the base scenario of TABLE C.15 and Moodys' 8×8 transition matrix $\boldsymbol{P}_{0,1}^{\text{Moodys}}$ in TABLE C.12 used as proxy representing the credit credit quality of the cover pool. Thereby, we also utilise the already established credit weightings of TABLE 5.14. At first we investigate the default behaviour of the Pfandbrief position for different maturity gaps between assets and liabilities. Thereby, we increase the maturity gap to five, six, seven, nine and twelve years, respectively. The results of TABLE 6.10 are solely

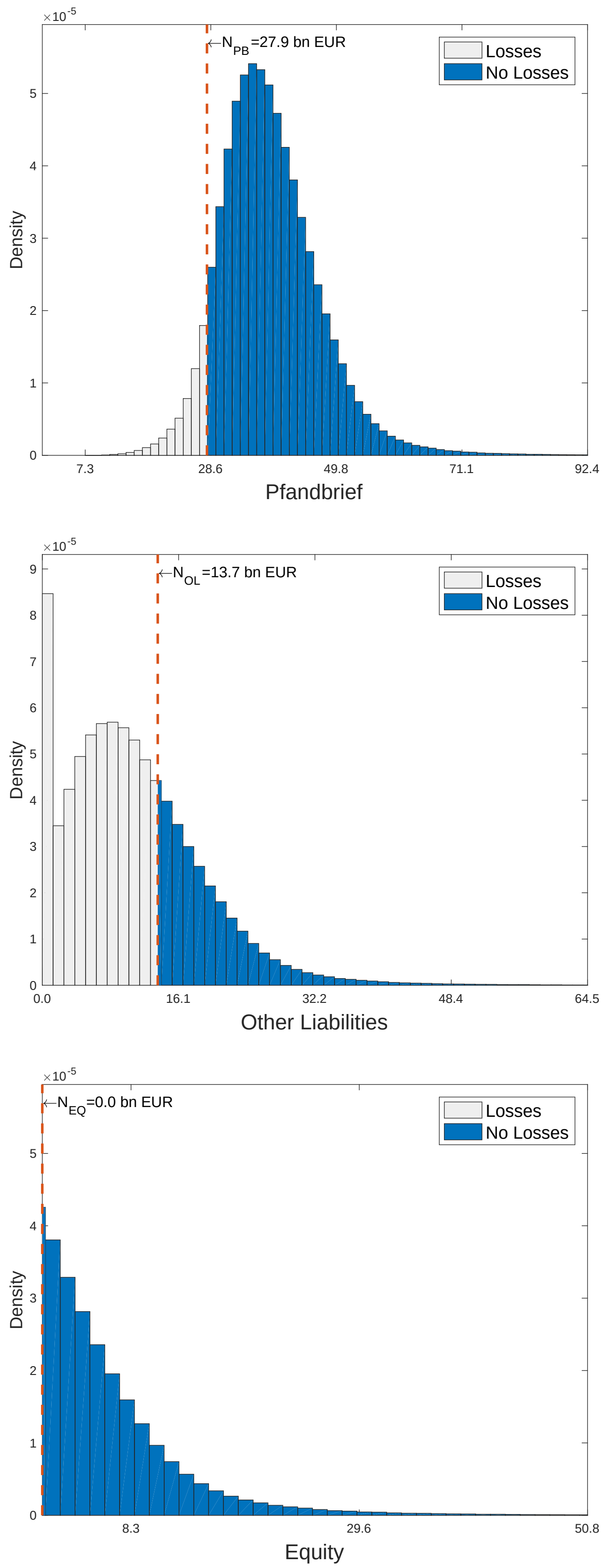

Figure 6.2.: Structural model: MHB's liability distributions of Pfandbrief (3.11), other liabilities (3.14) and equity (3.15) at time T_1.

Bank	D_{PB}	PD_{PB} (in%)	EAD_{PB} (in € mn)	LGD_{PB} (in%)	EL_{PB} (in € mn)	UL_{PB} (in € mn)
AAR	22,851	2.3	12,204.6	7.0	19.5	19.1
BHH	274,029	27.4	16,126.4	7.0	309.3	224.6
MHB	387,049	38.7	27,913.1	7.0	756.3	463.6
MMW	418,790	41.9	1,320.1	7.0	38.7	22.5
NAT	56,564	5.7	937.9	7.0	3.7	3.5
WBP	23,911	2.4	2,691.5	7.0	4.5	4.4
WIB	302,897	30.3	3,643.7	7.0	77.3	53.9

Table 6.8.: Structural model: Resulting credit risk measures of selected mortgage Pfandbrief banks wrt the PB position. Simulations are based on LSMC approach of stressed scenario 'Vola-Jump II' with 1,000,000 paths at $T_1 = 3$ and $T_2 = 7$.

based on the base scenario of Table C.15 for the Pfandbrief bank MHB. As expected, the higher the maturity gap between assets and liabilities the higher also the resulting PDs become and, consequently, EL and UL, see Table 6.10. This analysis of asset maturities $T_2 \geq 7$ give Pfandbrief investors additional valuable information regarding their investments wrt banks' asset-liability mismatch. For example, for the maturity set '$T_1 = 3$,$T_2 = 15$' 5,390 defaults occur where EL and UL amount to €105.3 mn and €99.6 mn, respectively.

Next we define stressed scenarios on which the reduced-form model is applied. Several possibilities exist where parameters can be modified on the asset side regarding the cover pool in order to force a deterioration of the overall Pfandbrief credit quality. E.g., as in Section 5.7 we let the cover pool default probabilities of $\boldsymbol{P}_{0,1}^{\text{Moodys}}$ in Table C.12

$$PD_{CP} = [0.0000, 0.0003, 0.0001, 0.0016, 0.0146, 0.0706, 0.2616]$$

increase by 50bp, 100bp, 150bp and 200bp. Also, we can raise the risk premiums as specified in Table 6.9. Likewise, a combination of both is also conceivable given by 'PD_{CP} +200bp Prem I' and 'PD_{CP} +200bp Prem II'. We adduce 'PD_{CP} +200bp Prem II' as an example for the distribution outcomes for assets (Figure 6.3) and liabilities (Figure 6.4) at T_1. We see a flatter slope on the lower end tail of the cover pool and Pfandbrief distribution compared to the structural outcome of Figure 6.1 and Figure 6.2. For the scenario 'PD_{CP} +200bp Prem II' we obtain a PD_{PB} of 9.5% where the EL and UL amount to €185.6 mn and €168.0 mn, respectively. Overall, due to the more flat lower tail end of the Pfandbrief distribution at T_1 we also see a more gradual increase in PD_{PB} when stressing the underlying cover pool assets wrt the cover pool PDs and risk premiums compared to its structural counterpart in Section 6.3. Besides, via the reduced-form approach we have gained a more tangible method of accessing a Pfandbrief default profile since we can actually quantify the parameters causing the resulting credit risk measures to correspond to the stressed cover pool accordingly. Furthermore, the reduced-form model allows a more precise default analysis since additional parameters can be adjusted, in form of a 8×8 or larger transition matrix or the risk premium process of the EJLT model in Section 5.6. Ultimately, the rating based approach provides a realistic risk assessment of the Pfandbrief and interpretation thereof. Taking a look at the output of the stressed scenarios of Table 6.11 we observe a near-linear increase in PD_{PB} for the stressed PD_{CP}, and a near-exponential increase for the stressed risk

premiums.
Of course, one can assume that the credit class weights in TABLE 5.14 will also shift when the overall cover pool deteriorates. It may become difficult for an issuer to maintain an overall triple A status for the Pfandbrief. Manipulating the weights poses another possibility to further stress the Pfandbrief where a single A status may then become more realistic as specified in TABLE 6.12. In TABLE 6.13 the results of the seven mortgage Pfandbrief banks are displayed based on the scenario 'PD_{CP} +300bp Prem II'. Overall, we see an outcome which is consistent with its structural counterpart of TABLE 6.8. Yet, the results are less dramatic to the scenario of 'Vola-Jump II'. This has partly to do with the fact that here the OA position is not further stressed compared to 'Vola-Jump II'. This could easily be accomplished if desired by applying the structural approach additionally for OA. However, this is deliberately omitted since it is desired to solely see the effactes of the stressed CP. Once again, we see that AAR, NAT and WBP, as opposed to BHH, MHB, MMW and WIB, have the lowest risk of defaulting Pfandbriefe due to their sufficient means of collateral posed by OC and OA, see TABLE 6.2.

Parameter	Prem I	Prem II	Prem III	Prem IV
$\pi(0)$	5	7	9	11

TABLE 6.9.: Reduced-form model: Stressed sets for risk premium parameters, while all other parameters in TABLE C.15 remain unchanged.

Maturity	D_{PB}	PD_{PB} (in%)	EAD_{PB} (in € mn)	LGD_{PB} (in%)	EL_{PB} (in € mn)	UL_{PB} (in € mn)
$T_1 = 3, T_2 = 7$	139	0.1	27,913.1	7.0	2.7	2.7
$T_1 = 3, T_2 = 8$	338	0.3	27,913.1	7.0	6.6	6.6
$T_1 = 3, T_2 = 9$	667	0.7	27,913.1	7.0	13.0	12.9
$T_1 = 3, T_2 = 10$	1,089	1.1	27,913.1	7.0	21.3	21.0
$T_1 = 3, T_2 = 12$	2,451	2.5	27,913.1	7.0	47.9	46.7
$T_1 = 3, T_2 = 15$	5,390	5.4	27,913.1	7.0	105.3	99.6

TABLE 6.10.: Reduced-form model: Resulting credit risk measures of MHB wrt the PB position for different maturities. Simulations are based on asset maturities $T_2 = \{7, 8, 9, 10, 12, 15\}$ with a sample size of 100,000 at $T_1 = 3$.

6.5. Summary

Due to formula (3.11) above risk assessment is rather conservative. Nevertheless, it is paramount for a Pfandbrief investor to be assured that sufficient funding exists during financial distress of the issuer. As already alluded above it is arguable how much voluntary OC (>2%) and OA is actually utilised as collateral for the Pfandbrief in the case of an issuer's default. However, the applied models, the viable structural and reduced-form approaches, provide verifiable and plausible results regarding the default outcomes wrt the PB position. We argue that the reduced-form model, a rating based approach, delivers a more accurate and subtle modelling option due to the numerous adjustment

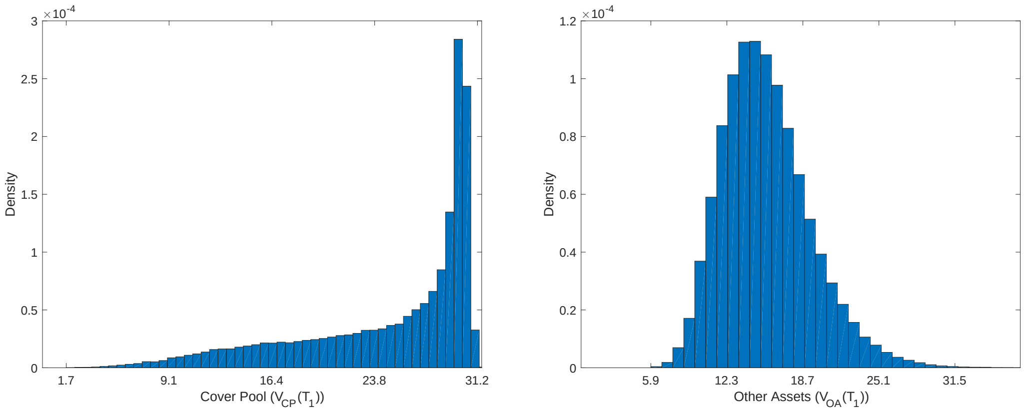

FIGURE 6.3.: Reduced-form model: MHB's asset present values of cover pool (3.5) and other assets (3.8) at time T_1

Scenario	D_{PB}	PD_{PB} (in%)	EAD_{PB} (in € mn)	LGD_{PB} (in%)	EL_{PB} (in € mn)	UL_{PB} (in € mn)
PD_{CP} +50bp	490	0.5	27,913.1	7.0	9.6	9.5
PD_{CP} +100bp	991	1.0	27,913.1	7.0	19.4	19.2
PD_{CP} +150bp	1,594	1.6	27,913.1	7.0	31.1	30.6
PD_{CP} +200bp	2,310	2.3	27,913.1	7.0	45.1	44.1
Prem I	712	0.7	27,913.1	7.0	13.9	13.8
Prem II	1,900	1.9	27,913.1	7.0	37.1	36.4
Prem III	3,818	3.8	27,913.1	7.0	74.6	71.8
Prem IV	6,188	6.2	27,913.1	7.0	120.9	113.4
PD_{CP} +200bp Prem I	5,559	5.6	27,913.1	7.0	108.6	102.6
PD_{CP} +200bp Prem II	9,500	9.5	27,913.1	7.0	185.6	168.0

TABLE 6.11.: Reduced-form model: Resulting credit risk measures of MHB wrt the PB position for different stressed sets. Simulations are based on various stressed scenarios with a sample size of 100,000 at $T_1 = 3$ and $T_2 = 7$.

Rating Category	AAA	AA	A	BBB	BB	B	CCC-C
Holdings (in %)	8.5%	9.0%	62.8%	15.3%	2.2%	1.5%	0.7%

TABLE 6.12.: Stressed cover Pool portfolio quality breakdown to the percentage holdings in the portfolio.

possibilities given by the underlying cover pool transition matrix, risk premium process and credit quality weights. Furthermore, the incorporation of random recovery rate into the loss distribution at T_1 lets us additionally control the recovery rate on the asset side. There is reason to assume that the recovery rate is high among the mortgage assets in the cover pool due to the standards enforced by the PfandBG wherein the minimum mortgage lending value of 60% ensures a high asset quality. In the structural model, downside risk can only be controlled by the jump component where fine tuning the jump amplitude remains a challenge to adequately capture the default behaviour of the

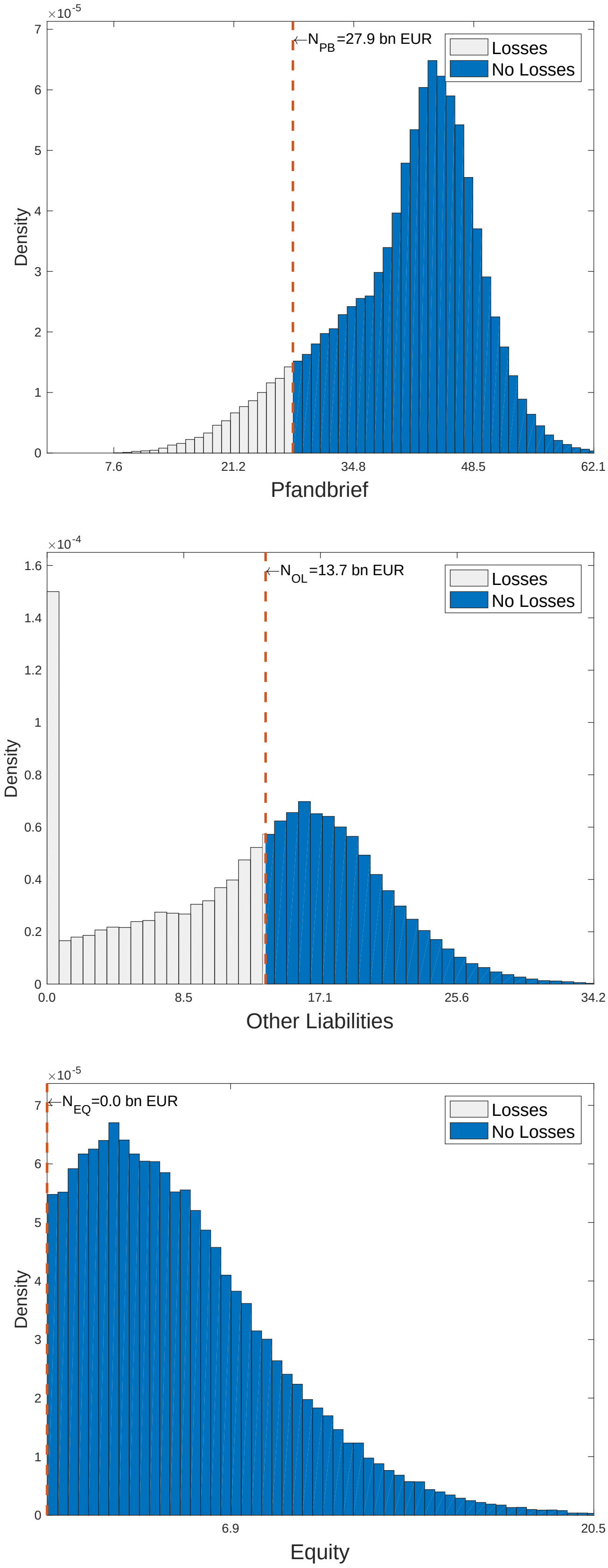

FIGURE 6.4.: Reduced-form model: MHB's liability distributions of Pfandbriefe (3.11), other liabilities (3.14) and equity (3.15) at time T_1 and $T_2 = 7$.

Bank	D_{PB}	PD_{PB} (in%)	EAD_{PB} (in € mn)	LGD_{PB} (in%)	EL_{PB} (in € mn)	UL_{PB} (in € mn)
AAR	0	0.0	12,204.6	7.0	0.0	0.0
BHH	5,613	5.6	16,126.4	7.0	63.4	59.8
MHB	14,156	14.2	27,913.1	7.0	276.6	237.4
MMW	15,646	15.6	1,320.1	7.0	14.5	12.2
NAT	120	0.1	937.9	7.0	0.1	0.1
WBP	0	0.0	2,691.5	7.0	0.0	0.0
WIB	10,256	10.3	3,643.7	7.0	26.2	23.5

Table 6.13.: Reduced-form model: Resulting credit risk measures of selected mortgage Pfandbrief banks wrt the PB position. Simulations are based on stressed scenario 'PD_{CP} +300bp Prem II' with a sample size of 100,000 at $T_1 = 3$ and $T_2 = 7$.

underlying cover pool assets, and ultimately of the Pfandbrief itself.

7. Conclusion

The overall objective was to provide a mark-to-market risk assessment methodology for the Pfandbrief in a one-period setting which comprises the most important characteristics of a mortgage Pfandbrief bank. Ultimately, the motivation of deriving a credit risk model is the situation during the financial crisis and aftermath where covered bond spreads were on the rise and the liquidity squeeze largely affected Pfandbrief banks. Even though not one single Pfandbrief has ever defaulted in its over 200 year history, the nimbus of non-defaulting issuers is broken and the perception of practically risk-free Pfandbriefe is at least since 2009 questionable. Three Pfandbrief banks needed to be bailed out by the German government including one of the largest — HRE.
In Chapter 6 we present an application to real balance sheet and §28 Reporting data. Unfortunately, we do not have complete information at our disposal which an issuing Pfandbrief bank has, meaning the resulting credit risk assessment needs to be treated with certain caution. Nevertheless, the main takeaways are, firstly, sufficient collateral in the form of OC and OA is paramount for the assurance towards the Pfandbrief creditor. Secondly, market changes or balance sheet mismanagement (asset-liability mismatch) by the underlying Pfandbrief bank the creditworthiness may deteriorate and, simultaneously, the outlook for its issued Pfandbriefe. Therefore, stressed scenarios are considered and analysed to obtain a more complete picture of the business practices of the issuer. Moreover, different maturity gaps between assets and liabilities give further insight for long-term investments where, as expected, the risk of defaulting rises with longer maturities. Certainly, refinements regarding the actual allocation of collateral is something further to look into, particularly, on how to distribute the OA adequately. Should CP proceeds not suffice for the debt service the creditors of the bonds, normally, rank pari passu with creditors of senior unsecured debt, hence have equal claim to the issuer's assets.
We have introduced quantitative methods for efficiently modelling the Pfandbrief in a one-period setting based on §28 Reporting and balance sheet data of the respective Pfandbrief bank. In light of Chapter 2, a certain trend towards the gaining importance of the mortgage Pfandbrief type compared to the public type could be established. The decline of the public Pfandbrief will according to market data and publications (e.g. by the VDP or ECBC) most likely further persist. Seven mortgage Pfandbrief banks were identified suitable for further analysis which predominantly issue mortgage Pfandbriefe. Next, a viable Pfandbrief framework (Chapter 3) was derived providing a foundation for the underlying structural (Chapter 4) and reduced-form (Chapter 5) model. The framework has its origins in Merton (1974) where a typical mortgage bank's balance sheet structure and regulatory requirements imposed by PfandBG are considered (see Spangler and Werner (2014)). In Chapter 3 we also find an extensive search for an appropriate interest rate model which adequately reflects and handles the current market situation of negative rates. A graphical depiction of both approaches is best summarised by FIGURE 7.1. On the left hand side the structural model is represented where paths are generated into the future and on the right we see a depiction of the reduced-form model

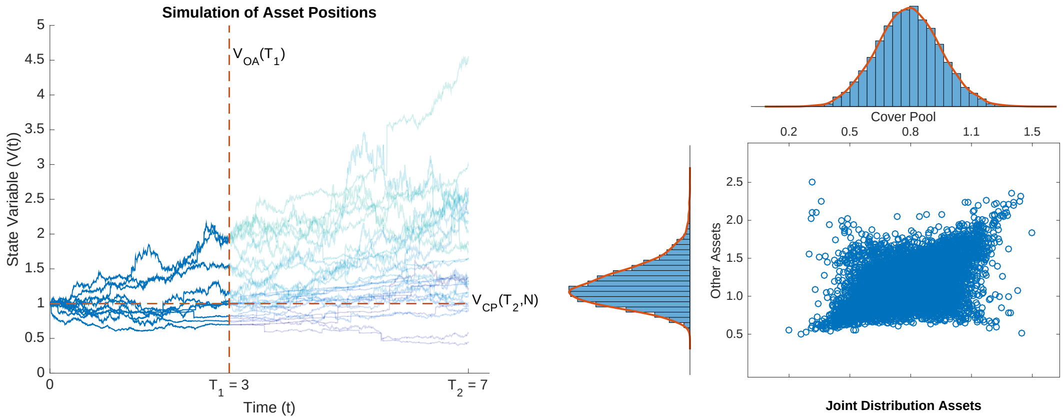

FIGURE 7.1.: Summary of one-period approaches. Left: Structural model; Right: Reduced-form model

where we draw random variables from a bivariate copula at T_1. Although concentrating on the mortgage type Pfandbrief in this work, a separate treatment of public sector and mortgage PB types with corresponding CP positions (FIGURE 3.1) is also conceivable by combining the presented structural (Chapter 4) and reduced-form (Chapter 5) approaches into one modelling framework, if required.

The structural model (Chapter 4) proposed by Sünderhauf (2006) is modelled via a Lévy process with stochastic interest rates, volatility and jumps in order to simulate the present values of CP and OA. Correlated Brownian motions are generated in order to capture the dependencies between SDEs. Six cover pool, six other assets, two market and ten correlation parameters are needed for the full model of (4.32). Significant improvements could be gained wrt simulation time and accuracy by introducing advanced algorithms for the volatility and jump component. An enhanced LSMC procedure is proposed where an almost perfect fit to the nested Monte Carlo values was accomplished while keeping the complexity of the linear regression low. Besides, model flexibility could be gained by deriving the forward and real-world representations of the underlying SDE to simulate CP and OA. Onward research may be well-invested in the field of variance reduction techniques in order to, potentially, further enhance the efficiency of Monte Carlo simulations.

In the reduced-form setting the CP is modelled by combining a random recovery factor model and assuming a LHP (Chapter 5) which constitutes the newly proposed model. Forward probabilities can be obtained via forecasting the (given) annual transition matrix where additional credit risk relevant constraints (Hughes and Werner, 2016) to the embedding problem in continuous time can be added. A risk-neutral setting is ensured by the EJLT model where stochastic risk premiums are incorporated. For capturing the underlying dependency between CP and OA we resort to a copula model. A log-normal distribution is assumed for OA. Altogether, four parameters are allocated to the factor model, three for the EJLT model, two for the log-normal distribution and one to two parameters for the copula. The probability bucketing approach, initially proposed by Andersen et al. (2003) and Hull and White (2004), can help to model the cover pool in a more granular sense should, for example, weightings of rating classes be more evenly distributed. The numerical procedure then consists of iteratively building up the loss distribution for a heterogeneous finite portfolio. Alternative factor models, e.g. Marshall-Olkin copula (Andersen and Sidenius, 2004), the Student-t copula (Schlögl and O'Kane, 2005), the double-t distribution in (Hull and White, 2004), the class of Archimedean copulas (Schönbucher, 2002) and normal inverse Gaussian factor copula model (Kalemanova et al., 2007) represent promising alternatives. Apart from the random recovery LHP model also stochastic correlation can be considered as an additional stochastic factor (Andersen and Sidenius, 2004).

Both approach possess a 'raison d'être', however, we argue that the reduced-form model for modelling the cover pool is superior as opposed to the structural model for a number reasons. The downside risk of the CP can be controlled via the given transition matrix where, for example, the PDs can be modified due to structural changes in the bank or a changed housing market situation. A clear relationship between input PDs on the CP side and output PDs on the PB side is comprehensible. Thus, a more adaptive modelling procedure is given. Furthermore, as pointed out, rating agencies appear to use the same approaches for the risk assessment of the cover pool. Fitch, for example, identifies two important risk sources when stressing for timely payments of the cash flows with recourse to the cover pool, namely "the credit risk of cover assets inferred from default probabilities and recovery expectations (credit loss component), and the cost of bridging maturity mismatches.", cf. (ECBC, 2016, p. 501-542). In our model we assume a given one-year transition matrix. However, one level beneath lies the challenge to correctly determine the level of borrower loan losses. Moody's includes a collateral score for mortgage loans based on "the range and distribution of LtVs, and the quality of the loan underwriting and, in particular, the calculation of whether the borrower can afford the loan.", cf. (ECBC, 2016, p. 501-542). Since the credit quality of the cover pool may vary over time Moody's has a monitoring system implemented which calculates the collateral score on a quarterly basis. Thus, a collateral score analysis in conjunction with a LtV analysis is certainly an area worthwhile for further investigation in the context of modelling the risk assessment of Pfandbriefe. Lastly, regulatory developments also seem to favour a rating based approach: "Due to the magnitude of banks' exposure to other banks, it is imperative that they have risk rating capabilities that incorporate all available information and rapidly refreshes ratings when material information becomes available.", cf. (BIS, 2001).

A. Implementation

Some insights regarding the implementation of the Pfandbrief framework (Chapter 3) with its models (Chapter 4 and Chapter 5) are described here. Emphasis is laid upon the object oriented structure and efficient programming, specifically, for MATLAB's vector based language.

A.1. The Pfandbrief Framework Object Oriented (OO)

In FIGURE A.1 and FIGURE A.2 the structure[1] of the OO Pfandbrief framework is depicted. The implemented framework makes use of the inheritance principle built upon object oriented classes. The folder structure is as follows:

+data Here data access objects (DAO) are provided representing an interface to databases which can be anything from .csv or .xml files to relational database management systems (RDBMS). Hence, methods in the `.m` files are provided for handling the data import which is necessary for modelling the Pfandbrief.

+model Main classes of the mathematical implementation of the underlying models are invoked by calling a constructor and contain multiple calculation steps. Example A.1 depicts the inheritance logic behind an implemented model — here, the reduced-form model of Chapter 5. Any model inherits from the so called `BaseModel` class which calls the methods `getInput()` — handles retrieving and processing of input data needed for the model calculation, `model()` — contains the implementation of the model logic and `getOutput()` — handles results of the calculation model and processes the output.

+script Main execution scripts of methods and models are provided here.

+test Test scripts can be executed for initial testing of methods and models.

+utility Utility methods are provided here which are then invoked globally by the respective models. FIGURE A.2 depicts all classes which are associated with utility type of methods. Thereby, business utility holds methods related to mathematical models and technical utility provides auxiliary functions which simplify and standardise frequently used steps or transformations.

+visualise Visualisation methods are gathered here which are repeatedly used to produce plots specifically for the depiction of important results.

Example A.1.

```
classdef PfandbriefReducedFormModel < com.pfandbrief.model.BaseModel

   properties
        logger;
        configID;
```

[1] My expression of gratitude to DEVnet GmbH for providing the underlying structure.

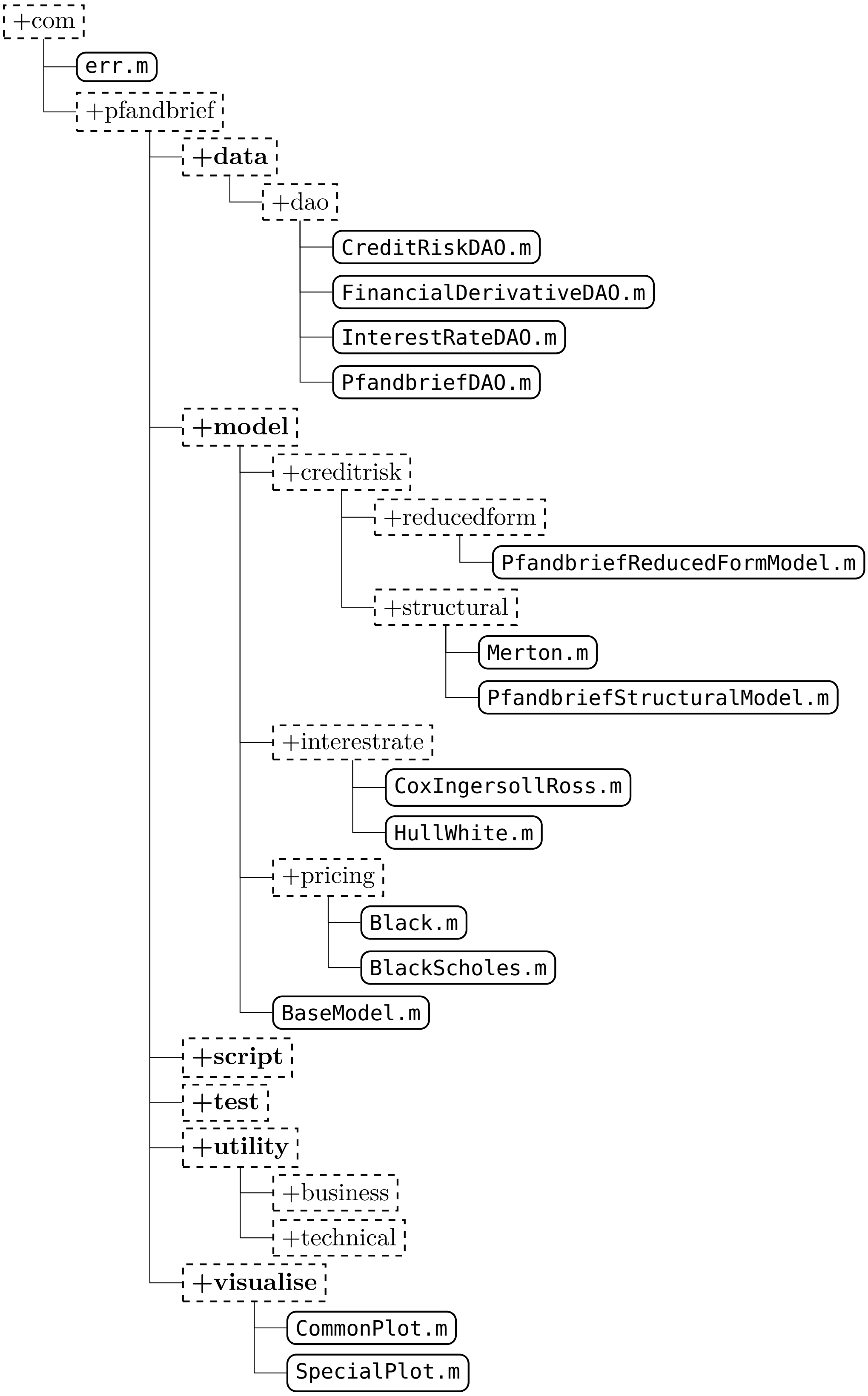

FIGURE A.1.: Class structure of the OO Pfandbrief framework.

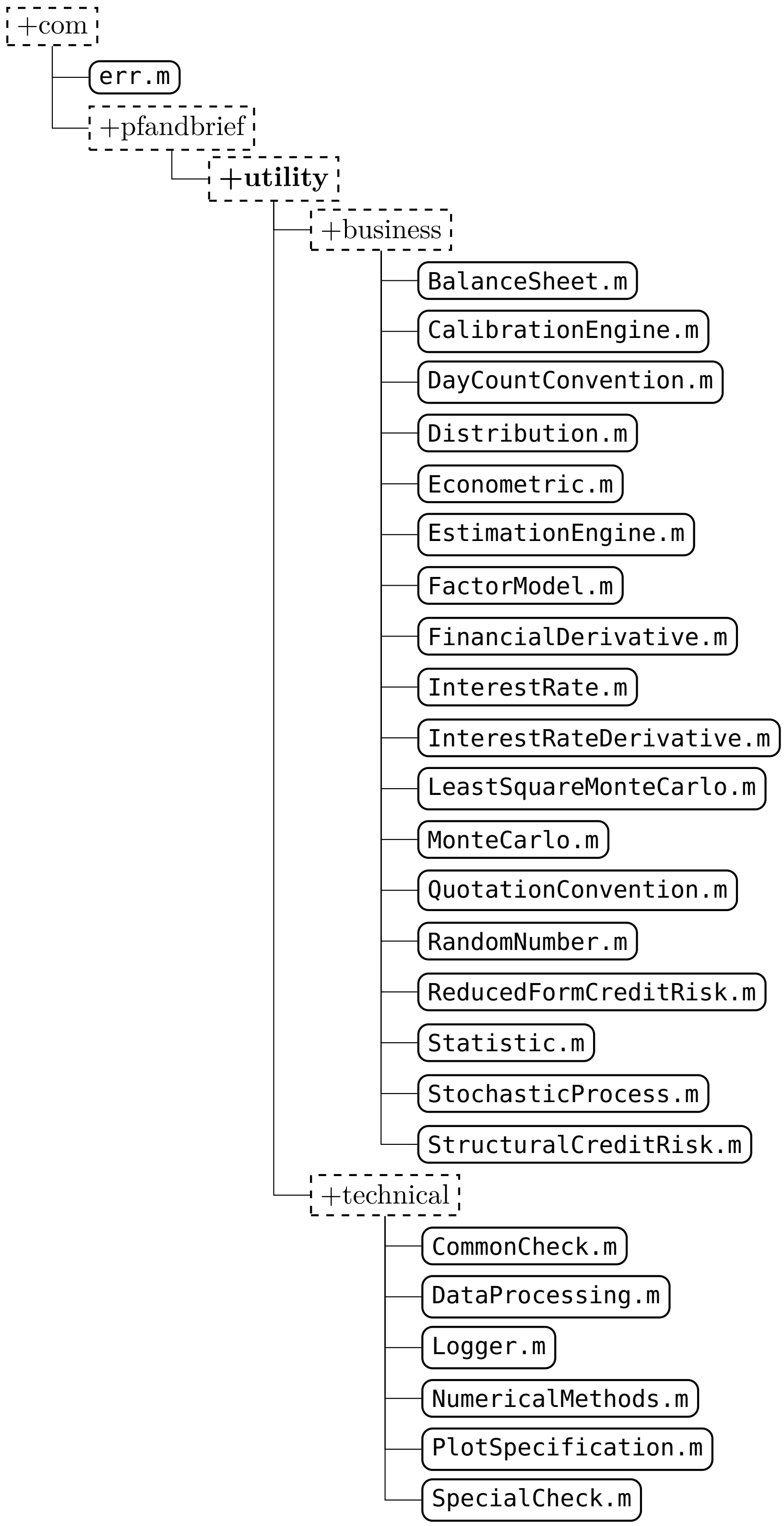

FIGURE A.2.: Business and technical utility methods.

```
        referenceTimestamp;
    end

     % Contains the three methods (getInput, model, getOutput) that
     % have to be accessible within a model.
     methods (Access = public)

         %%
         function [input,parameter] = getInput(this, parameter)
             % Input for the model calculation should be handled in
             % this method. The input should be stored in the 'input'
             % attribute of this class.

             % < ... put your code here ... >

         % eof
         end

         %%
         function result = model(this, parameter, input)
             % All model calculations are conducted in this method
             % containing specific model relevant functions only
             % accessible within this class.

             % < ... put your code here ... >

         % eof
         end

         %%
         function outputData = getOutput(this, parameter, result)
             % Results of the model calculation are handled in this
             % method. This includes result transformations to other
             % data structures. The output can be returned by this
             % method.

             % < ... put your code here ... >

         % eof
         end

     end

     methods (Access = private)

         % < ... put your code here ... >

     end

end
```

A.2. Efficient Programming

Important and elementary efficient programming features are

· preallocation of storage,

· vectorisation and

· parallelisation.

Parallelisation may not always be feasible or not available due to special necessary software packages. Here emphasis is laid upon vectorisation which is best demonstrated on simulating stochastic differential equations (SDEs). A typical equation is of the form

$$\mathrm{d}X(t) = \mu(X(t), t)\mathrm{d}t + \sigma(X(t), t)\mathrm{d}W(t), \tag{A.1}$$

where $W(t)$ denotes a Wiener process. On the basis of (A.1) coding examples are presented as a surrogate to the whole framework implementation in Appendix A.1. The conveying of code vectorisation is emphasised upon where enormous gains in performance can be made in MATLAB. If possible loops should, in general, be avoided and rather resort to native functions in order to take full advantage of MATLAB's vectorised programming language. However, one negative side effect might be that the code itself becomes abstract and difficult to read. The following basic examples are backed by the corresponding theory and can be executed straight away.

A.2.1. Loop over Time

If the time-dependent component is attached to other components in a non-additive or non-multiplicative fashion then one loop over time is necessary. Still, the vectorisation for the propagation step works perfectly fine for the path dimension, see Example A.2.

Example A.2 (HW1F Model).

$$\begin{aligned} X(t) &= r(t) \\ \mu(X(t), t) &= \theta(t) - \kappa r(t) \\ \sigma(X(t), t) &= \sigma \end{aligned}$$

```
nTimeSteps = 50; % Number of time steps
nPaths = 1000; % Number of paths
T = 1.0; % Simulation time horizon
dt = T/nTimeSteps; % Simulation time step
t = dt:dt:T; % Time

kappa = 0.1; % Mean reversion speed
sigma = 0.3; % Volatility level

Fc = repmat(0.05, nTimeSteps+1, 1); % Flat instantaneous forward curve

RN = randn(nTimeSteps,nPaths); % Draw random numbers
r = nan(nTimeSteps+1,nPaths); % Preallocate storage
```

```
r(1,:) = 0.05; % Assign starting vector

for i = 1:nTimeSteps
  theta(i) = (Fc(i+1) - Fc(i))/dt + kappa*Fc(i) + sigma^2/(2*kappa)*(1 - exp
      (-2*kappa*t(i)));
  r(i+1,:) = r(i,:) + (theta(i) - kappa*r(i,:))*dt + sigma*RN(i,:)*sqrt(dt);
end
```

A.2.2. Full Vectorisation

If the time-dependent component can be incorporated in an additive or multiplicative manner then one can resort to `cumsum()` or `cumprod()` which are fully vectorised, see Example A.3.

Example A.3 (Geometric Brownian Motion (GBM)).

$$\begin{aligned} X(t) &= S(t) \\ \mu(X(t),t) &= \mu S(t) \\ \sigma(X(t),t) &= \sigma S(t) \end{aligned}$$

$$\mathrm{d}S(t) = \mu S(t)\mathrm{d}t + \sigma S(t)\mathrm{d}W,$$

$$S(t_i)/S(t_{i-1}) = \exp\left(\left(\mu - \frac{1}{2}\sigma^2\right)\Delta t + \sigma\sqrt{\Delta t}Z_{t_i}\right)$$

with drift rate μ and volatility respectively σ being constants.

```
nTimeSteps = 50; % Number of time steps
nPaths = 1000; % Number of paths
T = 1.0; % Simulation time horizon
dt = T/nTimeSteps; % Simulation time step

sigma = 0.3; % Annual volatility
mu = 0.05; % Annual drift rate

RN = randn(nTimeSteps-1,nPaths); % Draw random numbers
S = nan(nTimeSteps,nPaths); % Preallocate storage
S(1,:) = 100; % Asset price at t=0

S(2:end,:) = exp((mu - 0.5*sigma^2)*dt + sigma*sqrt(dt)*RN);
S = cumprod(S,1);
```

B. Underlying Theory

Supplementary parts of the underlying theory can be found in this appendix chapter. Fundamentals in mathematical finance (Section B.1) and interest rate (Section B.2) theory are provided. Additionally, Markovian theory with application in credit risk can be accessed in Section B.3. Applied special distributions (Section B.4) and copulas (Section B.5) in the modelling framework are displayed, completing the theoretical supplements.

B.1. Mathematical Finance

Here we shall provide some useful mathematical tools and building blocks needed in finance. The theory behind mathematical finance is vast and, thus, we shall only give an excerpt of definitions and theorems which are frequently used in this thesis, namely, Itô's Formula (Section B.1.1), Girsanov Theorem (Section B.1.2) and change of numeraire (Section B.1.3). We refer to the literature for additional insights in the underlying theory in mathematical finance, see for example Björk (2004), Brigo and Mercurio (2007), Schlüchtermann and Pilz (2010), Shreve (2004) and Shreve (2012), amongst many others.

B.1.1. Itô's Formula

Itô's formula is based on some substantial stochastic calculus theory which represents a key element in financial modelling since it provides a technique to integrate stochastic processes, mainly consisting of the Wiener process W. Throughout this section we assume that (W_t) is a Wiener process on the filtered probability space $(\Omega, \mathcal{F}, (\mathcal{F}_t), \mathcal{P})$. Furthermore, we have a generic stochastic process X of the form

$$\begin{cases} \mathrm{d}X(t) = \mu(t, X(t))\mathrm{d}t + \sigma(t, X(t))\mathrm{d}W(t), \\ X(0) = a \end{cases} \tag{B.1}$$

where $X(0)$ is non-random and $\mu(t, X(t))$ and $\sigma(t, X(t))$ are stochastic processes. Main properties of a stochastic process are given in Definition B.1 and Definition B.2 which are crucial building blocks for constructing a stochastic integral and deriving Itô's formula.

Definition B.1 (Information and measurable, adaptive processes (Björk, 2004)). *The symbol $\mathcal{F}_t^X$ denotes "the information generated by X on the interval $[0, t]$", or alternatively "what has happened to X over the interval $[0, t]$". If, based upon* *observations of the trajectory $\{X(s) : 0 \leq s \leq t\}$, it is possible to decide whether a given event A has occurred or not, then we write this as*

$$A \in \mathcal{F}_t^X,$$

or say that "A is $\mathcal{F}_t^X$-measurable".
If the value of a given stochastic variable Z can be completely determined given observations of the trajectory $\{X(s) : 0 \leq s \leq t\}$, then we also write

$$Z \in \mathcal{F}_t^X.$$

If Y is a stochastic process such that we have

$$Y(t) \in \mathcal{F}_t^X$$

for all $t \geq 0$ then we say that Y is adapted to the filtration $\{\mathcal{F}_t^X\}_{t \geq 0}$.

Definition B.2 (Martingale Concept (Björk, 2004)). *A stochastic process X wrt $\mathcal{P}$ is called a $(\mathcal{F}_t)$-martingale if the following conditions hold.*

- *X is adapted to the filtration $\{\mathcal{F}_t\}_{t \geq 0}$.*
- *X is integrable for all t, if*

$$\mathbb{E}[|X(t)|] < \infty.$$

- *For all s and t with $s \leq t$ the following relation holds*

$$\mathbb{E}[X(t) \,|\, \mathcal{F}_s] = X(s).$$

Now, naturally, it is the objective to determine (solution to (B.1))

$$X(t) = a + \int_0^t \mu(s, X(s))\mathrm{d}s + \int_0^t \sigma(s, X(s))\mathrm{d}W(s) \tag{B.2}$$

where the ordinary Riemann-Stieltjes integral fails for integrating $\mathrm{d}W$. To be able to obtain the representation of X in (B.2) the concept of the Itô integral in Theorem B.3 is introduced where the trajectory-wise integration of $\mathrm{d}W$-integral is relaxed. Instead, for a large class of processes g in $\mathcal{L}^2$-space, integrals of the form

$$\int_0^t g(s)\mathrm{d}W(s) \tag{B.3}$$

are defined. The objective is now to define the stochastic integral for a process $g \in \mathcal{L}^2$. Consider the following simplification (Björk, 2004): Suppose that there exist deterministic points in time $a = t_0 < t_1 < \cdots < t_n = b$, such that g is constant on each subinterval. In other words we assume that $g(s) = g(t_k)$ for $s \in [t_k, t_{k+1})$. Then we can define the stochastic integral by

$$\int_a^b g(s)\mathrm{d}W(s) = \sum_{k=0}^{n-1} g(t_k)[W(t_{k+1}) - W(t_k)].$$

In order to guarantee the existence of the stochastic integral we have to impose integrability conditions (Definition B.3 with Theorem B.1) on g where the class $\mathcal{L}^2$ turns out to be natural. Further results are given by Theorem B.2, Corollary B.1 and Lemma B.1, respectively.

Definition B.3 (Conditions Stochastic Integral (Björk, 2004)).

1. *We say that the process g belongs to the class $\mathcal{L}^2[a,b]$ if the following conditions are satisfied:*
   - $\int_a^b \mathbb{E}[g^2(s)]\mathrm{d}s < \infty$
   - *The process g is adapted to the $\mathcal{F}_t^W$-filtration.*
2. *We say that the process g belongs to the class $\mathcal{L}^2$ if $g \in \mathcal{L}^2[0,t]$ for all $t > 0$.*

Theorem B.1 (Relations Stochastic Integral (Björk, 2004)). *Let g be a process satisfying the conditions 1. of Definition B.3. Then the following relations hold:*

$$\mathbb{E}\left[\int_a^b g(s)\mathrm{d}W(s)\right] = 0 \tag{B.4}$$

$$\mathbb{E}\left[\left(\int_a^b g(s)\mathrm{d}W(s)\right)^2\right] = \int_a^b \mathbb{E}[g^2(s)]\mathrm{d}s \tag{B.5}$$

$$\int_a^b g(s)\mathrm{d}W(s) \text{ is } \mathcal{F}_b^W\text{-measurable} \tag{B.6}$$

Remark B.1. *It is possible to define the stochastic integral for a process g satisfying only the weak condition*

$$\mathrm{Prob}\left(\int_a^b g^2(s)\mathrm{d}s < \infty\right) = 1.$$

For such a general g we have no guarantee that the properties (B.4) and (B.5) hold. Property (B.6) is, however, still valid.

Theorem B.2 ((Björk, 2004)). *For any process $g \in \mathcal{L}^2[s,t]$ the following holds:*

$$\mathbb{E}\left[\int_s^t g(u)\mathrm{d}W(u)\,\middle|\,\mathcal{F}_s^W\right] = 0.$$

Corollary B.1 ((Björk, 2004)). *For any process $g \in \mathcal{L}^2$, the process X, defined by*

$$X(t) = \int_0^t g(s)\mathrm{d}W(s),$$

is an $(\mathcal{F}_t^W)$-martingale. In other words, modulo an integrability condition, every stochastic integral is a martingale.

Lemma B.1 ((Björk, 2004)). *Within the framework above, and assuming enough integrability, a stochastic process X (having a stochastic differential) is a martingale iff the stochastic differential has the form*

$$\mathrm{d}X(t) = g(t)\mathrm{d}W(t),$$

i.e. X has no d*t-term.*

Theorem B.3 (Itô(-Doeblin)'s formula (Björk, 2004)). *Assume that the process X has a stochastic differential given by*

$$\mathrm{d}X(t) = \mu(t)\mathrm{d}t + \sigma(t)\mathrm{d}W(t),$$

where μ and σ are adapted processes, and let f be a $C^{1,2}$-function (i.e. f is once continuously differentiable in its first argument and twice continuously differentiable in its second argument). Define the process Z by $Z(t) = f(t, X(t))$. Then Z has a stochastic differential given by

$$\mathrm{d}f(t, X(t)) = \left(\frac{\partial f}{\partial t} + \mu\frac{\partial f}{\partial x} + \frac{1}{2}\sigma^2\frac{\partial^2 f}{\partial x^2}\right)\mathrm{d}t + \sigma\frac{\partial f}{\partial x}\mathrm{d}W(t). \tag{B.7}$$

Hence, Itô's formula (B.7) is obtained by a second order Taylor expansion

$$\mathrm{d}f = \frac{\partial f}{\partial t}\mathrm{d}t + \frac{\partial f}{\partial x}\mathrm{d}X + \frac{1}{2}\frac{\partial^2 f}{\partial x^2}(\mathrm{d}X)^2 \tag{B.8}$$

where we use the following formal multiplication table:

$$\begin{cases} (\mathrm{d}t)^2 = 0, \\ \mathrm{d}t \cdot \mathrm{d}W = 0, \\ (\mathrm{d}W)^2 = \mathrm{d}t \end{cases}$$

Remark B.2. *Strictly speaking, according to Schlüchtermann and Pilz (2010), stochastic integrals rely on the class of progressively measurable processes g (Definition B.3) which poses a stronger property than the notion of being adapted processes (see Definition B.1). A progressively measurable process is important because it implies the stopped process is measurable. In Schlüchtermann and Pilz (2010) we find the following conditions:*

1. *Every elementary adaptive process to the filtration $(\Omega, \mathcal{F}, (\mathcal{F}_t), \mathcal{P})$ is progressively measurable.*
2. *All continuous adaptive processes to the filtration $(\Omega, \mathcal{F}, (\mathcal{F}_t), \mathcal{P})$ are progressively measurable.*

Generally speaking, not every adaptive process is progressively measurable. However, as pointed out by Schlüchtermann and Pilz (2010), when imposing additional technical prerequisites to the filtration $(\Omega, \mathcal{F}, (\mathcal{F}_t), \mathcal{P})$ there exists to every adaptive process a corresponding version which is progressively measurable. Above conditions pose a sufficiently large class of progressively measurable processes.

B.1.2. Girsanov Theorem

The groundwork for the Girsanov Theorem is given by Section B.1.1. More precisely, in a 'Wiener world', the integrability of the Girsanov kernel $\mathfrak{g}$ is guaranteed by the conditions defined in Definition B.3 with the relations in Theorem B.1. Particularly, we imply that the stochastic integral is a square integrable martingale wrt the Wiener process. The Girsanov Theorem allows us to conduct continuous measure transformations which is

based on the mathematical tool of the Radon-Nikodým Theorem (see Björk (2004) or Schlüchtermann and Pilz (2010) for more details).
We denote the likelihood process for the measure change from $\mathcal{P}$ to $\mathcal{Q}$ (and vice versa) with L. The existence of L is covered by the Radon-Nikodým Theorem so that L_T will be the Radon-Nikodým derivative of $\mathcal{Q}$ wrt $\mathcal{P}$ so that $\mathcal{Q} << \mathcal{P}$ ($\mathcal{Q}$ is absolutely continuous wrt $\mathcal{P}$) on $\mathcal{F}_T$ which ensures also $\mathcal{Q} << \mathcal{P}$ on $\mathcal{F}_t$ for all $t \leq T$. For Theorem B.4 assume that the filtration $\underline{\mathcal{F}}$ is defined as

$$\mathcal{F}_t = \mathcal{F}_t^W, \qquad t \in [0, T].$$

Theorem B.4 (Girsanov Theorem (Björk, 2004)). *Let $W^{\mathcal{P}}$ be a d-dimensional standard $\mathcal{P}$-Wiener process on $(\Omega, \mathcal{F}, \mathcal{P}, \underline{\mathcal{F}})$ and let $\mathfrak{g}$ be any d-dimensional adapted column vector process. Choose a fixed T and define the process L on $[0, T]$ by*

$$\begin{aligned} \mathrm{d}L_t &= \mathfrak{g}_t^\top L_t \mathrm{d}W_t^{\mathcal{P}}, \\ L_0 &= 1, \end{aligned}$$

i.e.

$$L_t = \mathrm{e}^{\int_0^t \mathfrak{g}_s^\top \mathrm{d}W_s^{\mathcal{P}} - \frac{1}{2}\int_0^t \|\mathfrak{g}_s\|^2 \mathrm{d}s}.$$

Assume that

$$\mathbb{E}_{\mathcal{P}}[L_T] = 1, \tag{B.9}$$

and define the new probability measure $\mathcal{Q}$ on $\mathcal{F}_T$ by

$$L_T = \frac{\mathrm{d}\mathcal{Q}}{\mathrm{d}\mathcal{P}}, \quad \text{on } \mathcal{F}_T.$$

Then

$$\mathrm{d}W_t^{\mathcal{P}} = \mathfrak{g}_t \mathrm{d}t + \mathrm{d}W_t^{\mathcal{Q}},$$

where $W^{\mathcal{Q}}$ is a Q-Wiener process.

Remark B.3. *An equivalent, but perhaps less suggestive, way of formulating the conclusion of the Girsanov Theorem B.4 is to say that the process $W^{\mathcal{Q}}$, defined by*

$$W_t^{\mathcal{Q}} = W_t^{\mathcal{P}} - \int_0^t \mathfrak{g}_s \mathrm{d}s$$

is a standard $\mathcal{Q}$-Wiener process.

Lemma B.2 (The Novikov Condition (Björk, 2004)). *Assume that the Girsanov kernel $\mathfrak{g}$ is such that*

$$\mathbb{E}_{\mathcal{P}}\left[\mathrm{e}^{\frac{1}{2}\int_0^T \|\mathfrak{g}_t\|^2 \mathrm{d}t}\right] < \infty.$$

Then L is a martingale and in particular $\mathbb{E}_{\mathcal{P}}[L_T] = 1$.

Remark B.4. *Following Björk (2004), we need to assume that* $\mathfrak{g}$ *is such that* L *is a martingale, Equation (B.9), in the Girsanov Theorem (Theorem B.4). In general it can be that* $\mathbb{E}_{\mathcal{P}}[L_T] < 1$. *The problem is to give a condition on* $\mathfrak{g}$ *only, which guarantees the martingale property of* L. *The most general result so far, apart from when the process* $L \cdot \mathfrak{g}$ *is in* $\mathcal{L}^2$, *is the 'Novikov Condition' (Lemma B.2) which guarantees the martingale property of* L, *respectively (B.9).*

B.1.3. Change of Numeraire

With Girsanov's Theorem (Theorem B.4) we additionally provide the following change of measure toolkit represented by Theorem B.6. Likewise to Theorem B.4, the introduced tools rely on the Radon-Nikodým Theorem (see Björk (2004) or Schlüchtermann and Pilz (2010)).

Definition B.4 (Numeraire (Brigo and Mercurio, 2007)). *A numeraire is any positive non-dividend-paying asset.*

Theorem B.5 (Change-of-numeraire (Brigo and Mercurio, 2007)). *Assume there exists a numeraire* $\mathfrak{n}$ *and a probability measure* $\mathcal{Q}_{\mathfrak{n}}$, *equivalent to the initial* $\mathcal{Q}_0$, *such that the price of any traded asset* X *(without intermediate payments) relative to* $\mathfrak{n}$ *is a martingale under* $\mathcal{Q}_{\mathfrak{n}}$, *i.e.*

$$\frac{X_t}{\mathfrak{n}_t} = \mathbb{E}_{\mathfrak{n}}\left(\frac{X_T}{\mathfrak{n}_T}\,\middle|\,\mathcal{F}_t\right), \qquad 0 \leq t \leq T.$$

Let $\mathfrak{u}$ *be an arbitrary numeraire. Then there exists a probability measure* $\mathcal{Q}_{\mathfrak{u}}$, *equivalent to the initial* $\mathcal{Q}_0$, *such that the price of any attainable claim* Y *normalised by* $\mathfrak{u}$ *is a martingale under* $\mathcal{Q}_{\mathfrak{u}}$, *i.e.*

$$\frac{Y_t}{\mathfrak{u}_t} = \mathbb{E}_{\mathfrak{u}}\left(\frac{Y_T}{\mathfrak{u}_T}\,\middle|\,\mathcal{F}_t\right), \qquad 0 \leq t \leq T.$$

Moreover, the Radon-Nikodým derivative defining the measure $\mathcal{Q}_{\mathfrak{u}}$ *is given by*

$$\frac{\mathrm{d}\mathcal{Q}_{\mathfrak{u}}}{\mathrm{d}\mathcal{Q}_{\mathfrak{n}}} = \frac{\mathfrak{u}_T \mathfrak{n}_0}{\mathfrak{u}_0 \mathfrak{n}_T}.$$

Theorem B.6 (Change-of-numeraire toolkit (Brigo and Mercurio, 2007)). *We consider a numeraire* C *with its associated measure* $\mathcal{Q}_C$. *We also consider an* n*-vector diffusion process* X *whose dynamics under* $\mathcal{Q}_C$ *is given by*

$$\mathrm{d}X_t = \mu_t^C(X_t)\mathrm{d}t + \sigma_t(X_t)R\mathrm{d}W_t^C,$$

where μ_t^C *is a* $n \times 1$ *vector and* σ_t *is a* $n \times n$ *diagonal matrix, and where we explicitly point out the measure under which the dynamics is defined. Here* W^C *is an* n*-dimensional standard Brownian motion under* $\mathcal{Q}_C$, *and the* $n \times n$ *matrix* R *is introduced to model correlation in the resulting noise (*$R\mathrm{d}W$ *is equivalent to an* n*-dimensional Brownian motion with instantaneous correlation matrix* $\rho = RR^\top$*).*
Now suppose we are interested in expressing the dynamics of X *under the measure associated with a new numeraire* D. *The new dynamics will then be*

$$\mathrm{d}X_t = \mu_t^D(X_t)\mathrm{d}t + \sigma_t(X_t)R\mathrm{d}W_t^D,$$

where W^D is an n-dimensional standard Brownian motion under $\mathcal{Q}_D$.
When changing the numeraire from D to C we use the following result: Let us assume that the two numeraires C and D evolve under $\mathcal{Q}_D$ according to

$$\mathrm{d}C_t = (\ldots)\mathrm{d}t + \sigma_t^C R\mathrm{d}W_t^D,$$
$$\mathrm{d}D_t = (\ldots)\mathrm{d}t + \sigma_t^D R\mathrm{d}W_t^D,$$

where both σ_t^C and σ_t^D are $1 \times n$ vectors, W^D is the usual n-dimensional driftless (under $\mathcal{Q}_D$) standard Brownian motion and R is a $n \times n$ correlation matrix of the resulting noise. Then, the drift of the process X under the numeraire D is

$$\mu_t^D(X_t) = \mu_t^C(X_t) - \sigma_t(X_t)\rho \left(\frac{\sigma_t^C}{C_t} - \frac{\sigma_t^D}{D_t} \right)^\top . \tag{B.10}$$

Remark B.5 ((Brigo and Mercurio, 2007)). *See the complete derivation of Theorem B.5 in Brigo and Mercurio (2007). Generically, we can express the derived formula (B.10) as*

$$\mathrm{drift}_{\mathrm{asset}}^{\mathrm{Num2}} = \mathrm{drift}_{\mathrm{asset}}^{\mathrm{Num1}} - \mathrm{Vol}_{\mathrm{asset}}\mathrm{Corr}\left(\frac{\mathrm{Vol}_{\mathrm{Num1}}}{\mathrm{Num1}} - \frac{\mathrm{Vol}_{\mathrm{Num2}}}{\mathrm{Num2}} \right)^\top .$$

This formula allows us to compute the drift in dynamics of an asset price when moving from a first numeraire (Num1) to a second one (Num2), when we know the asset drift in the original numeraire, the asset volatility (that, as all instantaneous volatilities and correlations, does not depend on the numeraire), and the instantaneous correlation in the asset price dynamics as well as the volatilities of the two numeraires.

B.2. Interest Rate

The modelling of interest rates is an essential part of the Pfandbrief model in a one-period setting. The underlying theory is vast so that only excerpts thereof relevant to the Pfandbrief model for adequately capturing interest rate risks are displayed here. We mainly refer to Björk (2004), Brigo and Mercurio (2007) and Schlüchtermann and Pilz (2010).

B.2.1. Fundamentals

In this section we present the fundamental definitions in interest rate theory which build the basis for any derived interest rate model. We solely use the definitions and notation thereof as stated in Brigo and Mercurio (2007).

Definition B.5 (Bank (money-market) account (Brigo and Mercurio, 2007)). *We define $B(t)$ to be the value of a bank account at time $t \geq 0$. We assume $B(0) = 1$ and that the bank account evolves according to the following differential equation:*

$$\mathrm{d}B(t) = r_t B(t)\mathrm{d}t, \quad B(0) = 1, \tag{B.11}$$

where r_t is a positive function of time. As a consequence,

$$B(t) = \exp\left(\int_0^t r(s)\mathrm{d}s\right). \tag{B.12}$$

Remark B.6. Definition B.5 *tells us that investing a unit amount at time* 0 *yields at time t the value in (B.12), and $r(t)$ is the instantaneous rate at which the bank account accrues. The instantaneous rate is usually referred to as instantaneous spot rate, or briefly short rate. In fact, a first order expansion in Δt gives*

$$B(t + \Delta t) = B(t)(1 + r(t)\Delta t),$$

which amounts to say that, in any arbitrarily small time interval $[t, t + \Delta t)$,

$$\frac{B(t + \Delta t) - B(t)}{B(t)} = r(t)\Delta t.$$

Definition B.6 (Stochastic discount factor (Brigo and Mercurio, 2007)). *The (stochastic) discount factor $D(t, T)$ between two time instants t and T is the amount at time t that is 'equivalent' to one unit of currency payable at time T, and is given by*

$$D(t, T) = \frac{B(t)}{B(T)} = \exp\left(-\int_t^T r(s)\mathrm{d}s\right).$$

Definition B.7 (Zero-coupon bond (Brigo and Mercurio, 2007)). *A T-maturity zero coupon bond (pure discount bond) is a contract that guarantees its holder the payment of one unit of currency at time T, with no intermediate payments. The contract value at time $t < T$ is denoted by $P(t, T)$. Clearly, $P(T, T) = 1$ for all T.*

Definition B.8 (Time to maturity (Brigo and Mercurio, 2007)). *The time to maturity $T - t$ is the amount of time (in years) from the present time t to the maturity time $T > t$.*

Definition B.9 (Year fraction, Day-count convention (Brigo and Mercurio, 2007)). *We denote by $\mathfrak{d}(t, T)$ the chosen time measure between t and T, which is usually referred to as year fraction between the dates t and T. When t and T are less than one-day distant (typically when dealing with limit quantities involving time to maturities tending to zero), $\mathfrak{d}(t, T)$ is to be interpreted as the time difference $T - t$ (in years). The particular choice that is made to measure the time between two dates reflects what is known as the day-count convention.*

Definition B.10 (Continuously-compounded spot interest rate (Brigo and Mercurio, 2007)). *The continuously-compounded spot interest rate prevailing at time t for the maturity T is denoted by $R(t, T)$ and is the constant rate at which an investment of $P(t, T)$ units of currency at time t accrues continuously to yield a unit amount of currency at maturity T. In formulas:*

$$R(t, T) := -\frac{\ln P(t, T)}{\mathfrak{d}(t, T)}$$

Remark B.7. *The short rate is obtainable as a limit of* Definition B.10*, that is for each t,*

$$r(t) = \lim_{T \to t^+} R(t, T).$$

Definition B.11 (Zero-coupon curve (Brigo and Mercurio, 2007)). *The zero-coupon curve (sometimes also referred to as 'yield curve') at time t is the graph of the function*

$$T \mapsto \begin{cases} L(t,T) & t < T \leq t+1 \textit{ (years)}, \\ Y(t,T) & T > t+1 \textit{ (years)}, \end{cases}$$

where $L(t,T)$ is the simply-compounded spot interest rate and $Y(t,T)$ is the annually-compounded spot interest rate[1].

Remark B.8. *Continuing* Definition B.11*, the continuously-compounded spot interest rate is defined as follows*

$$T \mapsto R(t,T), \quad T > t,$$

which is the preferred rate used throughout this elaboration. The term 'zero-coupon curve' or 'yield curve' is used for any compounding convention.

Definition B.12 (Zero-bond curve (Brigo and Mercurio, 2007)). *The zero-bond curve at time t is the graph of the function*

$$T \mapsto P(t,T), \quad T > t,$$

which because of the positivity of interest rates, is a T-decreasing function starting from $P(t,t) = 1$. Such s curve is also referred to as term structure of discount factors.

Definition B.13 (Instantaneous forward interest rate (Brigo and Mercurio, 2007)). *The instantaneous forward interest rate prevailing at time t for the maturity $T > t$ is denoted by $f(t,T)$ and is defined as*

$$f(t,T) := \lim_{S \to T^+} F(t;T,S) = -\frac{\partial \ln P(t,T)}{\partial T}, \tag{B.13}$$

so that we also have

$$P(t,T) = \exp\left(-\int_t^T f(t,u)\mathrm{d}u\right).$$

Remark B.9. *The instantaneous forward interest rate is derived from the simply-compounded forward interest rate*

$$F(t;T,S) := \frac{1}{\mathfrak{d}(T,S)}\left(\frac{P(t,T)}{P(t,S)} - 1\right).$$

When the maturity of the forward rate collapses towards its expiry, we have the notion of the instantaneous forward rate. Indeed, let us consider the limit

$$\begin{aligned} \lim_{S \to T^+} F(t;T,S) &= -\lim_{S \to T^+} \frac{1}{P(t,S)} \frac{P(t,S) - P(t,T)}{S-T} \\ &= -\frac{1}{P(t,T)} \frac{\partial P(t,T)}{\partial T} \end{aligned}$$

[1] Definitions for $L(t,T)$ and $Y(t,T)$ can be found in Brigo and Mercurio (2007).

$$= -\frac{\partial \ln P(t,T)}{\partial T},$$

where we use our convention $\mathfrak{d}(T,S) = S - T$ when S is extremely close to T.

B.2.2. Change of Measure

Following Musiela and Rutkowski (2006) and applying Theorem B.5, an arbitrage-free family $P(t,T)$ of bond prices and the related saving account B are given. Note that by assumption, $0 < P(0,T) = \mathbb{E}_{\mathcal{Q}}(B_T^{-1}) < \infty$.

Definition B.14. *A probability mesure $\mathcal{Q}_T$ on $(\Omega, \mathcal{F}_T)$ equivalent to $\mathcal{Q}$, with the Radon-Nikodým derivative given by the formula*

$$\frac{\mathrm{d}\mathcal{Q}_T}{\mathrm{d}\mathcal{Q}} = \frac{B_T^{-1}}{\mathbb{E}_{\mathcal{Q}}(B_T^{-1})} = \frac{1}{B_T P(0,T)}, \quad \mathcal{Q} - \text{a.s.}, \tag{B.14}$$

is called the forward martingale measure (or briefly, the forward measure) for the settlement date T.

Notice that the above Radon-Nikodým derivative, when restricted to the σ-field $\mathcal{F}_t$, satisfies for every $t \in [0,T]$

$$\eta_t \stackrel{\text{def}}{=} \frac{\mathrm{d}\mathcal{Q}_T}{\mathrm{d}\mathcal{Q}}\,|_{\mathcal{F}_t} = \mathbb{E}_{\mathcal{Q}}\left(\frac{P(T,T)}{B_T P(0,T)}\,\middle|\,\mathcal{F}_t\right) = \frac{P(t,T)}{B_t P(0,T)},$$

with $P(T,T) = 1$.
Now, let X be a $\mathcal{F}_T$-measurable random number and (B.14) be the change of measure, where $\mathcal{Q}_T$ is the forward measure and $\mathcal{Q}$ is the risk neutral measure, then:

$$B_t \mathbb{E}_{\mathcal{Q}}\left(B_T^{-1} X\,\middle|\,\mathcal{F}_t\right) = P(t,T)\mathbb{E}_{\mathcal{Q}_T}\left(X \mid \mathcal{F}_t\right)$$

Proof.

$$\begin{aligned}
P(t,T)\mathbb{E}_{\mathcal{Q}_T}\left(X \mid \mathcal{F}_t\right) &= \frac{P(t,T)\mathbb{E}_{\mathcal{Q}}\left(\eta_T X \mid \mathcal{F}_t\right)}{\mathbb{E}_{\mathcal{Q}}\left(\eta_T \mid \mathcal{F}_t\right)} \\
&= \frac{P(t,T)\mathbb{E}_{\mathcal{Q}}\left(\frac{1}{B_T P(0,T)} X\,\middle|\,\mathcal{F}_t\right)}{\frac{P(t,T)}{B_t P(0,T)}} \\
&= B_t P(0,T)\mathbb{E}_{\mathcal{Q}}\left(\frac{1}{B_T P(0,T)} X\,\middle|\,\mathcal{F}_t\right) \\
&= B_t \mathbb{E}_{\mathcal{Q}}\left(B_T^{-1} X\,\middle|\,\mathcal{F}_t\right)
\end{aligned} \tag{B.15}$$

where $\eta_T = \frac{\mathrm{d}\mathcal{Q}_T}{\mathrm{d}\mathcal{Q}} = \frac{1}{B_T P(0,T)}$, $\mathbb{E}_{\mathcal{Q}}\left(\eta_T \mid \mathcal{F}_t\right) = \frac{P(t,T)}{B_t P(0,T)} (= \eta_t)$ and $B_t = \exp\left(\int_0^t r(s)\mathrm{d}s\right)$ denotes the bank account and numeraire under $\mathcal{Q}$. ∎

B.2.3. Affine Term Structure

The underlying interest rate theory is based on the idea of the so-called 'term structure equation' (Theorem B.8) which represents the most important equation in theory of interest rates. We will, however, deliberately omit delivering a complete picture and derivation of an arbitrage free and complete representation for pricing bonds (and other interest rate derivatives). Instead we shall present main results in form of assumptions and established theorems in order to uniquely determine the bond prices under the equivalent martingale measure (EMM) driven by the short rate dynamics, $r(t)$. We refer to the literature for more exhaustive insights into short rate, bond and generally speaking interest rate modelling in this context, see for example Björk (2004), Brigo and Mercurio (2007) and Schlüchtermann and Pilz (2010), amongst many others.

B.2.3.1. Preliminaries

Two fundamental assumptions regarding the modelling environment of interest rates are (Vašìček, 1977):

Assumption B.1. *The spot rate follows a continuous Markov process.*

Assumption B.2. *The market is efficient; that is, there are no transaction costs, information is available to all investors simultaneously, and every investor acts rationally (prefers more wealth to less, and uses all available information).*

Let us define a final time horizon T^* where $T \in [0, T^*]$. Two key elements of interest rate modelling are the spot rate process, $\{r(t) : t \leq T \leq T^*\}$, over the term of the bond and the term structure in form of the zero-coupon bond (Definition B.7), $P(t, T)$, at present time t with maturity T and $t < T$ which are embodied in Assumption B.3 (Björk, 2004), respectively Assumption B.4 (Björk, 2004).

Assumption B.3. *The term structure as well as the prices of all other interest rate derivatives are completely determined by specifying the r-dynamics under the martingale measure Q.*

Assumption B.4. *We assume that there is a market for T-bonds for every choice of T. Furthermore, we assume that for every T the price of a T-bond has the form*

$$P(t, T) = F(t, r(t); T)$$

where F is a smooth function of three real variables, with the boundary condition $F(T, r; T) = 1$.

A first important result is given by Theorem B.7 which allows us to perform a risk-neutral valuation of the bond prices. By utilising the technique of partial differential equations (PDE) on the term structure equations one obtains the Feynman-Kač solution writing the bond price as the conditional expectation (B.17) in Theorem B.7 (Björk, 2004). In particular, the zero-coupon bond price (B.17) at time t for maturity T is characterised by a unit amount of currency available at time T, so that a contingent claim with payoff is given by $H_T = 1$ at time T and we obtain

$$\begin{aligned} P(t,T) &= \mathbb{E}_{\mathcal{Q}}\left(\exp\left(-\int_t^T r(s)\mathrm{d}s\right) H_T \,\middle|\, \mathcal{F}_t\right) \\ &= \mathbb{E}_{\mathcal{Q}}\left(\exp\left(-\int_t^T r(s)\mathrm{d}s\right) \cdot 1 \,\middle|\, \mathcal{F}_t\right). \end{aligned} \tag{B.16}$$

Theorem B.7 (Risk-neutral valuation). *Bond prices are given by the formula $P(t,T) = F(t, r(t); T)$ where*

$$F(t,r;T) = \mathbb{E}_{\mathcal{Q}}\left(\mathrm{e}^{-\int_t^T r(s)\mathrm{d}s} \,\middle|\, \mathcal{F}_t\right). \tag{B.17}$$

Here, the conditional expectation on past information $\mathcal{F}_t$ under the martingale measure $\mathcal{Q}$ shall be taken given the following dynamics for the short rate:

$$\mathrm{d}r(t) = [\mu_{\mathcal{P}}(t,r(t)) - \varphi(t,r(t))\sigma_{\mathcal{P}}(t,r(t))]\mathrm{d}t + \sigma(t,r(t))\mathrm{d}W^{\mathcal{Q}}(t) \tag{B.18}$$

where $\mu_{\mathcal{P}}$ is the drift term, $\sigma_{\mathcal{P}}$ is the diffusion term, φ is the market price of risk and $\mathrm{d}W^{\mathcal{Q}}(t)$ is a Wiener process on $(\Omega, \mathcal{F}, \mathcal{Q}, (\mathcal{F}_t)_{0\le t\le T^*})$.

We take a step back and shall briefly outline the attainment of a risk-neutral representation of the bond price and short rate process of Theorem B.7 which arises from deriving an arbitrage-free price for any interest rate derivative based on a suitable locally-riskless portfolio as in Black and Scholes (1973). Originally, referring to the seminal work of Vašìček (1977), the instantaneous spot rate dynamics are specified under the real-world measure $\mathcal{P}$. Further, there exists one exogenously defined traded asset, namely the cash account (Definition B.5)

$$\mathrm{d}B(t) = r(t)B(t)\mathrm{d}t$$

with the short rate of interest under the real-world measure $\mathcal{P}$ solving

$$\mathrm{d}r(t) = \mu_{\mathcal{P}}(t,r(t))\mathrm{d}t + \sigma_{\mathcal{P}}(t,r(t))\mathrm{d}W^{\mathcal{P}}(t), \tag{B.19}$$

which is modelled as an Itô diffusion and is therefore Markovian (Assumption B.1). The drift and volatility parameters, $\mu_{\mathcal{P}}$ and $\sigma_{\mathcal{P}}$, are time-dependent deterministic functions which also may depend on the short rate r, satisfying the usual Lipschitz and boundedness conditions that guarantee existence and uniqueness of solutions of the stochastic differential equation. From Itô's formula (Theorem B.3) we get the process for the zero-coupon bond price ($\mathrm{d}W^{\mathcal{P}}(t)$ is a Wiener process on $(\Omega, \mathcal{F}, \mathcal{P}, (\mathcal{F}_t)_{0\le t\le T^*})$)

$$\mathrm{d}P(t,T) = m(t,r;T)P(t,T)\mathrm{d}t + v(t,r;T)P(t,T)\mathrm{d}W^{\mathcal{P}}(t)$$

where

$$\begin{aligned} m(t,r;T)F(t,r;T) = \frac{\partial F(t,r;T)}{\partial t} + \mu_{\mathcal{P}}(t,r)\frac{\partial F(t,r;T)}{\partial r} &+ \\ \frac{1}{2}\sigma_{\mathcal{P}}(t,r)^2\frac{\partial^2 F(t,r;T)}{\partial r^2}&, \end{aligned} \tag{B.20}$$

$$v(t,r;T)F(t,r;T) = \sigma_{\mathcal{P}}(t,r)\frac{\partial F(t,r;T)}{\partial r}. \tag{B.21}$$

The process $m(t,r;T)$ is regarded as a time-dependent drift parameter of the bond price which is additionally dependent on the bond's maturity T, whereas $v(t,r;T)$ represents the volatility structure.

In the context of interest rate modelling an inherent issue arises, namely the (bond) market is not necessarily complete. According to Björk (2004)'s heuristical approach, the number of tradable assets (excluding the risk free asset $B(t)$) need to be equal to the number of random sources (in form of Brownian motions) to ensure an arbitrage free and complete market. Here, unlike in the Black-Scholes model, the short term rate $r(t)$ is not a tradable asset (per definition it is a rate and not a price). Consequently, there are fewer tradable assets than sources of randomness and, thus, the market is incomplete, respectively, uniqueness of $\mathcal{Q}$ is not guaranteed. In order to overcome this issue a 'benchmark bond' is constructed from a portfolio consisting of two bonds at two fixed maturities S and T $(S < T)$ with which all other bond prices can be uniquely be determined. This 'benchmark bond' represents a tradable asset which has the r-dynamics as underlying — resulting to one asset with one random source. Hence, we have a arbitrage free and complete market (see Björk (2004) or Schlüchtermann and Pilz (2010) for the complete derivation).

Once the S and T dependencies are successfully separated and assuming that the bond market is arbitrage-free, we conclude that there exists an adaptive process $\varphi(t, r(t))$ denoting the market price of risk, given by

$$\frac{m(t,r(t)) - r(t)}{v(t,r(t))} = \varphi(t,r(t)) \tag{B.22}$$

for each maturity T, with φ that may depend on t and r but not on T (the maturities of the claims constituting the portfolio). In other words, "in a no arbitrage market all bonds will, regardless of maturity of time, have the same market price of risk", (Björk, 2004).

Remark B.10. *The market price of risk is also referred to the risk premium per unit risk or the sharp ratio. The numerator, $m(t,r(t)) - r(t)$, is called the risk premium for the T-bond denoting the excess return over the risk-free rate of return on the market (as opposed to simply investing money in a riskless bank account). The denominator, $v(t,r(t))$, represents the volatility for the T-bond, thus dividing by the amount of risk we are exposed to. Hence, the quotient amounts to the 'market price of risk' (or 'risk premium per unit of volatility') for the T-bond.*

Substitution of the expressions (B.20) and (B.21) into the equation (B.22) yield the arbitrage-free bond prices $F(t,r;T)$ satisfying one of the most important equations in the theory of interest rates — the term structure equation in Theorem B.8.

Theorem B.8 (Term structure equation). *In an arbitrage free bond market,*

$F(t, r; T)$ will satisfy the term structure equation

$$\begin{cases} \dfrac{\partial F(t,r;T)}{\partial t} + [\mu_{\mathcal{P}}(t,r) - \varphi(t,r)\sigma_{\mathcal{P}}(t,r)]\dfrac{\partial F(t,r;T)}{\partial r} + \\ \qquad\qquad \dfrac{1}{2}\sigma^2(t,r)\dfrac{\partial^2 F(t,r;T)}{\partial r^2} - rF(t,r;T) = 0 \\ \qquad\qquad F(T,r;T) = 1. \end{cases} \tag{B.23}$$

The term structure equation will yield the term of a basic (zero-coupon) T-bond ('benchmark bond') driven by a short rate process of interest. With these two components, the term structure equation allows one to determine all other bond prices.
According to Björk (2004), by fixing (t, r) and applying Itô's formula (Theorem B.3) to the process

$$\exp\left(-\int_t^s r(u)\mathrm{d}u\right) F(s, r(t), T)$$

where $F(s, r(t), T)$ satisfies (B.23), we obtain the Feynman-Kač representation (B.17) in Theorem B.7.

Remark B.11. *Comparing (B.19) and (B.18) we also see that the risk-neutral representation of the short rate process (B.18) of Theorem B.7 is obtained with the help of Girsanov (Theorem B.4) with which we can move from the real-world to the risk-neutral measure. More precisely, there exists a risk-neutral measure $\mathcal{Q}$ that is equivalent to the real-world measure $\mathcal{P}$ and is defined by the Radon-Nikodým derivative*

$$\frac{\mathrm{d}\mathcal{Q}}{\mathrm{d}\mathcal{P}}\Big|_{\mathcal{F}_t} = \exp\left(-\frac{1}{2}\int_0^t \varphi^2(s,r)\mathrm{d}s - \int_0^t \varphi(s,r)\mathrm{d}W^{\mathcal{P}}(s)\right) \tag{B.24}$$

where $\mathcal{F}_t$ is the σ-field generated by r up to time t, $W^{\mathcal{P}}(t)$ is a $\mathcal{P}$-Brownian motion and φ denotes the market price of risk[2]. As a consequence with (B.24) and (B.22), the initial process (B.19) under $\mathcal{P}$ then evolves under $\mathcal{Q}$ according to (B.18) of Theorem B.7 with $\mathrm{d}W^{\mathcal{Q}}(t) = \mathrm{d}W^{\mathcal{P}}(t) + \varphi(t,r)\mathrm{d}t$.

We see that a complete specification of an one-factor spot rate model amounts to specifying both dynamics of the short rate $r(t)$ as an Itô diffusion under $\mathcal{P}$ and the market price of risk process $\varphi(t) = \varphi(t, r(t))$. This is equivalent to selecting one equivalent martingale measure $\mathcal{Q}$ of the form (B.24) and an Itô diffusion for the $\mathcal{Q}$-dynamics of r. Either way, interest rate derivatives can then be priced by expectations of their final pay-off with respect to $\mathcal{Q}$. Hence, the market (implicitly) determines $\mathcal{Q}$ and φ. Referring to Björk (2004) we know that the term $\mu_{\mathcal{P}}(t, r(t)) - \varphi(t, r(t))\sigma_{\mathcal{P}}(t, r(t))$ in (B.18) of Theorem B.7 resembles the desired drift term under the martingale measure $\mathcal{Q}$ of the short rate process. However, under $\mathcal{Q}$ it is not necessary to specify $\mu_{\mathcal{P}}(t, r(t))$ and $\varphi(t, r(t))$, so that the market price of risk will be implicit in the underlying dynamics. Instead one models the short rate $r(t)$ directly under the martingale measure $\mathcal{Q}$ with a generic drift term $\mu(t, r(t))$, with

$$\varphi(t, r(t)) = \frac{\mu_{\mathcal{P}}(t, r(t)) - \mu(t, r(t))}{\sigma_{\mathcal{P}}(t, r(t))}$$

[2] Note the following relationship between the market price of risk (φ) the Girsanov kernel ($\mathfrak{g}$): $\varphi(t) = -\mathfrak{g}(t)$.

$$\sigma_{\mathcal{P}}(t, r(t)) = \sigma(t, r(t))$$

which leads to Assumption B.5.

Assumption B.5. *We assume that the dynamics of the short term rate is given by*

$$\mathrm{d}r(t) = \mu(r(t), t)\mathrm{d}t + \sigma(r(t), t)\mathrm{d}W^{\mathcal{Q}}(t) \tag{B.25}$$

where $W(t)$ is a Wiener process and $\mu(r(t), t)$ is the drift and $\sigma(r(t), t)$ the volatility, both deterministic functions dependent on the short rate r and time t in the general form, driving the behaviour of the short term rate.

The bond price dynamics under the risk-neutral measure are constituted by Theorem B.9 which is derived from Girsanov's Theorem B.4 (Schlüchtermann and Pilz, 2010).

Theorem B.9. *The scalar stochastic differential equation, in time t for each fixed time of maturity T, of the bond price $P(t, T)$ under the risk-neutral measure $\mathcal{Q}$ is*

$$\mathrm{d}P(t, T) = P(t, T)r(t)\mathrm{d}t + P(t, T)v(t, T)\mathrm{d}W^{\mathcal{Q}}(t) \tag{B.26}$$

where $r(t)$ is the short-term risk-free interest rate at time t and $v(t, T)$ is the volatility of $P(t, T)$, an adapted process parametrised by time of maturity T.

Henceforth, we shall postulate an equivalent martingale measure for all presented interest rate models and introduced model parameters, if not explicitly stated otherwise.

Remark B.12. *We postulate the general specification with drift*

$$\mu(r(t), t) = \theta(t) - \kappa(t)r(t)$$

and volatility

$$\sigma(r(t), t) = \sigma(t)[r(t)]^{\beta}.$$

Then, under the risk-neutral measure $\mathcal{Q}$ the mean-reverting process (B.25) evolves according to

$$\mathrm{d}r(t) = (\theta(t) - \kappa(t)r(t))\mathrm{d}t + \sigma(t)[r(t)]^{\beta}\mathrm{d}W^{\mathcal{Q}}(t), \quad r(0) = r_0, \tag{B.27}$$

where $\theta(t)$, $\kappa(t) > 0$ and $\sigma(t) > 0$ are time-varying and $W^{\mathcal{Q}}(t)$ is a Wiener process. The parameter $\beta \geq 0$ basically determines the underlying short rate model. From this general specification of (B.27) the following well known and widely used short rate models can be derived:

Vašiček *The Vašiček model (Vašiček, 1977) is obtained by setting $\beta = 0$ and constant parameters $\theta(t) = \theta$, $\kappa(t) = \kappa$, $\sigma(t) = \sigma$.*

HW1F *The Hull-White one-factor model (Hull and White (1990) or Hull and White (1993)) is defined by possessing a time-dependent mean reversion parameter $\theta(t)$, with $\beta = 0$ and constant parameters $\kappa(t) = \kappa$, $\sigma(t) = \sigma$.*

CIR1F *The Cox-Ingersoll-Ross one-factor model (Cox et al., 1985) is received by setting $\beta = 0.5$ and constant parameters $\theta(t) = \theta$, $\kappa(t) = \kappa$, $\sigma(t) = \sigma$.*

ExtVašíček *With $\beta = 0$ (everything else unchanged) we obtain the extended Vašíček (1977) model specified in Hull and White (1990) or Hull and White (1993).*

ExtCIR1F *With $\beta = 0.5$ (everything else unchanged) the extended Cox et al. (1985) model emerges, as specified in Hull and White (1990) or Hull and White (1993).*

The above model selection is far from exhaustive, however, these particular short rate models are frequently mentioned throughout Section B.2.5 and should provide some orientation without going into too much theoretical detail. In-depth model descriptions can be found, for example, in Brigo and Mercurio (2007).

B.2.3.2. Tractability

From Section B.2.3.1 we know that modelling interest rates is driven by an underlying short rate process $r(t)$. However, the zero-coupon bond object of (B.16) is still not satisfyingly tangible. A tractable solution delivers the so called 'affine term structure' (ATS) representation (Definition B.15) where (B.16) is reformulated to an affine equation (B.28), compare Björk (2004). In the affine models, the functions $A(t,T)$ and $B(t,T)$ are deterministic and must be continuously differentiable, otherwise the Riccati differential equations can not be formulated. This is essential to obtain closed form solutions for the respective models.

Definition B.15. *If the term structure (bond value) has the form*

$$P(t,T) = F(t, r(t); T), \tag{B.28}$$

where F has the form

$$F(t, r; T) = \mathrm{e}^{A(t,T) - B(t,T)r}$$

and where A and B are deterministic functions and $A, B : \mathbb{R}^2 \to \mathbb{R}$ continuously differentiable, then the model is said to possess an ATS.

Remark B.13. *Interest rate models assigned the term 'affine' (linear plus a constant) is motivated by the term structure of interest rates (Definition B.10) being an affine function with the short rate as argument, namely*

$$R(t,T) = -\frac{A(t,T)}{T-t} + \frac{B(t,T)}{T-t} r(t). \tag{B.29}$$

We make use of the partial differential equation (PDE) approach to briefly introduce, yet provide some valuable insight thereof, the concept of the affine term structure. Thereby, (B.23) is utilised in order to derive the affine term structure (ATS) Theorem B.10, as can be found in Björk (2004). Theorem B.10 allows to derive the bond equations of interest rate models with an affine term structure. Furthermore, in order to obtain an ATS specification of μ and σ in (B.25) the partial derivatives of $F(t, r; T)$ of Definition B.15 need to be computed which are

$$\begin{aligned}
\frac{\partial F(t,r;T)}{\partial t} &= F(t,r;T)\left(\frac{\partial A(t,T)}{\partial t} - \frac{\partial B(t,T)}{\partial t} r\right), \\
\frac{\partial F(t,r;T)}{\partial r} &= -F(t,r;T) B(t,T)
\end{aligned}$$

and

$$\frac{\partial^2 F(t,r;T)}{\partial r^2} = F(t,r;T)B^2(t,T).$$

After substitution and dividing by $F(t,r;T)$ Equation (B.23) amounts to

$$\frac{1}{2}\sigma^2(t,r)B^2(t,T) + \frac{\partial A(t,T)}{\partial t} - \left(1 + \frac{\partial B(t,T)}{\partial t}\right) r - \mu(t,r)B(t,T) = 0. \tag{B.30}$$

With $F(t,r;T) = 1$ it follows that $A(T,T) = B(T,T) = 0$ and by setting

$$\mu(r,t) = \alpha(t)r + \beta(t) \qquad \text{and} \qquad \sigma(r,t) = \sqrt{\gamma(t)r + \delta(t)},$$

one obtains

$$\left[\frac{\partial A(t,T)}{\partial t} - \beta(t)B(t,T) + \frac{1}{2}\delta(t)B^2(t,T)\right] - \\ \left(1 + \frac{\partial B(t,T)}{\partial t} + \alpha(t)B(t,T) - \frac{1}{2}\gamma(t)B^2(t,T)\right) r = 0. \tag{B.31}$$

As stated by Schlüchtermann and Pilz (2010), if (B.31) holds for all t, T and r and if $r \downarrow 0$ then the terms before r and in brackets $[\cdot]$ disappear, so that (B.32) and (B.33) emerge in Theorem B.10. Reversing the argumentation proves Theorem B.10.

Theorem B.10 (Affine term structure). *Assume that μ and σ are of the form*

$$\begin{cases} \mu(t,r) = \alpha(t)r + \beta(t), \\ \sigma(t,r) = \sqrt{\gamma(t)r + \delta(t)}. \end{cases}$$

Then the model admits an affine term structure (ATS) of the form (B.16), where A and B satisfy the system

$$\begin{cases} \dfrac{\mathrm{d}B(t,T)}{\mathrm{d}t} + \alpha(t)B(t,T) - \dfrac{1}{2}\gamma(t)B^2(t,T) = -1, \\ \qquad\qquad B(T,T) = 0 \end{cases} \tag{B.32}$$

and

$$\begin{cases} \dfrac{\mathrm{d}A(t,T)}{\mathrm{d}t} = \beta(t)B(t,T) - \dfrac{1}{2}\delta(t)B^2(t,T), \\ A(T,T) = 0. \end{cases} \tag{B.33}$$

First the Riccati equation (B.32) is solved (not depending on A) which can then be inserted into (B.33) and integrated in order to obtain A. Further, Schlüchtermann and Pilz (2010) provide a general solution of the PDEs for constant parameters α, β, γ and δ which is given in the following Corollary B.2 (from Theorem B.10).

Corollary B.2. *For time-independent functions α, β, γ ($\gamma \neq 0$) and δ solving the Riccati differential equations, yields for A with starting value $A(t,t) = 0$*

$$\frac{2}{\gamma}A(t,T) = a_2c_2\ln(a_2 - B(t,T)) + (c_2 + \frac{1}{2}\delta)a_1 \ln\left(\frac{B(t,T)+a_1}{a_1}\right) -$$

$$\frac{1}{2}\delta B(t,T) - a_2 c_2 \ln a_2 \quad \text{(B.34)}$$

and for B

$$B(t,T) = \frac{2(\mathrm{e}^{c_1(T-t)} - 1)}{(-\alpha + c_1)(\mathrm{e}^{c_1(T-t)} - 1) + 2c_1}, \tag{B.35}$$

with constants

$$a_1 = -\frac{\alpha - \sqrt{\alpha^2 + 2\gamma}}{\gamma}, \qquad a_2 = -\frac{-\alpha - \sqrt{\alpha^2 + 2\gamma}}{\gamma}$$

and

$$c_1 = \sqrt{\alpha^2 + 2\gamma}, \qquad c_2 = \frac{\beta - a_2\delta/2}{a_1 + a_2}.$$

Conclusively, we also state the stochastic differential equation, derivable via Itô's formula (Theorem B.3), for the bond price (B.36) of Theorem B.11.

Theorem B.11. *In an affine term-structure model in which the short rate satisfies the SDE (B.25) with μ and σ as in Theorem B.10, the bond price dynamics under the risk-neutral measure $\mathcal{Q}$ are*

$$\mathrm{d}P(t,T) = r(t)P(t,T)\mathrm{d}t - \sigma(t, r(t))B(t,T)P(t,T)\mathrm{d}W^{\mathcal{Q}}(t), \tag{B.36}$$

with $v(t,T) = \sigma(t, r(t))B(t,T)$ in (B.26).

Remark B.14. *Most short rate models possess a linear SDE which makes derivations of closed form solutions more easy. The existence of closed form solutions highly depends on the underlying distribution of $r(t)$. Plugging in normally distributed processes, such as the Vašíček (1977) or extended Vašíček (Hull and White, 1990) one-factor model (see Remark B.12), into bond price equation of (B.16) results in the computation of the expected value of a log-normal stochastic variable which is manageable. The Dothan (1978), Black et al. (1990) and Black and Karasinski (1991) belong to the class of log-normal short rate models. However, no closed form expressions for bond prices or options are available, thus also no ATS formulation exists.*

B.2.4. Hull-White One Factor (HW1F) Model — Extended

Here specific features of the HW1F model are elaborated to give a more complete picture of the underlying theory and parameter estimation techniques.

B.2.4.1. Derivation ZCB Pricing Formula

We apply the general theory of the ATS introduced in Appendix B.2.3 to the HW1F model. With $\mu(r,t) = \theta(t) - \kappa r(t)$ and $\sigma(r,t) = \sigma$, (B.30) becomes

$$\left[\frac{\partial A(t,T)}{\partial t} - \theta(t)B(t,T) + \frac{1}{2}\sigma^2 B^2(t,T)\right] - \left(1 + \frac{\partial B(t,T)}{\partial t} - \kappa B(t,T)\right) r = 0.$$

Again, by letting $r \downarrow 0$ the terms in brackets should be equal zero, so that (B.37) and (B.38) can be obtained. Alternatively, with the results of Theorem B.10 we can set $\alpha(t) = -\kappa$, $\beta(t) = \theta(t)$, $\gamma(t) = 0$ and $\delta(t) = \sigma^2$ resulting to

$$\begin{cases} \dfrac{\partial B(t,T)}{\partial t} = \kappa B(t,T) - 1, \\ B(T,T) = 0. \end{cases} \tag{B.37}$$

and

$$\begin{cases} \dfrac{\partial A(t,T)}{\partial t} = \theta(t)B(t,T) - \dfrac{1}{2}\sigma^2 B^2(t,T), \\ A(T,T) = 0. \end{cases} \tag{B.38}$$

Equation (B.37) is solved with the boundary condition $B(T,T) = 0$, so that $\frac{\partial B(t,T)}{\partial t} = \mathrm{e}^{-\kappa(T-t)}$ yielding (3.24). Deriving $A(t,T)$, Equation (3.23), is more involved where the integral (with $\int_t^T \frac{\partial A(t,T)}{\partial t} \mathrm{d}s = A(T,T) - A(t,T)$)

$$\begin{aligned} A(t,T) &= -\int_t^T \left(\theta(s)B(s,T) - \frac{1}{2}\sigma^2 B^2(s,T)\right) \mathrm{d}s \\ &= \underbrace{\frac{\sigma^2}{2}\int_t^T B^2(s,T)\mathrm{d}s}_{\text{(I)}} - \underbrace{\int_t^T \theta(s)B(s,T)\mathrm{d}s}_{\text{(II)}} \end{aligned} \tag{B.39}$$

needs to be calculated. The necessary equations are derived in the following.

(I):

$$\begin{aligned} &\frac{\sigma^2}{2}\int_t^T B^2(s,T)\mathrm{d}s \\ =& \frac{\sigma^2}{2\kappa^2}\int_t^T \left(1 - \mathrm{e}^{-\kappa(T-s)}\right)^2 \mathrm{d}s \\ =& \frac{\sigma^2}{2\kappa^2}\int_t^T \left(1 - 2\mathrm{e}^{-\kappa(T-s)} + \mathrm{e}^{-2\kappa(T-s)}\right) \mathrm{d}s \\ =& \frac{\sigma^2}{2\kappa^2}\left((T-t) + \frac{2}{\kappa}\left(1 - \mathrm{e}^{-\kappa(T-t)}\right) - \frac{1}{2\kappa}\left(1 - \mathrm{e}^{-2\kappa(T-t)}\right)\right) \end{aligned} \tag{B.40}$$

(II):

$$\begin{aligned} &\int_t^T \theta(s)B(s,T)\mathrm{d}s \\ =& \frac{1}{\kappa}\int_t^T \left(1 - \mathrm{e}^{-\kappa(T-s)}\right)\left(\frac{\partial f^M(0,s)}{\partial T} + \kappa f^M(0,s) + \frac{\sigma^2}{2\kappa}\left(1 - \mathrm{e}^{-2\kappa s}\right)\right) \mathrm{d}s \\ =& \underbrace{\frac{1}{\kappa}\int_t^T \left(\frac{\partial f^M(0,s)}{\partial T} + \kappa f^M(0,s)\right) \mathrm{d}s}_{\text{(III)}} - \end{aligned}$$

$$\underbrace{\frac{1}{\kappa}\int_t^T \mathrm{e}^{-\kappa(T-s)}\left(\frac{\partial f^M(0,s)}{\partial T}+\kappa f^M(0,s)\right)\mathrm{d}s}_{\text{(IV)}}+$$
$$\underbrace{\frac{\sigma^2}{2\kappa^2}\int_t^T\left(1-\mathrm{e}^{-\kappa(T-s)}\right)\left(1-\mathrm{e}^{-2\kappa s}\right)\mathrm{d}s}_{\text{(V)}} \tag{B.41}$$

(III):

$$\begin{aligned}&\frac{1}{\kappa}\int_t^T\left(\frac{\partial f^M(0,s)}{\partial T}+\kappa f^M(0,s)\right)\mathrm{d}s\\ =&\frac{1}{\kappa}\left(f^M(0,T)-f^M(0,t)\right)-\int_t^T f^M(0,s)\mathrm{d}s\end{aligned} \tag{B.42}$$

(IV):

$$\begin{aligned}&\frac{1}{\kappa}\int_t^T \mathrm{e}^{-\kappa(T-s)}\left(\frac{\partial f^M(0,s)}{\partial T}+\kappa f^M(0,s)\right)\mathrm{d}s\\ =&\frac{1}{\kappa}\int_t^T \mathrm{e}^{-\kappa(T-s)}\frac{\partial f^M(0,s)}{\partial T}+\int_t^T \mathrm{e}^{-\kappa(T-s)}f^M(0,s)\mathrm{d}s\\ =&\frac{1}{\kappa}\left(f^M(0,T)-\mathrm{e}^{-\kappa(T-t)}f^M(0,t)\right)-\int_t^T \mathrm{e}^{-\kappa(T-s)}f^M(0,s)\mathrm{d}s+\\ &\int_t^T \mathrm{e}^{-\kappa(T-s)}f^M(0,s)\mathrm{d}s\\ =&\frac{1}{\kappa}\left(f^M(0,T)-\mathrm{e}^{-\kappa(T-t)}f^M(0,t)\right)\end{aligned} \tag{B.43}$$

(V):

$$\begin{aligned}&\frac{\sigma^2}{2\kappa^2}\int_t^T\left(1-\mathrm{e}^{-\kappa(T-s)}\right)\left(1-\mathrm{e}^{-2\kappa s}\right)\mathrm{d}s\\ =&\frac{\sigma^2}{2\kappa^2}\int_t^T 1-\mathrm{e}^{-2\kappa s}-\mathrm{e}^{-\kappa(T-s)}+\mathrm{e}^{-\kappa(T-s)-2\kappa s}\mathrm{d}s\\ =&\frac{\sigma^2}{2\kappa^2}(T-t)+\\ &\frac{\sigma^2}{2\kappa^3}\left(\frac{1}{2}\left(\mathrm{e}^{-2\kappa T}-\mathrm{e}^{-2\kappa t}\right)+\left(1-\mathrm{e}^{-\kappa(T-t)}\right)-\left(\mathrm{e}^{-2\kappa T}-\mathrm{e}^{-\kappa(T+t)}\right)\right)\end{aligned} \tag{B.44}$$

For illustrating the exact yield curve fitting, the time-dependent mean reversion level function, $\theta(t)$, needs to be adapted in such a way that today's ($t=0$) theoretical bond price matches the market price $P^M(0,T)$ where $r(0)$ is today's observed short rate. Taking the logarithm of (B.28) and inserting (B.39) for $A(t,T)$ and (3.24) for $B(t,T)$ we find that $\theta(s)$ has to satisfy the integral

$$\begin{aligned}&-\int_0^T \theta(s)B(s,T)\mathrm{d}s\\ =&\log P(0,T)+r(0)B(0,T)-\frac{\sigma^2}{2}\int_0^T B^2(s,T)\mathrm{d}s\end{aligned}$$

$$= \log P(0,T) + \frac{r(0)}{\kappa}\left(1 - \mathrm{e}^{-\kappa T}\right) -$$
$$\frac{\sigma^2}{2\kappa^2}\left(T + \frac{2}{\kappa}\left(1 - \mathrm{e}^{-\kappa T}\right) - \frac{1}{2\kappa}\left(1 - \mathrm{e}^{-2\kappa T}\right)\right). \quad \text{(B.45)}$$

This equation can be solved for $\theta(T)$ by by differentiating twice wrt maturity T yielding

$$\begin{aligned}
\frac{\partial}{\partial T}\int_0^T \theta(s)B(s,T)\mathrm{d}s &= \theta(T)B(T,T) + \int_0^T \theta(s)\frac{\partial B(s,T)}{\partial T} \\
&= \int_0^T \theta(s)\mathrm{e}^{\kappa(s-T)}\mathrm{d}s \\
&= \mathrm{e}^{-\kappa T}\int_0^T \theta(s)\mathrm{e}^{\kappa s}\mathrm{d}s
\end{aligned}$$

and

$$\frac{\partial^2}{\partial T^2}\int_0^T \theta(s)B(s,T)\mathrm{d}s = \theta(T) - \kappa\mathrm{e}^{-\kappa T}\int_0^T \theta(s)\mathrm{e}^{\kappa s}\mathrm{d}s.$$

It follows that

$$\begin{aligned}
\theta(T) &= \frac{\partial^2}{\partial T^2}\int_0^T \theta(s)B(s,T)\mathrm{d}s + \kappa\frac{\partial}{\partial T}\int_0^T \theta(s)B(s,T)\mathrm{d}s \\
&= -\frac{\partial^2}{\partial T^2}\log P(0,T) - \kappa\frac{\partial}{\partial T}P(0,T) + \frac{\sigma^2}{2\kappa}(1 - \mathrm{e}^{-2\kappa T})
\end{aligned}$$

by inserting (B.45). Setting $P(0,T) = P^M(0,T)$ for all maturities $T > 0$ and with $f^{\mathrm{M}}(0,T) := \frac{-\partial \ln P^{\mathrm{M}}(0,T)}{\partial T}$ results to Equation (3.19).
Completing the model definition of the HW1F model, we state the bond price dynamics under the risk-neutral measure $\mathcal{Q}$ which can be easily obtained via Ito's formula, or via (B.36) with $\sigma(r,t) = \sigma$, amounting to

$$\mathrm{d}P(t,T) = r(t)P(t,T)\mathrm{d}t - B(t,T)P(t,T)\sigma\mathrm{d}W^{\mathcal{Q}}(t). \quad \text{(B.46)}$$

From Definition B.13 we know that $P^M(0,t) = \mathrm{e}^{-\int_0^t f^M(0,s)\mathrm{d}s}$ and $P^M(0,T) = \mathrm{e}^{-\int_0^T f^M(0,s)\mathrm{d}s}$, so that $\ln\left(\frac{P^M(0,T)}{P^M(0,t)}\right) = -\int_t^T f^M(0,s)\mathrm{d}s$. Inserting (B.40) and (B.41) with (B.42), (B.43) and (B.44) into (B.39) finally results to (3.23) in Section 3.7.3.1, the closed form solution of A and B to Definition B.15.

B.2.4.2. Alternative Measures

It may be useful for modelling purposes to represent (3.18) in alternative measures. The forward and real-world SDE formulations are derived in the following.

Forward Measure We resort to the change-of-numeraire toolkit (Theorem B.6) with (B.10) provided by Brigo and Mercurio (2007). For the HW1F model we have

- $C_t = B(t)$, the bank account numeraire (Definition B.5),
- $\sigma_t^C = 0$, the volatility of the bank account process is zero, and

- $D_t = P(t,T)$, the T-bond numeraire (Definition B.7).
- $X_t = r(t)$,
- $\mu_t^C(X_t) = \theta(t) - \kappa r(t)$, the old drift term of (3.18) under the risk-neutral measure $\mathcal{Q}$,
- $\sigma_t(X_t) = \sigma$, the volatility term of (3.18),
- $\rho = 1$, as $\mathrm{Corr}(\mathrm{d}W_t^D, \mathrm{d}W_t^D) = 1$ and
- $\sigma_t^D = -B(t,T)P(t,T)\sigma$, the volatility term of the bond price process (B.46).

Then we obtain the new drift under the T-forward measure $\mathcal{Q}_T$

$$\mu_t^D(X_t) = \theta(t) - \kappa r(t) - \sigma^2 B(t,T)$$

so that the SDE under $\mathcal{Q}_T$ becomes

$$\mathrm{d}r(t) = (\theta(t) - \kappa r(t) - \sigma^2 B(t,T))\mathrm{d}t + \sigma \mathrm{d}W^{\mathcal{Q}_T}(t). \tag{B.47}$$

Thus, under the forward measure, the short rate process remains a Hull-White process but the reversion level becomes $\frac{\theta(t)}{\kappa} - \frac{\sigma^2 B(t,T)}{\kappa}$ where $B(t,T)$ is an adapted process parametrised by time of maturity T.

Remark B.15. *Discounting under the forward measure, $\mathcal{Q}_T$, is deterministic where the discount factor no longer needs to be simulated as under $\mathcal{Q}$. This simplification results from including the additional term $-\sigma^2 B(t,T)$ in the drift of $r(t)$.*

Additionally, the $\mathcal{Q}_T$-Brownian motion $W^{\mathcal{Q}_T}$ can be determined, amounting to

$$\mathrm{d}W^{\mathcal{Q}_T}(t) = \mathrm{d}W^{\mathcal{Q}}(t) + \sigma B(t,T)\mathrm{d}t.$$

Real-World Measure Retaining a tractable short rate process for the HW1F model under the real-world measure $\mathcal{P}$, Assumption B.6 is postulated. Tractability under the objective measure can be helpful for historical-estimation purposes.

Assumption B.6. *The market price of risk process, $\varphi(t)$, needs to be of the particular functional form*

$$\varphi(t) = \varphi r(t), \tag{B.48}$$

where φ is a new parameter, contributing to the market price of risk.

With Assumption B.6 we obtain the Girsanov (Theorem B.4) change of measure

$$\frac{\mathrm{d}\mathcal{Q}}{\mathrm{d}\mathcal{P}} = \exp\left(-\frac{1}{2}\int_0^t \varphi^2 r(s)^2 \mathrm{d}s + \int_0^t \varphi r(s) \mathrm{d}W^{\mathcal{P}}(s)\right)$$

and the SDE under the real-world measure $\mathcal{P}$

$$\begin{aligned}\mathrm{d}r(t) &= (\theta(t) - \kappa r(t))\mathrm{d}t + \sigma\left(\mathrm{d}W^{\mathcal{P}}(t) - \varphi(t)\mathrm{d}t\right)\\ &= [\theta(t) - (\kappa + \sigma\varphi)r(t)]\mathrm{d}t + \sigma \mathrm{d}W^{\mathcal{P}}(t)\end{aligned} \tag{B.49}$$

where φ is the additional market price of risk parameter compared to the $\mathcal{Q}$-dynamics, affecting the drift term. Under the $\mathcal{P}$-dynamics the SDE is expressed again as a linear Gaussian stochastic differential equation as under $\mathcal{Q}$.

Remark B.16. *For $\varphi = 0$ the two dynamics coincide, i.e. there is no difference between the risk neutral and the real world.*

B.2.5. Model Selection

Here additional selection criteria are presented in order to choose an appropriate interest rate model for the underlying Pfandbrief model in a one-period setting.

B.2.5.1. Fitting the Yield Curve

Required components when fitting the yield curve (also known as inversion of the yield curve) basically consists of having (Björk, 2004)

· a theoretical term structure

$$P(0, T; \vartheta), \quad T \geq 0,$$

with an underlying short rate model under the $\mathcal{Q}$-dynamics as in Assumption B.5 expanded by a parameter vector ϑ, so that

$$\mathrm{d}r(t) = \mu(r(t), t; \vartheta)\mathrm{d}t + \sigma(r(t), t; \vartheta)\mathrm{d}W^{\mathcal{Q}}(t),$$

· and an observed (market) term structure

$$P^M(0, T), \quad T \geq 0.$$

A potential issue wrt calibration arises, namely for each T a corresponding equation needs to be solved consisting of the number of parameters contained in ϑ which can amount to a cumbersome problem to solve. The goodness-of-fit largely depends on how many parameters the model possesses. Naturally, a trade-off between model flexibility and complexity arises, meaning a model must have few enough parameters that a good fit is significant, and enough to ensure that a good fit is possible. Models where the term structure is given endogenously, generally, do not fit the initially observed term structure well, since the dynamics of the state variables need to be specified. For example the one-factor affine models, Vašìček (1977) or Cox et al. (1985), do not have a large range of shapes and will provide a poor fit to some initial yield curves which can be observed in Example B.1. We deliberately omit any in-depth theoretical description at this stage and refer to the literature, e.g. Brigo and Mercurio (2007) or also Section 4.1.3 for further details on the one-factor Cox-Ingersoll-Ross model (CIR1F) model (see Remark B.12). Emphasis is solely laid upon the calibration result.

Example B.1 (Calibration CIR1F). *For illustrating an unsatisfying calibration result we choose the CIR1F model (Remark B.12) which is fitted to the EURIBOR6M yield* *curve on 16/09/2008 (FIGURE 3.4). The non-linear least-square optimisation problem for the CIR1F model reads as follows*

$$
\begin{aligned}
&\min_{\vartheta} \sum_{k=1}^{m} \left(R_k^{\mathrm{CIR}}(\vartheta) - R_k^{\mathrm{M}} \right)^2, \qquad \text{(B.50)} \\
\text{subject to} \quad &\vartheta \in \Theta \subset \mathbb{R}_+^3, \\
&2\kappa\theta > \sigma^2
\end{aligned}
$$

where

- $\Theta \subset \mathbb{R}_+^3$ *is a non-empty and compact set,*
- $\vartheta = (\kappa, \theta, \sigma)$ *is a vector containing the CIR1F parameters to be calibrated, and*
- m *is the number of observations of the yield curve (zero yields).*

To ensure that the zero-coupon bonds, or other derivatives, are priced correctly in the model we perform the calibration by minimising the squared difference between model and market yield curves. We calculate the model rates by inserting the closed form solution, postulating that an ATS for the CIR1F model exists (see Section 4.1.3 for more details), of the CIR1F zero-coupon bond equation with the affine terms $A(t,T)$ and $B(t,T)$ into Equation (B.29), so that

$$
R^{CIR}(0, T_k) = -\frac{A(0, T_k)}{T_k} + \frac{B(0, T_k)}{T_k} r(0)
$$

where T_k are the different maturities, e.g. $T_k = \{\frac{1}{12}, \frac{1}{4}, \ldots, 1, 2, \ldots, 30\}$ (in years). We denote by R^M the vector of market yields and by R^{CIR} the vector of model yields. For today's short rate $r(0)$ we use the market yield R^M with the shortest maturity, e.g. one-month rate. Next, it is necessary to specify the initial parameters $(\kappa_0, \theta_0, \sigma_0) = (10^{-4}, 10^{-4}, 10^{-4})$, where the Matlab routine starts searching the minimum of (B.50). We use the inbuilt Matlab solver `fmincon()` with `'interior−point'` algorithm. Furthermore, we impose the non-linear constraint in form of the Feller condition $2\kappa\theta > \sigma^2$, guaranteeing non-negativity of the CIR1F model (see Section 4.1.3 for more details). The results of the calibration are displayed in TABLE B.1 containing the calibrated model parameters $(\widehat{\kappa}, \widehat{\sigma}, \widehat{\theta})$ and objective function value at the solution (sum of squared errors). Comparing the model curve to the market curve in FIGURE B.1 it becomes evident that the CIR1F model fails to deliver a satisfactory fit.

Date	$\widehat{\kappa}$	$\widehat{\sigma}$	$\widehat{\theta}$	Error
16/09/2008	1.4268	0.0474	0.3676	$2.31 \cdot 10^{-5}$

TABLE B.1.: Calibration results of CIR1F

B.2.5.2. Extensions

Certain extensions to a specific model may yield overall better modelling results. Model extensions can, however, also considerably contribute to the model complexity so that any model amendment needs to be treated with great care. Yet, in general it is of great

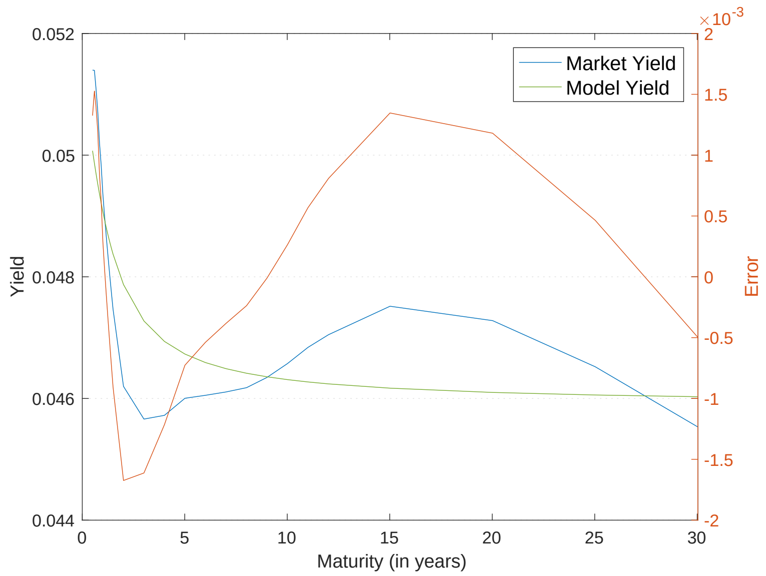

FIGURE B.1.: Calibration results of the CIR1F model of EURIBOR6M yield curve on 16/09/2008

advantage to possess some modelling flexibility within one model, rendering entire model substitutions unnecessary. In the following we shall elaborate on adding more factors to the model and allowing more flexibility through time varying parameters.

Factors In general, factor models assume that the term structure of interest rates is driven by a set of state variables or factors. An economic interpretation can be assigned to the chosen factors. Usually, the first factor is reserved for the short rate. Two factor models where the short-term rate is modelled as the first factor combined with a second factor consists of

· long-term rates (Brennan and Schwartz., 1979), respectively consol rates[3] (Brennan and Schwartz, 1982),

· inflation (Cox et al., 1985),

· spread between long and short-term rates, (Schaefer and Schwartz, 1987), and

· volatility of the short-term interest rate (Longstaff and Schwartz, 1992).

An example of a three factor model where the short-term interest rate, its volatility, and its long-run mean are identified as factors can be found in Chen (1996) and Balduzzi et al. (1996). Two main reasons stand out when incorporating more than one factor into a model, namely

· avoidance of correlation between yield curves with different maturity resulting from the model, and

· when a higher precision is desired, thus different sources may be responsible for variations in the yield curve.

[3]The consol rate (a long-term rate) is defined as the yield on a consol (perpetual) bond.

Thereby, we mainly refer to Brigo and Mercurio (2007) for introducing the idea of incorporating multiple factors into the model.
The issue regarding correlation between resulting yield curves can be summarised as follows. If yield curves with different maturities are monotonically dependent, then occurring shocks at some time point t are passed on throughout all yield curves. More precisely, the shock originates at the starting point of the yield curve which is in turn the corresponding short rate $r(t)$ at time t. Thus, any shift to a single yield largely causes a parallel shift to the whole yield curve in an one-factor model. Two or multiple factor models avoid this behaviour. For example, in a two-factor model the correlation is simply determined by the two underlying factors, thus a perfect correlation is not possible, or highly unlikely. However, one could argue that correlation between yield curves with different maturities is naturally high, particularly when maturities are not far apart (e.g. one and two years). Yet, correlation of one is still extremely unrealistic.
To quantify the variation in the yield curve explained by the factors a principal component analysis (PCA) can be conducted. The percent of variation of the first to last factor is given by the ordered eigenvalues of the covariance matrix, the principal components, of the standardised spot rate changes divided by the number of variables. We summarise the results of PCA analyses of Brigo and Mercurio (2007). Brigo and Mercurio (2007) references two PCA analyses by Jamshidian and Zhu (1996) and Rebonato (1998). While Rebonato (1998) concludes that the first component explains already 92% of the total variance, Jamshidian and Zhu (1996) come to an explanation of over 90% only after three components. Although both studies use historical yield curves (under the real-world measure) for their analysis the utilised input variables are not. Brigo and Mercurio (2007) summarises the outcomes as follows:

- Using a two or three factor model, thus a two- or three-dimensional process, is advisable for ensuring a realistic description of the yield curve.

- The same amount of factors (two to three) are also required when modelling under the risk-neutral probability measure, since the instantaneous covariance structure of the same process is invariant to measure changes.

Time Varying Parameters Another way of extending an existing model is to opt for time varying parameters, simply by replacing constant parameters in the model. This allows for additional flexibility. The motivation behind this extension is an economical one (Hull and White, 1990): "The time dependence can arise from the cyclical nature of the economy, expectations concerning the future impact of monetary policies, and expected trends in other macroeconomic variables." In Hull and White (1990) two extensions to the original (affine) one-factor models of Vašìček (Vašìček, 1977) and Cox-Ingersoll-Ross (Cox et al., 1985) are presented. The major advancements consist of firstly, being consistent with the current structure of interest rates and the current volatilities of all interest rates and secondly, the volatility parameter of the underlying short rate process can be a function of time. In the case of the extended Vašiček model analytical pricing formulas for bonds and other interest rate derivatives can be derived. For the extended Cox-Ingersoll-Ross model one must rely on numerical estimation procedures for determining model parameters. The most general representation of both model extensions, ExtVašiček and ExtCIR1F in Remark B.12, can be found in Hull and White (1993). The three functions of time in (B.27) provide additional degrees-of-freedom fulfilling different tasks. While the function $\theta(t)$ matches the prices of all discount bonds at the initial time, $\kappa(t)$ and $\sigma(t)$ are intended to match the initial volatility of all zero-coupon rates and the volatility of the short rate at all future times. The main advantage is that the generic representation of (B.27) can be calibrated exactly to the initial term structure, yet, at the cost of no longer having analytical tractability wrt bond and bond option pricing formulas. Furthermore, the issue of non-stationarity in the volatility term structure arises when $\kappa(t)$ and $\sigma(t)$ are time-varying. This phenomenon is thoroughly investigated and confirmed in Hull and White (1996) and may have some unwanted effects. For example, parameters can be a misspecified or misestimated resulting in potentially distorted option prices and thus, should be treated with great caution. Concluding, "Unless $\sigma(t)$ and $\kappa(t)$ are constants the volatility term structure is non-stationary. [...] Using all the degrees of freedom in the model to fit the volatility exactly constitutes an over-parameterisation of the model. It is our opinion that there should be no more than one time varying parameter used in Markov models of the term structure evolution and that this should be used to fit the initial term structure.", (Hull and White, 1996).

B.3. Markovian Theory with Application in Credit Risk

Estimating and forecasting in a Markovian setting is more involved, thus additional theory is introduced in the following. Basically, two kind of Markovian stochastic matrices are the objects of interest on which further credit risk related assessments are based on, namely

- transition matrix $\boldsymbol{P}$ containing transition and default probabilities of the Markov chain, and the continuous time equivalent
- generator matrix $\boldsymbol{G}$ containing rates at which the Markov chain jumps.

The relationship between the two matrices in the context of estimation and forecasting is briefly discussed in the following:

- Both matrices, $\boldsymbol{P}$ and $\boldsymbol{G}$, can be estimated from historical data if data is available based on various estimation methods. However, in research historical data is not always available.
- Usually, $\boldsymbol{P}$ is given as one-year stochastic matrices, denoted by $\boldsymbol{P}_{0,1}$. Particularly rating companies mostly publish the one-year transition matrix $\boldsymbol{P}_{0,1}$.
- Matrices transferred into the future, or also matrices projected to times less than one year, from a given or estimated transition matrix, $\boldsymbol{P}_{0,1}$, can be only accomplished in discrete time. For the generator matrix $\boldsymbol{G}$ future and past matrices can be obtained in continuous time.
- The most frequent case is having a given one-year transition matrix $\boldsymbol{P}_{0,1}$ where it becomes necessary to embed into continuous time which is known as the 'embedding problem'. A non-linear optimisation procedure is presented in Hughes and Werner (2016) for obtaining Markovian credit migration matrices in continuous time.
- Even if historical default data is available and an one-year transition matrix $\boldsymbol{P}_{0,1}$ or generator matrix $\boldsymbol{G}$ can be estimated certain corrections wrt default probabilities or migration rates to the resulting matrix ($\boldsymbol{P}_{0,1}$ or $\boldsymbol{G}$) may be desirable which can be seen in Hughes and Werner (2016) incorporating credit risk relevant constraints.

To this end we still owe some information on what $\boldsymbol{P}$, respectively $\boldsymbol{P}_{0,1}$, or $\boldsymbol{G}$ exactly are. Both the transition and generator matrix have their theoretical foundations in Markovian theory, more precisely, the underlying process is a Markov chain in discrete-time and continuous-time, respectively. We shall close this gap in the following. A more complete picture of credit risk modelling and Markovian theory can be found for example in Bielecki and Rutkowski (2004).

We start off by introducing the transition matrix embedded in the context of credit risk modelling. Let us assume a frictionless, discrete-time trading economy with a finite horizon $[0, T^*]$, with $t \leq T \leq T^*$ and a finite state space $\mathcal{S} = \{1, 2, \ldots, K\}$ where state 1 represents the best rating, $K-1$ the worst and K defines the default state (see also Remark B.18 for further details). Moving from state i to state j in one step is quantified by its corresponding probability

$$p_{ij} = \mathrm{Prob}(X_{t+1} = j \,|\, X_t = i) \tag{B.51}$$

where X_t denotes a time-homogeneous Markov chain in discrete time which is stated in Definition B.16 (Jarrow et al., 1997).

Definition B.16. *The discrete time, time-homogeneous finite state space Markov chain $\{X_t : 0 \leq t \leq T^*\}$ is specified by a $K \times K$ transition matrix*

$$\boldsymbol{P} = (p_{ij}), \quad \forall i, j \in \mathcal{S}$$

where

$$\boldsymbol{P} = \begin{pmatrix} p_{1,1} & p_{1,2} & p_{1,3} & \cdots & p_{1,K-1} & p_{1,K} \\ p_{2,1} & p_{2,2} & p_{2,3} & \cdots & p_{2,K-1} & p_{2,K} \\ \vdots & \vdots & \vdots & \ddots & \vdots & \vdots \\ p_{K-1,1} & p_{K-1,2} & p_{K-1,3} & \cdots & p_{K-1,K-1} & p_{K-1,K} \\ 0 & 0 & 0 & \cdots & 0 & 1 \end{pmatrix}, \tag{B.52}$$

and

$$p_{ii} = 1 - \sum_{\substack{j=1 \\ j \neq i}}^{K} p_{ij},$$

with $i = 1, \ldots, K$ and probabilities (B.51).

Properties B.1 of $\boldsymbol{P}$ follow immediately (Bluhm et al., 2002):

Property B.1.

(a) $\boldsymbol{P}$ has only non-negative entries: $p_{ij} \geq 0$ for $i, j = 1, \ldots, K$.

(b) All row sums of $\boldsymbol{P}$ are equal to 1: $\sum_{j=1}^{K} p_{ij} = 1$ for $i = 1, \ldots, K$.

(c) The last column contains the 1-year default probabilities: $p_{iK} = p_i^D$ for $i = 1, \ldots, K-1$.

(d) The default state is absorbing: $p_{Kj} = 0$ for $j = 1, \ldots, K-1$ and $p_{KK} = 1$. This means that there is no escape from the default state.

(e) *Low-risk states should never show a higher default probability than high-risk states, i.e.* $p_{i,K} \leq p_{i+1,K}$ *for* $i = 1, \ldots, K-1$.

(f) *It should be more likely to migrate to closer states than to more distant states (row monotony towards the diagonal),*

$$p_{i,i+1} \geq p_{i,i+2} \geq p_{i,i+3} \cdots$$
$$p_{i,i-1} \geq p_{i,i-2} \geq p_{i,i-3} \cdots$$

(g) *The chance of migration into a certain rating class should be greater for more closely adjacent rating categories (column monotony towards the diagonal).*

$$p_{i+1,i} \geq p_{i+2,i} \geq p_{i+3,i} \cdots$$
$$p_{i-1,i} \geq p_{i-2,i} \geq p_{i-3,i} \cdots$$

(h) *Insofar as a lower rating presents a higher credit risk:* $\sum_{j \geq k} p_{ij}$ *is a non-decreasing function of* i *for every fixed* k*, which is equivalent to requiring that the underlying Markov chain be stochastically monotonic.*

Now we can generalise the defined one-step $\boldsymbol{P}$ transition matrix (Definition B.16) to a t-step time horizon denoted by $\boldsymbol{P}_{0,t}$. This means that $p_{ij}(0,t)$ is the probability going from state i at time 0 to state j at time t. Under homogeneity the t-step transition matrix $\boldsymbol{P}_{0,t} = \boldsymbol{P}^t$ which amounts to the t-fold matrix product of $\boldsymbol{P}$. The most frequent representation one finds is an one-year ($t = 1$) transition matrix. This gives rise to some additional Properties B.2 given in Kreinin and Sidelnikova (2001) where the term 'regular credit migration model' (RCMM) is introduced.

Property B.2 (Regular Credit Migration Model (RCMM)).

(a) *The determinant of the annual transition matrix* $\boldsymbol{P}_{0,1}$ *is not equal to zero, and the eigenvalues are distinct (this allows us to compute the logarithm of* $\boldsymbol{P}_{0,1}$*).*

(b) *For the (given) one-year transition matrix* $\boldsymbol{P}_{0,1}$ *the diagonal probabilities (probability of staying in the corresponding credit grade within the first year) dominate the distribution of probability mass (i.e.* $p_{ii} > p_{ij}$*). This is a weak property as it is not always the case, but should be kept in mind when addressing the embedding problem. When moving on in time (*$t > 1$*) a dominant diagonal disappears.*

(c) *Eventually, with sufficient amount of time passed all companies in any starting credit grade will default, thus*

$$\lim_{t \to \infty} \boldsymbol{P}_{0,t} = \begin{pmatrix} 0 & 0 & \cdots & 1 \\ 0 & 0 & \cdots & 1 \\ \vdots & \vdots & \ddots & \vdots \\ 0 & 0 & \cdots & 1 \end{pmatrix}.$$

Now, let us assume a continuous-time trading economy with a finite horizon $[0, T^*]$, with $t \leq T \leq T^*$ and a finite state space $\mathcal{S} = \{1, 2, \ldots, K\}$. A continuous-time Markov chain

$X(t)$ jumps from state i to j at rate

$$g_{ij} = \lim_{h \to 0} \frac{\text{Prob}(X(t+h) = j \mid X(t) = i)}{h}, \tag{B.53}$$

with $i \neq j$ yielding Definition B.17.

Definition B.17 (Generator matrix). *A continuous-time, time-homogeneous Markov chain $\{X(t) : 0 \leq t \leq T^*\}$ is specified in terms of its $K \times K$ generator matrix*

$$\boldsymbol{G} = (g_{ij}), \quad \forall i, j \in \mathcal{S}$$

where

$$\boldsymbol{G} = \begin{pmatrix} g_{1,1} & g_{1,2} & g_{1,3} & \cdots & g_{1,K-1} & g_{1,K} \\ g_{2,1} & g_{2,2} & g_{2,3} & \cdots & g_{2,K-1} & g_{2,K} \\ \vdots & \vdots & \vdots & \ddots & \vdots & \vdots \\ g_{K-1,1} & g_{K-1,2} & g_{K-1,3} & \cdots & g_{K-1,K-1} & g_{K-1,K} \\ 0 & 0 & 0 & \cdots & 0 & 0 \end{pmatrix}, \tag{B.54}$$

and

$$g_{ii} = -\sum_{\substack{j=1 \\ j \neq i}} g_{ij},$$

with $i = 1, \ldots, K$ and intensities (B.53).

We can assign the following Properties B.3 to Definition B.17:

Property B.3.

(a) *Off-diagonal entries are non-negative:* $g_{ij} \geq 0, \quad \forall i \neq j$ *and* $i, j = 1, \ldots, K$

(b) *Row sums amount to zero:* $\sum_{j=1}^{K} g_{ij} = 0, \quad i = 1, \ldots, K$

The necessary and sufficient conditions (a) and (b) of Properties B.3 defining a generator matrix can be derived in three different ways, as can be seen in Norris (1998). A formal proof thereof is given in Asmussen (2008).

Remark B.17. *Note that for a generator matrix of Definition B.17, the $(K-1) \times (K-1)$ sub-matrix of $\boldsymbol{G}$ has the structure of a birth-death chain and the default intensities in the Kth column do not decrease as a function of row number. The last row of zeros in $\boldsymbol{G}$ implies that bankruptcy (state K) is absorbing which amounts to (d) of Properties B.1. Equivalent monotonicity conditions to (e) - (g) of Properties B.1 can be made for the generator matrix simply by replacing $\boldsymbol{P}$ by $\boldsymbol{G}$. The equivalent condition of (h) needs to be reformulated to (compare Jarrow et al. (1997))*

$$\sum_{j \geq k} g_{ij} \leq \sum_{j \geq k} g_{i+1,j}$$

for all i, k such that $k \neq i+1$.

Remark B.18. *When applying Markov chain theory to credit risk, ratings are introduced which stand for the corresponding states. An example of rating grades defined by the major rating companies Moody's, Fitch and S&P is given in* Table *B.2. The rating granularity can vary, thus the size of a given one-year transition matrix changes with the ratings (states). Most annual transition matrices published by the rating agencies have eight credit states. The ratings are to be viewed as an ordinal scale, in descending order, with 'triple A' being the best rating and where default is denoted as 'D' corresponding to the worst case. Reformulated transition or migration probabilities*[4] *from one rating class to another with ratings are e.g.* $p_{AAA,AA+}(t,t+1) = \text{Prob}(X_{t+1} = AAA \,|\, X_t = AA+)$, $p_{AA+,AAA}(t,t+1) = \text{Prob}(X_{t+1} = AA+ \,|\, X_t = AAA)$ *or* $p_{D,C}(t,t+1) = \text{Prob}(X_{t+1} = D \,|\, X_t = C)$. *The difference (more precisely additional assumption) to above general definition of a transition matrix (Definition B.16) is the default state, corresponding to the last row* K *in (B.52), which in credit risk frameworks is absorbing. Hence once a company migrated to 'D' (*$\hat{=}$ *default) there is no possibility of an upgrade. Markov chains in the context of RCMM can conveniently be grouped into transient states which are the non-default rating classes (*Table *B.2) and an absorbing state (default probabilities).*

Class	Moody's	Fitch	S&P
1	Aaa,Aa1,Aa2,Aa3	AAA,AA+,AA,AA-	AAA,AA+,AA,AA-
2	A1,A2,A3	A+,A,A-	A+,A,A-
3	Baa1,Baa2,Baa3	BBB+,BBB,BBB-	BBB+,BBB,BBB-

Table B.2.: Excerpt of rating grades of the three major rating companies Moody's, Fitch and S&P.

B.3.1. Relationships

We introduce the hazard rate and Chapman-Kolmogorov equations emphasising on their connections to the general Markovian theory and models used in this chapter. These noteworthy relationships are briefly addressed which are mainly taken from Aalen et al. (2008) where more in-depth explanations are given.

Hazard Rate We start off with the hazard rate since it connects the already introduced Markovian theory of Definition B.17 and is an elementary component of survival modelling in upcoming sections. The derivation of exponential default probability term structure is based on the idea that credit dynamics can be viewed as a two-state time-homogeneous Markov-chain, the two states being survival and default, and the unit time between two time steps being $\Delta t = t_i - t_{i-1}$ as in Definition B.18 (Lando, 2004).

Definition B.18 (Hazard Function). *Let* τ *be a positive random variable whose distribution can be described in terms of a hazard function* λ, *i.e.*

$$S(t) = \text{Prob}(\tau > t) = \exp\left(-\int_0^t \lambda(s)\mathrm{d}s\right). \tag{B.55}$$

[4] In some notations these are also denoted as $\text{Prob}(AA+ \to AAA)$, $\text{Prob}(AAA \to AA+)$ or $\text{Prob}(C \to D)$ which maybe gives a more intuitive representation.

Then, the standard definition of the hazard rate $\lambda(t)$ of τ is

$$\lim_{\Delta t \to 0} \frac{1}{\Delta t} \operatorname{Prob}(t \leq \tau < t + \Delta t \mid \tau \geq t) = \lambda(t), \tag{B.56}$$

so $\lambda(t)\Delta t$ is approximately the conditional probability of a default in a small interval after t given survival up to and including t where Δt is 'infinitesimally small', that is, the probability of something happening in the immediate future conditional on survival until time t.

It is common to assume that the survival function $S(t)$ (B.55) is absolutely continuous, and let us do so for the moment. Let $f(t)$ be the density of τ. Then $\lambda(t)$ is obtainable from $S(t)$ by

$$\lambda(t) = \frac{f(t)}{S(t)} = -\frac{S'(t)}{S(t)}. \tag{B.57}$$

Inversely, when $\lambda(t)$ is available $S(t)$ solves the differential equation $S'(t) = -\lambda(t)S(t)$, which leads to $S(t) = \exp(-\Lambda(t))$, where $\Lambda(t) = \int_0^t \lambda(s)\mathrm{d}s$ is the cumulative hazard rate. Note that τ does not have to be finite; if $\operatorname{Prob}(\tau = \infty) > 0$ then $\int_0^\infty f(s)\mathrm{d}s < 1$ and $\int_0^\infty \lambda(s)\mathrm{d}s < \infty$, which is sometimes referred to as a defective survival distribution.

Remark B.19. *The similarity of Definition B.17 with (B.53) to (B.56) is now more clear. The hazard measures the infinitesimal probability of going from 'alive' to 'dead' at time t; the Markov intensity measures the more general infinitesimal probability of going from state i to state j at time t. This is a basic connection between event history analysis and Markov theory.*

Chapman-Kolmogorov Equations Primarily, we are interested in modelling in continuous time, thus concentrating on the continuous-time representation of Chapman-Kolmogorov equations and, intentionally, omitting the full discrete-time formulation. However, we begin this section with the discrete-time formulation for a better understanding of the overall theory. Thereby, we mainly follow Aalen et al. (2008).
In general, it is of interest to be able to determine a n-step transition probability, meaning what is the probability that n time units later the chain will be in state j given it is now (at time m) in state i. Mathematically, this amounts to: Compute the n-step transition matrix $\boldsymbol{P}^{(n)} = (p_{ij}^n)$, $n \geq 1$, where $p_{ij}^n = \operatorname{Prob}(X_{m+n} = j \mid X_m = i)$, given a Markov chain $\{X_n\}$ with transition matrix $\boldsymbol{P}$. We can set $m = 0$ so that $p_{ij}^n = \operatorname{Prob}(X_n = j \mid X_0 = i)$, since transition probabilities do not depend on the time $m \geq 0$ at which the initial condition is chosen. Summing over all intermediate time points yields the equations given in Theorem B.12 where the Markov property holds. Given $X_n = k$, the future after time n is independent of the past, so the probability that the chain m time units later (at time $n+m$) will be in state j is p_{kj}^m, yielding the product $p_{ik}^n p_{kj}^m$.

Theorem B.12. *Let $\{X_k\}_{k\in\mathbb{N}_0}$ be a Markov chain with transition matrix $\boldsymbol{P}$ and state space $\mathcal{S}$. Then for all $n \geq 0$, $m \geq 0$, $i, j \in \mathcal{S}$*

$$\begin{aligned} p_{ij}^{n+m} &= \sum_{k\in\mathcal{S}} p_{ik}^n p_{kj}^m \\ &= \sum_{k\in\mathcal{S}} \operatorname{Prob}(X_{m+n} = i \mid X_m = j) \operatorname{Prob}(X_m = i \mid X_0 = j) \end{aligned}$$

$$= \text{Prob}(X_{m+n} = i \mid X_0 = j).$$

Preparing for the Chapman-Kolmogorov forward and backward equations we restate Definition B.17, again by following (Aalen et al., 2008). The Chapman-Kolmogorov equations describe the relationship between $\boldsymbol{P}$ and $\boldsymbol{G}$ where we can extend the numerator of (B.53) to the matrix notation

$$\begin{aligned}\boldsymbol{P}(t+\Delta t) - \boldsymbol{P}(t) &= \boldsymbol{P}(t)\boldsymbol{P}(\Delta t) - \boldsymbol{P}(t)\\ &= \boldsymbol{P}(t)(\boldsymbol{P}(\Delta t) - \boldsymbol{I})\\ &\approx \boldsymbol{P}(t)\boldsymbol{G}\Delta t.\end{aligned} \tag{B.58}$$

In fact, the Chapman-Kolmogorov equations are the matrix equivalents of (B.57). With

$$\boldsymbol{G} = \boldsymbol{P}'(0) = \lim_{\Delta t \to 0} \frac{1}{\Delta t}(\boldsymbol{P}(\Delta t) - \boldsymbol{P}(0)). \tag{B.59}$$

we arrive at Theorem B.13 for time-homogeneous Markov chains (see full proof for example in Norris (1998)) since $\boldsymbol{P}(0) = \boldsymbol{I}$.

Theorem B.13 (Kolmogorov forward and backward ODEs). *Let $\{X(t)\}_{t\in\mathbb{R}_0^+}$ be a right-continuous process and $i, j \in \mathcal{S}$ a finite set. The transition probabilities satisfy both*

- *the Kolmogorov forward differential equations*

$$p'_{ij}(t) = \sum_k p_{ik}(t) g_{kj} \qquad \textit{for all } i,\ j,$$

  or in matrix notation

$$\boldsymbol{P}(t)' = \boldsymbol{P}(t)\boldsymbol{G};$$

- *and the Kolmogorov backward differential equations*

$$p'_{ij}(t) = \sum_k g_{ik} p_{kj}(t) \qquad \textit{for all } i,\ j,$$

  or in matrix notation

$$\boldsymbol{P}(t)' = \boldsymbol{G}\boldsymbol{P}(t)$$

  where $\boldsymbol{P}(0) = \boldsymbol{I}$.

The matrix equations in Theorem B.13 have exponential matrix solutions. Subject to the boundary condition $\boldsymbol{P}_0 = \boldsymbol{I}$ ($\boldsymbol{I}$ is the identity matrix), these equations have the formal solution (care is needed when $\mathcal{S}$ is not finite)

$$\boldsymbol{P}(t) = \exp(t\boldsymbol{G}) := \boldsymbol{I} + t\boldsymbol{G} + \frac{(t\boldsymbol{G})^2}{2!} + \frac{(t\boldsymbol{G})^3}{3!} + \ldots = \sum_{n=0}^{\infty} \frac{\boldsymbol{G}^n t^n}{n!}, \quad \forall\, t \in \mathbb{R}_0^+, \tag{B.60}$$

where $\boldsymbol{G}^0 = \boldsymbol{I}$. Therefore, the transition probabilities are specified by the matrix of transition rates $\boldsymbol{G}$, and so the chain is specified by $\boldsymbol{G}$ and the initial distribution $p(0)$. Differentiating $\exp(\boldsymbol{G}t)$ wrt t will satisfy the Kolmogorov-Chapman equations.

Remark B.20. *Aalen et al. (2008) points out that "time-discrete and time-continuous homogeneous processes behave in a similar fashion and the resulting transition probabilities behave like exponential (or geometric) functions of time", cf. Aalen et al. (2008).*

Finally, let us formulate the inhomogeneous Kolmogorov-Chapman equations. Therefore, we need to extend by an additional time parameter for the transition probabilities where $\boldsymbol{P}(s,t)$ with $p_{ij}(s,t) = \mathrm{Prob}(X(t) = j \,|\, X(s) = i)$. Furthermore, the generator $\boldsymbol{G}$ additionally depends on the time parameter t to meet the additional complexity. With (B.58) the Kolmogorov forward equation amounts to

$$\frac{\partial}{\partial t}\boldsymbol{P}(s,t) = \boldsymbol{P}(s,t)\boldsymbol{G}(t),$$

with

$$\boldsymbol{G}(t) = \lim_{\Delta t \to 0} \frac{1}{\Delta t}(\boldsymbol{P}(t, t+\Delta t) - \boldsymbol{I}).$$

B.3.2. Estimation

In general we assume that $\boldsymbol{P}_{0,1}$ or $\boldsymbol{G}$ as given. However, this may not always be the case. Then it becomes necessary to estimate transition or generator matrices from historical default data. In the following we therefore present three different widely used estimation procedures. Furthermore, in classical rating settings firms of a particular industry are subject of investigation where transition probabilities are estimated. However, we are interested in estimates for cover pool assets consisting of mortgages. Hence we reformulate the well-established estimation techniques to suit our needs.
First we look at the simplest estimation form at discrete times $t = 0, \ldots, T$. We assume a sample of N mortgages with observed transitions between different states to be independent. We mainly follow Lando (2004) adopting the notation and derivation of the discrete-time estimator:

- $n_i(t)$ is the number of mortgages in state i at time t.
- $n_{ij}(t)$ is the number of mortgages which went from state i at time t to j at date $t+1$.
- $N_i(T) = \sum_{t=0}^{T-1} n_i(t)$ is the total number of mortgage exposures recorded at the onsets of transition periods.
- $N_{ij}(T) = \sum_{t=1}^{T} n_{ij}(t)$ is the total number of transitions from i to j over the entire period.

Assuming that rating migrations are independent across mortgages, we get products of the individual likelihoods and hence the complete likelihood function takes the form

$$L(\vartheta) = \prod_{i=1}^{K} \prod_{j=1}^{K} p_{ij}^{N_{ij}(T)},$$

where $\vartheta = (p_{ij})_{1\le i,j\le K}$ (the transition matrix entries) and $p^0_{ij} = 1$. Then, the log-likelihood is

$$l(\vartheta) = \sum_{i=1}^{K}\sum_{j=1}^{K} N_{ij}(T)\log p_{ij}.$$

Since we have the restriction $\sum_{j=1}^{K} p_{ij} = 1$ for every i, we have to maximise

$$\widehat{\vartheta} = \arg\max_{\vartheta} \sum_{i,j=1}^{K} N_{ij}(T)\log p_{ij}$$
$$\text{subject to} \sum_{j=1}^{K} p_{ij} = 1.$$

Solving this is a standard Lagrange multiplier exercise and one arrives at Definition B.19.

Definition B.19 (Discrete-Time Homogeneous ML Estimator). *The ML estimator in discrete time, or also referred to as the multinomial estimator, amounts to*

$$\widehat{p}_{ij} = \frac{N_{ij}(T)}{N_i(T)},$$

for all $i, j \in \mathcal{S}$.

Remark B.21. *As pointed out by Lando (2004) the estimator in Definition B.19 does not, strictly speaking, resemble a multinomial estimator since the number of mortgage exposures* $N_i(T)$ *in each category is random which would be true if* N_i *were fixed.*

In Jarrow et al. (1997) (also in Lando (2004)) we find the homogeneous estimator in continuous time (Definition B.20), adopted from Küchler and Sorensen (2006), where we assume that we have observed a collection of mortgages between time 0 and time T. The generator matrix is constructed in the following way. A mortgage asset remains in rating state i for an exponentially distributed amount of time with parameter

$$g_{ii} = -\sum_{\substack{j=1\\ j\neq i}} g_{ij}.$$

When a transition takes place the new rating is determined by a multinomial experiment in which the probability of a transition from state i to state j is given by g_{ij}/g_{ii} which leads to the estimator for the generator matrix as in Definition B.20.

Definition B.20 (Continuous-Time Homogeneous ML Estimator). *To estimate the elements of the generator under an assumption of time-homogeneity we use the MLE*

$$\widehat{g}_{ij} = \frac{N_{ij}(T)}{\int_0^T Y_i(s)\mathrm{d}s}$$

where

- $Y_i(s)$ *is the number of mortgages in rating class* i *at time* s, *and*

- $N_{ij}(T)$ *is the total number of transitions over the period from* i *to* j, $i \neq j$ *over the period* $[0, T]$.

Note that Definition B.20 is the continuous-time analogue of the MLE in Definition B.19. The major difference of Definition B.20 to Definition B.19 is that now all information between the time points 0 and T is being used. The numerator counts the number of observed transitions from i to j over the entire periods of observation whereas the denominator represents the total time spent in state i by all mortgages in the cover pool, respectively data set.

Lando and Skodeberg (2002) state an inhomogeneous estimator in continuous-time in form of the Aalen-Johansen estimator (see also Küchler and Sorensen (2006)) in Definition B.21. This method is a useful tool for replacing the methods Definition B.19 or Definition B.20 over longer periods of time. Consider a non-homogeneous continuous-time Markov process with finite state space $\mathcal{S} = \{1, 2, \dots, K\}$ whose transition probability matrix for the period from time s to time t is given by $\boldsymbol{P}_{s,t}$. Hence, the ij-th element of this matrix describes the probability that the chain starting in state i at time s is in state j at time t.

Definition B.21 (Continuous-Time Inhomogeneous Estimator). *When we do not assume homogeneity we can estimate the transition matrix* $\boldsymbol{P}$ *by the Aalen-Johansen estimator*

$$\widehat{\boldsymbol{P}}_{s,t} = \prod_{h=1}^{m} (\boldsymbol{I} + \Delta \widehat{\boldsymbol{G}}(T_h)),$$

where $\boldsymbol{I}$ *is the identity matrix,* T_h *is the jump time in the interval* $(s, t]$ *and*

$$\Delta \widehat{\boldsymbol{G}}(T_h) = \begin{pmatrix} -\frac{\Delta N_1(T_h)}{Y_1(T_h)} & \frac{\Delta N_{12}(T_h)}{Y_1(T_h)} & \cdots & \cdots & \frac{\Delta N_{1K}(T_h)}{Y_1(T_h)} \\ \frac{\Delta N_{21}(T_h)}{Y_2(T_h)} & -\frac{\Delta N_2(T_h)}{Y_2(T_h)} & \cdots & \cdots & \frac{\Delta N_{2K}(T_h)}{Y_2(T_h)} \\ \vdots & \vdots & \ddots & \ddots & \vdots \\ \frac{\Delta N_{K-1,1}(T_h)}{Y_{K-1}(T_h)} & \frac{\Delta N_{K-1,2}(T_h)}{Y_{K-1}(T_h)} & \cdots & -\frac{\Delta N_{K-1}(T_h)}{Y_{K-1}(T_h)} & \frac{\Delta N_{K-1,K}(T_h)}{Y_{K-1}(T_h)} \\ 0 & 0 & \cdots & \cdots & 0 \end{pmatrix}$$

where

- $\Delta N_{ij}(T_h)$ *denotes the number of transitions observed from state* i *to* j *at date* T_h,
- $\Delta N_k(T_h)$ *counts the total number of transitions away from state* k *at date* T_h*, and*
- $Y_k(T_h)$ *is the number of mortgages in state* k *right before date* T_h.

The diagonal element in row k counts, at a given date T_h, the fraction of the exposed mortgages $Y_k(T_h)$ which leaves the state at date T_h. The off-diagonal elements count the specific types of transitions away from the state divided by the number of exposed mortgages. The general findings of Lando and Skodeberg (2002) are that difference between the time-inhomogeneous estimator of Definition B.21 to the time-homogeneous estimator of Definition B.20 are small, however, significant accuracy is gained compared to the cohort method of Definition B.19. For more details refer for example to Lando

and Skodeberg (2002).
Plenty of numerical examples exist in the literature for estimating above transition or generator matrix entries, for example Jarrow et al. (1997), Lando and Skodeberg (2002), Lando (2004) and Trueck and Rachev (2009) amongst many others. Hence we shall not give additional examples at this point and refer to the literature, since we do not have access to any historical default data on mortgages to base any estimation on. Instead we would like to address the issue of non-fulfilment of the conditions (e) - (h) of Properties B.1 by transition matrices sampled from historical data as also pointed out Bluhm et al. (2002). In Hughes and Werner (2016) we show how to rectify violations of the particular conditions either for transition matrices directly or for the generator matrices, their continuous-time equivalents. This means whatever the estimation outcomes are of the above proposed estimation techniques it is possible to obtain an appropriate transition matrix posterior to any estimation by applying the non-linear optimisation in combination with additional constraints in form of conditions (e) - (h).

Remark B.22. *In Hughes and Werner (2016) condition (f) of Properties B.1 is not included in the selection of additional constraints, however, it is very similar to condition (e) and thus can be easily replaced or amended.*

B.4. Special Distributions

If not stated otherwise, the distributions introduced in this section are taken from Johnson et al. (1992), Johnson et al. (1994) and Johnson et al. (1995).

Definition B.22 (Chi-squared distribution). *If $Z_1, Z_2, \dots, Z_\nu$ are independent standard normal variables, then $\sum_{i=1}^{\nu} Z_i^2$ has a chi-square distribution with ν degrees of freedom (here ν has to be an integer by definition, but the distribution is defined for any real $\nu > 0$).*
Let us denote a chi-square random variable with ν degrees of freedom by χ^2_ν. Then the probability density function of χ^2_ν is

$$p_{\chi^2_\nu}(x) = \frac{1}{2^{\nu/2}\Gamma(\nu/2)} \exp(-x/2) x^{\nu/2-1}, \quad x \geq 0, \tag{B.61}$$

where $\Gamma(\cdot)$ is the (complete) gamma function with

$$\Gamma(\alpha) = \int_0^\infty \mathrm{e}^{-u} u^{\alpha-1} \mathrm{d}u.$$

Equation (B.61) is referred to as a χ^2 distribution with ν degrees of freedom for any positive ν ($\nu > 0$). The abbreviated formulation of Definition B.22 is $X \sim \chi^2_\nu$.

Definition B.23 (Non-central chi-squared distribution). *If $Z_1, Z_2, \dots, Z_\nu$ are independent standard normal variables and $\delta_1, \delta_2, \dots, \delta_\nu$ are constants then the distribution of*

$$\sum_{j=1}^{\nu} (Z_j + \delta_j)^2$$

depends on $\delta_1, \delta_2, \ldots, \delta_\nu$ only through the sum of their squares. It is called the non-central χ^2 distribution with ν degrees of freedom and non-centrality parameter $\lambda = \sum_{j=1}^{\nu} \delta_j^2$. The probability density function can be expressed as a mixture of central χ^2 pdfs (Definition B.22):

$$\begin{aligned} p_{\chi_\nu'^2(\lambda)}(x) &= \sum_{j=0}^{\infty} \left(\frac{(\frac{1}{2}\lambda)^j}{j!} \exp(-\lambda/2) \right) p_{\chi_{\nu+2j}'^2(0)}(x) \\ &= \frac{\exp\left(-\frac{1}{2}(\lambda + x)\right)}{2^{\nu/2}} \sum_{j=0}^{\infty} \left(\frac{\lambda}{4}\right)^j \frac{x^{\nu/2+j-1}}{j!\Gamma\left(\frac{1}{2}\nu + j\right)} \\ &= \mathrm{e}^{-(\lambda+x)/2} \frac{1}{2} \left(\frac{x}{\lambda}\right)^{(\nu-2)/4} I_{(\nu-2)/2}(\sqrt{\lambda x}), \qquad x > 0 \end{aligned} \tag{B.62}$$

where

$$I_a(y) = \left(\frac{y}{2}\right)^a \sum_{j=1}^{\infty} \frac{(y^2/4)^j}{j!\Gamma(a + j + 1)}$$

is the modified Bessel function of the first kind of order a (for integer or positive a) and $\Gamma(\cdot)$ is the (complete) gamma function with

$$\Gamma(\alpha) = \int_0^{\infty} \mathrm{e}^{-u} u^{\alpha-1} \mathrm{d}u.$$

Note:

- *The distribution defined in (B.62) is a proper distribution for any positive ν.*
- *The abbreviated formulation of Definition B.23 is $X \sim \chi_\nu'^2(\lambda)$.*
- *If $\lambda = 0$, the non-central χ^2-distribution ($\chi_\nu'^2(\lambda)$) becomes a central χ^2-distribution (χ_ν^2) (see Definition B.22), so that $p_{\chi_{\nu+2j}'^2(0)}(x)$ becomes $p_{\chi_{\nu+2j}^2}(x)$ with $\nu + 2j$ degrees of freedom.*
- *Distribution limits: If $X \sim \chi_\nu'^2(\lambda)$, then*

$$\frac{X - (\nu + \lambda)}{\sqrt{2(\nu + 2\lambda)}} \xrightarrow{d} \mathrm{N}(0, 1)$$

(converges in distribution) when $\nu \to \infty$ or $\lambda \to \infty$. This is briefly outlined by decomposing $X \sim \chi_\nu'^2(\lambda)$ of Definition B.23 into a random variable $X_\chi = Z_1^2 + \ldots + Z_\nu^2$ which has a (central) chi-square distribution with ν degrees of freedom, and the term $X_\mathrm{N} = 2\delta Z_1 + \delta^2$ which has a normal distribution $\mathrm{N}(\delta^2, 4\delta^2)$ where $Z_i \sim \mathrm{N}(0, 1)$, $i = 1, \ldots, \nu$ are independent standard normal variables. Since X depends only on the sum $\delta_1^2 + \ldots + \delta_\nu^2$ and not on the individual means δ_i we can assume (without loss of generality) that $\delta_1 = \delta$ and $\delta_2 = \ldots = \delta_\nu = 0$ and consequently we have

$$\lambda = \delta^2$$

and

$$X = (Z_1+\delta)^2 + Z_2^2 + \ldots + Z_\nu^2 = \underbrace{Z_1^2 + \ldots + Z_\nu^2}_{X_\chi} + \underbrace{2\delta Z_1 + \delta^2}_{X_\mathrm{N}}.$$

Moreover, variables Z_1^2 *and* Z_1 *are uncorrelated, so that* X_χ *and* X_N *are uncorrelated. Further, the first two moments of* X_χ *are* $\mathbb{E}(X_\chi) = \nu$ *and* $\mathbb{V}(X_\chi) = 2\nu$*. Then the non-central chi-square distribution gets approximated by the normal distribution* $\mathrm{N}(\nu + \lambda, 2(\nu + 2\lambda))$*, when:*

- $\lambda \to \infty$*: For large values of the non-centrality parameter* λ*, the term* X_N *becomes dominant and hence the corresponding non-central chi-square distribution could be well approximated by the normal distribution.*
- $\nu \to \infty$*: Increasing the number of degrees of freedom* ν*, the distribution of random variable* X_χ *(Definition B.22) approaches normal since it is defined by the sum of* ν *i.i.d. random variables and thus the central limit theorem holds.*

Definition B.24 (Vašìček distribution). *According to Vašiček (1987) the Vašìček distribution is defined as follows:*

$$x \sim \mathrm{Vasi}(p, \varrho)$$
$$p(x) = \sqrt{\frac{1-\varrho}{\varrho}} \exp\left(\frac{1}{2}\left(\Phi^{-1}(x)^2 - \left(\frac{\sqrt{1-\varrho}\Phi^{-1}(x) - \Phi^{-1}(p)}{\sqrt{\varrho}}\right)^2\right)\right),$$

with probability $0 < p < 1$*, correlation* $0 < \varrho < 1$ *and* $\Phi^{-1}(x)$ *being the inverse cdf of the standard normal distribution.*

B.5. Special Copulas

A copula is a multivariate distribution function C defined on the unit hypercube $[0,1]^d$, with uniformly distributed marginals. There exist two formal definitions of a d-dimensional copula, namely Definition B.25 and Definition B.26. Knowing both definitions is of advantage depending on the given situation. The former is a probabilistic definition via distribution functions while the latter, equivalently, defines copulas purely analytically. Literature on copulas is given for example by Mai and Scherer (2012) and Mai and Scherer (2014) on which this section is mainly based.

Definition B.25 (d-dimensional copula — probabilistic). *A function* $C : [0,1]^d \to [0,1]$ *is called a 'copula' if there is a random vector* $(U_1, \ldots, U_d)$ *such that each component* U_k *has a uniform distribution on* $[0,1]$*,* $k = 1, \ldots, d$ *and*

$$\mathrm{C}(u_1, u_2, \ldots, u_d) = \mathrm{Prob}(U_1 \le u_1, U_2 \le u_2, \ldots, U_d \le u_d) \tag{B.63}$$

with $u_1, u_2, \ldots, u_d \in [0,1]$*.*

Definition B.26 (d-dimensional copula — analytic). $C : [0,1]^d \to [0,1]$ *is a d-dimensional copula with properties:*

- $C(u_1, \ldots, u_{k-1}, 0, u_{k+1}, \ldots, u_d) = 0$, *the copula is zero if one of the arguments is zero (grounded property). This reflects* $0 \leq \text{Prob}(U_1 \leq u_1, \ldots, U_k \leq 0, \ldots, U_d \leq u_d) \leq \text{Prob}(U_k \leq 0) = 0$.
- $C(1, \ldots, 1, u_k, 1, \ldots, 1) = u_k$, *the copula is equal to* u_k *if one argument is* u_k *and all others* 1 *(normalised marginals property). This reflects the uniform marginals property, since* $\text{Prob}(U_1 \leq 1, \ldots, U_k \leq u_k, \ldots, U_d \leq 1) = \text{Prob}(U_k \leq u_k) = u_k$.
- *For each d-dimensional rectangle* $\times_{k=1}^{d}[a_k, b_k]$, *being a subset of* $[0,1]^d$, *one has:*

$$0 \leq \sum_{(c_1,\ldots,c_d)\in\times_{k=1}^{d}\{a_k,b_k\}} (-1)^{\{|k:c_k=a_k|\}} C(c_1, \ldots, c_d) \leq 1.$$

An example in form of the bivariate case of Definition B.26 is given in Example B.2.

Example B.2 (Bivariate case). $C : [0,1] \times [0,1] \to [0,1]$ *is a bivariate copula if* $C(0,u) = C(u,0) = 0$, $C(1,u) = C(u,1) = u$ *and* $C(u_2, v_2) - C(u_2, v_1) - C(u_1, v_2) + C(u_1, v_1) \geq 0$ *for all* $0 \leq u_1 \leq u_2 \leq 1$ *and* $0 \leq v_1 \leq v_2 \leq 1$.

In summary, Theorem B.14 (Sklar, 1959) states that every multivariate cumulative distribution function of a random vector $(X_1, X_2, \ldots, X_d)$ can be expressed in terms of its marginals and a copula.

Theorem B.14 (Sklar's theorem). *A function* $F : \mathbb{R}^d \to [0,1]$ *is the distribution function of some random vector* $(X_1, \ldots, X_d)$ *if and only if there are a copula* $C : [0,1]^d \to [0,1]$ *and univariate distribution functions* $F_1, \ldots, F_d : \mathbb{R} \to [0,1]$ *such that*

$$F(x_1, \ldots, x_d) = C\left(F_1(x_1), \ldots, F_d(x_d)\right), \tag{B.64}$$

with $x_1, \ldots, x_d \in \mathbb{R}$.

The copula function from (B.63) can be rewritten to

$$C(u_1, u_2, \ldots, u_d) = \text{Prob}(X_1 \leq F_1^{-1}, X_2 \leq F_2^{-1}, \ldots, X_d \leq F_d^{-1}).$$

With a given procedure to generate a sample $(U_1, U_2, \ldots, U_d)$ from the copula distribution, then the desired sample can be obtained by

$$(X_1, X_2, \ldots, X_d) = (F_1^{-1}(U_1), F_2^{-1}(U_2), \ldots, F_d^{-1}(U_d)).$$

We will consider the bivariate cases, in particular, the bivariate (log)-density functions (denoted with a small c) and give examples with subjectively chosen dependency parameters in form of plots.

B.5.1. Gaussian Copula

Definition B.27 (Gaussian copula). *Bivariate copula (Schepsmeier and Stöber, 2014):*

$$c(u_1, u_2; \rho) = \frac{1}{\sqrt{1-\rho^2}} \exp\left(-\frac{\rho^2(x_1^2 + x_2^2) - 2\rho x_1 x_2}{2(1-\rho^2)}\right),$$

with $x_k = \Phi^{-1}(u_k)$, $k = 1, 2$ *and* $\rho \in [-1, 1]$.

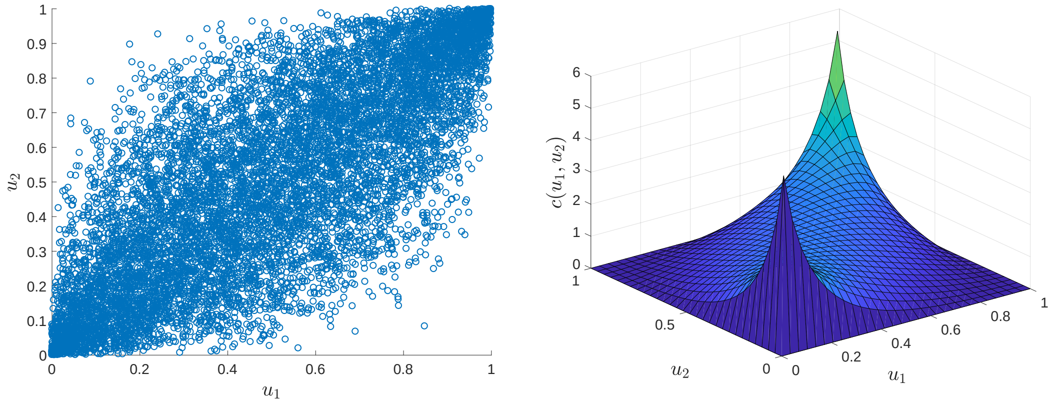

FIGURE B.2.: Bivariate Gaussian copula with $\rho = 0.7$

B.5.2. Student's T Copula

Definition B.28 (Student's T copula). *Bivariate copula (Schepsmeier and Stöber, 2014):*

$$c(u_1, u_2; \rho, \nu) = \frac{1}{2\pi\sqrt{1-\rho^2}} \frac{1}{d_t(x_1; \nu) d_t(x_2; \nu)} \left(1 + \frac{x_1^2 + x_2^2 - 2\rho x_1 x_2}{\nu(1-\rho^2)}\right)^{-\frac{\nu+2}{2}},$$

with $d_t(x_k; \nu) = \frac{\Gamma\left(\frac{\nu+1}{2}\right)}{\Gamma\left(\frac{\nu}{2}\right)\sqrt{\pi\nu}} \left(1 + \frac{x_k^2}{\nu}\right)^{-\frac{\nu+1}{2}}$, $x_k = t_\nu^{-1}(u_k)$, $k = 1, 2$, $\rho \in [-1, 1]$ *and* $\nu > 0$.

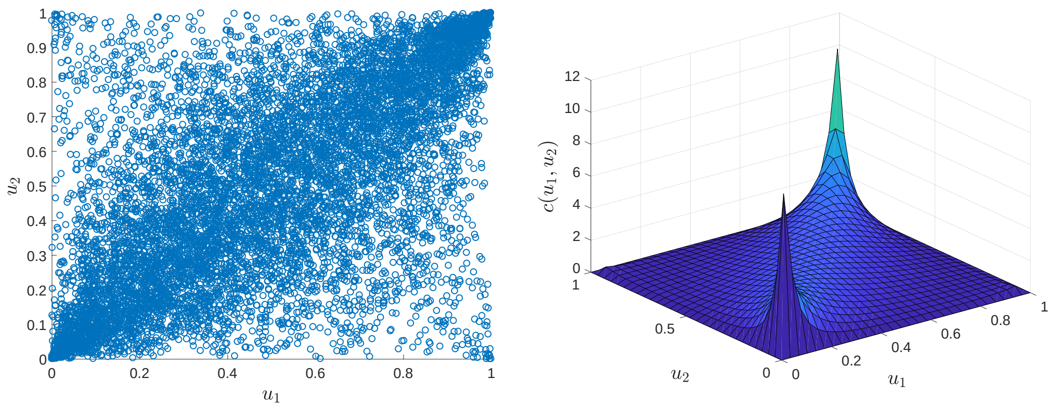

FIGURE B.3.: Bivariate Student's T copula with $\rho = 0.7$ and $\nu = 2$

B.5.3. Clayton Copula

Definition B.29 (Clayton copula). *Bivariate copula (Schepsmeier and Stöber,* *2014):*

$$c(u_1, u_2; \alpha) = (1+\alpha)(u_1 u_2)^{-1-\alpha}(u_1^{-\alpha} + u_2^{-\alpha} - 1)^{-\frac{1}{\alpha}-2},$$

where $\alpha \in [0, \infty]$.

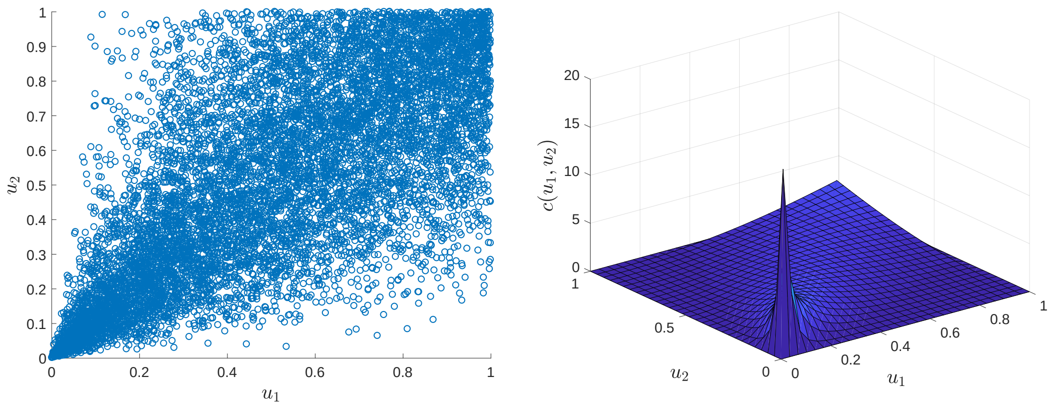

FIGURE B.4.: Bivariate Clayton copula with $\alpha = 3$

B.5.4. Frank Copula

Definition B.30 (Frank copula). *Bivariate copula (Schepsmeier and Stöber, 2014):*

$$c(u_1, u_2; \alpha) = \frac{\alpha(1-\exp(-\alpha))\exp(-\alpha(u_1+u_2))}{(1-\exp(-\alpha)) - (1-\exp(-\alpha u_1))(1-\exp(-\alpha u_2))^2},$$

where $\alpha \in [-\infty, \infty] \setminus \{0\}$.

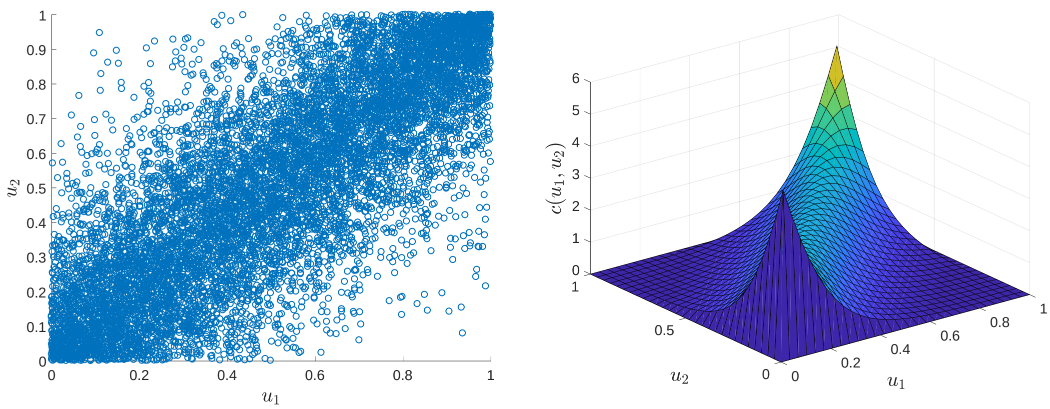

FIGURE B.5.: Bivariate Frank copula with $\alpha = 8$

B.5.5. Gumbel Copula

Definition B.31 (Gumbel copula). *Bivariate copula (Schepsmeier and Stöber,* *2014):*

$$c(u_1, u_2; \alpha) = C(u_1, u_2; \alpha)\frac{1}{u_1 u_2}(h_1 + h_2)^{-2+\frac{2}{\alpha}}(\ln(u_1)\ln(u_2))^{\alpha-1} \times \left(1 + (\alpha - 1)(h_1 + h_2)^{-\frac{1}{\alpha}}\right), \quad \text{(B.65)}$$

with $C(u_1, u_2; \alpha) = \exp\left(-(h_1 + h_2)\right)$, $h_k = (-\ln(u_k))^{\alpha}$, $k = 1, 2$ *and* $\alpha \in [1, \infty]$.

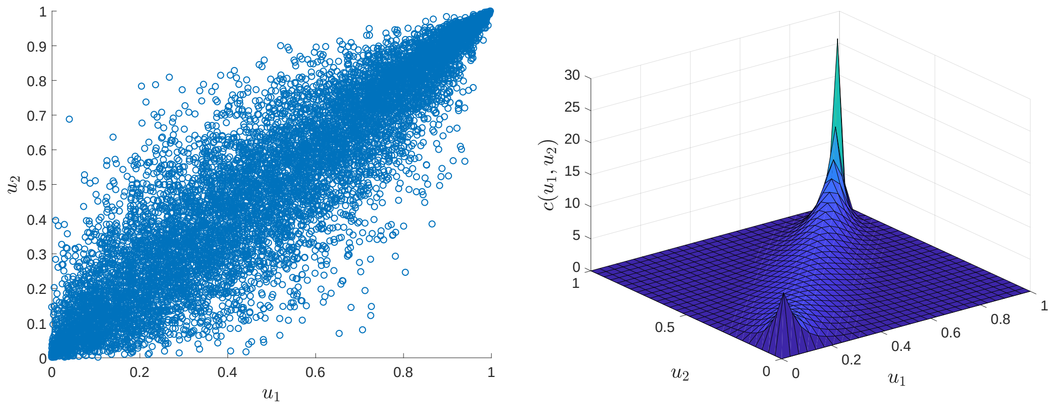

FIGURE B.6.: Bivariate Gumbel copula with $\alpha = 4$

C. Data Catalogue

C.1. Covered Bonds by Country and Bank

Country	Abbr.	Model	Public Sector		Mortgage	
			Outstanding	Onset	Outstanding	Onset
Australia	AUS	model V	no	-	yes	2011
Austria	AUT	model III	yes	pre 2008	yes	pre 2008
Belgium	BEL	model III	yes	2014	yes	2012
Canada	CAN	model V	no	-	yes	pre 2008
Cyprus	CYP	model III	no	-	yes	2011
Czech Republic	CZE	model IV	no	-	yes	pre 2008
Denmark	DNK	model II	no	-	yes	pre 2008
Finland	FIN	model I	no	-	yes	pre 2008
France	FRA	model I	yes	pre 2008	yes	pre 2008
Germany	DEU	model III	yes	pre 2008	yes	pre 2008
Greece	GRC	model IV	no	-	yes	2008
Hungary	HUN	model II	no	-	yes	pre 2008
Iceland	ISL	model III	no	-	yes	pre 2008
Ireland	IRL	model I	yes	pre 2008	yes	pre 2008
Italy	ITA	model V	yes	pre 2008	yes	2008
Latvia	LVA	model III	no	-	no	-
Luxembourg	LUX	model II	yes	pre 2008	no	-
New Zealand	NZL	model V	no	-	yes	2010
Norway	NOR	model I	yes	-	yes	2009
Panama	PAN	other	no	-	yes	2012
Poland	POL	model II	no	-	yes	pre 2008
Portugal	PRT	model IV	yes	2008	yes	pre 2008
Singapore	SGP	model V	no	-	yes	2015
Slovakia	SVK	model IV	no	-	yes	pre 2008
South Korea	KOR	model IV	no	-	yes	2009
Spain	ESP	model IV	yes	pre 2008	yes	pre 2008
Sweden	SWE	model I	no	-	yes	pre 2008
Switzerland	CHE	model I	no	-	yes	pre 2008
Turkey	TUR	other	no	-	yes	2016
The Netherlands	NLD	model V	no	-	yes	pre 2008
United Kingdom	GBR	model V	yes	pre 2008	yes	2009
United States	USA	other	no	-	yes	pre 2008

Table C.1.: Issuing covered bond countries in 2016.

C.2. Balance Sheet and §28 Reporting Data — Adjusted Values

Position	AAR	BHH	MHB	MMW	NAT	WBP	WIB
Equity	6,715.5	2,711.1	4,418.4	241.8	525.8	1,644.8	1,279.4
Total	55,268.7	29,427.7	45,443.4	2,087.8	2,787.4	11,192.6	6,430.5

Table C.3.: Equity and total sum of liability and assets.

Bank	Abbr.	Category	Cover Pool Share			Pfandbrief Share			
			Mortgage	Public	$\sum$	Mortgage	Public	$\sum$	
Verband deutscher Pfandbriefbanken e.V.	VDP	-	-	-	-	-	-	-	
Aareal Bank AG	AAR	Hyp	29.07	5.83	34.90	22.43	4.99	27.42	
Bayerische Landesbank	BLB	Other	3.47	11.11	14.58	1.92	7.65	9.57	
Berlin Hyp AG	BHH	Hyp	48.06	11.80	59.86	44.92	10.83	55.75	
Bremer Landesbank	BRL	Other	4.43	11.47	15.90	2.76	10.82	13.58	
Commerzbank AG	DSB	Other	3.90	2.66	6.56	3.08	2.31	5.39	
DekaBank Deutsche Girozentrale	DEKA	Other	0.38	4.32	4.70	0.10	3.07	3.17	
Deutsche Apotheker- und Ärztebank eG	APO	Other	11.71	0.00	11.71	8.26	0.00	8.26	
Deutsche Genossenschafts-Hypothekenbank AG	DGH	Hyp-Oef	35.58	26.88	62.46	27.94	22.12	50.06	
Deutsche Hypothekenbank (Actien-Gesellschaft)	DTH	Hyp-Oef	36.35	24.24	60.59	32.71	20.89	53.60	
Deutsche Kreditbank AG	DKB	Other	11.10	11.75	22.85	6.41	5.43	11.84	
Deutsche Pfandbriefbank AG	HRE	Hyp-Oef	29.87	33.53	63.40	24.94	28.45	53.39	
Deutsche Postbank AG	DPB	Other	3.69	0.20	3.89	2.56	0.14	2.70	
Düsseldorfer Hypothekenbank AG	DHB	Other	10.88	29.84	40.72	6.75	27.29	34.04	
DVB Bank SE	DVB	Other	0.00	0.00	0.00	0.00	0.00	0.00	
Hamburger Sparkasse AG	HASP	Other	16.01	0.00	16.01	11.37	0.00	11.37	
HSH Nordbank AG	HSH	Other	6.89	5.10	11.99	6.13	4.60	10.73	
Hypothekenbank Frankfurt AG	EH	-	-	-	-	-	-	-	
ING-DiBa AG	DIBA	Other	2.14	0.00	2.14	0.82	0.00	0.82	
Kreissparkasse Köln	KSK	Other	19.08	2.45	21.53	11.55	1.75	13.30	
Landesbank Baden-Württemberg	LBBW	Other	6.86	6.39	13.25	4.67	3.95	8.62	
Landesbank Berlin AG	LBB	Other	8.50	3.07	11.57	7.48	1.89	9.37	
Landesbank Hessen-Thüringen (Helaba)	HLB	Other	8.10	12.64	20.74	5.98	10.53	16.51	
Münchener Hypothekenbank eG	MHB	Hyp	58.44	12.59	71.03	52.60	12.28	64.88	
M.M.Warburg & CO Hypothekenbank AG	MMW	Hyp	70.11	1.57	71.68	65.30	0.32	65.62	
Natixis Pfandbriefbank AG	NAT	Hyp	52.79	0.00	52.79	37.35	0.00	37.35	
Nord/LB Norddeutsche Landesbank Girozentrale	NLB	Other	2.05	10.33	12.38	1.05	8.05	9.10	
PSD Bank Nürnberg eG	PSD	Other	7.58	0.00	7.58	5.31	0.00	5.31	
SaarLB	SAAR	Other	4.40	15.83	20.23	2.95	11.59	14.54	
SEB AG	SEB	Other	14.49	9.21	23.70	8.64	5.95	14.59	
Sparkasse KölnBonn	SKB	Other	16.05	0.95	17.00	12.04	0.17	12.21	
UniCredit Bank AG	HVB	Other	10.11	2.45	12.56	6.01	1.55	7.56	
VALOVIS BANK AG	KHB	Other	29.99	0.00	29.99	11.40	0.00	11.40	
Westdeutsche ImmobilienBank AG	WIB	Hyp	61.70	11.45	73.15	49.38	6.08	55.46	
WL BANK AG	WEL	Hyp-Oef	46.18	31.35	77.53	42.09	27.72	69.81	
Wüstenrot Bank AG Pfandbriefbank	WBP	Hyp	36.70	0.00	36.70	26.28	0.00	26.28	
			20.78	8.79	29.58	16.27	7.07	23.34	mean
			20.00	9.93	24.20	17.70	8.69	21.70	s.d.
			70.11	33.53	77.53	65.30	28.45	69.81	max
			0.00	0.00	0.00	0.00	0.00	0.00	min

TABLE C.2.: Percentage cover pool and Pfandbrief shares of all Pfandbrief banks in 4^{th} quarter 2016 (in %).

AAR, 4th Quarter 2016 (in mn €)			Cover Pool (CP)	Other Assets (OA)	Pfandbrief (PB)	Other Liabilities (OL)
Present Value	total		15,933.3	—	12,300.0	—
Nominal Value	total		15,797.3	39,471.3	12,204.6	37,048.1
	maturity	0.50	1,030.2	—	1,448.8	—
		1.00	929.4	—	1,034.1	—
		1.25	947.2	—	1,747.4	—
		1.75	1,142.0	—	1,182.4	—
		2.50	3,337.1	—	2,099.1	—
		3.50	2,657.1	—	719.0	—
		4.50	1,736.9	—	704.0	—
		7.50	2,948.4	—	2,443.5	—
		12.50	1,068.9	—	826.2	—

Table C.4.: Input data for the present values and adjusted nominals when allowing coupon payments of Aareal Bank AG, according to Section 6.2.

BHH, 4th Quarter 2016 (in mn €)			Cover Pool (CP)	Other Assets (OA)	Pfandbrief (PB)	Other Liabilities (OL)
Present Value	total		17,301.6	—	16,258.8	—
Nominal Value	total		17,140.1	12,287.6	16,126.3	11,773.2
	maturity	0.50	1,885.1	—	2,476.7	—
		1.00	1,508.7	—	468.9	—
		1.25	1,203.3	—	1,847.8	—
		1.75	1,154.1	—	1,596.6	—
		2.50	1,173.5	—	2,863.8	—
		3.50	1,819.4	—	1,323.6	—
		4.50	2,061.4	—	1,420.2	—
		7.50	5,083.5	—	2,433.1	—
		12.50	1,251.1	—	1,695.8	—

Table C.5.: Input data for the present values and adjusted nominals when allowing coupon payments of Berlin Hyp AG, according to Section 6.2.

MHB, 4th Quarter 2016 (in mn €)			Cover Pool (CP)	Other Assets (OA)	Pfandbrief (PB)	Other Liabilities (OL)
Present Value	total		32.550.1	—	28,321.9	—
Nominal Value	total		32,116.1	13,327.2	27,913.0	13.658,0
	maturity	0.50	1,267.1	—	675.5	—
		1.00	1,262.5	—	1,264.8	—
		1.25	1,496.7	—	865.8	—
		1.75	1,327.2	—	954.9	—
		2.50	2,425.1	—	1,658.0	—
		3.50	2,705.0	—	2,218.8	—
		4.50	2,403.7	—	1,800.6	—
		7.50	10,860.3	—	1,848.8	—
		12.50	8,368.0	—	11,319.8	—

Table C.6.: Input data for the present values and adjusted nominals when allowing coupon payments of Münchener Hypothekenbank eG, according to Section 6.2.

MMW, 4th Quarter 2016 (in mn €)			Cover Pool (CP)	Other Assets (OA)	Pfandbrief (PB)	Other Liabilities (OL)
Present Value	total		1,492.9	—	1,332.9	—
Nominal Value	total		1,476.6	611.2	1,320.0	595.9
	maturity	0.50	62.9	—	74.3	—
		1.00	30.8	—	65.0	—
		1.25	102.6	—	55.3	—
		1.75	88.5	—	124.1	—
		2.50	183.4	—	231.1	—
		3.50	145.2	—	115.3	—
		4.50	138.1	—	167.3	—
		7.50	678.3	—	464.0	—
		12.50	46.3	—	23.2	—

Table C.7.: Input data for the present values and adjusted nominals when allowing coupon payments of M. M. Warburg & CO Hypothekenbank AG, according to Section 6.2.

NAT, 4th Quarter 2016 (in mn €)			Cover Pool (CP)	Other Assets (OA)	Pfandbrief (PB)	Other Liabilities (OL)
Present Value	total		1,428.8	—	947.3	—
Nominal Value	total		1,412.5	1,374.8	937.9	1,448.6
	maturity	0.50	51.4	—	15.9	—
		1.00	40.8	—	51.4	—
		1.25	31.2	—	24.1	—
		1.75	26.2	—	32.0	—
		2.50	237.7	—	236.5	—
		3.50	224.9	—	76.1	—
		4.50	92.0	—	162.8	—
		7.50	600.2	—	338.6	—
		12.50	107.7	—	0	—

Table C.8.: Input data for the present values and adjusted nominals when allowing coupon payments of Natixis Pfandbriefbank AG, according to Section 6.2.

WBP, 4th Quarter 2016 (in mn €)			Cover Pool (CP)	Other Assets (OA)	Pfandbrief (PB)	Other Liabilities (OL)
Present Value	total		3,942.9	—	2,713.0	—
Nominal Value	total		3,908.6	7,284.0	2,691.5	7,171.2
	maturity	0.50	468.3	—	578.7	—
		1.00	252.6	—	332.6	—
		1.25	328.9	—	181.4	—
		1.75	291.6	—	151.6	—
		2.50	489.8	—	299.0	—
		3.50	389.2	—	189.9	—
		4.50	368.9	—	91.1	—
		7.50	1,120.5	—	712.3	—
		12.50	198.3	—	154.5	—

Table C.9.: Input data for the present values and adjusted nominals when allowing coupon payments of Wüstenrot Bank AG Pfandbriefbank, according to Section 6.2.

WIB, 4th Quarter 2016 (in mn €)			Cover Pool (CP)	Other Assets (OA)	Pfandbrief (PB)	Other Liabilities (OL)
Present Value	total		4,498.6	—	3,677.1	—
Nominal Value	total		4,466.1	1,964.3	3,643.6	2,392.9
	maturity	0.50	434.6	—	434.8	—
		1.00	443.1	—	389.7	—
		1.25	462.0	—	305.2	—
		1.75	489.1	—	224.4	—
		2.50	819.3	—	488.6	—
		3.50	351.5	—	216.3	—
		4.50	265.1	—	292.6	—
		7.50	1,015.1	—	931.6	—
		12.50	186.0	—	360.0	—

Table C.10.: Input data for the present values and adjusted nominals when allowing coupon payments of Westdeutsche ImmobilienBank AG, according to Section 6.2.

Segment	Sub-Segment	PD (pd_s)	Intra Correlation (ic_s)	Weights (w_s)
Germany (D)	residential	0.348	10.00	55.429
	commercial	0.856	46.55	10.722
PIGS(*)	residential	0.856	10.00	0.000
	commercial	4.746	44.76	0.343
Central Europe (CE)	residential	0.541	10.00	0.000
	commercial	1.365	18.00	0.000
Europe (ex D, PIGS, CE)	residential	0.348	10.00	6.776
	commercial	0.856	52.00	3.915
Rest of World	residential	0.348	10.00	1.773
	commercial	0.856	44.76	9.022
Supranational	residential	0.541	10.00	0.000
	commercial	1.365	52.00	0.000
Residual	—	0.541	52.00	12.021

Table C.11.: PDs, intra correlations (see for example Fisher (1992) for its computation) and weights of the Münchener Hypothekenbank eG, in % (source: Moody's). ((∗) PIGS states consist of Portugal, Ireland, Greece and Spain.)

C.3. Parameter Input

$\boldsymbol{P}_{0,1}^{\text{S\&P}}$	AAA	AA	A	BBB	BB	B	CCC-C	D
AAA	0.9193	0.0746	0.0048	0.0008	0.0004	0.0000	0.0000	0.0000
AA	0.0064	0.9180	0.0676	0.0060	0.0006	0.0011	0.0003	0.0000
A	0.0007	0.0227	0.9168	0.0512	0.0056	0.0025	0.0001	0.0004
BBB	0.0004	0.0027	0.0556	0.8789	0.0483	0.0102	0.0017	0.0023
BB	0.0004	0.0010	0.0061	0.0775	0.8148	0.0789	0.0111	0.0101
B	0.0000	0.0010	0.0028	0.0046	0.0695	0.8280	0.0396	0.0546
CCC-C	0.0019	0.0000	0.0037	0.0074	0.0243	0.1212	0.6046	0.2370
D	0.0000	0.0000	0.0000	0.0000	0.0000	0.0000	0.0000	1.0000

$\boldsymbol{P}_{0,1}^{\text{Moodys}}$	Aaa	Aa	A	Baa	Ba	B	Caa-C	D
Aaa	0.8866	0.1030	0.0102	0.0000	0.0003	0.0000	0.0000	0.0000
Aa	0.0108	0.8870	0.0955	0.0034	0.0015	0.0015	0.0000	0.0003
A	0.0006	0.0288	0.9021	0.0592	0.0074	0.0018	0.0001	0.0001
Baa	0.0005	0.0034	0.0707	0.8523	0.0605	0.0101	0.0008	0.0016
Ba	0.0003	0.0008	0.0056	0.0568	0.8358	0.0808	0.0053	0.0146
B	0.0001	0.0004	0.0017	0.0065	0.0660	0.8270	0.0276	0.0706
Caa-C	0.0000	0.0000	0.0066	0.0105	0.0305	0.0611	0.6297	0.2616
D	0.0000	0.0000	0.0000	0.0000	0.0000	0.0000	0.0000	1.0000

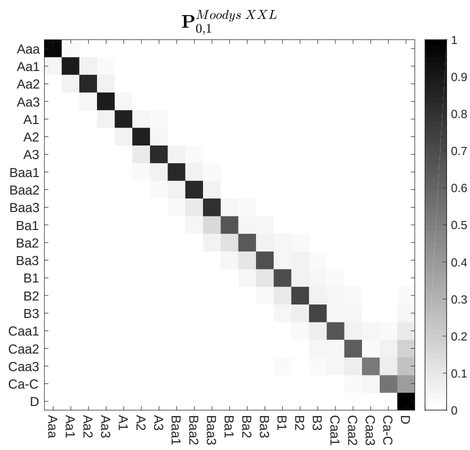

TABLE C.12.: Selection of transition matrices containing the 8×8 matrices $\boldsymbol{P}_{0,1}^{\text{S\&P}}$ and $\boldsymbol{P}_{0,1}^{\text{Moodys}}$ adopted from Israel et al. (2001) and the visual depiction of the 21×21 matrix $\boldsymbol{P}_{0,1}^{\text{Moodys XXL}}$ (companies without ratings (WR) are simply removed by computing $p_{ij}^{\text{WR}} = \frac{p_{ij}}{1-p_{i,WR}}$ for $i, j = 1, \ldots, K$) is given as in Metz and Cantor (2007).

$\boldsymbol{G}^{\text{Moodys}}$	Aaa	Aa	A	Baa	Ba	B	Caa-C	D
Aaa	-0.1212	0.1160	0.0051	0.0000	0.0001	0.0000	0.0000	0.0000
Aa	0.0121	-0.1223	0.1069	0.0002	0.0012	0.0015	0.0000	0.0003
A	0.0005	0.0321	-0.1075	0.0674	0.0061	0.0014	0.0000	0.0000
Baa	0.0006	0.0025	0.0805	-0.1650	0.0713	0.0085	0.0008	0.0008
Ba	0.0003	0.0007	0.0036	0.0671	-0.1857	0.0970	0.0054	0.0116
B	0.0001	0.0004	0.0014	0.0049	0.0787	-0.1952	0.0380	0.0717
Caa-C	0.0000	0.0000	0.0080	0.0124	0.0380	0.0825	-0.4644	0.3236
D	0.0000	0.0000	0.0000	0.0000	0.0000	0.0000	0.0000	0.0000

TABLE C.13.: Example of a resulting valid generator matrix based on BAM and (G1), (G2).

(a) For a general modelling setup the starting values for the cover pool and other assets are set to one.

(b) Setting the nominal value of the cover pool to one is motivated by its defintion of a risky zero coupon bond.

(c) Parameters for the Hull-White model are simply taken from Hull and White (1993), compare Sünderhauf (2006).

(d) At first, Sünderhauf (2006) derives the constant volatility ς_x in an iterative procedure (together with the zero-coupon bond nominals and state present values), by considering the risk-neutral default probability in case of the cover pool pd^Q_{CP}, which in turn are obtained from the real-world default probability. The equality $\varsigma^2_x(0) = \theta_{\varsigma_x} = \varsigma^2_x$ holds.

(e) The given values are obtained from the basic and realistic scenario as in Sünderhauf (2006).

(f) As the overall result in Sünderhauf (2006) is that correlation risk has low impact on results, the parameters are simply set to a moderate positive correlation value.

(g) The maturities from assets and liabilities can be derived from the amount in each maturity range divided by its total amount and multiplied by the mean maturity of its corresponding maturity range (see Sünderhauf (2006) for more details). The maximum maturity gap between assets and liabilities is 3.3 years, as calculated in Sünderhauf (2006).

	Description	CP	OA	CP & OA
State Variable[(a)]	Initial state variable value ($t=0$)	$V_{CP}(0)=1$	$V_{OA}(0)=1$	—
Nominal[(b)]	Nominal value at $t=T_2$ for CP	$N_{CP}=1$	—	—
Interest Rate[(c)]	Initial short rate value ($t=0$)	—	—	$r(0)=0.05$
	Level of flat instantaneous forward rate	—	—	$f^M(0,t)=0.05$
	Mean reversion speed	—	—	$\kappa_r=0.1$
	Volatility level	—	—	$\sigma_r=0.014$
Volatility[(d)]	Initial volatility value ($t=0$)	$\varsigma^2_{CP}(0)=(0.06)^2$	$\varsigma^2_{OA}(0)=(0.09)^2$	—
	Mean reversion level	$\theta_{\varsigma CP}=(0.06)^2$	$\theta_{\varsigma OA}=(0.09)^2$	—
	Mean reversion speed	$\kappa_{\varsigma CP}=0.1$	$\kappa_{\varsigma OA}=0.1$	—
	Volatility level	$\sigma_{\varsigma CP}=0.1$	$\sigma_{\varsigma OA}=0.1$	—
Jump Process[(e)]	Jump intensity	$\lambda_{V_{CP}}=0.2693$	$\lambda_{V_{OA}}=0.6484$	—
	Jump height mean	$\mu_{\pi_{V_{CP}}}=0$	$\mu_{\pi_{V_{OA}}}=0$	—
	Jump height volatility	$\sigma_{\pi_{V_{CP}}}=0.1$	$\sigma_{\pi_{V_{OA}}}=0.1$	—
Correlation[(f)]	State variables ($\tilde{W}_{V_{CP}},\tilde{W}_{V_{OA}}$)	—	—	$\rho_{V_{CP}V_{OA}}=0.3$
	Interest rate & volatility ($\tilde{W}_r,\tilde{W}_{\varsigma_x}$)	$\rho_{r\varsigma_{CP}}=0.3$	$\rho_{r\varsigma_{OA}}=0.3$	—
	State variable & volatility ($\tilde{W}_{V_x},\tilde{W}_{\varsigma_x}$)	$\rho_{V_{CP}\varsigma_{CP}}=0.3$	$\rho_{V_{OA}\varsigma_{OA}}=0.3$	—
	State variable & interest rate ($\tilde{W}_{V_x},\tilde{W}_r$)	$\rho_{V_{CP}r}=0.3$	$\rho_{V_{OA}r}=0.3$	—
Maturity[(g)]	Maturities of assets (in years)	$T_2=7$	$T_1=3$	—

TABLE C.14.: Structural model: Basis scenario set of parameters, starting values and maturities for simulations for CP and OA.

	Description	CP	OA	CP & OA
Nominal	Nominal value at $t = T_2$ for CP	$N_{CP} = 1$	—	—
Factor model	Maximum loss	$l^{\max} = 1$	—	—
	Factor Loading	$a = 0.5$	—	—
	Factor Loading	$b_{\tilde{\delta}} = 0.2$	—	—
	Variance idiosyncratic factors	$\sigma_{\xi}^2 = 0.01$	—	—
	Constant	$\mu_{\tilde{\delta}} = 0.4$	—	
	Expectation recovery rate	$\mathbb{E}[\tilde{\delta}] = 0.6$	—	—
	Variance recovery rate	$\mathbb{V}[\tilde{\delta}] = 0.01$	—	—
	Dependence recovery rate - asset returns	$\tau(\tilde{\delta}, X) = 0.8$	—	—
Risk Premium	Initial risk premium	$\pi(0) = 3$	—	—
	Mean reversion speed	$\alpha_{\pi} = 0.1$	—	—
	Mean reversion level	$\mu_{\pi} = 1$	—	—
	Volatility level	$\sigma_{\pi} = 1$	—	—
Log-normal	Mean	—	$\mu_{OA} = 0.129$	—
	Variance	—	$\sigma_{OA}^2 = 0.235^2$	—
Dependence	Copula	—	—	t
	Dependence OA and CP	—	—	$\rho_{CP,OA} = 0.5$
	Dof OA and CP	—	—	$\nu_{CP,OA} = 2$
Maturity$^{(g)}$	Maturities of assets (in years)	$T_2 = 7$	$T_1 = 3$	—

TABLE C.15.: Reduced-form model: Basis scenario set of parameters and maturities for simulations for CP and OA.

D. Supplementary Graphics

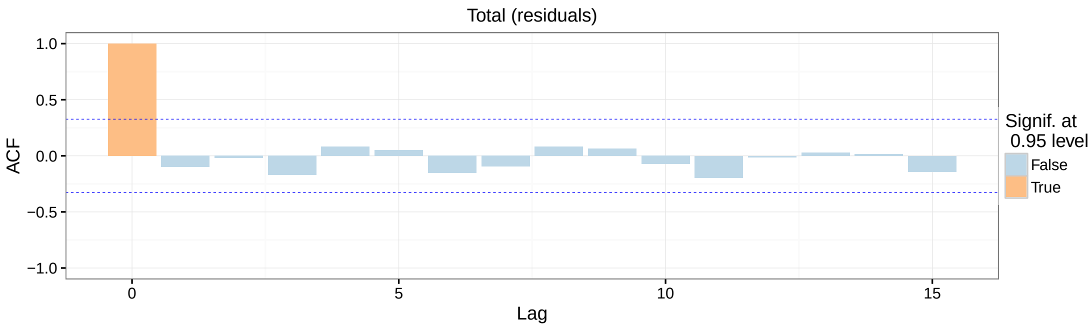

FIGURE D.1.: ACF plot of asset and liability positions with ARIMA fit

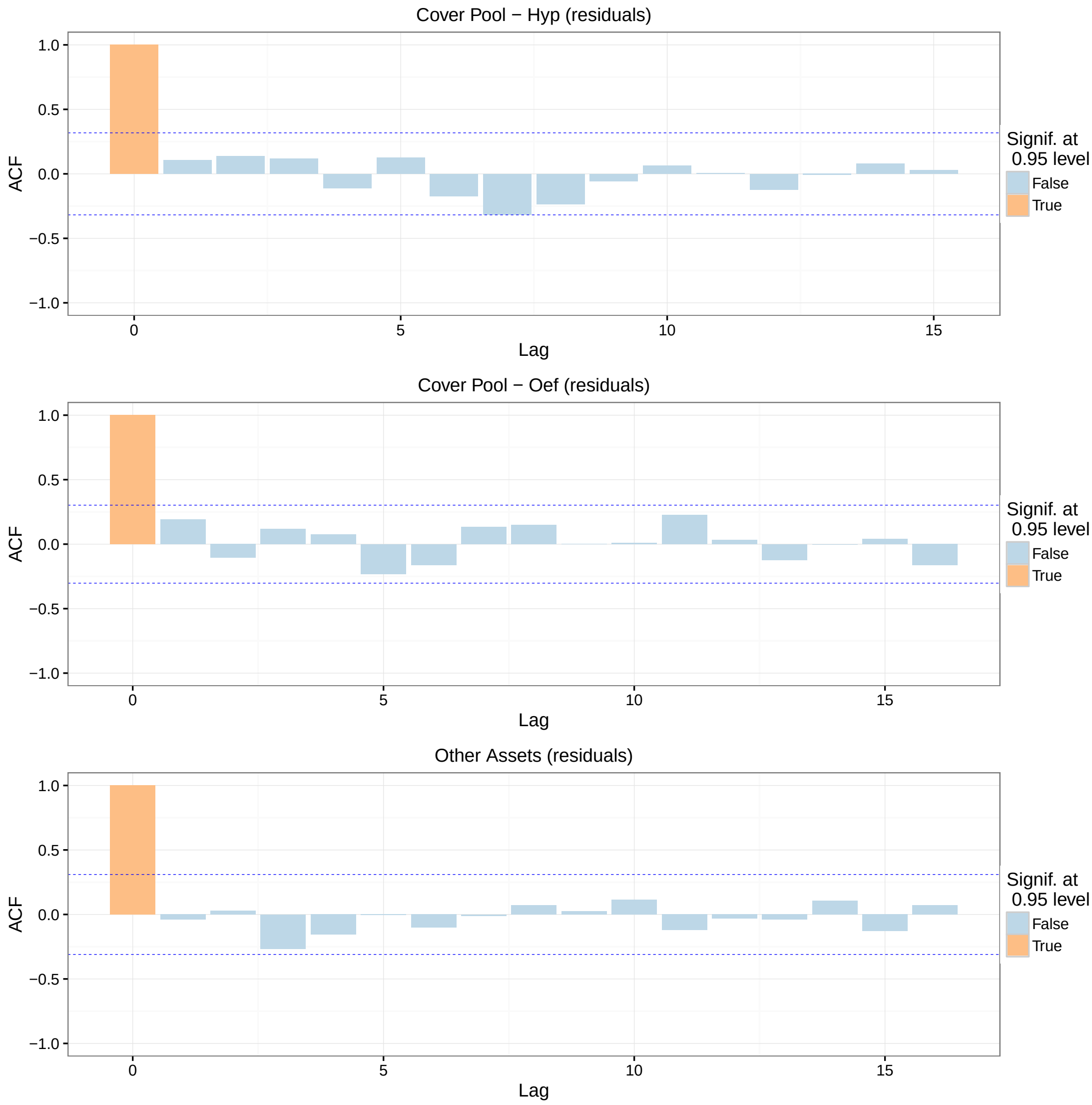

FIGURE D.2.: ACF plot of asset positions with ARIMA fit

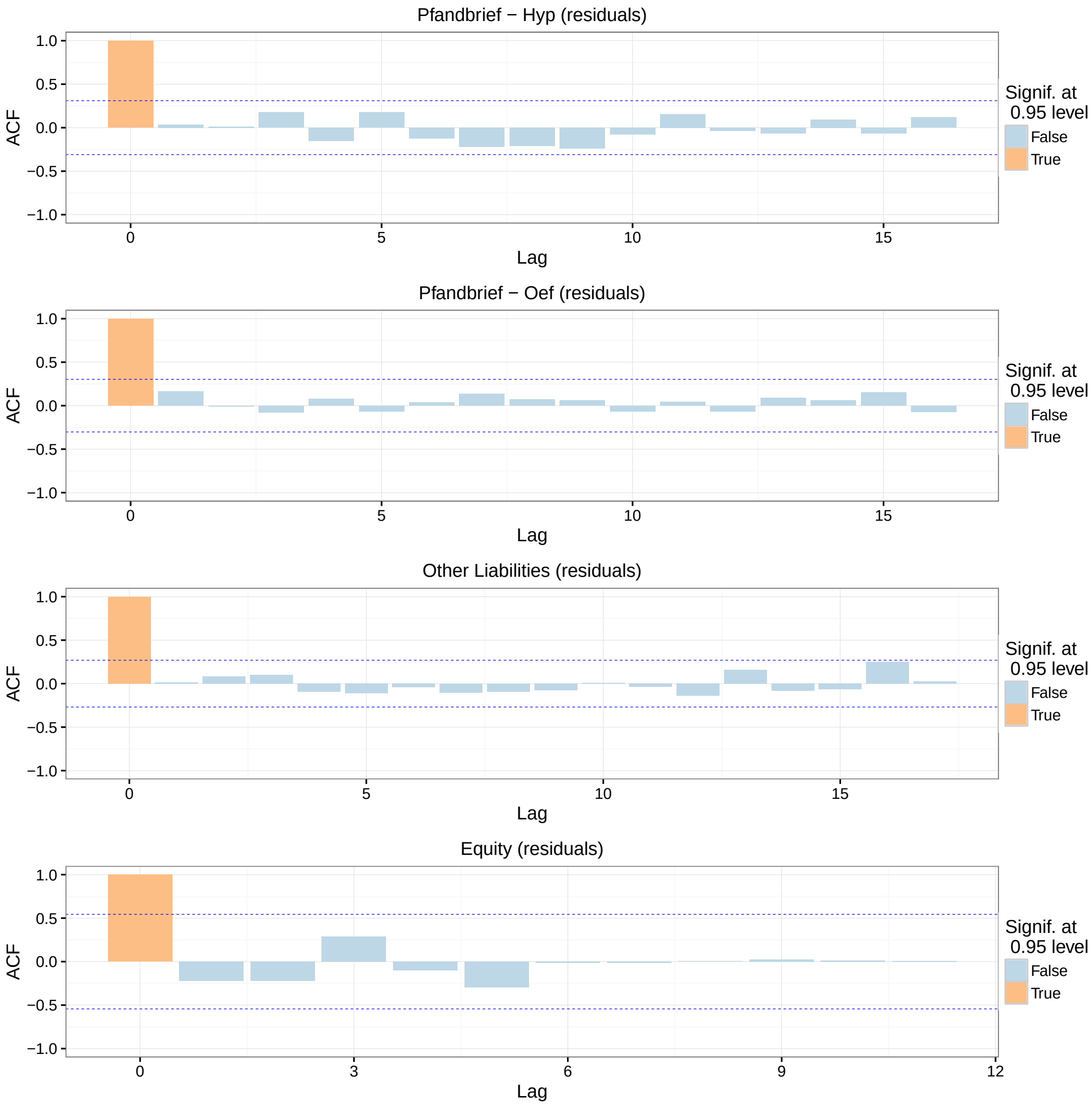

FIGURE D.3.: ACF plot of liability positions with ARIMA fit

Bibliography

Aalen, O., Borgan, O., and Gjessing, H. (2008). *Survival and Event History Analysis: A Process Point of View*. Statistics for Biology and Health. Springer New York.

AAR (2015). *Geschäftsbericht 2015*. Aareal Bank Group.

AAR (2016). *Geschäftsbericht 2016*. Aareal Bank Group.

Agrawal, D., Arora, N., and Bohn, J. (2004). Parsimony in Practice: An EDF-based Model of Credit Spreads. *Moody's KMV*.

Allianz SE (2016). *Annual Report 2016*. Allianz Group.

Andersen, L. (2008). Simple and efficient simulation of the Heston stochastic volatility model. *Journal of Computational Finance*, **11**(3):1–42.

Andersen, L. and Sidenius, J. (2004). Extensions to the Gaussian copula: random recovery and random factor loadings. *Journal of Credit Risk*, **1**(1):29–70.

Andersen, L., Sidenius, J., and Basu, S. (2003). All Your Hedges in One Basket. *RISK*, **16**(11):67–72.

Andersen, L. B., Jäckel, P., and Kahl, C. (2010). Simulation of square-root processes. *Encyclopedia of Quantitative Finance*.

Anderson, R. W. and Cakici, N. (1999). The Value of Deposit Insurance in the Presence of Interest Rate and Credit Risk. *Financial Markets, Institutions & Instruments*, **8**:45–62.

Arvanitis, A., Gregory, J., and Laurent, J.-P. (1999). Building models for credit spreads. *Journal of Derivatives*, **6**(3):27–43.

Asmussen, S. (2008). *Applied Probability and Queues*. Stochastic Modelling and Applied Probability. Springer New York.

Bachelier, L. (1900). Théorie de la spéculation. *Annales scientifiques de l'École Normale Supérieure*, **17**:21–86.

Balduzzi, P., Das, S. R., Foresi, S., and Sundaram, R. K. (1996). A Simple Approach to Three-Factor Affine Term Structure Models. *The Journal of Fixed Income*, **6**(3):43–53.

Bates, D. S. (1991). The Crash of '87: Was It Expected? The Evidence from Options Markets. *The Journal of Finance*, **46**(3):1009–1044.

Bates, D. S. (1996). Jumps and Stochastic Volatility: Exchange Rate Processes Implicit in Deutsche Mark Options. *The Review of Financial Studies*, **9**(1):67–107.

Baxter, M. and Rennie, A. (1996). *Financial Calculus: An Introduction to Derivative Pricing*. Cambridge University Press.

Beckers, M. (2009). *Hypothekenpfandbriefe und Mortgage Backed Securities: Hintergründe, Funktionsweisen und Risikovergleich in Zeiten der Finanzmarktkrise.* VDM Verlag Müller.

Beirne, J., Dalitz, L., Ejsing, J., Grothe, M., Manganelli, S., Monar, F., Sahel, B., Sušec, M., Tapking, J., and Vong, T. (January 2011). The Impact of the Eurosystem's Covered Bond Purchase Programme on the Primary and Secondary Markets. *European Central Bank*, **122**.

Berkaoui, A., Bossy, M., and Diop, A. (2008). Euler scheme for sdes with non-lipschitz diffusion coefficient: strong convergence. *ESAIM: Probability and Statistics*, **12**:1–11.

Bertalot, L., Dierks, L., Bertram, H., and Kullig, S. (2011). *The Euromoney Covered Bonds Handbook 2011.* Euromoney Books.

BHH (2015). *Geschäftsbericht 2015.* Berlin Hyp.

Bielecki, T. and Rutkowski, M. (2004). *Credit Risk: Modeling, Valuation and Hedging.* Springer Finance. Springer Berlin Heidelberg.

Bingham, N. and Kiesel, R. (2013). *Risk-Neutral Valuation: Pricing and Hedging of Financial Derivatives.* Springer Finance. Springer London.

BIS (2001). *The Internal Ratings-Based Approach.* Bank for International Settlements.

BIS (2013). *Basel III: The Liquidity Coverage Ratio and liquidity risk monitoring tools.* Bank for International Settlements.

Björk, T. (2004). *Arbitrage Theory in Continuous Time.* Oxford Finance Series. OUP Oxford.

Black, F. (1976). The Pricing of Commodity Contracts. *Journal of Financial Economics*, **3**(1–2):167–179.

Black, F., Derman, E., and Toy, W. (1990). A one-factor model of interest rates and its application to treasury bond options. *Financial Analysts Journal*, **46**(1):33–39.

Black, F. and Karasinski, P. (1991). Bond and option pricing when short rates are lognormal. *Financial Analysts Journal*, **47**(4):52–59.

Black, F. and Scholes, M. (1973). The Pricing of Options and Corporate Liabilities. *Journal of Political Economy*, **81**(3):637–654.

Bluhm, C., Overbeck, L., and Wagner, C. (2002). *An Introduction to Credit Risk Modeling.* Chapman & Hall/CRC financial mathematics series. Taylor & Francis.

Brennan, M. J. and Schwartz., E. S. (1979). A Continuous-Time Approach to the Pricing of Bonds. Research Program in Finance Working Papers 85, University of California at Berkeley.

Brennan, M. J. and Schwartz, E. S. (1982). An Equilibrium Model of Bond Pricing and a Test of Market Efficiency. *Journal of Financial and Quantitative Analysis*, **17**(3):301–329.

Brigo, D. and Mercurio, F. (2007). *Interest Rate Models — Theory and Practice: With Smile, Inflation and Credit.* Springer Finance. Springer Berlin Heidelberg.

Briys, E. and de Varenne, F. (1997). Valuing risky fixed rate debt: An extension. *Journal of Financial and Quantitative Analysis*, **32**(2):239–248.

Bushman, B. J. and Wang, M. C. (1995). A Procedure for Combining Sample Correlation Coefficients and Vote Counts to Obtain an Estimate and a Confidence Interval for the Population Correlation Coefficient. *Psychological Bulletin*, **117**(3):530–546.

Carette, P. (1995). Characterizations of Embeddable 3×3 Stochastic Matrices with a Negative Eigenvalue. *New York Journal of Mathematics*, **1**:120–129.

Chan-Lau, J. A. and Oura, H. (2014). Bail-in Clause, Depositor Preference, and Asset Encumbrance: The End of Cheap Senior Unsecured Debt? A Structural Pricing Prespective. *SSRN Electronic Journal*.

Chen, L. (1996). *A Three-Factor Model of the Term Structure of Interest Rates*, pages 1–36. Springer Berlin Heidelberg, Berlin, Heidelberg.

Chung, K. (1960). *Markov Chains with Stationary Transition Probabilities*. Die Grundlehren der mathematischen Wissenschaften. Springer.

Commission Staff Working Paper (2011). National measures and practices to avoid foreclosure procedures for residential mortgage loans. *SEC*, **357 final**.

Corey, D. M., Dunlap, W. P., and Burke, M. J. (1998). Averaging Correlations: Expected Values and Bias in Combined Pearson rs and Fisher's z Transformations. *The Journal of General Psychology*, **125**(3):245–261.

Cox, J. C., Ingersoll, J. E., and Ross, S. A. (1985). A Theory of the Term Structure of Interest Rates. *Econometrica*, **53**(2):385–407.

Culver, W. J. (1966). On the Existence and Uniqueness of the Real Logarithm of a Matrix. *Proceedings of the American Mathematical Society*, **17**(5):1146–1151.

Cuthbert, J. (1972). On Uniqueness of the Logarithm for Markov Semi-Groups. *J. London Math. Soc.*, **4**:623–630.

Cuthbert, J. (1973). The Logarithmic Function for Finite-State Markov Semi-Groups. *J. London Math. Soc.*, **6**:524–532.

Davies, E. (2010). Embeddable Markov Matrices. *Electronic Journal of Probability*, **15**(47):1474–1486.

Deelstra, G. and Delbaen, F. (1998). Convergence of discretized stochastic (interest rate) processes with stochastic drift term. *Applied Stochastic Models and Data Analysis*, **14**(1):77–84.

Dereich, S., Neuenkirch, A., and Szpruch, L. (2012). An euler-type method for the strong approximation of the cox–ingersoll–ross process. *Proceedings of the Royal Society of London A: Mathematical, Physical and Engineering Sciences*, **468**(2140):1105–1115.

DGHYP (August 2012). *The German Pfandbrief Market 2012 / 2013*. Deutsche Genossenschafts-Hypothekenbank AG.

Dothan, L. U. (1978). On the term structure of interest rates. *Journal of Financial Economics*, **6**(1):59–69.

Draper, N. and Smith, H. (1998). *Applied regression analysis*. Number Bd. 1 in Wiley series in probability and statistics: Texts and references section. Wiley.

Dübel, H. J. (2010). Reformerfordernisse bei Pfandbriefen und Pfandbriefbanken vor dem Hintergrund der Finanzmarktkrise. *Technical and policy paper*.

Dubrana, L. (2011). A Stochastic Model for Credit Spreads Under a Risk-Neutral Framework Through the Use of an Extended Version of the Jarrow, Lando and Turnbull Model. *SSRN*.

Duffie, D. J. (1999). Credit Swap Valuation. *Financial Analysts Journal*, **55**(1):73–87.

Dufresne, D. (2001). *The Integrated Square-root Process*. Research paper. Centre for Actuarial Studies, Department of Economics, University of Melbourne.

EBA (December 2016). *EBA Report on Covered Bonds*. European Banking Authority.

EBF (2014). *Study on Internal Rating Based (IRB) models in Europe — Residential Mortgages*. EBF Risk Assessment Working Group.

ECBC (August 2016). *European Covered Bond Fact Book*. European Covered Bond Council, 11th edition.

ECBC (August 2017). *European Covered Bond Fact Book*. European Covered Bond Council, 12th edition.

Eilers, F. (2017a). Prognosen zur langfristigen Preisentwicklung auf den deutschen Immobilienmärkten. *Association of German Pfandbrief Banks*, page 9.

Eilers, F. (2017b). vdpresearch stellt Immobilienmarktprognosen Deutschland 2017 - 2021 vor. *Association of German Pfandbrief Banks*, page 5.

Elfving, G. (1937). Zur Theorie der Markoffschen Ketten. *Acta Societatis Scientiarum Fennicae*, **A.2.**(8):1–17.

EPRS (2015). Covered bonds — ripe for expansion? *European Parliamentary Research Service*.

Fahrmeir, L., Brachinger, W., Hamerle, A., and Tutz, G. (1996). *Multivariate statistische Verfahren*. de Gruyter.

Fahrmeir, L., Kneib, T., Lang, S., and Marx, B. (2013). *Regression: Models, Methods and Applications*. Springer Berlin Heidelberg.

Fisher, R. A. (1992). *Statistical Methods for Research Workers*, volume Breakthroughs in Statistics of *Springer Series in Statistics (Perspectives in Statistics)*. Springer, New York, NY.

Frydman, H. (1980). The Embedding Problem for Markov Chains with Three States. *Mathematical Proceedings of the Cambridge Philosophical Society*, **87**:285–294.

Fuglede, B. (1988). On the Imbedding Problem for Stochastic and Doubly Stochastic Matrices. *Probability Theory and Related Fields*, **80**(2):241–260.

Glasserman, P. (2004). *Monte Carlo Methods in Financial Engineering*. Applications of mathematics: stochastic modelling and applied probability. Springer.

Glosten, L. R., Jagannathan, R., and Runkle, D. E. (1993). On the Relation between Expected Value and the Volatility of the Nominal Excess Return on Stocks. *The Journal of Finance*, **48**(5):1779–1801.

Gogarn, J. (2015). *Capital Requirements Regulation – CRR: Verordnung über Aufsichtsanforderungen an Kreditinstitute und Wertpapierfirmen, Stand: November 2013: Die amtlichen EU-Texte Deutsch – Englisch*. Books on Demand.

Golin, J. (2006). *Covered Bonds: Beyond Pfandbriefe: Innovations, Investment and Structured Alternatives*. Euromoney books. Euromoney Books.

Goodman, G. S. (1970). An Intrinsic Time for Non-Stationary Finite Markov Chains. *Zeitschrift für Wahrscheinlichkeitstheorie und Verwandte Gebiete*, **16**:165–180.

Grimmett, G. and Stirzaker, D. (2001). *Probability and Random Processes*. Probability and Random Processes. OUP Oxford.

Guerry, M.-A. (2013). On the Embedding Problem for Discrete-Time Markov Chains. *J. Appl. Probab.*, **50**(4):918–930.

Guerry, M.-A. (2014). On the Embedding Problem for Three-State Markov Chains. *Proceedings of the World Congress on Engineering 2014*, **II**.

Guo, X., Jarrow, R. A., and Zeng, Y. (2009). Credit risk models with incomplete information. *Mathematics of Operations Research*, **34**(2):320–332.

Hagen, L. (2002). LGD-Grading der Hypothekenbanken: ein offenes Modell für Dritte. *Immobilien & Finanzierung*, **11**.

Hagen, L. (2018). Regulierungsumfeld gewinnt Konturen. *Börsen-Zeitung*, **163**.

Hagen, L. and Marburger, C. (2002). Auswirkungen von Basel II auf die Hypothekenbanken und ihre Kunden — eine Zwischenbilanz. *Immobilien & Finanzierung*, **3**.

Heath, D., Jarrow, R., and Morton, A. (1992). Bond Pricing and the Term Structure of Interest Rates: A New Methodology for Contingent Claims Valuation. *Econometrica*, **60**(1):77–105.

Hertz, D. B. (1964). Risk Analysis in Capital Investment. *Harvard Business Review*, **1**:95–106.

Heston, S. L. (1993). A closed-form solution for options with stochastic volatility with applications to bond and currency options. *Review of Financial Studies*, **6**(2):327–343.

Higham, D. J. (2001). An Algorithmic Introduction to Numerical Simulation of Stochastic Differential Equations. *Society for Industrial and Applied Mathematics*, **43**(3):525–546.

Higham, D. J. and Mao, X. (2005). Convergence of Monte Carlo simulations involving the mean-reverting square root process. *Journal of Computational Finance*, **8**(3):35–61.

Hillenbrand, F. (2013). Covered Bonds in der Insolvenz — ein systematischer Überblick. *I&F*, **14**:483–485.

Ho, T. S. Y. and Lee, S.-b. (1986). Term structure movements and pricing interest rate contingent claims. *Journal of Finance*, **41**(5):1011–1029.

Homey, J. and Soldera, J. (2010). Moody's Analysis of Legal Framework For German Pfandbrief. *Moody's Investor Service, Inc.*

Homey, J. and Soriano, J. P. (2010). Announcement: Moody's assigns Aaa rating to Muenchener Hypothekenbank's mortgage covered bonds. *Moody's Investors Service, Inc.*

Hughes, M. and Werner, R. (2016). Choosing markovian credit migration matrices by nonlinear optimization. *Risks*, **4**(31).

Hull, J. (2009). *Options, Futures and Other Derivatives.* Options, Futures and Other Derivatives. Pearson/Prentice Hall.

Hull, J. and White, A. (1988). An Analysis of the Bias in Option Pricing Caused by a Stochastic Volatility. *Advances in Futures and Options Research*, **3**:29–61.

Hull, J. and White, A. (1990). Pricing Interest-Rate-Derivative Securities. *Review of Financial Studies*, **3**(4):573–592.

Hull, J. and White, A. (1993). One-Factor Interest-Rate Models and the Valuation of Interest-Rate Derivative Securities. *Journal of Financial and Quantitative Analysis*, **28**(2):235–254.

Hull, J. and White, A. (1994). Branching Out. *Risk*, **7**:34–37.

Hull, J. and White, A. (Winter 2004). Valuation of a CDO and an n^{th} to Default CDS Without Monte Carlo Simulation. *Journal of Derivatives*, **12**(2):8–23.

Hull, J. C. (2015). *Risk Management and Financial Institutions.* Wiley Finance. Wiley.

Hull, J. C. and White, A. D. (1996). Using Hull-White Interest Rate Trees. *The Journal of Derivatives*, **3**(3):26–36.

Ineke, J., Barton, S., and Bradley, M. (2006). *Covered Bonds: Beyond Pfandbriefe: Innovations, Investment and Structured Alternatives*, chapter Basel II and covered bonds, pages 42–54. Euromoney books. Euromoney Books.

Isopel, I. and Lanza, M. (2017). Ratings Affirmed On Wuestenrot Bausparkasse's German Mortgage Covered Bonds Following Program Transfer. *Standard & Poor's Financial Services LLC.*

Israel, R. B., Rosenthal, J. S., and Wei, J. Z. (2001). Finding Generators for Markov Chains via Empirical Transition Matrices, with Applications to Credit Ratings. *Mathematical Finance*, **11**(2):245–265.

Izzi, L., Oricchio, G., and Vitale, L. (2012). *Basel III Credit Rating Systems: An Applied Guide to Quantitative and Qualitative Models.* Finance and Capital Markets Series. Palgrave Macmillan.

Jamshidian, F. and Zhu, Y. (1996). Scenario simulation: Theory and methodology. *Finance and Stochastics*, **1**(1):43–67.

Jarrow, R. A., Lando, D., and Turnbull, S. M. (1997). A Markov Model for the Term Structure of Credit Risk Spreads. *Review of Financial Studies*, **10**(2):481–523.

Jarrow, R. A. and Turnbull, S. M. (1995). Pricing derivatives on financial securities subject to credit risk. *The Journal of Finance*, **50**(1):53–85.

Johansen, S. (1974). Some Results on the Imbedding Problem for Finite Markov Chains. *J. London Math. Soc*, **2**(8):345–351.

Johnson, N., Kotz, S., and Balakrishnan, N. (1994). *Continuous univariate distributions*, volume **1** of *Wiley series in probability and mathematical statistics: Applied probability and statistics*. Wiley & Sons.

Johnson, N., Kotz, S., and Balakrishnan, N. (1995). *Continuous univariate distributions*, volume **2** of *Wiley series in probability and mathematical statistics: Applied probability and statistics*. Wiley & Sons.

Johnson, N., Kotz, S., and Kemp, A. (1992). *Univariate discrete distributions*. Wiley series in probability and mathematical statistics: Probability and mathematical statistics. John Wiley & Sons.

Just, T. and Maennig, W. (2012). *Understanding German Real Estate Markets*. Management for Professionals. Springer.

Kahl, C. (2008). *Modelling and Simulation of Stochastic Volatility in Finance*. Universal Publishers.

Kalemanova, A., Schmid, B., and Werner, R. (2007). The Normal Inverse Gaussian Distribution for Synthetic CDO Pricing. *The Journal of Derivatives*, **14**(3):80–94.

Kealhofer, S., Kwok, S., and Weng, W. (1998). Uses and abuses of bond default rates. *KMV Corporation*.

Kenyon, C. (2009). Pricing Covered Bonds. *SSRN*.

Kijima, M. and Komoribayashi, K. (1998). A Markov Chain Model for Valuing Credit Risk Derivatives. *The Journal of Derivatives*, **6**(1):97–108.

Kingman, J. F. C. (1962). The Imbedding Problem for Finite Markov Chains. *Zeitschrift für Wahrscheinlichkeitstheorie und Verwandte Gebiete*, **1**:14–24.

Kleiber, C. and Zeileis, A. (2008). *Applied Econometrics with R*. Use R! Springer New York.

Kloeden, P. and Platen, E. (2011). *Numerical Solution of Stochastic Differential Equations*. Stochastic Modelling and Applied Probability. Springer Berlin Heidelberg.

Korn, R., Korn, E., and Kroisandt, G. (2010). *Monte Carlo Methods and Models in Finance and Insurance*. Chapman and Hall/CRC Financial Mathematics Series. CRC Press.

Kreinin, A. and Sidelnikova, M. (2001). Regularization Algorithms for Transition Matrices. *Algo Research Quarterly*, **4**(1):23–40.

Küchler, U. and Sorensen, M. (2006). *Exponential Families of Stochastic Processes*. Springer Series in Statistics. Springer New York.

Lando, D. (2004). *Credit Risk Modeling: Theory and Applications*. Princeton Series in Finance. Princeton University Press.

Lando, D. and Skodeberg, T. M. (2002). Analyzing rating transitions and rating drift with continuous observations. *Journal of Banking & Finance*, **26**(2-3):423–444.

Lassen, T. (December 2005). Specialization of Covered Bond Issuers in Europe. *HOUSING FINANCE INTERNATIONAL*, pages 3–12.

Laurent, J.-P. and Gregory, J. (Summer 2005). Basket Default Swaps, CDO's and Factor Copulas. *Journal of Risk*, **7**(4):103–122.

Lenhard, M. (2017). Aareal Bank AG Mortgage Covered Bonds: German Covered Bonds. *Moody's Investors Service, Inc.*

Li, D. X. (2000). On Default Correlation: A Copula Function Approach. *The Journal of Fixed Income*, **9**(4):43–54.

Lin, L. (2011). *Roots of Stochastic Matrices and Fractional Matrix Powers*. PhD thesis, University of Manchester.

Litterman, R. B. and Iben, T. (1991). Corporate bond valuation and the term structure of credit spreads. *The Journal of Portfolio Management*, **17**(3):52–64.

Longstaff, F. and Schwartz, E. S. (1992). Interest rate volatility and the term structure: A two-factor general equilibrium model. *Journal of Finance*, **47**(4):1259–82.

Longstaff, F. A. and Schwartz, E. S. (1995). A Simple Approach to Valuing Risky Fixed and Floating Rate Debt. *The Journal of Finance*, **50**(3):789–819.

Longstaff, F. A. and Schwartz, E. S. (2001). Valuing American options by simulation: A simple least-squares approach. *Review of Financial Studies*, pages 113–147.

Lord, R., Koekkoek, R., and van Dijk, D. (2006). A Comparison of Biased Simulation Schemes for Stochastic Volatility Models. *Tinbergen Institute Discussion Paper*, **46**(4).

Mai, J. and Scherer, M. (2012). *Simulating Copulas: Stochastic Models, Sampling Algorithms, and Applications*. Series in quantitative finance. Imperial College Press.

Mai, J. and Scherer, M. (2014). *Financial Engineering with Copulas Explained*. Financial Engineering Explained. Palgrave Macmillan UK.

Mastroeni, O. (2000). Pfandbrief-style products in Europe. *European Central Bank*.

McNeil, A., Frey, R., and Embrechts, P. (2005). *Quantitative Risk Management: Concepts, Techniques, and Tools*. Princeton Series in Finance. Princeton University Press.

Merton, R. (1974). On the Pricing of Corporate Debt: The Risk Structure of Interest Rates. *The Journal of Finance*, **29**:449–470.

Merton, R. C. (1973). An Intertemporal Capital Asset Pricing Model. *Econometrica*, **41**(5):867–887.

Merton, R. C. (1976). Option pricing when underlying stock returns are discontinuous. *Journal of Financial Economics*, **3**(1-2):125–144.

Metz, A. and Cantor, R. (2007). Moody's Credit Policy — Introducing Moody's Credit Transition Model. *Moody's Special Comment*.

MHB (2005). *Geschäftsbericht 2005*. Münchener Hypothekenbank eG.

MHB (2006). *Geschäftsbericht 2006*. Münchener Hypothekenbank eG.

MHB (2007a). *Geschäftsbericht 2007*. Münchener Hypothekenbank eG.

MHB (2007b). *Halbjahresfinanzbericht 2007*. Münchener Hypothekenbank eG.

MHB (2008). *Geschäftsbericht 2008*. Münchener Hypothekenbank eG.

MHB (2016). *Geschäftsbericht 2016*. Münchener Hypothekenbank eG.

Mikosch, T. (2009). *Non-Life Insurance Mathematics: An Introduction with the Poisson Process*. Universitext. Springer Berlin Heidelberg.

MMW (2016). *Geschäftsbericht 2016*. M.M.Warburg & CO Hypothekenbank AG.

Moreno, M. and Navas, J. F. (2003). On the Robustness of Least-Squares Monte Carlo (LSM) for Pricing American Derivatives. *Review of Derivatives Research*, **6**:107–128.

Musiela, M. and Rutkowski, M. (2006). *Martingale Methods in Financial Modelling*. Stochastic Modelling and Applied Probability. Springer.

Norris, J. R. (1998). *Markov Chains*. Number 2008 in Cambridge Series in Statistical and Probabilistic Mathematics. Cambridge University Press.

Packer, F., Stever, R., and Upper, C. (2007). The Covered Bond Market. *BIS Quarterly Review*.

PBB (2009). *Annual Report 2009*. Deutsche Pfandbriefbank.

Peña, D., Tiao, G., and Tsay, R. (2001). *A course in time series analysis*. Wiley series in probability and statistics: Probability and statistics. Wiley.

Philipp, A. (2008). *Internationale Covered Bonds - Eine Untersuchung der Produkt- und Preisbestandteile*. GRIN Verlag.

Pinedo, A. and Tanenbaum, J. (2010a). *Covered Bonds Handbook*, volume **1** of *Covered Bonds Handbook*. Practising Law Institute.

Pinedo, A. and Tanenbaum, J. (2010b). *Covered Bonds Handbook*, volume **2** of *Covered Bonds Handbook*. Practising Law Institute.

Prokopczuk, M. and Vonhoff, V. (2012). Risk premia in covered bond markets. *Journal of Fixed Income*, **22**(2):19–29.

Rast, M. and Soriano, J. P. (2013). Rating Action: Moody's assigns definitive Aaa to NATIXIS Pfandbriefbank's mortgage covered bonds. *Moody's Investors Service, Inc.*

Rebonato, R. (1998). *Interest-rate option models: understanding, analysing and using models for exotic interest-rate options*. Wiley series in financial engineering. John Wiley & Sons.

Rudolf, M. and Saunders, A. (2009). *Refinancing Real Estate Loans: Lessons to be Learned from the Subprime Crisis*. Schriftenreihe des Verbandes Deutscher Pfandbriefbanken. Vdp.

Runnenberg, J. T. (1962). On Elfving's Problem of Imbedding a Time-discrete Markov Chain in a Time-Continuous One for Finitely many States I. *Koninklijke Nederlandsche Akademie van Wetenschappen*, Proceedings, Series A, Math. Sci. **65**(5):536–541.

Samuelson, P. A. (1965). Proof that Properly Anticipated Prices Fluctuate Randomly. *IMR; Industrial Management Review (pre-1986)*, **6**(2):41–49.

Schachermayer, W. and Teichmann, J. (2008). How close are the option pricing formulas of Bachelier and Black-Merton-Scholes? *Mathematical Finance*, **18**(1):155–170.

Schaefer, S. M. and Schwartz, E. S. (1987). Time-Dependent Variance and the Pricing of Bond Options. *Journal of Finance*, **42**(5):1113–1128.

Schepsmeier, U. and Stöber, J. (2014). Derivatives and Fisher information of bivariate copulas. *Statistical Papers*, **55**(2):525–542.

Schich, S. T. (1996). Alternative Spezifikationen der deutschen Zinsstrukturkurve und ihr Informationsgehalt hinsichtlich der Inflation. *Volkswirtschaftliche Forschungsgruppe der Deutschen Bundesbank*, **8**(96).

Schlögl, L. and O'Kane, D. (2005). A note on the large homogeneous portfolio approximation with the Student-t copula. *Finance and Stochastics*, **9**(4):577–584.

Schlüchtermann, G. and Pilz, S. (2010). *Modellierung derivater Finanzinstrumente: Theorie und Implementierung*. Studienbücher Wirtschaftsmathematik. Vieweg+Teubner Verlag.

Schönbucher, P. J. (2002). Taken to the Limit: Simple and Not-so-Simple Loan Loss Distributions. *Available at SSRN: https://ssrn.com/abstract=378640*.

Schönfeld, D. (2012). Knappes Gut Pfandbrief. *Immobilien & Finanzierung — Der Langfristige Kredit*, **14**:22–23.

Shreve, S. (2004). *Stochastic Calculus for Finance II: Continuous-Time Models*. Number v. 11 in Springer Finance / Springer Finance Textbooks. Springer.

Shreve, S. (2012). *Stochastic Calculus for Finance I: The Binomial Asset Pricing Model*. Springer Finance. Springer.

Siewert, J. and Vonhoff, V. (2011). Liquidity and credit risk premia in the Pfandbrief market. *Working paper*.

Singer, B. and Spilerman, S. (1976). The Representation of Social Processes by Markov Models. *The American Journal of Sociology*, **82**(1):1–54.

Sklar, M. (1959). *Fonctions de Répartition À N Dimensions Et Leurs Marges*. Université Paris 8.

Spangler, M. (2018). *Modelling German Covered Bonds*. Mathematische Optimierung und Wirtschaftsmathematik. Springer Spektrum.

Spangler, M. and Werner, R. (2014). *German Covered Bonds*. SpringerBriefs in Finance. Springer.

Staff Team of IMF (2011). The Future of German Mortgage-Backed Covered Bond (Pfandbrief) and Securitization Markets. *IMF Country Report*, **11**(369).

Stöcker, O. (Winter 2011). Covered bond models in Europe: fundamentals on legal structures. *HOUSING FINANCE INTERNATIONAL*, pages 32–40.

Sünderhauf, R. (2006). *Bewertung des Ausfallrisikos deutscher Hypothekenbank-Pfandbriefe*. Neue betriebswirtschaftliche Studienbücher. BWV, Berliner Wissenschafts-Verlag.

Tasche, D. (2016). Fitting a distribution to value-at-risk and expected shortfall, with an application to covered bonds. *Journal of Credit Risk*, **12**(2):77–111.

Trueck, S. and Rachev, S. (2009). *Rating Based Modeling of Credit Risk: Theory and Application of Migration Matrices*. Academic Press Advanced Finance. Elsevier Science.

Tsay, R. (2010). *Analysis of Financial Time Series*. CourseSmart. Wiley.

Tsay, R. (2013). *Multivariate Time Series Analysis: With R and Financial Applications*. Wiley Series in Probability and Statistics. Wiley.

Vašìček, O. A. (1977). An Equilibrium Characterisation of the Term Structure. *Journal of Financial Economics*, **5**(2):177–188.

Vašìček, O. A. (1987). Probability of Loss on Loan Portfolio. *KMV Corporation, San Francisco, California, USA*.

VDP (2016). Daten und Fakten 2016. *Association of German Pfandbrief Banks*.

VDP (2017). Daten und Fakten 2017. *Association of German Pfandbrief Banks*.

VDP (August 2009). *The Pfandbrief 2009 | 2010*. Association of German Pfandbrief Banks, 14th edition.

VDP (August 2010). *The Pfandbrief 2010 | 2011*. Association of German Pfandbrief Banks, 15th edition.

VDP (August 2011). *The Pfandbrief 2011 | 2012*. Association of German Pfandbrief Banks, 16th edition.

VDP (August 2012). *The Pfandbrief 2012 | 2013*. Association of German Pfandbrief Banks, 17th edition.

Volk, B. (2009). Overview Covered Bonds: Adjusting to the new market. *Deutsche Bank: Global Markets Research*.

Volk, B. (2011). Covered Bond Market — set for further structural changes. *Deutsche Bank: Global Markets Research*.

Volk, B. (2017). CBPP3, Tapering und Pfandbriefe. *Der Pfandbrief 2017 | 2018*.

WBP (2015). *Geschäftsbericht 2015*. Wüstenrot Bank AG Pfandbriefbank.

WBP (2016). *Geschäftsbericht 2016*. Wüstenrot Bank AG Pfandbriefbank.

WIB (2015). *Geschäftsbericht 2015*. Westdeutsche ImmobilienBank AG.

WIB (2016). *Geschäftsbericht 2016*. Westdeutsche ImmobilienBank AG.

Widmayer, P. and Yamanaka, H. (2018). Berlin Hyp AG — Mortgage Covered Bonds. *Moody's Investors Service, Inc.*

Wilmott, P. (2006). *Paul Wilmott on Quantitative Finance*. The Wiley Finance Series. John Wiley & Sons.

Wolf, D. (2010). Schuldenkrise hinterlässt Spuren am Covered-Bond-Markt. *Börsen-Zeitung*, **170**.

Zeileis, A., Leisch, F., Hornik, K., and Kleiber, C. (2002). strucchange: An R Package for Testing for Structural Change in Linear Regression Models. *Journal of Statistical Software*, **7**(2):1–38.

Zhou, C. (1997). *A jump-diffusion approach to modeling credit risk and valuing defaultable securities.* Finance and economics discussion series. Division of Research & Statistics and Monetary Affairs, Federal Reserve Board.

Zhou, C. (2001). The term structure of credit spreads with jump risk. *Journal of Banking & Finance*, **25**(11):2015–2040.